

A Unified Approach to Resveratrol-Derived Natural Products:
Harnessing the Reactivity of Persistent Radical and Quinone Methide
Intermediates for Complex Molecule Synthesis

by

Mitchell Henry Keylor

A dissertation submitted in partial fulfillment
of the requirements for the degree of
Doctor of Philosophy
(Chemistry)
in The University of Michigan
2016

Doctoral Committee:

Professor Corey R. J. Stephenson, Chair
Professor John Montgomery
Professor Melanie S. Sanford
Professor David H. Sherman

To Fred, Sara, Ben and Hillary — for your steadfast support

ACKNOWLEDGEMENTS

“Achieving the summit of a mountain was tangible, immutable, concrete. The incumbent hazards lent the activity a seriousness of purpose that was sorely missing from the rest of my life.”

—Jon Krakauer, *Into Thin Air*

The completion of this dissertation constitutes the pinnacle of my academic career, my proudest achievement. The ascent was undoubtedly the most challenging and formative experience of my life. I am incredibly fortunate to have been granted this opportunity, and I must express my gratitude to those who have made it possible. First and foremost I must thank my advisor, Professor Corey Stephenson. Corey’s continuous and intense presence, his unspoken expectations of excellence and diligence, produced a unique atmosphere of enthusiasm and challenge. I am grateful to Corey for his generous support of my travel to and attendance at various conferences over the past several years, which fostered the development of my scientific communication skills and exposed me to some wonderful science. His guidance and the freedom of inquiry that he enabled were instrumental to my development as a scientist and professional. In his book *Outliers*, Malcolm Gladwell defines meaningful work as that which provides autonomy, complexity, and a connection between effort and reward — qualities which I was fortunate to experience in my PhD research.

The training I received during my time at Boston University in reaction mechanisms, physical organic chemistry, and spectroscopy served as the foundation for development as a synthetic chemist, and I must thank Professors Ramesh Jasti and John Snyder for their excellent instruction. I thank my dissertation committee members Professors John Montgomery, Melanie Sanford, and David Sherman — you have each been generous with your time and mentorship

during my tenure at the University of Michigan. I would also like to thank the wonderful administrative support here at UM — specifically that of Cornelius Wright, Margarita Bekiares, and Liz Oxford — you have truly made my integration into this department as seamless as possible. Finally, I would like to thank the excellent technical support here at UM, including that of Eugenio Alvarado and Chris Kojiro (NMR), Jim Windak and Paul Lennon (Mass Spectrometry), and Jeff Kampf (X-Ray Crystallography).

I have benefited immensely from the good fortune of working with a group of incredibly talented and hard-working individuals throughout my time in the Stephenson lab. I would like to specifically thank the early members of the group — Jagan Narayanam, Joe Tucker, Laura Furst, Bryan Matsuura, and John Nguyen for being role models — Jagan with his inventiveness, Joe with his industriousness and efficiency, Laura with her experimental adroitness, Bryan with his insatiable thirst for knowledge, and John with his leadership and humor. You each truly set the tone for the lab.

Bryan is deserving of special mention, as he had a hand in essentially all components of the work described herein. While I have benefited from the assistance of a number of skilled colleagues these past few years, Bryan worked with me through the most difficult parts of this research, and is likely the only one who will ever fully appreciate what it took to advance the project to its current state. Brilliant and outspoken, Bryan was able to find something interesting about just about anything and defend it articulately — with rhetoric fortified by his previous acting career (which he used for *mostly* good influence). Replete with idiosyncrasies that each of us who were fortunate enough to work with him remembers fondly, Bryan is one of the most creative minds I have encountered and I owe a significant amount of my development as a scientist to his mentorship.

I would also like to directly mention other contributors to the project. Mariia (Masha) Kirillova is a remarkable experimentalist who joined our lab for ten weeks in the summer of 2015. She played a significant role in helping us to advance our radical–arene cross coupling method and could grow crystals of just about anything. Oliver Fischer and Ryan Harding were fantastic apprentices who were instrumental to the completion of the tetramer syntheses through their assistance with the preparation of an advanced intermediate. Finally, I would like to thank Professor Derek Pratt of the University of Ottawa who has been a wonderful collaborator. I would also like to thank the members of his group who have been involved with this collaboration, including Bo Li, YuXuan Lin, Shelby Allison, and Markus Griesser. His group’s expertise in the study of free radical oxidation chemistry has been of tremendous value for helping to re-shape the thinking about the biological role of resveratrol-derived natural products and analogues through their systematic evaluation of the physical and biological properties of these compounds. Their skillful characterization of these systems extends far beyond what we would have been able to accomplish in lieu of their assistance.

A special thanks to James Douglas, Bryan Matsuura, Joel Beatty, John Nguyen, Markus Kaerkaes, Verner Lofstrand, Liz Swift, Daryl Staveness, Alex Nett, Evan Darzi, and Gina Kim for their camaraderie — there are too many good memories to share but I look forward to future encounters where we can re-live them. Finally, I would like to thank the various other labmates who I have had the pleasure of working with these past few years, including David Freeman, Carl-Johan (Calle) Wallentin, James Devery, Milena Czyz, Lara Cala, Irene Bosque-Martinez, Tim Monos, Gabe Magallanes, Martin Sevrin, Theresa Williams, Rory McAtee, Alex Sun, Kevin Romero, and Taylor Sodano. I would also like to acknowledge our extended lab family — the Schindler group — for always keeping things interesting, with special mention of Rebecca

Watson and Haley Albright, who have each become dear friends. Finally, I would like to thank Daryl, Markus, Verner, and Irene for their useful comments and suggestions during the preparation of this document.

“We live entirely by the imposition of a narrative line upon disparate images, by the ‘ideas’ with which we have learned to freeze the shifting phantasmagoria which is our actual experience”
–Joan Didion, *The White Album*

Though highly cynical, anyone who has experienced graduate studies in the physical sciences would likely agree that this quote captures the essence of those few years. You conquer previously existing limitations of your physical and intellectual capacity only to come barreling into new ones, all the while trying to prove your worth to your superiors, your peers, and most importantly, to yourself. The whole experience is uniquely humbling, a form of ‘accelerated maturation’. In traversing these years, my path was held true by the wonderful support of my family, friends, and partner, and to them I must extend my thanks. My father, Frederick Keylor, embodies courage. Hard-working, principled, and stoic, you lead by example and the opportunity to pursue higher education would not have been possible without your unwavering support and guidance. Thank you, Dad. My Mother, Sara Keylor, has and always will be my moral compass. Since childhood you have encouraged my curiosity and learning, and your unconditional love and strength inspires me. No one understands me (for better or worse) as well as my brother, Ben Keylor. It is you whose advice I seek whenever faced with a challenging decision and your honesty and wisdom has been invaluable. Hillary Tellier, I do not even know where to begin. Distance and the demands of my studies have put immense strain on our relationship, and through it all you have been nothing but loving and supportive. Your patience and composure never cease to amaze me, and your companionship keeps me grounded.

Finally, I must thank Joel Beatty, who over the past five years has become family to me. Joel is the most intelligent person that I have ever met, and now that we are each departing from the group, I can admit that upon joining the group I was intimidated to have him as my classmate. Competitive, sharp-witted (and tongued), and never-satisfied, Joel's intensity and discipline are unrivaled, and set an example for each of his co-workers (myself included) to aspire to. More importantly, however, Joel is a great friend. I am fortunate to have shared this experience with him, and have surpassed what I could have accomplished on my own by virtue of his friendship. I will miss the lively repartee with Joel, James, and Bryan, and hope to find such camaraderie in future employment.

TABLE OF CONTENTS

DEDICATIONS:.....	ii
ACKNOWLEDGEMENTS.....	iii
LIST OF FIGURES	xi
LIST OF TABLES.....	xv
LIST OF ABBREVIATIONS.....	xvii
ABSTRACT.....	xxi
CHAPTER 1: BIOSYNTHESIS AND BIOLOGICAL ACTIVITY OF RESVERATROL- DERIVED NATURAL PRODUCTS	1
1.1 Introduction.....	1
1.2 Biosynthesis of Resveratrol and Resveratrol Dimers	3
1.3 Biosynthesis of Higher-Order Resveratrol Oligomers.....	7
1.4 Therapeutic Potential of Resveratrol and its Oligomers	8
1.5 Possible Mechanisms of Action.....	12
1.6 Resveratrol and its Oligomer as Antioxidants	16
1.7 Conclusions and Outlook.....	19

CHAPTER 2: DEVELOPMENT OF A SCALABLE BIOMIMETIC RESVERATROL DIMERIZATION: APPLICATION IN TOTAL SYNTHESIS AND SYSTEMATIC EVALUATION OF RADICAL TRAPPING ANTIOXIDANT ACTIVITY	21
2.1 Introduction.....	21
2.2 Biomimetic Synthesis of Resveratrol Dimers.....	22
2.3 Biomimetic Syntheses using Modified Resveratrol Derivatives	28
2.4 Selected <i>de Novo</i> Synthetic Approaches to Resveratrol Dimers	31
2.5 Development of a Scalable Biomimetic Synthesis of 8–8' Resveratrol Dimers.....	34
2.6 Biomimetic Total Synthesis of Quadrangularin A and Pallidol	41
2.7 Systematic Evaluation of Antioxidant Activity	44
2.8 Conclusions.....	49
2.9 Experimental Procedures and Spectral Data.....	51
CHAPTER 3: TOTAL SYNTHESIS OF RESVERATROL TETRAMERS NEPALENSINOL B AND VATERIAPHENOL C.....	119
3.1 Introduction.....	119
3.2 Existing Approaches to the Synthesis of Higher-Order Resveratrol Oligomers ..	120
3.3 Concept for Biomimetic Synthesis of Higher-Order Resveratrol Oligomers.....	125
3.4 Discovery of Unusual Persistent Radical Character of Bis-Quinone Methides ...	127
3.5 Preliminary Explorations in Tetramer Synthesis	131

3.6	Strategies for Dihydrobenzofuran Synthesis	136
3.7	Applications of Persistent Radicals to Dihydrobenzofuran Synthesis.....	140
3.8	The Total Synthesis of Nepalensinol B and Vateriaphenol C	143
3.9	History and Biological Activities of Tetramers	158
3.10	Conclusions.....	160
3.11	Experimental Procedures and Spectral Data.....	162
CHAPTER 4: EFFORTS TOWARD THE TOTAL SYNTHESIS OF TRIMERIC RESVERATROL NATURAL PRODUCTS.....		314
4.1	Introduction.....	314
4.2	Toward the Synthesis of Indane-Derived Resveratrol Trimers	316
4.3	Concept for Biomimetic Trimer Synthesis and Efforts Toward this End.....	324
4.4	Future Directions: Applications of Persistent Radical Chemistry to Trimer Synthesis	330
4.5	Experimental Procedures and Spectral Data.....	335
APPENDIX A: X-RAY CRYSTALLOGRAPHIC DATA		389
REFERENCES CITED:.....		448

LIST OF FIGURES

Figure 1.1 Resveratrol Biosynthesis	3
Figure 1.2 Formation and Dimerization of Resveratrol-Derived Phenoxy Radicals.....	4
Figure 1.3 Potential Role of Dirigent Proteins in Stereoselective Coupling of Resveratrol.....	6
Figure 1.4 Divergent Biosynthesis of 8–10' Resveratrol Trimers	8
Figure 1.5 Biochemical Pathways Postulated to be influenced by Resveratrol Oligomers	14
Figure 1.6 A) Naturally-occurring small molecules which modify cysteine residues of Keap1 leading to Nrf2 derepression; B) Autoxidation and C) Oligomerization of resveratrol results in the formation of similarly reactive electrophiles	18
Figure 2.1 Regiocontrol and Product Oxidation Present Challenges for Biomimetic Resveratrol Oxidation.....	23
Figure 2.2 Whole Cell <i>B. Cinerea</i> -Mediated Dimerization of XX.....	24
Figure 2.3 Biomimetic Synthesis of Vitisin B by Sako and Co-workers	27
Figure 2.4 Regioselective Dimerizations of di- ^t Bu-4-hydroxy Styrenes and Stilbenes	28
Figure 2.5 Synthesis of Quadrangularin A by Hou, Li, et al.	29
Figure 2.6 Snyder's <i>de Novo</i> Synthetic Strategy to 8–10' (top) and 8–8' (bottom) Derived Resveratrol Dimers	32
Figure 2.7 Studer's <i>de Novo</i> Approach to Resveratrol Dimers using Pd Catalysis.....	34
Figure 2.8 Reductive and Oxidative Quenching Manifolds in Photoredox Catalysis	36
Figure 2.9 Photocatalytic Deprotection of Electron-rich Benzylic Ethers	37
Figure 2.10 Hypothesis for Photocatalytic Resveratrol Dimerization	38

Figure 2.11 A) Facial Presentation of Resveratrol Monomers During Dimerization and B) Diastereodivergence during Friedel–Crafts Cyclization.....	42
Figure 2.12 Scalable Biomimetic Synthesis of Quadrangularin A and Pallidol.....	43
Figure 2.13 A) Lipid Peroxidation; B) Inhibition by Radical Trapping Antioxidant (RTA)	44
Figure 2.14 Kinetic Product Distributions of Peroxyl Radical Trapping of Methyl Linoleate	46
Figure 2.15 Inhibited Oxidations of Phosphatidylcholine Liposomes.....	48
Figure 3.1 Biogenic Studies on A) 8–8' Trimers, B) 8–10' Trimers, and C) 8–8' Tetramers	121
Figure 3.2 Transformation of Indane Dimers to [3.2.1] and [3.3.0] Bicyclooctanes.....	122
Figure 3.3 Paradigm for DHB Synthesis through Iterative Homologation	123
Figure 3.4 Snyder's Synthesis of [3.2.1] and [3.3.0] Bicyclooctane Resveratrol Trimers and Tetramers via Desymmetrization or Two-Directional Synthesis from Dimeric Cores	124
Figure 3.5 Concept for Unified Biomimetic Synthesis of Resveratrol Oligomers	126
Figure 3.6 Experimental Results Inconsistent with Prototropic Rearrangement.....	128
Figure 3.7 Thermal Crossover Experiment Provides Insight to Free Radical Equilibrium.....	129
Figure 3.8 Persistent Radicals Discovered by Gomberg and Becker	130
Figure 3.9 Possible Configurations of Tetrameric Bis-quinone Methide (R = ^t Bu or TMS)	132
Figure 3.10 Preparation of Benzofuran Aldehyde Precursor.....	133
Figure 3.11 Preparation of <i>tert</i> -Butyl Viniferifuran Derivative.....	134
Figure 3.12 Unusual Disproportionation of Tetrameric Bis-quinone Methide.....	135
Figure 3.13 C–H Insertion for the Synthesis of Dihydrobenzofurans	137
Figure 3.14 Selected Methods Attempted for A) Benzophenone Synthesis and B) PG Incorporation for DHB Synthesis	138
Figure 3.15 Dimeric Resveratrol Indanone Resistant to Functionalization.....	140

Figure 3.16 Attempted Thermal Rearrangement of Bis-Quinone Methide Dimer	141
Figure 3.17 Dihydrobenzofuran Synthesis using Persistent Radical	142
Figure 3.18 Early Efforts to Promote DHB Synthesis through Radical Cross Coupling	143
Figure 3.19 Route to Key Aldehyde Intermediate used in Total Synthesis of Caraphenol A	144
Figure 3.20 Wittig Reaction Uniquely Effective for Synthesis of Viniferin Derivative	146
Figure 3.21 Regiodivergent Cyclization Pathways from Tetrameric Bis-Quinone Methide.....	147
Figure 3.22 Model Study for Stability of Dihydrobenzofuran to De-tert-butylation	151
Figure 3.23 Thwarted Efforts to Dealkylate Nepalensinol B Precursor	152
Figure 3.24 Model Study for Blocking Group Alternatives (Unoptimized Sequence)	153
Figure 3.25 First Generation Route to TMS-Viniferin Derivative	155
Figure 3.26 Preparation of Phosphorus-Based Olefination Reagents.....	156
Figure 3.27 Total Synthesis of Nepalensinol B, Vateriaphenol C, and Hopeaphenol.....	157
Figure 4.1 Synthesis of Caraphenol A by Snyder and Wright.....	315
Figure 4.2 Synthesis of Vaticanol A by Snyder and Co-workers.....	316
Figure 4.3 Trimeric Structures based on the Core of Quadrangularin A.....	317
Figure 4.4 Probing the Feasibility of Intermolecular Quinone Methide Functionalization.....	318
Figure 4.5 Attempted Regioselective 1,6 Additions to Quinone Methide.....	319
Figure 4.6 Friedel–Crafts Trimerization Reaction.....	321
Figure 4.7 A) Desired Cascade Cyclization and B) Unexpected Skeletal Rearrangement	322
Figure 4.8 Proposed Biomimetic Oxidative (3+2) Annulation for Trimer Synthesis	324
Figure 4.9 Dihydrobenzofuran Synthesis through Formal Oxidative (3+2) Cycloadditions	325
Figure 4.10 A) $\text{BCl}_3/\text{Me}_5\text{-Benzene}$ Mediated Debenzylation of Trimers; B) Failed Attempts at Intramolecular Oxidative (3+2) Annulation	327

Figure 4.11 A) Friedel–Crafts Trimerization of ^t Bu Resveratrol Derivative; B) Deprotection and Chemoselective Dehydrogenation of ^t Bu Trimer	328
Figure 4.12 Hexamer Formation Occurs in Preference to Intramolecular Cyclization	329
Figure 4.13 Late-Stage Dihydrobenzofuran Synthesis using Persistent Phenoxy Radicals	331
Figure 4.14 Access to tert-Butylated Natural Product Cores.....	332
Figure 4.15 A) Likely Biogenesis of Resveratrol Trimers; B) Cross Coupling Attempt Leads to only Homocoupled Products; C) Formal Cross Coupling of Resveratrol and Viniferin through Thermal Radical Crossover.....	334

LIST OF TABLES

Table 1.1 Cytotoxicities of Resveratrol Oligomers Against Various Cancer Cell Lines	11
Table 1.2 Intracellular Effects of Representative Bioactive Resveratrol Oligomers	14
Table 2.1 Enzymatic and Non-Enzymatic Dimerization Reactions of Resveratrol.....	25
Table 2.2 Dimerizations of <i>tert</i> -Butylated Resveratrol and Protected Derivatives	30
Table 2.3 Optimization of Oxidative Resveratrol Dimerization.....	40
Table 2.4 RTA Activity of Resveratrol Dimers and Derivatives.....	47
Table 3.1 Variable Product Distribution in Friedel–Crafts Cylization.....	128
Table 3.2 Optimization of Tetramer Cyclization.....	149
Table 3.3 Comparison of ¹ H-NMR Spectrum of 3.67 with Reported Literature Data	211
Table 3.4 Comparison of ¹³ C-NMR Spectrum of 3.67 with Literature Reported Data	212
Table 3.5 Comparison of ¹ H-NMR Spectrum of 3.68 with Literature Reported Data	213
Table 3.6 Comparison of ¹³ C-NMR Spectrum of 3.68 with Literature Reported Data	214
Table 3.7 Comparison of ¹ H-NMR Spectrum of 3.69 with Literature Reported Data	215
Table 3.8 Comparison of ¹³ C-NMR Spectrum of 3.69 with Literature Reported Data	216
Table A.1 Crystal Data and Structural Refinement for 2.52.....	389
Table A.2 Atomic coordinates (x10 ⁴) and equivalent isotropic displacement parameters (Å ² x 10 ³) for 2.52	390
Table A.3 Bond Lengths [Å] and Angles [°] for 2.52	392
Table A.4 Anisotropic Displacement Parameters (Å ² x 10 ³) for 2.52	403

Table A.5 Hydrogen Coordinates ($\times 10^4$) and Isotropic Displacement Parameters ($\text{Å}^2 \times 10^3$) for 2.52.....	405
Table A.6 Torsion Angles [$^\circ$] for 2.52.....	407
Table A.7 Crystal Data and Structural Refinement for 4.12.....	412
Table A.8 Atomic coordinates ($\times 10^4$) and equivalent isotropic displacement parameters ($\text{Å}^2 \times 10^3$) for 4.12	413
Table A.9 Bond Lengths [Å] and Angles [$^\circ$] for 4.12	415
Table A.10 Torsion Angles [$^\circ$] for 4.12.....	425
Table A.11 Crystal Data and Structural Refinement for 4.20.....	429
Table A.12 Atomic coordinates ($\times 10^4$) and equivalent isotropic displacement parameters ($\text{Å}^2 \times 10^3$) for 4.20	430
Table A.13 Bond Lengths [Å] and Angles [$^\circ$] for 4.20	432
Table A.14 Torsion Angles [$^\circ$] for 4.20.....	443

LIST OF ABBREVIATIONS

°C	degrees Celsius
δ	chemical shift in parts per million
μL	microliters
μM	micromolar
α -TOH	alpha-tocopherol
5-LOX	arachidonate 5-lipoxygenase
abs	absorbance
Ac	acetyl
ACE	angiotensin converting enzyme
AChE	acetylcholinesterase
AIBN	azobisisobutyronitrile
Akt	protein kinase B
APPH	2,2'-azobis-(2-amidinopropane)-dihydrochloride
ARE	antioxidant response element
ATRA	atom transfer radical addition
A β	amyloid- β
aq.	aqueous
Ar	aryl
BAD	BCL-2-associated death promoter
BAX	BCL-2-associated X protein
BCL-2	B-cell lymphoma 2
BCL-XL	B-cell lymphoma-extra large
BDE	bond dissociation energy
BHT	2,6-di- <i>tert</i> -butyl-4-hydroxytoluene
Bn	benzyl
Boc	<i>tert</i> -butyloxycarbonyl
Bu	<i>n</i> -butyl
bpy	2,2'-bipyridine
bpz	2,2'-bipyrazine
caspase	cysteine-dependent aspartate-directed proteases
cm	centimeters
COX-1	cyclooxygenase-1
Cp	cyclopentadienyl
Cys	cysteine
d	doublet
DBU	1,8-diazabicyclo[5.4.0]undec-7-ene
dd	doublet of doublets
DDQ	2,3-dichloro-5,6-dicyano-1,4-benzoquinone
dF(CF ₃)ppy	2-(2,4-difluorophenyl)-5-(trifluoromethyl)pyridine

DFT	density functional theory
DHB	dihydrobenzofuran
DIBAL-H	diisobutylaluminum hydride
DISC	death-inducing signaling complex
DMF	dimethylformamide
DMP	Dess-Martin periodinane
DMSO	dimethylsulfoxide
DNA	deoxyribonucleic acid
DP	dirigent protein
DPPH	2,2-diphenyl-1-picrylhydrazyl
dr	diastereomeric ratio
dtbbpy	4,4'-di-tert-butyl-2,2'-bipyridine
EC ₅₀	half maximal effective concentration
EDG	electron-donating group
ee	enantiomeric excess
E^{ox}_{p}	standard oxidation potential
EPR	electron paramagnetic resonance
eq.	equation
equiv	molar equivalents
ERK	extracellular-signal-regulated kinases
ESI	electrospray ionization
Et	ethyl
EtOH	ethanol
EWG	electron-withdrawing group
<i>fac</i>	facial
FADD	Fas-Associated protein with Death Domain
FTIR	Fourier transform infrared spectroscopy
g	grams
GPCR	G-protein-coupled receptors
GPx	glutathione peroxidase
GSH	glutathione
GSK	GlaxoSmithKline
h	hours
H ₂ B-PMHC	BODIPY-2,2,5,7,8-pentamethyl-6-hydroxy-chromane
HAT	hydrogen atom transfer
HCV	hepatitis c virus
HIF-1	hypoxia-inducible factor 1
HMDS	hexamethyldisilazide
HO-1	heme oxygenase-1
HPLC	high performance liquid chromatography
HRMS	high resolution mass spectrometry
HRP	horseradish peroxidase
Hz	Hertz
IC ₅₀	half maximal inhibitory concentration
IFN	interferon
IL	interleukin

iNOS	inducible nitric oxide synthase
I κ B	inhibitor of κ B
IR	infrared
<i>J</i>	coupling constant in units of Hertz
Keap1	Kelch-like ECH-associated protein 1
L	liters
LFP	laser flash photolysis
LPS	lipopolysaccharide
m	multiplet
M	molar concentration
MAPK	mitogen-activated protein kinases
Me	methyl
MeCN	acetonitrile
MeOAMVN	2,2'-azobis(4-methoxy-2,4-dimethylvaleronitrile)
MeOH	methanol
mg	milligrams
MHz	megahertz
min	minutes
mL	milliliters
MLCT	metal to ligand charge transfer
mm	millimeters
mmol	millimoles
MMP-1	matrix metalloproteinase-1
mol	moles
MRP1	multidrug resistance-associated protein 1
NBS	<i>N</i> -bromosuccinimide
<i>n</i> -BuOH	<i>n</i> -butanol
NF- κ B	nuclear factor kappa-light-chain-enhancer of activated B cells
nM	nanomolar
nm	nanometers
NMR	nuclear magnetic resonance
Nrf2	nuclear transcription factor erythroid 2-related factor 2
[O]	oxidant
PARP1	poly(ADP-ribose) polymerase 1
PC	photocatalyst
PET	photoinduced electron transfer
PI3K	phosphatidylinositol 3-kinase
PIDA	[diacetoxyiodo]benzene
PIFA	[bis(trifluoroacetoxy)iodo]benzene
PG	protecting group
PKC	protein kinase C
PMB	<i>para</i> -methoxybenzyl protecting group
PPAR	peroxisome proliferator-activated receptors
ppm	parts per million
ppy	2-phenylpyridine
q	quartet

ROS	reactive oxygen species
RT	room temperature
RTA	radical trapping antioxidant
s	singlet
SAR	structure activity relationship
SCE	saturated calomel electrode
SPLET	sequential proton loss electron transfer
STAT-1	Signal transducer and activator of transcription 1
t	triplet
T3SS	type III secretion system
TBAF	tetra- <i>n</i> -butyl ammonium fluoride
TBS	<i>tert</i> -butyl-dimethylsilyl
^t Bu	<i>tert</i> -butyl
THF	tetrahydrofuran
TLC	thin layer chromatography
TMS	trimethylsilyl
Topo II	topoisomerase II
tRNA	transfer ribonucleic acid
TXN	thioredoxin
TYR	tyrosinase
TyrRS	tyrosyl transfer-RNA (tRNA) synthetase
UV	ultraviolet
V	volts
VSMC	vascular smooth muscle cells
YopE	<i>Yersinia pseudotuberculosis</i> outer protein E
YopH	<i>Yersinia pseudotuberculosis</i> outer protein H

ABSTRACT

Numerous reports of therapeutically relevant biological activities of resveratrol (3,4',5-trihydroxy-*trans*-stilbene) and oligomers derived therefrom have stimulated widespread interest in these natural products. In spite of this, their chemical synthesis has only recently been targeted. This is largely a symptom of the historically enigmatic mechanisms of action of polyphenols, which has precluded their clinical development. If the therapeutic potential of polyphenolic natural products such as the resveratrol oligomers is to be realized, synthetic advances must be made in order to confirm/refute the biological activities ascribed to oligomers obtained from isolates, to determine which scaffolds hold promise as small molecule chemopreventives and/or chemotherapeutics, and to enable structural modification for both structure-activity relationship (SAR) studies and the development of more potent congeners. The work described herein seeks to address the above issues through collaborative research, combining novel methods for chemical synthesis, physical chemistry and chemical biology in an effort to elucidate the mechanism(s) of biological activity of resveratrol and its derivatives and shed light on potential of plant-derived antioxidants in pathophysiology wherein oxidative stress has been implicated. Chapter 1 summarizes the biosynthesis and biological activities of resveratrol-derived natural products in order to contextualize our biomimetic synthetic strategy and provide justification for our research objectives. Chapter 2 describes the development of a highly efficient and scalable oxidative dimerization of *tert*-butylated resveratrol derivatives, which for the first time has rendered biomimetic synthesis a viable approach for the controlled preparation of useful quantities of resveratrol oligomers. This method was showcased in the

synthesis of dimeric natural products pallidol (6 steps/26% yield) and quadrangularin A (5 steps/54% yield), each representing the most efficient synthesis (either biomimetic or *de novo*) to date. Recently, the concise biomimetic total synthesis of resveratrol tetramers nepalensinol B, vateriaphenol C, and hopeaphenol was accomplished, representing just the second reported total synthesis of tetrameric resveratrol oligomers, and the first to these specific targets. The details of these efforts are provided in Chapter 3. The final chapter delineates our preliminary and ongoing efforts toward the application of this biomimetic strategy to the synthesis of resveratrol trimers.

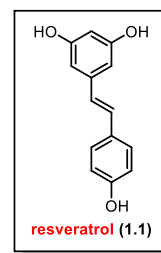
CHAPTER 1: BIOSYNTHESIS AND BIOLOGICAL ACTIVITY OF RESVERATROL-DERIVED NATURAL PRODUCTS

*Portions of this chapter have been published in:

Keylor, M. H.; Matsuura, B. S.; Stephenson, C. R. J. *Chem. Rev.* **2015**, *115* (17), 8976–9027.

1.1 Introduction

The level of public interest in the health benefits of antioxidant supplements is astounding. The global nutraceutical market, currently valued at US \$182.6B, is projected to reach \$278.96B by 2021.¹ The popularity of these products is driven by the belief — on the basis of epidemiological evidence — that the consumption of foods that are rich in antioxidants is associated with lower incidence of degenerative disease and an increase in longevity.^{2,3} Despite the staggering amount of literature regarding antioxidants, studies often present inconsistent results on the potency and/or mechanism of action for a given compound or class of compounds. Resveratrol (**1.1**) is a particularly striking example given that it has captivated both the scientific community and general public, yet little is understood about the mode or extent of its biological activity. This ambiguity is even more prominent for the seemingly endless number of natural products (dimers and oligomers) derived from it. In fact, the relative abundance of resveratrol (**1.1**) in the skin of red grapes (and wine made therefrom) has been credited as the key to the so-called French Paradox: the low incidence of cardiovascular disease in the French population despite elevated



risk factors.^{4,5} Although the reality of the French Paradox remains contentious,^{6,7} research into the health benefits of resveratrol has exploded as a result.

Given the widespread public interest in resveratrol supplementation as a prophylactic measure (an industry earning \$30 million per annum in the U.S. alone⁸), it is imperative that we understand the biological mode of action of **1.1** and its various metabolites as well as their impact on human health. The vast range of activities and differing potencies attributed to resveratrol in hundreds of *in vitro* studies may be more easily accounted for if one of its many possible oxidation products — including the naturally-occurring dimers and oligomers — were responsible. These higher products offer significantly more intricate architectures than resveratrol itself, the three-dimensionality of which imbues a much higher probability for selective binding within a cell. Thus, the wealth of proposed modes of action for resveratrol may be partially, or even solely, due to highly potent activities of the various oligomeric contaminants. To deconvolute this issue, each potential active agent must be analyzed separately. However, isolation efforts have supplied only minimal quantities of single materials through extensive purification and *de novo* synthesis of these targets has not yet become general enough to provide sufficient quantities for rigorous evaluation. The lack of a reliable supply necessitates the development of new synthetic strategies. The research described herein details our efforts to address this demand through the development of a unified synthetic approach to resveratrol-derived natural products — an approach enabled largely by the discovery of new methods to both access and harness the reactivity of unusual persistent radical and quinone methide intermediates.

This chapter succinctly summarizes the biosynthesis and biological activities of resveratrol-derived natural products in order to contextualize our synthetic strategy and provide

justification for these research objectives. Subsequent chapters present the results of these studies, which establish a unified biomimetic strategy for the chemical synthesis of the resveratrol oligomers. Additional literature precedent germane to the content of each chapter will be supplemented throughout.

1.2 Biosynthesis of Resveratrol and Resveratrol Dimers

In producing organisms, the biosynthetic pathway to resveratrol — namely, the phenylpropanoid polymalonate pathway — is common to a variety of natural scaffolds, including the cinnamic acid, coumarin, and lignan families natural products.⁹ Phenylalanine (**1.2**), a product of the shikimate pathway, undergoes a series of enzymatic reactions to produce the linear tetraketide **1.3** (Figure 1.1). Under normal cellular conditions, chalcone synthase — a type III polyketide synthase — is constitutively expressed, resulting in the cyclization of **1.3** to chalcone (not depicted) and ultimately leading to the production of flavonoid natural products such as naringenin (**1.4**).¹⁰ The gene encoding stilbene synthase, on the other hand, is transcribed only in response to stress factors whose expression is induced by external stimuli such as pathogenic invasion or UV irradiation.¹¹ Resveratrol and its derivatives can thus be defined as phytoalexins¹² — plant-derived secondary metabolites generated for defensive purposes — and are vital to the maintenance of the functional integrity of plant cells under stressing conditions.

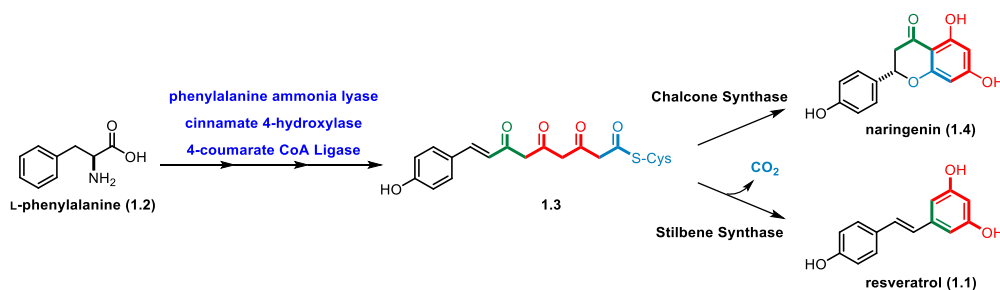


Figure 1.1 Resveratrol Biosynthesis

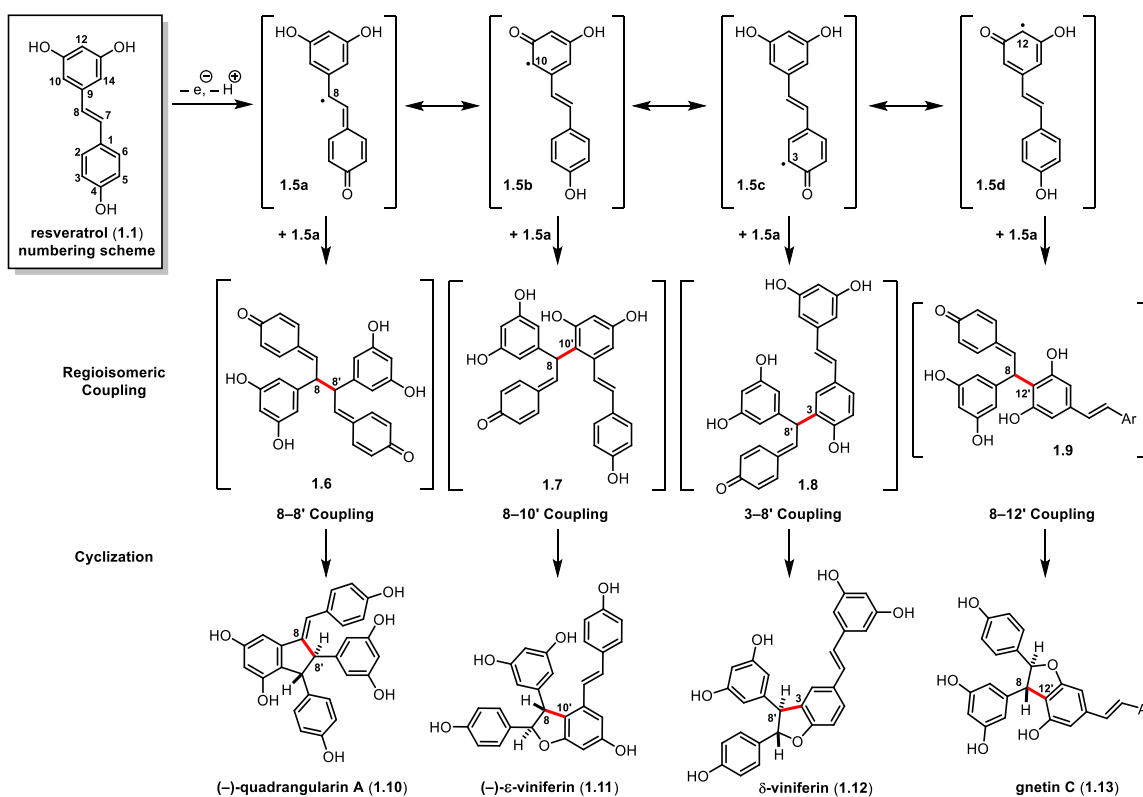


Figure 1.2 Formation and Dimerization of Resveratrol-Derived Phenoxy Radicals

Once formed, the fates of **1.1** are myriad. Various derivatizations (e.g. glycosylation, methylation) serve to modify the physical properties of **1.1**, such as its reduction potential,¹³ or to facilitate its storage and translocation within the plant tissues.¹⁴ The extended conjugation and electron rich nature of resveratrol — particularly the presence of the 4-hydroxy stilbene moiety — renders it susceptible to oxidation ($E_p^{ox} = +1.14$ V vs SCE in MeCN)¹⁵ under physiological conditions,^{16,17} let alone in times of duress when reactive oxygen species (ROS) are known to be present at higher concentrations.¹⁸ While the pathway of resveratrol biosynthesis has been elucidated, the cellular constituents responsible for its oxidative oligomerization remain to be identified. In fact, most of what is currently understood about this process has been inferred through biomimetic oxidation studies. Nonetheless, there is compelling evidence that the biogenesis of resveratrol oligomers takes place via single electron oxidation processes (Figure 1.2), yielding reactive quinone methide intermediates en route to a diverse series of complex

polyphenols.¹⁹ Regardless of whether laccases,^{20–23,13} peroxidases,^{24–28} or simple autoxidation¹⁶ promote this event, removal of a proton and electron from resveratrol (**1.1**) generates phenoxyl radical **1.5**, the reactivity of which is best described by resonance hybrids **1.5a–d**.

The regioisomeric preferences during dimerization are largely dictated by the localization of the unpaired electron on carbons where it is captodatively stabilized as a quinone methide (**1.5a**) or semiquinone (**1.5b–d**) radical. As phenoxyl radical **1.5a** participates in each of the depicted oxidative couplings, the putative biogenic intermediates that result (**1.6 – 1.9**) each bear highly-reactive *para*-quinone methides which can undergo numerous regiodivergent Friedel–Crafts reactions, nucleophilic trappings, or tautomerizations. Operating on this widely accepted biosynthetic hypothesis, a survey of the literature renders it clear that the 8–8' coupling (as found in quadrangularin A (**1.10**)^{29,30} and 8–10' (ϵ -viniferin (**1.11**))³¹ coupling modes are the most prevalent in nature, whereas the 3–8' coupling mode (δ -viniferin (**1.12**))^{25,26} predominates in the vast majority of biomimetic studies. Products derived from 3–12' coupling (gnetin C (**1.13**)),³² on the other hand, are relatively uncommon. The underlying factors controlling the stereo- and regiochemical outcome of resveratrol dimerization in plants are unknown, though it is tempting to draw parallels between the biosynthesis of resveratrol oligomers and that of plant lignans, polyphenolic substances formed via the oxidative dimerization of substituted cinnamyl alcohols.

In 1997, Davin and Lewis isolated, expressed, and characterized a previously unknown protein, *FiDIR1*, which exhibited the unique ability to convert (*E*)-coniferyl alcohol (**1.14**) — via the intermediacy of putative bis-*para*-quinone methide intermediate **1.15** — to the optically active lignan, (+)-pinoresinol (**1.16**) in the presence of peroxidases or inorganic oxidants (Figure 1.3).^{33,34} They termed the unprecedented *FiDIR1* a “dirigent protein” (DP) (Latin: *dirigere*, to

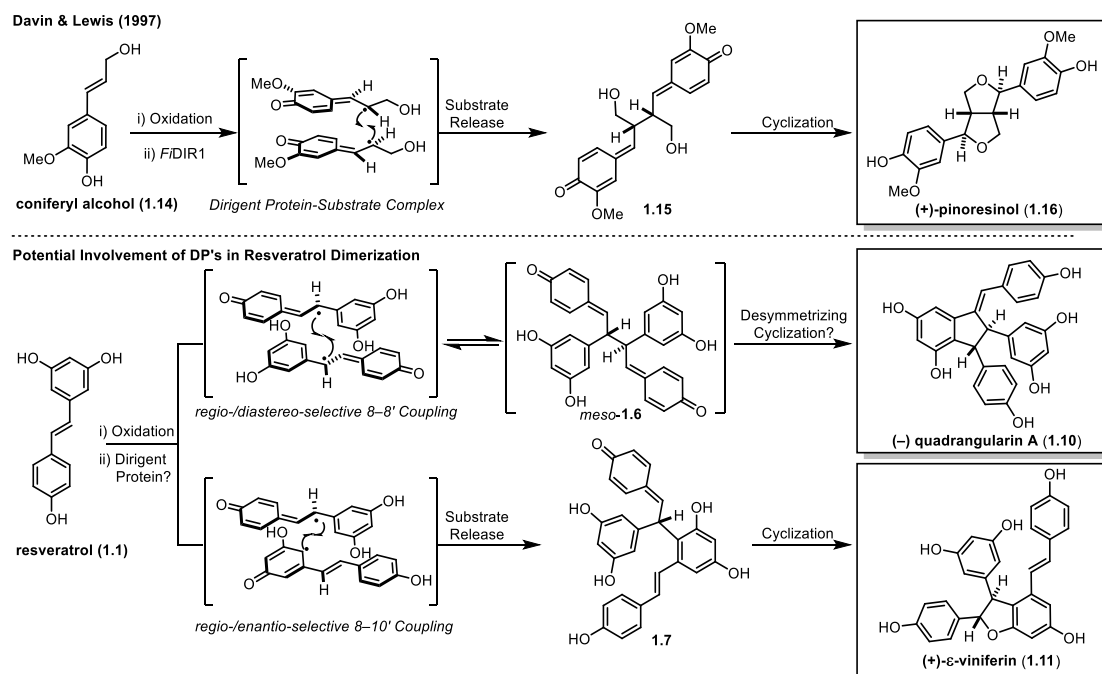


Figure 1.3 Potential Role of Dirigent Proteins in Stereoselective Coupling of Resveratrol

align or guide) based on its ability to dictate the regio- and stereo-chemical outcome of monolignol dimerization. The structural similarity of the resveratrol oligomers and lignans, their shared origin (phenylpropanoid pathway), and their common role as phytoalexins has engendered speculation that product distributions during resveratrol dimerization may too be influenced by dirigent proteins.^{35–37} For instance, (–)-quadrangularin A (**1.10**) is likely formed through cyclization and tautomerization of *meso*-**1.6**. Thus, the isolation of optically active (–)-quadrangularin A (**1.10**) implies the participation of a chiral entity, such as a DP, to promote the enantioselective desymmetrization of prochiral **1.6**. Likewise, ϵ -viniferin (**1.11**) is isolated from nature in optically active form; (–)- ϵ -viniferin is found in several plant families including Dipterocarpaceae, Gnetaceae, Cyperaceae, and Fabaceae (Leguminosae), while its enantiomer, (+)- ϵ -viniferin, is exclusively found in plants from the family Vitaceae. Hence, it would seem plausible that a DP-like protein controls the stereochemical outcome in the conversion of **1.1** to

putative biosynthetic intermediate **1.7**, although no such protein has been discovered to substantiate this hypothesis.

1.3 Biosynthesis of Higher-Order Resveratrol Oligomers

The resveratrol dimers are almost universally generated by an initial oxidative radical coupling. In contrast, the higher-order oligomers (trimers – octamers) can be the product of *either* an oxidative coupling to resveratrol (**1.1**)/ ϵ -viniferin (**1.11**) *or* an intermolecular Friedel–Crafts reaction. In addition to the dihydrobenzofuran, indane, bicyclic [3.2.1], and bicyclic [3.3.0] ring systems that characterize the resveratrol dimers, higher oligomers introduce several distinctive architectures which rapidly increase both the complexity of individual structures and the diversity across the natural product class. Among these are six-, seven-, eight-, and nine-membered carbocycles, and even bicyclic [6.2.1] ring systems. Given the vast structural diversity emblematic of the higher oligomers, a detailed discussion of their likely biogenic pathways is beyond the purview of this chapter, and the reader is instead directed to our recent review of this topic.¹⁹ Suffice it to say that for a majority of the resveratrol dimers, trimers and tetramers, oligomerization occurs through an *intermolecular* radical coupling, followed by *intramolecular* Friedel–Crafts cyclization(s).

In 2012, Pan *et al.* were able to recapitulate the biosynthetic relationship between ϵ -viniferin (**1.11**), resveratrol (**1.1**), and miyabenol C (**1.17**)³⁸ through a biomimetic horseradish peroxidase (HRP)-mediated crossed trimerization reaction (Figure 1.4).³⁹ As a representative example, the oxidative crossed dimerization between the C₈-position of ϵ -viniferin (**1.11**) and the C₁₀-position of resveratrol (**1.1**) would yield quinone methide intermediate **1.18**, which is poised for rapid diversification through regiodivergent annulation pathways. An oxa-conjugate addition of the pendant resorcinol (Path A) affords miyabenol C (**1.17**), which can undergo a subsequent

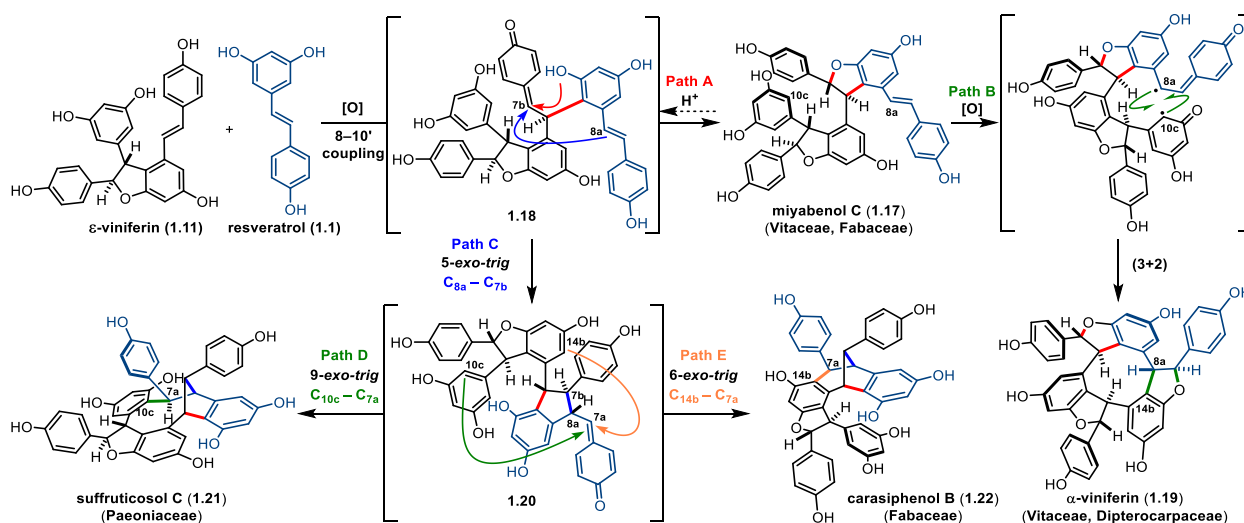


Figure 1.4 Divergent Biosynthesis of 8–10' Resveratrol Trimers

oxidative (3+2) dihydrofuran annulation (Path B) to form the bioactive cyclotrimer, α -viniferin (1.19).²⁶ Alternatively, 1.18 — perhaps formed reversibly from 1.17 in the presence of acid — can be trapped through a vinyllogous Friedel–Crafts reaction from the adjacent 4-hydroxy stilbene (Path C), in turn generating a new quinone methide intermediate 1.20. From here, dichotomous 9-*exo-trig* (Path D) and 6-*exo-trig* (Path E) cyclizations provide the bicyclic cores of suffruticosol C (1.21)⁴⁰ and carasiphenol B (1.22),⁴¹ respectively.

1.4 Therapeutic Potential of Resveratrol and its Oligomers

Since the popularization of resveratrol at the end of the 20th century, an enormous number of studies have been undertaken in an effort to define its pharmacological profile. Initial excitement spawned from a 1997 report by Pezzuto and co-workers describing cancer chemopreventive activity of 1.1 through anti-initiation, anti-promotion, and antipromotion activity.^{42,43} In the wake of this study, a series of high-impact publications appeared over the next decade from Sinclair and co-workers reporting that resveratrol behaved as a sirtuin activating compound in various models, including *Saccharomyces cerevisiae* (yeast),⁴⁴ metazoans (including *C. elegans* and *Drosophila melanogaster*),⁴⁵ and ultimately in mouse models.⁴⁶ The sirtuins are a family of

protein deacetylases whose activity is proposed to underly the life-extending properties of caloric restriction. These discoveries led to the founding of Sirtris Pharmaceuticals, a start-up which was acquired by GlaxoSmithKline (GSK) in 2008 for \$720 million. However, clinical trials were later terminated (ClinicalTrials.gov Identifier: NCT00920556), and the company was absorbed by GSK where sirtuins remain an active area of research and development. More recently, a study by Sajish and Schimmel implicates human tyrosyl transfer-RNA (tRNA) synthetase (TyrRS) as a poly(ADP-ribose) polymerase 1 (PARP1)-activating effector target for resveratrol, and TyrRS-mediated PARP1-activation was demonstrated to occur at lower *in vitro* concentrations of resveratrol (**1.1**) than observed for binding to other targets.⁴⁷

In spite of hundreds of additional publications detailing the biological activity of resveratrol, including antioxidant,^{48,49} anticancer,⁵⁰ and cardioprotective⁵¹ activity, its therapeutic potential and mode of action remain highly contentious.⁵²⁻⁵⁵ The promiscuity of resveratrol as a ligand in biological systems has been acknowledged,^{56,57} and its implementation in human therapeutic applications is forestalled by its poor bioavailability^{58,59} and an incomplete understanding of its pharmacodynamics. Similar to its role in the plant, where resveratrol dimers and higher oligomers are much more potent as antifungal phytoalexins than their parent monomer,³¹ the “broad spectrum” biological activity of resveratrol *in vitro* is likely a reflection of the intrinsic reactivity of the trihydroxylated stilbene as a redox-active molecule. Given how readily resveratrol autoxidizes under ambient conditions,¹⁶ it is possible, if not likely, that dimerization and further oligomerization of resveratrol takes place spontaneously. As such, the many biological activities of resveratrol may, in fact, be due to the *in situ* formation of these compounds, which subsequently act as potent ligands or exert their activity through further reactivity as either radical-trapping antioxidants or electrophiles. Indeed, the probability of

selective modulation of targets within a chiral cellular environment is rapidly enhanced as a small, two-dimensional molecule (resveratrol) is transformed into a complex three-dimensional structure.

In fact, many of the resveratrol oligomers have demonstrated potent activity as enzyme inhibitors and/or cytotoxic compounds. For example, the resveratrol tetramers nepalensinol B and vitisin B have been found to inhibit topoisomerase II ($IC_{50} = 11$ nM) and the NS3 helicase involved in hepatitis C virus (HCV) replication ($IC_{50} = 3$ nM), respectively.^{60,61} Additionally, a large number of related trimers and tetramers have exhibited micromolar EC_{50} values against various cancer cell lines (Table 1.1).¹⁹ The anticarcinogenic effects of resveratrol and its oligomers have principally been ascribed to cytotoxicity and induction of apoptosis, although antimutagenic and antiproliferative activities have also been observed.

From a structure-activity relationship (SAR) standpoint, salient features of the resveratrol oligomers include 2,3-dihydrobenzofurans (DHBs), indanes, and medium-sized rings. Indanes and DHBs are highly attractive scaffolds for medicinal chemistry due to the combination of aliphatic and aromatic properties within a rigid ring system and the ability for diversification of both the identity and relative configuration of substituents at each of the contiguous sp^3 -hybridized ring carbons.⁶² Ligands containing the indane substructure are among those with the highest affinities for G-coupled protein receptors (GPCRs), and structures highly analogous to those comprising the cores of resveratrol dimers and higher oligomers — such as enrasentan — have been implemented as potent endothelin receptor antagonists.⁶³ The 2,3-dihydrobenzofuran also represents a privileged scaffold present in a variety of biologically active molecules, including those with reported activity against pathologies such as cancer, HIV, tuberculosis, and

Table 1.1 Cytotoxicities of Resveratrol Oligomers Against Various Cancer Cell Lines

Cell lines; ^{refs}	Most active compd	(EC ₅₀ , μ M) ^a	Cell lines; ^{refs}	Most active compd	(EC ₅₀ , μ M) ^a
Cervical (Adeno)carcinoma			Colon (Adeno)carcinoma		
HeLa; ⁶⁴⁻⁶⁶	pauciflorol B	2.8	SW-480; ⁶⁷⁻⁷⁰	vaticanol C	3.2
HSG; ⁷¹	sophorastilbene A	108.0	DLD-1; ^{67,69}	vaticanol C	—
KB; ^{64,66,72-75}	peracetyl ampelopsin A	0.8	COLO-201; ^{67,69}	vaticanol C	—
Ovarian (Adeno)carcinoma			Lung (Adeno)carcinoma		
1A9; ⁷⁴	peracetyl ampelopsin A	1.0	A549; ^{70,72,80-75}	<i>cis</i> -vitisin A	0.93
SK-OV-3; ⁷⁷	<i>cis</i> -vitisin A	0.17	NCI-H446; ⁷⁹⁻⁸¹	α -viniferin	16.1
Breast (Adeno)carcinoma			NCI-H460; ⁸⁰	kobophenol A	200
MCF-7; ^{65,74,76,78,82-86}	peracetyl ampelopsin A	2.8	NCI-H1299; ⁷⁶	vaticanol A	19.7
MDA-MB-231; ^{76,86,87}	hopeachinol E	14.3	SPC-A-1; ⁸⁰	—	—
BJMC-3879; ⁸⁸	vaticanol C	8.0	Liver Carcinoma		
BC-1; ⁷³	(-)-vatdiospyroidol	4.2	Hep-G2; ^{78,82,83,87,89}	hopeachinol J	12.4
Leukemia			SMMC-7721; ⁸⁷	hopeachinol F	10.4
P388; ^{90,91}	(-)-hopeaphenol	5.2	Clear Cell Renal Carcinoma		
EHEB; ⁹²	—	—	Caki-1; ⁷⁴	peracetyl ampelopsin A	5.5
WSU-CLL and ESKOL; ⁹²	ϵ -viniferin	6.7	Prostate (Adeno)carcinoma		
Jurkat; ⁹³	miyabenol C	29.4	LNCaP; ⁶⁷	vaticanol C	N/A
HL-60; ^{65,67,71,78,87,91,94-97}	vaticanol C	3.0	PC-3; ⁶⁷	α -viniferin	N/A
K562; ^{67,93}	miyabenol C	18.7	Neuroblastoma		
Myeloma			SH-SY57; ^{69,85}	vaticanol C	N/A
U266; ⁹³	miyabenol C	12.1	C6; ⁸³	gnetin H	18.7
RPMI-8226; ⁹³	miyabenol C	20.8	Sarcoma		
Lymphoma			S-180; ⁹⁹	extract- <i>Vat. indica</i>	29.5
U937; ^{67,93,100}	heyneanol A	6.6	SaOS-2; ⁷⁴	peracetyl ϵ -viniferin	11.3
Colon (Adeno)carcinoma			Oral Squamous Carcinoma		
HCT-116; ^{68,81,86,87}	α -viniferin	6.6	HSC-2; ⁷¹	sophorastilbene A	27.0
HT-29; ^{81-83,86}	α -viniferin	32.6	HSC-3; ⁷¹	(+)- α -viniferin	60.0
Caco-2; ⁸¹	α -viniferin	16.1	Malignant Melanoma		
Col-2; ⁷³	(-)-vatdiospyroidol	2.1	SK-MEL-2; ^{74,77}	vitisin B	4.9
HCT-8; ⁷⁴	peracetyl ampelopsin A	5.7			

^aAll values reported as (μ g/mL) have been converted to EC₅₀ (μ M) for the sake of comparison.

malaria, as well as those with reported inhibition of specific targets including hypoxia-inducible factor 1 (HIF-1), NF- κ B, α -glucosidase, arachidonate 5-lipoxygenase (5-LOX), and the muscarine M₃ receptor.^{101,102} Finally, the medium-sized rings found in many resveratrol trimers and tetramers have also proven to be privileged structural motifs in biologically active natural products, including Taxol, vinblastine, and colchicine. The synthesis of medium-sized rings is challenging due to various unfavorable enthalpic and entropic factors, including torsional, transannular, and large-angle strain, and therefore new strategies must be devised to address this demand.¹⁰³

1.5 Possible Mechanisms of Action

Hundreds of studies have been conducted in which observed responses in phenotypic assays have been used to justify claims to specific mechanisms of action for resveratrol and a select number of its oligomers. For example, modes of action identified for resveratrol include inhibition of cellular differentiation, cell invasion, and angiogenesis,¹⁰⁴ and induction of phase II drug-metabolizing enzymes.^{42,105} Conversely, **1.1** has also been associated with induction of apoptosis through mitochondrial membrane depolarization via up-regulation of pro-apoptotic BAX and various caspases (cysteine-dependent aspartate-directed proteases) with concomitant reductions in levels of anti-apoptotic BCL-2 and BCL-XL.^{93,56}

Like resveratrol, the postulated modes of action of its dimers and higher oligomers are numerous. However, few investigations were performed with sufficient rigor to be worthy of discussion. The resveratrol oligomers ϵ -viniferin (**1.11**), α -viniferin (**1.19**) and vaticanol C (**1.23**) are arguably the most well-studied resveratrol dimer, trimer, and tetramer, respectively, in the context of biological activity (Table 1.2). Thus, a brief discussion of their purported biological activities and corresponding modes of action (Figure 1.5) provided as an implication of the extensive therapeutic potential within the broader class of resveratrol oligomers. The resveratrol dimer ϵ -viniferin (**1.11**) is perhaps the most important of the resveratrol oligomers not only because it serves as the biogenic precursor to nearly all higher-order oligomers (*vide supra*), but also because it exhibits diverse biological activity in its own right (although spontaneous transformations of **1.11** to other oligomers *in situ* may contribute to observed activities).

ϵ -Viniferin exhibits activity primarily as an antiproliferative/cytotoxic plant metabolite with additional influence over various processes affecting cellular redox homeostasis. A comparative study of the antiproliferative and apoptotic effects of resveratrol, ϵ -viniferin, and vine shoot-

derived polyphenols (vineatrols) on chronic B lymphocytic leukemia cells and normal human lymphocytes found that **1.11** exhibits only moderate pro-apoptotic capacities.¹⁰⁶ However, peracetylation of **1.11** resulted in a marked improvement in the efficiency of the compound in this regard, promoting apoptosis of immortalized B-cell lines and in primary chronic lymphocytic leukemia (B-CLL) cells.⁹² The acetyl derivative was shown to inhibit inducible nitric oxide synthase (*i*NOS) expression and NO production. The compound was also found to induce DNA fragmentation in both the WSU-CLL cell line and in primary B-CLL cells. Various mitochondrial events associated with apoptosis, including dissipation of transmembrane potential and reduction in the levels of anti-apoptotic protein BCL-2 were observed. Additionally, increases in the activity of effector caspase-3 were induced by treatment with the acetyl derivative of ϵ -viniferin.⁹² A related study indicated that ϵ -viniferin arrests cell cycle progression of the myeloma cell line U266 in the G2/M phase.⁹³ This study also found that the compound does not act directly on the mitochondrial membrane, but induces activation of upstream caspases (specifically caspase-8) independently of Fas/FasL interaction, although it remains possible that it promotes apoptosis by forming a death-inducing signaling complex (DISC) involving Fas, FADD, and procaspase 8 in the absence of any interaction with FasL.

It has also been shown that ϵ -viniferin can influence the redox environment of vascular smooth muscle cells (VSMCs) through derepression of Nrf2 (nuclear transcription factor erythroid 2-related factor 2) resulting in increased expression of heme oxygenase-1 (HO-1), which catalyzes the degradation of heme to biliverdin, carbon monoxide, and iron.¹⁰⁷ It is known that mitogen-activated protein kinases (MAPKs) and the phosphatidylinositol 3-kinase (PI3K)/protein kinase B (Akt) can alter cytoprotective and anti-inflammatory responses by contributing to the accumulation of Nrf2 in the nucleus.^{108,109} ϵ -Viniferin was shown to induce

Table 1.2 Intracellular Effects of Representative Bioactive Resveratrol Oligomers

Intracellular Effect; ^{refs}	Intracellular Effect; ^{refs}	Intracellular Effect; ^{refs}
↓iNOS; ⁹²	↓PKC; ^{110,111}	↑Caspase-3; ⁸⁸
↓BCL-2; ⁹²	↓COX-I; ^{112,113} ↓COX-2; ^{112,113}	↑Caspases-8,-9; ⁸⁸
↑Caspase-3; ⁹²	↓iNOS; ^{112,113}	↓PI3K/Akt; ⁸⁸
↑Caspase-8; ⁹³	↓PI3K/Akt/NFκβ; ¹¹⁴	↑PPAR-α; ¹¹⁵ ↑PPAR-β/δ; ¹¹⁵
↑Nrf2; ¹⁰⁷	↓IFN-γ/ERK-1/STAT-1; ¹¹³	↓MEK/ERK; ⁸⁸
↑HO-1; ¹⁰⁷	↑Nrf2; ¹¹⁴	↓BCL-2; ⁸⁸
↑Akt/p38/ERK-1 phosphorylation; ¹⁰⁷	↓TYR; ¹¹⁶ ↓AChE; ¹¹⁷ ↓Topo II; ⁶⁰ ↓MRP1; ^{118,119}	↑BAD; ⁸⁸

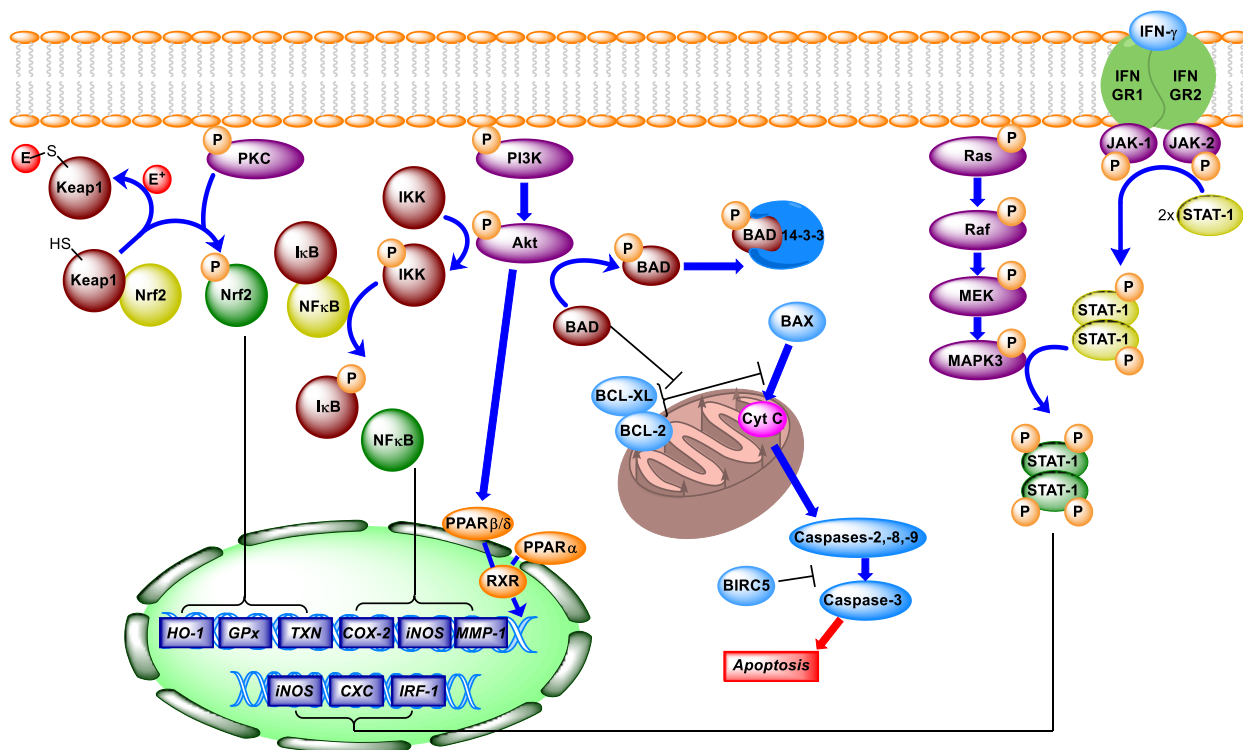


Figure 1.5 Biochemical Pathways Postulated to be influenced by Resveratrol Oligomers

the phosphorylation of Akt, p38, and the extracellular signal regulated kinases (ERK)-1/2, with ERK/p38 involved in ϵ -viniferin-mediated Nrf2 activation.¹⁰⁷

The cellular effects of the resveratrol cyclotrimer α -viniferin (**1.19**) are primarily affiliated with anti-inflammatory activity. This natural product has been reported to inhibit COX-1 (IC₅₀ = 7.0 μ M), and transcription of *COX-2* and *iNOS* genes in lipopolysaccharide (LPS)-activated murine macrophages.^{112,113} Subsequent studies in BV2 murine microglial cells revealed that the latter effect resulted from disruption of canonical NF- κ B activation (PI3K/Akt-mediated phosphorylation of IKK [inhibitor of κ B (I κ B) kinase]), which ultimately reduced levels of the anti-inflammatory gene products.¹¹⁴ α -Viniferin was also shown to influence autoimmune and inflammatory response mediated by the pleiotropic cytokine interferon (IFN)- γ .^{120,121} Specifically, **1.19** suppresses IFN- γ induced STAT-1 (signal transducer and activator of transcription 1) activation by inhibiting Ser⁷²⁷ phosphorylation by MAPK3 (mitogen-activated protein, also known as ERK-1). α -Viniferin was shown to increase expression levels of Nrf2.¹¹⁴ Indeed, it was found that **1.19** increased the activity of Nrf2 — the entity controlling HO-1 expression levels — in a dose-dependent manner, and increased the measurable levels of Nrf2 in the nuclear compartment. Although not cytotoxic, α -viniferin was found to inhibit the growth of human colon cancer cell lines.⁸¹ Furthermore, **1.19** did not induce apoptosis but arrested the cell cycle in the S phase (as compared to the G2/M phase for **1.11**) only in mutated colon cell lines (Caco-2, HT-29, HCT-116) and not in healthy colon cells (CCD-18Co). Finally, α -viniferin has been shown *in vitro* to inhibit protein kinase C (PKC),^{110,111} tyrosinase (TYR),¹¹⁶ acetylcholine esterase (AChE),¹¹⁷ topoisomerase II (Topo II),⁶⁰ and multidrug resistance-associated protein 1 (MRP1).^{118,119}

Vaticanol C (**1.23**) is a cytotoxic resveratrol tetramer containing a bicyclic [3.2.1] ring system at its core. Isolated from the Dipterocarpaceous plant *Vatica rassak* in 2002, **1.23** was found to induce apoptosis in three colon cancer cell lines, with observable changes to cell morphology including nuclear condensation/fragmentation and DNA ladder formation.⁶⁹ Like ϵ -viniferin (**1.11**), vaticanol C was found to exert an agonistic effect on both initiator and effector caspases involved in regulation of apoptosis.⁸⁸ Specifically, **1.23** activated the effector caspase-3, but not initiator caspase-8 in colon cancer cell lines, although it was later found that **1.23** does activate caspase-8 in mammary carcinoma cells BJMC 3879. Loss of mitochondrial transmembrane potential was observed upon treatment with vaticanol C, and initiator caspase-9 was found to be activated concurrently with the release of cytochrome c.⁸⁸ Further studies revealed that levels of phosphorylated MEK, ERK, and Akt were significantly reduced in cells treated with **1.23**, effects which were coupled with a corresponding reduction in BCL-2-associated death promoter (BAD) phosphorylation.^{91,122,123}

In spite of the pro-apoptotic effects observed *in vitro*, upon transitioning to *in vivo* models of mammary carcinoma vaticanol C did not show any ability to reduce tumor size.⁸⁸ It did, however, significantly reduce lymph node and lung metastases, suggesting a potential role as an adjuvant therapy in metastatic human breast cancer carrying *p53* mutations. Recently, it was found that vaticanol C activates the peroxisome proliferator-activated receptors (PPARs)- α and β/δ , ligand-dependent transcription factors that play various roles in lipid and carbohydrate metabolism as well as cell development and differentiation.¹¹⁵

1.6 Resveratrol and its Oligomer as Antioxidants

The incredibly broad biological profile of resveratrol-derived natural products has often been ascribed to radical-trapping antioxidant (RTA) activity⁴⁸ despite the fact that kinetic studies of

this reactivity have revealed that the rates of these reactions are uncompetitive with those of ubiquitous native antioxidants (e.g. α -tocopherol [α -TOH]) – not only in solution,¹²⁴ but as we have recently demonstrated,¹²⁵ in lipid bilayers as well as in cells. Collectively, the antioxidant literature involving resveratrol strongly suggests that other mechanisms *must* be operative for compounds producing phenotypic responses *in vitro*. One intriguing possibility is that resveratrol is exerting antioxidant-like effects through disruption of the Keap1-Nrf2 interaction (Keap1: Kelch-like ECH-associated protein 1). Keap1 directly inhibits Nrf2 translocation to the nucleus and facilitates its degradation.¹²⁶ Abolishing this protein-protein interaction releases free Nrf2, which then induces transcription of various antioxidant and anti-inflammatory elements¹²⁷ such as glutathione peroxidase (GPx), heme oxygenase (HO-1), thioredoxin (TXN), and enzymes involved in glutathione (GSH) biosynthesis (Figure 1.5).^{128,129} As would be expected, dysregulation of this pathway (termed the Keap1-Nrf2-ARE pathway; ARE: antioxidant response element) is generally associated with oxidative stress and inflammation — indications ubiquitous across a wide range of pathologies — and has been implicated in malignant tumor growth, multiple sclerosis, and diabetic nephropathy.^{128,129}

The proposed primary method for Nrf2 release is through irreversible allosteric bond-forming events between Keap1 and cytosolic electrophiles and oxidants.¹²⁶ A variety of phytochemicals that contain obvious electrophilic moieties (i.e., the Michael acceptors in Figure 1.6A) are suitable for this mode of reactivity by targeting nucleophilic cysteine residues of Keap1 (of the 27 total, Cys¹⁵¹ appears to be the most important). This covalent attachment induces a conformational change that releases Nrf2, allowing it to escape ubiquitination, translocate to the nucleus, and induce ARE-controlled gene expression (Figure 1.5).¹²⁷ An alternate mode of allosteric regulation of this pathway involves the oxidation of cysteines,

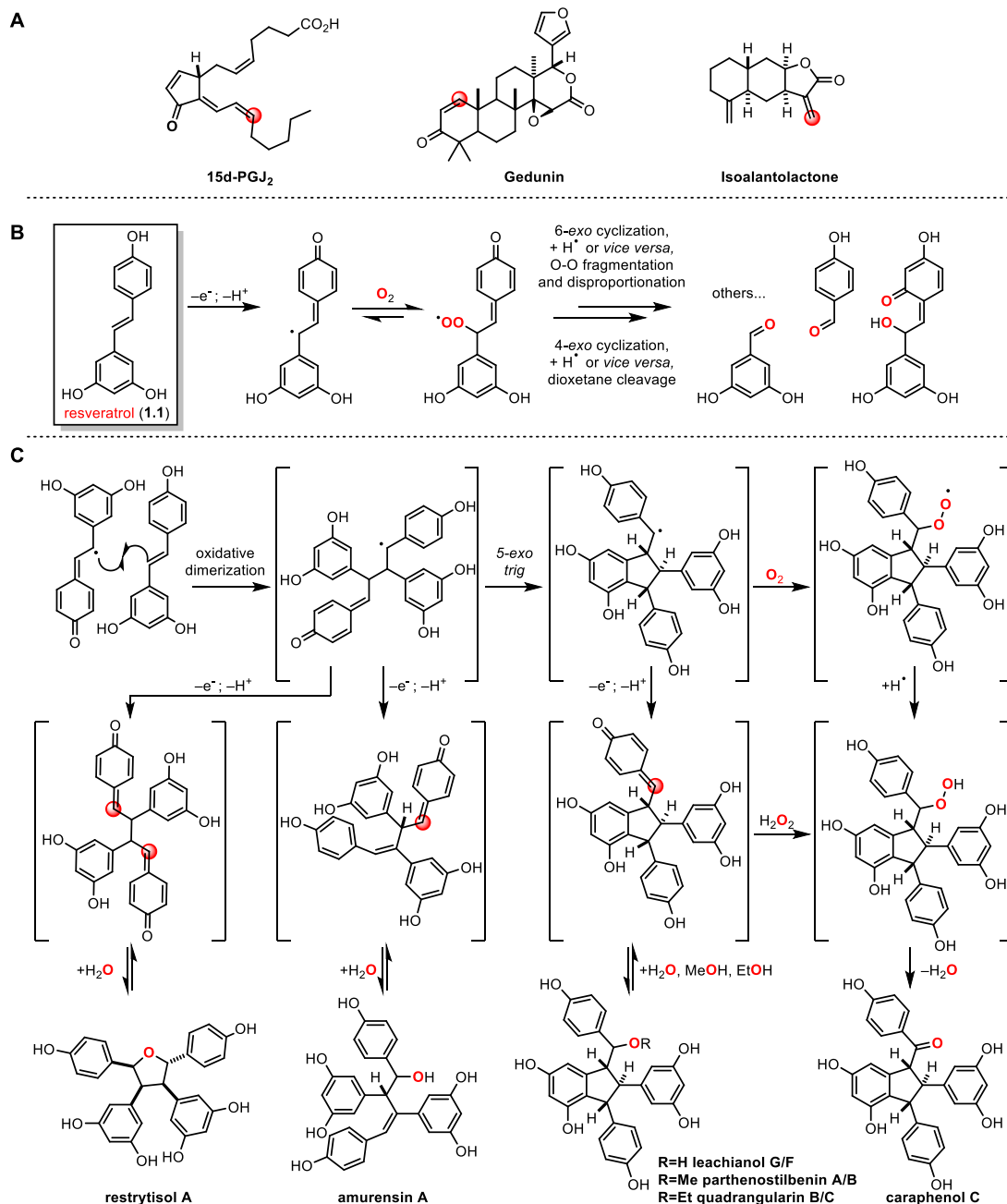


Figure 1.6 A) Naturally-occurring small molecules which modify cysteine residues of Keap1 leading to Nrf2 derepression; B) Autoxidation and C) Oligomerization of resveratrol results in the formation of similarly reactive electrophiles

including Cys¹⁵¹ (*intermolecular*) and Cys²²⁶/Cys⁶¹³ (*intramolecular*), to the corresponding disulfides.^{130,131} It is possible that the ‘antioxidant’ activity of resveratrol and its derivatives is not due to their reactivity to free radicals in a reductive capacity, but instead due to the paradoxical ability of the oxidized metabolites and redox byproducts (e.g. H₂O₂) to *oxidatively*

stimulate Nrf2 release through Keap1 antagonism (covalent adduction of Cys¹⁵¹ or disulfide bond formation, respectively).¹³²

Given how readily resveratrol autoxidizes under ambient conditions, it is likely that dimerization and further oligomerization takes place spontaneously. As such, the many biological activities of resveratrol may, in fact, be due to the *in situ* formation of these compounds and/or their intermediates and redox byproducts. However, given the highly complex product mixtures that arise upon autoxidation of **1.1** (Figure 1.6B), including the dozens of natural products resulting from its dimerization and oligomerization (Figure 1.6C), teasing out which may be responsible for the observed biological activities *and why* has been a challenging task.

1.7 Conclusions and Outlook

It is readily apparent that resveratrol, α -viniferin, and related natural products cannot possibly provide direct influence *each* of the biochemical pathways discussed above. To clarify, the author does not refute the authenticity of reported phenotypic responses, but rather the notion that these compounds could act as ligands for such a wide variety of intracellular targets. The observed promiscuity would seem to indicate that pleiotropic effects (such as the IFN- γ mediated processes discussed above) are the likely culprit. Unfortunately, many investigations in this area typically do not extend beyond initial toxicity studies of one or multiple oligomers against several cancer cell lines, which provide no information about their mechanism(s) of action. This deficiency is likely due to the requirement for laborious extraction and purification of resveratrol oligomers from plant matter. Therefore, access to these natural products through chemical synthesis will be instrumental to overcoming limitations imposed by material scarcity.

While several powerful *de novo* approaches to the total synthesis of these molecules have provided momentum to the field,^{133–144} to our knowledge only one of these studies has culminated in the biological evaluation of the target structures.¹³⁵ Furthermore, with the exception of two recent reports (one of which is our own preliminary work),^{125,142} existing synthetic routes do not deliver the final compounds in quantities amenable to systematic evaluation across a broad panel of biological assays. Synthetic scalability not only enables a complete picture of the medicinal chemistry of a target molecule,¹⁴⁵ but also provides opportunity for investigation of physical properties and relevant reaction kinetics,¹²⁵ and ultimately for the design of chemical probes to enable the identification of cellular targets.

To better understand the behavior of these molecules in biological systems and enable the development of more potent analogs, systematic structure–activity relationship (SAR) studies must be performed. Limited commentary on the structural features correlated to bioactivity exists in the literature, and typically consists of retrospective conjecture based on observed IC₅₀ values for a given set of isolated natural products. It would be beneficial for researchers to perform these studies on analogues that have been rationally designed, as this would enable a more generalized understanding of which physical properties can be exploited in the development of more potent congeners. To date, progress in this area has been hampered by existing synthetic technologies, which have largely been incapable of providing materials in sufficient quantities for their systematic evaluation, although several strategies have recently been reported that hold promise in this regard. While resveratrol oligomers are a relatively new target in the area of complex molecule synthesis, they offer unique challenges and therefore opportunities for valuable contributions to synthetic chemistry and an improved biological understanding of one of the most intriguing classes of natural products in the plant kingdom.

CHAPTER 2:
**DEVELOPMENT OF A SCALABLE BIOMIMETIC RESVERATROL
DIMERIZATION: APPLICATION IN TOTAL SYNTHESIS AND SYSTEMATIC
EVALUATION OF RADICAL TRAPPING ANTIOXIDANT ACTIVITY**

*Portions of this chapter have been published in:

Matsuura, B. S.; Keylor, M. H.; Li, B.; Lin, Y.; Allison, S.; Pratt, D. A.; Stephenson, C. R. J.
Angew. Chem. Int. Ed. **2015**, *54* (12), 3754–3757.

2.1 Introduction

The precision and efficiency with which nature achieves complex biochemical transformations, the result of millions of years of evolution, is a requirement for life as we know it. As synthetic chemists, we aspire to achieve such levels of chemoselectivity and catalysis in the flask, and cognizant of it or not, the bond disconnections that we elect to pursue are undoubtedly influenced by the fundamental laws of chemical reactivity shaped by the world in which we live, often resembling or “mimicking” analogous processes in nature. In many instances, consideration of nature’s hypothetical or established strategies is deliberately employed in the design of synthetic efforts in the laboratory, a sub-discipline of organic synthesis that has been termed “biomimetic” synthesis and whose birth is widely recognized in Robinson’s groundbreaking synthesis of tropinone.¹⁴⁶ While the biochemical processes resulting in serial polymers such as nucleic acids or peptides are both elegant and powerful, synthetic “biomimicry” more commonly refers to the construction of *natural products* or “secondary metabolites” — compounds which are not essential to cellular function but which exist for specialized purposes and influence gene expression, cell signaling, and cell survival through a

variety of pathways. Historically, natural products have served as a source of inspiration in drug discovery,^{147,148} and as a corollary, their biosynthesis has and will continue to shape small molecule synthesis. Although the biogenesis of natural products typically constitutes the most efficient route, it is often not possible to replicate in the laboratory the remarkable levels of control achieved by enzymes in the cell. Resveratrol oligomerization, which takes place via phenolic oxidative coupling, represents but one example of this challenge. Herein, we provide a brief history of seminal work in this area and how these findings have influenced our strategy for the synthesis of these natural products.

2.2 Biomimetic Synthesis of Resveratrol Dimers

The principal challenge in the biomimetic synthesis of resveratrol based natural products is controlling regiochemical outcomes. Indeed, the oxidation potential of resveratrol ($E_p^{\text{ox}} = +1.14$ V vs SCE in MeCN)¹⁵ is well within the range of a number of commonly used oxidants. Yet, the same property which renders this process so facile — electronic delocalization of the resultant phenoxyl radical — introduces difficulty in controlling the regiochemical outcomes during oxidative coupling. Additional problems of chemoselectivity arise from the fact that the products of dimerization — particularly those such as ϵ -viniferin (**1.11**) which preserve the 4-hydroxy stilbene moiety — possess similar electrochemical potentials ($E_p^{\text{ox}} = +1.15$ V vs SCE in MeCN)¹⁵ as resveratrol itself and are thus prone to over-oxidation.

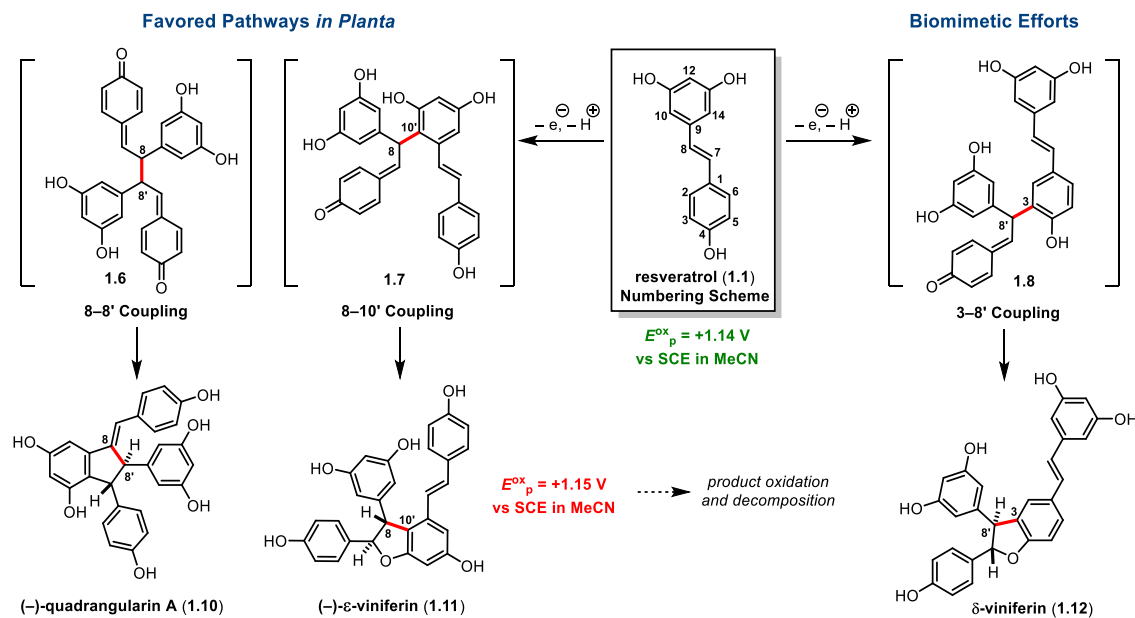


Figure 2.1 Regiocontrol and Product Oxidation Present Challenges for Biomimetic Resveratrol Oxidation

While the favored secondary metabolites formed in nature — quadrangularin A (**1.10**) and ϵ -viniferin (**1.11**) — are the result of 8–8' and 8–10' couplings, respectively (Figure 2.1), δ -viniferin (**1.12**, 3–8' coupling) represents the major constituent isolated from most biomimetic studies. Indeed, it was first inadvertently synthesized by Langcake and Pryce during their seminal isolation studies on grape phytoalexin compounds when they intended to produce ϵ -viniferin (**1.11**) from resveratrol using horseradish peroxidase (HRP) and H_2O_2 (Table 2.1, entry 9, *vide infra*).²⁵ More recently, Jeandet²¹ and Cichewicz²³ identified the metabolites formed (in <1% yield) by incubation of resveratrol with the pathogenic fungus *B. cinerea* as δ -viniferin (**1.12**), restrytisols A–C (**2.1/2.2/2.3**), pallidol (**2.4**), and leachinols F/G (**2.5/2.6**) (Figure 2.2). The 3–8' dimers formed through enzymatic/whole cell incubations are typically isolated as racemates, since laccases/peroxidases, which differ by the metal oxidant in their active sites (Cu^{20} vs Fe^{24} respectively), are fairly promiscuous enzymes capable of oxidizing a wide range of substrates. It is important to clarify that many of these studies were performed by natural product

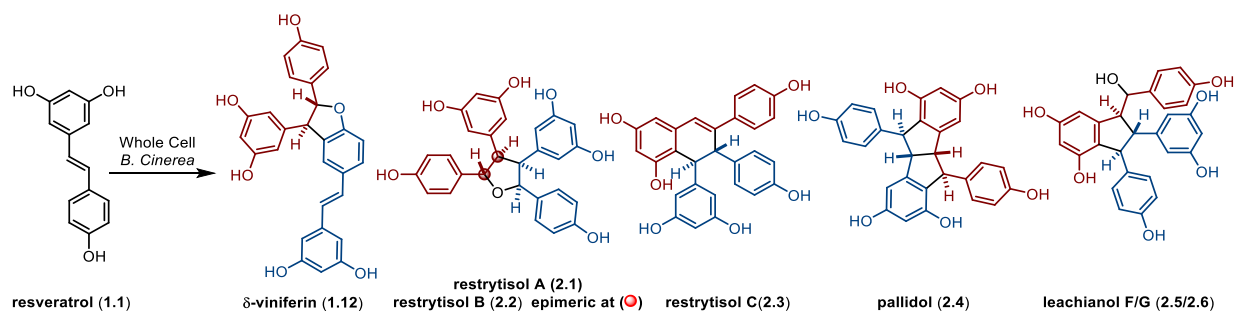
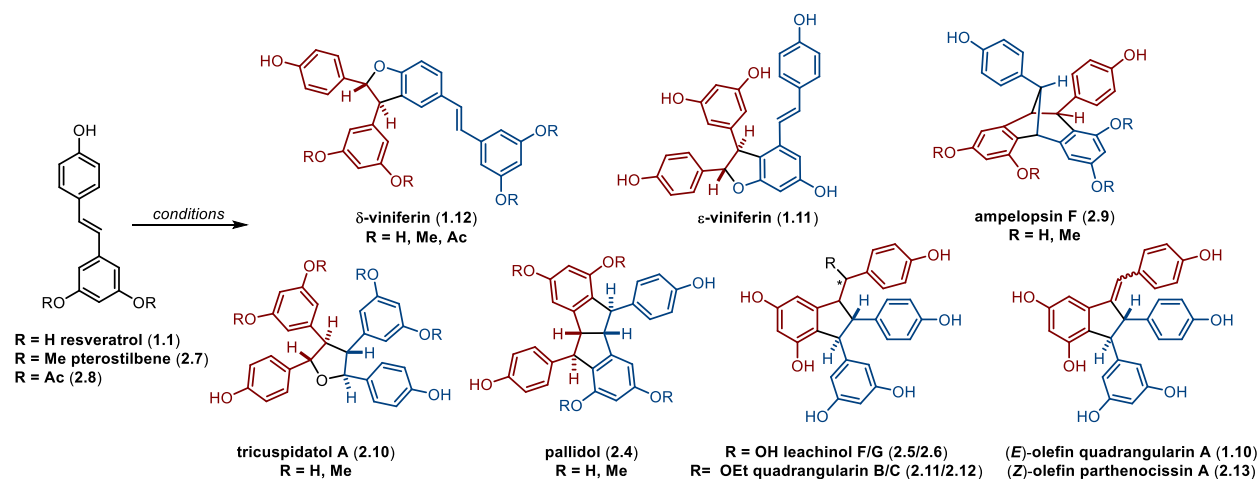


Figure 2.2 Whole Cell *B. cinerea*-Mediated Dimerization of XX

isolation groups whose objective was not total synthesis, but rather to support biogenic hypotheses and establish the absolute configuration of the natural products through semisynthesis.

Subjection of resveratrol (**1.1**), pterostilbene (**2.7**), or the acetyl derivative **2.8** to a variety of oxidation conditions including enzymatic,^{28,149,150} organic,^{151,152} inorganic,^{15,27,153} and photochemical oxidations¹⁵⁴ (Table 2.1) has predominantly resulted in the formation of the 3–8' dihydrobenzofuran regioisomer, δ -viniferin (**1.12**) (or the corresponding –Me or –Ac derivatives). While most of the early studies in this area employed enzymatic conditions (laccases/peroxidases in combination with H₂O₂), more recent uses of inorganic oxidants have dramatically improved both the yield and selectivity of these reactions. In a limited number of studies, the dihydrobenzofuran-containing dimer formed on oxidation of **1.1** has been claimed to be the 8–10' regioisomer, ϵ -viniferin (**1.11**). The selective formation of **1.11** would be much more impactful from a synthetic standpoint, since it constitutes the biogenic precursor for a majority of the resveratrol natural products. In one early example, Pezet

Table 2.1 Enzymatic and Non-Enzymatic Dimerization Reactions of Resveratrol



Entry	Reaction conditions, ^{ref}	1.12	1.11	2.9	2.10	2.4	2.5/2.6 2.11/2.12	1.10/2.13
Enzymatic								
1 ^a	Soybean (<i>Glycine max</i>) peroxidase, aq. EtOH ²⁷	12% ^d	—	—	—	10% ^d	14% ^{d,e}	—
2 ^a	Fungal (<i>Arthromyces ramosus</i>) peroxidase, aq. EtOH ²⁷	13% ^d	—	—	—	5% ^d	13% ^{d,e}	—
3 ^a	Horseradish peroxidase, aq. Acetone ²⁷	13% ^d	—	—	—	10% ^d	—	—
4 ^a	Fungal (<i>Arthromyces ramosus</i>) peroxidase, aq. Acetone ²⁷	18% ^d	—	—	—	7% ^d	5% ^{d,f}	—
5 ^a	Fungal (<i>T. pubescens</i>) laccase, EtOAc, pH 4.5 ¹⁴⁹	18%	—	—	—	—	—	—
6 ^b	Soybean (<i>Glycine max</i>) peroxidase, aq. Acetone ²⁷	21% ^d	—	—	—	7% ^d	2% ^{d,f}	—
7 ^c	Fungal (<i>M. thermophyla</i>) laccase, <i>n</i> -BuOH, pH 6.5 ¹⁴⁹	26%	—	—	—	—	—	—
8 ^a	Fungal (<i>M. thermophyla</i>) laccase, <i>n</i> -BuOH, pH 6.5 ¹⁴⁹	31%	—	—	—	—	—	—
9 ^a	Horseradish peroxidase, aq. Acetone ²⁵	41%	—	—	—	—	—	—
10 ^a	Horseradish peroxidase, aq. Acetone, pH 4.0 ²⁸	42% ^{g,h}	—	—	—	8% ^g	50% ^{f,g}	—
11 ^a	Horseradish peroxidase, aq. Acetone, pH 5.0 ²⁸	45% ^{g,h}	—	—	—	20% ^g	35% ^{f,g}	—
12 ^a	Horseradish peroxidase, aq. Acetone, pH 6.0 ²⁸	45% ^{g,h}	—	—	—	—	55% ^{f,g}	→ 50% ⁱ
13 ^a	Horseradish peroxidase, aq. Acetone, pH 8.0 ²⁸	89%	—	—	—	—	7% ^{f,g}	—
14 ^a	Fungal (<i>B. cinerea</i>) laccase-like stilbene oxidase ²²	—	86%	—	—	—	—	—
Non-Enzymatic								
15 ^a	NaNO ₂ , MeOH, pH 3.0 ¹⁵⁵	4%	—	—	1%	—	—	—
16 ^a	Cu ^{II} SO ₄ , MeCN ¹⁵³	16%	—	—	—	—	—	—
17 ^a	DPPH, MeOH ¹⁵¹	18%	—	—	—	—	—	—
18 ^a	Galvinoxyl radical, EtOH ¹⁵²	41%	—	—	—	—	—	—
19 ^a	Graphitic carbon nitride (<i>hν</i> , 410 nm), lutidine, air, MeCN ¹⁵⁴	85%	—	—	—	—	—	—
20 ^a	AgOAc, MeOH, 50 °C ¹⁵	86%	—	—	—	—	—	—
21 ^a	MnO ₂ , CH ₂ Cl ₂ ²⁷	91% ^d	—	—	—	—	—	—
22 ^a	FeCl ₃ , acetone ²⁷	97% ^d	—	—	—	—	—	—
23 ^a	FeCl ₃ , MeOH/H ₂ O ¹⁵⁶	—	30%	—	—	—	—	—
24 ^a	K ₃ Fe(CN) ₆ , K ₂ CO ₃ , MeOH/H ₂ O ²⁷	23% ^d	22% ^d	—	—	16% ^d	—	—
25 ^a	Ce(SO ₄) ₂ , MeOH, -50 °C ²⁷	8% ^d	4% ^d	—	—	—	—	—
26 ^a	Tl(NO ₃) ₃ , MeOH, -50 °C ²⁷	—	30% ^d	—	—	—	—	—
27 ^b	AgOAc, CH ₂ Cl ₂ ¹⁵⁷	36%	—	—	—	—	—	—
28 ^b	FeCl ₃ ·6H ₂ O, CH ₂ Cl ₂ /MeOH (7:3 v/v) ¹⁵⁷	—	—	—	29%	—	—	—
29 ^b	FeCl ₃ ·6H ₂ O, CH ₂ Cl ₂ ¹⁵⁷	—	—	7%	—	10%	—	—
30 ^j	Pt electrode, MeCN/0.2 M LiClO ₄ (+1.00 V vs Ag/AgNO ₃) ¹⁵⁸	—	—	8%	—	14%	—	—

^aR = H (1.1); ^bR = Me (2.7); ^cR = Ac (2.8); ^dDegree of transformation "DT" = ((mole of product x2)/(mole of resveratrol)) x 100; ^e2:1 mixture of 2.11/2.12; ^fOnly (2.5/2.6) obtained; ^gHPLC yield; ^hE/Z mixture; ⁱYield of (1.10) upon treatment of (2.5/2.6) with BF₃·OEt₂ (over 2 steps from 1.1). UV (>306 nm) afforded (2.13) in 38% over 3 steps; ^jPermethyl resveratrol was used in these studies.

and co-workers isolated a laccase-like stilbene oxidase from the fungal plant pathogen *B. cinerea* which was shown to be capable of dimerizing resveratrol to **1.11** in 86% yield (Table 2.1, entry 14).²² The observed selectivity for the 8–10' regioisomer is in contrast to all other laccases and peroxidases that have been investigated for this purpose, which typically afford a mixture of 3–8' and 8–8' regioisomers, the distribution of which is strongly influenced by the pH of the reaction medium (Table 2.1, entries 1–13). Unfortunately, the stilbene oxidase-mediated reaction was only performed on μg amounts of resveratrol, and likely does not represent a viable solution to the preparation of synthetically useful quantities of this material. In 2004, Yao and co-workers reported the use of FeCl_3 for the preparative (0.5 g) scale synthesis of ϵ -viniferin from resveratrol in 30% isolated yield, along with 40% recovery of starting resveratrol (Table 2.1, entry 23).¹⁵⁶ This method has since been implemented in the synthesis of related resveratrol dimers.¹⁵⁹ Niwa and co-workers performed a thorough investigation of product distribution as a function of oxidant — both enzymatic and non-enzymatic — and discovered that $\text{Tl}(\text{NO}_3)_3$ was also selective for ϵ -viniferin formation (30% yield with 56% starting material (SM) recovery, Table 2.1, entry 26), although careful temperature control was required to prevent oxidative decomposition and the high toxicity of thallium based oxidants renders this impractical for preparative synthesis.²⁷

In addition to the dihydrobenzofuran-containing 8–10' and 3–8' regioisomers (**1.11** and **1.12**, respectively), a number of conditions have been found to deliver products derived from the 8–8' mode of oxidative coupling (Table 2.1), including the bicyclo [3.2.1] octane ampelopsin F (**2.9**), tetrahydrofuran tricuspidatol A (**2.10**), diquinane pallidol (**2.4**), and indane epimers leachinols F/G (**2.5/2.6**) and quadrangularins B/C (**2.11/2.12**).^{27,28,157,158} Exposure of leachinols F/G (**2.5/2.6**) to $\text{BF}_3 \cdot \text{OEt}_2$ promoted their dehydration to quadrangularin A (**1.10**, Table 2.1, entry 12)

in 90% yield (50% from **1.1**), which could then be converted to the (*Z*)-olefin isomer, parthenocissin A (**2.13**) in 77% yield by irradiation with UV light (>306 nm).²⁸ Although the chemoselectivity of these biomimetic oxidations is — with the exception of δ -viniferin (**1.12**) — modest at best, these seminal studies demonstrate the feasibility of performing a reagent controlled dimerization of resveratrol. It is clear that a number of factors can have a profound influence over the chemoselectivity of resveratrol dimerization, including the identity of the oxidant, solvent selection, pH of the reaction medium, and temperature.

Notably, dimerization to δ -viniferin results in alkylation of the 4-hydroxy stilbene, which greatly attenuates the electron transfer potential of **1.12** as compared to **1.1**, thereby preventing product oxidation. The conditions developed by Sako and co-workers (Table 2.1, entry 20) are the most robust that have been reported to date for the direct dimerization of resveratrol, providing δ -viniferin in 86% isolated yield.¹⁵ To showcase the regio- and chemoselectivity (product stability under these conditions), the researchers subjected ϵ -viniferin (**1.11**) to their optimized conditions (AgOAc, MeOH, 50 °C), isolating the tetramer vitisin B (**2.14**) in 40% yield along with 32% of an unidentified tetrameric didehydrodimer for a remarkable combined yield of 72% (Figure 2.3). Vitisin B has recently been shown to exhibit high potency against replication of the hepatitis C virus (HCV, EC₅₀ = 6 nM),⁶¹ and therefore this method could find practical application for its synthetic preparation.

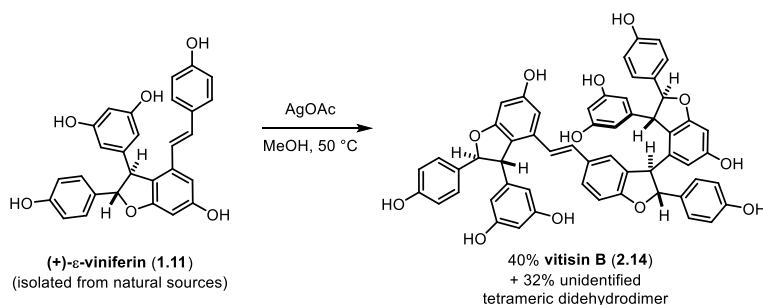


Figure 2.3 Biomimetic Synthesis of Vitisin B by Sako and Co-workers

2.3 Biomimetic Syntheses using Modified Resveratrol Derivatives

Studies such as those discussed above on the biomimetic dimerization of resveratrol or pterostilbene highlight the significant challenges in achieving high chemo- and regioselectivity, and synthetically useful yield, particularly on preparative scale. In an effort to address these shortcomings, several groups have demonstrated that the chemoselectivity of dimerization can be largely controlled by the use of modified resveratrol derivatives. Namely, by blocking the 3- and 5-positions of resveratrol, it is possible to overcome the preferred 3–8' coupling and enforce the 8–8' coupling mode. For this purpose, *tert*-butyl (^tBu) groups have been employed, which can later be removed under strongly acidic conditions through a retro-Friedel–Crafts reaction.^{160,161}

The selection of *tert*-butyl groups undoubtedly drew inspiration from the seminal work of Müller/Wallis and Becker,^{162–164} who established regioselective oxidative dimerizations of the ^tBu congeners of monolignols **2.15** and hydroxy stilbenes **2.16**, respectively. Interestingly, the dimerizations yielded stable forms of the dimeric bis-quinone methide intermediates **2.17** and **2.18** (Figure 2.4). These unusual structures are central to our own work, and this early evidence of their existence and stability has been highly inspirational to the evolution of our approach to resveratrol oligomerization.

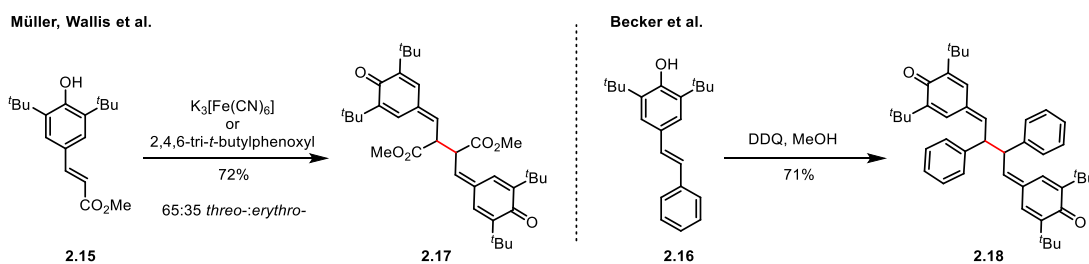


Figure 2.4 Regioselective Dimerizations of di-^tBu-4-hydroxy Styrenes and Stilbenes

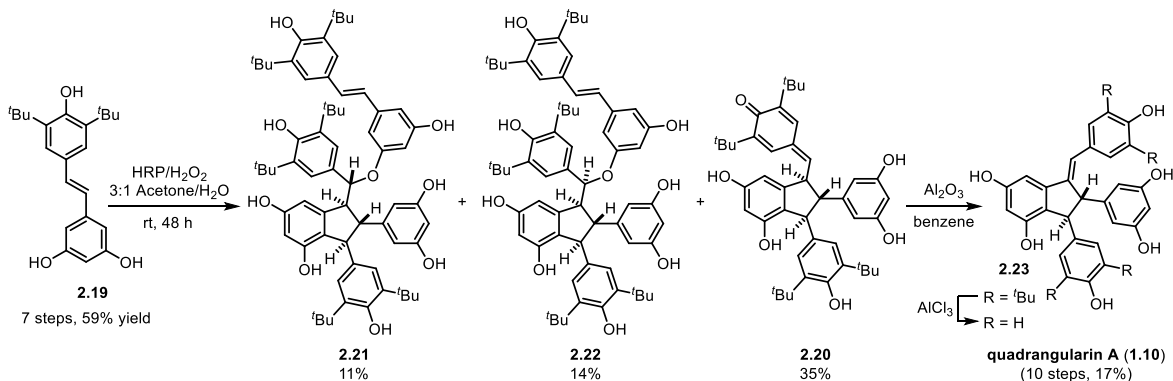


Figure 2.5 Synthesis of Quadrangularin A by Hou, Li, et al.

Hou and Li were the first to apply this strategy to resveratrol coupling, and treatment of the *tert*-butyl resveratrol derivative **2.19** with horseradish peroxidase (HRP)/H₂O₂ resulted in regioselective 8–8' coupling, affording the indane quinone methide isomer **2.20** in 35% over 48 hours (Figure 2.5).¹⁶⁵ Notably, **2.20** is not a stable intermediate, and is susceptible to nucleophilic trapping by, for instance, the free resorcinol –OH, yielding trimeric epimers **2.21** and **2.22**. Nonetheless, tautomerization/rearomatization of **2.20** can be accomplished by exposure to basic alumina, and de-*tert*-butylation of the resultant intermediate **2.23** was achieved by a Lewis acid-mediated retro-Friedel–Crafts reaction to reveal quadrangularin A (**1.10**) in ten total steps and 17% overall yield.

Since this seminal contribution, Li and co-workers have reported two extensions of this work, exploring the behavior of **2.19** and protected derivatives **2.24** and **2.25** in the presence of various solvent/oxidant combinations (Table 2.2).^{166,167} Unfortunately, reaction outcomes in this communication were reported as “reaction conversion” and percent recovered starting material, values which in several cases add to more than 100%, rendering yield estimation difficult. With the exception of ampelopsin F derivative **2.26**, which is derived from an 8–10' dimerization, each of **2.20**, pallidol derivative **2.27**, tricuspidatol A derivatives **2.28**, and restrytisol B derivatives **2.29** represent 8–8' dimeric isomers. In the case of acetyl- and Boc-derivatives **2.24** and **2.25**,

Table 2.2 Dimerizations of *tert*-Butylated Resveratrol and Protected Derivatives

$\text{R} = \text{H}$ **2.19**
 $\text{R} = \text{Ac}$ **2.24**
 $\text{R} = \text{Boc}$ **2.25**

2.20 **^tBu-ampelopsin F (2.26)** **^tBu-pallidol (2.27)** **H = β ^tBu-tricuspidatol A (2.28)**
H = α ^tBu-restrytisol B (2.29)
 $\text{R} = \text{Ac, Boc}$

Entry	Reaction conditions	2.20	2.26	2.27	2.28	2.29
1 ^a	Ag ₂ CO ₃ , CH ₂ Cl ₂	59% ^{a,d}	—	—	—	—
2 ^a	MnO ₂ , CH ₂ Cl ₂	54% ^{a,d}	—	—	—	—
3 ^{a,b,c}	FeCl ₃ •6H ₂ O, Benzene/Acetone 2:1	—	—	55% ^{a,d}	24% ^{b,d} ; 14% ^{c,d}	24% ^{b,d} ; 18% ^{c,d}
4 ^a	FeCl ₃ •6H ₂ O, CH ₂ Cl ₂	—	45% ^{a,d}	—	—	—

^aR = H (**2.19**); ^bR = Ac (**2.24**); ^cR = Boc (**2.25**); ^dReported as % conversion.

subjection to the conditions in Table 2.2, entry 3 effected their conversion to the tetraaryl furan diastereomers **2.28** and **2.29**.¹⁶⁷ The acetyl derivative was found to deliver higher yields of the dimeric products, and hydrolysis of OAc-**2.28/2.29** followed by triflic acid-mediated dehydration/de-*tert*-butylation yielded pallidol (**2.4**). Lewis acid (AlCl₃)-mediated de-*tert*-butylation of **2.26** and **2.27** was reportedly accomplished in 76% and 85% yields to afford ampelopsin F (**2.9**) and pallidol (**2.4**), respectively. In fact, the synthesis of **2.9** constitutes the first example of a selective, biomimetic synthesis of a 8–10' dimer. However, the dimerization reaction is reported as proceeding for more than 3 hours to give 45% conversion to **2.26** with 25% recovered **2.19**. In our hands, full conversion of **2.19** to a complex product mixture was observed within 1 h under the reported conditions, and just 14% of **2.26** could be isolated. In light of this, it would not be accurate to consider this reaction regioselective or chemoselective as stated in their communication.

2.4 Selected *de Novo* Synthetic Approaches to Resveratrol Dimers

As described in the preceding section, much of the early work in resveratrol oligomerization aimed to replicate nature's approach, which is postulated to take place via the coupling of oxidatively generated resveratrol-derived phenoxyl radicals.¹⁹ While the biomimetic construction of these molecules has provided support for this mode of biogenesis, efforts to date have largely resulted in low yields and/or complex mixtures of products. As a result, these strategies have failed to satisfy the material demand for systematic physical and biochemical evaluation of these potentially bioactive natural products. Recognizing this shortcoming, several research groups have designed powerful *de novo* synthetic approaches to a number of resveratrol oligomers, the vast majority of them dimers.¹⁹ As a prelude to our own studies, the two most pertinent total syntheses of quadrangularin A (**1.10**) and pallidol (**2.4**), those by Snyder and Studer,^{136,137,144} are summarized briefly at this juncture.

The strategy developed by Snyder and co-workers was not inspired by biosynthetic considerations in the forward sense, but rather through retrosynthetic analysis and pattern recognition. Specifically, the realization that indane-derived resveratrol dimers such as ampelopsin D (**2.30**) and quadrangularin A (**1.10**) differ only in the relative positioning of the phenol (A₁) and resorcinol (A₂) components of the resveratrol monomer whose ethylene bridge comprises C₁ and C₂ of the indane ring (Figure 2.6, inset) enabled the retrosynthetic design of triaryl starting materials **2.31** and **2.32**. Each of these materials bears a labile benzylic alcohol which is readily ionized on exposure to acid, facilitating intramolecular cyclization and subsequent nucleophilic trapping of the resultant *trans*-configured 2,3-diaryl indanyl cations **2.33** and **2.34**.¹³⁶ The use of trifluoroacetic acid afforded the solvolysis products (i.e. **2.35**, regioisomer not shown), which were then oxidized to the indanones **2.36** and **2.37**,

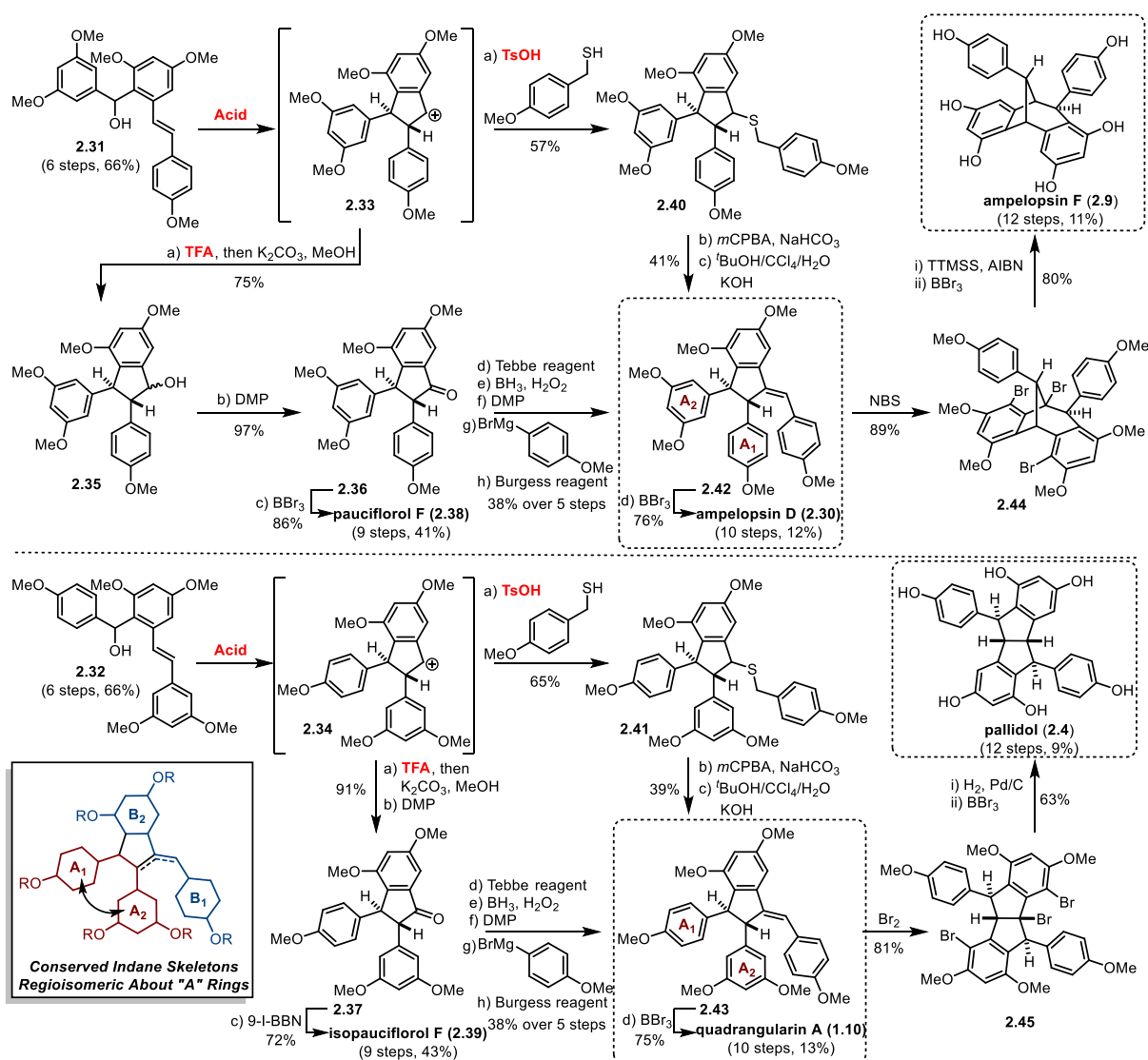


Figure 2.6 Snyder's *de Novo* Synthetic Strategy to 8–10' (top) and 8–8' (bottom) Derived Resveratrol Dimers

permethylated analogues of pauciflorol F (2.38) and isopauciflorol F (2.39), respectively. Alternatively, by the use of *p*-toluenesulfonic acid, cations 2.33 and 2.34 could be trapped by 4-methoxybenzyl mercaptan to produce adducts 2.40 and 2.41, which were subsequently channeled through a Ramberg–Bäcklund¹⁶⁸ sequence (Meyer's modification)¹⁶⁹ to afford 2.42 and 2.43, permethylated analogues ampelopsin D (2.30) and quadrangularin A (1.10), respectively.

In a subsequent report, Snyder and co-workers exploited the inherent polarization of the *para*-methoxy styrene moiety present in **2.30** and **1.10** to achieve their electrophilic bromine-mediated conversion to the bicyclo[3.2.1] **2.44** and diquinane **2.45** ring systems that comprise ampelopsin F (**2.9**) and pallidol (**2.4**), respectively.¹³⁷ These pioneering studies are not only impressive in their own right, but laid the foundation for a generalized synthetic approach to higher resveratrol oligomers.^{138,142,143}

More recently, a second elegant approach to each of the indane-based regioisomeric product classes was executed by Studer and co-workers.¹⁴⁴ Rather than preparing separate starting materials for access to the 8–8' and 8–10' connectivity (*vide supra*), the authors envisaged a retrosynthetic design that would proceed through the common intermediate **2.46** (Figure 2.7, inset). The group had previously developed methodologies for the regio- and stereospecific decarboxylative cross-coupling of allylic quaternary carboxylates with aryl iodides.¹⁷⁰ Application of their optimized conditions to **2.46** effected its conversion in moderate yield but with complete regioselectivity to the arylated indene products **2.47** and **2.48**. A subsequent nitroxide-mediated oxidative Mizoroki–Heck arylation delivered **2.43** and **2.42**, the permethylated analogues of quadrangularin A (**1.10**) and ampelopsin D (**2.30**). Notably the Heck arylations took place with complete regioselectivity for the C₂ position of the indene, with complete facial selectivity to provide the *trans*-configured product, and gave exclusively the (*E*)-alkene isomer of each product. Lewis acid (BBr₃) promoted demethylation yielded the desired natural products **1.10** and **2.30**, or alternatively quadrangularin A precursor **2.43** could be converted to the natural product pallidol (**2.4**) by a known two-step procedure.¹⁷¹

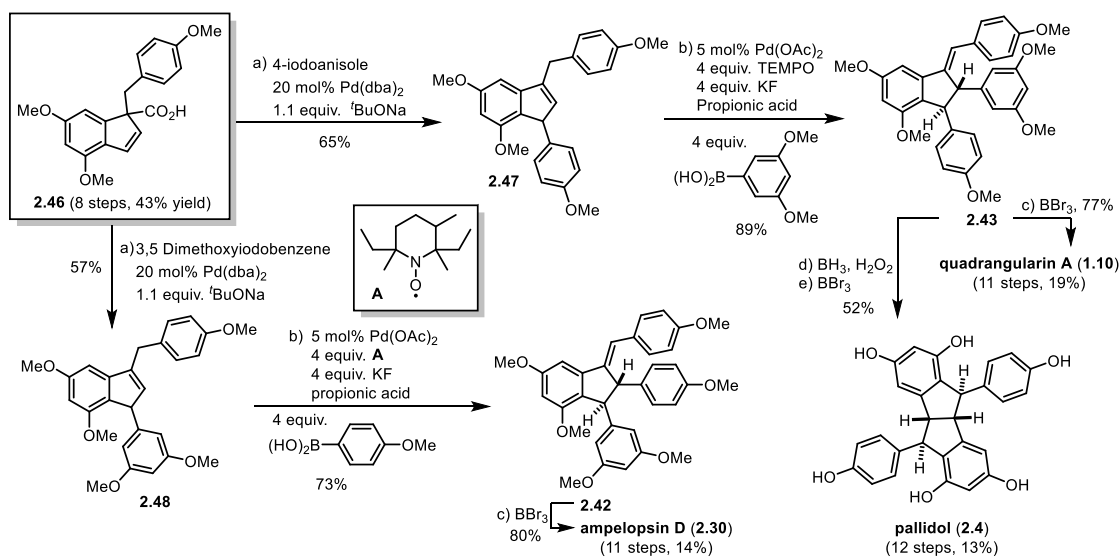


Figure 2.7 Studer's *de Novo* Approach to Resveratrol Dimers using Pd Catalysis

2.5 Development of a Scalable Biomimetic Synthesis of 8–8' Resveratrol Dimers

The crux of our research program — the application of free radical chemistry in both methodology and complex molecule synthesis — naturally attracted us to the prospect of developing this reactivity in the context of a biomimetic resveratrol oligomerization. However, contemporaneous with the outset of the project, the initial zeal surrounding the promising biological activities of resveratrol and its oligomers had been supplanted with skepticism and contention regarding their therapeutic potential, particularly considering their poor bioavailability and elusive mechanisms of action. Moreover, synthetic efforts of that time had revealed significant challenges for controlling the regio- and chemoselectivity of these processes (*vide supra*, Section 2.2). While a number of *de novo* synthetic approaches had displayed good stereo- and regiocontrol (Section 2.4), these approaches tended to be highly linear, were often directed toward a single architectural sub-type, and commonly utilized methoxy protecting groups, which require exceedingly harsh conditions for removal at a late-stage. We sought to combine lessons learned from each of these synthetic philosophies by developing a strategy that

would rapidly access chemical diversity from common intermediates in a *controlled* fashion, and to address lingering questions regarding the role of resveratrol-derived natural products as bioactive small molecules by providing access to the natural products as single materials for systematic biological evaluation.

Our initial foray into resveratrol oligomer synthesis was centered on the use of photoredox catalysis to effect the dimerization of resveratrol or an appropriately functionalized analogue. Photoredox catalysis has been developed as an attractive alternative to traditional methods of generating synthetically useful radical intermediates in complex settings.^{172,173} Generally, this mode of catalysis is predicated on the ability of metal polypyridyl complexes, such as the prototypical ruthenium tris-bipyridine $[\text{Ru}(\text{bpy})_3]^{2+}$, to absorb light in the visible range and use this energy to both initiate and catalyze single electron processes. Excitation with visible light produces a charge-separated excited state in which an electron has been transferred from the metal center to the ligand scaffold, resulting in a radical anion-like electronic structure on the ligand that can serve as a reductant, and a formal $n+1$ oxidation state at the metal center, which can serve as an oxidant. Channeling subsequent reactivity of the excited state complex can be achieved through catalyst-substrate matching and/or the use of stoichiometric electron donors or acceptors to enable net reductive, net oxidative, and redox neutral transformations to be performed chemoselectively (Figure 2.8).^{172,174,175}

Most commonly, (super)stoichiometric electron donors are used as additives to promote either the photoinduced electron transfer (PET) or catalyst turnover in the reductive and oxidative quenching manifolds, respectively. However, in several instances, the participation of the substrate itself in these discrete mechanistic steps has enabled selective functional group manipulations that are net-oxidative with respect to the substrate. For example, the participation

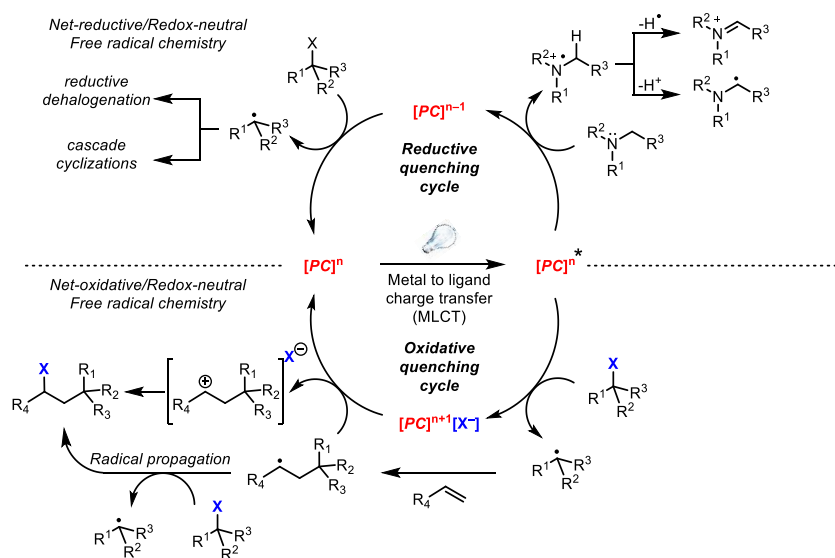
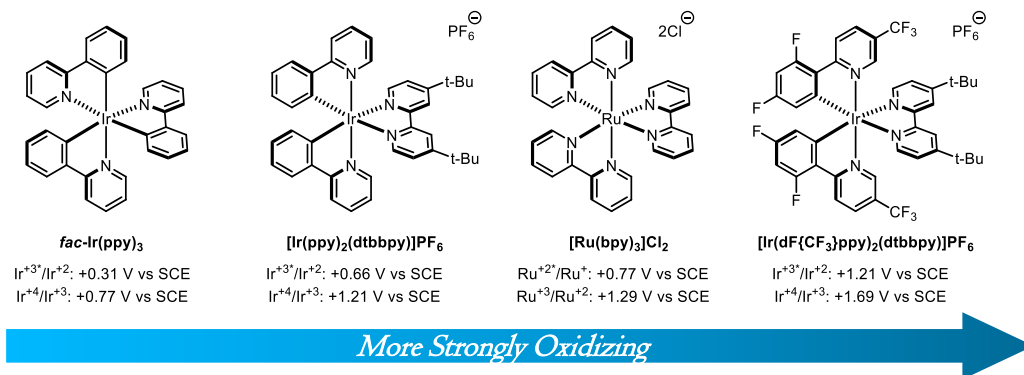


Figure 2.8 Reductive and Oxidative Quenching Manifolds in Photoredox Catalysis

of tertiary amine substrates in reductive quenching of the excited state photocatalyst generates transiently an amine radical cation (Figure 2.8, upper right quadrant), which can either lose a hydrogen atom to produce an electrophilic iminium species, or undergo deprotonation to yield a nucleophilic α -amino radical (the radical itself can also be further oxidized to the iminium).¹⁷⁶ However, the work that inspired our preliminary investigations into the application of visible light photoredox catalysis to resveratrol dimerization was an example from the alternative reaction manifold, where substrate oxidation takes place during the catalyst turnover step (Figure 2.8, lower left quadrant).

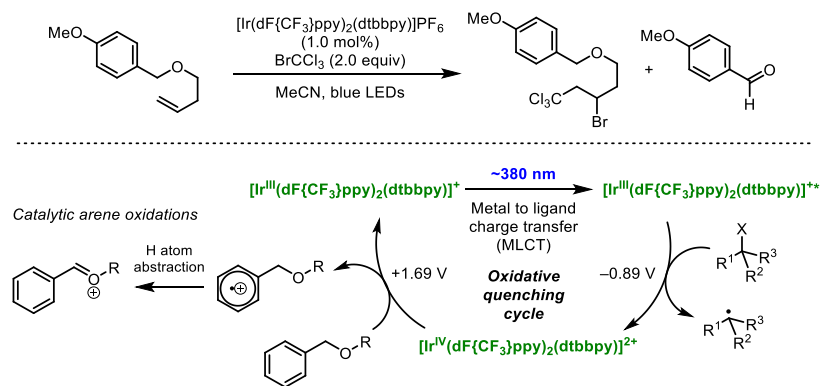


Figure 2.9 Photocatalytic Deprotection of Electron-rich Benzylic Ethers

Early experiments performed in our group utilizing the oxidative quenching cycle of the fluorinated iridium catalyst $[\text{Ir}(\text{dF}\{\text{CF}_3\}\text{ppy})_2(\text{dtbbpy})]\text{PF}_6$ ¹⁷⁷ illustrated the utility of this catalyst for processes that are net redox-neutral with respect to the substrates, such as the atom transfer radical additions (ATRA) of haloalkenes and α -halocarbonyls to olefins (Figure 2.8, bottom).¹⁷⁸ However, when performed using olefins bearing electron-rich benzylic ethers, the reactions yielded both ATRA products along with those resulting from a carbon-hydrogen bond oxidation pathway (Figure 2.9, top). This serendipitous finding was then optimized for the development of a mild and selective deprotection of *para*-methoxy benzyl (PMB) ethers (Figure 2.9, bottom).¹⁷⁹

There are a number of catalysts available whose excited state and return potentials are tunable by modification of both the metal center and the ligand scaffold (Figure 2.8). Owing to the electron-rich character of resveratrol, Bryan Matsuura, a very talented former colleague of mine, hypothesized that catalytic generation of the requisite phenoxy radical for dimerization should be possible under photocatalytic conditions (Figure 2.10). In considering reaction design, we drew inspiration from the seminal report of Hou and Li,¹⁶⁵ in which they demonstrated that horseradish peroxidase mediated oxidation of *tert*-butyl resveratrol derivative **2.19** yielded dimeric products derived from the regioselective 8–8' oxidative coupling mode (*vide supra*, Section 2.3). Whether resveratrol oxidation would take place directly from the catalyst excited

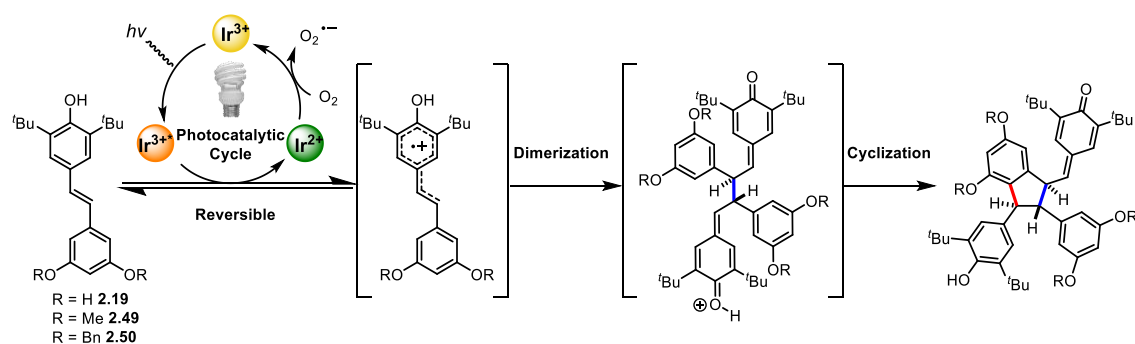


Figure 2.10 Hypothesis for Photocatalytic Resveratrol Dimerization

state or during catalyst turnover under photocatalytic conditions would be a function of catalyst identity, additive selection, and a number of other factors, such as pH of the reaction medium.

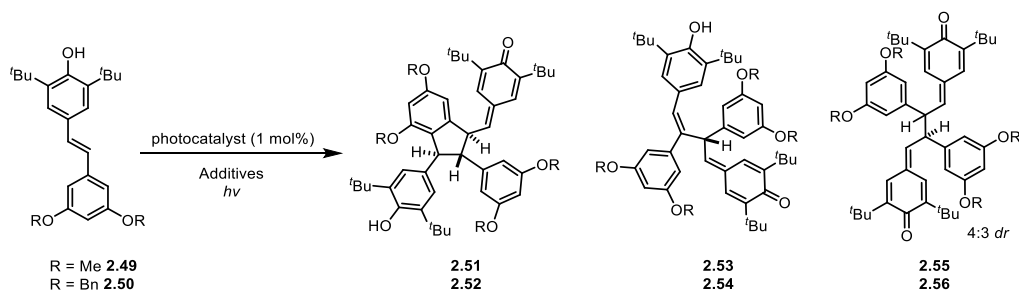
Initial efforts using the *tert*-butyl resveratrol derivative **2.19** indicated that it was not suitable for this purpose due to apparent issues with product instability, leading to over-oxidation and oligomerization of dimers in the reaction mixtures. Thus, we turned to the methyl-protected derivative **2.49** (and eventually the benzyloxy derivative **2.50**) for the remainder of our investigations (Table 2.3). Though seemingly trivial, this measure rendered both the starting material and products significantly more stable and improved substrate solubility in nonpolar solvents, an effect that proved to be critical to product chemoselectivity. We quickly learned that for many of the complexes, relaxation from the excited state through triplet energy transfer — presumably due to the extended π -conjugation of **2.49/2.50** — became highly competitive with the desired photoinduced electron transfer (PET) event, as evidenced by the observation of *cis/trans* stilbene isomerization in lieu of dimerization. Efforts to steer the reaction through the oxidative quenching pathway through the use of stoichiometric terminal oxidants under anaerobic conditions led to either starting material decomposition or only trace conversion (Table 2.3, entries 1–3). Conversely, under aerobic conditions the iridium(III) bis(terpyridine) complex $[\text{Ir}(\text{tpy})_2](\text{PF}_6)_3$, which possesses a strong excited state reduction potential ($E_{\text{red}}^* = -1.90$ V vs. SCE),¹⁸⁰ was found to promote low conversion to indane isomers **2.51/2.52** over the course

of two days (Table 2.3, entry 4), presumably through an inefficient reductive quenching mechanism. The use of the heteroleptic iridium(III) terpyridine catalyst [Ir(tpy)(tpy)](PF₆)₃, which has a slightly lower excited state oxidation potential ($E_{\text{red}}^* = -1.79$ V vs. SCE) but a longer excited state lifetime,^{180,181} improved the yield of **2.51/2.52** to 38% when performed in acetone (Table 2.3, entry 5).

In an effort to improve the efficiency of the reaction, base was added in order to convert **2.49/2.50** to their corresponding phenoxides. While the effects of pH on resveratrol dimerization had been explored previously (cf. Table 2.1),²⁸ the motivations for our decision were different. Namely, the previous study examined the influence of pH over a horseradish peroxidase mediated dimerization of resveratrol **1.1**, and the authors postulated that variable product distributions could be accounted for by pH-induced conformational changes caused by protonation/deprotonation of histidine residues within the heme cavity. In contrast, the use of base in our studies was inspired by an electrochemical study by Corduneanu and co-workers,¹⁷ who demonstrated incontrovertibly that anodic oxidation of the phenol moiety of resveratrol takes place first and is irreversible, and that *a linear relationship exists between the reduction potential of resveratrol and pH*. Thus, dimerization of the phenoxide of **2.49/2.50** was hypothesized to be more efficient by virtue of the fact that it is more strongly reducing and therefore SET to the [Ir(tpy)(tpy)](PF₆)₃ photocatalyst should take place more readily.

Indeed, treatment of the resveratrol derivatives with NaOMe in the presence of the photocatalyst in an acetone/MeOH solution open to air resulted in full consumption of starting material and a 47% yield of the isomeric dimers **2.53/2.54** after just five hours (Table 2.3, entry 6). Ultimately, control experiments revealed that the photocatalyst was unnecessary, and that

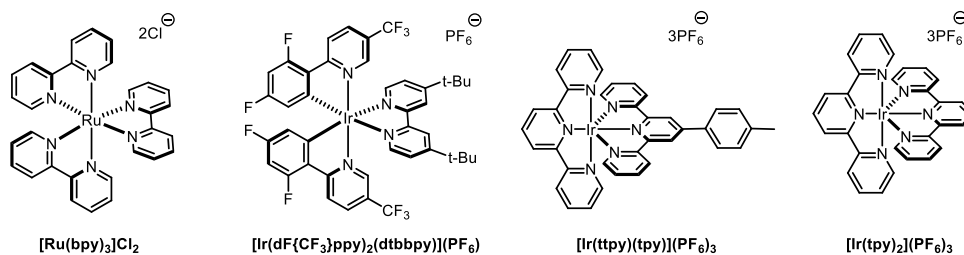
Table 2.3 Optimization of Oxidative Resveratrol Dimerization



Entry	Photocatalyst	Solvent	Oxidant	Additive	Time	Yield	Product
1	[Ru(bpy) ₃]Cl ₂	MeCN	BrCCl ₃	—	12 h	decomp.	—
2	[Ru(bpy) ₃]Cl ₂	MeCN	(NH ₄) ₂ S ₂ O ₈	—	2 h	decomp.	—
3	[Ir(dF(CF ₃)ppy) ₂ (dtbbpy)]PF ₆	CCl ₄	CCl ₄	—	72 h	—	2.49/2.50
4	[Ir(tpy) ₂](PF ₆) ₃	MeCN	O ₂	—	48 h	7% ^a	2.51/2.52
5	[Ir(tpy)(ppy)](PF ₆) ₃	acetone	O ₂	—	48 h	38%	2.51/2.52
6	[Ir(tpy)(ppy)](PF ₆) ₃	acetone/MeOH	O ₂	NaOMe	5 h	47%	2.53/2.54
7	—	acetone/MeOH	degassed	NaOMe	2 h	—	E/Z 2.49/2.50
8 ^b	—	acetone/MeOH	degassed	NaOMe	2 h	—	2.49/2.50
9 ^b	[Ir(tpy)(ppy)](PF ₆) ₃	acetone/MeOH	O ₂	NaOMe	5 h	45%	2.53/2.54
10 ^b	—	acetone/MeOH	O ₂	NaOMe	2 h	55%	2.53/2.54
11 ^b	—	CCl ₄	O ₂	KO ^t Bu	1 h	60-80%	2.55/2.56
12 ^c	—	THF	Cp ₂ FePF ₆	KHMDS	0.5 h	98%	2.55/2.56

^aIncomplete conversion; ^bReaction was shielded from light; ^cPerformed on decagram scale.

Photocatalyst Structure



each of the phenoxides were undergoing dimerization via an autoxidation mechanism under the aerobic reaction conditions (Table 2.3, entries 7–10). Upon discovering this, we optimized for the aerobic oxidation by performing the reaction in solvents which are known to possess high oxygen solubility.¹⁸² The yields and product distribution were found to be highly dependent on the solvent and the presence/absence of base. In CCl₄ and in the presence of KO^tBu, **2.49/2.50** undergo a remarkably efficient and selective dimerization to the unusual bis-quinone methide intermediates **2.55/2.56** (Table 2.3, entry 11). Each of the isomeric dimers (indane **2.51/2.52** and mono-quinone methide **2.53/2.54**) derive from the corresponding bis-quinone methide **2.55/2.56** via a Friedel–Crafts cyclization or tautomerization, respectively. Unfortunately, a significant

decrease in selectivity and reproducibility was observed on scaling the aerobic dimerization beyond ~500 mg, presumably due to difficulty in controlling oxygen diffusion into systems of increasing volume. To overcome this limitation, we exchanged O₂ for ferrocenium hexafluorophosphate — [Cp₂FePF₆] — as the stoichiometric oxidant, which reliably provided **2.55/2.56** in better than 95% yield on up to a decagram scale (Table 2.3, entry 12).¹²⁵ Despite the lability generally associated with quinone methides,¹⁸³ which are often generated and reacted *in situ*,¹⁴³ **2.55/2.56** could be purified by flash chromatography and were found to be indefinitely bench-stable. To the best of our knowledge, this represents the highest yield and largest scale yet reported for oxidative dimerization of a resveratrol derivative, and is the first truly viable biomimetic strategy for resveratrol oligomer synthesis.

2.6 Biomimetic Total Synthesis of Quadrangularin A and Pallidol

With optimized conditions for the scalable preparation of versatile bis-quinone methide intermediate **2.56** in hand, we set out to apply this method in the total synthesis of dimeric resveratrol natural products. During the dimerization, the monomers can approach each other either from opposite faces (*Re/Si*) or from the same face (*Re/Re* or *Si/Si*), resulting in a diastereomeric mixture (*d.r.* = 4:3) of products (Figure 2.11 A). The nearly statistical mixture obtained from this reaction indicates that there is little energetic preference for the *meso* versus the (*D/L*)-diastereomer. Nonetheless, the relative configuration of the vicinal stereogenic centers has important (and likely biogenically relevant) consequences for the synthesis of quadrangularin A (**1.10**) and pallidol (**2.4**).

Formation of the bicyclo[3.3.0]octane core of pallidol requires two sequential 5-*exo* Friedel–Crafts cyclizations. This outcome is not possible from *meso*-**2.56**, which, upon cyclization to **2.52**, orients the substituents in a *trans/trans*-relative configuration and introduces

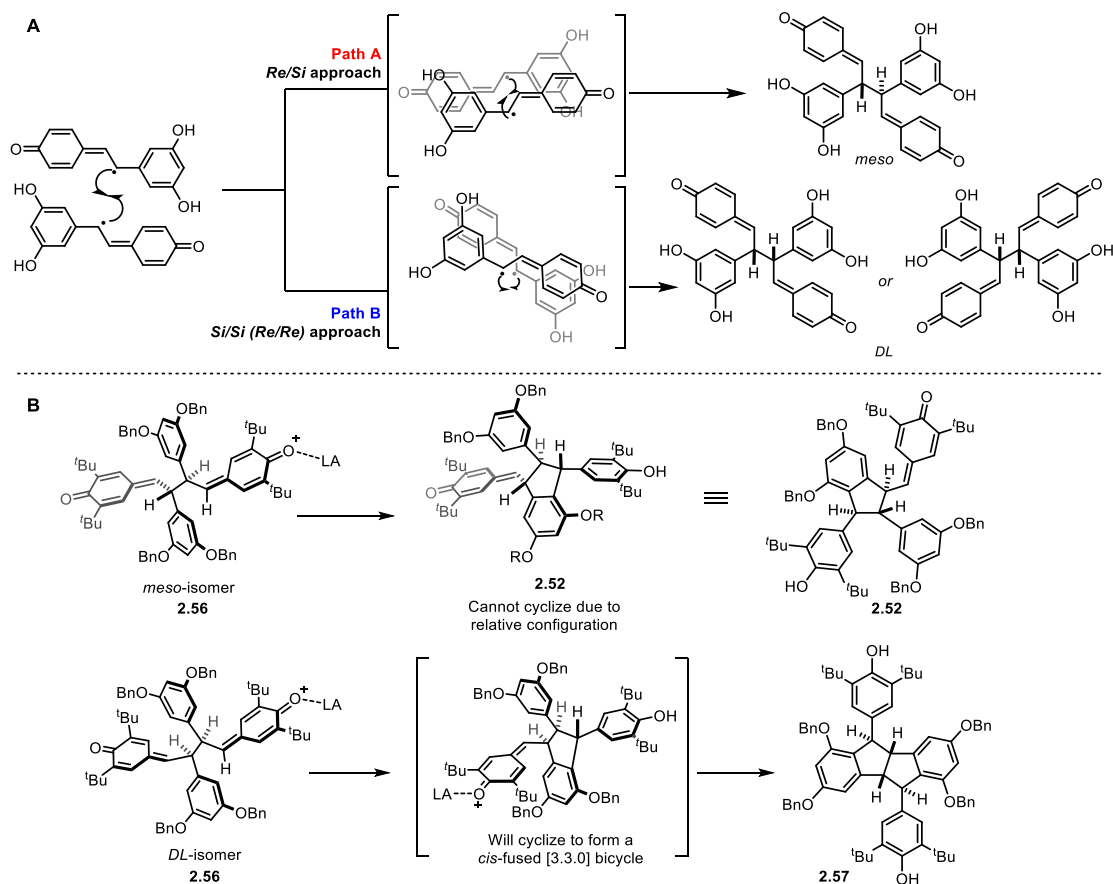


Figure 2.11 A) Facial Presentation of Resveratrol Monomers During Dimerization and B) Diastereodivergence during Friedel–Crafts Cyclization

a prohibitively high thermodynamic barrier for the unfavorable formation of a *trans*-fused bicyclo[3.3.0]octane (Figure 2.11 B).¹⁸⁴ Conversely, cyclization of (*D/L*)-**2.56** generates an indane quinone methide with a *cis/trans*-relative configuration. Thus, the quinone methide substituent at the C₃-position of this intermediate is disposed *cis* to the pendant nucleophilic resorcinol at C₂, and a 43% yield of the *cis*-fused [3.3.0] product **2.57** is obtained upon treatment of a dilute solution of **2.56** with BF₃·OEt₂ at –78 °C (Figure 2.12). The remaining mass balance on direct exposure of **2.56** to BF₃·OEt₂ consisted of varying amounts of **2.52** (up to 45% yield) and a complex mixture of oligomerized material (Figure 2.12). The natural product pallidol (**2.4**) was revealed through a two-step deprotection sequence involving hydrogenolysis to intermediate **2.27** and removal of the *tert*-butyl groups through a retro-Friedel–Crafts reaction.¹⁶¹

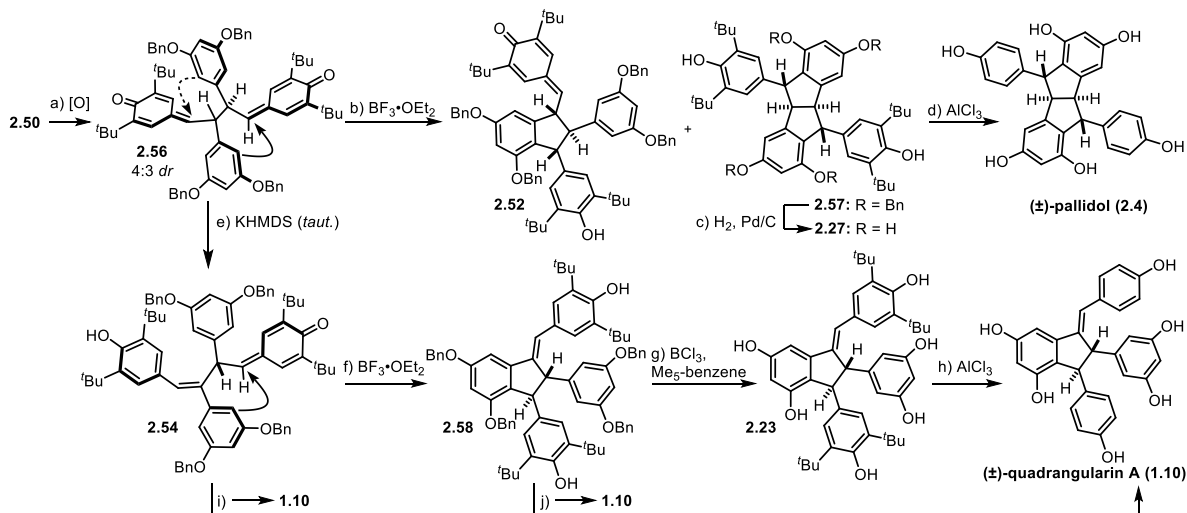


Figure 2.12 Scalable Biomimetic Synthesis of Quadrangularin A and Pallidol

a) KHMDS (1.05 equiv), FeCp_2PF_6 (1.05 equiv), THF, 0 °C, 30 min, 95%; b) $\text{BF}_3 \cdot \text{OEt}_2$ (2 equiv), CH_2Cl_2 , -78 °C, 40 min, 88% ~1:1; c) Pd/C (30 wt%), H_2 (1 atm), 3:2 EtOAc/MeOH, rt, 12 h, 95%; d) AlCl_3 (12 equiv, 2.25 M in CH_3NO_2), toluene, 60 °C, 30 min, 80%; e) KHMDS (1.05 equiv), FeCp_2PF_6 (1.05 equiv), THF, 0 °C, 30 min, then KHMDS (1.25 equiv), 15 min; f) $\text{BF}_3 \cdot \text{OEt}_2$ (2 equiv), CH_2Cl_2 , -78 °C, 5 min, 90% over 3 steps; g) BCl_3 (12 equiv), $\text{Me}_5\text{-benzene}$ (20 equiv), CH_2Cl_2 , -78 °C, 2 h, 82%; h) AlCl_3 (12 equiv, 2.25 M in CH_3NO_2), toluene, 60 °C, 30 min, 80%; i) $\text{Me}_5\text{-benzene}$ (40 equiv), AlCl_3 (25 equiv, 0.6 M in CH_3NO_2) slow add'n, CH_2Cl_2 , 0 °C, then 60 °C, 15 min, 51%; j) $\text{Me}_5\text{-benzene}$ (40 equiv), AlCl_3 (24 equiv, 0.5 M in CH_3NO_2) slow add'n, CH_2Cl_2 , 0 °C, then 60 °C, 1 h, 88%, 5:1 mixture of quadrangularin A (**3**) to its internal alkene isomer; Bn=benzyl, ^tBu=*tert*-butyl, *taut.*=tautomerization, KHMDS=potassium hexamethyldisilazide, FeCp_2PF_6 =ferrocenium hexafluorophosphate, THF=tetrahydrofuran, $\text{Me}_5\text{-benzene}$ =pentamethylbenzene.

For the synthesis of quadrangularin A (**1.10**), the mixture of diastereomers obtained on formation of **2.56** is inconsequential, as the stereochemical information at one of the centers is ultimately destroyed. Thus, upon full conversion of **2.50** to the bis-quinone methide (as determined by thin-layer chromatography), an additional equivalent of base is added to promote tautomerization and rearomatization of one of the quinone methides (Figure 2.12). The tautomerization is diastereoconvergent — the (*E*)-stilbene isomer of **2.54** is obtained exclusively. A subsequent Friedel–Crafts cyclization to **2.58**, global debenylation to **2.23**, and de-*tert*-butylation afforded the natural product quadrangularin A (**1.10**). Conditions were developed for achieving this sequence in one, two, or three steps in 51%, 73%, and 55% yields, respectively. In each case, Lewis acids were employed to promote all three events, while $\text{Me}_5\text{-benzene}$ was critical to preventing oxygen-to-carbon transfer of the benzyl protecting groups.^{185,186}

2.7 Systematic Evaluation of Antioxidant Activity

Oxidative damage to cellular constituents arising from lipid peroxidation (Figure 2.13 A)¹⁸⁷⁻¹⁸⁹ has long been implicated in the pathogenesis of a staggering number of degenerative diseases.¹⁹⁰ Phenolic compounds are known to be good *in vitro* inhibitors of lipid peroxidation (e.g. α -tocopherol (α -TOH), the most biologically active form of Vitamin E) because they often possess weak O–H bonds that enable fast H-atom transfer to chain-carrying peroxy radicals (Figure 2.13 B).^{191,192} Although hundreds of papers have purportedly detailed the radical-trapping antioxidant (RTA) activities of **1.1** (and other phenolic phytochemicals), these generally employ titrations of their reducing equivalents using colorimetric methods, such as in 2,2-diphenyl-1-picrylhydrazyl (DPPH) assays. Despite their widespread use, these assays offer poor estimates of the efficacies with which ‘antioxidants’ trap intracellular or lipid-embedded peroxy radicals since the oxidants are rarely peroxy radicals and the results provide no kinetic information – simply information on the position of a redox equilibrium.¹⁹³⁻¹⁹⁵ In reality, RTAs must outcompete (poly)unsaturated lipids (or other readily autoxidizable cellular components) for peroxy radicals (k_p vs. k_{inh}), making the *kinetics of their reactions with peroxy radicals* paramount. Furthermore, DPPH assays are typically conducted in ethanol or other polar protic media, in which the redox event proceeds via a sequential proton-loss-electron-transfer (SPLET) mechanism as opposed to the hydrogen atom transfer (HAT) mechanism that predominates in the

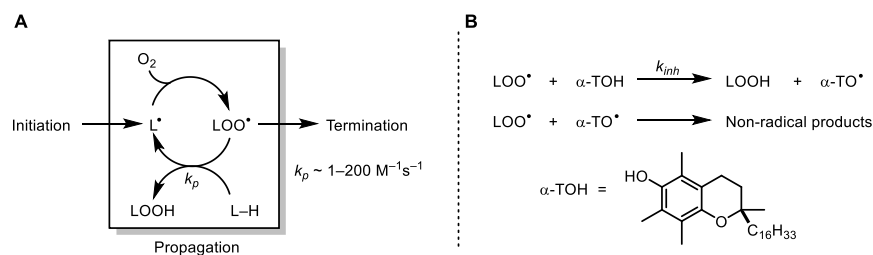


Figure 2.13 A) Lipid Peroxidation; B) Inhibition by Radical Trapping Antioxidant (RTA)

lipophilic environment of cellular membranes.

Despite the hype surrounding the antioxidant properties of resveratrol, it was not until 2003 that a kinetic study on its RTA activity was performed. Valgimigli and coworkers determined the rate of peroxy radical-trapping by resveratrol in homogeneous chlorobenzene solution to be $2.0 \times 10^5 \text{ M}^{-1} \text{ s}^{-1}$,¹²⁴ which is approximately 16 times lower than that of α -tocopherol, (α -TOH, $k_{inh} = 3.2 \times 10^6 \text{ M}^{-1} \text{ s}^{-1}$), nature's ubiquitous radical-trapping antioxidant.¹⁹¹ Enabled by the aforementioned synthetic advances, we recently collaborated with the Pratt group to evaluate the RTA activities of resveratrol (**1.1**) and two of its dimers – quadrangularin A (**1.10**) and pallidol (**2.4**) – in homogeneous organic solution, lipid bilayers, and cell culture.¹²⁵

Experiments in organic solution were carried out using the peroxy radical clock methodology^{196,197} or inhibited autoxidation methodology.¹⁹⁸ This method relies on the fact that the distribution of lipid autoxidation products is a function of a competition between a unimolecular reaction (β -fragmentation of peroxy radicals) having a known rate constant (k_{β}) and a bimolecular reaction (H-atom donation from a substrate to a peroxy radical) with an unknown rate constant (k_{inh}). For these studies, the lipid substrate used was methyl linoleate **2.59**, the autoxidation of which has been studied in great detail and is known to involve β -fragmentations of several intermediate peroxy radicals (Figure 2.14).^{187,199,200} Thus, MeOAMVN (**2.60**)-initiated formation of the methyl linoleate-derived pentadienyl radical **2.61** is followed by trapping with molecular oxygen to form three regioisomeric peroxy radicals, **2.62**, **2.63**, and **2.64**. Typically, β -fragmentation of the nonconjugated peroxy **2.63** is so fast that the corresponding hydroperoxide **2.65** is not observed. Efficient H-atom donors — where $k_{\beta II}$ from **2.62** and **2.64** is not kinetically competitive with k_{inh} — lend way to *cis,trans*-conjugated hydroperoxides **2.66** and **2.67**. Conversely, β -fragmentation ($k_{\beta II}$) to reform **2.61** becomes

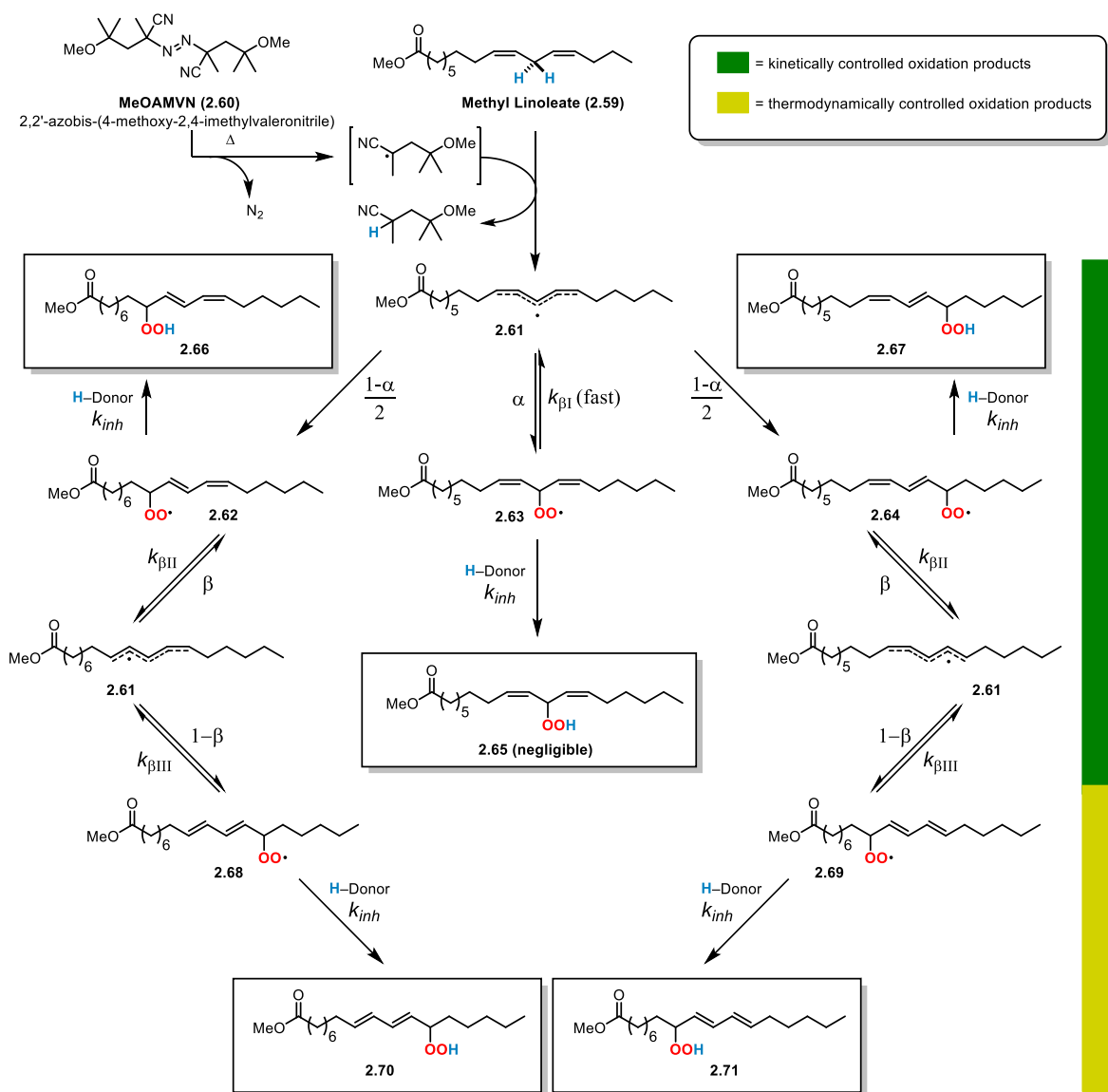
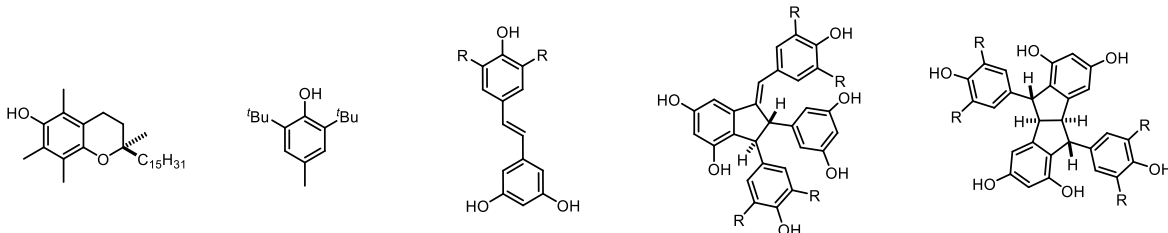


Figure 2.14 Kinetic Product Distributions of Peroxy Radical Trapping of Methyl Linoleate

$$\frac{[E,Z]}{[Z,Z]} = \frac{k_{\beta I}}{k_{inh}[\text{Antioxidant}]} \left(\frac{1-\alpha}{\alpha} \right) + \left(\frac{1-\alpha}{\alpha} \right) \quad (1)$$

$$\frac{[E,Z]}{[E,E]} = \frac{k_{inh}[\text{Antioxidant}]}{k_{\beta II}(1-\beta)} + \frac{k_{\beta III}}{k_{\beta II}} \left(\frac{\beta}{1-\beta} \right) \quad (2)$$

Table 2.4 RTA Activity of Resveratrol Dimers and Derivatives

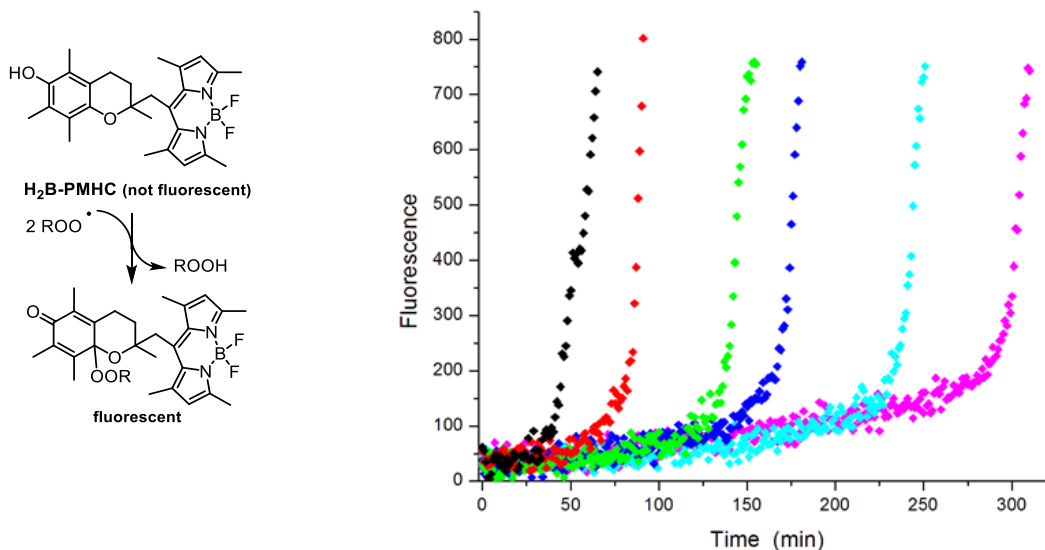


	Solution		Lipid Bilayers		Cells	Cytotoxicity
	k_{inh}^a (PhCl) / $M^{-1}s^{-1}$	$k_{rets}^b n^c$ ($ROO\bullet_{lipid}$) ^d	$k_{rets}^b n^c$ ($ROO\bullet_{aq}$) ^d	EC_{50} / μM	EC_{50} / μM	
resveratrol (1.1)	2.0×10^5 ^e	<0.01	<0.01	12.6 ± 0.9	118 ± 14	
pallidol (2.4) ^f	8.5×10^4 ^g	<0.01	<0.01	8.1 ± 0.9	205 ± 11	
quadrangularin A (1.10)	2.3×10^5 ^g	<0.01	<0.1	3.4 ± 0.4	63.5 ± 3.0	
α -tocopherol (α -TOH)	3.2×10^6 ^f	$1.8 \pm 0.2, 2.0$ ^h	$1.3 \pm 0.1, 2.0$ ^h	0.15 ± 0.01	>100	
^t Bu ₂ -resveratrol (2.19)	$(5.9 \pm 0.8) \times 10^4$ ⁱ	$17.9 \pm 3.3, 1.8 \pm 0.1$	$21.0 \pm 6.8, 1.8 \pm 0.1$	0.051 ± 0.004	10.2 ± 0.3	
^t Bu ₄ -pallidol (2.27) ^f	$(2.1 \pm 0.3) \times 10^4$ ⁱ	<0.01	<0.01	0.39 ± 0.07	10.2 ± 0.4	
^t Bu ₄ -quadrangularin A (2.23)	$(6.2 \pm 0.9) \times 10^4$ ⁱ	$7.5 \pm 0.6, 1.9 \pm 0.1$	<0.1	0.21 ± 0.03	8.7 ± 0.5	
BHT	$(2.2 \pm 0.1) \times 10^4$ ⁱ	<0.01	<0.01	12.7 ± 1.5	49.5 ± 2.0	

^aSecond order rate constant for the reaction with (linoleyl) peroxy radicals. ^bSecond order rate constant for the reaction with peroxy radicals relative to the fluorescent probe H₂B-PMHC. ^cNumber of peroxy radicals trapped per molecule of test compound. ^dInitiated with MeOAMVN and AAPH, respectively. ^eDetermined at 30 °C by the inhibited autoxidation of styrene. ^fSince two equivalent units exist on the same molecule, the observed rate constant has been divided by 2. ^gEstimated from the value for resveratrol and the relative reactivities of the corresponding synthetic precursors (*tert*-butylated analogs). ^hFrom ref. [124]. ⁱDetermined at 37°C by the peroxy radical clock methodology on resorcinol ring-protected (benzyl) compounds.

significant for poor radical trapping antioxidants, leading to formation of *trans,trans*-conjugated peroxy radicals **2.68** and **2.69**, and ultimately to their corresponding hydroperoxides **2.70** and **2.71**. Steady-state analysis leads to equations (1) and (2), which describe the product distribution as a function of oxygen partitioning (α), β -fragmentation, and antioxidant concentration for autoxidations carried out under kinetically or thermodynamically controlled conditions, respectively.

While the poor solubility of the natural products in chlorobenzene precluded direct determinations of their k_{inh} values, each of the benzylated synthetic precursors were soluble and values of k_{inh} were readily determined (Table 2.4), revealing that ^tBu₄-quadrangularin A **2.23** ($6.8 \times 10^4 M^{-1}s^{-1}$) was slightly more reactive than ^tBu₂-resveratrol **2.19** ($5.9 \times 10^4 M^{-1}s^{-1}$), while ^tBu₄-pallidol **2.27** ($2.5 \times 10^4 M^{-1}s^{-1}$) was less reactive. The k_{inh} value of **2.27**, which lacks an activating alkene, is indistinguishable from that of the common synthetic antioxidant BHT (once pallidol's two-fold statistical advantage is considered). The reactivities of the authentic natural



Fluorescence intensity-time profiles of MeOAMVN-mediated oxidation of H₂B-PMHC-embedded PC liposomes in phosphate-buffered saline (pH 7.4) as a function of increasing concentration of *t*-butylated resveratrol (**2.19**): 2.5 μM (black), 5.0 μM (red), 10 μM (green), 15 μM (blue), 20 μM (cyan), 30 μM (magenta). [MeOAMVN] = 0.68 mM, [H₂B-PMHC] = 15 μM, [PC] = 1 mM.

Figure 2.15 Inhibited Oxidations of Phosphatidylcholine Liposomes

products could be estimated from the relative rate constants given above and the known rate constant for resveratrol as reported by Valgimigli and co-workers.¹²⁴ These rate constants are all much lower than that of α -tocopherol (α -TOH, $k_{\text{inh}} = 3.2 \times 10^6 \text{ M}^{-1} \text{ s}^{-1}$), suggesting that neither resveratrol nor the dimers quadrangularin A and pallidol are likely to owe their biological activity to radical-trapping antioxidant activity.

Experiments in lipid bilayers were carried out using Cosa's pro-fluorescent H₂B-PMHC probe,²⁰¹ which functions as shown (Figure 2.15). In the lipid bilayers of unilamellar vesicles of egg phosphatidylcholine, resveratrol, pallidol and quadrangularin A were each almost entirely inactive – presumably due to their inability to partition significantly to the lipid phase. Interestingly, despite being far less reactive in solution, the *tert*-butylated synthetic precursors were much more effective than the natural products in lipid bilayers (Table 2.4). In fact, the *tert*-butylated resveratrol derivative (**2.19**) was one of the most potent compounds ever studied in lipid bilayers. Barclay,²⁰² Niki²⁰³ and others have shown that the inherent reactivity of RTAs to

peroxyl radicals (i.e. solution k_{inh} values) is far less important than their physical properties when in a lipid bilayer, and the findings in this study underscore this fact. Not only are the natural products expected to be less soluble than the *tert*-butylated analogs in the lipid milieu, but the reactivity of their key phenolic O–H groups will be reduced to a greater extent due to H-bonding with phosphatidylcholine moieties and/or water at the interface.

The RTA activity of resveratrol analogue **2.19** translated to cultures of human Tfla erythroblasts, where it was shown to be significantly more potent than α -TOH (Table 2.4). Collectively, the natural products were again far less effective at inhibiting lipid peroxidation than their *tert*-butylated synthetic precursors. In the case of pallidol and quadrangularin A, the difference in their EC₅₀ values is roughly 20-fold (8.1 and 3.4 vs. 0.39 and 0.21 μM , respectively), whereas for resveratrol, the difference is almost 250-fold (12.6 μM vs. 51 nM). Moreover, the effective concentrations for RTA activity were at least an order of magnitude lower than those for cytotoxicity for each of the natural product analogs. Curiously, although *t*Bu₂-pallidol **2.27** was inefficient at preventing lipid peroxidation in bilayers, it was surprisingly potent (EC₅₀ = 0.39 μM) in cell culture, suggesting that it likely operates through a mechanism other than direct radical trapping.

2.8 Conclusions

We embarked on the work summarized in Sections 2.5–2.7 with the intention of simultaneously addressing what, at the time, represented two underdeveloped areas in photoredox catalysis: (1) the use of this mode of catalysis to perform net-oxidative chemistry and (2) its applications in total synthesis. Our objectives, both immediate and long-term, have since evolved substantially. Through highly collaborative research, we have combined sophisticated methods for chemical synthesis, physical chemistry and chemical biology in an effort to

elucidate the mechanism(s) of biological activity of resveratrol and its derivatives and shed light on the preventive and/or therapeutic potential of plant-derived antioxidants in pathophysiology wherein oxidative stress has been implicated. Now that systematic studies of these types of compounds have extended past homogeneous solution into lipid bilayers and cell culture, they challenge the popular belief that the biological activities of resveratrol-derived natural products are due to their ability to trap radicals.

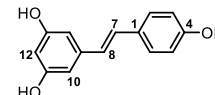
The development of a highly efficient and scalable oxidative dimerization of *tert*-butylated resveratrol derivative **2.50** has, for the first time, rendered biomimetic synthesis a viable approach for the controlled preparation of useful quantities of resveratrol oligomers. This method was showcased in the synthesis of dimeric natural products pallidol (**2.4**) (6 steps/26% yield) and quadrangularin A (**1.10**) (5 steps/54% yield), each representing the most efficient synthesis (either biomimetic or *de novo*) to date.¹²⁵ Moreover, access to uniquely stable and synthetically versatile *para*-quinone methide intermediates such as **2.56** has broad (and likely biogenically relevant) implications for the synthesis of resveratrol oligomers. Stable at neutral and mildly basic pH, the quinone methides become strong electrophiles in the presence of either Lewis or Brønsted acids. This property proved instrumental for the synthesis of quadrangularin A (**1.10**) and pallidol (**2.4**), enabling tautomerization under strongly basic conditions while maintaining “switchable” Friedel–Crafts reactivity under Lewis acidic conditions. The ability to harness the reactivity of persistent radical and quinone methide intermediates has facilitated the extension of this chemistry to the synthesis of complex resveratrol trimers and tetramers, which are the subject of the ensuing chapters.

2.9 Experimental Procedures and Spectral Data

General Procedures: Glassware was dried in a 150 °C oven or flame-dried under vacuum (~0.5 Torr) prior to use. Reaction vessels were equipped with Teflon/PTFE-coated magnetic stir bars and fitted with rubber septa, and reaction mixtures were maintained under a positive pressure of dry nitrogen unless otherwise noted. Air- and/or moisture-sensitive liquids were transferred using stainless steel needles or cannulae. Reaction progress was monitored by analytical thin-layer chromatography (TLC) using glass-backed plates pre-coated with 230–400 mesh silica gel (250 µm, Indicator F-254), available from Silicycle, Inc (cat #: TLG-R10011B-323). Thin layer chromatography plates were visualized by exposure to a dual short-wave/long-wave UV lamp and/or by exposure to ethanolic solutions of *p*-anisaldehyde or vanillin, or an aqueous solution of ceric ammonium molybdate (Hanessian's stain), and the stained plates were developed by warming with a heat gun. Flash column chromatography was performed according to the procedure described by Still et al.¹ either manually using 43–60 µm (230–400 mesh) silica gel or utilizing RediSep®R_F Gold silica columns with a Teledyne Isco CombiFlash R_F automated purification system. Upon reaction quenching and work up, organic solutions were dried over Na₂SO₄ or MgSO₄ and concentrated on Büchi rotary evaporators at ~10 Torr/35 °C, then at ~0.5 Torr/25 °C using a Welch vacuum pump.

Materials: Commercially available starting materials were used as received without further purification unless otherwise noted. Organic solvents (acetonitrile, dichloromethane, diethyl ether, dimethylformamide, dimethyl sulfoxide, methanol, tetrahydrofuran, toluene) and amine bases (triethylamine, pyridine, *N,N*-diisopropylethylamine, and diisopropylamine) were purified immediately prior to use by the method of Grubbs et al.² using a Phoenix Solvent Drying System (JC-Meyer Solvent Systems) or PureSolv Micro amine drying columns (Innovative Technology/Inert), respectively, and maintained under positive argon pressure. Solutions of organolithium reagents (*n*-BuLi, *t*-BuLi) and Grignard reagents were purchased from Acros Organics unless otherwise noted and titrated prior to use (1,10-phenanthroline/menthol) according to the method of Paquette.³

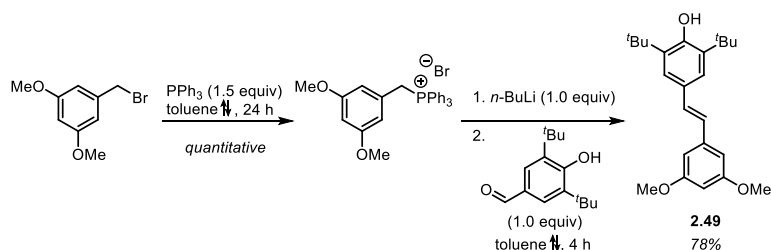
Product Analysis: Product names were generated using ChemDraw Ultra 14.0 (PerkinElmer). ¹H and ¹³C NMR spectra were recorded at the indicated temperature at 117 kG and 176 kG (¹H 500 MHz, 700 MHz; ¹³C 125 MHz and 175 MHz) using an internal deuterium lock on Varian Inova 500 or Varian VNMR 500 and 700 spectrometers. ¹H chemical shifts are expressed in parts per million (ppm) relative to the residual protio solvent resonance in CDCl₃ using δ 7.26 as standard for residual CHCl₃ or using the center line of the solvent signal as internal reference for acetone-*d*₆: δ 2.05, and DMSO-*d*₆: δ 2.50. Multiplicity is reported as follows: (br = broad, s = singlet, d = doublet, t = triplet, dd = doublet of doublets, ddd = doublet of doublet of doublets, m = multiplet), and the corresponding coupling constants are indicated as *J*-values in units of Hz. ¹³C NMR spectra were completely ¹H-decoupled (broadband) and the center line of the solvent signal was used as internal reference: CDCl₃ δ 77.23; acetone-*d*₆ δ 29.92; DMSO-*d*₆ δ 39.51. ¹³C chemical shifts are expressed in parts per million (ppm) to a single decimal place; in instances where multiple resonances approximate the same chemical shift value, two decimal places are used. For ¹H and ¹³C assignments, the following resveratrol numbering scheme was used, and each successive resveratrol equivalent was denoted with (a, b, c, etc.). Diastereotopic protons are denoted with (*), and protons found to exchange in the presence of D₂O are indicated with “exchangeable [D₂O]”. Infrared data were obtained on a Perkin-Elmer Spectrum BX FT-IR spectrophotometer using an ATR mount with a ZnSe crystal and are reported as follows: [frequency of absorption (cm⁻¹), intensity of absorption (s = strong, m = medium, w = weak, br = broad)]. High-resolution mass spectra (HRMS) were obtained on a Micromass AutoSpec Ultima Magnetic Sector mass spectrometer using electrospray ionization (ESI), positive ion mode—we thank James Windak and Paul Lennon at the University of Michigan Department of Chemistry instrumentation facility for conducting these experiments.



¹ Still, W. C.; Kahn, M.; Mitra, A. *J. Org. Chem.* **1978**, *43* (14), 2923–2925.

² Pangborn, A. B.; Giardello, M. A.; Grubbs, R. H.; Rosen, R. K.; Timmers, F. J. *Organometallics* **1996**, *15* (5), 1518–1520.

³ Lin, H.S.; Paquette, L. A. *Synth. Commun.* **1994**, *24* (17), 2503–2506; Watson, S. C.; Eastham, J. F. *J. Organomet. Chem.* **1967**, *9* (1), 165–168.



(E)-2,6-di-tert-butyl-4-(3,5-dimethoxystyryl)phenol (2.49): A round bottom flask equipped with a reflux condenser and magnetic stir bar was charged with commercially available 3,5-dimethoxy benzyl bromide (6.00 g, 26.0 mmol, 1.00 equiv). The material was dissolved in anhydrous toluene (60 mL, 0.43 M) at room temperature under N₂. To the stirring mixture, PPh₃ (10.2 g, 38.9 mmol, 1.5 equiv) was added in a single portion and the solution was heated to reflux for 24 h. The reaction mixture was allowed to cool to room temperature and the product collected by vacuum filtration. The solid was washed with hexanes and dried under vacuum to give the desired phosphonium salt as a crystalline white solid (12.8 g, 26.0 mmol 99% yield). The phosphonium salt (5.00 g, 10.1 mmol, 1.00 equiv) was suspended in anhydrous toluene (200 mL, 0.05 M) in a flame-dried, 3-neck 500 mL round bottom flask equipped with a reflux condenser and magnetic stir bar. To the stirring suspension at room temperature under N₂, *n*-BuLi (4.00 mL, 2.5 M soln. in hexanes, 1.00 equiv) was added slowly, turning the mixture a brilliant red. The mixture was allowed to equilibrate at this temperature for 30 minutes, at which point the solution of the ylide was heated to reflux. Once reflux temperature was reached, 3,5-di-*tert*-butyl-4-hydroxybenzaldehyde (2.38 g, 10.1 mmol, 1.00 equiv, recrystallized from toluene and dried from benzene 3x prior to use) was added as a solid, portion wise under a stream of N₂. The reaction was allowed to stir at this temperature for 4 hours; reaction progress was monitored by TLC in 9:1 Hexanes/EtOAc. At 4 h, the reaction was quenched with methanol and the solvent removed by rotary evaporation. The crude residue was treated with cold diethyl ether to precipitate triphenylphosphine oxide, and filtered through a fritted funnel packed with Celite and a filter paper. The crude filtrate was then purified by flash chromatography over SiO₂ (97:2:1 Hexanes/EtOAc/CH₂Cl₂) to afford stilbene **2.49** as an amorphous white solid (2.90 g, 7.87 mmol, 78% yield).

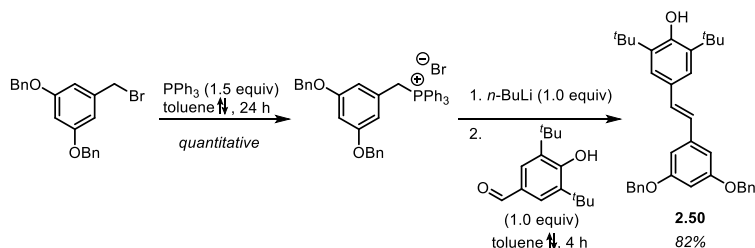
TLC (Hexanes/EtOAc, 90:10), R_f: 0.35 (UV, *p*-anisaldehyde (maroon));

¹H NMR (500 MHz, CDCl₃, 25 °C) δ: 7.34 (s, 2H), 7.05 (d, *J* = 16.1 Hz, 1H), 6.87 (d, *J* = 16.1 Hz, 1H), 6.66 (d, *J* = 2.2 Hz, 2H), 6.37 (t, *J* = 2.2 Hz, 1H), 5.29 (s, 1H), 3.84 (s, 6H), 1.48 (s, 18H);

¹³C NMR (175 MHz, CDCl₃, 25 °C) δ: 161.2, 154.2, 140.2, 136.4, 130.3, 128.6, 126.0, 123.7, 104.4, 99.8, 55.6, 34.6, 30.5;

HRMS (ESI): *m/z* calculated for C₂₄H₃₃O₃⁺ ([M+H]⁺) 369.2244, found 369.2426;

FTIR (neat) cm⁻¹: 3624, 2956, 1590, 1456, 1436, 1358, 1236, 1204, 1150, 1066.



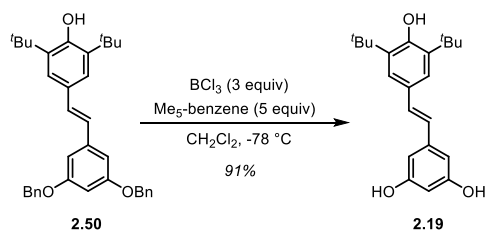
(E)-4-(3,5-bis(benzyloxy)styryl)-2,6-di-tert-butylphenol (2.50): A round bottom flask equipped with a reflux condenser and magnetic stir bar was charged with commercially available 3,5-dibenzyloxy benzyl bromide (10.1 g, 26.4 mmol, 1.00 equiv). The material was dissolved in anhydrous toluene (60 mL, 0.44 M) at room temperature under N₂. To the stirring mixture, PPh₃ (10.4 g, 39.6 mmol, 1.50 equiv) was added in a single portion and the solution was heated to reflux for 24 h. The reaction mixture was allowed to cool to room temperature and the product collected by vacuum filtration. The solid was washed with hexanes and dried under vacuum to give the desired phosphonium salt as a crystalline white solid (16.9 g, 26.2 mmol 99% yield). The phosphonium salt (13.5 g, 22.4 mmol, 1.00 equiv) was suspended in anhydrous toluene (225 mL, 0.10 M) in a flame-dried, 3-neck 500 mL round bottom flask equipped with a reflux condenser and magnetic stir bar. To the stirring suspension at room temperature under N₂, *n*-BuLi (9.39 mL, 2.5 M soln. in hexanes, 1.05 equiv) was added slowly, turning the mixture a brilliant red. The mixture was allowed to equilibrate at this temperature for 30 minutes, at which point the solution of the ylide was heated to reflux. Once reflux temperature was reached, 3,5-di-*tert*-butyl-4-hydroxybenzaldehyde (5.77 g, 24.6 mmol, 1.10 equiv, recrystallized from toluene and dried from benzene 3x prior to use) was added as a solid, portionwise under a stream of N₂. The reaction was allowed to stir at this temperature for 4 hours; reaction progress was monitored by TLC in 9:1 Hexanes/EtOAc. At 4 h, the reaction was quenched with methanol and the solvent removed by rotary evaporation. The crude residue was treated with cold diethyl ether to precipitate triphenylphosphine oxide, and filtered through a fritted funnel packed with Celite and a filter paper. The crude filtrate was purified by flash chromatography over SiO₂ (97:2:1 Hexanes/EtOAc/CH₂Cl₂) to afford stilbene **2.50** as an amorphous white solid (9.57 g, 18.4 mmol, 82% yield), which was further purified to a crystalline white powder by sonication in ¹PrOH and collected by vacuum filtration.

TLC (Hexanes/EtOAc, 90:10), R_f: 0.35 (UV, *p*-anisaldehyde (maroon));

¹H NMR (500 MHz, CDCl₃, 25 °C) δ: 7.46 – 7.32 (m, 10H), 7.04 (d, *J* = 16.1 Hz, 1H), 6.87 (d, *J* = 16.1 Hz, 1H), 6.77 (d, *J* = 2.2 Hz, 2H), 6.52 (t, *J* = 2.2 Hz, 1H), 5.29 (s, 1H), 5.08 (s, 4H), 1.48 (s, 18H);

All characterization data consistent with that reported.⁴

⁴ W. Li, H. Li, Y. Li, Z. Hou, *Angew. Chem. Int. Ed.* **2006**, *45*, 7609–7611; *Angew. Chem.* **2006**, *118*, 7771–7773.



(*E*)-5-(3,5-di-tert-butyl-4-hydroxystyryl)benzene-1,3-diol (2.19):⁵ A round bottom flask equipped with a septum and magnetic stir bar was charged with starting **2.50** (1.75 g, 3.36 mmol, 1.00 equiv) and Me₅-benzene (2.49 g, 16.8 mmol, 5 equiv). The mixture was dissolved in anhydrous CH₂Cl₂ (57 mL, 0.05 M) at room temperature under N₂ and cooled to -78 °C. To the stirring mixture, BCl₃ (10.1 mL, 1.0 M soln. in CH₂Cl₂, 3 equiv) was added slowly, turning the reaction deep maroon. Upon completion of the addition, the reaction was quickly transferred to a 0 °C ice bath and stirred for an additional 40 minutes at this temperature, over which the reaction turned a bright transparent red color. The reaction was quenched at -78 °C by pipet-wise addition of a 4:1 THF/sat. aq. NaHCO₃ mixture and the solution stirred vigorously under N₂ for several minutes as it decolorized. The contents were then transferred to a separatory funnel containing DI H₂O and the organic layer separated. The aqueous phase was extracted with CH₂Cl₂ (2x) and organic layers combined, dried over Na₂SO₄, and concentrated *in vacuo*. The resulting residue was purified by flash chromatography using a gradient 5% to 15% EtOAc in CHCl₃ mobile phase to give **2.19** as an amorphous white solid (1.05 g, 0.81 mmol, 91% yield) along with 45 mg (4%) of the corresponding (*Z*)-stilbene isomer. NOTE: **2.19** is unstable to prolonged storage in air at room temperature, but could be stored indefinitely at -20 °C in a container sealed under N₂.

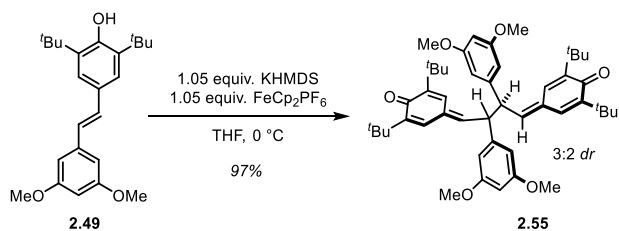
TLC (CH₂Cl₂/MeOH, 90:10), R_F: 0.48 (UV, *p*-anisaldehyde (purple));

¹H NMR (500 MHz, CDCl₃, 25 °C) δ: 7.31 (s, 2H), 7.02 (d, *J* = 16.4 Hz, 1H), 6.79 (d, *J* = 16.4 Hz, 1H), 6.56 (d, *J* = 2.2 Hz, 2H), 6.24 (t, *J* = 2.2 Hz, 1H), 5.30 (s, 1H), 4.66 (s, 2H), 1.47 (s, 18H).

All characterization data consistent with that reported.⁶

⁵ Procedure adapted from: Okano, K.; Okuyama, K.; Fukuyama, T.; Tokuyama, H. *Synlett* **2008**, No. 13, 1977–1980.

⁶ W. Li, H. Li, Y. Li, Z. Hou, *Angew. Chem. Int. Ed.* **2006**, *45*, 7609–7611; *Angew. Chem.* **2006**, *118*, 7771–7773.



4,4'-(2,3-bis(3,5-dimethoxyphenyl)butane-1,4-diylidene)bis(2,6-di-tert-butylcyclohexa-2,5-dien-1-one) (2.55):

In a round bottom flask equipped with a septum and magnetic stir bar, a solution of **2.49** (2.00 g, 5.43 mmol, 1.00 equiv) in anhydrous THF (55 mL, 0.1 M) was cooled to 0 °C in an ice bath under inert atmosphere. To this, KHMDS (5.7 mL, 1.0 M soln. in THF, 1.05 equiv) was added slowly, turning the pale yellow solution a dark forest green. (NOTE: KHMDS must be fresh for reproducible results). The solution was allowed to stir at temperature for 10 minutes, upon which the septum was removed and ferrocenium hexafluorophosphate (1.9 g, 97% purity, 5.70 mmol, 1.05 equiv.) was added in two 950 mg portions, separated by 15 minutes. The heterogeneous reaction slowly turns from blue-green to a dark yellow/orange color as the ferrocenium is reduced. After the reaction was deemed complete by TLC (ca. 30 min), the reaction mixture was dried on to Celite and the solvent removed completely under reduced pressure. The crude material was purified by flash chromatography over SiO₂ (100:0 Hexanes/EtOAc [to elute ferrocene], then gradient 95:2.5:2.5 to 90:5:5 Hexanes/EtOAc/CH₂Cl₂) to afford **2.55** as an amorphous yellow solid (1.94 g, 2.64 mmol, 97% yield), which further purified to a crystalline yellow powder by trituration from a minimum of CH₂Cl₂ with MeOH.

TLC (Hexanes/EtOAc, 90:10), R_F: 0.30 (UV, *p*-anisaldehyde (pale red));

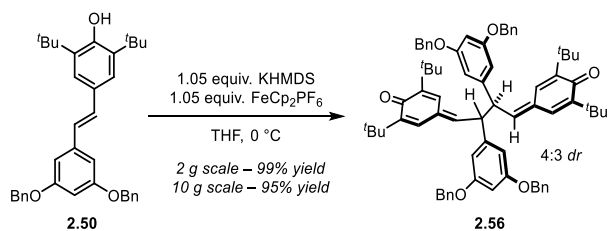
¹H NMR (700 MHz, CDCl₃, 25 °C) δ:⁷ 7.13 (major, d, *J* = 1.9 Hz, 2H), 7.09 (minor, d, *J* = 2.0 Hz, 2H), 6.82 (minor, d, *J* = 2.2 Hz, 2H), 6.71 (major, d, *J* = 2.2 Hz, 2H); 6.43 (minor, m, 2H), 6.33 (major, m, 2H), 6.35 (major, d, *J* = 2.1 Hz, 4H), 6.31 (major, t, *J* = 2.1 Hz, 2H), 6.29-6.27 (minor, overlap, 6H), 4.34 – 4.30 (minor, m, 2H), 4.30 – 4.26 (major, m, 2H), 3.74 (major, s, 12H), 3.70 (minor, s, 12H), 1.25 (minor, s, 18H), 1.24 (major, s, 18H), 1.23 (minor, s, 18H), 1.22 (major, s, 18H);

¹³C NMR (175 MHz, CDCl₃, 25 °C) δ: 186.67, 186.65, 161.3, 161.2, 149.2, 149.0, 147.7, 147.3, 145.3, 144.1, 143.3, 142.9, 134.8, 134.7, 133.1, 132.1, 126.1, 126.0, 106.9, 106.8, 99.0, 98.8, 55.54, 55.52, 51.6, 51.2, 35.6, 35.5, 35.1, 35.0, 29.7, 29.63, 29.62, 29.60;

HRMS (ESI): *m/z* calculated for C₄₈H₆₃O₆⁺ ([M+H]⁺) 735.4619, found 735.4613;

FTIR (neat) cm⁻¹: 2953, 1602, 1461, 1350, 1201, 1156, 1059, 925, 831, 696.

⁷ Dimer **2.55** exists as a rapidly equilibrating and therefore inseparable mixture of diastereomers



4,4'-(2,3-bis(3,5-bis(benzyloxy)phenyl)butane-1,4-diyldene)bis(2,6-di-tert-butylcyclohexa-2,5-dien-1-one)

(2.56): In a round bottom flask equipped with a septum and magnetic stir bar, a solution of **2.50** (1.88 g, 3.61 mmol, 1.00 equiv) in anhydrous THF (30 mL, 0.1 M) was cooled to 0 °C in an ice bath under inert atmosphere. To this, KHMDS (3.8 mL, 1.0 M soln. in THF, 1.05 equiv) was added slowly, turning the pale yellow solution a dark forest green. (NOTE: KHMDS must be fresh for reproducible results). The solution was allowed to stir at temperature for 10 minutes, upon which the septum was removed and ferrocenium hexafluorophosphate (1.25 g, 97% purity, 3.79 mmol, 1.05 equiv) was added in two 625 mg portions, separated by 15 minutes. The heterogeneous reaction turns from blue-green to a dark yellow/orange color as the ferrocenium is reduced. After the reaction was complete by TLC (ca. 30 min), the reaction mixture was dried on to Celite and the solvent removed completely under reduced pressure. The crude material was purified by flash chromatography over SiO₂ (100% Hexanes [to elute ferrocene], then gradient 95:2.5:2.5 to 90:5:5 Hexanes/EtOAc/CH₂Cl₂) to afford **2.56** (1.87 g, 1.81 mmol, 99% yield) as an amorphous yellow solid, which was further purified to a crystalline yellow powder by sonication in pH neutral CH₃NO₂. When ran on 10 gram scale, isolated 9.49 g of **2.56** (95% yield).

TLC (Hexanes/EtOAc, 90:10), R_F: 0.35 (UV, *p*-anisaldehyde (red-brown));

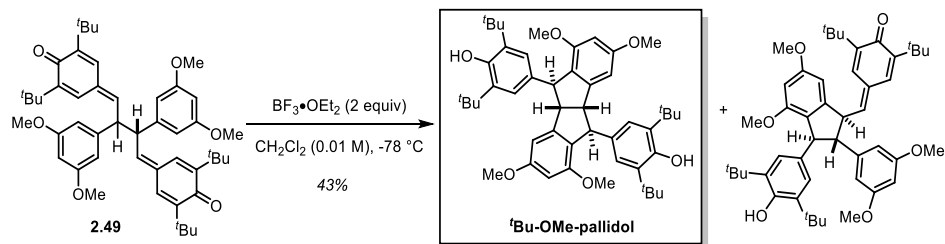
¹H NMR (700 MHz, CDCl₃, 25 °C) δ:⁸ 7.40 – 7.40 (m, 20H), 7.12 (major, d, *J* = 2.2 Hz, 2H), 7.02 (minor, d, *J* = 2.0 Hz, 2H), 6.82 (minor, d, *J* = 2.2 Hz, 2H), 6.72 (major, d, *J* = 2.0 Hz, 2H), 6.41 – 6.37 (minor, m, 2H), 6.33 – 6.29 (major, m, 2H), 6.48 (major, t, *J* = 2.1 Hz, 2H), 6.47 (minor, t, *J* = 2.2 Hz, 2H), 6.45 (major, d, *J* = 2.1 Hz, 4H), 6.38 (minor, d, *J* = 2.2 Hz, 4H), 4.96 (major, d, *J* = 11.5 Hz, 4H), 4.94 (major, d, *J* = 11.5 Hz, 4H), 4.91 (minor, d, *J* = 11.5 Hz, 4H), 4.89 (minor, d, *J* = 11.5 Hz, 4H), 4.28 (m, overlap, 4H), 1.26 (minor, s, 18H), 1.24 (major, s, 36H), 1.23 (minor, s, 18H);

¹³C NMR (175 MHz, CDCl₃, 25 °C) δ: 186.70, 186.66, 160.5, 160.4, 149.2, 149.1, 147.7, 147.4, 145.2, 143.9, 143.3, 142.9, 136.7, 136.6, 134.9, 134.7, 133.2, 132.2, 128.85 (2C), 128.4, 127.81, 127.79, 126.2, 126.0, 108.2, 108.0, 100.6, 100.57, 100.54, 70.5, 51.8, 51.2, 35.57, 35.55, 35.11, 35.05, 29.7, 29.64, 29.62;

HRMS (ESI): *m/z* calculated for C₇₂H₇₉O₆⁺ ([M+H]⁺) 1039.5832, found 1039.5871;

FTIR (neat) cm⁻¹: 2954, 1593, 1453, 1361, 1292, 1254, 1160, 1054, 930, 822, 734, 695.

⁸ Dimer **2.56** exists as a rapidly equilibrating and therefore inseparable mixture of diastereomers



4,4'-((4*S*,5*S*,9*S*,10*S*)-1,3,6,8-tetramethoxy-4*b*,5,9*b*,10-tetrahydroindeno[2,1-*a*]indene-5,10-diyl)bis(2,6-di-*tert*-butylphenol): A solution of **2.49** (20 mg, 0.027 mmol, 1.00 equiv) in anhydrous CH_2Cl_2 (10 mL, 0.003 M) was cooled to -78°C in a dry ice/acetone bath under inert atmosphere. To this, $\text{BF}_3 \cdot \text{OEt}_2$ (14 μL , 46.5% in diethyl ether, 2 equiv) was added dropwise, turning the reaction a brilliant magenta color (NOTE: temperature control is critical for the success of this reaction). The reaction was allowed to run for 40 minutes upon which the reaction was quenched with sat. aq. NaHCO_3 at temperature and allowed to warm to room temperature under vigorous stirring. The reaction was diluted with CH_2Cl_2 and transferred to a separatory funnel. The phases were separated and the aqueous layer was extracted with portions of CH_2Cl_2 . The organic layers were combined, washed with sat. aq. NaHCO_3 , brine, dried over sodium sulfate and concentrated *in vacuo*. The crude material was purified by column chromatography over SiO_2 (90:5:5 Hexanes/EtOAc/ CH_2Cl_2) to afford the pallidol derivative (8.5 mg, 0.012 mmol 43% yield) as a white amorphous solid. The remaining material was identified as the indane quinone methide product shown.

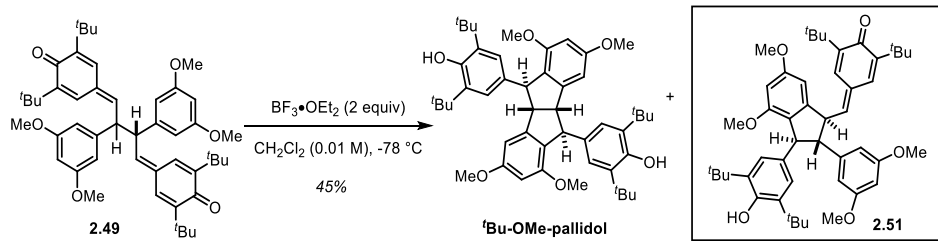
TLC (Hexanes/EtOAc, 90:10), R_f : 0.10 (UV);

^1H NMR (700 MHz, CDCl_3 , 25°C) δ : 7.12 (s, 4H), 6.66 (s, 2H), 6.23 (s, 2H), 5.03 (s, 2H, OH), 4.57 (s, 2H), 4.25 (s, 2H), 3.83 (s, 6H), 3.66 (s, 6H), 1.42 (s, 36H);

^{13}C NMR (175 MHz, CDCl_3 , 25°C) δ : 161.1, 157.1, 152.0, 148.5, 136.3, 135.4, 125.9, 124.3, 100.8, 97.6, 59.6, 55.7, 55.3, 54.2, 34.5, 30.6;

HRMS (ESI): m/z calculated for $\text{C}_{68}\text{H}_{63}\text{O}_6^+$ ($[\text{M}+\text{H}]^+$) 735.4650, found 735.4625;

FTIR (neat) cm^{-1} : 3646, 2988, 1600, 1436.



2,6-di-tert-butyl-4-(((1S,2S,3S)-3-(3,5-di-tert-butyl-4-hydroxyphenyl)-2-(3,5-dimethoxyphenyl)-4,6-dimethoxy-2,3-dihydro-1H-inden-1-yl)methylene)cyclohexa-2,5-dien-1-one (2.51):

Isolated in 45% as a byproduct of pallidol core synthesis (see previous page for experimental protocol).

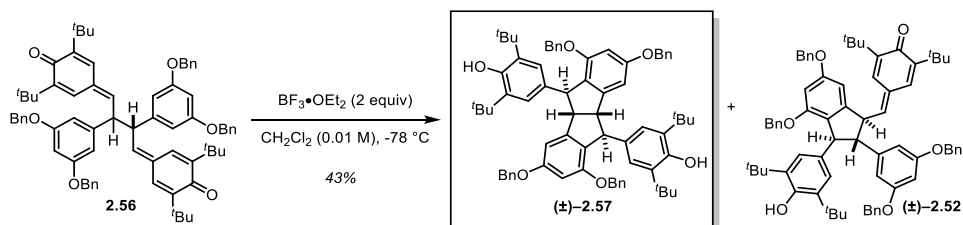
TLC (Hexanes/THF, 90:10), R_f : 0.33 (UV *p*-anisaldehyde (pale orange));

^1H NMR (500 MHz, CDCl_3 , 25 °C) δ : 6.97 (d, $J = 2.2$ Hz, 1H), 6.85 (d, $J = 2.2$ Hz, 1H), 6.70 (s, 2H), 6.42 (d, $J = 2.0$ Hz, 1H), 6.39 (d, $J = 10$ Hz, 1H), 6.34 – 6.30 (m, 4H), 4.96 (s, 1H), 4.58 (dd, $J = 9.2, 9.2$ Hz, 1H), 4.48 (d, $J = 7.8$ Hz, 1H), 3.83 (s, 3H), 3.70 (s, 6H), 3.61 (s, 3H), 3.08 (dd, $J = 8.1, 8.1$ Hz, 1H), 1.32 (s, 18H), 1.26 (s, 9H), 1.16 (s, 9H);

^{13}C NMR (125 MHz, CDCl_3 , 25 °C) δ : 186.8, 161.6, 161.0, 157.5, 152.1, 148.7, 147.8, 147.1, 146.7, 144.8, 135.1, 134.9, 133.9, 132.8, 127.0, 124.0, 123.8, 106.5, 100.9, 98.9, 98.7, 65.1, 56.6, 55.8, 55.5, 55.4, 52.9, 35.4, 35.0, 34.5, 30.6, 29.61, 29.56;

HRMS (ESI): m/z calculated for $\text{C}_{48}\text{H}_{63}\text{O}_6^+$ ($[\text{M}+\text{H}]^+$) 735.4619, found 735.4620;

FTIR (neat) cm^{-1} : 3640, 2953, 1594, 1460, 1434, 1360, 1202, 1152, 1070, 934, 882, 832 cm^{-1} ;



4,4'-((4*S*,5*S*,9*bS*,10*S*)-1,3,6,8-tetrakis(benzyloxy)-4*b*,5,9*b*,10-tetrahydroindeno[2,1-*a*]indene-5,10-diyl)bis(2,6-di-*tert*-butylphenol) (2.57): A solution of **2.56** (800 mg, 0.77 mmol, 1.00 equiv) in CH_2Cl_2 (77 mL, 0.01M) was cooled to $-78\text{ }^\circ\text{C}$ in a dry ice/acetone bath under inert atmosphere. To this, $\text{BF}_3 \cdot \text{OEt}_2$ (390 μL , 46.5% in diethyl ether, 2 equiv) was added dropwise, turning the reaction a brilliant magenta color. Temperature control is critical for the success of this reaction. The reaction was allowed to run for 40 minutes upon which the reaction was quenched with sat. aq. NaHCO_3 at temperature and allowed to warm to room temperature under vigorous stirring. The reaction was diluted with CH_2Cl_2 and transferred to a separatory funnel. The phases were separated and the aqueous layer was extracted with portions of CH_2Cl_2 . The organic layers were combined, washed with sat. aq. NaHCO_3 , brine, dried over sodium sulfate and concentrated *in vacuo*. The crude material was purified by column chromatography over SiO_2 (95:5 Hexanes/THF gradient to 90:10 Hexanes/THF) to afford **2.57** (340 mg, 0.33 mmol, 43% yield) as a white amorphous solid. The remaining material was identified as compound **2.52** (consult Section 3.11 for characterization data).

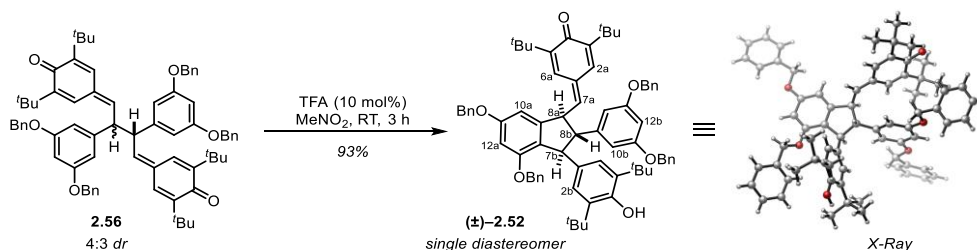
TLC (Hexanes/EtOAc, 95:5), R_f : 0.19 (UV *p*-anisaldehyde (pale orange));

^1H NMR (500 MHz, CDCl_3 , $25\text{ }^\circ\text{C}$) δ : 7.42 (d, $J = 7.5\text{ Hz}$, 4H), 7.35 (m, 5H), 7.29 (m, 2H), 7.22 (m, 5H), 7.03 (s, 4H), 7.01 (m, 4H), 6.73 (d, $J = 2.0\text{ Hz}$), 6.33 (d, $J = 2.0\text{ Hz}$), 5.04 (d, $J = 11.2\text{ Hz}$, 2H), 5.02 (d, $J = 11.2\text{ Hz}$, 2H), 5.01 (s, 2H, OH), 4.88 (d, $J = 11.7\text{ Hz}$, 2H), 4.82 (d, $J = 11.7\text{ Hz}$, 2H), 4.55 (s, 2H), 4.24 (s, 2H), 1.36 (s, 36H);

^{13}C NMR (175 MHz, CDCl_3 , $25\text{ }^\circ\text{C}$) δ : 160.2, 156.0, 152.1, 148.8, 137.3, 136.9, 135.6, 128.8, 128.6, 128.2, 127.9, 127.7, 127.1, 126.7, 124.3, 102.4, 99.5, 70.6, 69.6, 60.1, 55.4, 34.47 (2C), 30.6;

HRMS (ESI): m/z calculated for $\text{C}_{72}\text{H}_{79}\text{O}_6^+$ ($[\text{M}+\text{H}]^+$) 1039.5871, found 1039.5843;

FTIR (neat) cm^{-1} : 3636, 2954, 2908, 2870, 1598, 1433, 1316, 1135, 905, 727, 695.



4-(((1*R*,2*R*,3*R*)-4,6-bis(benzyloxy)-2-(3,5-bis(benzyloxy)phenyl)-3-(3,5-di-*tert*-butyl-4-hydroxyphenyl)-2,3-dihydro-1*H*-inden-1-yl)methylene)-2,6-di-*tert*-butylcyclohexa-2,5-dien-1-one (2.52): A suspension of starting bis-*para*-quinone methide **2.56** (4.00 g, 3.848 mmol, 1.00 equiv) was prepared in nitromethane (40.0 mL) under inert atmosphere. Trifluoroacetic acid (TFA, 29 μ L, 0.380 mmol, 0.10 equiv) was added in a single portion. While the starting material and product have identical R_F values, it is possible to monitor the reaction by TLC (aliquot must be dissolved in CH_2Cl_2 prior to spotting) by the use of *p*-anisaldehyde stain, the action of which turns **2.56** maroon and **2.52** yellow-orange. During the course of the reaction, the suspension will gradually change from the bright yellow color of the starting **2.56** to a very pale yellow. The reaction is allowed to stir at room temperature for ≥ 3 h, at which point **2.52** is collected from the reaction mixture by vacuum filtration, washing with nitromethane to afford a pale yellow free flowing solid (3.72 g, 3.59 mmol, 93% yield). Crystals of **2.52** suitable for X-ray diffraction studies were obtained by slow evaporation from $\text{MeOH}/\text{CH}_2\text{Cl}_2$.

TLC (Hex/EtOAc/DCM, 85:10:5), R_F : 0.35 (UV, *p*-anisaldehyde (yellow-orange));

^1H NMR (500 MHz, CDCl_3 , 25 $^\circ\text{C}$) δ : 7.47 – 7.28 (m, 15H, $-\text{OCH}_2\text{C}_6\text{H}_5$), 7.14 – 7.10 (m, 3H, $-\text{OCH}_2\text{C}_6\text{H}_5$), 7.02 (d, $J = 2.4$ Hz, 1H, $\text{C}_{6a}\text{-H}$), 6.89 (d, $J = 2.4$ Hz, 1H, $\text{C}_{2a}\text{-H}$), 6.80 (s, 2H, $\text{C}_{2/6b}\text{-H}$), 6.68 (d, $J = 2.0$ Hz, 1H, $-\text{OCH}_2\text{C}_6\text{H}_5$), 6.66 (d, $J = 2.0$ Hz, 1H, $-\text{OCH}_2\text{C}_6\text{H}_5$), 6.59 (d, $J = 2.0$ Hz, 1H, $\text{C}_{12a}\text{-H}$), 6.47 (t, $J = 2.2$ Hz, 1H, $\text{C}_{12b}\text{-H}$), 6.45 (d, $J = 2.0$ Hz, 1H, $\text{C}_{10a}\text{-H}$), 6.44 (d, $J = 9.5$ Hz, 1H, $\text{C}_{7a}\text{-H}$), 6.42 (d, $J = 2.2$ Hz, 2H, $\text{C}_{10b}\text{-H}$), 5.08 (d, $J = 11.2$ Hz, 1H, $-\text{OCH}_2\text{C}_6\text{H}_5$), 5.05 (d, $J = 11.2$ Hz, 1H, $-\text{OCH}_2\text{C}_6\text{H}_5$), 5.03 (s, 1H, $\text{C}_{4b}\text{-OH}$), 4.91 (d, $J = 11.2$ Hz, 1H, $-\text{OCH}_2\text{C}_6\text{H}_5$), 4.90 (d, $J = 11.2$ Hz, 2H, $-\text{OCH}_2\text{C}_6\text{H}_5$), 4.87 (d, $J = 11.2$ Hz, 2H, $-\text{OCH}_2\text{C}_6\text{H}_5$), 4.84 (d, $J = 11.2$ Hz, 1H, $-\text{OCH}_2\text{C}_6\text{H}_5$), 4.65 (dd, $J = 9.4, 9.4$ Hz, 1H, $\text{C}_{8a}\text{-H}$), 4.52 (d, $J = 8.5$ Hz, 1H, $\text{C}_{7b}\text{-H}$), 3.14 (dd, $J = 8.8, 8.8$ Hz, 1H, $\text{C}_{8b}\text{-H}$), 1.31 (s, 18H, $-\text{C}(\text{CH}_3)_3$), 1.28 (s, 9H, $-\text{C}(\text{CH}_3)_3$), 1.18 (s, 9H, $-\text{C}(\text{CH}_3)_3$);

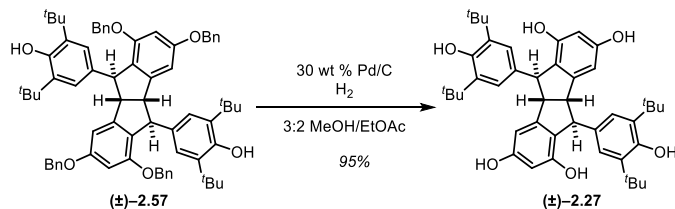
^{13}C NMR (175 MHz, CDCl_3 , 25 $^\circ\text{C}$) δ : 186.8 (C_{4a}), 160.7 (C_{11a}), 160.2 (C_{11b}), 156.2 (C_{13a}), 152.3 (C_{4b}), 148.8 (C_{3a}), 147.6 (C_{7a}), 147.2 (C_{5a}), 146.8 (C_{9a}), 144.0 (C_{9b}), 137.0 ($-\text{OCH}_2\text{C}_6\text{H}_5$), 136.9 ($-\text{OCH}_2\text{C}_6\text{H}_5$), 136.8 ($-\text{OCH}_2\text{C}_6\text{H}_5$), 135.5 (C_{3b}), 134.9 (C_{2a}), 134.2 (C_{1b}), 133.1 ($-\text{OCH}_2\text{C}_6\text{H}_5$), 128.82 ($-\text{OCH}_2\text{C}_6\text{H}_5$), 128.75 ($-\text{OCH}_2\text{C}_6\text{H}_5$), 128.4 ($-\text{OCH}_2\text{C}_6\text{H}_5$), 128.3 ($-\text{OCH}_2\text{C}_6\text{H}_5$), 128.2 ($-\text{OCH}_2\text{C}_6\text{H}_5$), 127.9 ($-\text{OCH}_2\text{C}_6\text{H}_5$), 127.8 ($-\text{OCH}_2\text{C}_6\text{H}_5$), 127.5 ($-\text{OCH}_2\text{C}_6\text{H}_5$), 127.1 (C_{6a}), 126.4 ($-\text{OCH}_2\text{C}_6\text{H}_5$), 124.8 (C_{14a}), 124.1 (C_{2b}), 107.6 (C_{10b}), 102.3 (C_{10a}), 100.5 (C_{12a}), 100.4 (C_{12b}), 70.7 ($-\text{OCH}_2\text{C}_6\text{H}_5$), 70.3 ($-\text{OCH}_2\text{C}_6\text{H}_5$), 69.6 ($-\text{OCH}_2\text{C}_6\text{H}_5$), 65.5 (C_{8b}), 57.0 (C_{7b}), 52.5 (C_{8a}), 35.4 ($-\text{C}(\text{CH}_3)_3$), 35.1 ($-\text{C}(\text{CH}_3)_3$), 34.5 ($-\text{C}(\text{CH}_3)_3$), 30.6 ($-\text{C}(\text{CH}_3)_3$), 29.66 ($-\text{C}(\text{CH}_3)_3$), 29.65 ($-\text{C}(\text{CH}_3)_3$);

HRMS (ESI):

m/z calculated for $\text{C}_{72}\text{H}_{79}\text{O}_6$ $[\text{M}+\text{H}]^+$: 1039.5871, found 1039.5849;

FTIR (neat) cm^{-1} : 3639 (w), 2956 (m), 1603 (s), 1559 (m), 1434 (s), 1378 (m), 1308 (m), 1157 (s), 1054 (s), 1029 (m);

X-Ray: For coordinates, see Appendix A.



(4*b*S,5*S*,9*b*S,10*S*)-5,10-bis(3,5-di-*tert*-butyl-4-hydroxyphenyl)-4*b*,5,9*b*,10-tetrahydroindeno[2,1-*a*]indene-1,3,6,8-tetraol (2.27**):** A heterogenous solution of **2.57** (250 mg, 0.24 mmol, 1 equiv) and 30 wt % Pd/C (770 mg) in 5 mL of 3:2 EtOAc/MeOH was sparged with hydrogen gas for 30 min at room temperature. The walls of the vessel were rinsed down with a minimum of MeOH and the septum fitted with a full balloon of H₂. The reaction was allowed to stir at room temperature overnight under an atmosphere of hydrogen. The reaction solution was filtered over a pad of celite and concentrated to provide **2.27** (155 mg, 0.23 mmol, 95% yield) as an amorphous white solid without need for further purification (NOTE: **2.27** is unstable to prolonged storage in air at room temperature, but could be stored indefinitely at -20 °C in a container sealed under N₂).

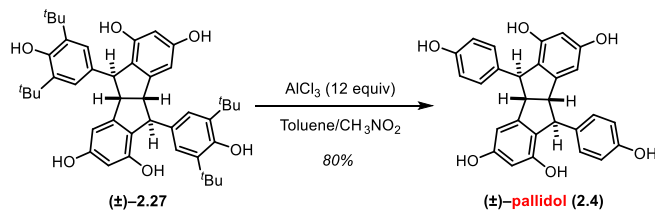
TLC (CH₂Cl₂/MeOH, 90:5), R_F: 0.09 (UV, *p*-anisaldehyde (red-purple));

¹H NMR (700 MHz, Acetone-*d*₆, 25 °C) δ: 7.09 (s, 4H), 6.64 (s, 2H), 6.21 (s, 2H), 4.61 (s, 2H), 3.94 (s, 2H), 1.38 (s, 36H);

¹³C NMR (175 MHz, Acetone-*d*₆, 25 °C) δ: 159.2, 155.3, 152.7, 150.3, 137.8, 124.5, 123.4, 103.4, 102.3, 60.7, 54.6, 35.1, 30.8;

HRMS (ESI): *m/z* calculated for C₄₄H₅₅O₆⁺ ([M+H]⁺) 679.3993, found 679.3989;

FTIR (neat) cm⁻¹: 3367, 2956, 1600, 1458, 1435, 1254, 1233, 1126, 1042.



Pallidol (2.4): The following procedure was adapted from Hou et. al.⁹ To a solution of **2.27** (150 mg, 0.22 mmol, 1 equiv) in anhydrous toluene (10.8 mL, 0.02 M) at room temperature under inert atmosphere, AlCl₃ (354 mg, 0.28 mmol, 12 equiv) was added as a solution in CH₃NO₂ (1.2 mL, 2.25 M). The reaction was immediately heated to 60 °C for 30 min upon which the reaction was removed from the heat source and transferred to a separatory funnel containing 1:1 ice/1 N HCl. The reaction flask was rinsed with EtOAc several times and the contents transferred to the separatory funnel. The phases were separated and the aqueous layer extracted with additional ethyl acetate (2x). The organic layers were combined, washed with sat. aq. NaHCO₃, brine, dried over Na₂SO₄, and concentrated *in vacuo*. The crude material was purified by flash chromatography over SiO₂ (95:5 CH₂Cl₂/MeOH gradient to 90:10 CH₂Cl₂/MeOH) to afford pallidol (**2.4**) (80 mg, 0.17 mmol, 80%) as white amorphous solid.

TLC (CH₂Cl₂/MeOH/Acetone, 85:10:5), R_f: 0.21 (UV, *p*-anisaldehyde (red));

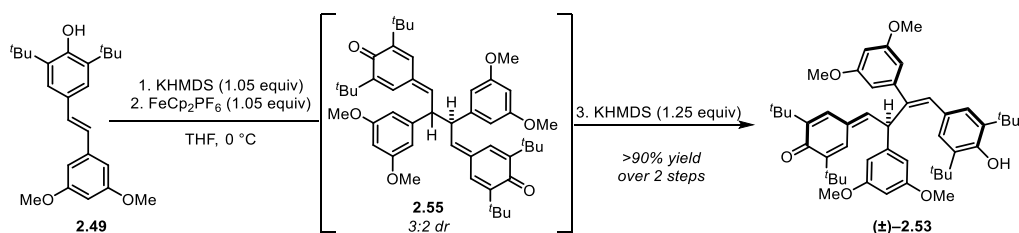
¹H NMR (500 MHz, Acetone-*d*₆, 25 °C) δ: 8.02 (s, 2H, OH), 8.00 (s, 2H, OH), 7.77 (s, 2H, OH), 6.98 (d, *J* = 8.5 Hz, 4H), 6.70 (d, *J* = 8.5 Hz, 4H), 6.62 (d, *J* = 2.0 Hz, 2H), 6.19 (d, *J* = 2.2 Hz, 2H) 4.57 (s, 2H), 3.81 (s, 2H);

¹³C NMR (175 MHz, Acetone-*d*₆, 25 °C) δ: 159.4, 156.4, 155.4, 150.4, 137.8, 129.1, 123.3, 115.9, 103.4, 102.6, 60.6, 54.0;

HRMS (ESI): *m/z* calculated for C₂₈H₂₃O₆⁺ ([M+H]⁺) 455.1450, found 455.1457;

FTIR (neat) cm⁻¹: 3296, 1598, 1508, 1464, 1334, 1238, 1128, 1147, 995, 831.

⁹ W. Li, H. Li, Y. Li, Z. Hou, *Angew. Chem. Int. Ed.* **2006**, *45*, 7609–7611; *Angew. Chem.* **2006**, *118*, 7771–7773.



(E)-2,6-di-tert-butyl-4-(4-(3,5-di-tert-butyl-4-hydroxyphenyl)-2,3-bis(3,5-dimethoxyphenyl)but-3-en-1-ylidene)cyclohexa-2,5-dien-1-one (2.53):

In a round bottom flask equipped with a septum and magnetic stir bar, a solution of **2.49** (1.88 g, 2.60 mmol, 1.00 equiv) in anhydrous THF (75 mL, 0.02 M) was cooled to 0 °C in an ice bath under inert atmosphere. To this, KHMDS (2.73 mL, 1.0 M soln. in THF, 1.05 equiv) was added slowly. The solution was allowed to stir at temperature for 10 minutes, upon which the septum was removed and ferrocenium hexafluorophosphate (932 mg, 97% purity, 2.73 mmol, 1.05 equiv) was added in two 466 mg portions, separated by 15 minutes. After the reaction was deemed complete by TLC (ca. 30 min), KHMDS (3.25 mL, 1.0 M soln. in THF, 1.25 equiv), was added, turning the solution from yellow-orange to opaque. After 15 min, the reaction mixture was quenched by the addition of sat. aq. NH₄Cl, turning the organic phase bright red. The reaction was diluted with EtOAc and transferred to a separatory funnel containing DI H₂O. The phases were separated and the aqueous layer extracted with additional EtOAc (2x). The organic layers were combined and washed with brine, dried over Na₂SO₄, and concentrated *in vacuo*. The crude residue was taken up in CH₂Cl₂ and dried on to Celite and the solvent removed completely under reduced pressure. The crude material was purified by flash chromatography over a short plug of SiO₂ (100:0 Hexanes/EtOAc [to elute ferrocene] then 100% CH₂Cl₂) to afford **2.53** (1.88 g, 1.30 mmol, crude), which was taken directly on to the cyclization. For characterization, the material can instead be eluted with a gradient 95:2.5:2.5 to 90:5:5 Hexanes/EtOAc/CH₂Cl₂ mobile phase.

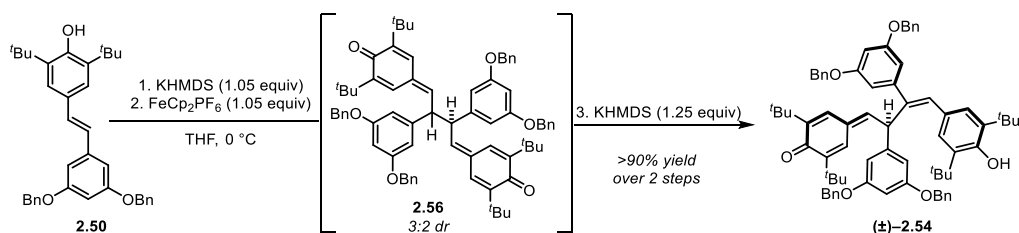
TLC (Hexanes/EtOAc, 95:5), *R_F*: 0.17 (UV, *p*-anisaldehyde (pale red));

¹H NMR (500 MHz, CDCl₃, 25 °C) δ: 6.92 (s, 2H), 6.73 (d, *J* = 2.9 Hz, 1H), 6.52 (d, *J* = 2.2 Hz, 2H), 6.39 (d, *J* = 2.2 Hz, 2H), 6.31 (t, *J* = 2.2 Hz, 1H), 6.24 (d, *J* = 2.7 Hz, 1H), 6.23 (t, *J* = 2.2 Hz, 1H), 5.80 (d, *J* = 1.7 Hz, 1H), 5.00 (s, 1H), 4.97 (dd, *J* = 9.6, 1.8 Hz, 1H), 3.7 (s, 6H), 3.68 (s, 6H), 1.37 (s, 18H), 1.30 (s, 9H), 0.91 (s, 9H);

¹³C NMR (175 MHz, CDCl₃, 25 °C) δ: 186.6, 160.9, 160.7, 152.8, 147.6, 146.6, 146.22, 146.15, 144.5, 141.6, 137.5, 135.4, 130.8, 127.8, 124.0, 106.9, 105.0, 100.2, 98.2, 65.3, 56.6, 55.5, 55.4, 54.6, 35.0, 34.8, 34.5, 30.5, 30.0, 29.3;

HRMS (ESI): *m/z* calculated for C₄₈H₆₃O₆⁺ ([M+H]⁺) 735.4619, found 735.4616;

FTIR (neat) cm⁻¹: 3630, 2956, 2359, 1653, 1590, 1457, 1356, 1204, 1153, 1065, 833, 738.



(E)-4-(2,3-bis(3,5-bis(benzyloxy)phenyl)-4-(3,5-di-tert-butyl-4-hydroxyphenyl)but-3-en-1-ylidene)-2,6-di-tert-butylcyclohexa-2,5-dien-1-one (2.54): In a round bottom flask equipped with a septum and magnetic stir bar, a solution of **2.50** (1.00 g, 1.92 mmol, 1.00 equiv) in anhydrous THF (75 mL, 0.02 M) was cooled to 0 °C in an ice bath under inert atmosphere. To this, KHMDS (1 M solution in THF, 1.61 mL, 1.05 equiv) was added slowly. The solution was allowed to stir at temperature for 10 minutes, upon which the septum was removed and ferrocenium hexafluorophosphate (655 mg, 97% purity, 2.04 mmol, 1.05 equiv) was added in two 328 mg portions, separated by 15 minutes. After the reaction was complete by TLC (ca. 30 min), KHMDS (1.92 mL, 1.0 M soln. in THF, 1.25 equiv), was added, turning the solution from yellow-orange to opaque. After 15 min, the reaction mixture was quenched by the addition of sat. aq. NH₄Cl. The reaction was diluted with EtOAc and transferred to a separatory funnel containing DI H₂O. The phases were separated and the aqueous layer extracted with EtOAc (2x). The organic layers were combined and washed with brine, dried over Na₂SO₄, and concentrated *in vacuo*. The crude residue was taken up in CH₂Cl₂ and dried on to Celite and the solvent removed under reduced pressure. Purification by flash chromatography over a short plug of SiO₂ (100% Hexanes [to elute ferrocene], then 100% CH₂Cl₂) afforded **2.54** (1.00 g, 0.96 mmol, crude), which was taken directly on to the cyclization. For characterization, the material can instead be eluted with a gradient 95:2.5:2.5 to 90:5:5 Hexanes/EtOAc/CH₂Cl₂ mobile phase.

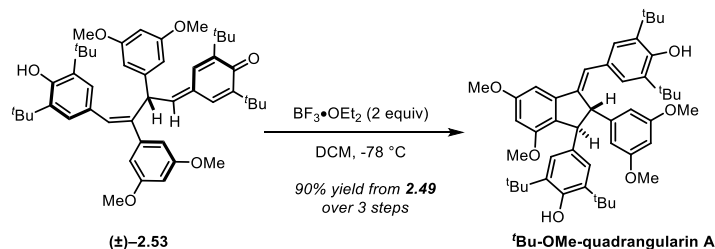
TLC (Hexanes/EtOAc/CH₂Cl₂, 85:10:5), R_f: 0.25 (UV, *p*-anisaldehyde (pale red));

¹H NMR (500 MHz, CDCl₃, 25 °C) δ: 7.39 – 7.29 (m, 20H), 6.91 (s, 2H), 6.71 (d, *J* = 2.7 Hz, 1H), 6.64 (d, *J* = 2.2 Hz, 2H), 6.52 (d, *J* = 2.2 Hz, 2H), 6.50 (t, *J* = 2.2 Hz, 1H), 6.42 (t, *J* = 2.2 Hz, 1H), 6.23 (d, *J* = 2.7 Hz, 1H), 5.79 (d, *J* = 2.0 Hz, 1H), 5.02 (s, 1H), 4.95 (d, *J* = 11.5 Hz, 2H), 4.94 (d, *J* = 11.5 Hz, 2H), 4.89 (d, *J* = 11.5 Hz, 2H), 4.88 (d, *J* = 11.5 Hz, 2H), 3.66 (d, *J* = 9.8 Hz, 1H), 1.38 (s, 18 H), 1.31 (s, 9H), 0.92 (s, 9H);

¹³C NMR (175 MHz, CDCl₃, 25 °C) δ: 186.6, 160.2, 159.9, 152.9, 147.6, 146.5, 146.2, 144.4, 141.6, 137.5, 137.0, 136.9, 135.4, 130.9, 128.80, 128.78, 128.76, 128.2, 127.9, 127.82, 127.76, 127.7, 124.0, 108.2, 106.3, 102.0, 100.3, 70.32, 70.27, 65.2, 56.6, 54.7, 35.0, 34.8, 34.5, 30.5, 30.0, 29.3;

HRMS (ESI): *m/z* calculated for C₇₂H₇₉O₆⁺ ([M+H]⁺) 1039.5832, found 1039.5838;

FTIR (neat) cm⁻¹: 3641, 2952, 1654, 1590, 1435, 1373, 1264, 1151, 1054, 1028, 834, 733, 696.



2,6-di-tert-butyl-4-((1S,2S)-3-((E)-3,5-di-tert-butyl-4-hydroxybenzylidene)-2-(3,5-dimethoxyphenyl)-5,7-dimethoxy-2,3-dihydro-1H-inden-1-yl)phenol:

A solution of crude **2.53** (260 mg, 0.35 mmol, 1.00 equiv) in anhydrous CH_2Cl_2 (35 mL, 0.01 M) was cooled to $-78\text{ }^\circ\text{C}$ in a dry ice/acetone bath. To this, $\text{BF}_3 \cdot \text{OEt}_2$ (175 μL , 46.5% in diethyl ether, 2 equiv) was added dropwise, turning the solution into a deep ruby red color. After 5 min, the reaction was quenched with sat. aq. NaHCO_3 at $-78\text{ }^\circ\text{C}$ and allowed to warm to room temperature with vigorous stirring. The reaction mixture was diluted with CH_2Cl_2 and transferred to a separatory funnel containing additional sat. aq. NaHCO_3 . The phases were separated and the aqueous layer was extracted with additional CH_2Cl_2 (2x). The organic layers were combined, washed with brine, dried over sodium sulfate and concentrated *in vacuo*. The crude residue was purified by flash chromatography using a 90:5:5 Hexanes/EtOAc/ CH_2Cl_2 mobile phase to afford the quadrangularin derivative (235 mg, 0.32 mmol, 90% yield from **2.49** over 3 steps) as a pale yellow amorphous solid.

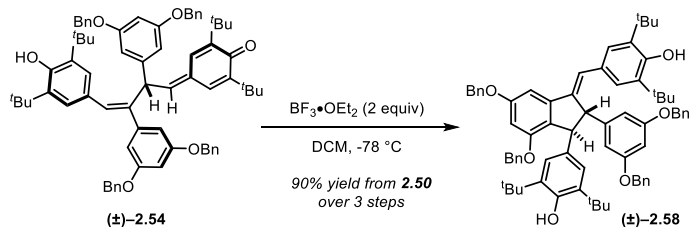
TLC (Hexanes/EtOAc, 90:10): R_f : 0.33 (UV);

^1H NMR (500 MHz, CDCl_3 , $25\text{ }^\circ\text{C}$) δ : 7.13 (s, 1H), 7.08 (s, 2H), 7.06 (s, 2H), 6.83 (d, $J = 1.7\text{ Hz}$, 1H), 6.50 (d, $J = 2.2\text{ Hz}$, 2H), 6.29 (d, $J = 2.0\text{ Hz}$, 2H), 5.18 (s, 1H), 4.99 (s, 1H), 4.49 (s, 1H), 4.32 (s, 1H), 3.92 (s, 3H), 3.73 (s, 6H), 3.65 (s, 3H), 1.35 (s, 18H), 1.31 (s, 18H);

^{13}C NMR (175 MHz, CDCl_3 , $25\text{ }^\circ\text{C}$) δ : 161.3, 161.0, 160.8, 157.5, 153.1, 152.0, 147.9, 145.1, 142.5, 136.3, 135.8, 135.3, 128.9, 127.2, 126.3, 125.9, 124.1, 123.9, 106.0, 104.9, 98.9, 98.3, 95.5, 58.8, 57.0, 55.8, 55.4, 55.3, 34.50, 34.45, 30.5, 30.4;

HRMS (ESI): m/z calculated for $\text{C}_{48}\text{H}_{63}\text{O}_6^+$ ($[\text{M}+\text{H}]^+$) 735.4625, found 735.4648;

FTIR (neat) cm^{-1} : 3633, 2965, 1593, 1435, 13783, 1304, 1234, 1153, 1050, 1028, 736.



4-((1S,2S)-5,7-bis(benzyloxy)-2-(3,5-bis(benzyloxy)phenyl)-3-((E)-3,5-di-tert-butyl-4-hydroxybenzylidene)-2,3-dihydro-1H-inden-1-yl)-2,6-di-tert-butylphenol (2.58**):** A solution of crude **2.54** (1.00 g, 0.96 mmol, 1.00 equiv) in anhydrous CH_2Cl_2 (96 mL, 0.01 M) was cooled to -78°C in a dry ice/acetone bath under inert atmosphere. To this, $\text{BF}_3 \cdot \text{OEt}_2$ (511 μL , 46.5% in diethyl ether 2 equiv) was added dropwise, turning the solution into a deep ruby red color. After 5 min, the reaction was quenched with sat. aq. NaHCO_3 at -78°C and allowed to warm to room temperature with vigorous stirring. The reaction mixture was diluted with CH_2Cl_2 and transferred to a separatory funnel containing additional sat. aq. NaHCO_3 . The phases were separated and the aqueous layer was extracted with additional CH_2Cl_2 (2x). The organic layers were combined, washed with brine, dried over sodium sulfate and concentrated *in vacuo*. The crude residue was purified by flash chromatography using a 90:5:5 Hexanes/EtOAc/ CH_2Cl_2 mobile phase to afford **2.58** (898 mg, 0.86 mmol, 90% yield over 3 steps from **2.50**) as a pale yellow amorphous solid.

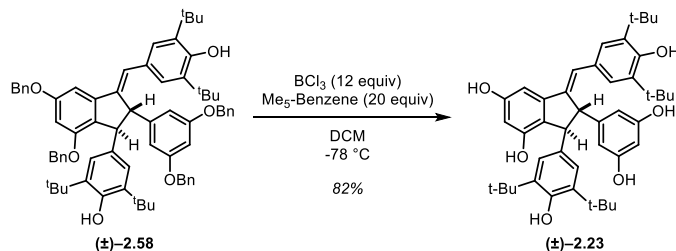
TLC (Hexanes/EtOAc/ CH_2Cl_2 , 85:10:5): R_f : 0.27 (UV);

^1H NMR (500 MHz, CDCl_3 , 25°C) δ : 7.50 (m, 2H), 7.41 – 7.28 (m, 13H, benzyl group overlap), 7.21 (m, 3H), 7.14 (d, $J = 0.7$ Hz, 1H), 7.04 (s, 2H), 7.03-7.01 (m, 2H, benzyl group H's), 7.00 (s, 2H), 6.95 (d, $J = 1.7$ Hz, 1H), 6.59 (d, $J = 2.2$ Hz, 2H), 6.42 (t, $J = 2.2$ Hz, 1H), 6.41 (d, $J = 1.7$ Hz, 1H), 5.30 (s, 2H), 5.16 (s, 1H, OH), 5.15 (s, 2H), 4.99 (s, 1H, OH), 4.95 (d, $J = 12.2$ Hz, 2H), 4.93 (d, $J = 12.2$ Hz, 2H), 4.90 (d, $J = 12.0$ Hz, 1H), 4.84 (d, $J = 12.0$ Hz, 1H), 4.40 (s, 1H), 4.32 (s, 1H), 1.31 (s, 18H), 1.29 (s, 18H);

^{13}C NMR (175 MHz, CDCl_3 , 25°C) δ : 160.5, 160.2, 156.4, 153.2, 152.1, 148.1, 145.3, 142.5, 137.3, 137.20, 137.16, 136.6, 135.7, 135.5, 128.9, 128.80, 128.77, 128.7, 128.6, 128.5, 128.21, 128.18, 128.1, 128.0, 127.9, 127.8, 127.7, 127.2, 127.1, 126.0, 124.2, 124.1, 107.1, 100.8, 100.1, 97.0, 70.6, 70.2, 69.6, 58.9, 57.6, 34.5, 34.4, 30.6, 30.5, 30.4;

HRMS (ESI): m/z calculated for $\text{C}_{72}\text{H}_{79}\text{O}_6^+$ ($[\text{M}+\text{H}]^+$) 1039.5871, found 1039.5829;

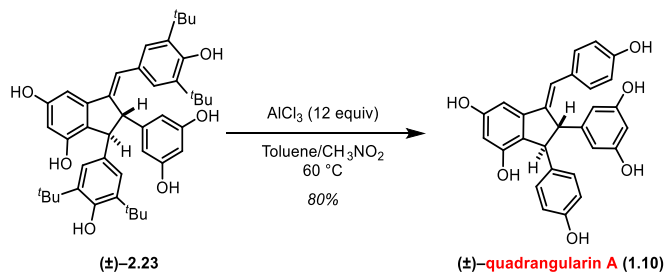
FTIR (neat) cm^{-1} : 3632, 2953, 1592, 1451, 1434, 1372, 1304, 1154, 1048, 774, 696.



(2S,3S)-1-((E)-3,5-di-tert-butyl-4-hydroxybenzylidene)-3-(3,5-di-tert-butyl-4-hydroxyphenyl)-2-(3,5-dihydroxyphenyl)-2,3-dihydro-1H-indene-4,6-diol (2.23):

A solution of **2.58** (460 mg, 0.44 mmol, 1.00 equiv) and pentamethylbenzene (1.30 g, 8.8 mmol, 20 equiv) in anhydrous CH_2Cl_2 (22 mL, 0.02 M) was cooled to $-78\text{ }^\circ\text{C}$ in a dry ice/acetone bath under inert atmosphere. To this, BCl_3 (5.3 mL, 1.0 M soln. in CH_2Cl_2 , 12 equiv) was added dropwise turning the yellow solution a brilliant magenta color. Reaction was maintained at $-78\text{ }^\circ\text{C}$ until deemed complete by TLC (ca. 2h). At this point, the reaction was quenched with a 4:1 THF/sat. aq. NaHCO_3 mixture at $-78\text{ }^\circ\text{C}$ and allowed to warm to room temperature while stirring vigorously. Upon thawing, the solution returned to a yellow color. The reaction was diluted with ethyl acetate (50 mL) and transferred to a separatory funnel containing additional sat. aq. NaHCO_3 . The phases were separated and the aqueous layer extracted with additional EtOAc (2x). The organic layers were combined and washed with brine, dried over Na_2SO_4 , and concentrated *in vacuo*. The crude residue was purified by flash chromatography over SiO_2 (98:2 $\text{CH}_2\text{Cl}_2/\text{MeOH}$ gradient to 90:10 $\text{CH}_2\text{Cl}_2/\text{MeOH}$) to afford **2.23** (245 mg, 0.36 mmol, 82% yield) as a white amorphous solid (NOTE: **2.23** is unstable to prolonged storage in air at room temperature, but could be stored indefinitely at $-20\text{ }^\circ\text{C}$ in a container sealed under N_2).

TLC ($\text{CH}_2\text{Cl}_2/\text{MeOH}$, 95:5): R_f :	0.09 (UV, <i>p</i> -anisaldehyde (red));
^1H NMR (700 MHz, Acetone- d_6 , $25\text{ }^\circ\text{C}$) δ :	8.13 (br. s., 4H, OH), 7.86 (br. s., 2H, OH), 7.15 (s, 2H), 7.12 (s, 1H), 7.05 (s, 2H), 6.80 (s, 1H), 6.38 (s, 2H), 6.29 (s, 1H), 6.20 (s, 1H), 5.99 (s, 1H), 5.73 (s, 1H), 4.33 (s, 1H), 4.26 (s, 1H), 1.34 (s, 18H), 1.31 (s, 18H);
^{13}C NMR (175 MHz, Acetone- d_6 , $25\text{ }^\circ\text{C}$) δ :	159.6, 159.5, 155.9, 154.0, 152.9, 148.8, 147.2, 143.0, 137.9, 137.8, 137.6, 130.0, 126.6, 124.4, 107.0, 103.6, 101.5, 98.8, 60.5, 58.0, 35.2, 30.8, 30.7;
HRMS (ESI):	m/z calculated for $\text{C}_{44}\text{H}_{55}\text{O}_6^+$ ($[\text{M}+\text{H}]^+$) 679.3993, found 679.3989;
FTIR (neat) cm^{-1} :	3376, 2957, 1599, 1547, 1467, 1434, 1341, 1237, 1157, 1006, 838.



Quadrangularin A (1.10): The following procedure was adapted from Hou et. al.¹⁰ To a solution of **2.23** (80.0 mg, 0.12 mmol, 1.00 equiv) in anhydrous toluene (5.4 mL, 0.022 M) at room temperature under inert atmosphere, AlCl_3 (190 mg, 1.44 mmol, 12.0 equiv) was added as a solution in CH_3NO_2 (600 μL , 2.33 M). The reaction was immediately heated to 60 °C for 30 min upon which the reaction was removed from the heat source and transferred to a separatory funnel containing 1:1 ice/1 N HCl. The reaction flask was rinsed with EtOAc several times and the contents transferred to the separatory funnel. The phases were separated and the aqueous layer extracted with additional ethyl acetate (2x). The organic layers were combined, washed with brine, dried over Na_2SO_4 , and concentrated *in vacuo*. The crude material was purified by flash chromatography over SiO_2 (95:5 $\text{CH}_2\text{Cl}_2/\text{MeOH}$ gradient to 90:10 $\text{CH}_2\text{Cl}_2/\text{MeOH}$) to afford quadrangularin A (**1.10**) (43 mg, 0.095 mmol 80%) as a tan amorphous solid.

TLC ($\text{CH}_2\text{Cl}_2/\text{MeOH}$, 95:5): R_f : 0.09 (UV, *p*-anisaldehyde (red));

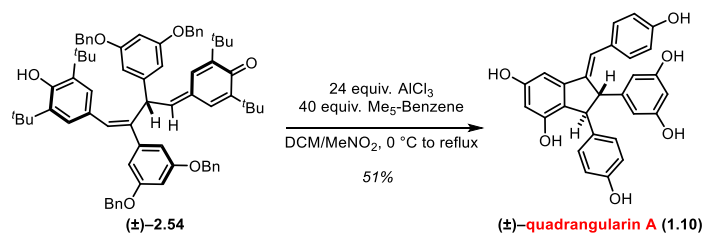
^1H NMR (500 MHz, Acetone- d_6 , 25 °C) δ : 8.16 (s, 6H), 7.21 (d, $J = 8.5$ Hz, 2H), 7.05 (d, $J = 1.0$ Hz, 1H), 6.92 (d, $J = 8.5$ Hz), 6.79 (d, $J = 2.0$ Hz, 1H), 6.68 (d, $J = 5.4$ Hz, 2H), 6.67 (d, $J = 5.4$ Hz, 2H), 6.31 (d, $J = 2.2$ Hz, 2H), 6.30 (d, $J = 2.0$ Hz, 1H), 6.19 (t, $J = 2.2 \times 2$ Hz, 1H), 4.27 (s, 1H), 4.14 (s, 1H);

^{13}C NMR (175 MHz, Acetone- d_6 , 25 °C) δ : 159.7, 159.7, 157.4, 156.6, 155.9, 149.1, 147.1, 142.7, 137.8, 131.1, 129.8, 128.8, 124.6, 123.0, 116.0, 115.9, 106.3, 103.7, 101.6, 98.4, 60.7, 57.7;

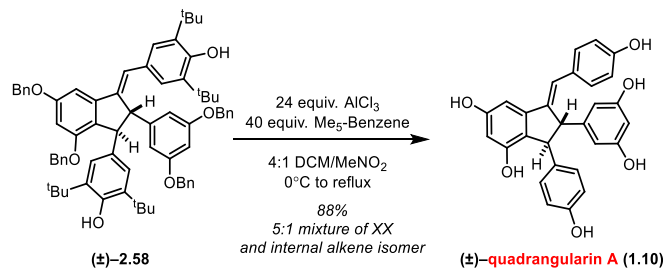
HRMS (ESI): m/z calculated for $\text{C}_{28}\text{H}_{23}\text{O}_6^+$ ($[\text{M}+\text{H}]^+$) 455.1489, found 455.1485;

FTIR (neat) cm^{-1} : 3245, 1596, 1509, 1446, 1334, 1233, 1172, 1147, 1005, 831.

¹⁰ W. Li, H. Li, Y. Li, Z. Hou, *Angew. Chem. Int. Ed.* **2006**, *45*, 7609–7611; *Angew. Chem.* **2006**, *118*, 7771–7773.



Friedel-Crafts Cyclization – Global Deprotection of 2.54 with AlCl₃: A solution of **1.10** (370 mg, 0.34 mmol, 1.00 equiv) and pentamethylbenzene (2.1 g, 14.1 mmol, 40 equiv) in anhydrous CH₂Cl₂ (57 mL, 0.005 M) was cooled to 0 °C in an ice bath under inert atmosphere. To this, AlCl₃ (1.14 g, 8.6 mmol, 25 equiv) was added slowly as a solution in CH₃NO₂ (14 mL, 0.6 M) via syringe turning the clear yellow solution a deep red color. Upon addition, the reaction flask was fitted with a reflux condenser and heated to 60 °C, allowing the reaction to stir at this temperature for 15 minutes. The reaction was removed from the heat and the contents transferred to a separatory funnel containing 1:1 ice/1N HCl. The reaction flask was rinsed with EtOAc several times and the contents transferred to the separatory funnel. The phases were separated and the aqueous layer extracted with additional ethyl acetate (2x). The organic layers were combined, washed with sat. aq. NaHCO₃, brine, dried over Na₂SO₄, and concentrated *in vacuo*. The dry crude material was dissolved in a minimal amount of diethyl ether using sonication. Hexanes was then added dropwise to the sonicating material to precipitate out crude quadrangularin A as a brown amorphous solid, which was collected by vacuum filtration. This crude material (nearly pure by NMR), was purified via flash chromatography (95:2.5:2.5 gradient to 90:5:5 Chloroform/Acetone/MeOH) to yield quadrangularin A (**1.10**) (82 mg, 0.18 mmol, 51%) as a tan amorphous solid (consult page XX for characterization data).



Global Deprotection of 2.58 with AlCl₃: A solution of **1.10** (30 mg, 0.03 mmol, 1.00 equiv) and pentamethylbenzene (170 mg, 1.14 mmol, 40 equiv.) in CH₂Cl₂ (4.5 mL, 0.005 M) was cooled to 0 °C in an ice bath under inert atmosphere. To this, AlCl₃ (92 mg, 0.70 mmol, 24 equiv) was added as a solution in CH₃NO₂ (1.5 mL, 0.48 M) via syringe, turning the clear yellow solution a deep red color. Upon addition, the reaction flask was fitted with a reflux condenser and heated to 60 °C, allowing the reaction to stir at this temperature for 1 hour. The reaction was cooled down to 0 °C, quenched with sat. aq. NaHCO₃, and stirred until the solution turned from red to clear yellow. The reaction was transferred to a separatory funnel and washed with ice cold 1N HCl (CO₂ evolution). The organic layer was removed and the aqueous layer was extracted with EtOAc (2x). The organic layers were combined, washed with sat. aq. NaHCO₃, brine, dried over Na₂SO₄, and concentrated *in vacuo*. The crude residue was purified by flash chromatography over SiO₂ (17:2:1 Chloroform/MeOH/Acetone) to yield quadrangularin A (**1.10**) (11.5 mg, 88%, 5:1 ratio of quadrangularin A and its internal alkene isomer)¹¹ as a tan amorphous solid (consult page XX for characterization data).

¹¹ Observed NMR resonances for internal alkene isomer consistent with those reported: Klotter, F.; Studer, A. *Angew. Chem. Int. Ed.* **2014**, *53* (9), 2473–2476; *Angew. Chem.* **2014**, *126*, 2505 – 2509.

SYSTEMATIC EVALUATION OF ANTIOXIDANT ACTIVITY OF RESVERATROL, QUADRANGULARIN A, PALLIDOL, AND DERIVATIVES

Materials. Methyl linoleate, egg phosphatidylcholine, Triton™ X-100 and penicillin-streptomycin were purchased from Sigma-Aldrich. C11-BODIPY^{581/591} (4,4-difluoro-5-(4-phenyl-1,3-butadienyl)-4-bora-3a,4a-diaza-s-indacene-3-undecanoic acid), MTT (3-(4,5-dimethylthiazol-2-yl)-2,5-diphenyltetrazolium bromide), RPMI-1640 media with/without phenol red, fetal bovine serum (FBS), Hank's balanced salt solution (HBSS) were purchased from Invitrogen (life technologies). Phosphate buffered saline (PBS), 2, 2'-azobis(4-methoxy-2,4-dimethylvaleronitrile) (MeOAMVN), 2,2'-azobis-(2-amidinopropane) monohydrochloride (AAPH) and all other chemicals were used as received. The H₂B-PMHC fluorescent probe was prepared according to the previous literature.^[1]

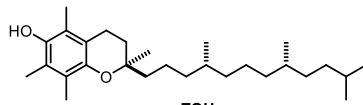
Radical Clock Experiments. Methyl linoleate (MeLn) was chromatographed on silica gel (5% EtOAc/ hexanes) prior to use. Stock solutions (0.02 M) of the tested compounds and methyl linoleate (1.0 M) were prepared in chlorobenzene separately. A stock solution of MeOAMVN (0.05 M) was prepared in benzene. Samples were prepared in 1.0 mL autosampler vials with a total reaction volume of 100 μ L. The solutions were added in the following order to avoid premature oxidation: inhibitor (final concentration is 0.002 - 0.01 M), amount of chlorobenzene required to dilute samples to 100 μ L, methyl linoleate (0.1 M), and MeOAMVN (0.01 M). The sealed samples were then incubated at 37 °C for 90 minutes. Stock solutions of BHT (1.0 M in hexanes) and PPh₃ (1.0 M in chlorobenzene) were prepared separately. Following the oxidation, the BHT solution (0.05 M) and then PPh₃ solution (0.05 M), were added to the samples and then diluted to 1 mL with HPLC grade hexanes, and analyzed by HPLC (0.5 % iPrOH/hexanes, 1.1 mL/min for 30 min, Sun-Fire Silica 5 mm 4.6 \times 250 mm column, detection at 234 nm). The ratio of products (*E,Z:E,E*) was plotted versus the concentration of the tested compound to determine k_{inh} according to the reported procedure.^[2]

Liposome Preparation and Oxidation. Liposome preparation and oxidations were performed following the procedure in one of our recent manuscripts.^[3] To individual 21.4 μ L aliquots of the 20 mM liposome solution were added increasing amounts (1.25, 2.5, 5, 7.5, 10 and 15 μ L, respectively) of a solution of the test antioxidant in DMSO (857.5 μ M) and 2.5 μ L of a solution of H₂B-PMHC in acetonitrile (25.8 μ M). Each resultant solution was then diluted to 400 μ L with 10 mM phosphate buffered-saline (PBS) solution containing 150 mM NaCl (pH 7.4), from which 280 μ L of each was loaded into a well of a 96-well microplate. The solution was equilibrated to 37 °C for 5 min, after which 20 μ L of a solution of azo compound (40.5 mM in 2,2'-azobis-(2-amidinopropane)monohydrochloride, AAPH, in PBS or 10.1 mM in 2,2'-azobis-(4-methoxy-2,4-dimethylvaleronitrile, MeOAMVN, in acetonitrile) was added to each well. The fluorescence was then monitored for 10 h at 60 s time intervals (λ_{ex} = 485 nm; λ_{em} = 520 nm). The final solutions in each well were 1 mM in lipids, 0.15 μ M in H₂B-PMHC, 2.7 mM in AAPH or 0.68 mM in MeOAMVN and either 2.5 μ M, 5.0 μ M, 10 μ M, 15 μ M, 20 μ M, 30 μ M in antioxidant. The rates of peroxy radical trapping by the test compounds relative to the probe H₂B-PMHC were determined by re-plotting the data as $-\ln\{(I_{\infty}-I_t)/(I_{\infty}-I_0)\}$ versus $-\ln(1-t/\tau)$ and determining the slope from the initial portion of the graph, which corresponds to $k_{inh}^{H_2B-PMHC}/k_{inh}^{unknown}$ as described in references [1] and [3].

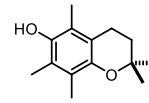
Cellular Lipid Peroxidation. TF1a cells were cultured in RPMI-1640 media (with phenol red) with 10 % FBS and 1 % penicillin-streptomycin. The cells (5×10^5 cells in 1 mL media) were treated with each antioxidant at final concentrations from 1.5 μ M to 50 μ M and incubated at 37 °C for 22 hours in phenol red-free RPMI-1640 media with 10 % FBS in humidified 5 % CO₂ atmosphere in 12-well plates. Cells were then treated with 1 μ M C11-BODIPY^{581/591} and incubated at 37 °C in the dark for 30 minutes after which oxidative stress was induced with diethylmaleate (9 mM) for 2 hours. Treated cells were then collected by centrifugation at 250 \times g for 4 minutes and washed with PBS. Cells were resuspended in PBS and analyzed by flow cytometry at a final concentration of 5×10^5 cells/ml (λ_{ex} = 488 nm; λ_{em} = 525 \pm 25 nm). Cells not treated with DEM were used as negative control. Cells not treated with antioxidants were used as positive control.

Cell Viability. TF1a cells (5×10^4 cells in 250 μL media) were treated with each antioxidant in DMSO at final concentrations ranging from 0.5 μM to 750 μM (final DMSO concentration was to not exceed 1% v/v) and incubated at 37°C for 22 hours in phenol red-free RPMI-1640 media with 10% FBS in a humidified 5 % CO_2 atmosphere on a 96-well plate. Each well was then treated with 50 μL of MTT (12.1 μM in HBSS) for 4h. The treated cells were collected by centrifugation at 250 \times g for 5 minutes and the solution was aspirated. The resultant purple crystals were dissolved with a 250 μL 1:4 water:DMSO (v/v) solution followed by 30 minutes incubation at room temperature. Absorbance ($\lambda = 570 \text{ nm}$) was measured by microplate reader. Results were compared to a negative control (1 % DMSO) and a positive control (1 % TritonTM X-100).

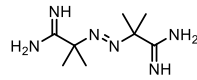
COMPOUND STRUCTURES FOR ANTIOXIDANT STUDIES



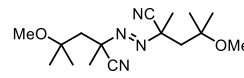
α -TOH
 α -Tocopherol



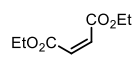
PMHC
2,2,5,7,8-pentamethyl-6-hydroxy-chromane



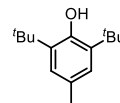
AAPH
2,2'-azobis-(2-amidinopropane)-dihydrochloride



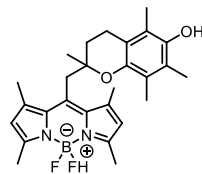
MeOAMVN
2,2'-azobis-(4-methoxy-2,4-dimethylvaleronitrile)



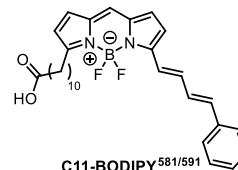
DEM
Diethylmaleate



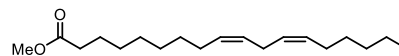
BHT
2,6-di-*tert*-butyl-4-hydroxytoluene



H₂B-PMHC
BODIPY-2,2,5,7,8-pentamethyl-6-hydroxy-chromane



C11-BODIPY^{581/591}



Methyl Lineolate

RADICAL CLOCK EXPERIMENTS

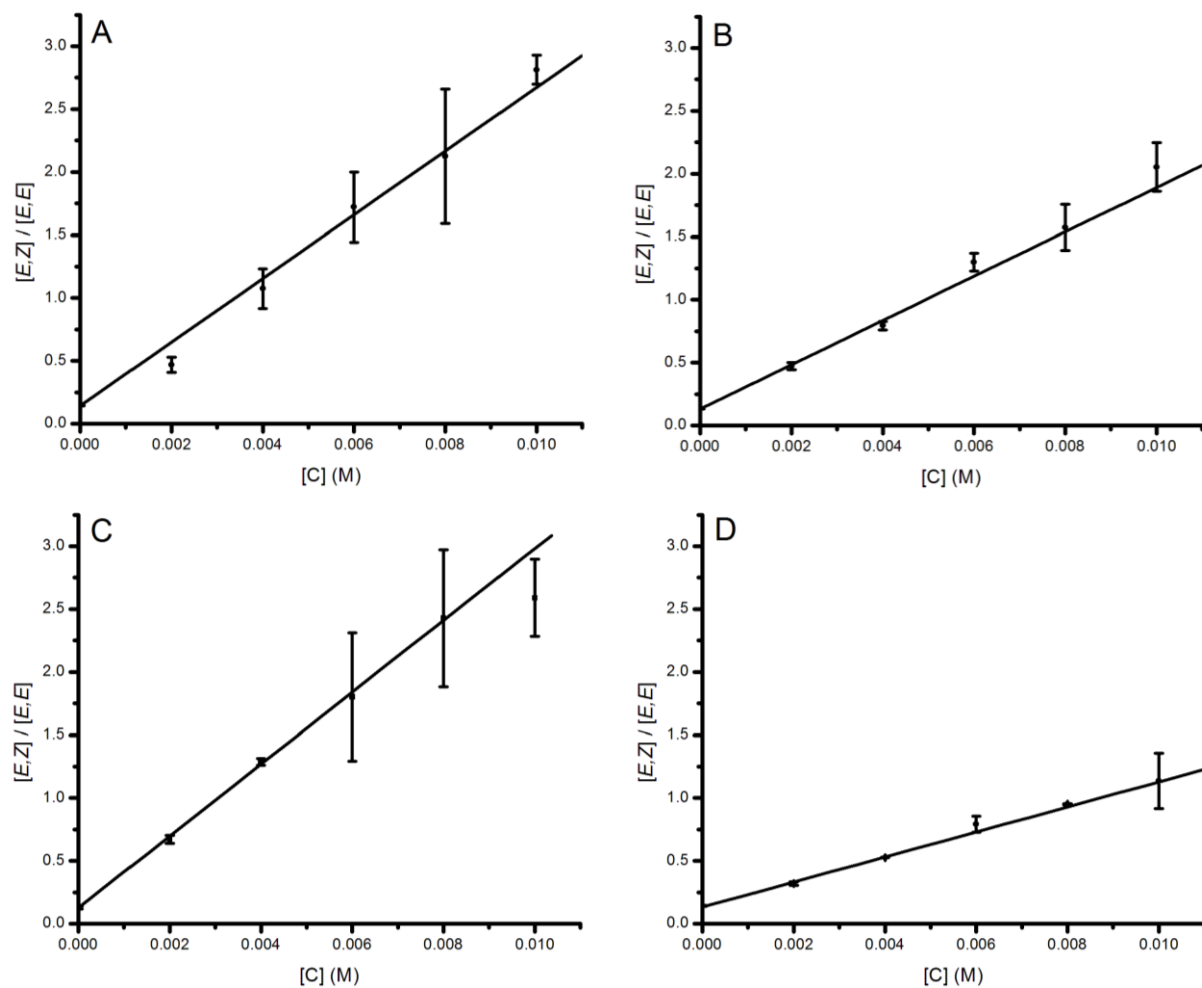


Figure S1. Ratio of [E,Z]:[E,E] products versus concentration of t -Bu₂-resveratrol (2.19) (A), t -Bu₂-pallidol (2.27) (B), t -Bu₂-quadrangularin A B (2.23) (C), and BHT (D) in the MeOAMVN-initiated (0.01 M) autoxidation of methyl linoleate (0.1 M) in chlorobenzene at 37°C.

INHIBITED OXIDATIONS OF PHOSPHATIDYLCHOLINE LIPOSOMES

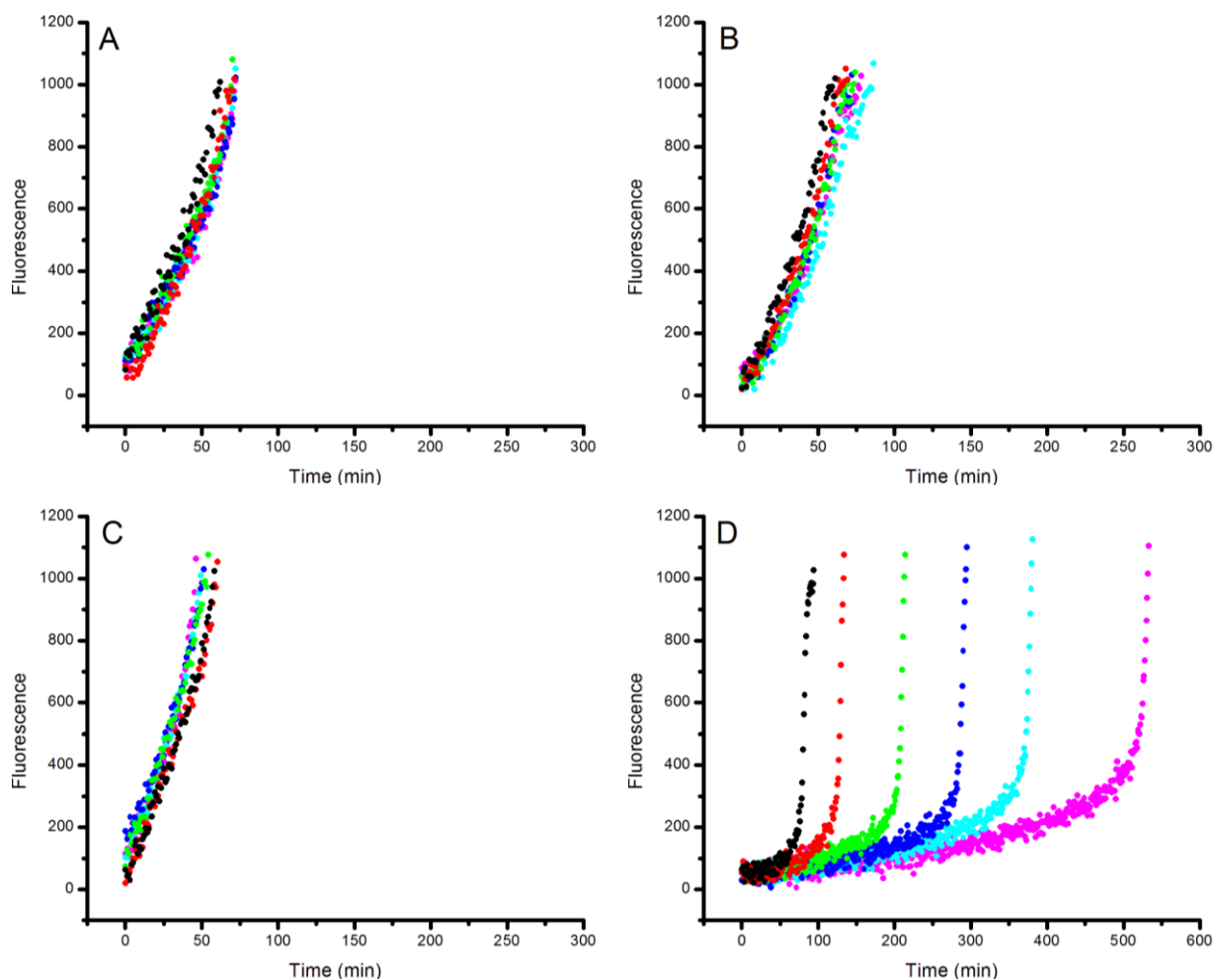


Figure S2. Representative fluorescence intensity-time profiles from MeOAMVN-mediated (0.68 mM) oxidations of egg phosphatidylcholine liposomes (1 mM in pH 7.4 PBS buffer) containing 0.15 μM H₂B-PMHC probe and increasing concentrations (2.5 μM , 5.0 μM , 10 μM , 15 μM , 20 μM , 30 μM) of resveratrol (**1.1**) (A), pallidol (**2.4**) (B), quadrangularin A (**1.10**) (C) and PMHC (D). Fluorescence ($\lambda_{\text{ex}} = 485 \text{ nm}$, $\lambda_{\text{em}} = 520 \text{ nm}$) was recorded every 60s.

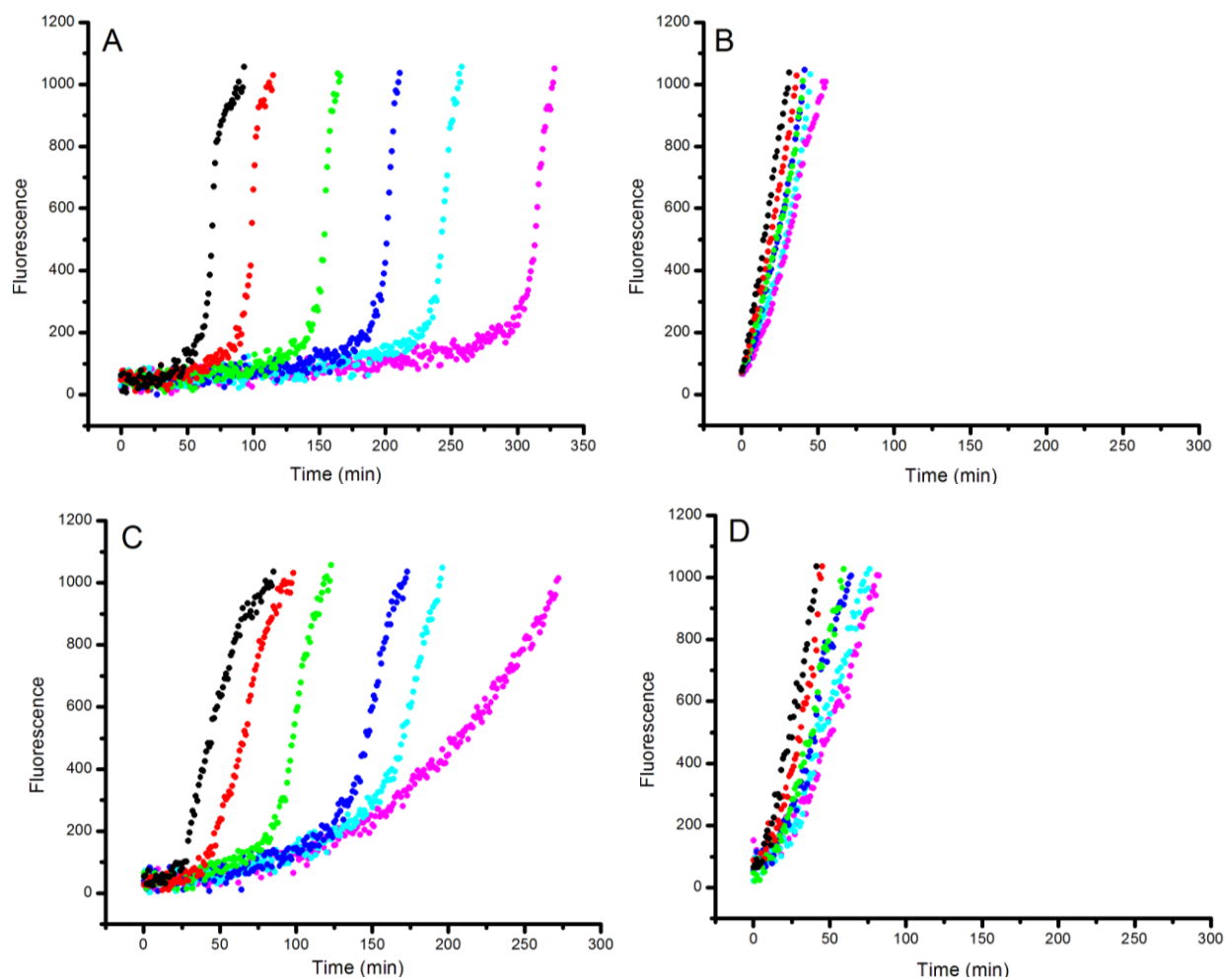


Figure S3. Representative fluorescence intensity-time profiles from MeOAMVN-mediated (0.68 mM) oxidations of egg phosphatidylcholine liposomes (1 mM in pH7.4 PBS buffer) containing 0.15 μ M H₂B-PMHC and increasing concentrations (2.5 μ M, 5.0 μ M, 10 μ M, 15 μ M, 20 μ M, 30 μ M) of *t*-Bu₂-resveratrol (**2.19**) (A), *t*-Bu₂-pallidol (**2.27**) (B), *t*-Bu₂-quadrangularin A (**2.23**) (C) and BHT (D). Fluorescence ($\lambda_{\text{ex}} = 485 \text{ nm}$; $\lambda_{\text{em}} = 520 \text{ nm}$) was recorded every 60s.

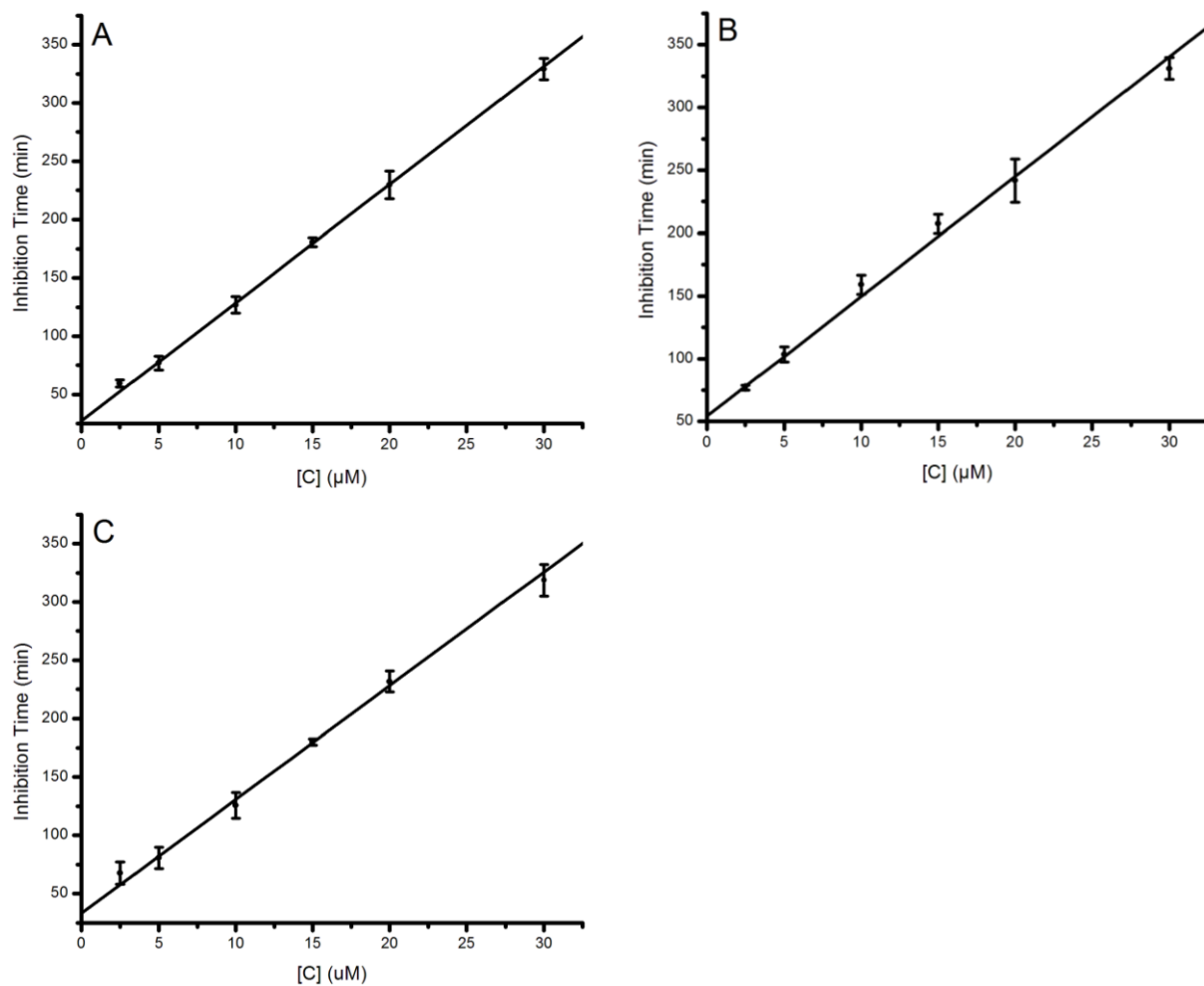


Figure S4. Inhibition time-concentration profiles from MeOAMVN-mediated (0.68 mM) oxidations of egg phosphatidylcholine liposomes (1 mM in pH 7.4 PBS buffer) containing 0.15 μM H₂B-PMHC and increasing concentrations (2.5 μM, 5.0 μM, 10 μM, 15 μM, 20 μM, 30 μM) of the inhibitors which display a clear inhibited period: PMHC (A), *t*-Bu₂-resveratrol (**2.19**) (B), and *t*-Bu₂-quadrangularin A (**2.23**) (C). The stoichiometric numbers (*n*) were calculated based on the slopes of the line of best fit relative to PMHC, for which *n*=2.

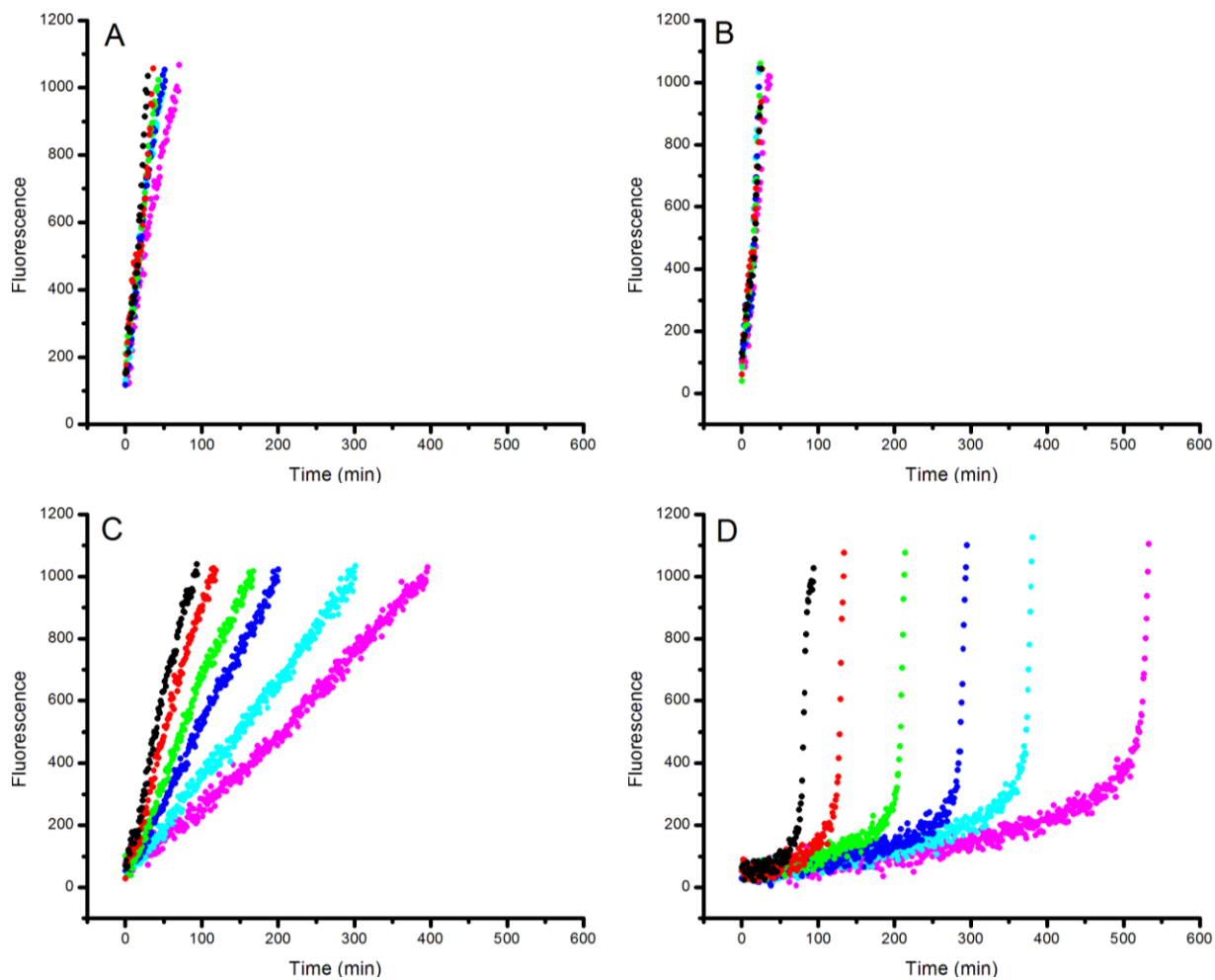


Figure S5. Representative fluorescence intensity-time profiles from AAPH-mediated (2.7 mM) oxidations of egg phosphatidylcholine liposomes (1 mM in pH 7.4 PBS buffer) containing 0.15 μM H₂B-PMHC and increasing concentrations (2.5 μM , 5.0 μM , 10 μM , 15 μM , 20 μM , 30 μM) of resveratrol (**1.1**) (A), pallidol (**2.4**) (B), quadrangularin A (**1.10**) (C) and PMHC (D). Fluorescence ($\lambda_{\text{ex}} = 485 \text{ nm}$; $\lambda_{\text{em}} = 520 \text{ nm}$) was recorded every 60s.

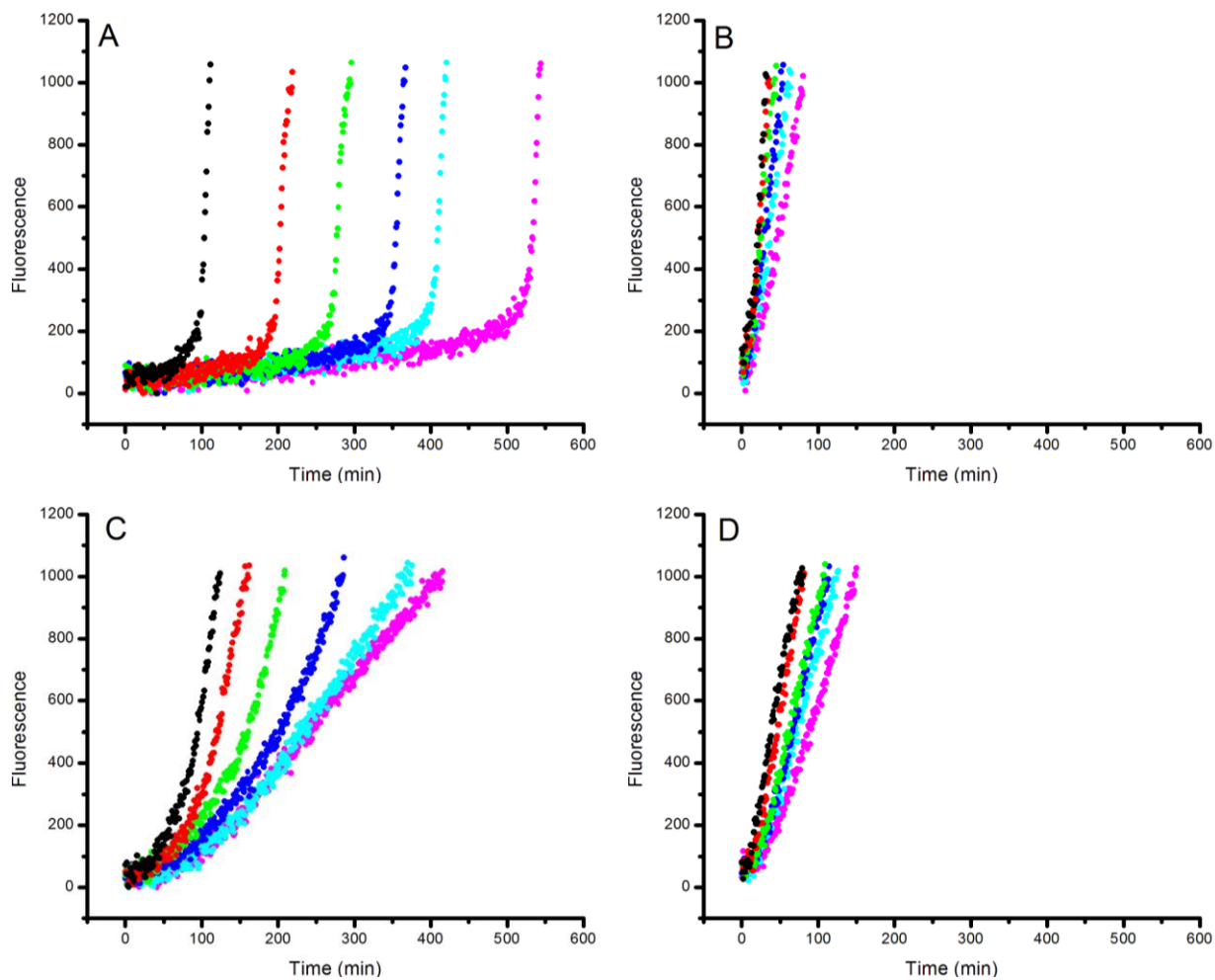


Figure S6. Representative fluorescence intensity-time profiles from AAPH-mediated (2.7 mM) oxidations of egg phosphatidylcholine liposomes (1 mM in pH 7.4 PBS buffer) containing 0.15 μM H₂B-PMHC and increasing concentrations (2.5 μM , 5.0 μM , 10 μM , 15 μM , 20 μM , 30 μM) of *t*-Bu₂-resveratrol (**2.19**) (A), *t*-Bu₂-pallidol (**2.27**) (B), *t*-Bu₂-quadrangularin A (**2.23**) (C) and BHT (D). Fluorescence ($\lambda_{\text{ex}} = 485 \text{ nm}$; $\lambda_{\text{em}} = 520 \text{ nm}$) was recorded every 60s.

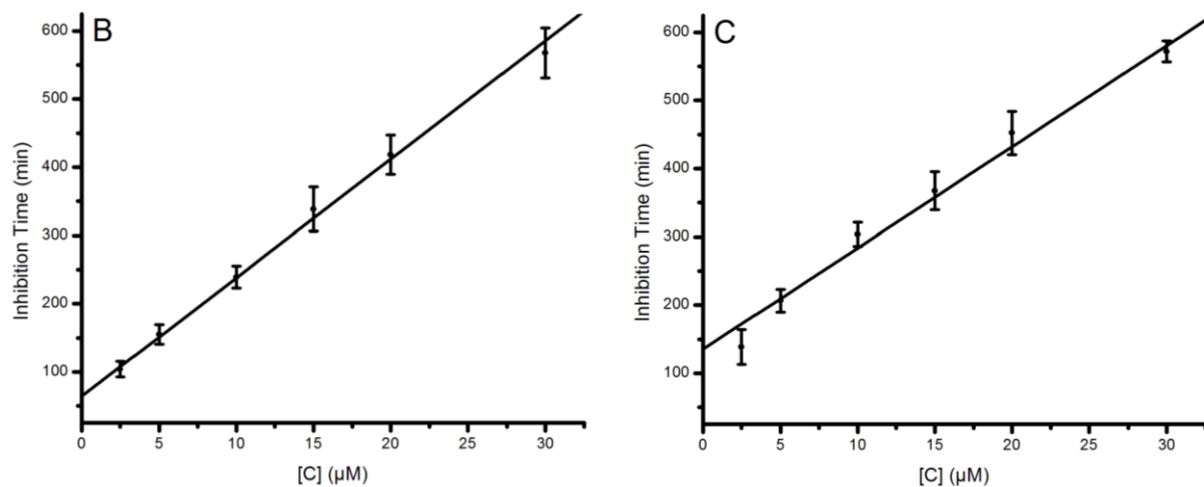


Figure S7. Inhibition time-concentration profiles from AAPH-mediated (2.7 mM) oxidations of egg phosphatidylcholine liposomes (1 mM in pH 7.4 PBS buffer) containing 0.15 μM H₂B-PMHC and increasing concentrations (2.5 μM, 5.0 μM, 10 μM, 15 μM, 20 μM, 30 μM) of the inhibitors which display a clear inhibited period: PMC (B) and *t*-Bu₂-resveratrol (**2.19**) (C). The stoichiometric numbers (*n*) were calculated based on the slopes of the line of best fit relative to PMHC, for which *n*=2.

CELLULAR LIPID PEROXIDATION ASSAY

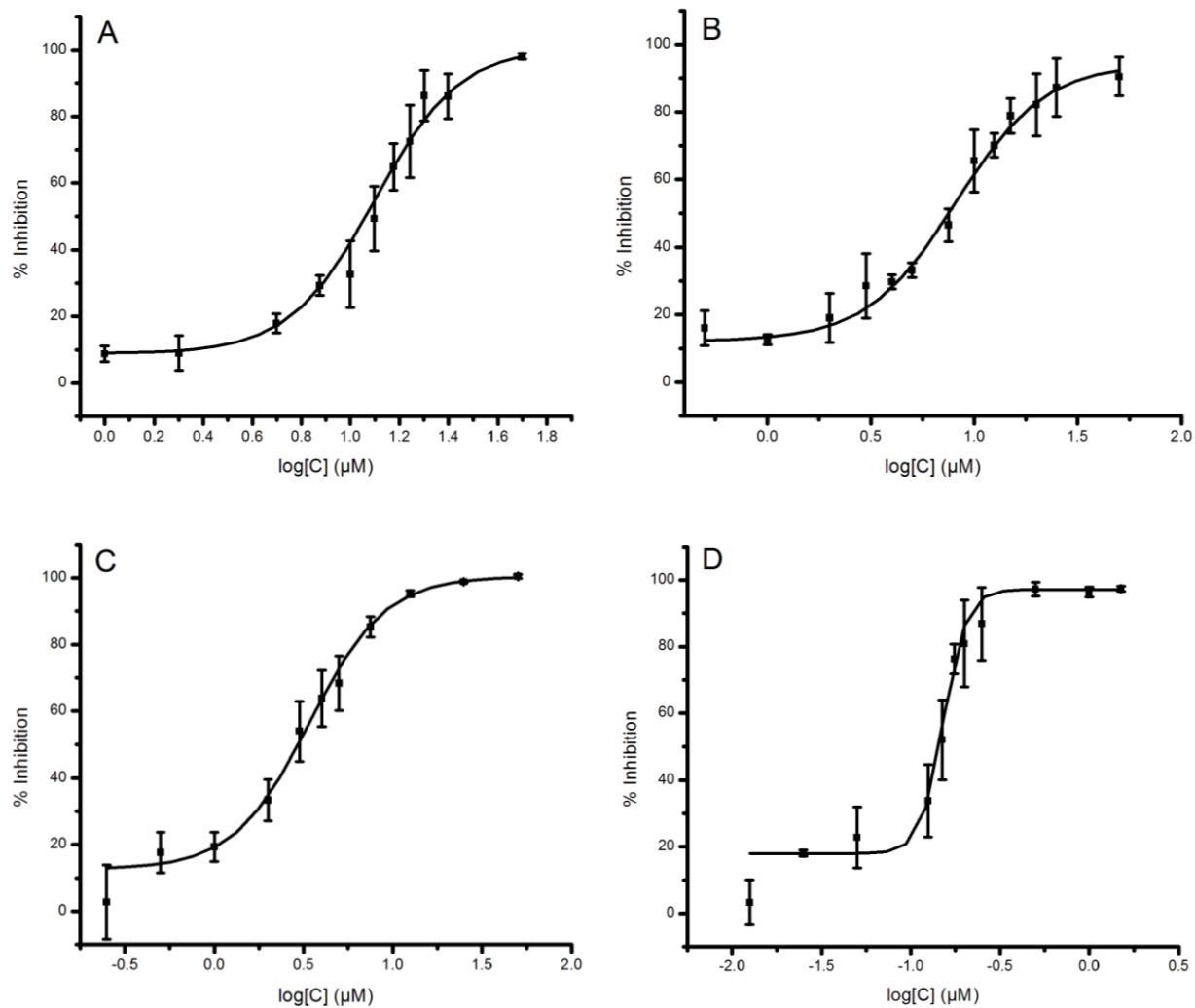


Figure S8. Dose-response curves obtained from flow cytometry (5×10^5 cells/ mL; $\lambda_{\text{ex}} = 488$ nm, $\lambda_{\text{em}} = 525 \pm 25$ nm; 10,000 events) following induction of oxidative stress with diethylmaleate (DEM, 9 mM) in TF1a cells grown in media containing resveratrol (**1.1**) (A), pallidol (**2.4**) (B), quadrangularin A (**1.10**) (C) and α -tocopherol (D) (0.015-50 μM) for 22 hours at 37 °C. Cells were incubated with the lipid peroxidation reporter C11-BODIPY^{581/591} (1 μM) for 30 minutes prior to DEM treatment.

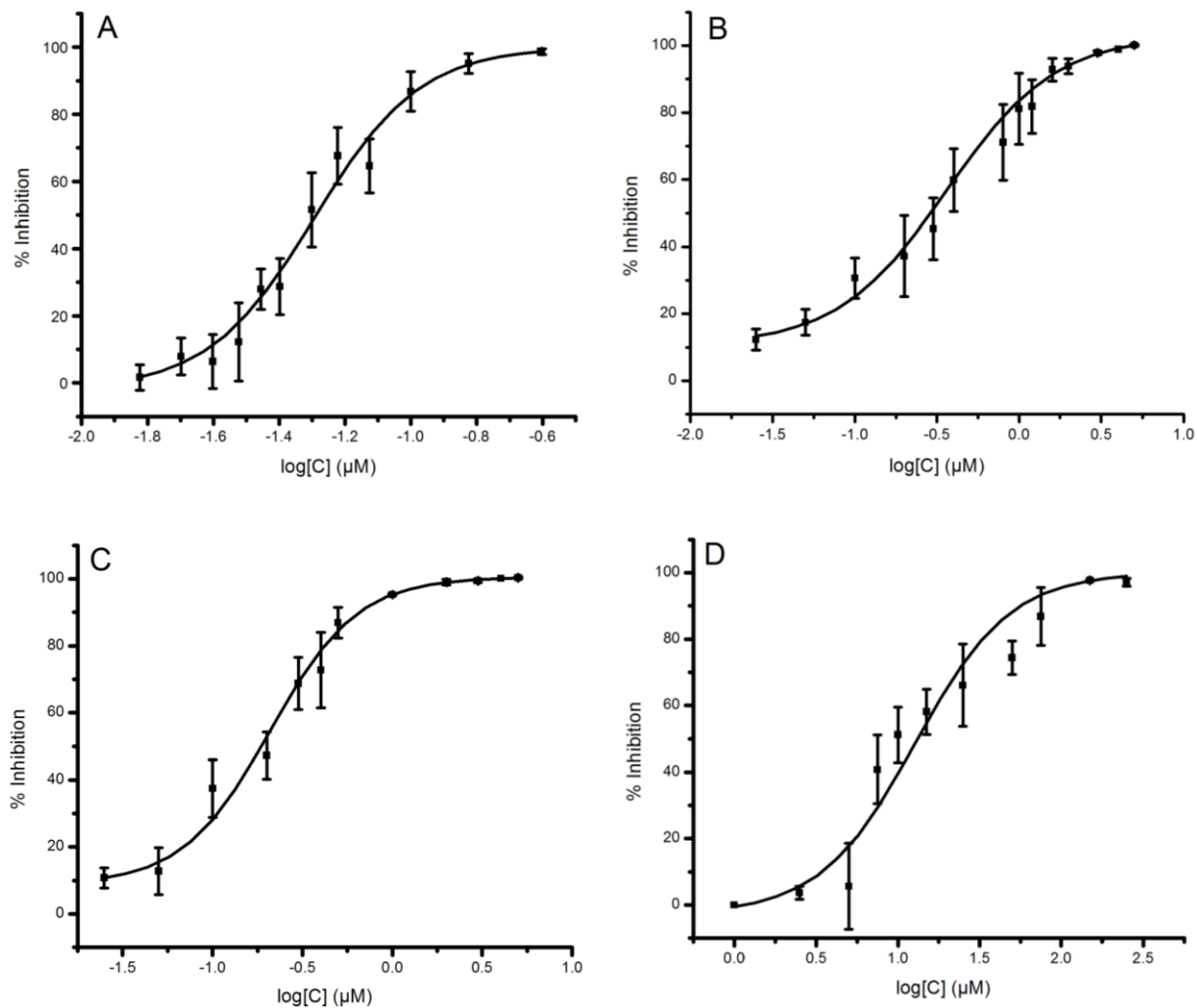


Figure S9. Dose-response curves obtained from flow cytometry (5×10^5 cells/ mL; $\lambda_{\text{ex}} = 488$ nm, $\lambda_{\text{em}} = 525 \pm 25$ nm; 10,000 events) following induction of oxidative stress with diethylmaleate (DEM, 9 mM) in TF1a cells grown in media containing *t*-Bu₂-resveratrol (**2.19**) (A), *t*-Bu₂-pallidol (**2.27**) (B), *t*-Bu₂-quadrangularin A (**2.23**) (C) and BHT (D) (0.015-50 μ M) for 22 hours at 37 °C. Cells were incubated with the lipid peroxidation reporter C11-BODIPY^{581/591} (1 μ M) for 30 minutes prior to DEM treatment.

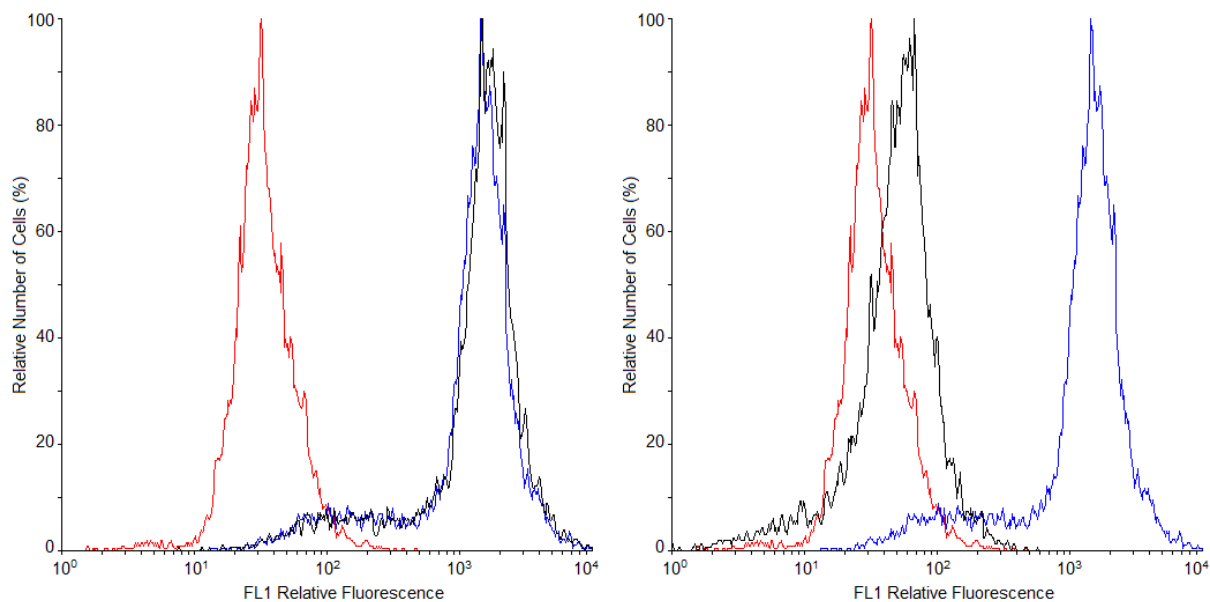


Figure S10. Representative histograms obtained from flow cytometry (5×10^5 cells/ mL; $\lambda_{\text{ex}} = 488$ nm, $\lambda_{\text{em}} = 525 \pm 25$ nm; 10,000 events) following induction of oxidative stress with diethylmaleate (DEM, 9 mM) in TF1a cells grown in media containing resveratrol (left black: 5 μM , right black: 50 μM) for 22 hours at 37 °C. Cells were incubated with the lipid peroxidation reporter C11-BODIPY^{581/591} (1 μM) for 30 minutes prior to DEM treatment. Cells not treated with DEM were used as negative control (red). Cells not treated with antioxidants were used as positive control (blue).

CELL VIABILITY STUDIES

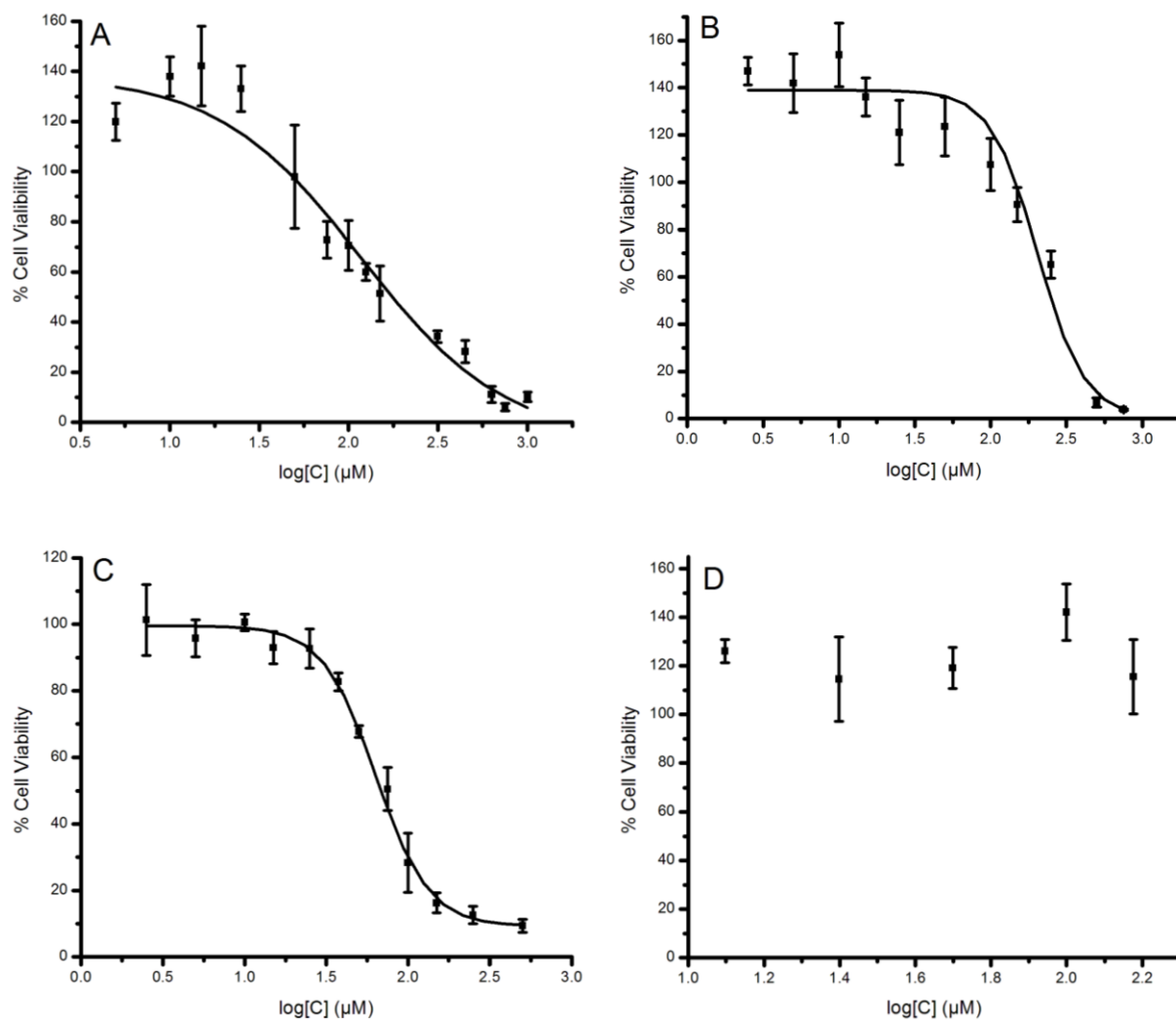


Figure S11. Dose-response curves obtained from MTT cell viability studies with TF1a erythroblasts (0.2×10^6 cells/ mL) containing varying concentrations of resveratrol (**1.1**) (A), pallidol (**2.4**) (B), quadrangularin A (**1.10**) (C), α -tocopherol (D) incubated at 37 °C for 22h.

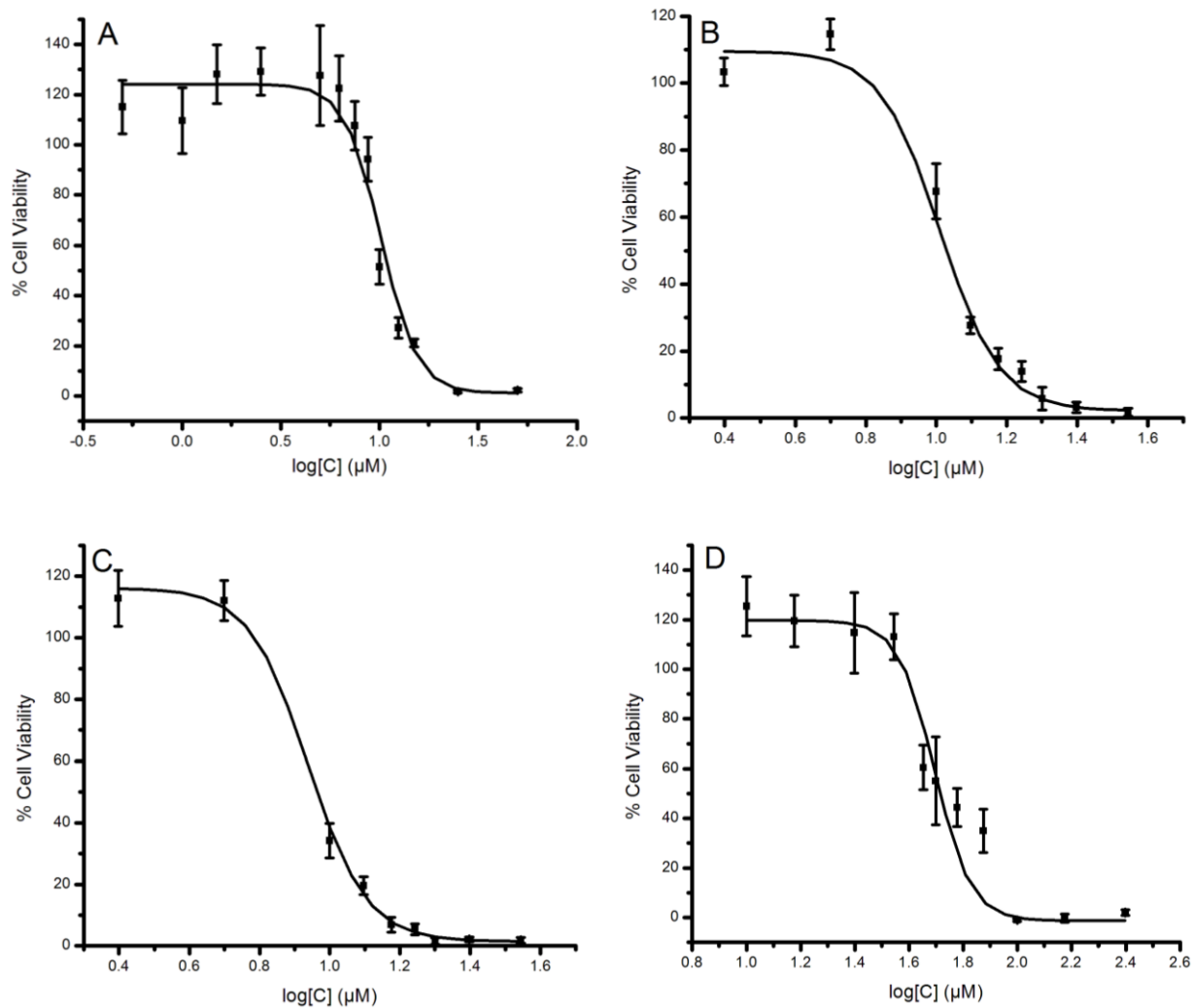
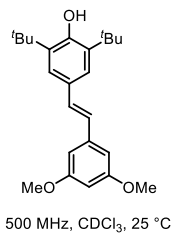
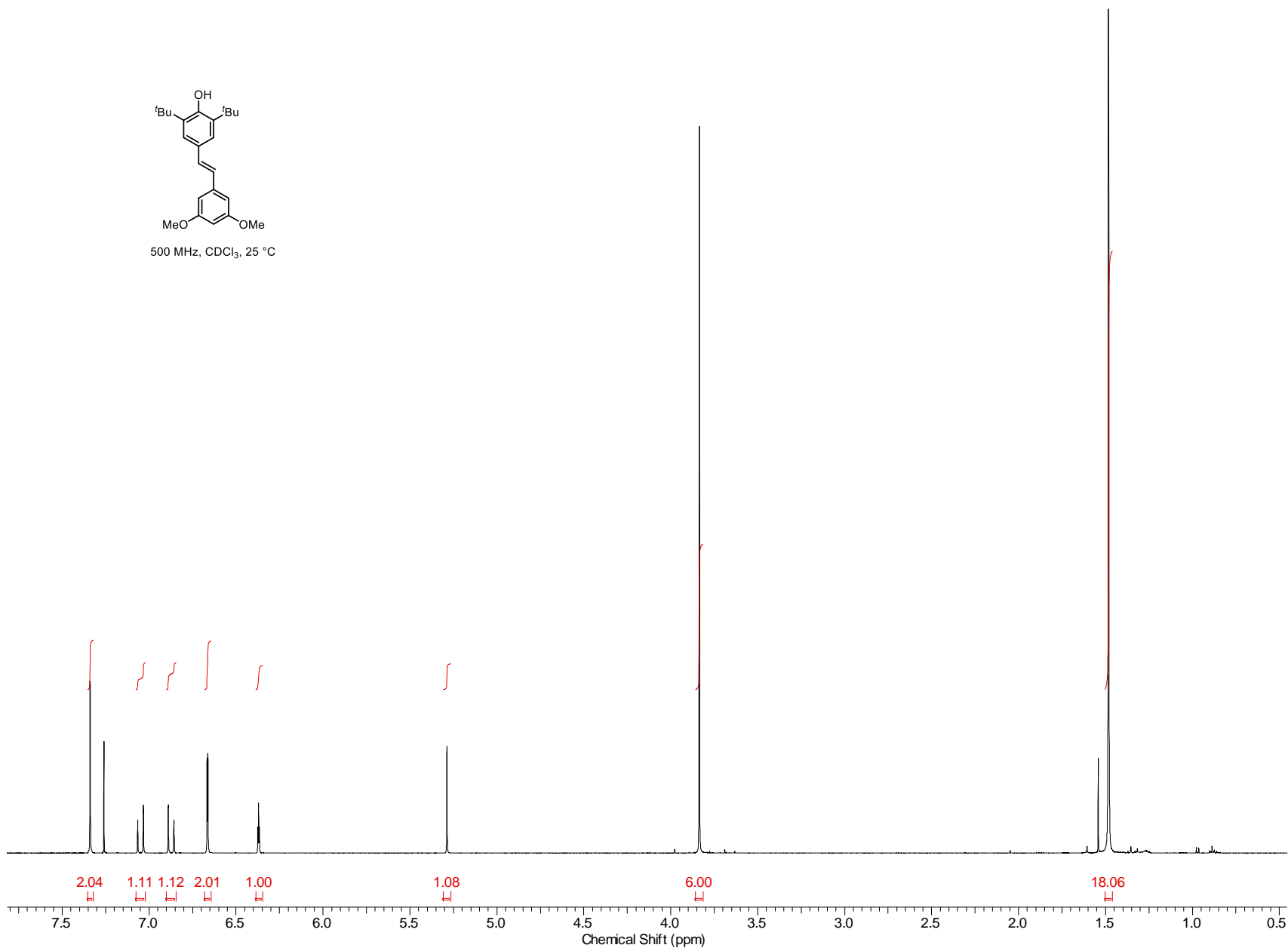
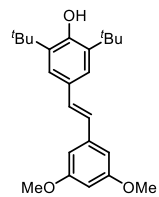


Figure S12. Dose-response curves obtained from MTT cell viability studies with TF1a erythroblasts (0.2×10^6 cells/ mL) containing varying concentrations of *t*-Bu₂-resveratrol (**2.19**) (A), *t*-Bu₂-pallidol (**2.27**) (B), *t*-Bu₂-quadrangularin A (**2.23**) (C), BHT (D) incubated at 37 °C for 22h.

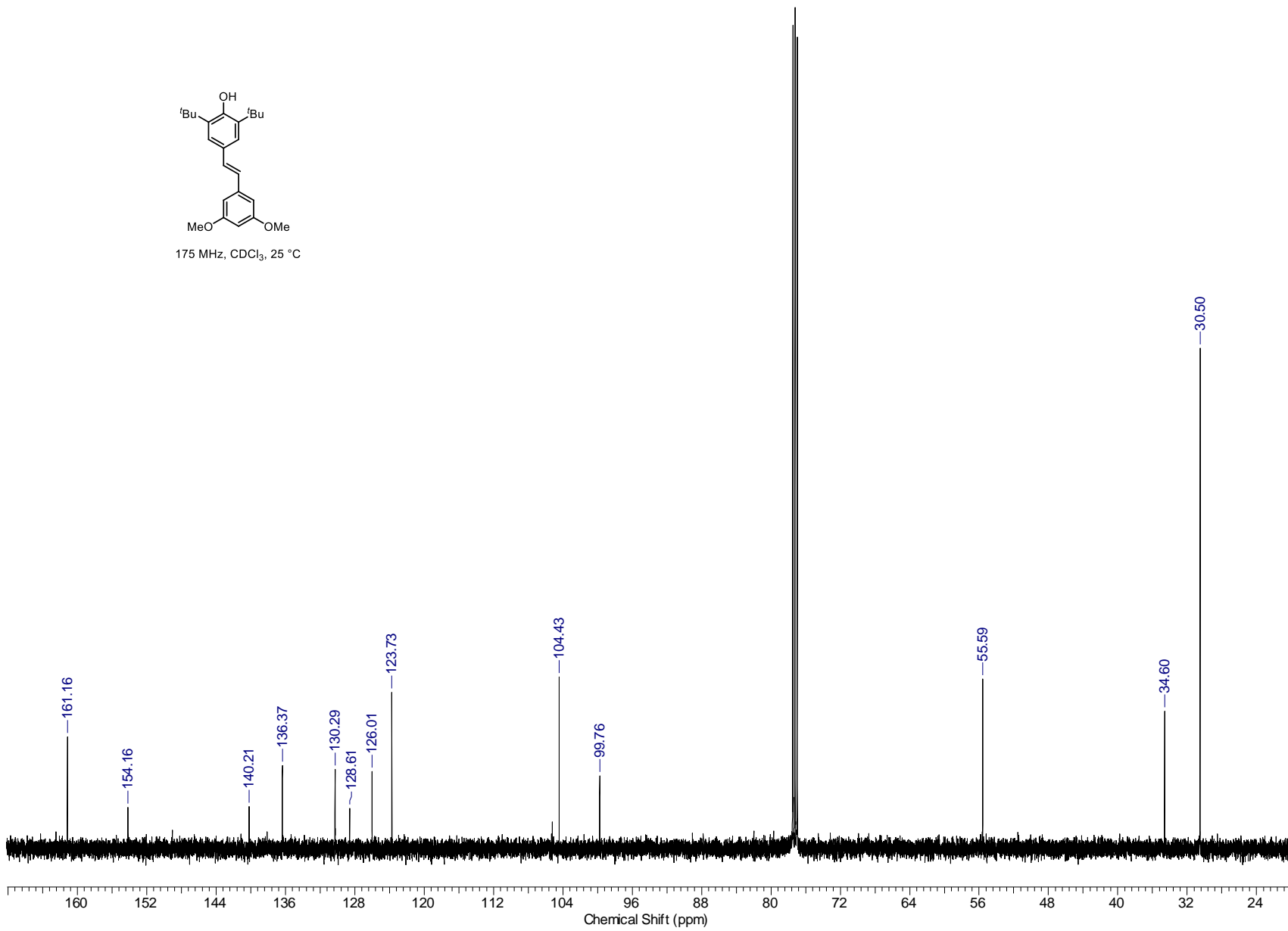


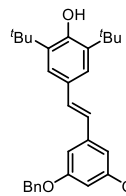
87





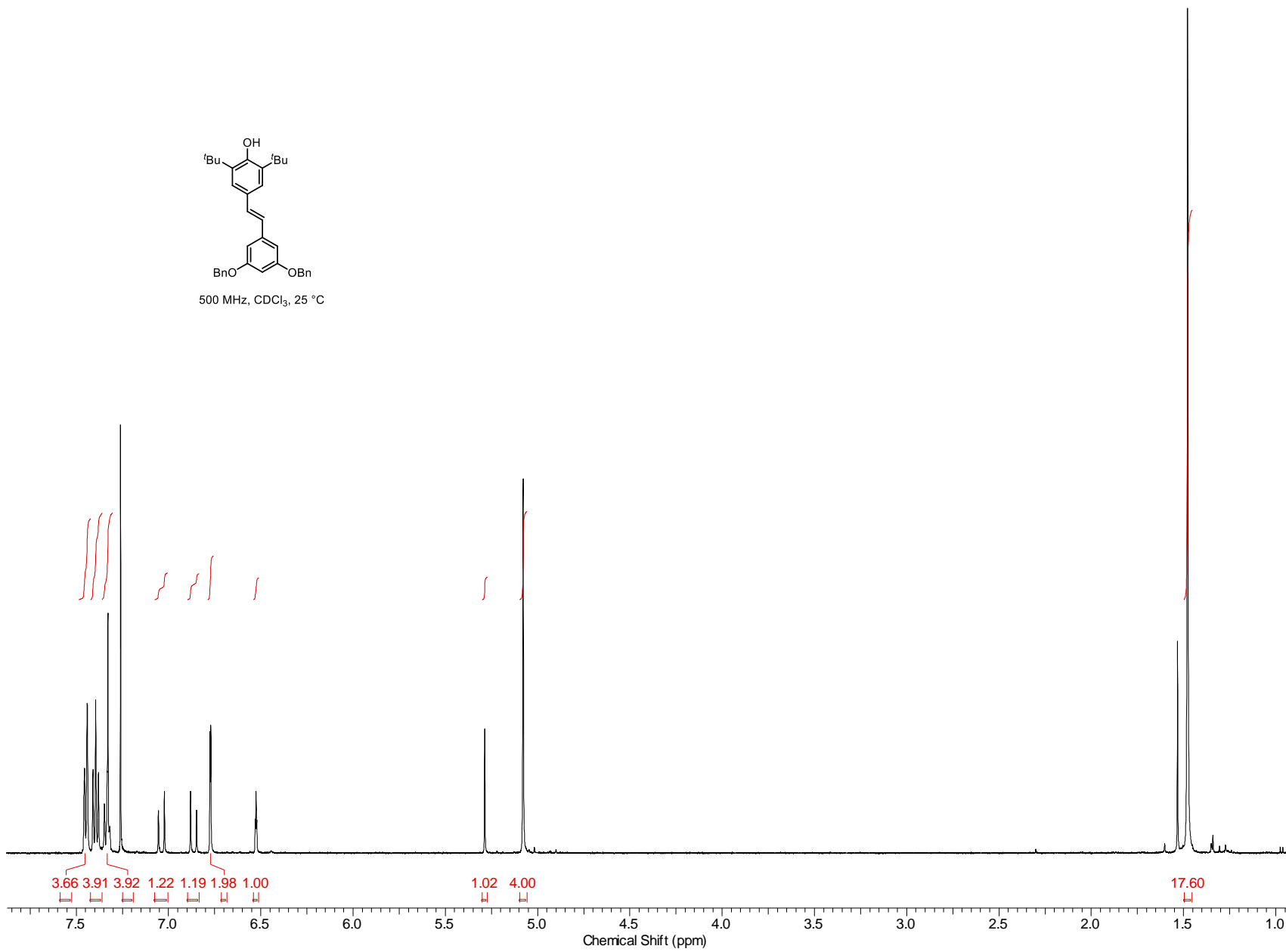
175 MHz, CDCl₃, 25 °C



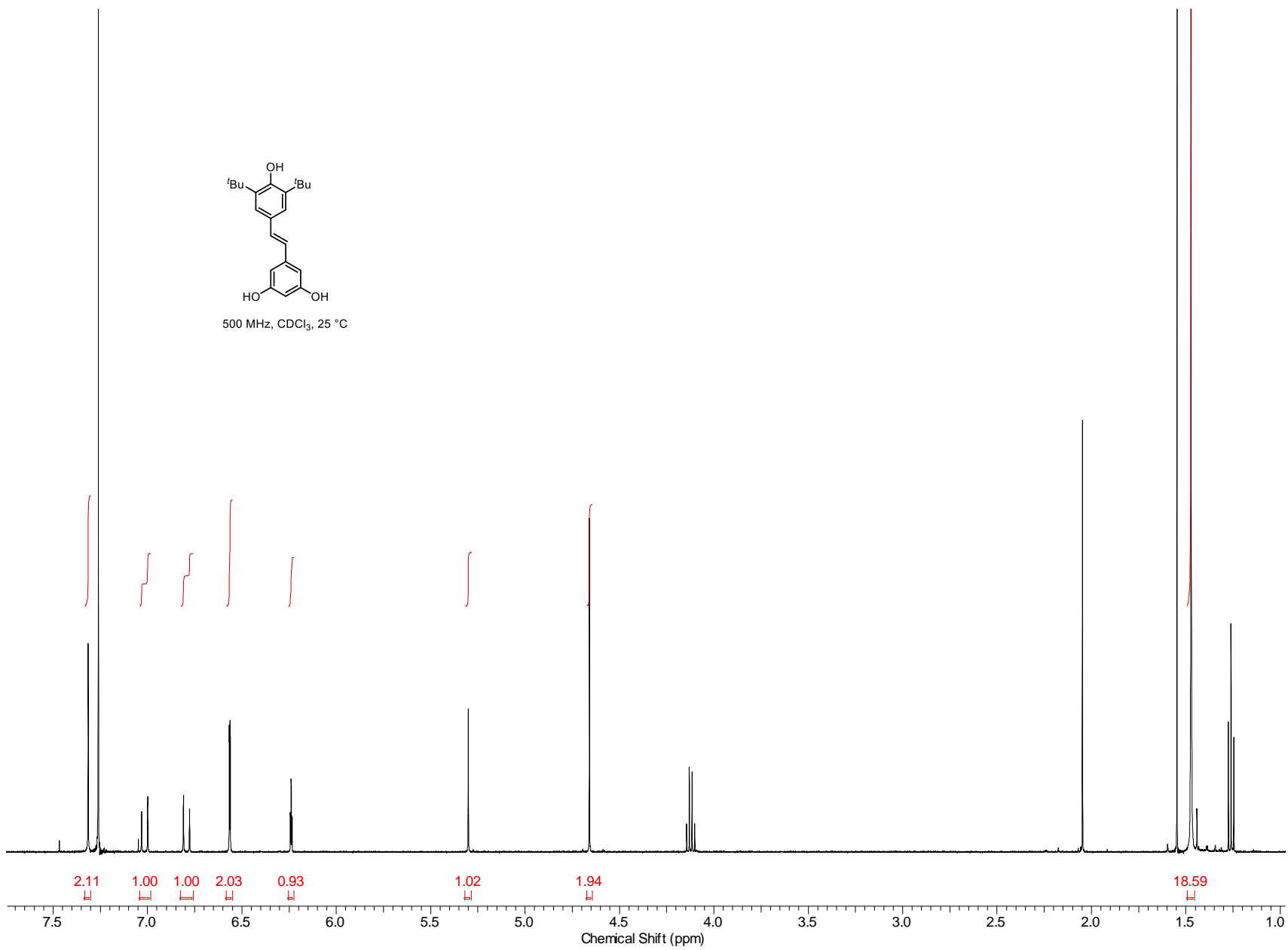
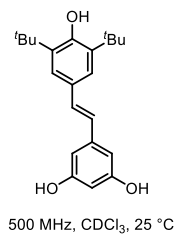


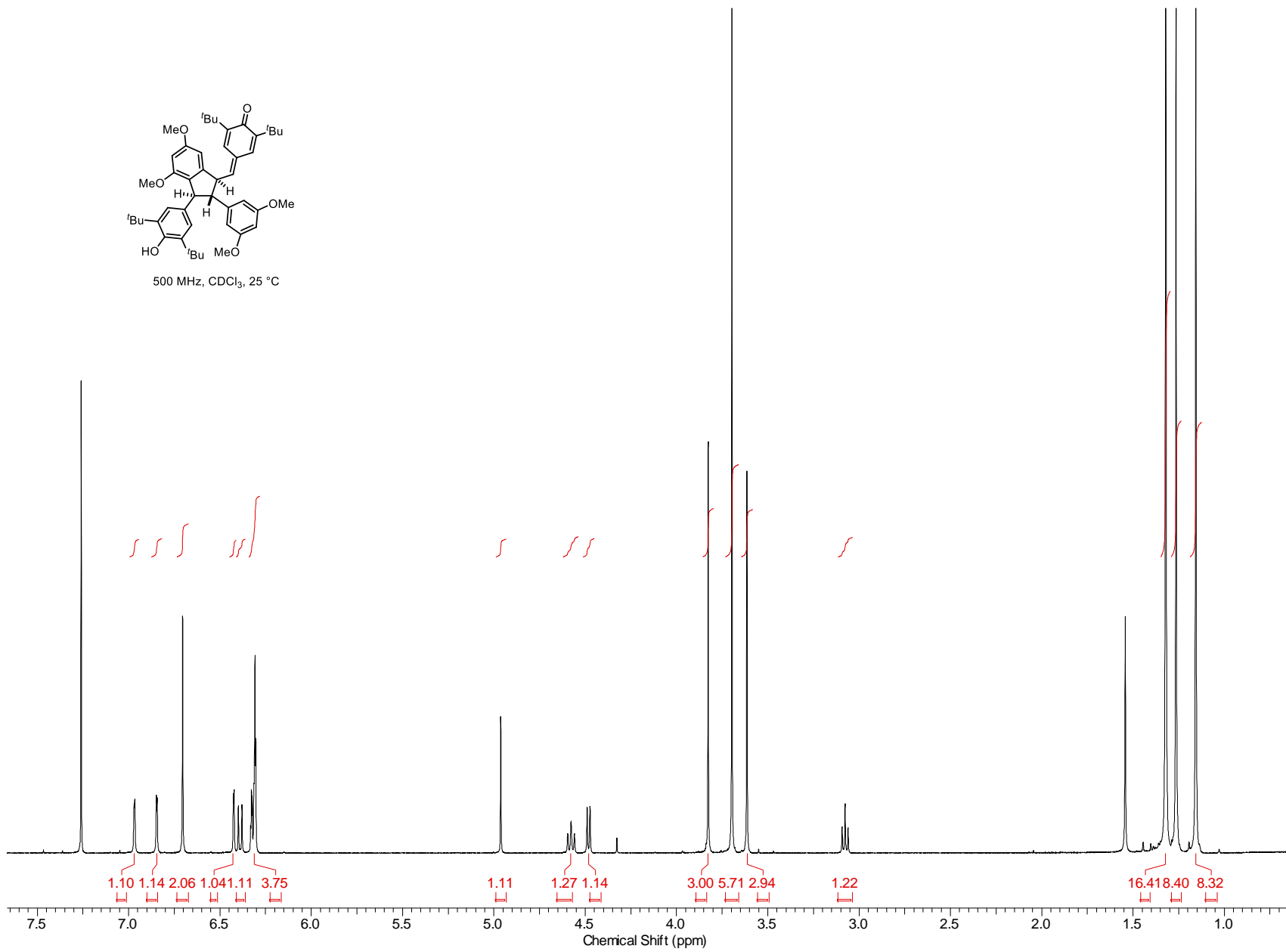
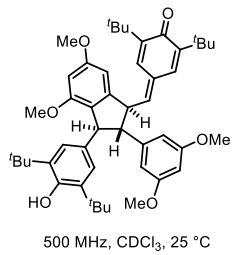
500 MHz, CDCl₃, 25 °C

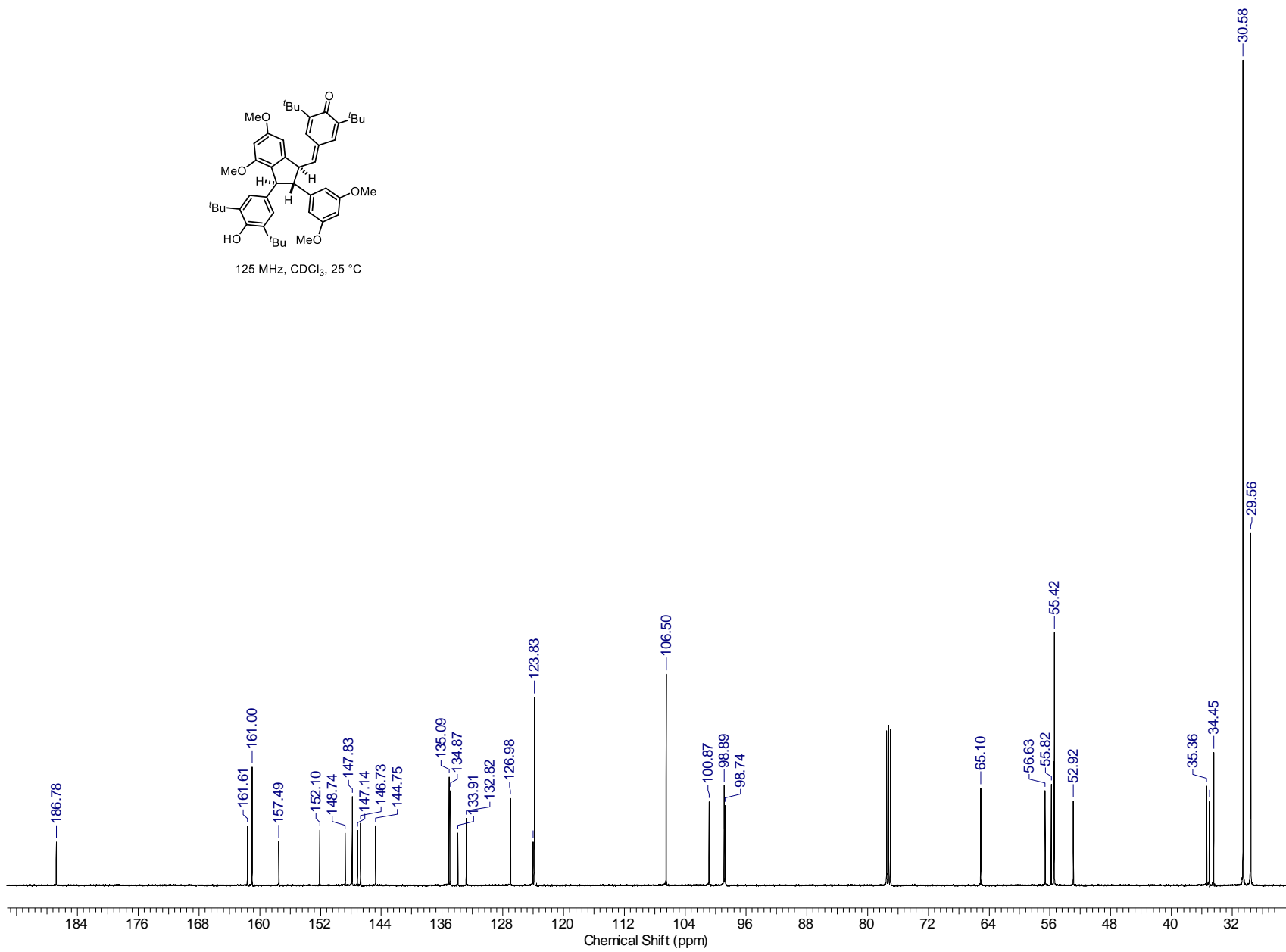
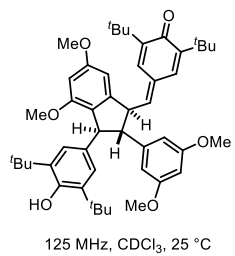
68

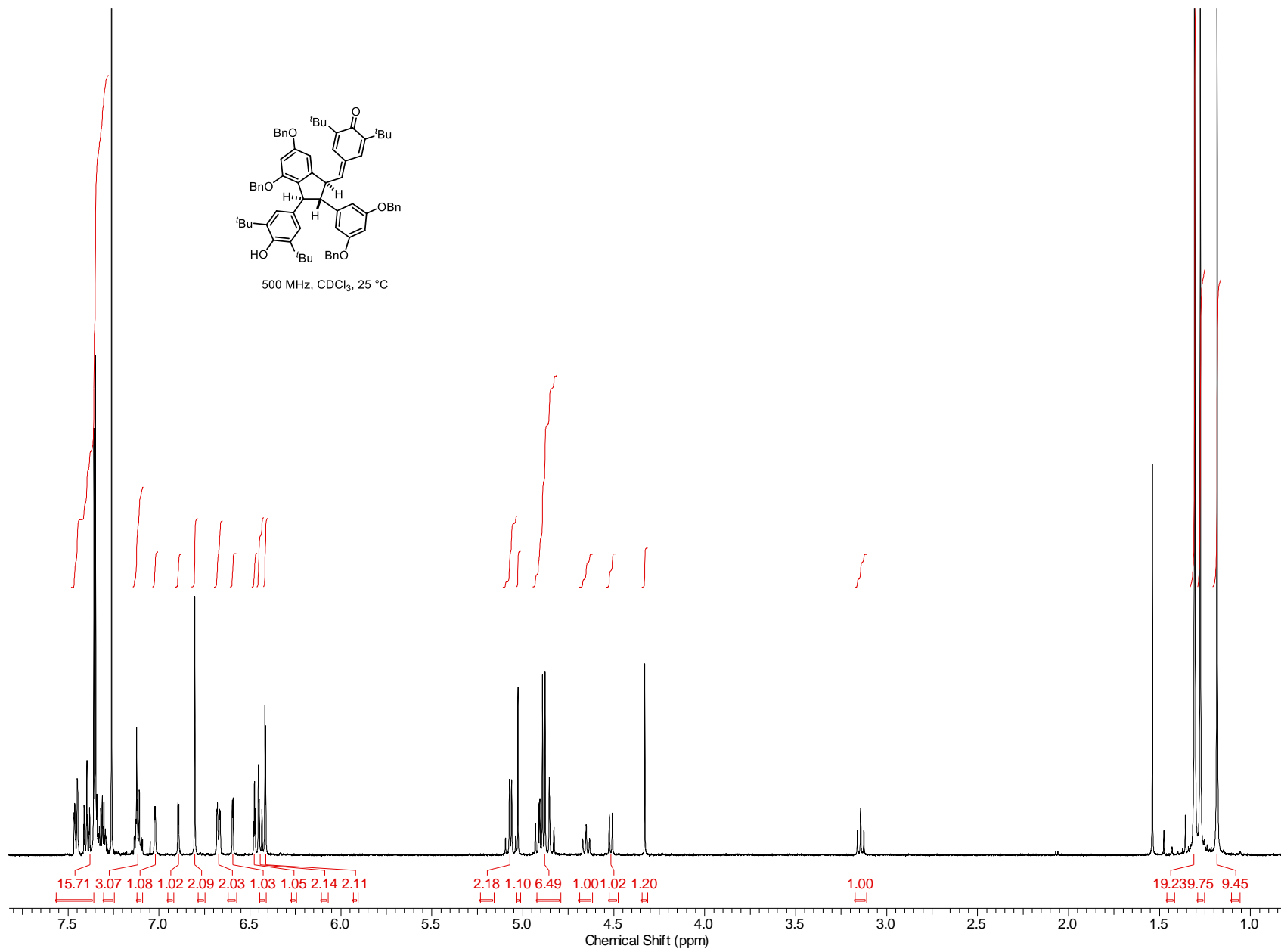


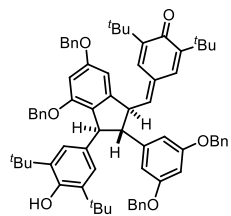
06



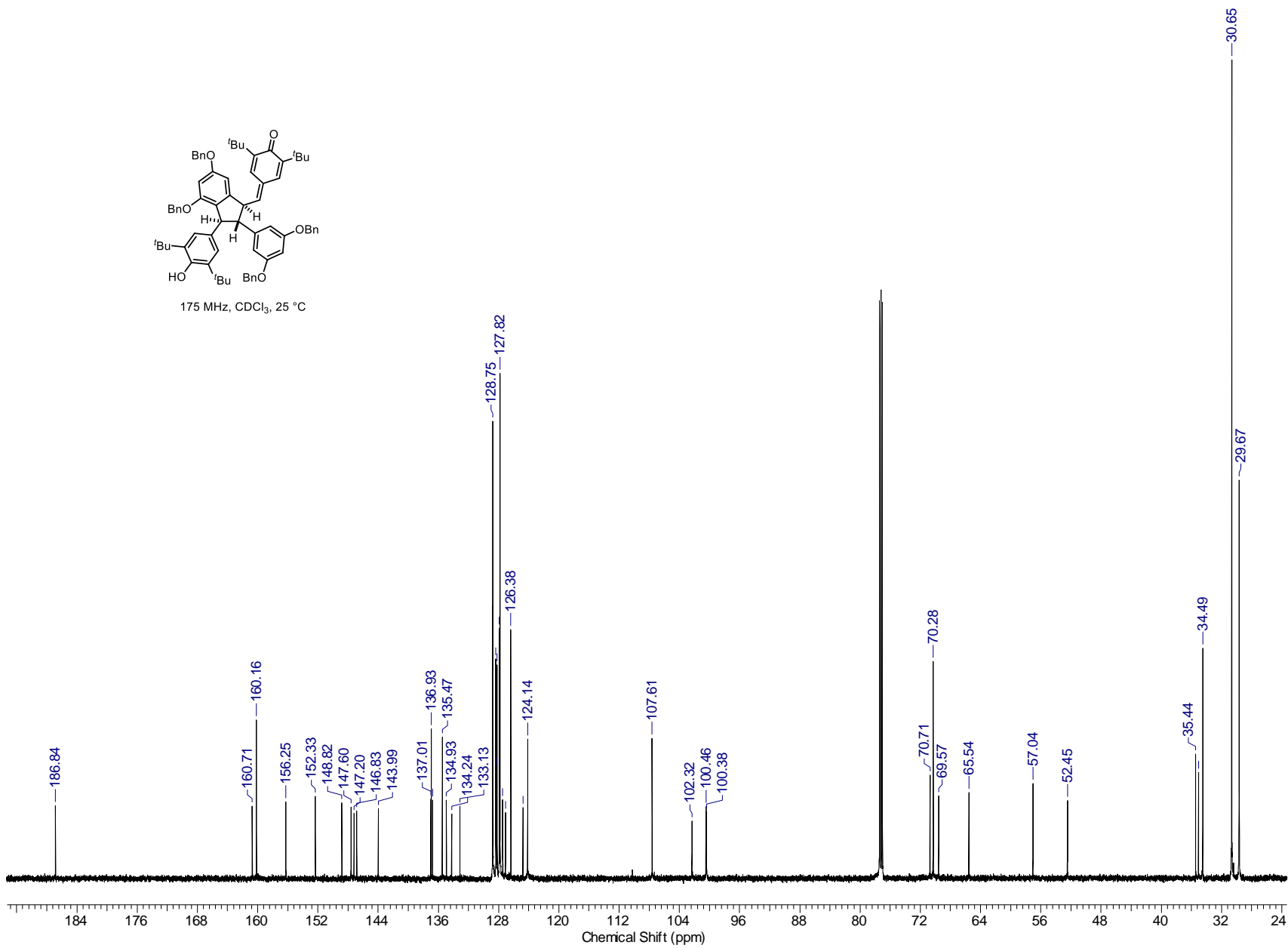


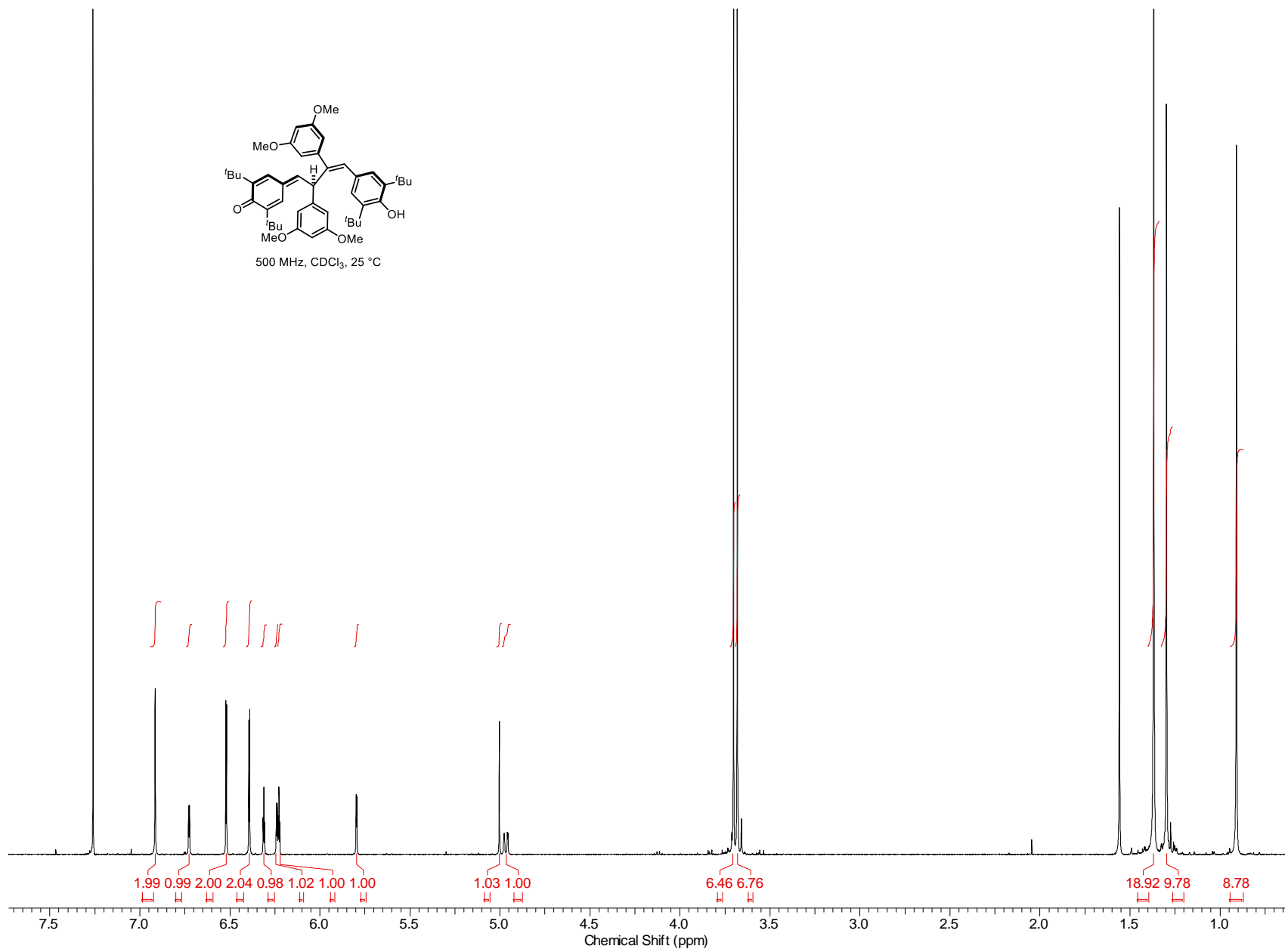


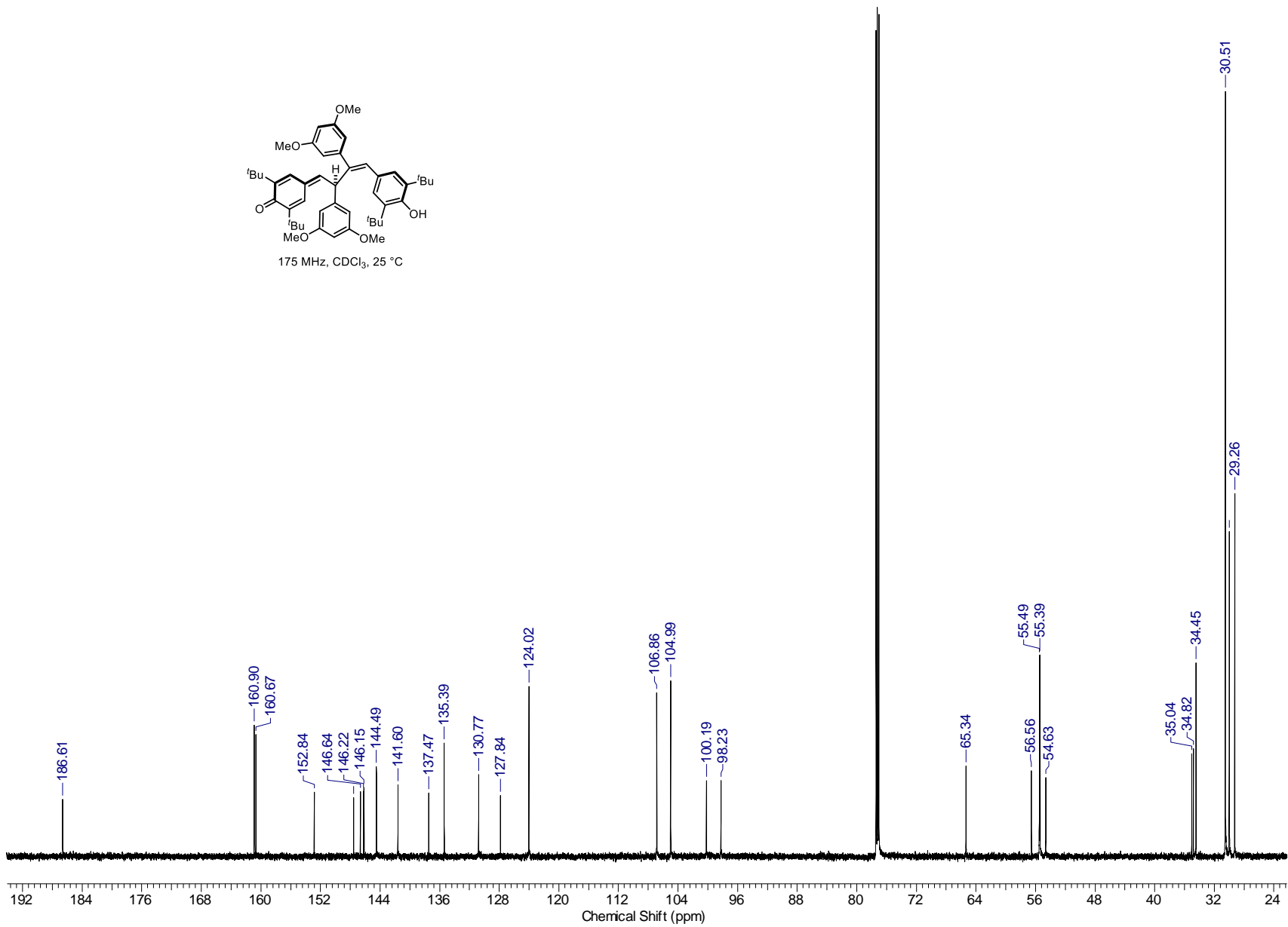
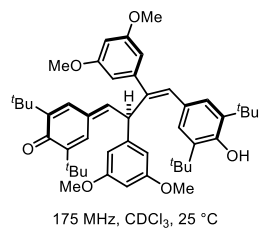


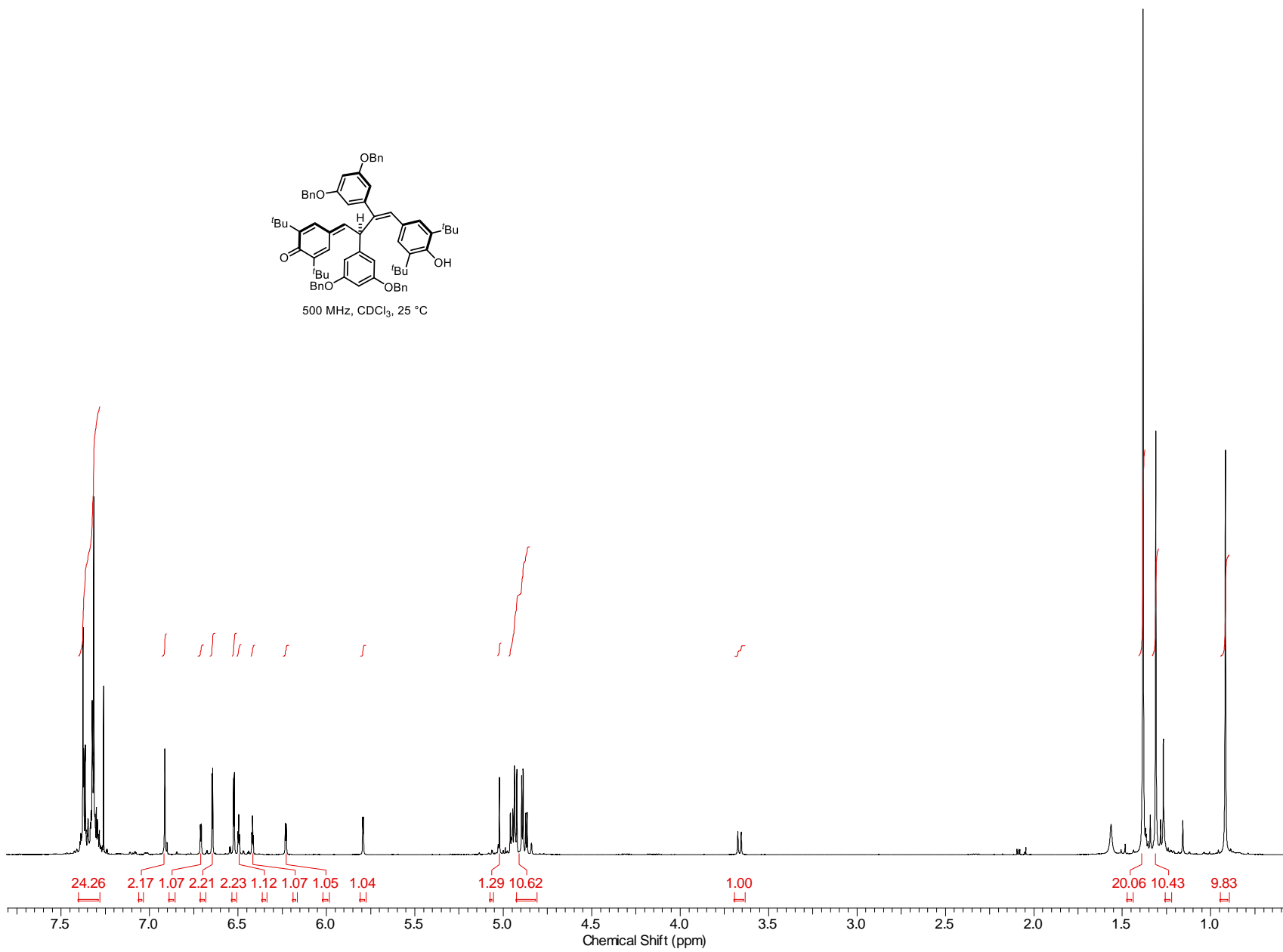
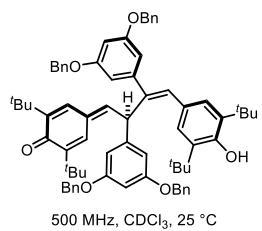


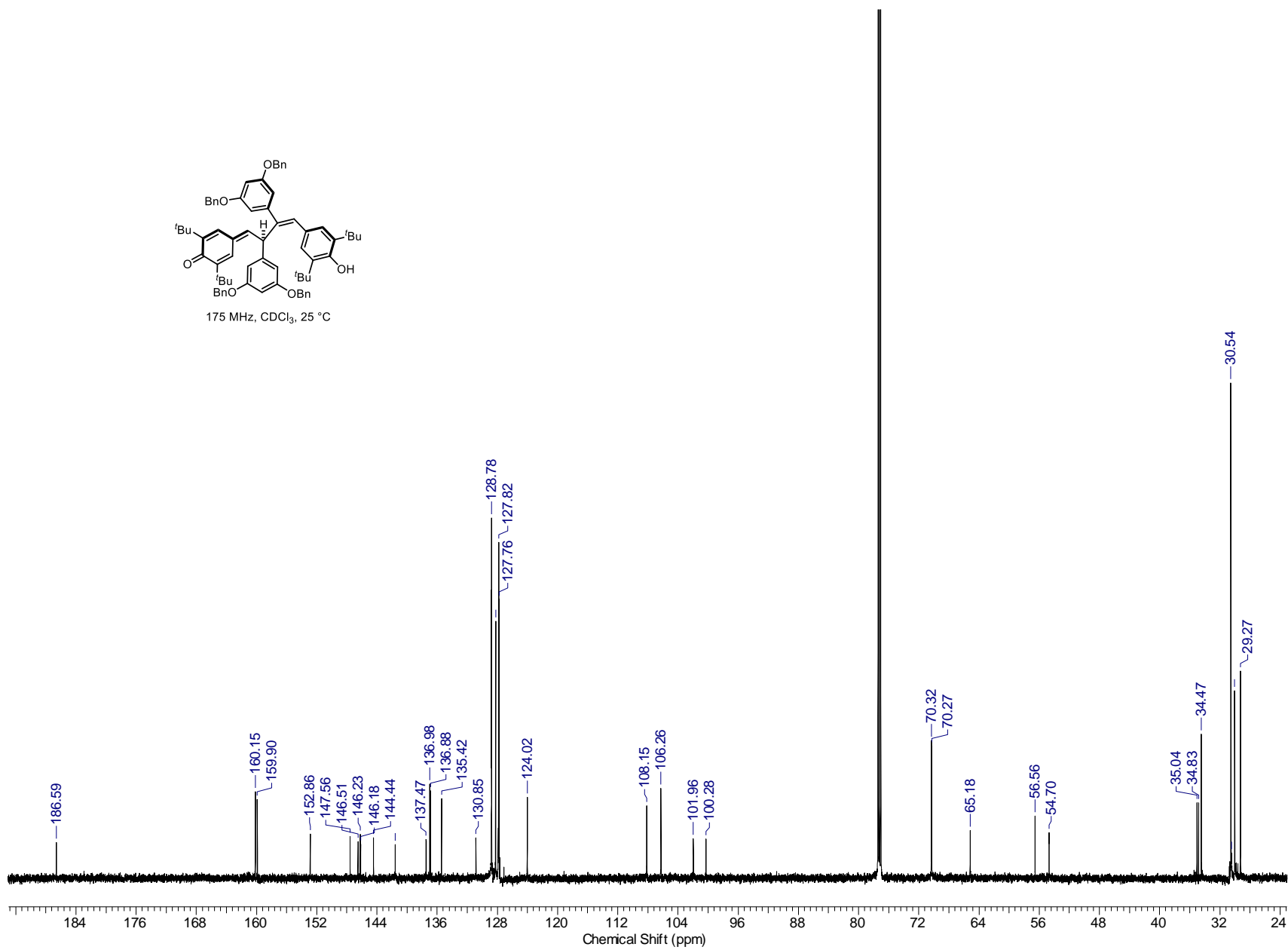
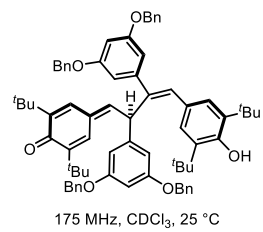
175 MHz, CDCl₃, 25 °C

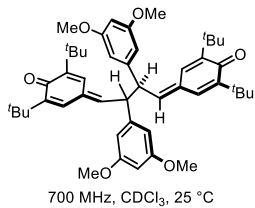




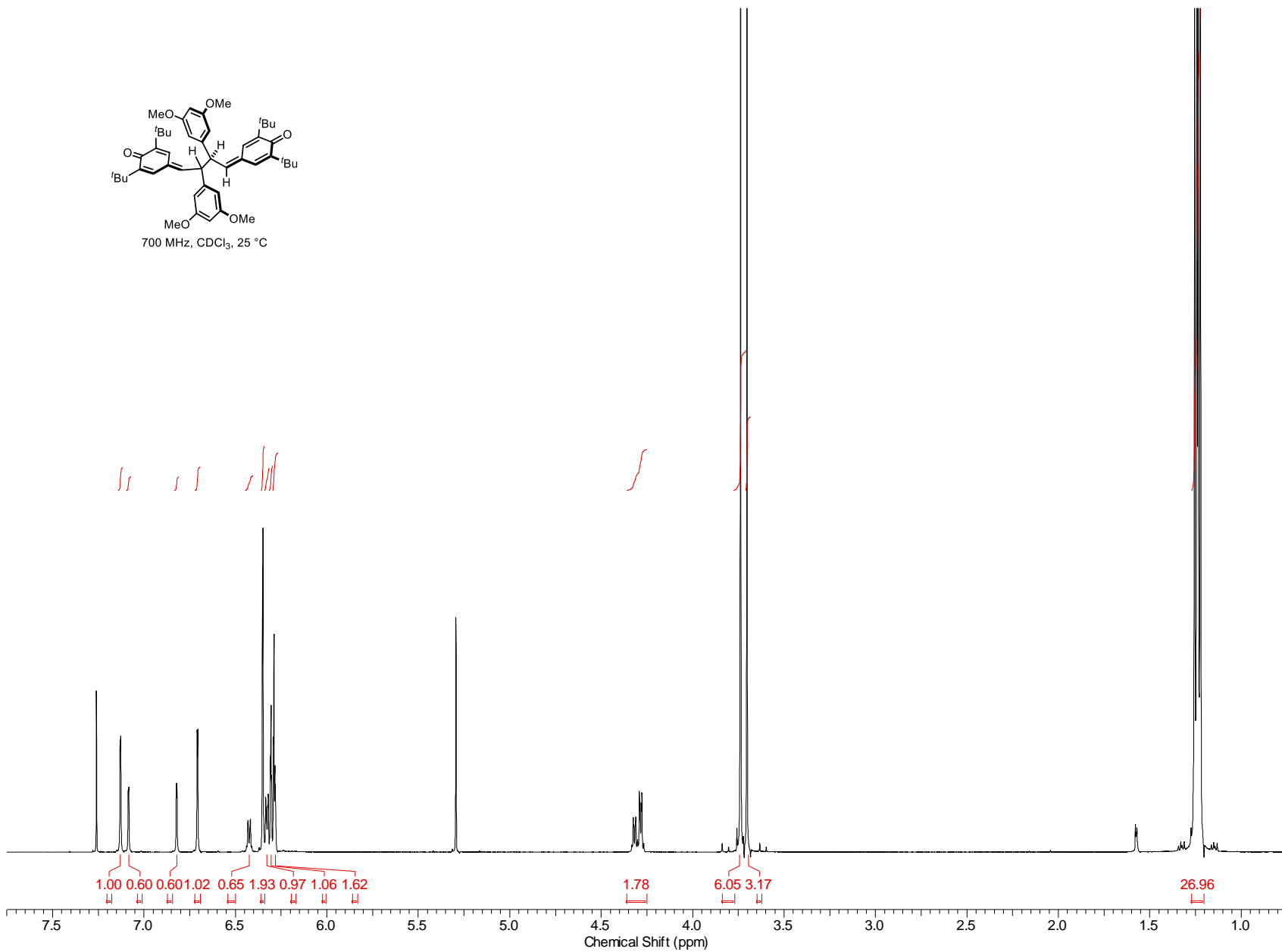




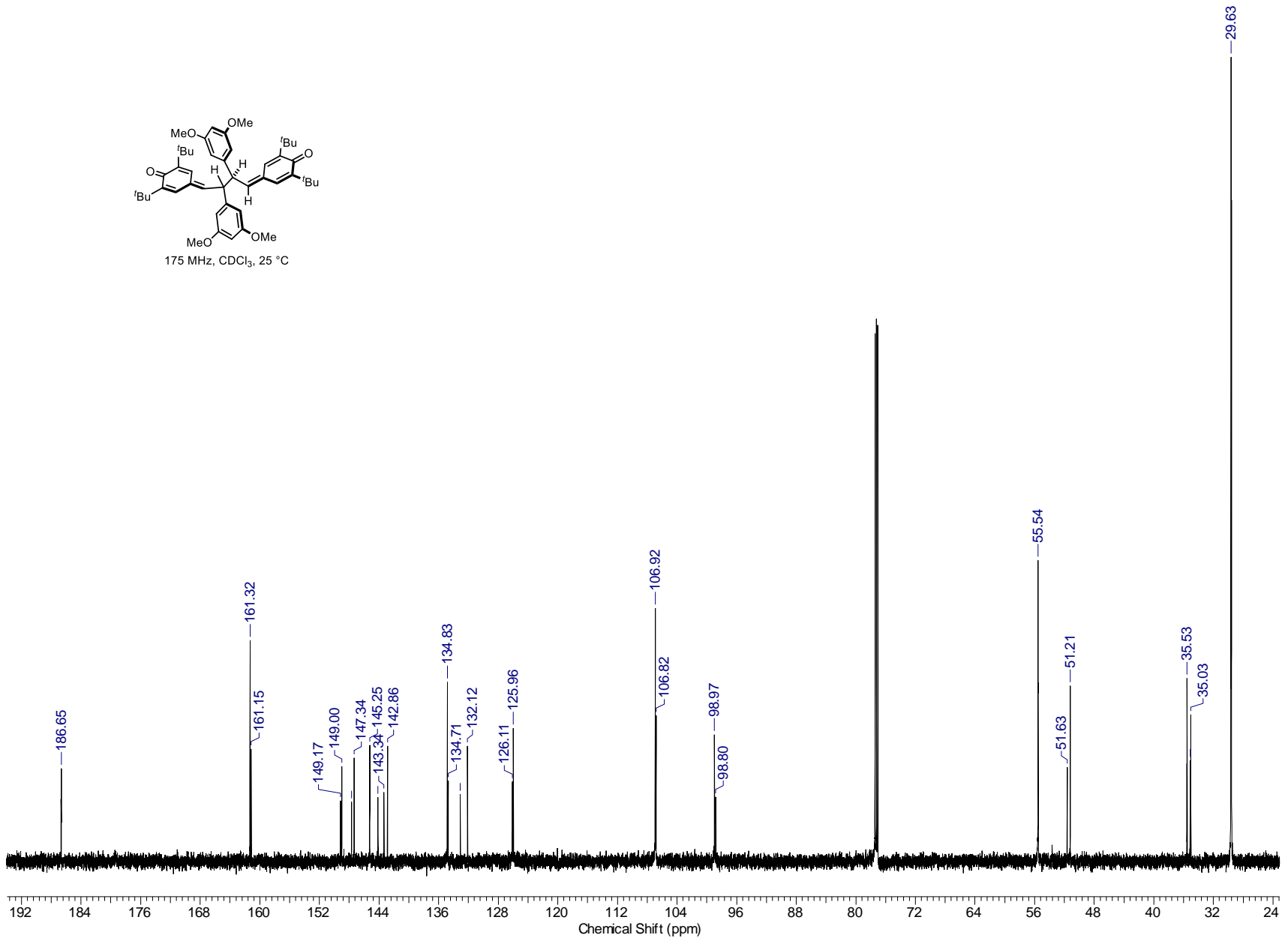
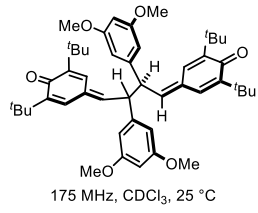


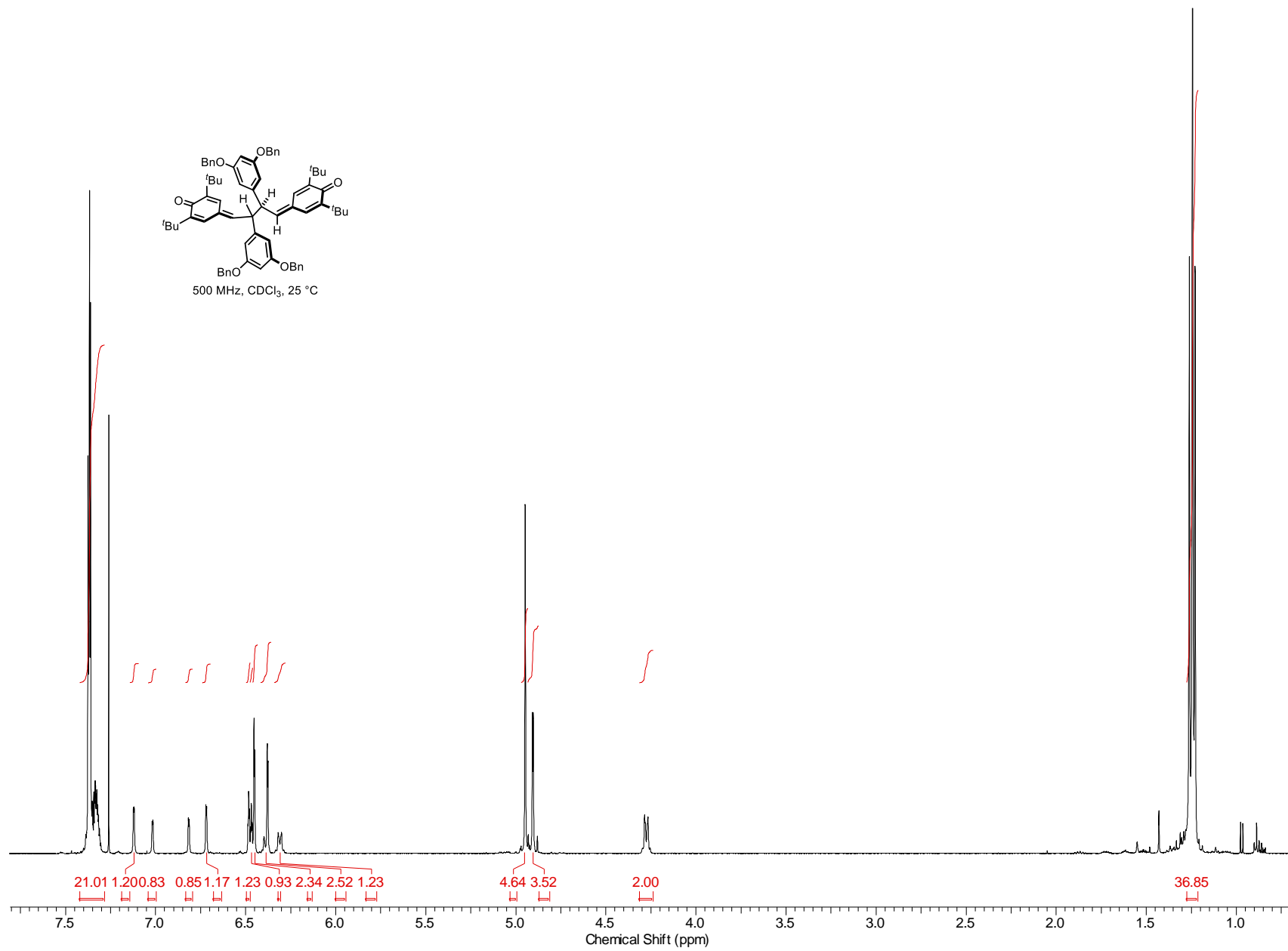


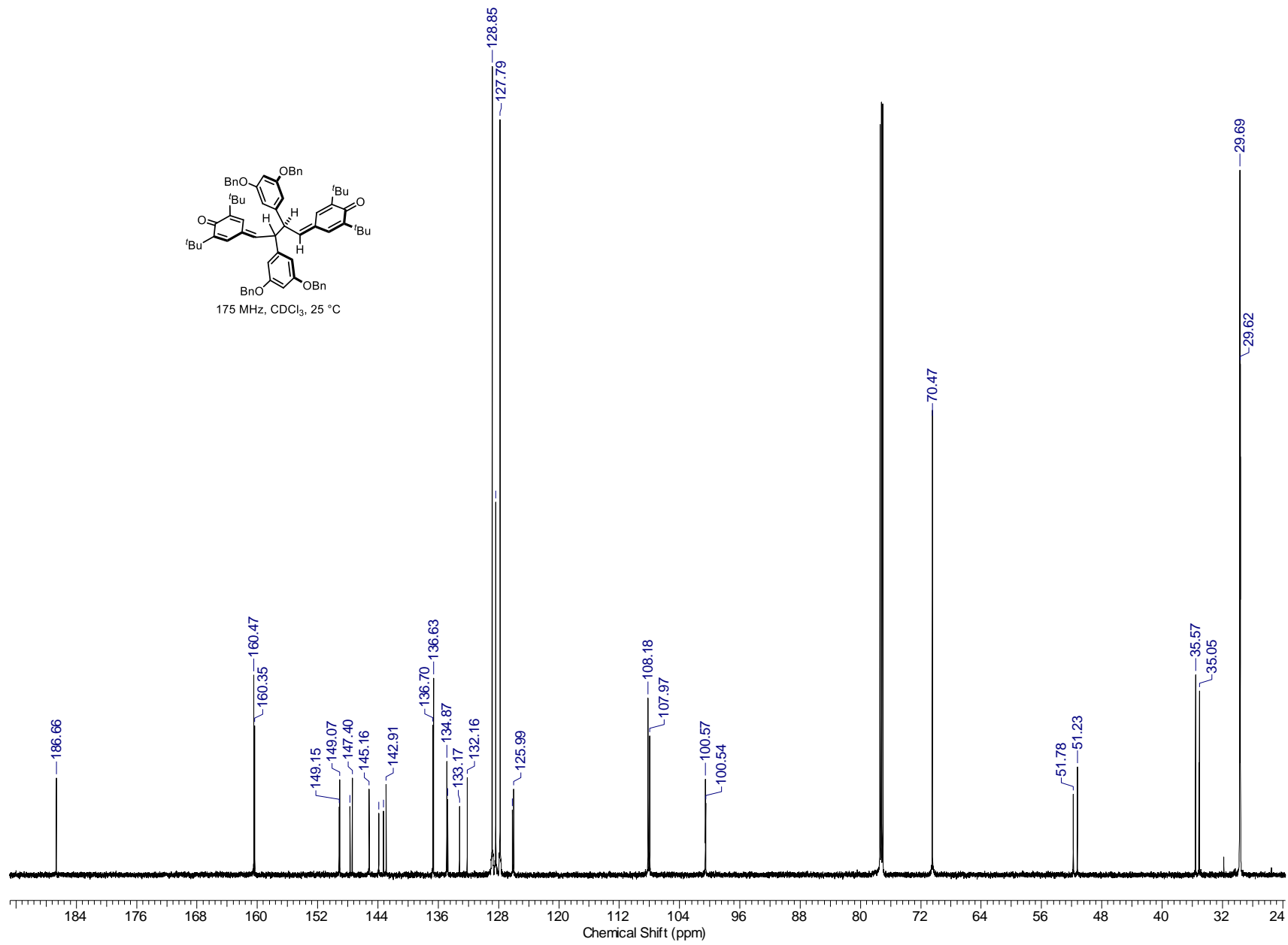
66

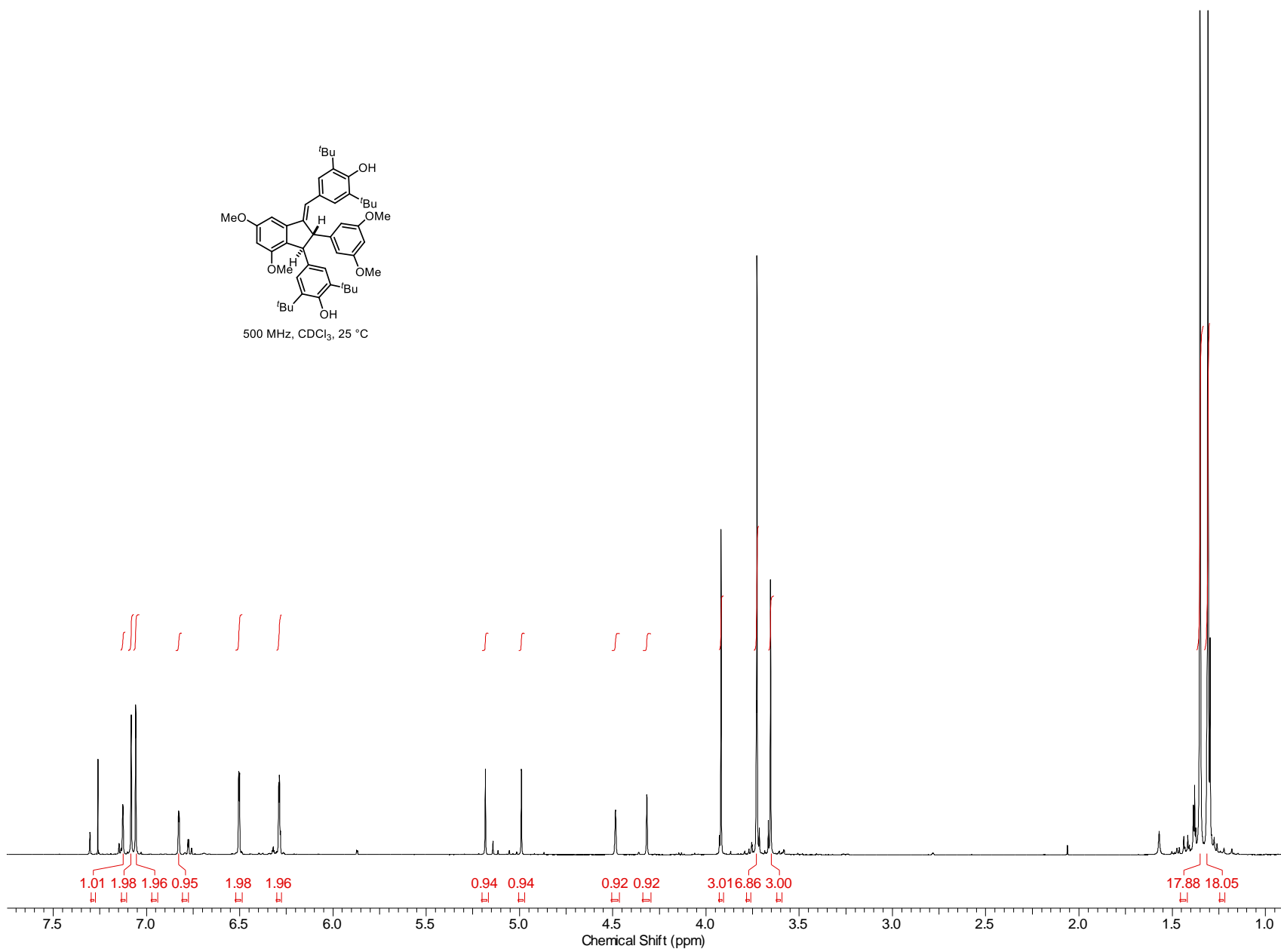
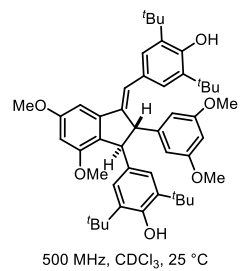


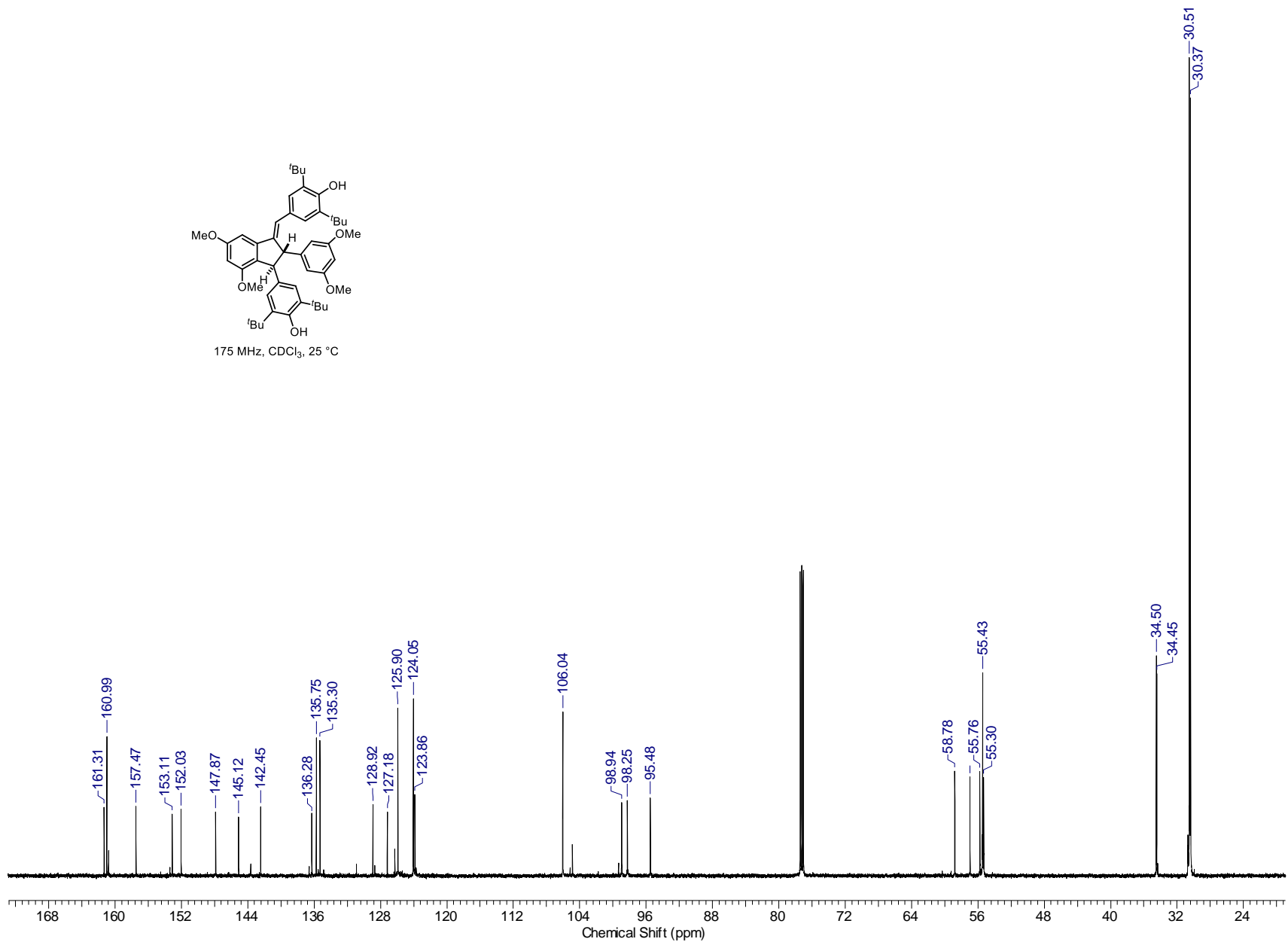
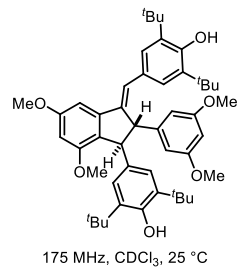
001

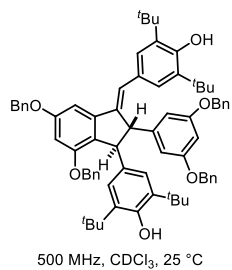




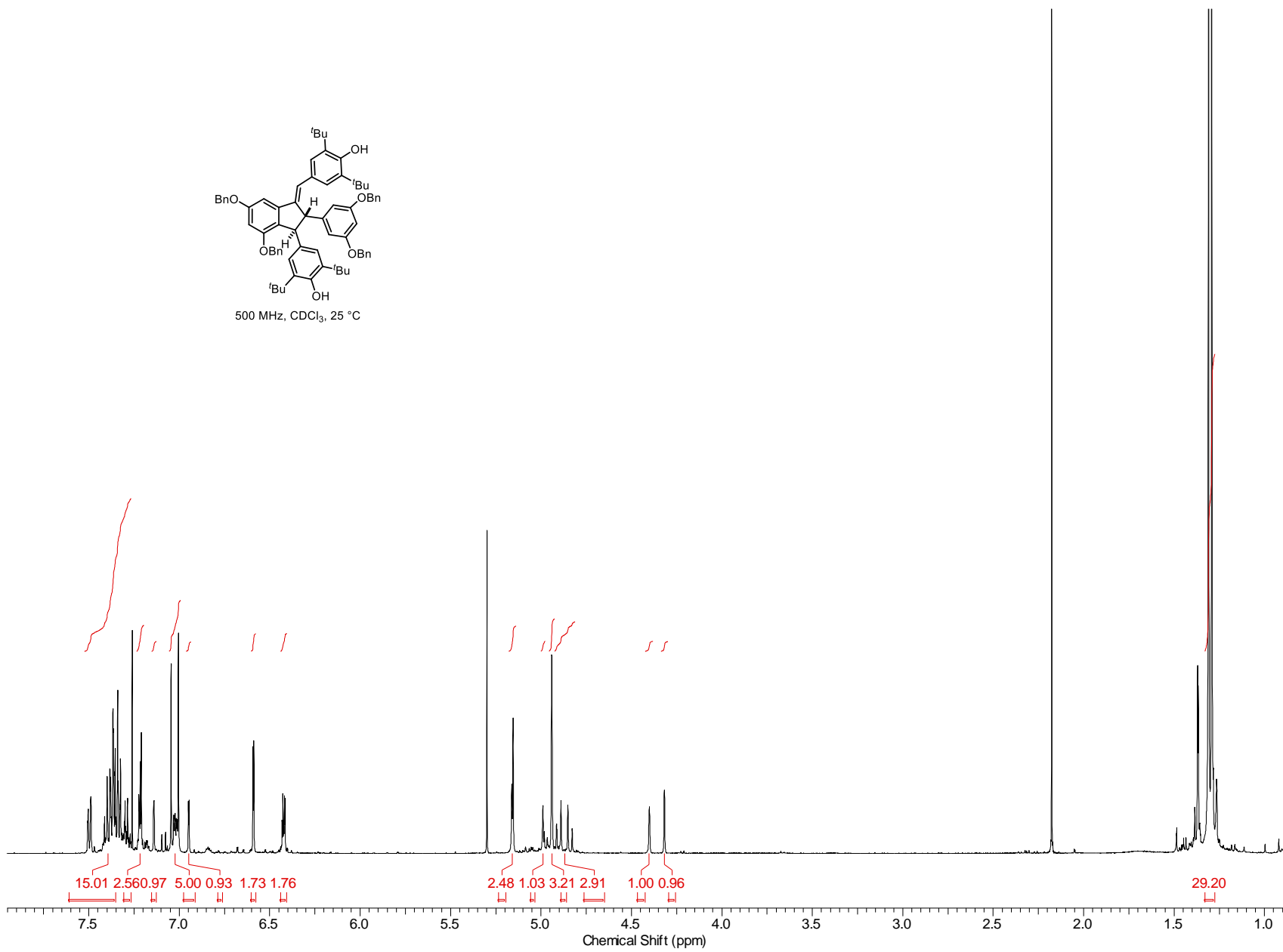


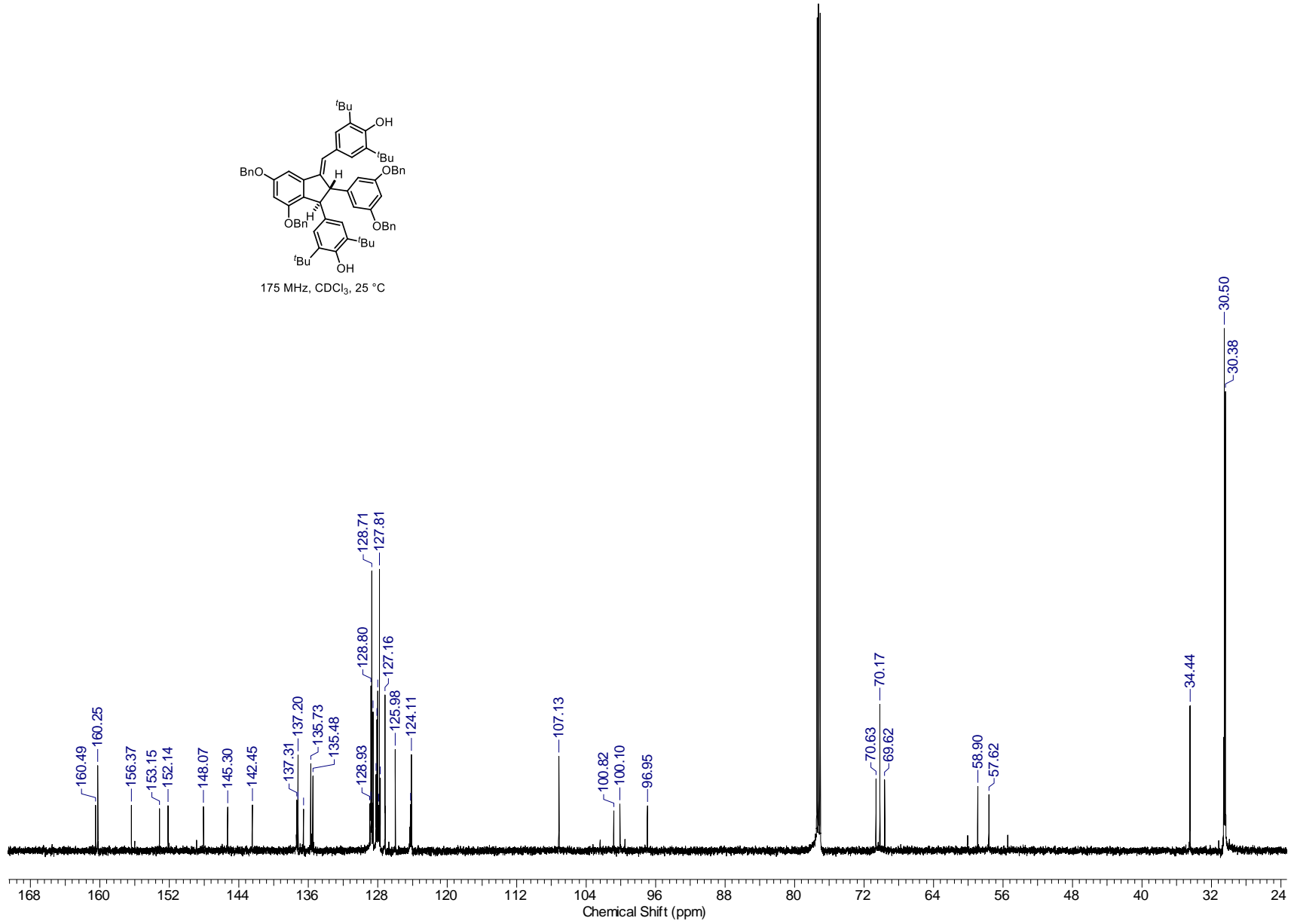
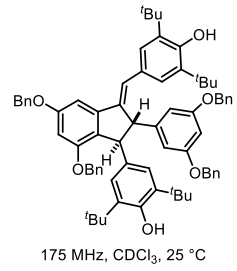


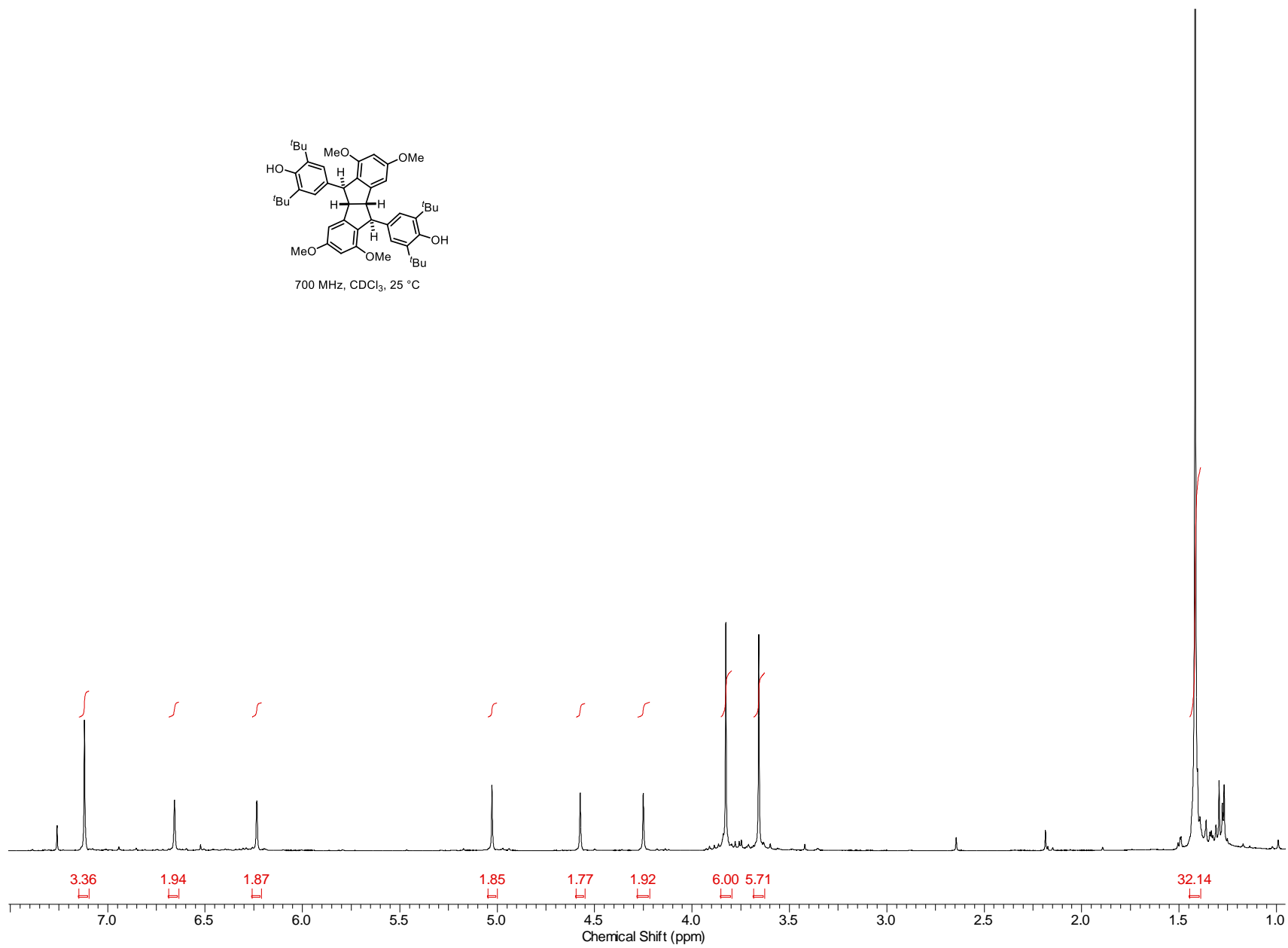
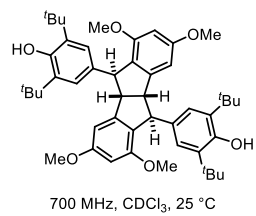


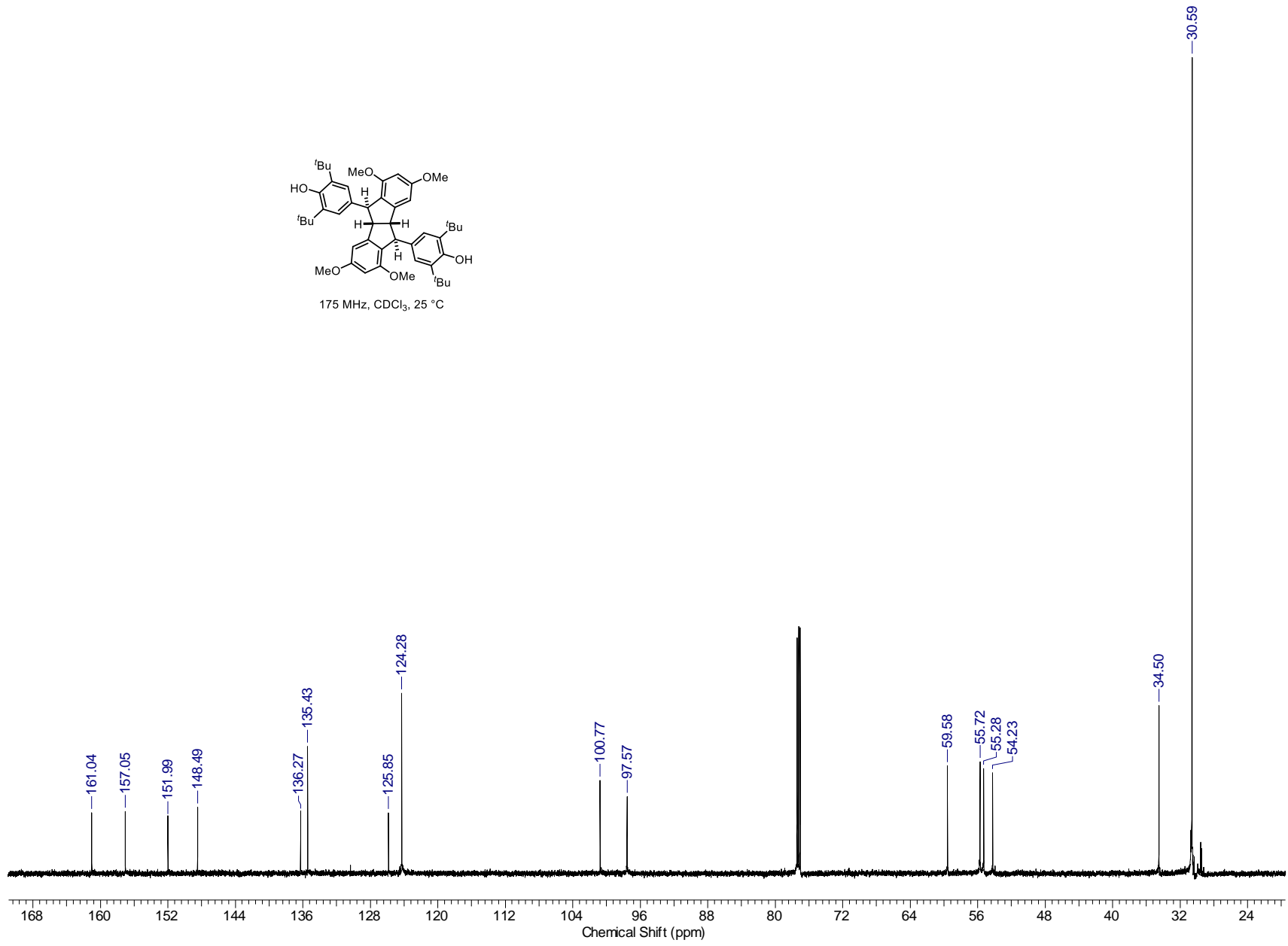
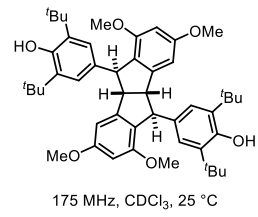


105

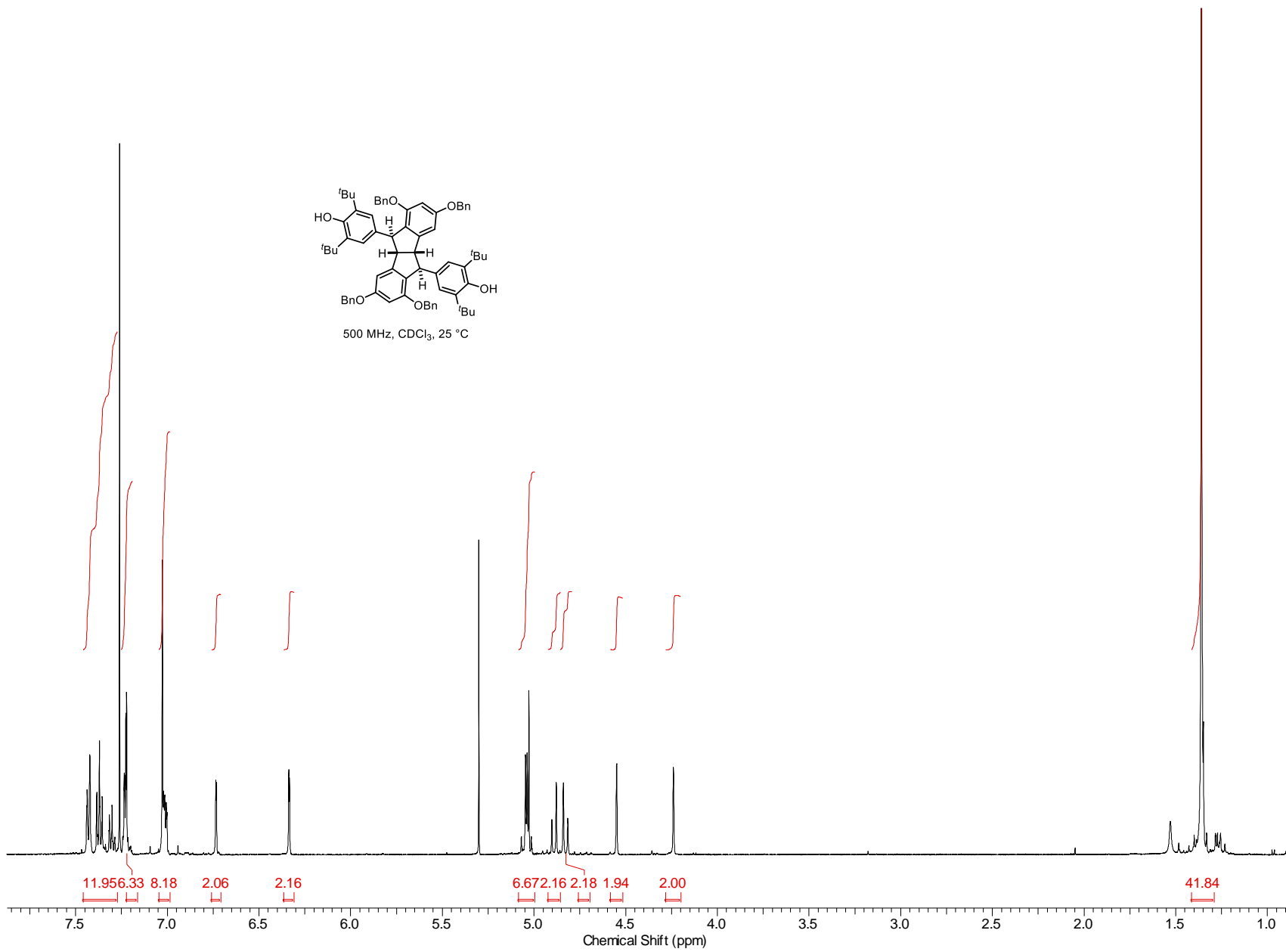
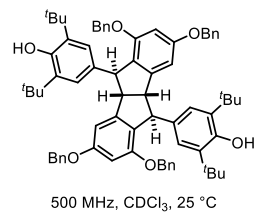


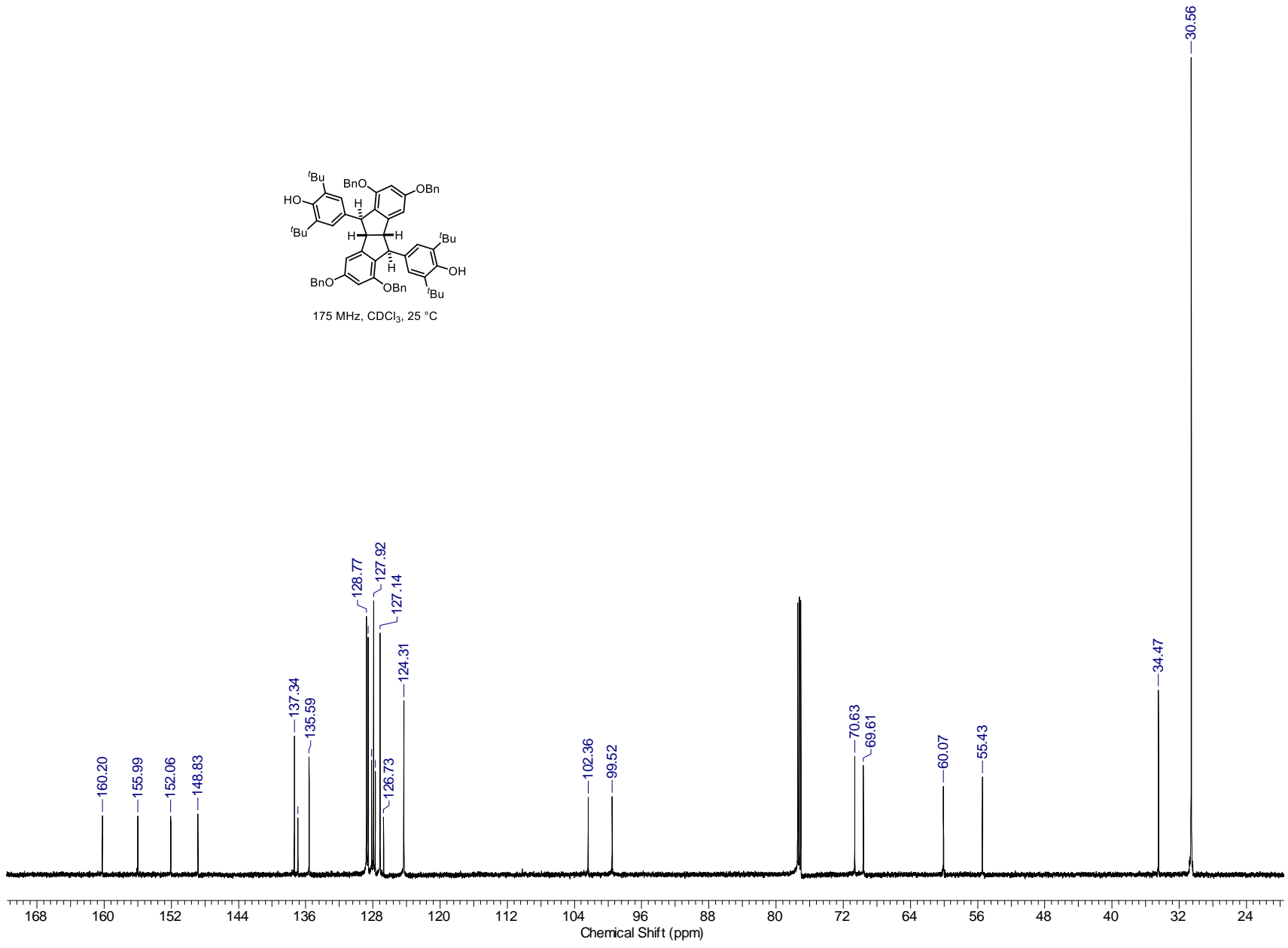
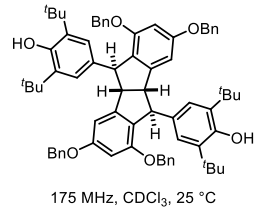


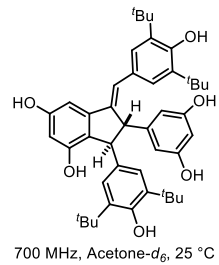




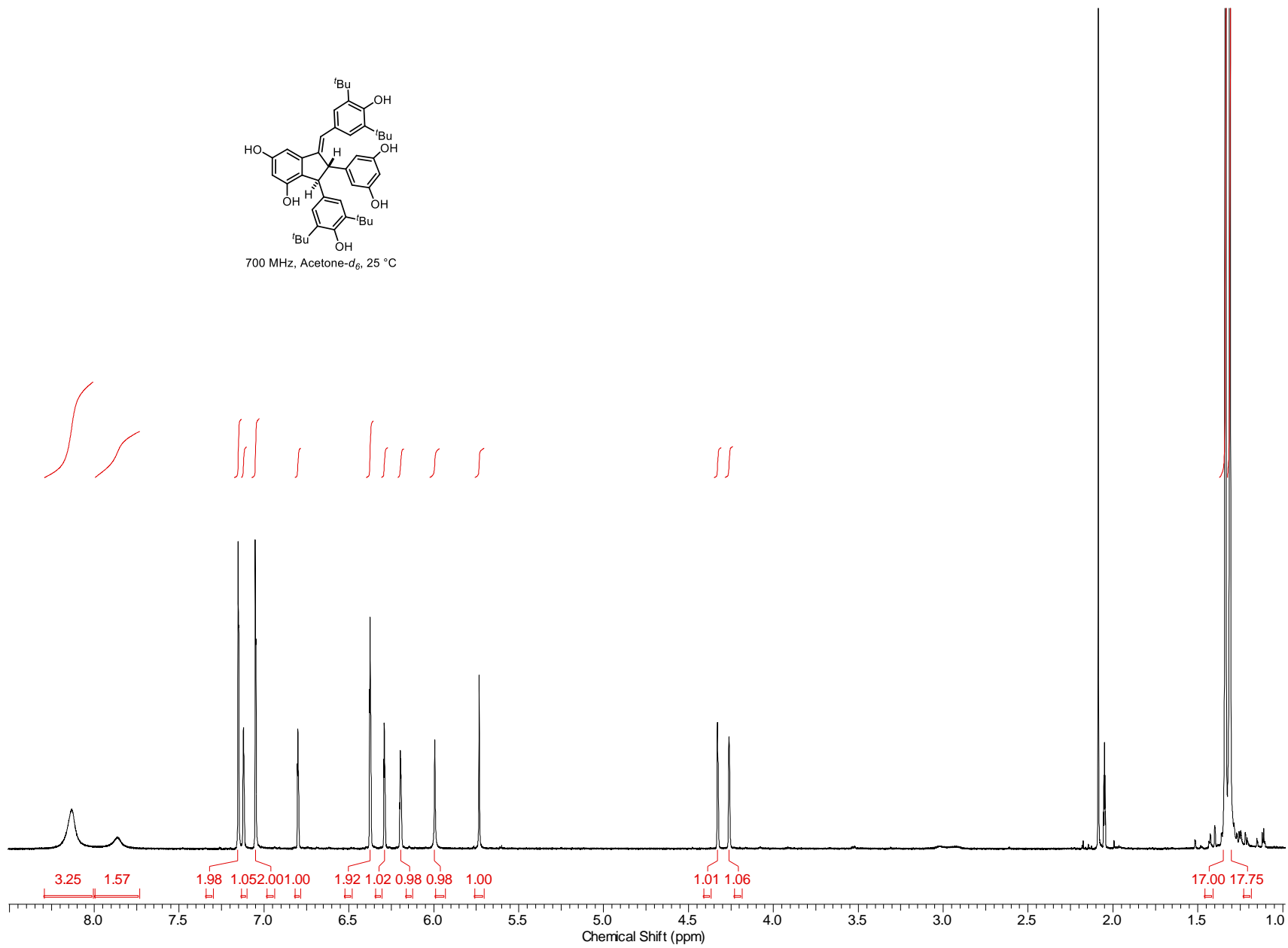
109

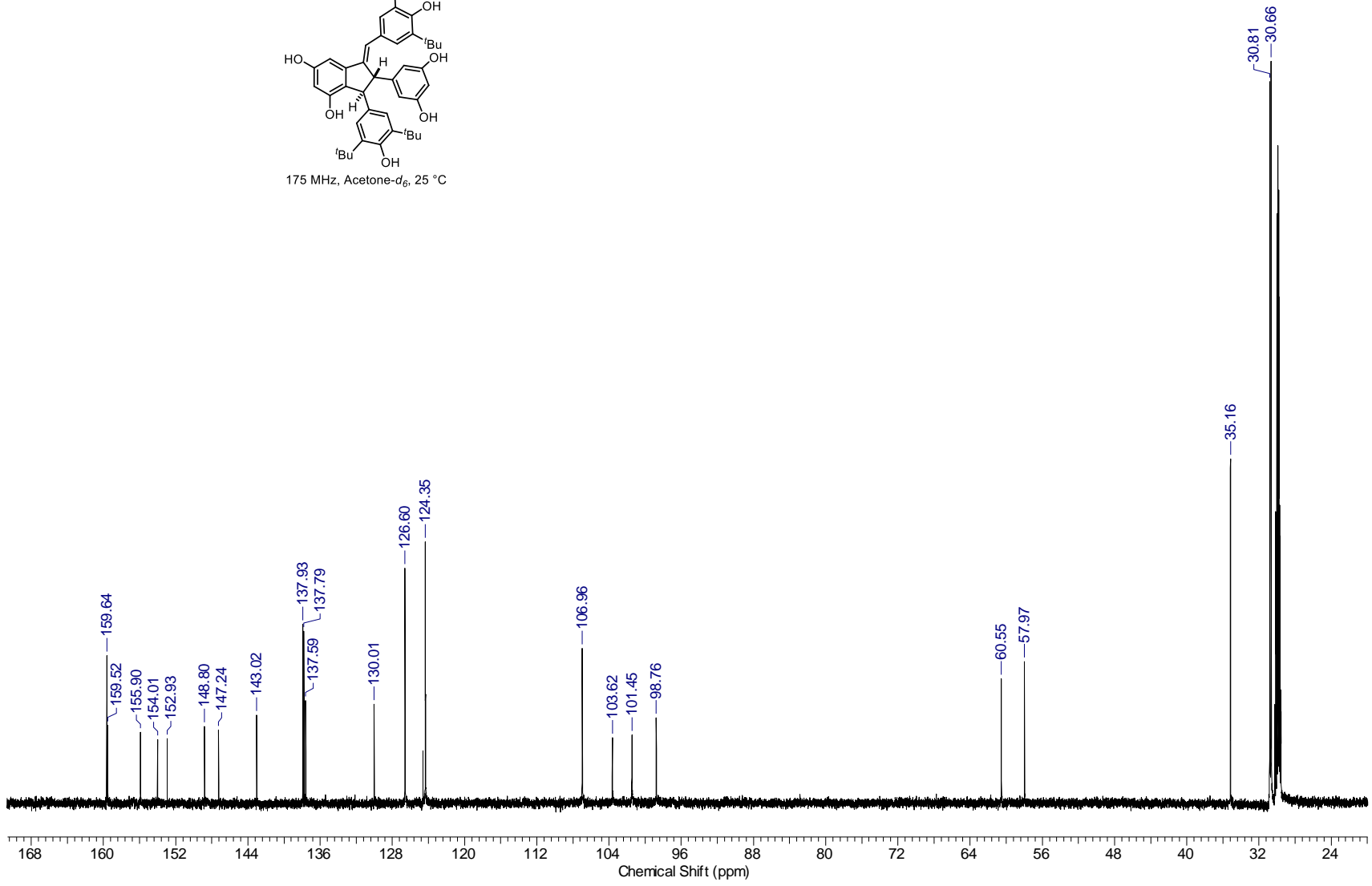
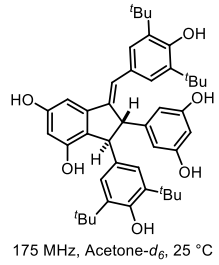


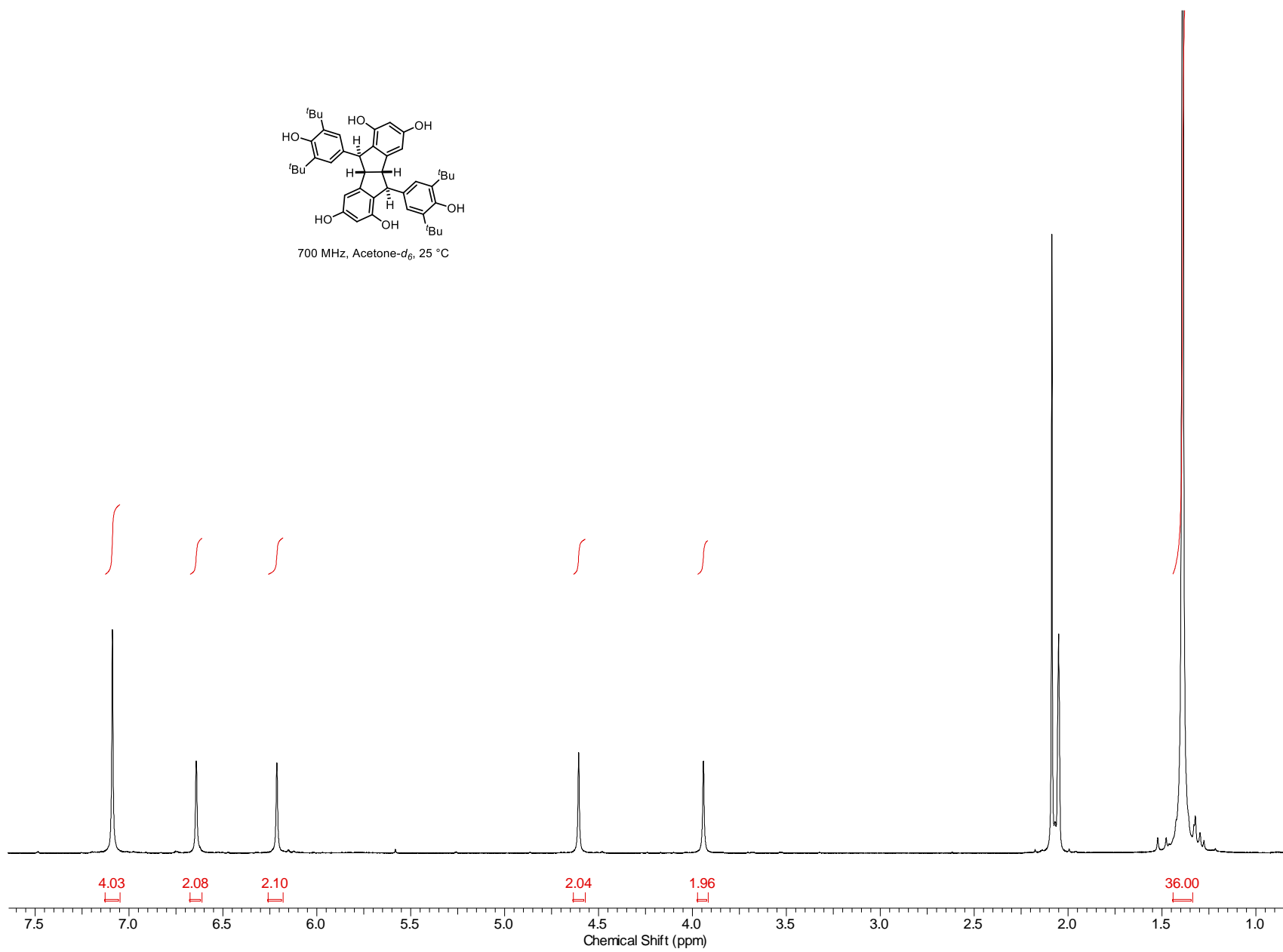
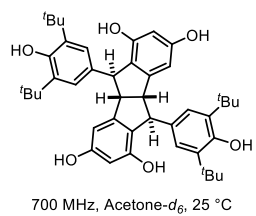


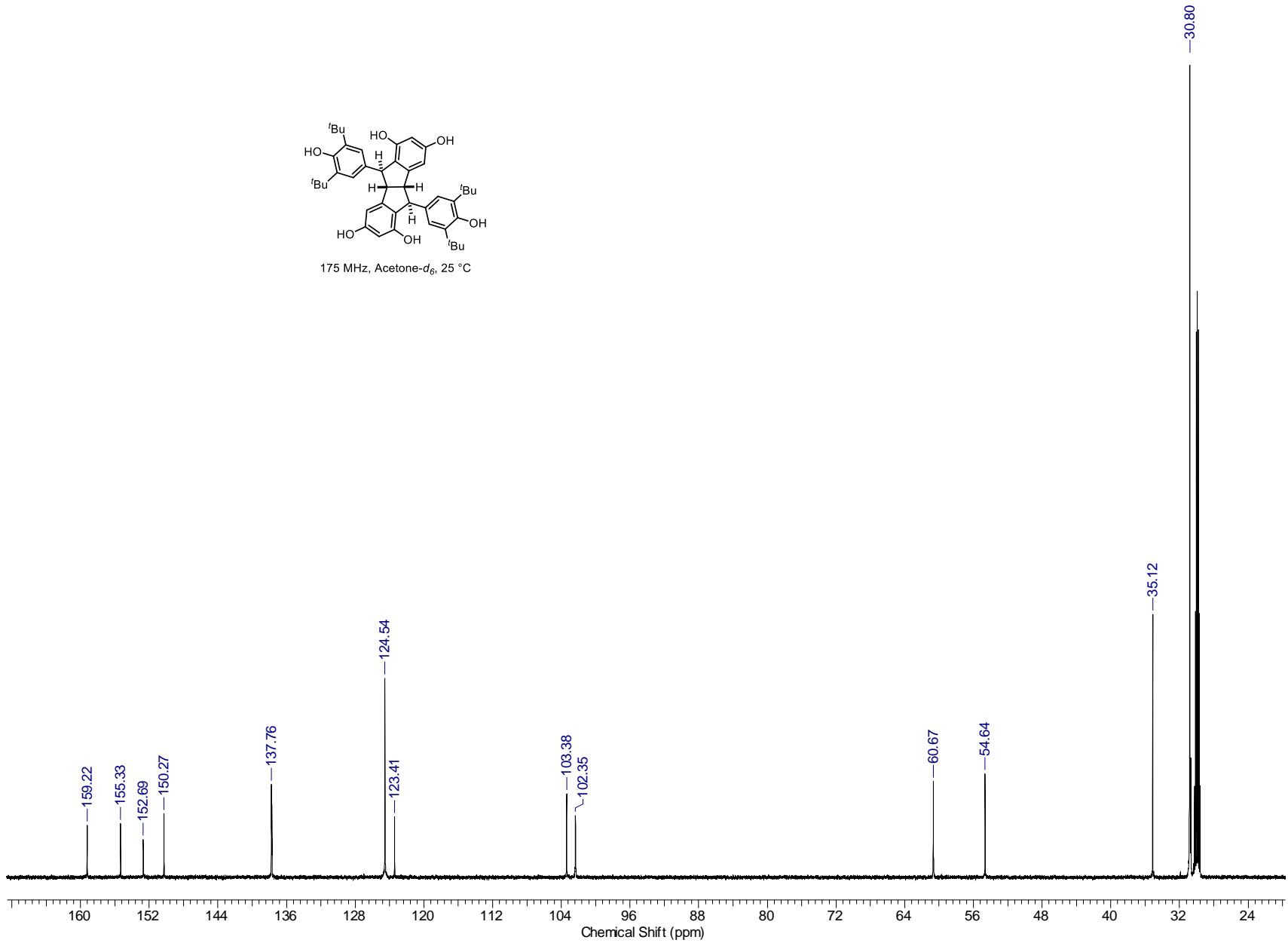
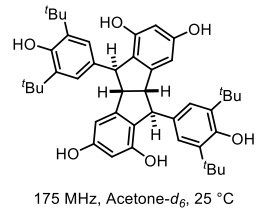


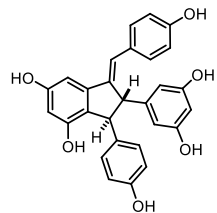
111





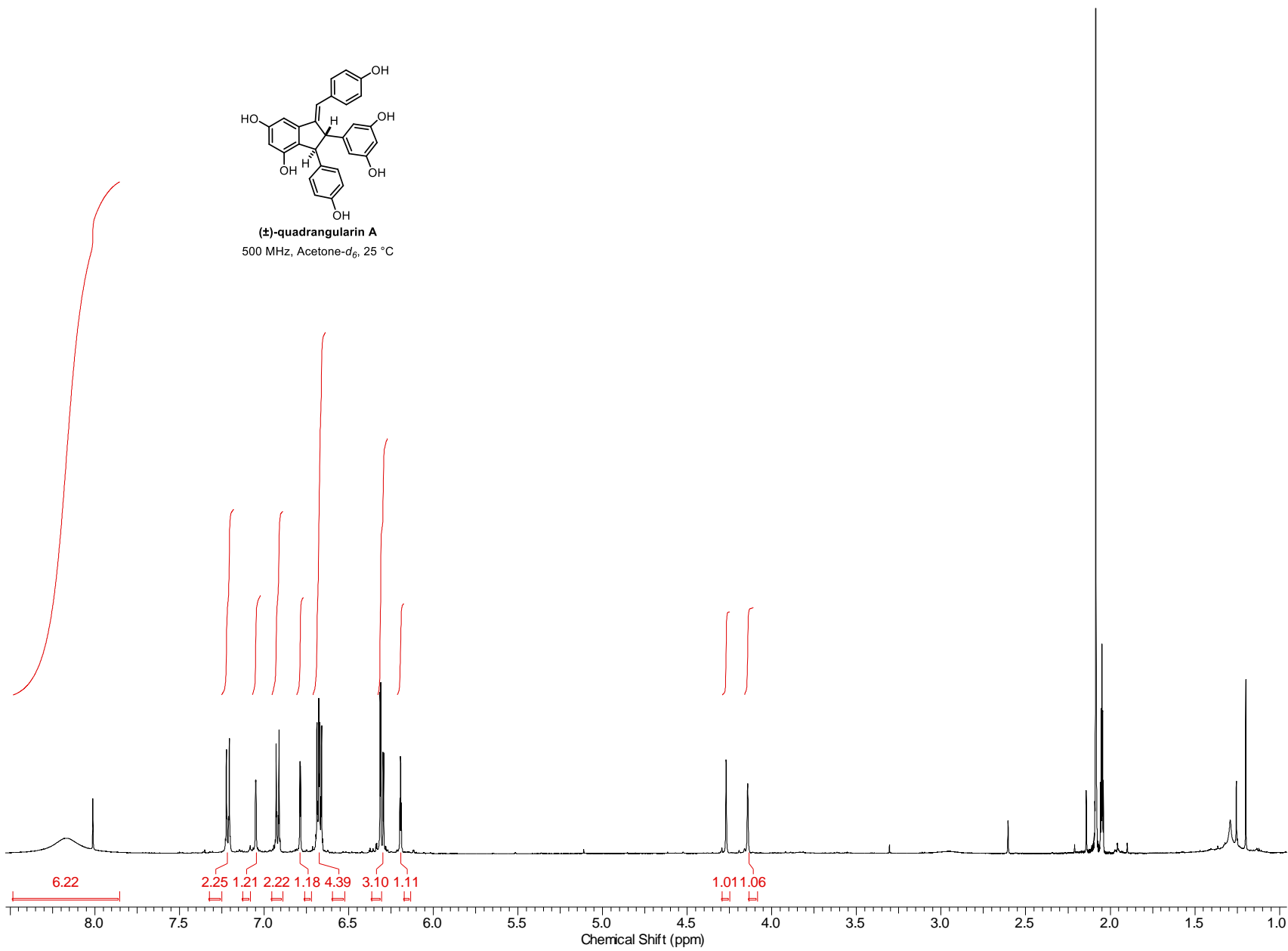


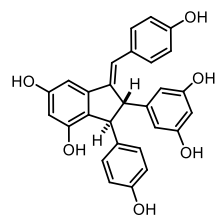
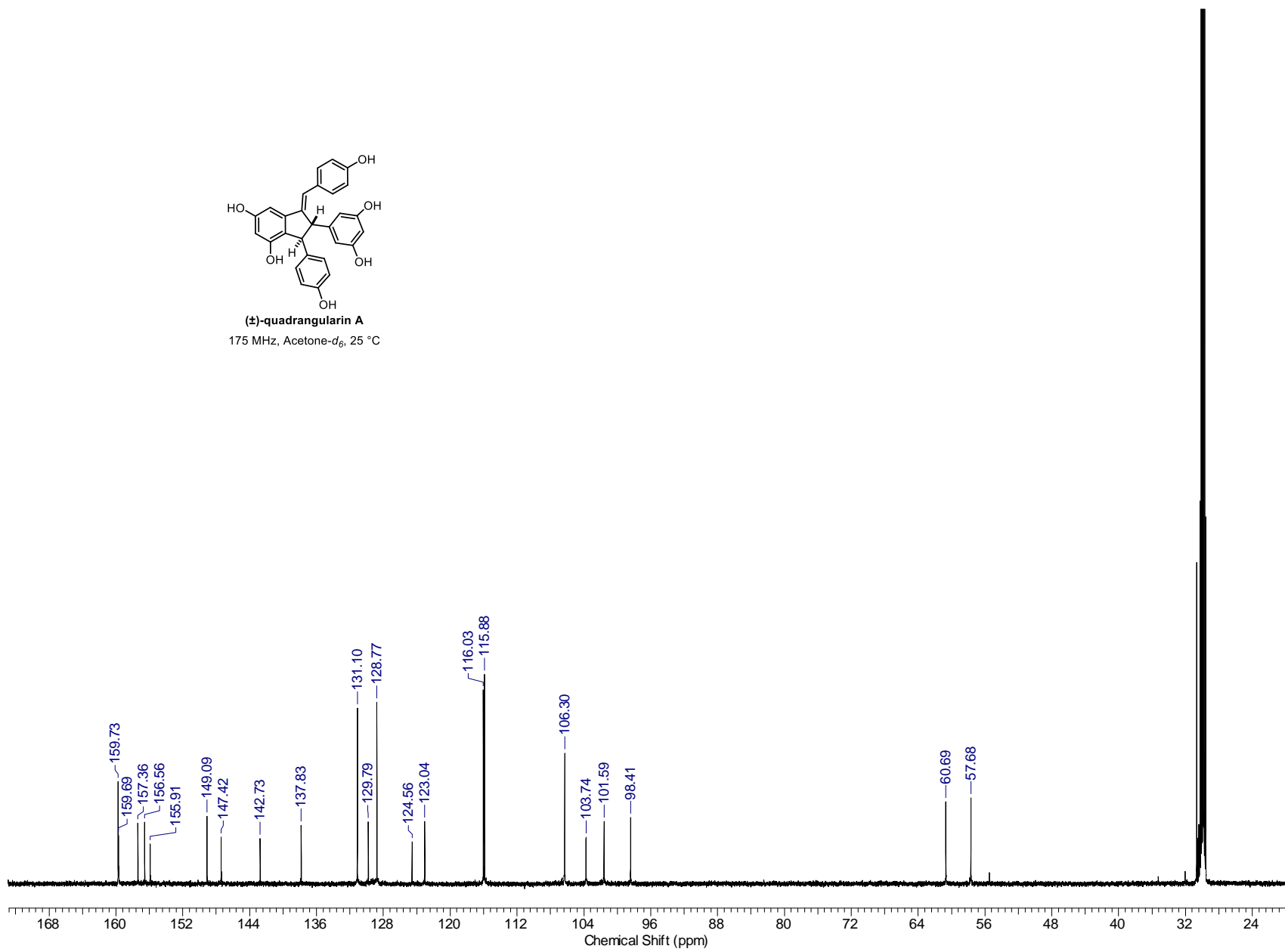


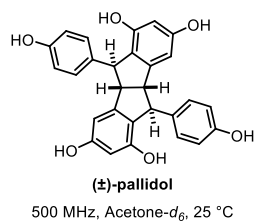


(±)-quadrangularin A
500 MHz, Acetone- d_6 , 25 °C

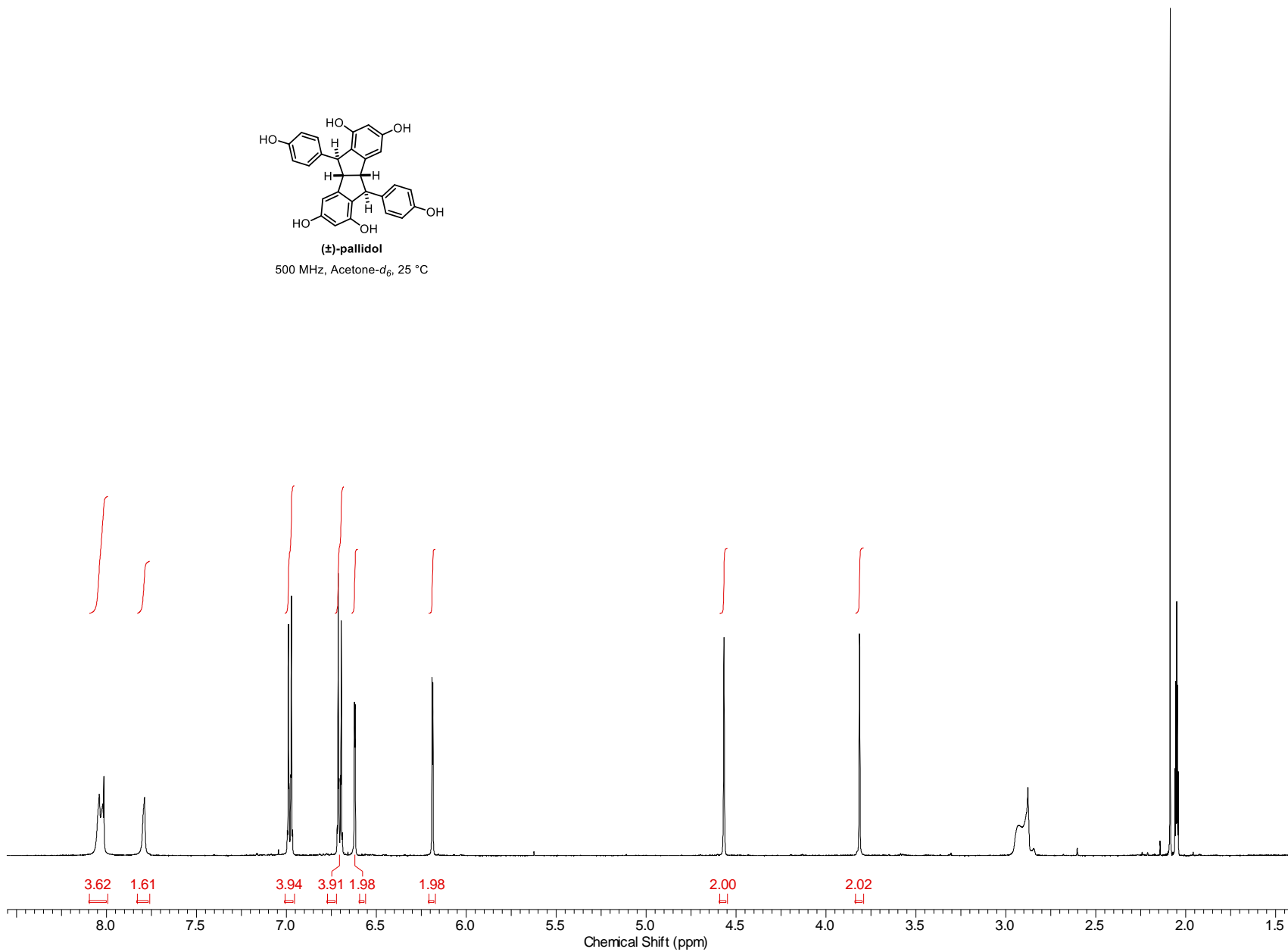
115

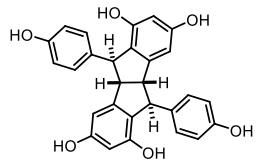
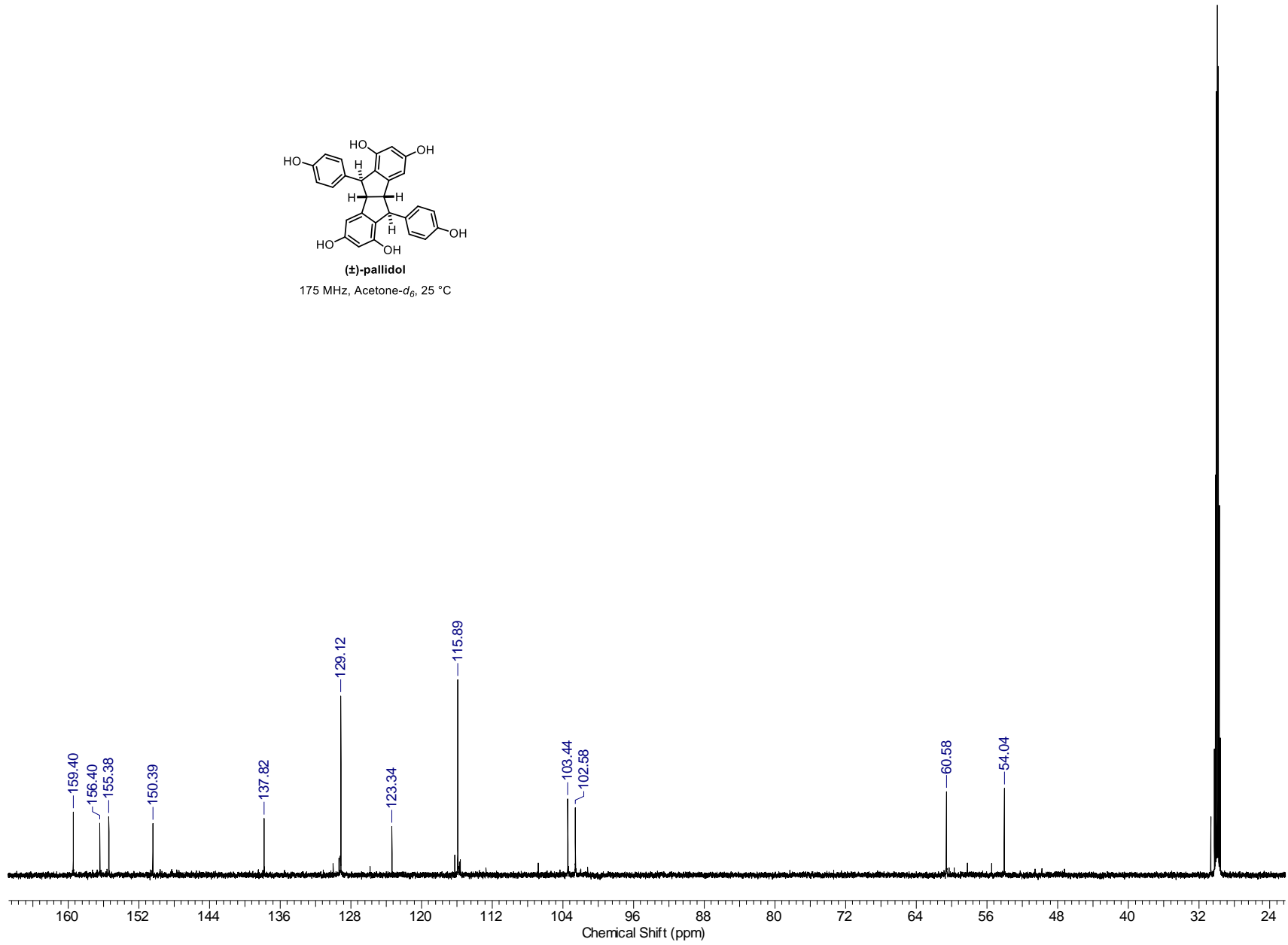


**(±)-quadrangularin A**175 MHz, Acetone- d_6 , 25 °C



117



**(±)-pallidol**175 MHz, Acetone- d_6 , 25 °C

**CHAPTER 3:
TOTAL SYNTHESIS OF RESVERATROL TETRAMERS
NEPALENSINOL B AND VATERIAPHENOL C**

3.1 Introduction

The precise role of resveratrol (**1.1**) and its oligomers in the plant is unknown. Due to the fact that the biosynthetic machinery responsible for resveratrol synthesis is not constitutively expressed but rather produced in response to biotic and abiotic environmental stresses, the stilbene product and its various derivatives have been broadly categorized as “phytoalexins”: antimicrobial defense metabolites which accumulate rapidly at sites of pathogenesis to neutralize invasive microorganisms and promote plant survival.^{12,204} Indeed, chemical defense against pathogenic invasion represents one of the most fundamental aspects of plant survival, part of the perpetual evolutionary arms race between the invasive species and host organisms. Most phytoalexins can be classified as either masked phenolics (isoflavonoids, stilbenes, phenanthrenes, benzofurans) or as terpenoids.²⁰⁵ Each of these frameworks originate from highly versatile building blocks, a common attribute that has enabled the natural creation of diverse libraries of complex molecules through oligomerizations, skeletal rearrangements, corresponding variations in stereochemical configuration and positional oxidation states, etc.²⁰⁶ This logic would imply that the secondary metabolites generated through these pathways can sample exponentially greater chemical space than — and therefore access a range of biological activities not available to — the starting monomer. While the goal in this scenario is likely random, uncontrolled production of chemical diversity, it is clear that a number of scaffolds have

emerged from this chaos through various selection pressures as a result of the advantages which they provide for plant survival.

As witnessed with terpenoids in the 20th century, the conversion of isoprene by living organisms into varied and complex secondary metabolites with important biological functions often leads to chemical frameworks with broadly useful pharmacological properties that transcend their natural role. It stands to reason that this is also true of other natural product families. Yet, for medicinally relevant complex terpenoids, progress in our understanding of their biological activity has largely been made possible through procurement from natural sources of advanced biogenic precursors which can be transformed to the target of interest through semi-synthesis and adapted for human use.²⁰⁷ The same cannot be said of other classes of compounds, including the resveratrol oligomers. Indeed, the relatively nascent biological investigations of resveratrol and its oligomers appear to reveal a correlation between complexity and biological activity, at least in the early stages (monomer – tetramer) of oligomerization (see Sections 1.4 – 1.6). Thus, synthetic advances must be made in order to confirm/refute the biological activities ascribed to oligomers obtained from isolates, to determine which scaffolds hold potential as small molecule chemopreventives and/or chemotherapeutics, and to enable structural modification for both structure-activity relationship (SAR) studies and the development of more potent congeners.

3.2 Existing Approaches to the Synthesis of Higher-Order Resveratrol Oligomers

Resveratrol dimers have been targeted through a variety of synthetic approaches, both biomimetic (Sections 2.2, 2.3, 2.6) and *de novo* (Section 2.4 and reference [19]). In contrast, only a single synthetic strategy — a *de novo* approach developed by Snyder and co-workers — exists for the preparation of higher-order resveratrol oligomers.^{138,142,143} With the exception of Sako's

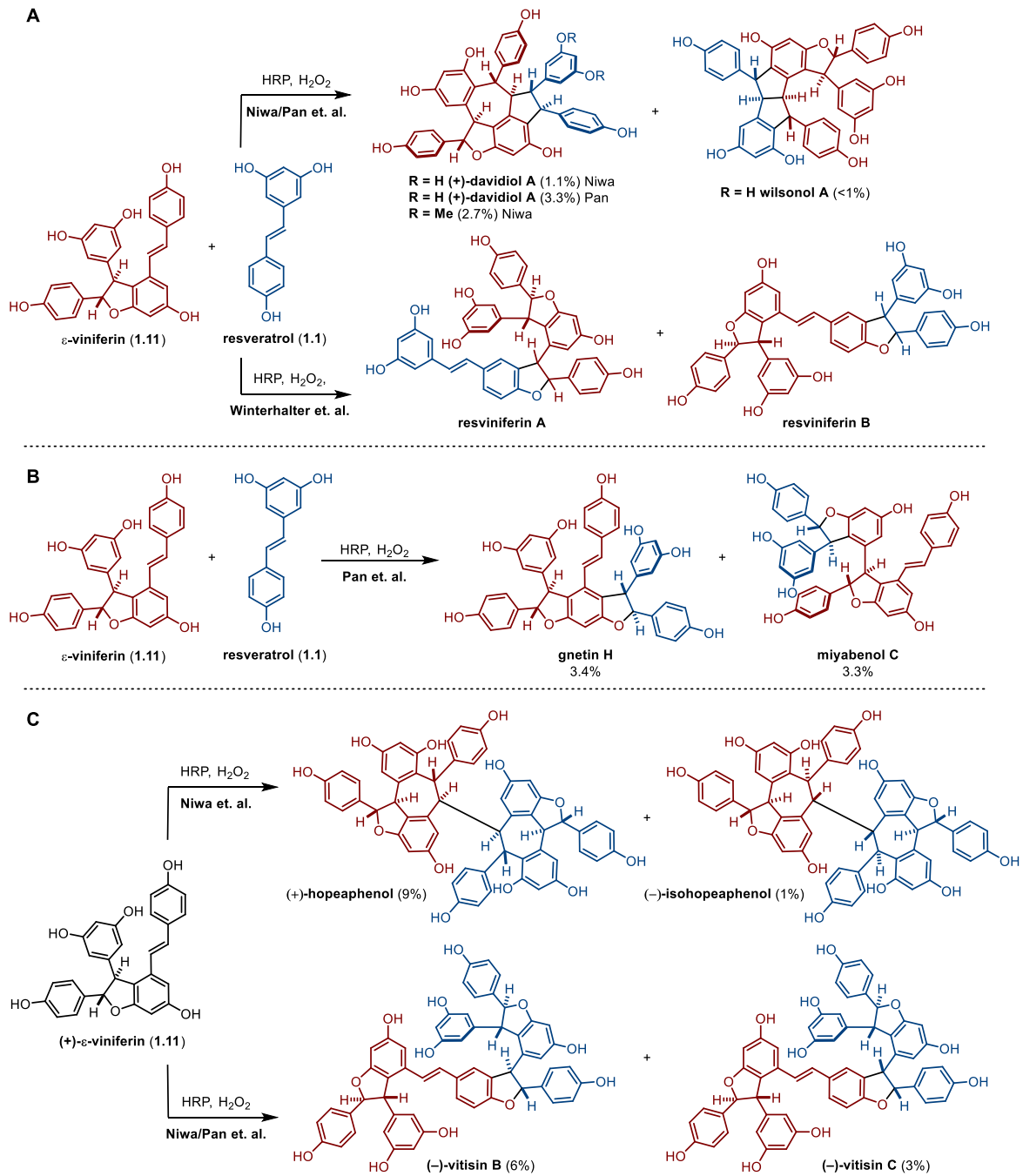


Figure 3.1 Biogenic Studies on A) 8–8' Trimers, B) 8–10' Trimers, and C) 8–8' Tetramers

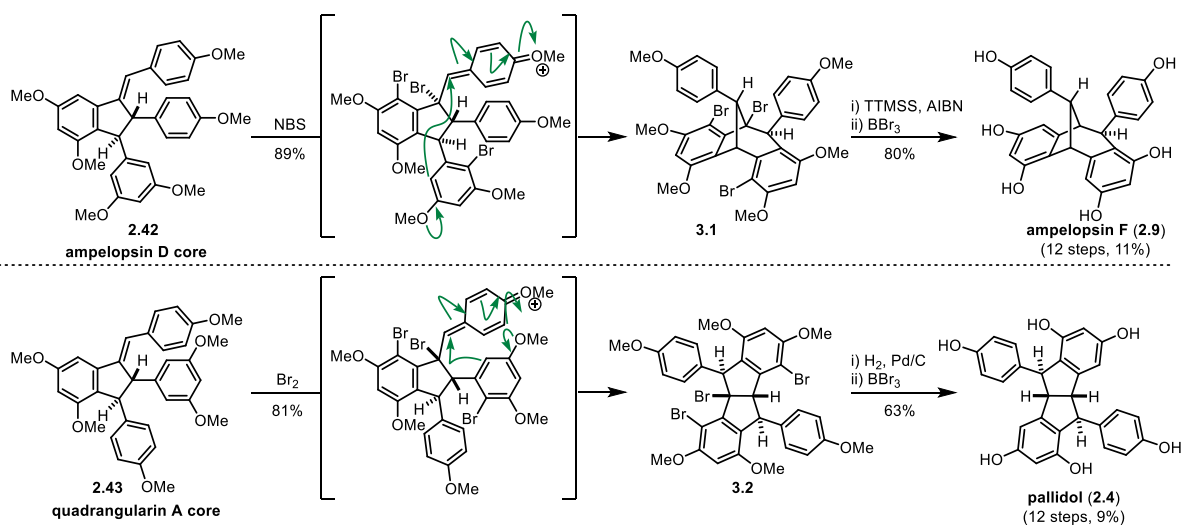


Figure 3.2 Transformation of Indane Dimers to [3.2.1] and [3.3.0] Bicyclooctanes

remarkable synthesis of the tetramer vitisin B (**2.14**) (Figure 2.3),¹⁵ biomimetic studies in this vein have been performed exclusively with the goal of providing empirical support for the biogenesis of these compounds and establishing their absolute configurations. The most relevant examples of this chemistry are presented in Figure 3.1,^{39,208–210} and the yields isolated from the complex mixtures that were obtained in these studies illustrate the fact that biomimetic semisynthesis is not yet a feasible concept for the preparation of these compounds.

In an initial extension of their synthetic strategy to indane-containing resveratrol dimers (Section 2.4), Snyder and co-workers sought to exploit the inherent polarization of the methoxy styrene moiety present in compounds **2.42** and **2.43** to effect their interconversion to the remaining two dimeric structural sub-types: the bicyclo[3.2.1]octanes (e.g. ampelopsin F (**2.9**)) and the bicyclo[3.3.0]octanes (e.g. pallidol (**2.4**)).¹³⁷ Each of these transformations was accomplished via electrophilic bromine-mediated activation of these olefins which smoothly transformed **2.42** and **2.43** to the trihalo- natural product precursors **3.1** and **3.2** (Figure 3.2). Sequential hydrodehalogenation and demethylation provided the natural products ampelopsin F (**2.9**) and pallidol (**2.4**).¹³⁷

While the requirement for removal of the bromides negatively impacts the step- and atom-economy for the synthesis of dimeric natural products, the complete regioselectivity observed during their introduction has enabled the synthesis of a number of higher-order oligomers. These seemingly extraneous aryl bromides provide functional handles with which to target the construction of 2,3-diaryldihydrobenzofurans for the synthesis of trimeric and tetramer resveratrol-derived oligomeric natural products (*vide infra*). The development by Snyder and co-workers of a robust synthetic sequence for the conversion of *ortho*-bromo phenols to 2,3-disubstituted dihydrobenzofurans (DHBs) was truly an enabling technology for the chemical synthesis of higher-order resveratrol oligomers.^{138,142,143}

In spite of the prevalence of DHBs in bioactive molecules,^{101,102} there are a paucity of methods for their construction in complex settings, particularly for sterically demanding variants bearing substitution at the 2-, 3-, and 4-positions. Snyder and co-workers were able to develop a nine-step homologation sequence of *ortho*-bromo phenols featuring a Johnson–Corey–Chaykovsky epoxidation^{211,212} and Meinwald rearrangement²¹³ to ultimately afford the desired 2,3-diaryl DHB (Figure 3.3). The application of this strategy to the [3.2.1] (**3.3**) and [3.3.0] (**3.2** and **3.4**) bicyclooctane cores provided access to five distinct trimers and tetramers in a groundbreaking synthetic effort (Figure 3.4).¹³⁸

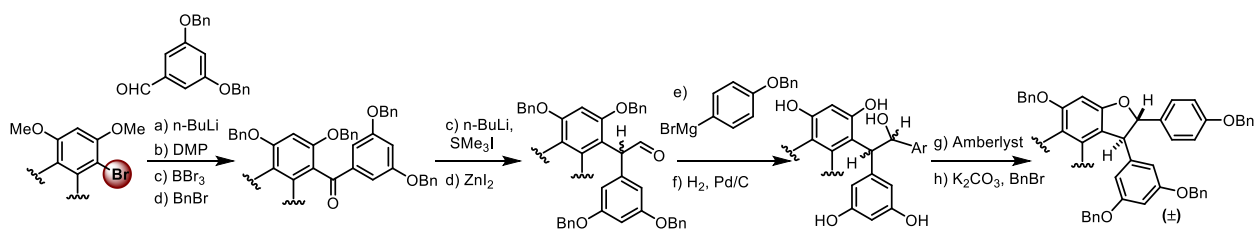


Figure 3.3 Paradigm for DHB Synthesis through Iterative Homologation

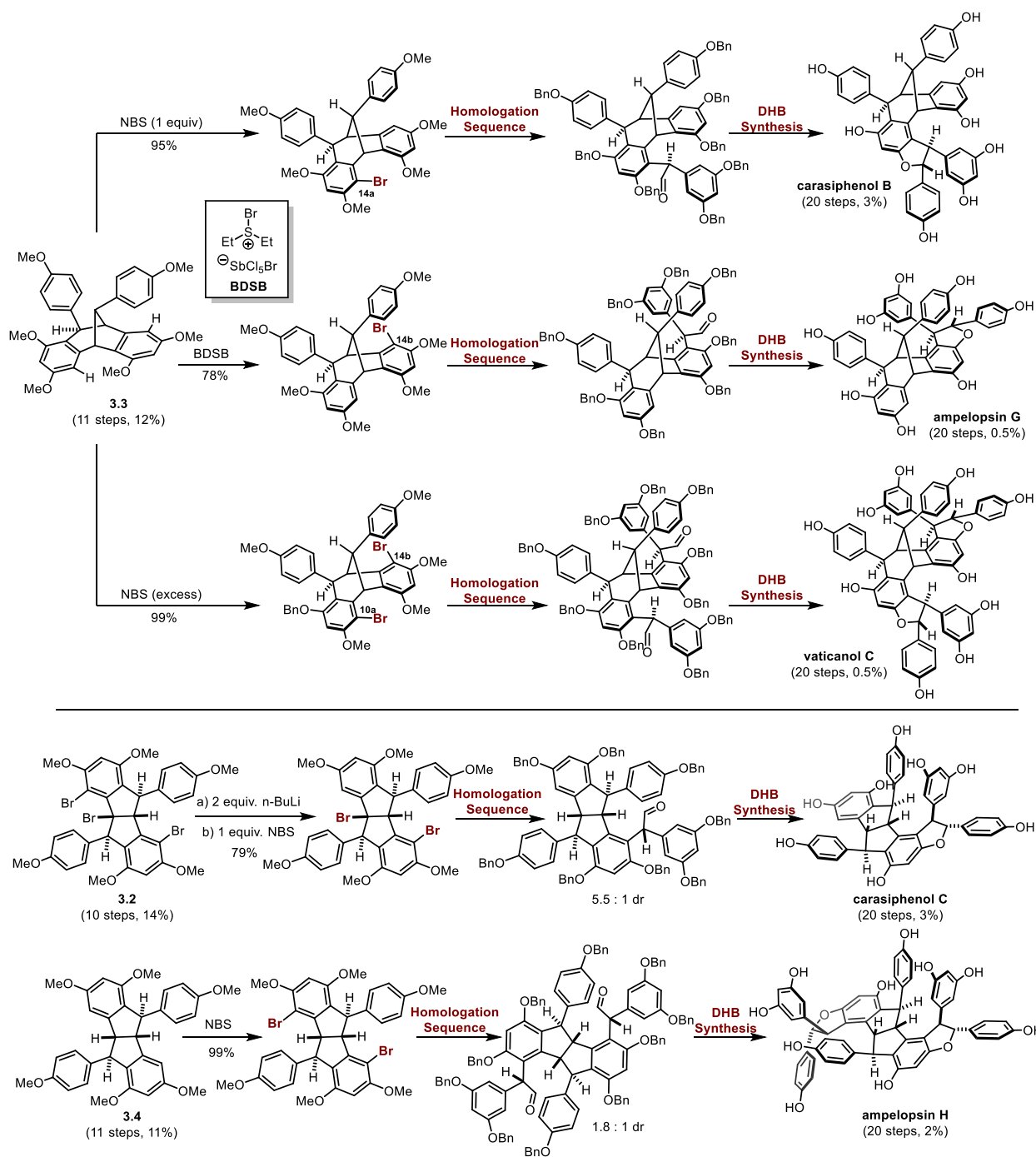


Figure 3.4 Snyder's Synthesis of [3.2.1] and [3.3.0] Bicyclooctane Resveratrol Trimers and Tetramers via Desymmetrization or Two-Directional Synthesis from Dimeric Cores

3.3 Concept for Biomimetic Synthesis of Higher-Order Resveratrol Oligomers

Conceptually, Snyder's strategy for higher-oligomer synthesis is orthogonal to commonly accepted hypotheses regarding the biosynthesis of these compounds. Namely, this *de novo* approach entails either desymmetrization of, or two-directional^{214,215} synthesis from, dimeric cores for the construction of trimers and tetramers respectively, via iterative homologation reactions in a fashion similar to the biogenesis (and chemical synthesis) of polyketide natural products.²¹⁶ Compare this with the convergent assembly of ϵ -viniferin (**1.11**) and resveratrol (**1.1**) fragments through oxidative coupling pathways (Figure 3.1) that are evocative of those employed during the biogenesis of resveratrol dimers (cf. Sections 1.2 – 1.3).

Based on this analogy, we began to consider whether it would be possible to target the synthesis of higher-order resveratrol oligomers — specifically trimers and tetramers — utilizing a similar biomimetic strategy to that which was implemented for the preparation of quadrangularin A (**1.10**) and pallidol (**2.4**) (Section 2.6).¹²⁵ Central to the execution of that synthesis was the development of conditions which provided scalable access to key bis-quinone methide intermediate **2.56**. Of course, the extension of this chemistry to the synthesis of higher-order oligomers would require the identification of those natural products whose biosynthesis conceivably proceeds via an analogous 8–8' coupling. Indeed, in their studies on the structural elucidation and biogenesis of resveratrol oligomers, Niwa and co-workers invoke bis-quinone methides as common intermediates for the biosynthesis of a number of tetramers from ϵ -viniferin (**1.11**). Application of this logic to retrosynthetic design reduces the synthesis of all 8–8' linked resveratrol oligomers to three possible combinations of the C₈-centered free radicals derived from the oxidation of resveratrol analogue **2.50** and ϵ -viniferin analogue **3.5** (Figure 3.5). These include the homo- and hetero-coupled bis quinone methide intermediates **2.56**, **3.6**, and

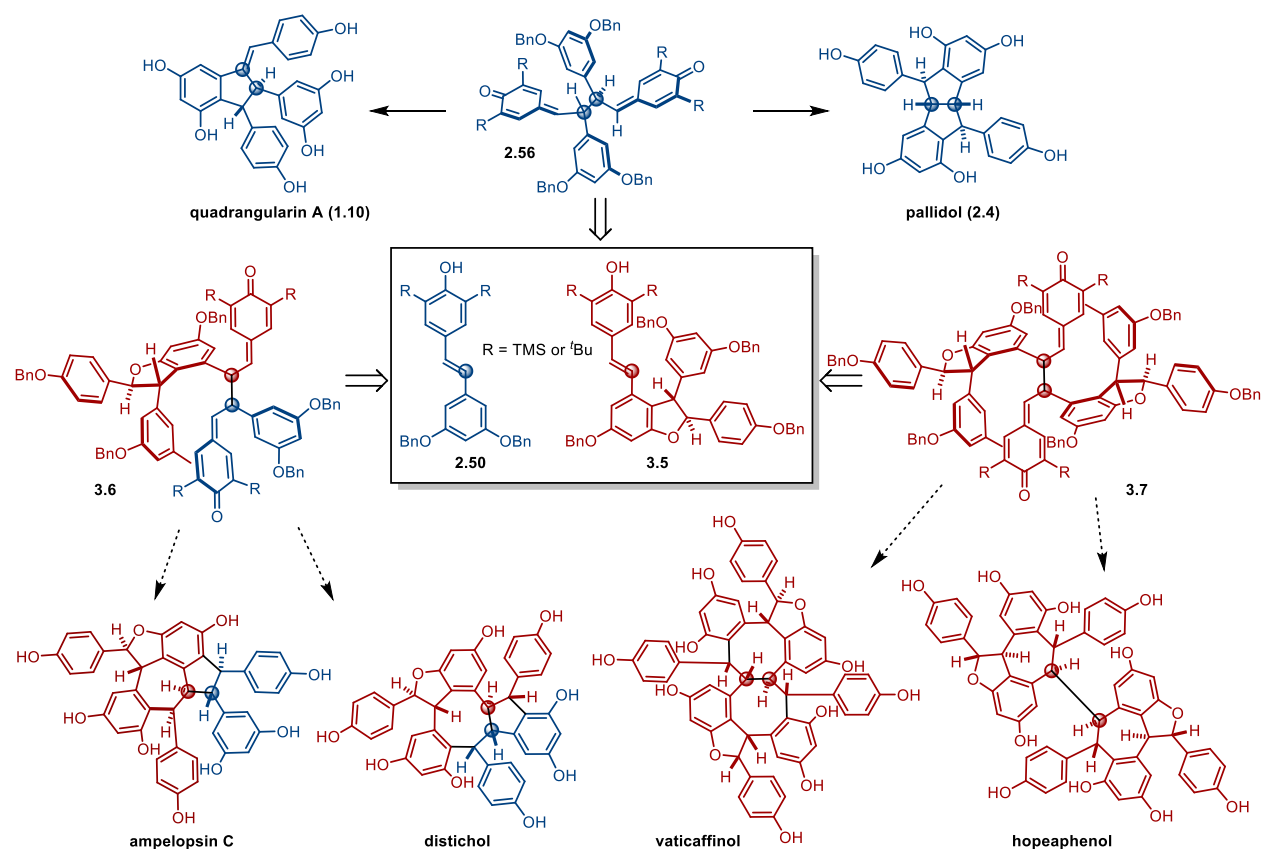


Figure 3.5 Concept for Unified Biomimetic Synthesis of Resveratrol Oligomers

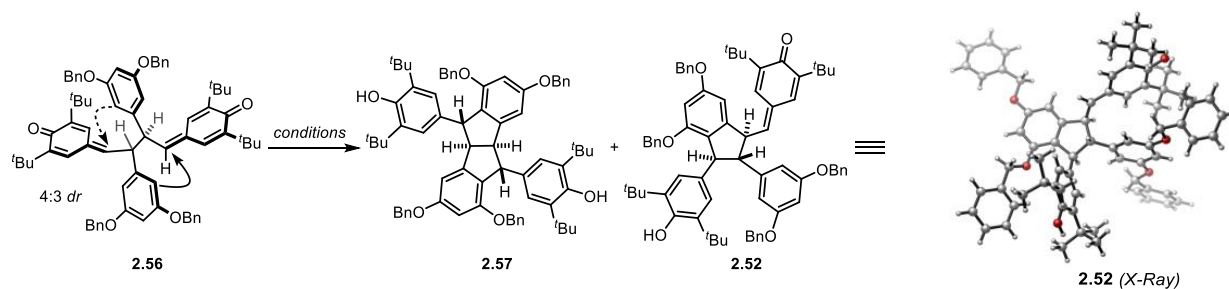
3.7, which are each poised for regio- and stereo-divergent cyclization pathways to produce a diverse series of complex natural products. Having executed this strategy for the synthesis of resveratrol dimers, we sought to explore the utility of the method for trimer and tetramer synthesis, and our efforts in this regard constitute the remainder of this dissertation. Our motivations for these investigations were two-fold: 1) The efficient synthesis of higher-oligomers of resveratrol would facilitate a more thorough examination of their biological activities, and 2) bis-quinone methides such as **2.56**, **3.6**, and **3.7** have received limited attention from the scientific community despite their immense potential as synthons for complex molecule synthesis, and therefore a demonstration of this potential and accompanying characterization of

their physical and chemical properties would promote their adoption by the synthetic community at large.

3.4 Discovery of Unusual Persistent Radical Character of Bis-Quinone Methides

Recall that in our previously disclosed synthesis of the resveratrol dimers quadrangularin A (**1.10**) and pallidol (**2.4**) (Section 2.6, Figure 2.12), the existence of linear bis-quinone methide dimer **2.56** as a mixture of *meso* and *DL* diastereomers had important consequences on the cyclization pathways available upon exposure of this intermediate to Lewis acid (Figure 2.11 B). Interestingly, we also discovered stoichiometry to have a profound influence over the product distribution obtained (Table 3.1). Specifically, in order for substantial quantities (~40% yield) of the desired diquinane product **2.57** to be obtained, a significant excess (>2 equiv) of $\text{BF}_3 \cdot \text{OEt}_2$ had to be employed. As the equivalents of Lewis acid were decreased, a dramatic change in the relative proportions of **2.52** and **2.57** was observed, shifting in favor of **2.52**. The influence of reaction conditions on product distribution became even more pronounced when Brønsted acid was used instead to promote the cyclization, resulting in exclusive formation of the *trans,trans*-indane isomer **2.52**. Crystals of **2.52** suitable for X-ray diffraction studies were obtained by slow evaporation from $\text{MeOH}/\text{CH}_2\text{Cl}_2$ — we thank Masha Kirillova for her skilled crystal growth and Jeff Kampf for conducting the XRD study and analysis.

Table 3.1 Variable Product Distribution in Friedel–Crafts Cyclization



Entry	Reaction Conditions	2.57 ^a	2.52 ^a
1	BF ₃ ·OEt ₂ (200 mol%), CH ₂ Cl ₂ (0.005 M), -78 °C, 0.75 h	45%	43%
2	BF ₃ ·OEt ₂ (10 mol%), CH ₂ Cl ₂ (0.005 M), -78 °C, 0.75 h	78%	10%
3	TFA (10 mol%), MeNO ₂ (0.1 M), RT, 5 h	93%	—

^aIsolated yields

As compound **2.52** can only arise from cyclization of *meso*-**2.56** (cf. Figure 2.11 B), its quantitative isolation suggests a dynamic equilibrium between the (*D/L*)- and *meso*-**2.56** whereby depletion of *meso*-**2.56** via acid-promoted desymmetrization to **2.52** results in epimerization of (*D/L*)-**2.56** as the system compensates for the shifted equilibrium. Initially, we postulated that the epimerization takes place by a mechanism involving prototropic rearrangement of (*D/L*)-**2.56** to the corresponding stilbene, **2.54**, followed by stereorandom protonation of the intermediate sp²-hybridized center. However, independent preparation of **2.54** and subjection to the standard reaction conditions did not result in the formation of an observable amount of **2.52** (Figure 3.6).

The protected quadrangularin A derivative **2.58** was also found not to isomerize to **2.52**.

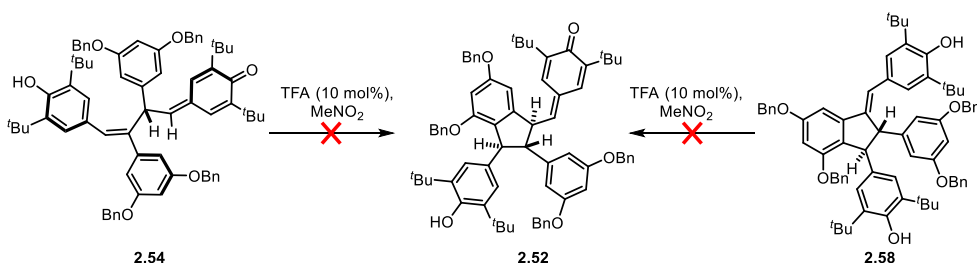


Figure 3.6 Experimental Results Inconsistent with Prototropic Rearrangement

In 1969, Becker reported that bis-quinone methides similar to **2.56** (cf. Figure 2.4) spontaneously dissociate (via homolytic C–C bond scission) into their monomeric phenoxy radical precursors in solution ($K_{\text{eq}} = 10^{-2}$ at room temperature).¹⁶³ To probe this possibility, we subjected a 1:1 mixture of OMe-**2.55** and OBn-**2.56** to a thermal crossover experiment in CDCl_3 (Figure 3.7). Upon heating, a dramatic color change took place—consistent with Becker’s observations for phenoxy radicals of type **3.8**—and the formation of a new product of intermediate R_f was observed by thin layer chromatography. $^1\text{H-NMR}$ and HRMS experiments on the reaction mixture support the formation of crossover product **3.9**. With this information in hand, we could account for the foregoing mechanism of epimerization.

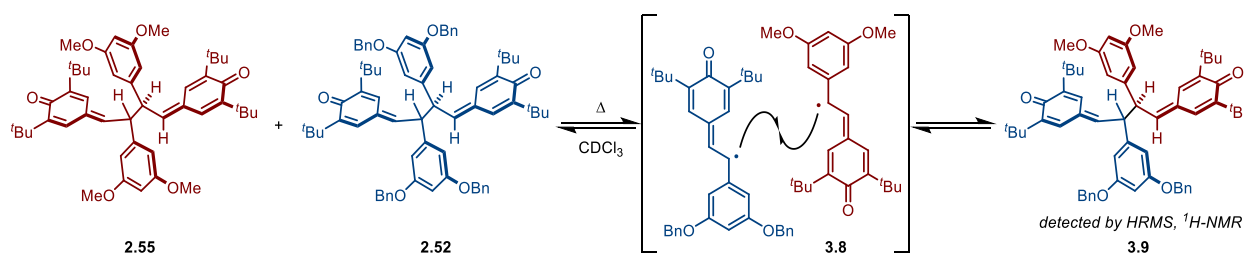


Figure 3.7 Thermal Crossover Experiment Provides Insight to Free Radical Equilibrium

In organic chemistry, carbon-centered free radicals are generally considered to be transient intermediates due to the rates at which they react with either closed shell species or with other free radicals in solution. Even in the absence of favorable pathways for radical reactivity with closed-shell species, carbon-centered free radicals typically combine or disproportionate at rates approaching the diffusion limit, reducing their “lifetime” to the order of micro–milliseconds.²¹⁷ The term “persistent” is used to describe those radicals which exhibit a significant lifetime relative to some standard transient radical under similar conditions in non-viscous solvents.²¹⁸ Though electronic (mesomeric, hyperconjugative, captodative) *stabilization* of a radical contributes significantly to the ease with which it forms, radical *persistence* is primarily a

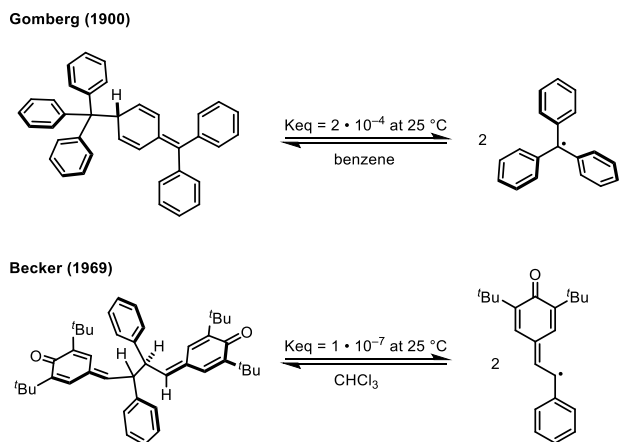


Figure 3.8 Persistent Radicals Discovered by Gomberg and Becker

consequence of steric effects, which retard termination and disproportionation events and attenuate reactivity to oxygen.²¹⁸

In 1900, Moses Gomberg, then a professor here at the University of Michigan, discovered the existence of organic free radicals in the form of the triphenylmethyl (trityl) radical (Figure 3.8).^{219–221} This seminal contribution is regarded as the birth of free radical chemistry, which has had a tremendous impact not only within organic chemistry, but in physical and life sciences as a whole. It is known that like **3.8**, the triphenylmethyl radical exists in equilibrium with its dimer, the correct quinoid structure of which was not identified until 68 years after its discovery.²²¹ The dimer-monomer homolytic dissociation equilibria for each of Gomberg and Becker's persistent radicals has associated with it a corresponding equilibrium constant (Figure 3.8). The concentration of the free radical in Gomberg's system is remarkably high ($K_{eq} = 2 \cdot 10^{-4}$ at room temperature). While that for Becker's bisquinone methide is significantly lower (by approximately 2000-fold), there is nonetheless evidence for the presence of free radicals in solutions of these compounds at room temperature.

In collaboration with the Pratt group (Univ. of Ottawa), we are currently characterizing this property for our compounds using a gamut of characterization techniques including variable

temperature UV-Visible spectroscopy, electron paramagnetic resonance (EPR) studies with accompanying density functional theory (DFT) calculations, and nanosecond laser flash photolysis (LFP). From these studies, we will be able to ascertain the bond-dissociation energies (BDE), equilibrium constants and forward rate constants for each dimer/monomer equilibria, as well as the extinction coefficients for each radical and the rate constant for their recombination. This work will be published elsewhere, but our preliminary data indicates that the BDEs for these molecules are remarkably low: on the order of $\sim 16 \text{ kcal}\cdot\text{mol}^{-1}$ for the *tert*-butyl quinone methide dimers and as low as $\sim 8 \text{ kcal}\cdot\text{mol}^{-1}$ for the corresponding trimethylsilyl derivatives (*vide infra*). Becker's important discovery, and the identification of this property for our compounds, has enabled us to complete a highly efficient biomimetic synthesis of resveratrol tetramers and to develop new strategies for the use of persistent radicals for oxidative cycloaddition chemistry. The details of these studies are described in the ensuing sections.

3.5 Preliminary Explorations in Tetramer Synthesis

Recall that our synthetic endeavors began with bis-quinone methides of type **2.56**. To achieve our goals of furthering the utility of these our continuation of the study of these intermediates for complex molecule synthesis, the related compounds **3.6** and **3.7** (Figure 3.5) would need to be prepared and their reactivity evaluated. As **3.7** represents a homocoupled product (versus the heterocoupled product **3.6**), it was clear that pursuit of the former was the logical choice with respect to feasibility. This raised several important considerations at the outset of this project. For instance, our previous studies with **2.56** had revealed that the compound exists as a mixture of diastereomers. Thus, it was expected that the hypothetical compound of type **3.7** would demonstrate similar behavior. However, the absence of stereoselectivity on dimerization of resveratrol derivative **2.50** was minimally disruptive to (and

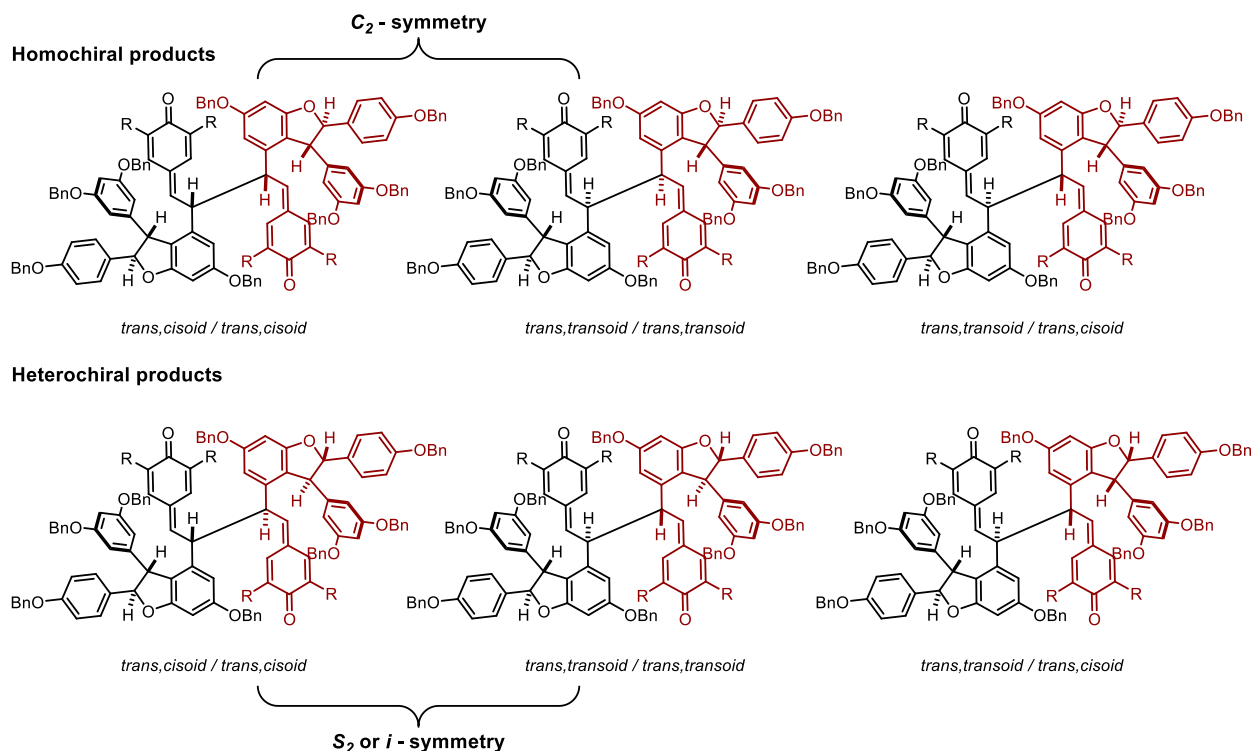


Figure 3.9 Possible Configurations of Tetrameric Bis-quinone Methide (R = ^tBu or TMS)

actually advantageous for) the synthesis of resveratrol dimers, as there were no other stereogenic centers present in the starting monomer. This is not true of the proposed precursor to **3.7**, ϵ -viniferin analogue **3.5**, which contains a dihydrobenzofuran moiety and therefore introduces two stereocenters in addition to the prochiral C₈ position of the olefin. Assuming that racemic **3.5** would be prepared as exclusively the *trans*-configured 2,3-diaryldihydrobenzofuran, analysis of the hypothetical configurations of bis-quinone methide **3.7** reveals that there are six diastereomers that could possibly be formed (Figure 3.9). It was unclear whether oxidation of the racemic starting material would reveal any preference for dimerization of (–)**3.5** with a second molecule of itself (homochiral coupling), if it would prefer to couple with its (+) antipode (heterochiral coupling), or if the product **3.7** would simply be obtained as a statistical mixture of all possible combinations. Therefore, to simplify product analysis and determine whether the oxidative coupling were even possible in this complex setting, we elected to first pursue the

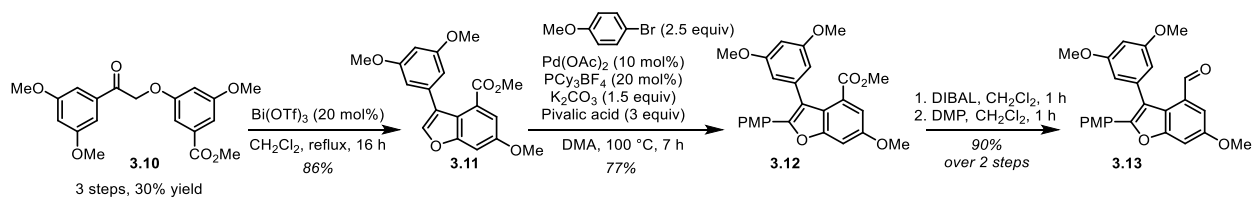


Figure 3.10 Preparation of Benzofuran Aldehyde Precursor

synthesis of the corresponding benzofuran congener of **3.5**, a derivative of a natural product known as viniferifuran.²²²

The requisite aldehyde was prepared according to procedures described by Kim and Choi for the synthesis of permethylated analogues of the resveratrol dimers viniferifuran, malibatol A, and shoreaphenol (Figure 3.10).²²³ Notably, this approach has since been used for the synthesis of ϵ -viniferin (**1.11**).²²⁴ In this sequence, a regioselective Bi(OTf)₃-catalyzed cyclodehydration of intermediate **3.10** (available in 3 steps from commercially available materials) provided the C₃-substituted benzofuran **3.11**. A subsequent C–H arylation using modified Fagnou conditions^{225,226} afforded the 2,3-diarylbenzofuran **3.12**. Final redox manipulations using standard conditions yielded the key aldehyde precursor **3.13**.

With access to aldehyde **3.13**, we began to explore olefination conditions for effecting its conversion to the desired *tert*-butylated viniferifuran derivative. Thus, the *O*-acetyl and *O*-trimethylsilyl phosphonate esters **3.14** and **3.15** were each prepared in three steps from commercially available butylated hydroxytoluene (BHT)¹² through a sequence involving protection, Wohl–Ziegler bromination,^{227,228} and a Michaelis–Arbuzov reaction.²²⁹ Notably, standard conditions (DMAP, acetyl chloride) proved ineffective for the acetylation of BHT, and the use of acid catalysis (Sc(OTf)₃, Ac₂O) was required.²³⁰ Likewise, silyl protection of the phenol demanded the use of *N,O*-bis(trimethylsilyl)acetamide, a highly reactive silyl donor.²³¹

¹² See supporting information for experimental details

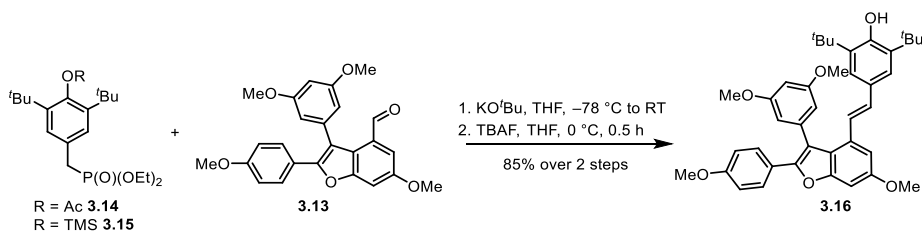


Figure 3.11 Preparation of *tert*-Butyl Viniferifuran Derivative

Unfortunately, all attempts to use **3.14** for olefination via a Horner–Wadsworth–Emmons protocol with either **3.13** or simpler aldehyde model systems were unsuccessful, presumably due to competitive deprotonation of the protecting group. Initial attempts using **3.15** also failed, but it was eventually found that deprotonation of **3.15** in the presence of **3.13** led to the formation of the desired viniferifuran derivative **3.16** in good yield (Figure 3.11). Conveniently, the silyl protecting group could be removed in a one-pot procedure by simply treating the reaction mixture with TBAF upon full consumption of starting material.

With the viniferifuran derivative **3.16** in hand, we were able to investigate the proposed oxidative coupling reaction (Figure 3.12). On subjection of **3.16** to our optimized ferrocenium-mediated dimerization conditions, we observed clean conversion to a product of lower R_F . However, isolation of tetrameric product **3.17** (~1:1 mixture of diastereomers) by flash chromatography resulted in a far lower yield than anticipated (27%), along with a mixture of (*E*) and (*Z*)-isomers of the starting **3.16**. This finding has significant mechanistic implications as only the pure (*E*)-isomer of **3.16** was used in the reaction and was apparently fully consumed in the reaction conditions as determined by TLC analysis. Thus, it is proposed that the presence of the benzofuran moiety in conjugation with the newly formed 8–8' linkage of the bis-quinone methide tetramer **3.17** renders it highly susceptible to disproportionation, forming **3.16** as the reduction product and postulated vinylogously stabilized oxocarbenium **3.18**, which is highly electrophilic and leads to various decomposition products.

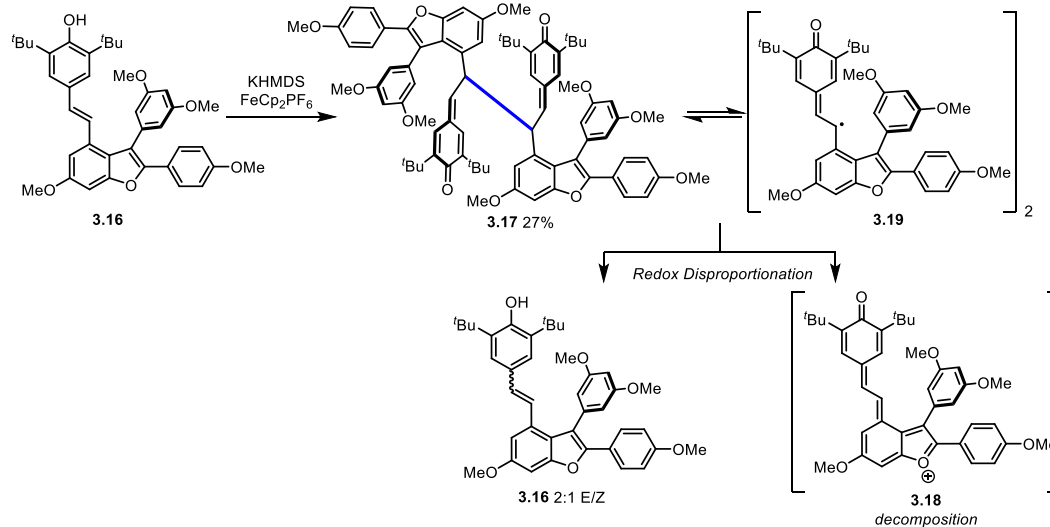


Figure 3.12 Unusual Disproportionation of Tetrameric Bis-quinone Methide

While possible to draw an ionic mechanism for this transformation, it is known that bisquinone methides such as **3.17** exist in equilibrium with their monomeric phenoxyl radicals (e.g. **3.19**, *vide supra*, Section 3.4), and it would seem more likely that this represents a radical–radical disproportionation reaction.²³² This aligns well with Becker’s observation that the degree of dissociation of bisquinone methides into phenoxyl radicals depends on the electronic nature of their substituents rather than on their steric influence, with electron donating methoxy groups promoting higher concentrations of free radicals.¹⁶³ Furthermore, exposure of **3.17** to **BF₃·OEt₂** did not lead to the desired cyclization products, but once again afforded a mixture of *E* and *Z*-isomers of the starting viniferiferifuran derivative **3.16**. In this instance, it is perhaps more accurate to draw an ionic mechanism whereby complexation of the Lewis acid by a quinone methide carbonyl activates the 8–8’ bond for an E₁-elimination assisted by vinylogous donation from the benzofuran oxygen.

While we deliberately targeted the unsaturated derivative **3.16** to reduce the number of possible diastereomers of **3.17**, our preliminary investigations with this compound indicated that it would not be possible to overcome these adverse electronic effects. Since we were tentatively

attributing the instability of **3.17** to donation of the benzofuran oxygen through conjugation, we sought to probe this hypothesis by saturating this olefin to the corresponding dihydrobenzofuran. Furthermore, while the use of methyl protecting groups was beneficial during our pilot studies for simplification of spectral analysis, we anticipated their late-stage removal to be problematic, and therefore sought to develop a route that enabled the use instead of benzyl groups either through protecting group exchange at an early intermediate or introduction at the beginning of the synthesis. Thus, the new target became viniferin derivative **3.5**, which reintroduced the possibility that we would simply obtain a complex mixture of stereoisomers upon oxidative coupling. Indeed, the small amount of **3.17** that we were able to isolate gave a ¹H-NMR spectrum consistent with the presence of both possible diastereomers.

3.6 Strategies for Dihydrobenzofuran Synthesis

At this point, we considered a number of strategies for preparation of 2,3-diaryldihydrobenzofurans, and soon became aware that there are very few broadly useful methods available for their synthesis. The nine-step homologation sequence of *ortho*-bromo phenols developed by Snyder and co-workers (cf. Figure 3.3), while robust, highlights the general challenges associated with their preparation: existing methods are lengthy and are generally not amenable to enantioselective synthesis.

We were pleased to discover a highly auspicious report from the Shaw lab describing a catalytic method for the asymmetric preparation of 2,3-diaryl dihydrobenzofurans.²³³ Largely pioneered by Davies and Hashimoto, C–H insertion had previously been applied in the synthesis of dihydrobenzofurans,^{234–236} a method which has since witnessed usage in a number of total syntheses.^{237–240} However, common to each of these applications is the requirement for at least one neighboring π -acceptor functionality, which confers stability to the diazo metal-carbenoid

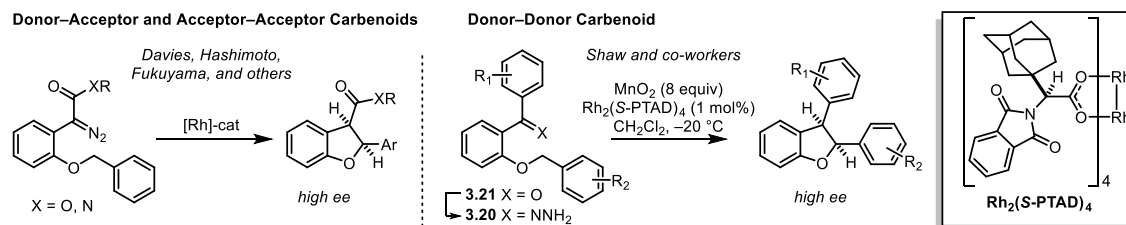


Figure 3.13 C–H Insertion for the Synthesis of Dihydrobenzofurans

precursor (Figure 3.13, left). Conversely, Shaw and co-workers demonstrated that diaryldiazomethanes **3.20** — readily prepared from the corresponding benzophenones **3.21** — are also suitable precursors for C–H insertion reactions of “donor-donor” rhodium-carbenoids (Figure 3.13, right). This method was applied for the enantioselective synthesis of dihydrobenzofurans using Davies’ $\text{Rh}_2(\text{S-PTAD})_4$ catalyst.²⁴¹

Shaw’s approach is highly advantageous for the synthesis of 2,3-diaryl dihydrobenzofurans as it eliminates the requirement for functional group interconversion on advanced intermediates. Notably, the *cis*-2,3-diaryl dihydrobenzofuran diastereomer is favored regardless of the electronic nature (A/A, D/A, D/D) of the diazo precursor and intermediate metal-carbenoid. However, it has been shown that *cis*-dihydrofurans bearing an anisole or phenol at the 2-position can be fully epimerized under mild conditions while retaining the stereochemical integrity of the C-3 chiral center.^{236,242} Shaw and co-workers were able to leverage this method for the asymmetric synthesis of δ -viniferin (**1.12**).

Seeking to implement this chemistry for the enantioselective synthesis of ϵ -viniferin derivative **3.5**, we turned toward the preparation of benzophenones of type **3.21**. Benzophenones were attractive starting materials for the synthesis of highly substituted dihydrobenzofurans since they provide opportunity for incorporation of the phenolic protecting group into the product. Since each enantiomer of the $\text{Rh}_2(\text{PTAD})_4$ catalyst is commercially available, this would in principle provide access to both enantiomers of **3.5**, enabling the synthesis of the natural isomers

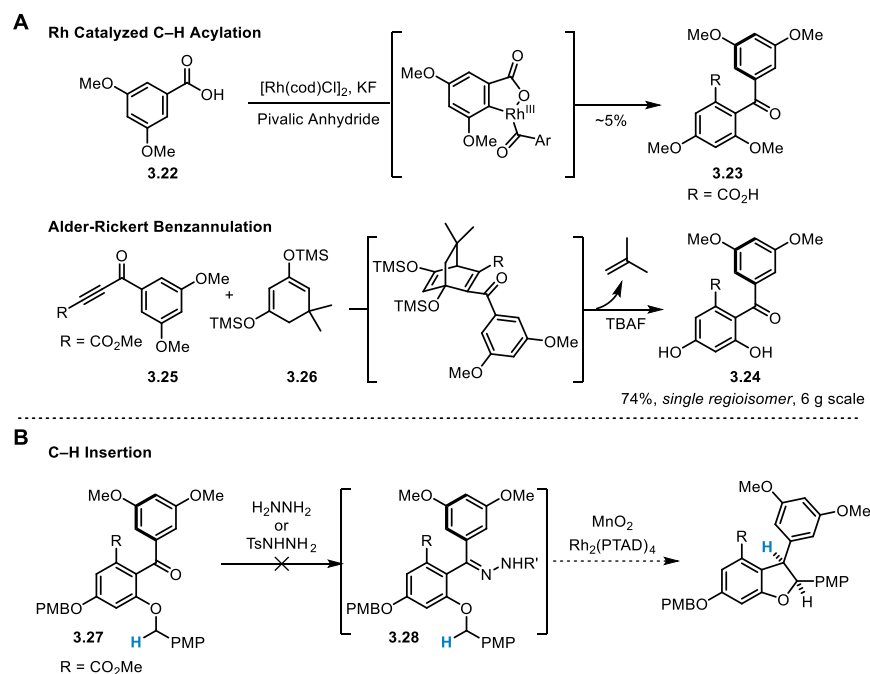


Figure 3.14 Selected Methods Attempted for A) Benzophenone Synthesis and B) PG Incorporation for DHB Synthesis

of Vitaceous and Diptereocarpaceous resveratrol oligomers, respectively.¹⁹ One uncertainty was whether the *ortho,ortho*-substitution pattern of the requisite benzophenone (more accurately its derived diazodiarylmethane) would be tolerated by the bulky catalyst.

In the course of our studies we identified several distinct approaches that would provide an efficient synthesis of the desired highly functionalized benzophenone (Figure 3.14, A). In lieu of detailed discussion of each of the approaches studied, selected examples are presented. Typical Friedel–Crafts acylations²⁴³ or nucleophilic fragmentations of substituted phthalic anhydrides²⁴⁴ were found to be unsuitable for this task due to poor reactivity or poor regioselectivity. Since acid-promoted Fries rearrangements of the benzoic anhydride derived from acid **3.22** failed, we instead attempted a rhodium-catalyzed *ortho*-acylation method reported by Goößen and co-workers.²⁴⁵ However, this catalytic system was found to be intolerant of the steric demands of the *ortho,ortho*' disubstitution found in **3.22**, yielding only trace

quantities of the desired benzophenone **3.23**. Previously reported strategies toward this challenging structural motif include the nucleophilic addition of an aryl anion to a benzaldehyde derivative followed by oxidation,²⁴⁶ carbonylative cross coupling,²⁴⁷ or anionic Fries-type rearrangements.¹⁴² While successful in preparing highly substituted benzophenone derivatives, each of these strategies require multi-step syntheses of pre-functionalized starting materials.

Our first major success came in the development of a regioselective Alder-Rickert reaction (Figure 3.14, A, bottom),²⁴⁸ a methodology popularized by Danishefsky in his syntheses of the macrolide natural products cycloproparadicicol and xestodecalactone A.^{249–252} The advantage of this approach is that it is highly convergent. Benzophenone **3.24** was prepared on multigram scale in high yield by heating a neat mixture of the aryl propiolate **3.25** and dimedone-derived siloxydiene **3.26** — each available in two steps^{251,253} — which promoted a regioselective [4+2] cycloaddition/cycloreversion sequence that proceeds through the intermediacy of a [2.2.2] dihydrobarrelene intermediate (Figure 3.14, A, bottom). With **3.24** in hand, *O*-alkylation with PMB-Cl under standard conditions afforded the starting material **3.27** for our investigations of the proposed C–H functionalization (Figure 3.14, B).

At this stage condensation of hydrazine or *p*-toluenesulfonyl hydrazide onto the benzophenone was anticipated to provide the corresponding hydrazones **3.28**, which would be converted to the requisite diazo carbenoid precursor by oxidation or base-mediated decomposition, respectively. We were dismayed to find that, despite fairly extensive experimentation, we were unable to identify conditions for this seemingly trivial functional group interconversion. Only under relatively forcing conditions (50 °C, HOAc (1 equiv), XS hydrazine) was consumption of the starting material observed, and the product formed was consistent with the phthalazinone product of double condensation across the ketone and ester.

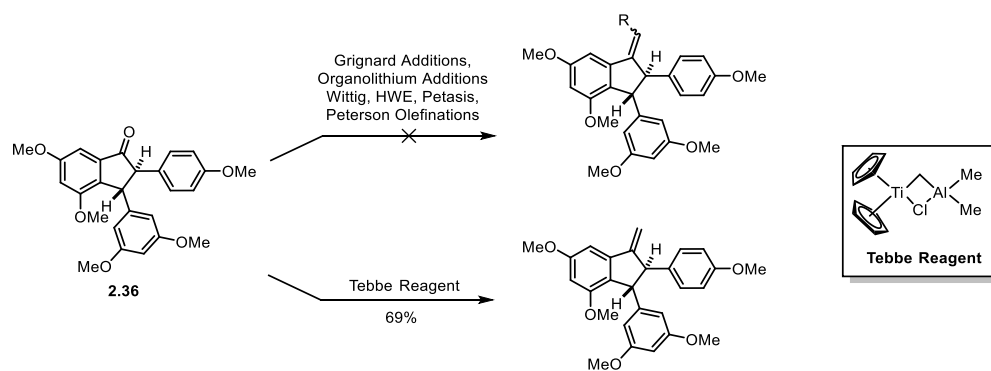


Figure 3.15 Dimeric Resveratrol Indanone Resistant to Functionalization

Though disappointing, the resistance of benzophenone **3.27** toward nucleophilic attack can be rationalized by both steric and electronic effects. It is expected that steric clashing of the *ortho*-substituents of one arene with the *ortho*-hydrogens of the other forces one of them to twist out of plane. In this conformation, the Bürgi–Dunitz trajectory for nucleophilic addition would be significantly encumbered.²⁵⁴ Furthermore, the benzophenone is in conjugation with both *ortho*- and *para*-disposed benzyloxy ethers, which presumably each donate electron density to the carbonyl moiety and attenuate its reactivity. Indeed, related aryl ketones have historically been challenging to functionalize, and attempts by other research groups to use permethyl (iso)pauciflorol F **2.36/2.37** as a precursor for the synthesis of other resveratrol oligomers have failed, leading to either no reaction or simply α -deprotonation (Figure 3.15).^{137,171,255} Notably, the most effective system for functionalization of this carbonyl was the Tebbe reagent,²⁵⁶ which afforded a good yield of the methenylated product.

3.7 Applications of Persistent Radicals to Dihydrobenzofuran Synthesis

Our efforts thus far to apply existing methods in new settings for (dihydro)benzofuran synthesis were met with several unforeseen challenges. It appeared as though the optimization of these methods on the substrates described would constitute entire projects of their own, and we

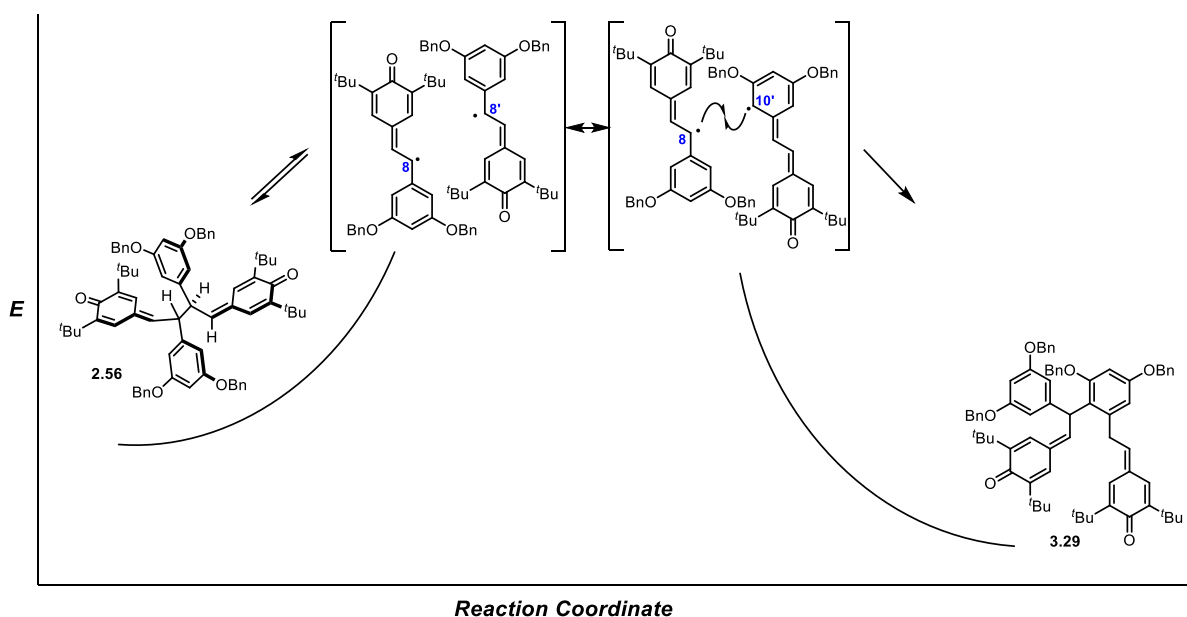


Figure 3.16 Attempted Thermal Rearrangement of Bis-Quinone Methide Dimer

did not want to lose sight of the primary objective: the development of a biomimetic approach to resveratrol tetramers. However, through our discovery that bis-quinone methide dimers exist as persistent radicals in solution, an opportunity had presented itself to devise a new solution for this purpose.

Our previously optimized dimerization (cf. Section 2.5) yielded exclusively the 8–8' coupled product (resveratrol numbering system), in which carbon-carbon bond formation has taken place between the benzylic positions of each monomer. The development of a regio-complementary 8–10' coupling method would be of tremendous value for the synthesis of resveratrol oligomers, as a majority of these natural products (e.g. ϵ -viniferin (**1.11**) and oligomers derived therefrom) are fused in this manner. We reasoned that perhaps thermally induced homolytic cleavage of dimer **2.56** would enable the resultant free radical to eventually combine through the resorcinol ring to afford the regioisomer **3.29** (Figure 3.16). The intent was that subsequent rearomatization would render this process irreversible, and that the bis-quinone methide could, upon prolonged heating, eventually be funneled entirely to this thermodynamic

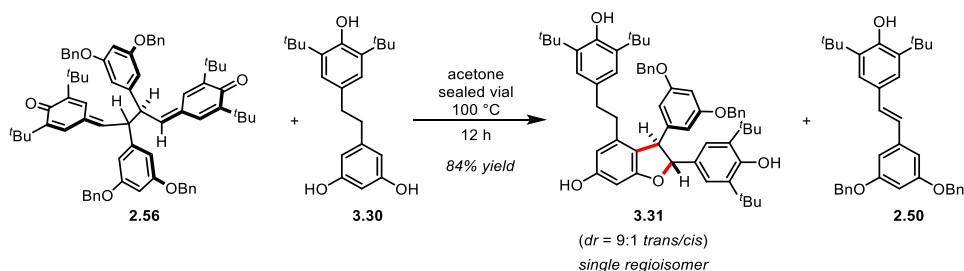


Figure 3.17 Dihydrobenzofuran Synthesis using Persistent Radical

well. However, we found that thermal cycling of the dimers could be performed indefinitely without observing any of the desired rearranged product, with the only observed changes being oxidative decomposition of the material in non-degassed solvents, or occasionally radical–radical disproportionation to yield some of the stilbene monomer.

The latter result led us to consider the potential of intercepting one of the monomeric free radicals with a closed-shell species, as the resultant free radical could potentially be oxidized by a second monomeric free radical through a similar disproportionation event. If the closed-shell species were an arene (e.g. a phenol), oxidation of an intermediate cyclohexadienyl radical and ensuing rearomatization would represent an irreversible capture of the persistent radical. Indeed, we found that thermal homolysis of **2.56** in the presence of dihydroresveratrol derivative **3.30** results in the formation of ϵ -viniferin analogue **3.31** as the exclusive regioisomer in high yield and with good diastereoselectivity, and was accompanied by the formation of a stoichiometric amount of stilbene **2.50**, indicative of a disproportionation mechanism. We were quite pleased with the isolated yield of **3.31** (84%), and the byproduct **2.50** could readily be recycled to **2.56** using our optimized dimerization conditions.

Although we have only recently been successful with this transformation, the idea of intercepting the phenoxyl radical with a phenol was conceived of several years ago when we were initially investigating aerobic dimerization conditions. Interestingly, previous attempts to

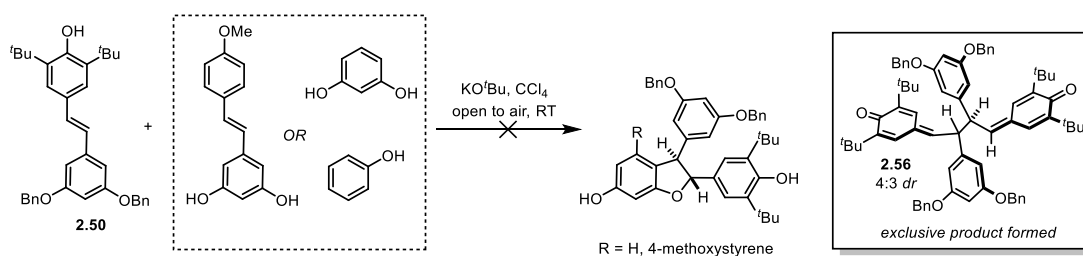


Figure 3.18 Early Efforts to Promote DHB Synthesis through Radical Cross Coupling

promote the cross coupling of various phenols with ^tBu-resveratrol-derived phenoxy radical at room temperature under our aerobic oxidative dimerization conditions were unsuccessful, yielding exclusively the bis-quinone methide homodimer **2.56** (Figure 3.18).

Work to further develop this chemistry for the concise synthesis of ϵ -viniferin analogue **3.5** and its subsequent implementation in tetramer synthesis is underway. Additional exploration into the reactivity of dimeric “radical donors” of type **2.56** — and their so-formed monomeric free radicals — with other heteroatom-bearing radicophiles such as anilines, thiophenols, enamines, and enol ethers is ongoing. This would provide a novel means of constructing five-membered heterocycles including indolines, dihydrobenzothiophenes, dihydropyrroles, and dihydrofurans, respectively.

3.8 The Total Synthesis of Nepalensinol B and Vateriaphenol C

With our aim re-centered on completing the synthesis of the targeted resveratrol tetramers, we sought a strategy to ϵ -viniferin derivative **3.5** that would enable flexibility with respect to the blocking groups at the 3- and 5-positions of the 4-hydroxy stilbene, as removal of these groups in the final step of the synthesis must be tolerant of the increased functionality present in these molecules as compared to the previously synthesized dimeric natural products.¹²⁵ We therefore targeted aldehyde **3.32**, which would conceivably serve as a precursor to the required materials through an olefination reaction. Conveniently, Snyder and Wright had just recently disclosed a

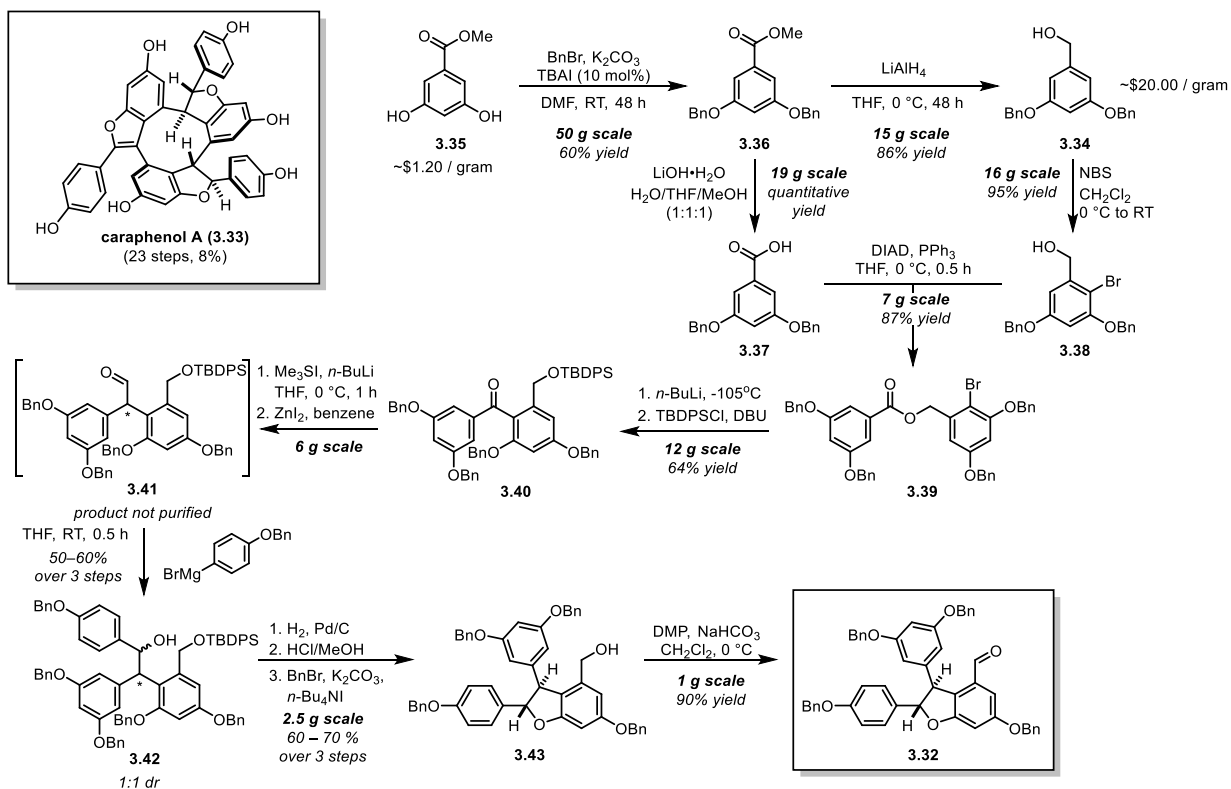


Figure 3.19 Route to Key Aldehyde Intermediate used in Total Synthesis of Caraphenol A

preparation of **3.32** as an intermediate for their synthesis of caraphenol A (**3.33**), a resveratrol trimer belonging to a subclass of resveratrol oligomers containing strained 9-membered rings.¹⁴²

We elected to use this route to allow us to investigate the feasibility of our synthetic end-game while concurrently investigating new strategies for the synthesis of ϵ -viniferin (**1.11**) and analogue **3.5**. I gratefully acknowledge Oliver Fischer and Ryan Harding — two conscientious mentees of mine — for their assistance with the preparation of key intermediate **3.32**.

The scale and yield for each reaction as performed by us are represented in Figure 3.19. While Snyder and Wright commence their synthesis from 3,5-dibenzoyloxybenzyl alcohol **3.34**, we elected to instead source methyl 3,5-dihydroxybenzoate **3.35** for this synthesis due to its lower cost. Alkylation with benzyl bromide afforded the 3,5-dibenzoyloxy methylbenzoate **3.36**, which served as a versatile intermediate for this synthesis. Hydrolysis under standard conditions proceeded smoothly in quantitative yield to the corresponding acid **3.37**, whereas reduction using

lithium aluminum hydride afforded benzyl alcohol **3.34**, also in high yield. Regioselective bromination yielded **3.38**, which was subsequently coupled with **3.37** to yield ester **3.39**. At this point, key benzophenone intermediate **3.40** was produced by a one-pot anionic Fries-rearrangement/TBDPS protection.²⁵⁷ This compound was competent for the general homologation strategy previously developed by Snyder and co-workers (cf. Figure 3.3 and Figure 3.4). Thus, aldehyde **3.41** was prepared through a Johnson–Corey–Chaykovsky epoxidation^{211,212} and Meinwald rearrangement,²¹³ and was subjected without purification to Grignard addition using the commercially available 4-benzyloxyphenyl magnesium bromide. The resultant adduct **3.42** was obtained as a diastereomeric mixture, which was carried through a three-step sequence involving global debenylation, acid-promoted dihydrobenzofuran cyclization, and final re-protection to afford benzyl alcohol **3.43**. Notably, the acid-mediated cyclization is diastereoconvergent, yielding almost exclusively the *trans*-dihydrofuran diastereomer as a racemic mixture. A final oxidation using Dess–Martin periodinane proceeded uneventfully to deliver the requisite aldehyde **3.32**.

At this point, we were well-positioned to execute the biomimetic synthesis of resveratrol tetramers derived from the 8–8' dimerization of ϵ -viniferin (**1.11**). Our previous synthetic experience had revealed benzyl protecting groups to be optimal with respect to stability, solubility, and ease of removal. Moreover, we had already developed a synthesis of the *tert*-butyl phenol-derived phosphonate ester **3.15**, and developed conditions for its successful implementation in the Horner–Wadsworth–Emmons olefination of benzofuran aldehyde **3.13** for the preparation of viniferifuran derivative **3.16** (cf. Section 3.5, Figure 3.11).

We were immediately confronted with difficulty, as aldehyde **3.32** was found to be unreactive toward phosphonate ester. A number of reaction parameters were varied, including

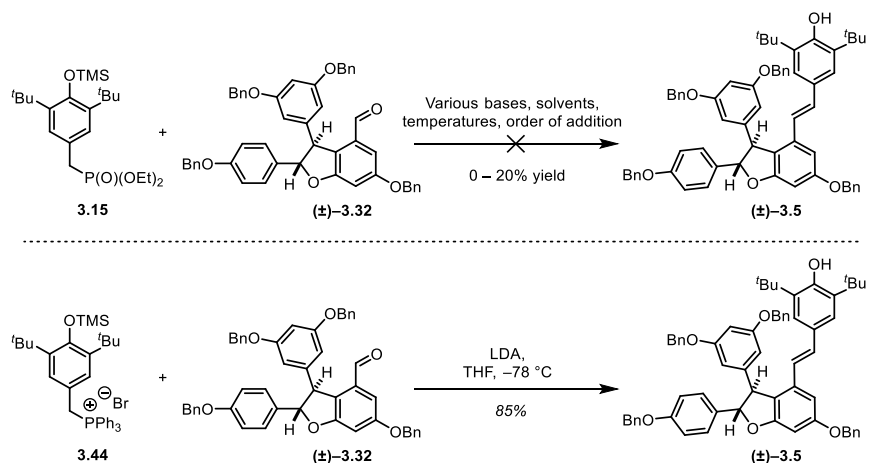


Figure 3.20 Wittig Reaction Uniquely Effective for Synthesis of Viniferin Derivative

the base, order of addition, and solvent, but the reaction was found to give either low (<20%) or no conversion in all cases, including with the use of 3,5-dibenzoyloxy benzaldehyde as a model system. Hence, it would seem that aldehyde **3.13** was uniquely matched for this olefination reaction, which we found to be counterintuitive given the vinylogous conjugation of **3.13** with the benzofuran, an electronic effect that would be expected to decrease electrophilicity. Although it was unclear what the fate of the phosphonate ester was in these reactions, we speculated that *O*-desilylation was likely becoming a competitive pathway due to slow reactivity with **3.32**, which could perhaps be attributed to the high steric demand of each of the reaction partners.

Benzyl phosphonium salts (ylid precursors) have a pK_a of ~ 17 as compared to a value of ~ 27 for the corresponding phosphonate esters.^{258,259} Consistent with this large (ten orders of magnitude) difference, the phosphonium ylid formed upon deprotonation has attenuated nucleophilicity and basicity as compared to the phosphonate-stabilized carbanion, and we reasoned that this could possibly mitigate deleterious or unproductive pathways, such as *O*-desilylation. The BHT-derived phosphonium salt **3.44** was prepared in a similar manner to the phosphonate ester **3.15** by simply reacting the intermediate benzyl bromide with

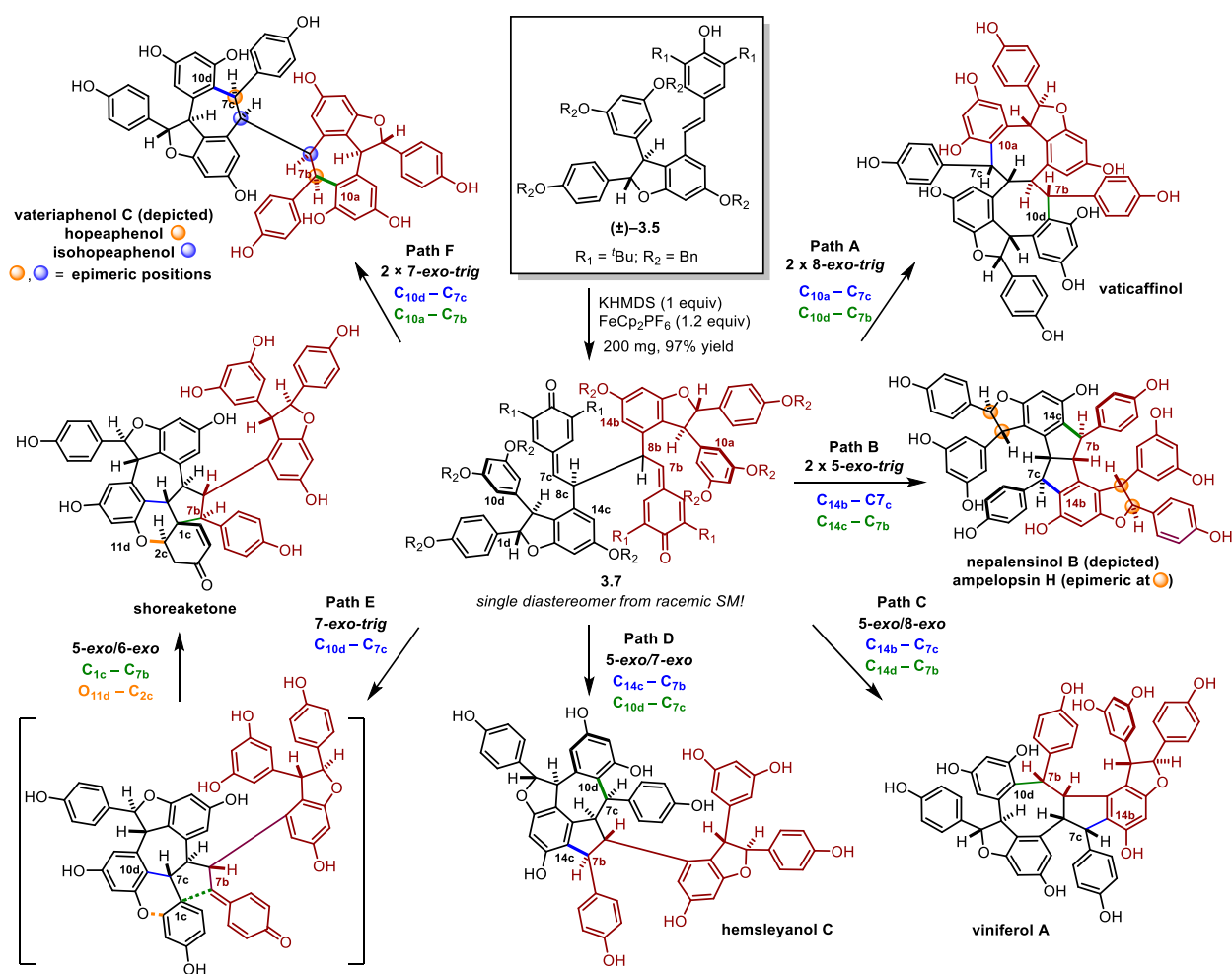


Figure 3.21 Regiodivergent Cyclization Pathways from Tetrameric Bis-Quinone Methide

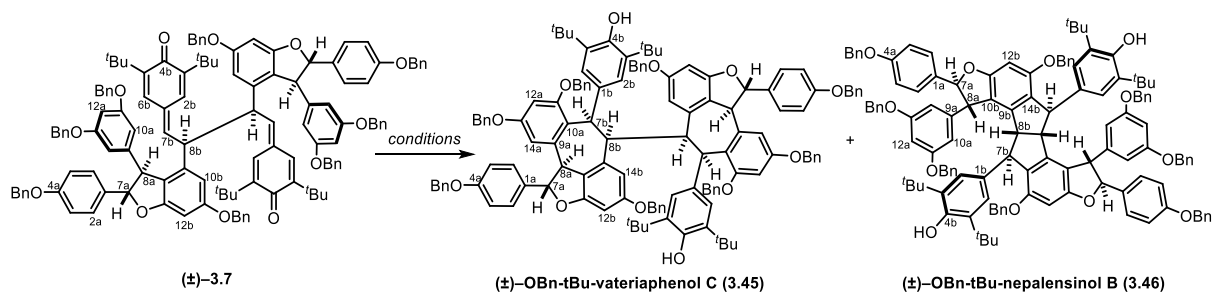
triphenylphosphine rather than triethylphosphite.¹³ Gratifyingly, our first reaction conditions for the olefination of **3.44** with **3.32** (*n*-BuLi, THF, 0 °C) yielded 45% of the desired ϵ -viniferin derivative **3.5**, already more than double our highest yield previously using the phosphonate ester **3.15**. With some optimization, this yield was improved to 85% on a 500 mg scale. The use of LDA at -78 °C was found to be uniquely effective for this transformation. Again, the silyl protecting group could be conveniently removed in a one-pot procedure by simply treating the reaction mixture with TBAF upon full consumption of starting material.

¹³ See supporting information for experimental details

We now finally had access to sufficient quantities of the *tert*-butyl benzyloxy ϵ -viniferin derivative **3.5**, and were eager to pursue the synthesis of resveratrol tetramers from this intermediate. In our initial pilot scale reaction we were excited to find that benzyloxy **3.5** (more accurately its phenoxide) was a competent substrate for ferrocenium-mediated oxidative coupling. Gratifyingly, the corresponding tetramer **3.7** was isolated in 92% yield as what appeared to be a *single diastereomer* (Figure 3.21). Though we could not identify whether **3.7** was the product of homochiral or heterochiral coupling (cf. Figure 3.9), it was clear by NMR that it contained one or more symmetry elements (mirror plane, inversion center, rotation axis). Scale up of this reaction to 200 mg resulted in a remarkable 97% isolated yield of **3.7** (Figure 3.21).

With access to significant quantities of putative biogenic intermediate **3.7**, we were now faced with another challenge — promoting its intramolecular cyclization (Table 3.2). As shown in Figure 3.21, there are a number of regioisomeric Friedel–Crafts cyclization pathways hypothetically available to this intermediate. Provided that ϵ -viniferin (**1.11**) is dimerized to a bis-quinone methide intermediate similar to **3.7** during the biogenesis of resveratrol tetramers, it would appear that the relative configuration across the newly formed 8–8' stereogenic centers would have important implications for subsequent bond-forming events. For example, the products formed through paths A and D would require the (*R*)/(*S*) or (*S*)/(*R*) configuration across these vicinal stereocenters, whereas those formed through Paths B, C, E, and F each derive from the (*R*)/(*R*) or (*S*)/(*S*) configured bis-quinone methide.

Given our success with the dynamic desymmetrization of dimeric bis-quinone methide **2.56** (Section 3.3, Table 3.1), we initially attempted to promote the desired cyclization using trifluoroacetic acid in nitromethane (Table 3.2, entry 1). As was true of the dimer, the tetrameric quinone methide *tert*-butyl benzyloxy **3.7** formed a heterogeneous suspension under these

Table 3.2 Optimization of Tetramer Cyclization

Entry	Reaction Conditions	3.7^a	3.45^a	3.46^a
1	TFA (1 equiv), MeNO ₂ , RT, ultrasound then stir 3 h	100%	—	—
2	BF ₃ ·OEt ₂ (4 equiv), CH ₂ Cl ₂ (0.01 M), -78 °C, 0.5 h	71%	7%	—
3 ^b	BF ₃ ·OEt ₂ (4 equiv), CH ₂ Cl ₂ (0.01 M), -40 °C 2 h, then warm to RT	—	16%	59%
4	BF ₃ ·OEt ₂ (4 equiv), CH ₂ Cl ₂ (0.01 M), 0 °C to 5 °C, 0.75 h	—	—	28%
5 ^c	BF ₃ ·OEt ₂ (4 equiv), CH ₂ Cl ₂ (0.01 M), -60 °C to -30 °C, then 2.5 h	—	9%	44%

^aIsolated yields; ^bPerformed on 10 mg scale; ^cPerformed on 75 mg scale.

conditions. However, ¹H-NMR of the crude material after removal of volatiles indicated that entirely starting material remained. We found that on exposure of **3.7** to BF₃·OEt₂ at -78 °C in CH₂Cl₂, a faint color change took place. However, due to the nearly identical R_F values and staining profile of the cyclized products and the starting material, it was very difficult to discern whether starting material consumption was occurring. Furthermore, if the aliquot in the spotting capillary was allowed to warm at all, a more pronounced color change to a maroon was observed, leading us to become skeptical of the validity of this method for monitoring the progress of this reaction. Indeed, on quenching at this temperature, ¹H-NMR revealed that a significant amount of starting material remained (~70%), although we isolated 7% of a new product whose structure was tentatively assigned as a bis-7-*exo* adduct **3.45** (Table 3.2, entry 2). Increasing the temperature (-40 °C to RT) resulted in a significant improvement in conversion, now yielding a 4:1 mixture of a new product and **3.45**, respectively, in ~75% combined yield (Table 3.2, entry 3). The structure of the new compound was consistent with the [3.3.0] bicyclooctane connectivity of the nepalensinol B core **3.46**. Alternatively, a reaction run between 0–5 °C showed rapid consumption of starting material, but the crude mixture formed was highly complex, containing a significant amount of oligomerized/polymerized material (Table 3.2, entry

4). From this mixture, we were able to isolate cyclization product **3.46** in 28% yield. Finally, it was found that initiating the cyclization reaction at $-60\text{ }^{\circ}\text{C}$ and allowing it to slowly warm to $-30\text{ }^{\circ}\text{C}$ over several hours was optimal for promoting cyclization while sequestering indiscriminate polymerization. Under these conditions, the yield of the diquinane structure **3.46** improved to 44%, and 9% of product **3.45** was obtained for a combined cyclization yield of 53% (Table 3.2, entry 5).

Though we were reasonably confident in the proposed connectivity, at the time we were unable to assign the relative configuration of each product. Notably, vicinal coupling constants are notoriously poor predictors of relative configuration within the five- and seven-membered ring systems which are prevalent in this class of natural products,³⁵ leading to a number of structural misassignments²⁶⁰ and revisions.^{261,262} We have since learned that the initially assigned connectivity was indeed correct, and that the relative configurations correspond to those depicted, which represent the cores of the natural products vateriaphenol C and nepalensinol B, respectively.^{261,263}

Given that the Path B and Path F products (Figure 3.21) each derive from the (*R*)/(*R*) or (*S*)/(*S*) configured bis-quinone methide **3.7**, it is tempting to conclude that this must be the preferred diastereomer during the dimerization event. While it is not impossible that the dimerization event itself is diastereoselective, it is far more likely that initial coupling produces a mixture of diastereomers which rapidly equilibrate in solution via bond homolysis–recombination. Therefore it remains possible that the (*R*)/(*S*) diastereomer is preferred but that the (*R*)/(*R*) or (*S*)/(*S*) configuration is the only one conducive to cyclization. In this scenario, depletion of the the (*R*)/(*R*) or (*S*)/(*S*) diastereomer would promote epimerization of the (*R*)/(*S*) configured dimer (via C–C bond homolysis/combination) to compensate for the shifted

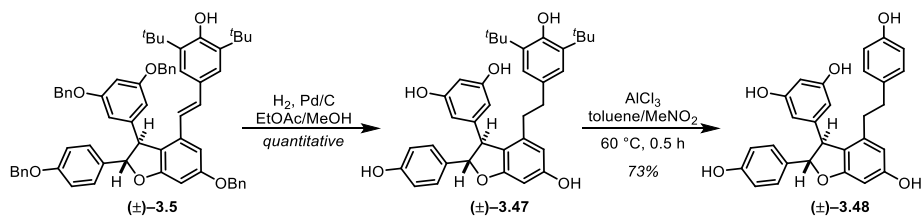


Figure 3.22 Model Study for Stability of Dihydrobenzofuran to De-*tert*-butylation

equilibrium. This possibility is highly analogous to what was observed during our work with dimeric bis-quinone methide **2.56** during its dynamic, acid-promoted desymmetrization to **2.52** (Table 3.1).

At the outset of our campaign for the total synthesis of resveratrol tetramers, we were cognizant of the fact that these more advanced architectures may not be tolerant of the harsh conditions ($AlCl_3$, 60 °C) required for removal of the *tert*-butyl groups via a retro-Friedel–Crafts reaction. While this method proved successful during our synthesis of the resveratrol dimers pallidol and quadrangularin A (cf. Figure 2.12), neither of those scaffolds contain a dihydrobenzofuran moiety, which we anticipated could be susceptible to acid-mediated ionization and decomposition. Thus, to probe this possibility, we performed a model system study. A hydrogenation/hydrogenolysis of the *tert*-butyl, benzyloxy ϵ -viniferin derivative **3.5** was performed to afford derivative **3.47** in quantitative yield (Figure 3.22). A solution of this compound in toluene at 60 °C was treated with a 0.5 M solution of $AlCl_3$ in MeNO₂, turning the mixture to a golden yellow color. Complete conversion was observed within 0.5 h, and workup and purification yielded the desired **3.48** in 73% yield.

Our immediate success with model system **3.47** — and our previous success with de-*tert*-butylation of pallidol and quadrangularin A derivatives **2.27** and **2.23** — was highly encouraging for the feasibility of this strategy for higher oligomer synthesis. Thus, debenylation of the major tetrameric product, nepalensinol B derivative **3.46** was achieved via Pd/C-mediated

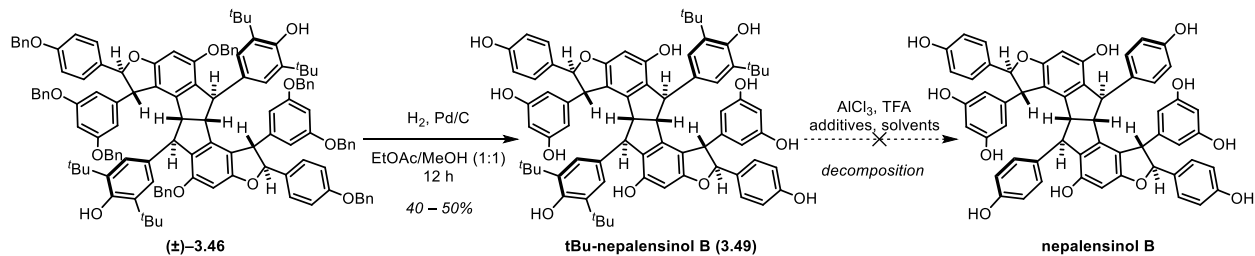


Figure 3.23 Thwarted Efforts to Dealkylate Nepalensinol B Precursor

hydrogenolysis (Figure 3.23), yielding the penultimate intermediate **3.49** in 40 – 50% yield (although the yield could likely be improved with a higher catalyst loading). Intermediate **3.49** was subjected to a range of conditions in an effort to promote cleavage of the *tert*-butyl groups, including AlCl₃, AlCl₃/biphenyl, and TFA, at various temperatures and in various solvents, but in all cases complete decomposition of the starting material was observed. Though the mixtures were intractable, the sheer number of *tert*-butyl resonances in the ¹H-NMR spectra of crude reaction mixtures was suggestive that indiscriminate intramolecular transfer of the *tert*-butyl cation was occurring in preference to alkylation of toluene. The aphorism famously attributed to R. B. Woodward — “the only model system worth using is the enantiomer” — is decidedly apropos for our sentiments upon receiving these disappointing results.

Rather than continuing to explore conditions for de-*tert*-butylation, we considered whether it would be possible to replace them with an alternative functional group that could be removed under milder conditions. In order for this strategy to be viable, a number of criteria needed to be met, including: 1) Can the groups be readily introduced from commercially available materials in a manner that does not require complete revision of the synthesis?, 2) Are the conditions for their removal orthogonal to those it will be exposed to in the key steps of the synthesis? 3) Will they facilitate the oxidative dimerization in the same way as the *tert*-butyl

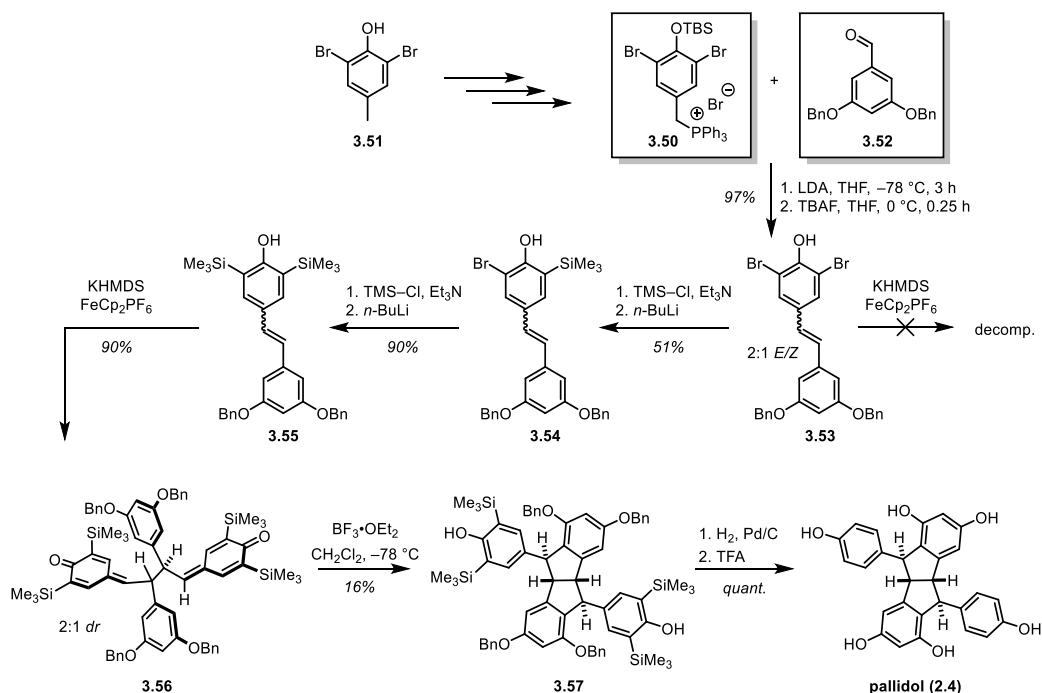


Figure 3.24 Model Study for Blocking Group Alternatives (Unoptimized Sequence)

groups? and 4) Will the resultant bis-quinone methides persist through homolytic dissociation equilibria and enable the diastereoselective preparation of **3.7**?

A survey of the literature and evaluation of our criteria narrowed the targeted blocking groups down to bromo- and trimethylsilyl (TMS) moieties. The bromo-derivatives would provide opportunity for removal under reductive conditions, whereas the TMS group can be removed by protodesilylation under much more mildly acidic conditions than those required for *de-tert*-butylation. Furthermore, the TMS group is readily introduced from the corresponding *ortho*-bromo phenol through a retro-Brook rearrangement, and therefore the same materials would allow ready access to each of the sought after derivatives.

We planned to first explore these derivatives in the context of the chemistry developed for the synthesis of resveratrol dimers (cf. Section 2.6), as this would allow us to address each of the aforementioned criteria with the exception of (4). Thus, we set out for the preparation of the corresponding bromo- and TMS-derivatives of *tert*-butyl resveratrol analogue **2.50**. Given our

success with the Wittig reaction (cf. Figure 3.20), we aimed to prepare phosphonium salt **3.50**. A three-step sequence was developed from commercially available 2,6-dibromo-4-methylphenol **3.51** involving silyl protection, Wohl-Ziegler bromination,^{227,228} and phosphonium salt formation (Figure 3.24). A subsequent Wittig olefination with 3,5-dibenzyloxy benzaldehyde **3.52** proceeded in high yield, but delivered the resveratrol derivative **3.53** as a mixture of (*E*)- and (*Z*)-olefin isomers. Attempts to directly dimerize **3.53** led only to decomposition, indicating that the use of bromides as blocking groups was not feasible for our synthetic strategy. However, the bromide **3.53** was then converted to the corresponding mono- **3.54** and bis- **3.55** TMS-derivatives by means of a retro-Brook sequence. Pleasingly, the TMS-derivative **3.55** was found to dimerize to bis-quinone methide **3.56** under our optimized oxidative coupling conditions, and the TMS groups tolerated BF₃·OEt₂ promoted cyclization to diquinane **3.57**. Most importantly, after global debenylation by hydrogenolysis, the TMS groups were removed quantitatively by exposure to dilute trifluoroacetic acid (TFA) at room temperature, delivering the natural product pallidol (**2.4**) in nearly pure form by simple removal of volatiles. Thus, with our proof of concept study we were able to identify TMS as a suitable replacement for the *tert*-butyl blocking group, and therefore we set out to apply this chemistry for our tetramer synthesis.

As was true of resveratrol derivative **3.53**, Wittig olefination (not shown) of **3.50** using benzaldehyde **3.32** afforded the dibromo- ϵ -viniferin analogue **3.58** (Figure 3.25) as a mixture of geometric isomers. While this is ultimately inconsequential, it renders product analysis difficult and the mixture of isomers must be carried through several steps prior to destruction of this stereochemical information. Although we had previously been unsuccessful with the application of a Horner-Wadsworth-Emmons (HWE) olefination for the synthesis of ϵ -viniferin derivatives (cf. Figure 3.20), our suspicion that the poor reactivity was due to the instability of the *O*-TMS

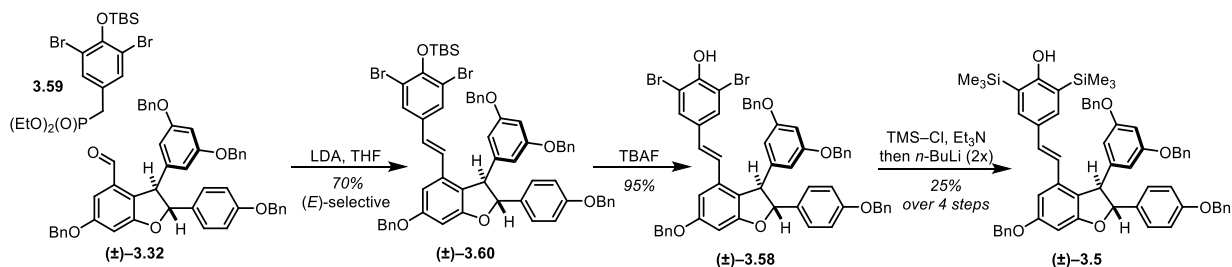


Figure 3.25 First Generation Route to TMS-Viniferin Derivative

group under these conditions led us to re-visit this for the bromo derivative, which sterically tolerates a more robust *tert*-butyldimethylsilyl (TBS) ether. The requisite phosphonate ester **3.59** was easily prepared from the same benzyl bromide precursor used for preparation of **3.50** through a Michaelis–Arbuzov reaction.²²⁹ Gratifyingly, the HWE reaction was immediately successful, providing ϵ -viniferin derivative **3.60** in 70% yield as exclusively the (*E*)-isomer (Figure 3.25).

While the subsequent tetra-*n*-butylammonium fluoride (TBAF)-mediated desilylation proceeded smoothly, it was not possible to isolate product **3.58** from the greasy contaminants derived from the reagent. Only using a special work-up protocol developed by Kaburagi and Kishi were we able to isolate **3.58** in pure form.²⁶⁴ Upon complete desilylation as determined by TLC, the reaction mixture is treated with an excess of CaCO₃, which forms the insoluble salt CaF₂. At this point, the solution phase contains predominantly the tetra-*n*-butylammonium phenoxide, and treatment with DOWEX-50WX8-400, a sulfonic acid resin, results in ion-exchange to liberate the phenol and trap the tetrabutylammonium as a sulfonate counterion. After stirring for >1 h, the mixture is simply filtered and concentrated to dryness to yield the desired product free of greasy contaminants.

The pure **3.58** was then subjected to the previously described retro-Brook sequence to provide the TMS-derivative **3.5**. However, despite variations in base (*n*-BuLi/*t*-BuLi), temperature, and solvent, the highest yields that could be obtained for these reactions were ~50%

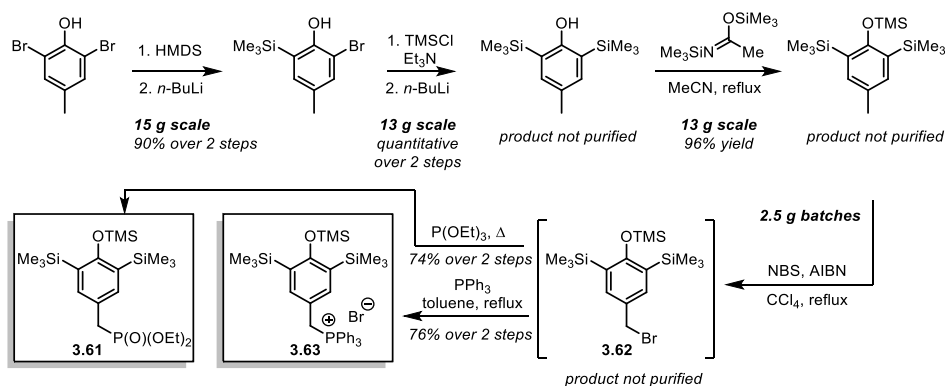


Figure 3.26 Preparation of Phosphorus-Based Olefination Reagents

per step. Fortunately, the remaining mass balance consisted almost entirely of the *O*-desilylated material **3.58**, which could then be recycled through the sequence. Eventually, 33 mg of the desired trimethylsilyl ϵ -viniferin derivative was obtained, and while this route has since been abandoned, this batch of material ultimately enabled the initial completion of our total synthesis.

A more attractive and convergent route would involve the direct conversion of aldehyde **3.32** to **3.5**, which would mitigate issues associated with late-stage introduction of the TMS groups while reducing the linear step count by three steps and five synthetic operations. Based on our most recent success using an HWE olefination for the preparation of **3.58**, we initially set out to prepare phosphonate ester **3.61** (Figure 3.26).¹⁴ Notably, only a single column purification was required throughout the sequence (at Step 1) and all reactions were found to be high yielding at scale. Also of note is the instability of bromide **3.62**, which must be carried on directly as the crude residue. As was true of the *tert*-butyl derivative **3.15** (Figure 3.20), the phosphonate ester **3.61** was found to be unreactive toward **3.32**, lending further support to the incompatibility of TMS-protected phenols in the presence of phosphonate-stabilized carbanions. Conversely, the corresponding phosphonium salt **3.63** provided the TMS ϵ -viniferin derivative **3.5** in 80% isolated yield as exclusively the (*E*)-isomer.

¹⁴ See supporting information for details

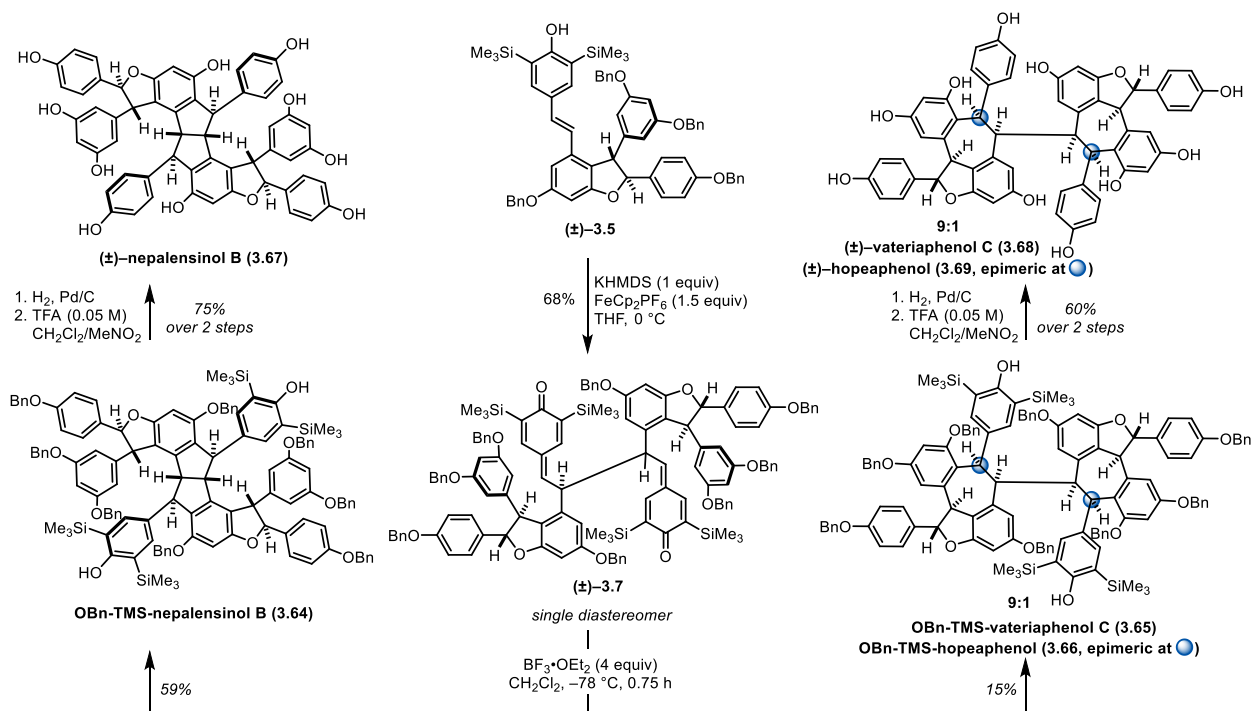


Figure 3.27 Total Synthesis of Nepalensinol B, Vateriaphenol C, and Hopeaphenol

Ionization of TMS–**3.5** and treatment of the resulting phenoxide with ferrocenium hexafluorophosphate FeCp_2PF_6 resulted in smooth conversion to the bis-quinone methide intermediate **3.7** as a single diastereomer (Figure 3.27). The slightly lower yields obtained for these reactions as compared to that of the corresponding *tert*-butyl derivative can be accounted for by the more electron-rich nature of the bis-quinone methide, which leads to more facile homolysis and disproportionation of the resultant phenoxyl radicals. Interestingly, the subsequent $\text{BF}_3 \cdot \text{OEt}_2$ promoted cyclization took place rapidly even at -78°C , suggesting a greater degree of conformational flexibility of TMS–**3.7** as compared to its *tert*-butyl congener. However, a temperature dependence of the product distribution was observed. In each case, the nepalensinol B core **3.64** was isolated as the major product, and the minor bis-7-*exo* product was formed as a 9:1 mixture of vateriaphenol C core **3.65** to hopeaphenol core **3.66**. The ensuing deprotections of these compounds proceeded smoothly. Global hydrogenolysis delivered near-pure samples of

each of the debenzylated materials (not shown) on simple filtration, and the resultant crude materials were used directly in the TFA-mediated protodesilylation reactions. Simple removal of volatiles at this stage yielded nearly pure samples of nepalensinol B (**3.67**) and a 9:1 inseparable mixture of vateriaphenol C (**3.68**) and hopeaphenol (**3.69**), which were each brought to analytical purity via preparative thin layer chromatography. Interestingly, allylic strain minimization would predict the hopeaphenol isomer to be preferred, yet vateriaphenol C is isolated as a significant majority, indicating a likely contribution of transannular strain and/or conformational restrictions in controlling the diastereoselectivity of the 7-*exo* Friedel–Crafts cyclization.

3.9 History and Biological Activities of Tetramers

On completion of the synthesis of the three tetramers, we could now finally be confident in the assignment of both their connectivities and relative configurations by comparison with the isolation reports. Originally isolated as “stenophyllol C”²⁶⁵ from the roots of *Sophora stenophylla* (Fabaceae) and later as “nepalensinol B” from the stem of *Kobresia nepalensis* (Cyperaceae),²⁶³ compound **3.67** has been isolated from a number of plant families and has been shown to exhibit several interesting biological activities. For instance, **3.67** isolated from *Vatica albiramis* (Dipterocarpaceae) was found to have a strong inhibitory effect (at 1 μ M) on interleukin (IL)-1 β -induced matrix metalloproteinase (MMP)-1 production in human dermal fibroblasts.²⁶⁶ Expression and activity of MMPs are known to increase with the progression of disease and with aging, causing degradation and remodeling of the structural extracellular matrix.²⁶⁷ Nepalensinol B was also found to exhibit potent activity against topoisomerase II (IC₅₀ = 0.02 μ g/mL),²⁶³ 3000 times stronger than etoposide (VP-16, IC₅₀ = 70 μ g/mL),²⁶⁸ a clinically approved chemotherapeutic that is on the WHO model list of essential cytotoxic and adjuvant medicines.²⁶⁹ Stenophyllol C was also shown to significantly reduce amyloid- β (A β)-40 and

A β 42 levels in N2a695 (mouse neuroblastoma) cells at low concentrations ($\leq 8 \mu\text{M}$), albeit not via a mechanism involving (α , β , or γ) secretase inhibition.²⁷⁰

The structure assigned to vateriaphenol C (**3.68**) on isolation was found to be identical with the structure reported in the literature for the resveratrol tetramer isohopeaphenol (cf. Figure 3.21), and the structure of isohopeaphenol has since been revised and confirmed through ^1H , ^1H -NOESY experiments.^{271,261} Thus, it is difficult to conclude with certainty whether biological studies prior to this fairly recent discovery (2008) were in fact using **3.68** or isohopeaphenol. Conversely, hopeaphenol (**3.69**) constitutes the first resveratrol oligomer ever characterized, which was accomplished by Coggon and co-workers in 1966 using single-crystal X-ray diffraction of a dibromo-decamethyl ether derivative.^{272,273} The structure was later confirmed by Kawabata and co-workers using advanced NMR techniques.²⁷⁴ Compound **3.69** was found to have an even stronger inhibitory effect (at $1 \mu\text{M}$) than stenophyllol C (**3.67**) on interleukin (IL)- 1β -induced matrix metalloproteinase (MMP)-1 production in human dermal fibroblasts.²⁶⁶ This scaffold also appears to be privileged for topoisomerase II inhibition, as each diastereomer of the bis-7-*exo* product **3.68** and **3.69** has been shown to have inhibitory activity ($\text{IC}_{50} = 4 \mu\text{M}$ and $6 \mu\text{M}$, respectively). Hopeaphenol was also found to inhibit angiotensin converting enzyme (ACE, $\text{IC}_{50} = 1.5 \mu\text{M}$), indicating a potential role as an antihypertensive agent.²⁷⁵ Moreover, **3.69** displayed activity against the bacterial virulence type III secretion system (T3SS), specifically against *Yersinia pseudotuberculosis* outer proteins E and H (YopE and YopH), with IC_{50} values of $8.8 \mu\text{M}$ and $2.9 \mu\text{M}$, respectively.^{276,277}

These structures have also demonstrated promising anti-cancer activities. Hopeaphenol (**3.69**) was found to be cytotoxic toward murine leukemia (P-388) cells ($\text{IC}_{50} = 5.2 \mu\text{M}$),⁹⁰ and demonstrated anti-proliferative effects in the canine glioblastoma cell line D-GBM ($\text{IC}_{50} = 1.8$

μM) and the canine histiocytic sarcoma cell line DH82 ($\text{IC}_{50} = 8.8 \mu\text{M}$).²⁷⁸ Furthermore, the anti-proliferative effect in D-GBM cells was found to be dependent on initiator caspase 9 induced activation of effector caspases 3 and 7. A separate study revealed potent cytotoxicity of **3.69** against a number of human cancer cell lines, including KB (cervical carcinoma, $\text{ED}_{50} = 1.2 \mu\text{M}$), A549 (lung carcinoma, $\text{ED}_{50} = 4.8 \mu\text{M}$), MCF-7 (breast adenocarcinoma, $\text{ED}_{50} = 4.2 \mu\text{M}$), and 1A9 (ovarian carcinoma, $\text{ED}_{50} = 7.8 \mu\text{M}$).⁷⁴ A subsequent study by Akao and co-workers investigated the cytotoxic effects of twenty resveratrol oligomers at various concentrations in nine human cancer cell lines.⁶⁷ Hopeaphenol (**3.69**) was found to inhibit the growth of SW480 (colon adenocarcinoma) and HL60 (promyelocytic leukemia) cell lines at a broadly screened concentration of $10 \mu\text{M}$. Alternatively, isohopeaphenol (likely vateriaphenol C (**3.68**)) was found to inhibit LNCaP (prostate carcinoma), SH-SY5Y (neuroblastoma), and HL60 cell lines at this concentration. The IC_{50} values for hopeaphenol against SW480 and HL60 cell lines were determined to be moderate, at 28.6 and $21.3 \mu\text{M}$, and that of isohopeaphenol/vateriaphenol C against HL60 was $36.2 \mu\text{M}$.

3.10 Conclusions

The concise biomimetic total synthesis of resveratrol tetramers nepalensinol B, vateriaphenol C, and hopeaphenol has been accomplished. This represents just the second reported total synthesis of tetrameric resveratrol oligomers,¹³⁸ and was achieved in seven fewer steps and higher overall yield than the previously reported route. Our initial observation of the dependency of cyclization product distribution on Lewis acid stoichiometry (cf. Table 3.1), careful consideration of the stereochemical implications of this process, and logical control studies allowed us to identify the homolytic dissociation equilibria of bis-quinone methide intermediates as previously discovered by Becker.¹⁶³ Although this unusual physical property

was initially disclosed as a mechanistic curiosity, we were able to recognize the synthetic potential of this process for dynamic stereocontrol, and implement it for the diastereoselective synthesis of resveratrol tetramers from racemic starting materials. The observed diastereoselectivity in the oxidative coupling of racemic ϵ -viniferin analog **3.5** indicates that the enantioselective preparation of this compound represents a viable entry to the asymmetric preparation of resveratrol tetramers in the 8–8' series.

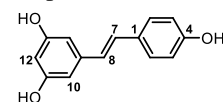
The wealth of biological activities surrounding these natural product scaffolds renders their efficient synthesis a significant achievement, as it will allow for a more thorough understanding of the bioactivity of not only the natural products, but their tert-butylated precursors and other analogues. Indeed, the NIH's National Center for Advancing Translational Sciences (NCATS) has launched a program to revitalize the pursuit of natural products research in drug discovery, including a high-throughput screen against a panel of over 30 whole-cell assays designed to encompass a broad diversity of biologies. The natural products prepared through our synthetic route have been submitted to this screening effort, and we eagerly await the results.

3.11 Experimental Procedures and Spectral Data

General Procedures: Glassware was dried in a 150 °C oven or flame-dried under vacuum (~0.5 Torr) prior to use. Reaction vessels were equipped with Teflon/PTFE-coated magnetic stir bars and fitted with rubber septa, and reaction mixtures were maintained under a positive pressure of dry nitrogen unless otherwise noted. Air- and/or moisture-sensitive liquids were transferred using stainless steel needles or cannulae. Reaction progress was monitored by analytical thin-layer chromatography (TLC) using glass-backed plates pre-coated with 230–400 mesh silica gel (250 μm, Indicator F-254), available from Silicycle, Inc (cat #: TLG-R10011B-323). Thin layer chromatography plates were visualized by exposure to a dual short-wave/long-wave UV lamp and/or by exposure to ethanolic solutions of *p*-anisaldehyde or vanillin, or an aqueous solution of ceric ammonium molybdate (Hanessian's stain), and the stained plates were developed by warming with a heat gun. Flash column chromatography was performed according to the procedure described by Still et al.¹⁵ either manually using 43-60 μm (230–400 mesh) silica gel or utilizing RediSep®R_F Gold silica columns with a Teledyne Isco CombiFlash R_F automated purification system. Upon reaction quenching and work up, organic solutions were dried over Na₂SO₄ or MgSO₄ and concentrated on Büchi rotary evaporators at ~10 Torr/35 °C, then at ~0.5 Torr/25 °C using a Welch vacuum pump.

Materials: Commercially available starting materials were used as received without further purification unless otherwise noted. Organic solvents (acetonitrile, dichloromethane, diethyl ether, dimethylformamide, dimethyl sulfoxide, methanol, tetrahydrofuran, toluene) and amine bases (triethylamine, pyridine, *N,N*-diisopropylethylamine, and diisopropylamine) were purified immediately prior to use by the method of Grubbs et al.¹⁶ using a Phoenix Solvent Drying System (JC-Meyer Solvent Systems) or PureSolv Micro amine drying columns (Innovative Technology/Inert), respectively, and maintained under positive argon pressure. Solutions of organolithium reagents (*n*-BuLi, *t*-BuLi) and Grignard reagents were purchased from Acros Organics unless otherwise noted and titrated prior to use (1,10-phenanthroline/menthol) according to the method of Paquette.¹⁷

Product Analysis: Product names were generated using ChemDraw Ultra 14.0 (PerkinElmer). ¹H and ¹³C NMR spectra were recorded at the indicated temperature at 117 kG and 176 kG (¹H 500 MHz, 700 MHz; ¹³C 125 MHz and 175 MHz) using an internal deuterium lock on Varian Inova 500 or Varian VNMR 500 and 700 spectrometers. ¹H chemical shifts are expressed in parts per million (ppm) relative to the residual protio solvent resonance in CDCl₃ using δ 7.26 as standard for residual CHCl₃ or using the center line of the solvent signal as internal reference for acetone-*d*₆: δ 2.05, and DMSO-*d*₆: δ 2.50. Multiplicity is reported as follows: (br = broad, s = singlet, d = doublet, t = triplet, dd = doublet of doublets, ddd = doublet of doublet of doublets, m = multiplet), and the corresponding coupling constants are indicated as *J*-values in units of Hz. ¹³C NMR spectra were completely ¹H-decoupled (broadband) and the center line of the solvent signal was used as internal reference: CDCl₃ δ 77.23; acetone-*d*₆ δ 29.92; DMSO-*d*₆ δ 39.51. ¹³C chemical shifts are expressed in parts per million (ppm) to a single decimal place; in instances where multiple resonances approximate the same chemical shift value, two decimal places are used. For ¹H and ¹³C assignments, the following resveratrol numbering scheme was used, and each successive resveratrol equivalent was denoted with (a, b, c, etc.). Diastereotopic protons are denoted with ('), and protons found to exchange in the presence of D₂O are indicated with "exchangeable [D₂O]". Infrared data were obtained on a Perkin-Elmer Spectrum BX FT-IR spectrophotometer using an ATR mount with a ZnSe crystal and are reported as follows: [frequency of absorption (cm⁻¹), intensity of absorption (s = strong, m = medium, w = weak, br = broad)]. High-resolution mass spectra (HRMS) were obtained on a Micromass AutoSpec Ultima Magnetic Sector mass spectrometer using electrospray ionization (ESI), positive ion mode—we thank James Windak and Paul Lennon at the University of Michigan Department of Chemistry instrumentation facility for conducting these experiments. X-ray crystallographic data were collected on a Rigaku AFC10K Saturn 944+ CCD-based X-ray diffractometer—we thank Dr. Jeff W. Kampf for conducting these experiments.



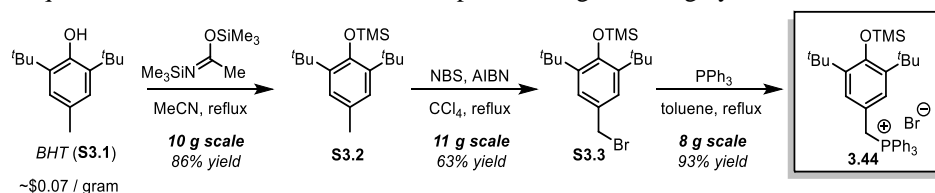
¹⁵ Still, W. C.; Kahn, M.; Mitra, A. J. *Org. Chem.* **1978**, *43* (14), 2923–2925.

¹⁶ Pangborn, A. B.; Giardello, M. A.; Grubbs, R. H.; Rosen, R. K.; Timmers, F. J. *Organometallics* **1996**, *15* (5), 1518–1520.

¹⁷ Lin, H.S.; Paquette, L. A. *Synth. Commun.* **1994**, *24* (17), 2503–2506; Watson, S. C.; Eastham, J. F. *J. Organomet. Chem.* **1967**, *9* (1), 165–68.

Preparation of Phosphonium Salt 3.44:

The requisite phosphonium salt was prepared according to the scheme depicted below from commercially available 2,6-Di-*tert*-butyl-4-methylphenol (BHT, CAS #: 128-37-0). Notably, no column purification was required throughout the sequence and all reactions were found to perform in good to high yield at scale.



Starting BHT (**S3.1**) (10.0 g, 45.4 mmol, 1.00 equiv) was added to a flame-dried round bottom flask fitted with a reflux condenser and equipped with stir bar. The material was dissolved in anhydrous MeCN (180 mL) and *N,O*-bistrimethylsilylacetaimide (95% purity, 13.32 mL, 54.5 mmol, 1.20 equiv) was added at room temperature. The reaction mixture was then heated to reflux under inert atmosphere for 15 h. The mixture was removed from heat and allowed to slowly cool to room temperature. The solution was then placed in an ice bath and cooled while gently stirring, inducing crystallization of the desired **S3.2**, which was collected by filtration as a white crystalline solid (11.4 g, 38.8 mmol, 86% yield).

¹H NMR (500 MHz, CDCl₃, 25 °C) δ: 7.04 (s, 2H), 2.26 (s, 3H), 1.40 (s, 18H), 0.40 (s, 9H).

The TMS-protected phenol **S3.2** (11.35 g, 38.8 mmol, 1.00 equiv) was dissolved in anhydrous CCl₄ (260 mL) in a flame-dried round bottom flask fitted with a reflux condenser and equipped with a magnetic stir bar. NBS (recrystallized, 7.596 g, 42.68 mmol, 1.10 equiv) then AIBN (319 mg, 1.94 mmol, 0.05 equiv) were added sequentially to the stirring solution at room temperature, and the mixture was immediately heated to reflux for 3 h. The solution was then cooled and filtered over a sinter funnel fitted with filter paper. The CCl₄ was removed *in vacuo* and the crude oil was recrystallized from MeCN (low melting solid so initiate recrystallization at lower temperature to prevent oiling out). The desired **S3.3** was isolated in pure form as white needles (9.07 g, 24.4 mmol, 63% yield).

¹H NMR (500 MHz, CDCl₃, 25 °C) δ: 7.27 (s, overlap, 2H), 4.49 (s, 2H), 1.40 (s, 18H), 0.41 (s, 9H).

A flame-dried round bottom flask equipped with a reflux condenser and magnetic stir bar was charged with the starting bromide **S3.3** (8.07 g, 21.73 mmol, 1.00 equiv). The material was dissolved in toluene (105 mL) under inert atmosphere and triphenylphosphine (8.548 g, 32.59 mmol, 1.50 equiv) was added in a single portion. The mixture was then heated at reflux for 12 h, at which point it was allowed to cool to room temperature. The phosphonium salt was collected by filtration and the source flask and filter cake rinsed repeatedly with hexanes. The desired phosphonium **3.44** was thus obtained as a white crystalline solid (12.75 g, 20.1 mmol, 93% yield).

¹H NMR (500 MHz, DMSO-*d*₆, 25 °C) δ: 7.90 (t, *J* = 7.6 Hz, 3H), 7.73 (ddd, *J* = 3.4, 7.8, 7.8 Hz, 6H), 7.57 (dd, *J* = 7.3, 12.5 Hz), 6.81 (d, *J* = 2.7 Hz, 2H), 5.00 (d, *J* = 14.9 Hz, 2H), 1.13 (s, 18H), 0.36 (s, 9H);

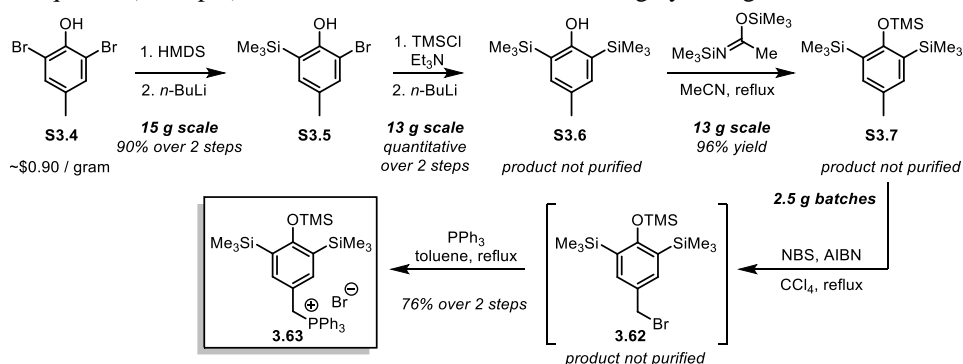
¹³C NMR (125 MHz, DMSO-*d*₆, 25 °C) δ: 140.8 (d, *J* = 3.8 Hz), 134.9 (d, *J* = 2.9 Hz), 134.0 (d, *J* = 9.5 Hz), 130.0 (d, *J* = 12.4 Hz), 128.5 (d, *J* = 87.7 Hz), 128.6 (d, *J* = 5.7 Hz), 118.9 (d, *J* = 8.6 Hz), 118.3 (s), 117.7 (s), 34.6 (s), 30.7 (s), 3.33 (s);

HRMS (EI): *m/z* calculated for C₃₆H₄₆OPSi [M-Br]⁺: 553.3056, found 553.3054;

FTIR (neat) cm⁻¹: 2950 (m), 2361 (m), 1434 (s), 1420 (s), 1393 (m), 1269 (m), 1252 (m), 1230 (s), 1215 (s), 1111 (s), 910 (s), 837 (s), 692 (s).

Preparation of Phosphonium Salt 3.63:

The requisite phosphonium salt was prepared according to the scheme depicted below from commercially available 2,6-dibromo-4-methylphenol (CAS #: 2432-14-6). Notably, only a single column purification was required throughout the sequence (at Step 1) and all reactions were found to be high yielding at scale.



2-bromo-4-methyl-6-(trimethylsilyl)phenol (S3.5): Prepared from 2,6-dibromo-4-methylphenol **S3.4** (15.0 g, 56.4 mmol, 1.00 equiv) according to the method reported by Akai and co-workers.¹⁸ After column chromatography (100% hexanes), **S3.5** was obtained in pure form as a clear/colorless oil (13.1 g, 50.5 mmol, 90% yield). ¹H-NMR data for **S3.5** is reported below:

¹H NMR (400 MHz, CDCl₃, 25 °C) δ: 7.28 (m, 1H), 7.07 (m, 1H), 5.53 (s, -OH), 2.26 (s, 3H), 0.30 (s, 9H).

4-methyl-2,6-bis(trimethylsilyl)phenol (S3.6): Prepared from **S3.5** (13.05 g, 50.3 mmol, 1.00 equiv) according to the method reported by Akai and co-workers.¹⁹ After work-up, the desired **S3.6** was obtained in pure form as clear/colorless stacked plate crystals (12.7 g, 50.3 mmol, quantitative yield). ¹H-NMR data for **S3.6** is reported below:

¹H NMR (500 MHz, CDCl₃, 25 °C) δ: 7.15 (s, 2H), 4.84 (s, 1H), 2.28 (s, 3H), 0.33 (s, 9H).

(5-methyl-2-((trimethylsilyl)oxy)-1,3-phenylene)bis(trimethylsilane) (S3.7): Starting **S3.6** (12.7 g, 50.3 mmol, 1.00 equiv) was added to a flame-dried round bottom flask fitted with a reflux condenser and equipped with stir bar. The material was dissolved in anhydrous MeCN (200 mL) and N,O-bis(trimethylsilyl)acetamide (95% purity, 15.53 mL, 60.4 mmol, 1.20 equiv) was added at room temperature. The reaction mixture was then heated to reflux under inert atmosphere for 15 h. The byproduct, trimethylsilylacetamide, was removed by sublimation (80 °C, <5 Torr) to afford a viscous oil which was taken up in toluene and filtered through a pad of Celite. The filtrate was concentrated *in vacuo* to yield the desired product **S3.7** in pure form an amorphous white solid (15.7 g, 48.4 mmol, 96% yield).

¹H NMR (400 MHz, CDCl₃, 25 °C) δ: 7.17 (s, 2H), 2.27 (s, 3H), 0.30 (s, 18H), 0.22 (s, 9H);

¹³C NMR (125 MHz, CDCl₃, 25 °C) δ: 162.9, 138.1, 129.81, 129.76, 20.8, 21.5, 1.28;

HRMS (EI): *m/z* calculated for C₁₆H₃₃OSi₃ [M+H]⁺: 324.1761, found 324.1771;

FTIR (neat) cm⁻¹: 2958 (m), 2902 (m), 1552 (w), 1386 (s), 1247 (s), 1210 (s), 1121 (m), 1103 (m), 930 (s), 890 (s), 818 (s).

¹⁸ Akai, S.; Ikawa, T.; Takayanagi, S.; Morikawa, Y.; Mohri, S.; Tsubakiyama, M.; Egi, M.; Wada, Y.; Kita, Y. *Angew. Chem. Int. Ed.* **2008**, *47* (40), 7673–7676.

¹⁹ Ikawa, T.; Nishiyama, T.; Shigeta, T.; Mohri, S.; Morita, S.; Takayanagi, S.; Terauchi, Y.; Morikawa, Y.; Takagi, A.; Ishikawa, Y.; Fujii, S.; Kita, Y.; Akai, S. *Angew. Chem. Int. Ed.* **2011**, *50* (25), 5674–5677.

(3,5-bis(trimethylsilyl)-4-((trimethylsilyl)oxy)benzyl)triphenylphosphonium bromide (3.62): Starting **S3.7** (2.50 g, 7.70 mmol, 1.00 equiv) was dissolved in CCl₄ (77 mL) in a flame-dried round bottom flask equipped with a stir bar and fitted with a reflux condenser. NBS (recrystallized, 1.507 g, 8.470 mmol, 1.10 equiv) then AIBN (63 mg, 0.385 mmol, 0.05 equiv) were added sequentially to the stirring solution at room temperature, and the mixture was immediately heated to reflux for 3 h. The solution was then cooled and filtered over a sinter funnel fitted with filter paper, eluting with hexanes. The filtrate was concentrated *in vacuo* to afford the intermediate bromide **3.62** in nearly pure form as a yellow oil (quantitative yield assumed, ¹H-NMR of crude material included). (NOTE: Intermediate **3.62** is unstable and should be carried on directly and shielded from light).

¹H NMR (500 MHz, CDCl₃, 25 °C) δ: 7.39 (s, 2H), 4.49 (s, 2H), 0.32 (s, 3H), 0.23 (s, 9H).

The bromide **3.62** was dissolved in toluene (38 mL) under inert atmosphere and triphenylphosphine (3.029 g, 11.55 mmol, 1.50 equiv) was added in a single portion. The mixture was then heated at reflux for 1 h, at which point it was allowed to cool to room temperature. The phosphonium salt was collected by filtration and the source flask and filter cake rinsed repeatedly with hexanes. The desired phosphonium **3.63** was thus obtained as a white crystalline solid (3.9 g, 5.86 mmol, 76% yield over 2 steps).

¹H NMR (500 MHz, DMSO-*d*₆, 25 °C) δ: 7.91 (m, 4H), 7.73 (ddd, 3.4, 7.9, 7.9 Hz, 6H), 7.58 (dd, *J* = 7.1, 12.4 Hz, 6H), 7.01 (d, *J* = 2.7 Hz, 2H), 5.06 (d, *J* = 15.1 Hz, 2H), 0.18 (s, 9H), 0.09 (s, 18H);

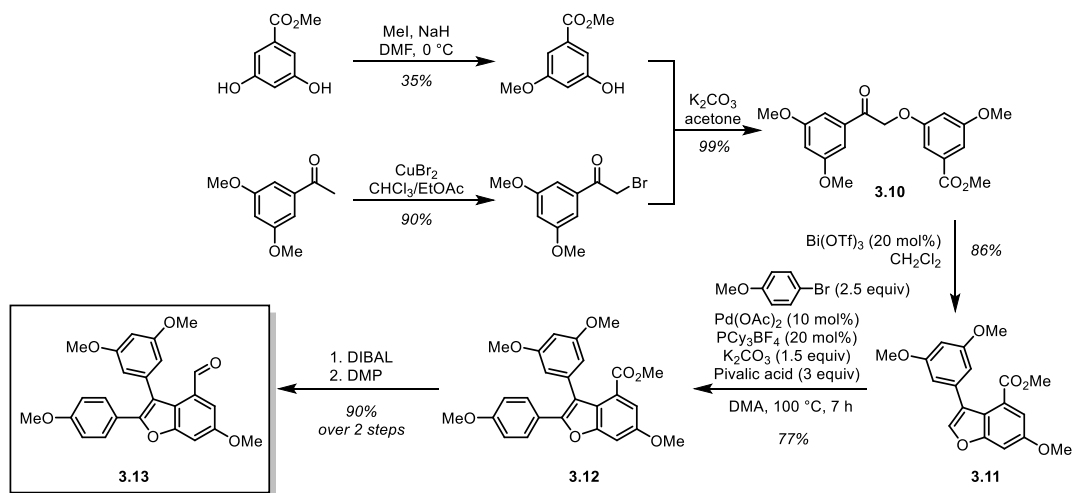
¹³C NMR (125 MHz, DMSO-*d*₆, 25 °C) δ: 139.7 (d, *J* = 4.8 Hz), 135.0 (s), 134.0 (d, *J* = 9.5 Hz), 130.2 (s), 130.0 (d, *J* = 12.4 Hz), 128.5 (d, *J* = 86.8 Hz), 125.3 (s), 118.2 (s), 117.5 (s), 1.42 (s), 0.64 (s);

HRMS (ESI): *m/z* calculated for C₁₆H₃₃OSi₃ [M+H]⁺: 585.2594, found 585.2590;

FTIR (neat) cm⁻¹: 2951 (m), 2878 (m), 1437 (m), 1384 (s), 1252 (m), 1213 (m), 1112 (s), 937 (m), 902 (m), 829 (s).

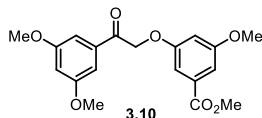
Preparation of Aldehyde 3.13:

The requisite aldehyde was prepared according to the scheme depicted below using procedures described by Kim and Choi.²⁰ For the C₂-arylation of benzofuran **3.11**, a modified procedure using Fagnou's conditions was employed.²¹ Because these are reported procedures, synthetic protocols are not included here. However, ¹H-NMR data are reported for all compounds beginning with intermediate **3.10** in the following pages and the corresponding authentic spectra are included.



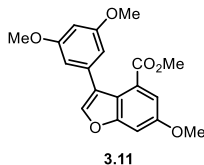
²⁰ Kim, I.; Choi, J. *Org. Biomol. Chem.* **2009**, *7* (13), 2788–2795.

²¹ (a) Liégault, B.; Lapointe, D.; Caron, L.; Vlassova, A.; Fagnou, K. *J. Org. Chem.* **2009**, *74* (5), 1826–1834; (b) Kim, K.; Kim, I. *Org. Lett.* **2010**, *12* (22), 5314–5317.



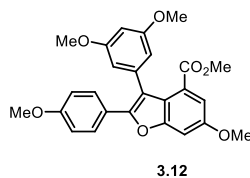
Methyl 3-(2-(3,5-dimethoxyphenyl)-2-oxoethoxy)-5-methoxybenzoate (3.10):

$^1\text{H NMR}$ (400 MHz, CDCl_3 , 25 °C) δ : 7.23 (dd, $J = 1.2, 2.4$ Hz, 1H), 7.18 (dd, $J = 1.2, 2.4$ Hz, 1H), 7.11 (d, $J = 2.4$ Hz, 2H), 6.74 (t, $J = 2.4$ Hz, 1H), 6.70 (t, $J = 2.4$ Hz, 1H), 5.28 (s, 2H), 3.90 (s, 3H), 3.85 (s, 6H), 3.83 (s, 3H).



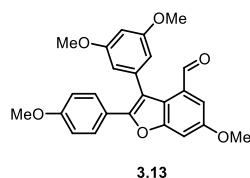
Methyl 3-(3,5-dimethoxyphenyl)-6-methoxybenzofuran-4-carboxylate (3.11):

$^1\text{H NMR}$ (500 MHz, CDCl_3 , 25 °C) δ : 7.62 (s, 1H), 7.34 (d, $J = 2.5$ Hz, 1H), 7.22 (d, $J = 2.5$ Hz, 1H), 6.49 (d, $J = 2.2$ Hz, 2H), 6.47 (t, $J = 2.2$ Hz, 1H), 3.90 (s, 3H), 3.80 (s, 6H), 3.32 (s, 3H).



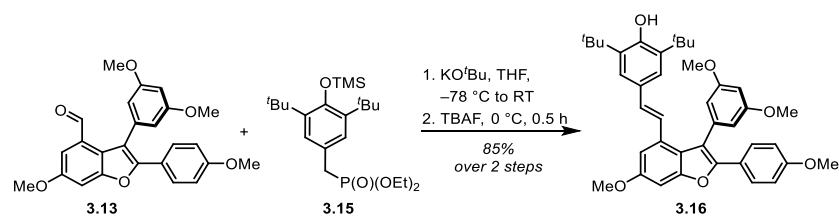
Methyl 3-(3,5-dimethoxyphenyl)-6-methoxy-2-(4-methoxyphenyl)benzofuran-4-carboxylate (3.12):

$^1\text{H NMR}$ (500 MHz, CDCl_3 , 25 °C) δ : 7.49 (d, $J = 9.0$ Hz, 2H), 7.24 (d, $J = 2.2$ Hz, 1H), 7.22 (d, $J = 2.2$ Hz, 1H), 6.82 (d, $J = 9.0$ Hz, 2H), 6.50 (s, overlap, 3H), 3.90 (s, 3H), 3.80 (s, 3H), 3.77 (s, 6H), 3.24 (s, 3H).



3-(3,5-dimethoxyphenyl)-6-methoxy-2-(4-methoxyphenyl)benzofuran-4-carbaldehyde (3.13):

$^1\text{H NMR}$ (400 MHz, CDCl_3 , 25 °C) δ : 9.77 (s, 1H), 7.53 (d, $J = 9.1$ Hz, 2H), 7.46 (d, $J = 2.4$ Hz, 1H), 7.33 (d, $J = 2.4$ Hz, 1H), 6.83 (d, $J = 9.1$ Hz, 2H), 6.61 (d, $J = 2.4$ Hz, 2H), 6.55 (t, $J = 2.4$ Hz, 1H), 3.92 (s, 3H), 3.80 (s, 3H), 3.79 (s, 6H).



(E)-2,6-di-tert-butyl-4-(2-(3-(3,5-dimethoxyphenyl)-6-methoxy-2-(4-methoxyphenyl)benzofuran-4-yl)vinyl)phenol (3.16):

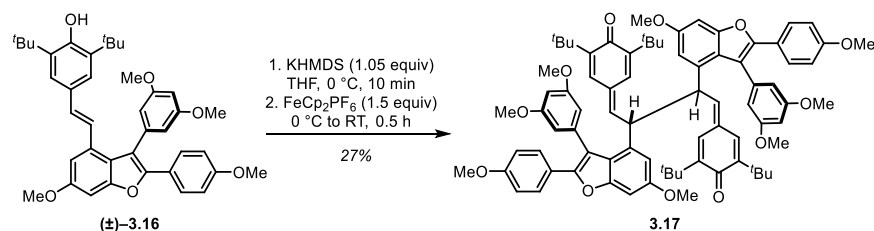
A solution of starting aldehyde **3.13** (139 mg, 0.332 mmol, 1.00 equiv) and phosphonate ester **3.15** (214 mg, 0.498 mmol, 1.50 equiv), was prepared in THF (6 mL). The mixture was degassed by freeze-pump-thaw (3x), with the final thaw cycle in a $-78\text{ }^{\circ}\text{C}$ dry ice/acetone bath. To the stirring solution at this temperature was added KO^tBu (1.0 M sol'n in THF, 498 μL , 1.50 equiv), turning it bright red. The reaction was then equilibrated to $0\text{ }^{\circ}\text{C}$ and allowed to stir overnight and slowly warm to RT. At 15 h, cooled reaction back to $0\text{ }^{\circ}\text{C}$ and added TBAF (1.0 M sol'n in THF, 498 μL , 1.50 equiv). The reaction was stirred for 0.5 h then quenched with sat. aq. NH_4Cl , diluted with EtOAc, and transferred to a separatory funnel where the phases were separated. The aqueous phase was extracted with additional EtOAc and the combined organic layers were washed with brine, dried over Na_2SO_4 , and concentrated *in vacuo*. The crude material was purified by flash chromatography over SiO_2 (10% of a 2:1 EtOAc/ CH_2Cl_2 mixture in hexanes) to yield the viniferifuran derivative **3.16** (175 mg, 0.282 mmol, 85% yield) as a white foam.

TLC (Hexanes/EtOAc/ CH_2Cl_2 , 80:15:5), R_f : 0.36 (UV);

^1H NMR (500 MHz, CDCl_3 , $25\text{ }^{\circ}\text{C}$) δ : 7.44 (d, $J = 9.1\text{ Hz}$, 2H), 7.15 (d, $J = 2.2\text{ Hz}$, 1H), 7.00 (d, overlap, $J = 2.2\text{ Hz}$), 6.99 (s, 2H), 6.94 (d, $J = 16.1\text{ Hz}$, 1H), 6.86 (d, $J = 16.1\text{ Hz}$, 1H), 6.80 (d, $J = 9.1\text{ Hz}$, 2H), 6.63 (d, $J = 2.2\text{ Hz}$, 2H), 6.53 (t, $J = 2.2\text{ Hz}$, 1H), 5.25 (s, 1H), 3.93 (s, 3H), 3.79 (s, 3H), 3.70 (s, 6H), 1.42 (s, 18H);

^{13}C NMR (175 MHz, CDCl_3 , $25\text{ }^{\circ}\text{C}$) δ : 161.2, 159.4, 158.1, 155.2, 154.0, 150.1, 136.9, 136.2, 132.9, 130.9, 128.7, 127.7, 123.7, 123.6, 122.0, 121.9, 116.7, 114.0, 108.6, 107.1, 101.3, 94.9, 56.1, 55.5, 55.4, 34.5, 30.5;

HRMS (ESI): m/z calculated for $\text{C}_{40}\text{H}_{45}\text{O}_6$ $[\text{M}+\text{H}]^+$: 621.3211, found 621.3205.

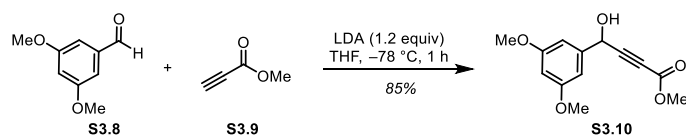


4,4'-((2R)-2,3-bis(3-(3,5-dimethoxyphenyl)-6-methoxy-2-(4-methoxyphenyl)benzofuran-4-yl)butane-1,4-diylidene)bis(2,6-di-tert-butylcyclohexa-2,5-dien-1-one) (3.17): Starting **3.16** (37 mg, 0.053 mmol, 1.00 equiv) was dissolved in THF (5.20 mL) and cooled to 0 °C under inert atmosphere. KHMDS (1.0 M sol'n in THF, 56 μ L, 0.056 mmol, 1.05 equiv) was then added slowly, turning the solution bright red. FeCp_2PF_6 (23 mg, 0.067 mmol, 1.25 equiv) was then added in a single portion. At 0.5 h, the reaction was filtered through a cotton plug and the filtrate concentrated *in vacuo*. The crude material was then purified by flash chromatography over SiO_2 (5–20% gradient of 2:1 $\text{CH}_2\text{Cl}_2/\text{EtOAc}$ mixture in Hexanes) to afford **3.17** (9 mg, 0.007 mmol, 27% yield) as a mixture of diastereomers.

TLC (Hexanes/EtOAc/ CH_2Cl_2 , 80:15:5), R_f : 0.22 (UV, *p*-anisaldehyde (green));

$^1\text{H NMR}$ (500 MHz, CDCl_3 , 25 °C) δ : 7.34 (d, $J = 9.0$ Hz, 4H), 7.22 (d, $J = 9.0$ Hz, 4H), 7.06 (br s, 2H), 6.93 (d, overlap, $J = 2.2$ Hz, 2H), 6.92 (d, overlap, $J = 2.2$ Hz, 2H), 6.79 (d, $J = 9.0$ Hz, 4H), 6.76 (d, overlap, $J = 9.0$ Hz, 4H), 6.76 (d, overlap, $J = 2.0$ Hz), 6.63 (d, $J = 2.2$ Hz, 2H), 6.60 (d, $J = 2.0$ Hz, 2H), 6.57 (t, $J = 2.2$ Hz, 2H), 6.51 (br s, 2H), 6.49 (t, $J = 2.2$ Hz, 2H), 6.42 (d, $J = 2.0$ Hz, 2H), 6.41 (br s, 2H), 6.26 (br d, $J = 7.1$ Hz, 2H), 6.20 (m, overlap, 4H), 6.17 (d, $J = 2.2$ Hz, 2H), 6.10 (br s, 2H), 4.55 (m, overlap, 4H), 3.93 (s, 6H), 3.79 (s, 12H), 3.78 (s, 6H), 3.77 (s, 6H), 3.76 (s, 6H), 3.75 (s, 6H), 3.59 (s, 6H), 3.17 (s, 6H), 1.18 (s, 18H), 1.15 (s, 18H), 1.12 (s, 18H), 0.98 (s, 18H).

HRMS (ESI): m/z calculated for $\text{C}_{80}\text{H}_{86}\text{O}_{12}$ $[\text{M}+\text{NH}_4]^+$: 1256.6458, found 1256.6420.



Methyl 4-(3,5-dimethoxyphenyl)-4-hydroxybut-2-ynoate (S3.10):²² A solution of diisopropylamine (2.03 mL, 14.51 mmol, 1.20 equiv) in THF (28 mL) was cooled to $-78\text{ }^\circ\text{C}$ and treated with *n*-butyllithium (2.5 M sol'n in hexanes, 5.56 mL, 13.91 mmol, 1.15 equiv). After 15 minutes of stirring at this temperature under inert atmosphere, methyl propiolate **S3.9** (1.24 mL, 13.91 mmol, 1.15 equiv) was added slowly, turning the solution yellow–orange. Meanwhile, a solution of 3,5-dimethoxybenzaldehyde **S3.8** (2.01 g, 12.1 mmol, 1.00 equiv) was prepared in THF (12 mL) and cooled to $-78\text{ }^\circ\text{C}$. At 15 minutes, the aldehyde solution was transferred by cannula to the stirring solution of lithium acetylide. The reaction was stirred at $-78\text{ }^\circ\text{C}$ for 1 h at which point it was quenched by the addition of sat. aq. NH_4Cl . The mixture was then diluted with diethyl ether and transferred to a separatory funnel where the phases were separated. The aqueous phase was extracted with additional portions of diethyl ether. The combined organic layers were washed with brine, dried over Na_2SO_4 , and concentrated *in vacuo*. The crude material was then purified by flash chromatography over SiO_2 (15–35% EtOAc/Hexanes) to afford the propargylic alcohol **S3.10** as a yellow oil (2.708 g, 10.8 mmol, 85% yield).

TLC (Hexanes/EtOAc, 85:15), R_f : 0.21 (UV);

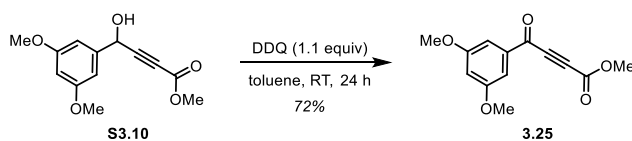
$^1\text{H NMR}$ (500 MHz, CDCl_3 , $25\text{ }^\circ\text{C}$) δ : 6.66 (d, $J = 2.2\text{ Hz}$, 2H), 6.44 (t, $J = 2.2\text{ Hz}$, 1H), 5.50 (s, 1H), 3.81 (s, 6H), 3.79 (s, 3H);

$^{13}\text{C NMR}$ (175 MHz, CDCl_3 , $25\text{ }^\circ\text{C}$) δ : 160.8, 153.9, 140.9, 104.5, 100.5, 86.9, 77.0, 63.7, 55.3, 52.8;

HRMS (ESI): m/z calculated for $\text{C}_{13}\text{H}_{15}\text{O}_5$ $[\text{M}+\text{H}]^+$: 251.0914, found 251.0918;

FTIR (neat) cm^{-1} : 3422 (m, br), 2953 (w), 2839 (w), 1715 (s), 1596 (s), 1457 (s), 1430 (s), 1249 (s), 1203 (s), 1154 (s), 1059 (s), 1016 (s), 962 (m), 910 (m), 838 (m, br).

²² Procedure adapted from: Pünner, F.; Schieven, J.; Hilt, G. *Org. Lett.* **2013**, *15* (18), 4888–4891.



Methyl 4-(3,5-dimethoxyphenyl)-4-oxobut-2-ynoate (3.25):²³ A solution of starting **S3.10** (2.425 g, 9.69 mmol, 1.00 equiv) was prepared in toluene (20 mL). To the stirring mixture at room temperature was added DDQ (2.42 g, 10.66 mmol, 1.10 equiv) in a single portion. The reaction turned a deep red/black and was allowed to stir at room temperature over night, during which time it became red-orange and heterogeneous. At 24 h, the reaction mixture was diluted with EtOAc and transferred to a separatory funnel where the phases were separated. The organic layer was then washed with sat. aq. Na₂CO₃ until the aqueous washes were only faintly colored. The organic layer was then washed with brine, dried over Na₂SO₄, and concentrated *in vacuo*. The crude material was purified by flash chromatography over SiO₂ (10–20% EtOAc in Hexanes) to afford **3.25** (1.900 g, 7.65 mmol, 72% yield) as a yellow solid.

TLC (Hexanes/EtOAc, 85:15), R_f: 0.21 (UV);

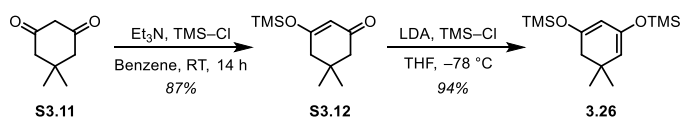
¹H NMR (700 MHz, CDCl₃, 25 °C) δ: 7.25 (d, *J* = 2.2 Hz, 2H), 6.74 (t, *J* = 2.2 Hz, 1H), 3.89 (s, 3H), 3.85 (s, 6H),

¹³C NMR (175 MHz, CDCl₃, 25 °C) δ: 175.6, 161.0, 152.6, 137.3, 107.6, 107.3, 80.0, 79.8, 55.7, 53.4;

HRMS (ESI): *m/z* calculated for C₁₃H₁₃O₅ [M+H]⁺: 249.0757, found 249.0760;

FTIR (neat) cm⁻¹: 2939 (w), 1716 (s), 1654 (s), 1589 (m), 1472 (m), 1445 (m), 1429 (m), 1355 (s), 1305 (s), 1266 (s), 1203 (s), 1160 (s), 1067 (m), 1044 (m), 981 (m), 925 (m), 897 (m), 848 (m), 824 (m), 741 (s), 680 (s).

²³ Procedure adapted from: Pünner, F.; Schieven, J.; Hilt, G. *Org. Lett.* **2013**, *15* (18), 4888–4891.



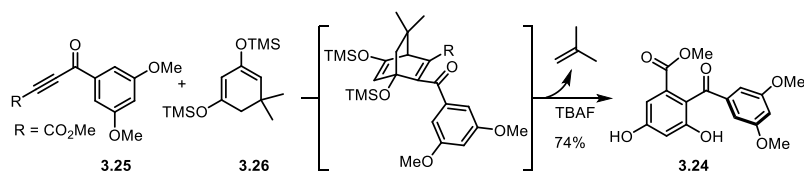
((5,5-dimethylcyclohexa-1,3-diene-1,3-diyl)bis(oxy))bis(trimethylsilane) (3.26):²⁴ To a suspension of dimedone **S3.11** (10.0 g, 71.3 mmol, 1.00 equiv) in benzene (100 mL) at room temperature was added Et₃N (12.93 mL, 92.7 mmol, 1.30 equiv), turning the mixture homogeneous. Next, chlorotrimethylsilane (11.8 mL, 92.7 mmol, 1.30 equiv) was added, causing salt precipitation (NOTE: stir vigorously). The suspension was stirred under inert atmosphere for 14 h, at which point the precipitated salts were removed by filtration and the solvent was removed *in vacuo*. The residue was distilled under high vacuum at 160 °C (air condenser) to afford the intermediate silyl enol ether **S3.12** as a white solid (13.16 g, 62 mmol, 87% yield).

¹H NMR (400 MHz, CDCl₃, 25 °C) δ: 5.38 (s, 1H), 2.23 (s, 2H), 2.19 (s, 2H), 1.07 (s, 6H), 0.29 (s, 9H).

To a solution of diisopropylamine (15.62 mL, 111.5 mmol, 1.8 equiv) in THF (100 mL) was added *n*-butyllithium (1.6 M sol'n in hexanes, 68 mL, 108.3 mmol, 1.75 equiv) at -78 °C. A solution of the silyl enol ether **S3.12** (13.15 g, 62 mmol, 1.00 equiv) was prepared in THF (125 mL) and added slowly to the stirring solution of LDA at -78 °C. After the mixture had been stirred for 1 h at -78 °C, chlorotrimethylsilane (17.3 mL, 136.2 mmol, 2.2 equiv) was added and the solution was allowed to stir overnight and slowly warm to RT. Pentanes was then added to the stirring mixture to precipitate LiCl which was then removed by filtration over a pad of Celite. The filtrate was then concentrated *in vacuo* and the crude residue purified by distillation under high vacuum/160 °C using a bulb-to-bulb distillation apparatus with a water condenser and an external vacuum trap to prevent a white solid from sublimating into the the manifold. The product **3.26** (16.5 g, 58 mmol, 94% yield) was collected as a clear oil.

¹H NMR (700 MHz, CDCl₃, 25 °C) δ: 4.91 (dd, *J* = 1.2, 2.3 Hz, 1H), 4.41 (d, *J* = 2.3 Hz, 1H), 2.05 (d, *J* = 1.2 Hz, 2H), 1.02 (s, 6 H), 0.23 (s, 9H), 0.18 (s, 9H).

²⁴ Procedure adapted from: Langer, P.; Schneider, T.; Stoll, M. *Chem. – Eur. J.* **2000**, *6* (17), 3204–3214.



Methyl 2-(3,5-dimethoxybenzoyl)-3,5-dihydroxybenzoate (3.24): Starting aroyl propiolate **3.25** (5.85 g, 23.57 mmol, 1.00 equiv) and diene **3.26** (16.76 g, 58.9 mmol, 2.50 equiv) were combined in a round bottom flask equipped with a stir bar and sealed with a rubber septum under inert atmosphere. The neat mixture was then heated to 120 °C, melting the materials into a homogeneous red-orange mixture. The reaction was stirred for 15 h at this temperature, at which point it was fitted directly with a distillation apparatus and heated to 160 °C under high vacuum. In this way, excess diene **3.26** (6 g, 36%) was recovered. The remaining crude material was cooled to room temperature, dissolved in THF (190 mL), and cooled to 0 °C under inert atmosphere. To the stirring solution was added TBAF (1 M sol'n in THF, 47.1 mL, 47.1 mmol, 2.00 equiv), turning it a deep red. After 45 minutes, the reaction was quenched by the addition of sat. aq. NH₄Cl, diluted with EtOAc, and transferred to a separatory funnel where the phases were separated. The aqueous phase was extracted with additional portions of EtOAc, and combined organic layers were washed with brine, dried over Na₂SO₄, and concentrated *in vacuo*. Partial purification achieved by flash chromatography over SiO₂ (25–50% EtOAc/Hexanes, NOTE: Product has low solubility). The semi-pure material was then brought to purity by recrystallization from boiling toluene, affording **3.24** (5.80 g, 17.5 mmol, 74% yield) as a white crystalline solid as a single regioisomer (confirmed to be the desired regioisomer by 2D NMR).

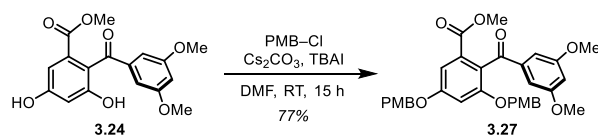
TLC (Hexanes/EtOAc, 75:25), R_F: 0.49 (UV, before desilylation); 0.08 (UV, after desilylation)

¹H NMR (700 MHz, Acetone-*d*₆, 25 °C) δ: 9.85–8.95 (br s, 2H), 6.95 (d, *J* = 2.3 Hz, 1H), 6.85 (d, *J* = 2.3 Hz, 2H), 6.69 (d, *J* = 2.3 Hz, 1H), 6.68 (t, *J* = 2.3 Hz, 1H), 3.80 (s, 6H), 3.47 (s, 3H);

¹³C NMR (175 MHz, Acetone-*d*₆, 25 °C) δ: 196.5, 167.2, 161.8, 160.92, 159.6, 142.1, 134.4, 118.9, 109.9, 107.33, 107.29, 105.1, 55.9, 52.4;

HRMS (ESI): *m/z* calculated for C₁₇H₁₇O₇ [M+H]⁺: 333.0969, found 333.0972;

FTIR (neat) cm⁻¹: 3327 (m, br), 1717 (m), 1700 (s), 1684 (m), 1653 (s), 1616 (s), 1591 (s), 1558 (s), 1540 (m), 1506 (m), 1457 (s), 1436 (m), 1347 (s, br), 1206 (s), 1157 (s), 1065 (m), 1027 (m).



Methyl 2-(3,5-dimethoxybenzoyl)-3,5-bis((4-methoxybenzyl)oxy)benzoate (3.27): A round bottom flask was charged with starting **3.24** (1.40 g, 4.22 mmol, 1.00 equiv) and TBAI (311 mg, 0.842 mmol, 20 mol%). The materials were dissolved in DMF (20 mL) and cooled to 0 °C, and Cs₂CO₃ (3.02 g, 9.27 mmol, 2.20 equiv), was added in a single portion. After stirring for 20 minutes at this temperature, PMB–Cl (1.20 mL, 8.85 mmol, 2.10 equiv) was added slowly. At 1 h, the ice bath was removed and the reaction was allowed to stir at room temperature overnight. The reaction mixture was then diluted with EtOAc and transferred to a separatory funnel containing ice cold DI H₂O. The phases were separated and the aqueous phase was extracted with additional portions of EtOAc. The combined organic layers were washed with DI H₂O (2x), 5% aq. LiCl, and brine. The organic phase was then dried over Na₂SO₄ and concentrated *in vacuo*. The crude material was purified by flash chromatography over SiO₂ (20–35% EtOAc/Hexanes) to afford **3.27** (1.85 g, 3.23 mmol, 77% yield) as a white amorphous solid.

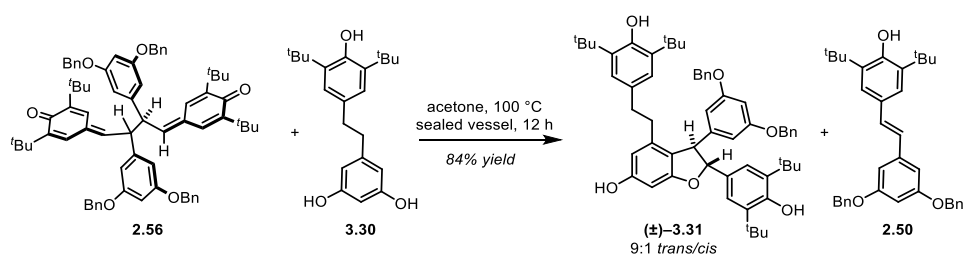
TLC (Hexanes/EtOAc, 60:40), R_F: 0.31 (UV)

¹H NMR (700 MHz, CDCl₃, 25 °C) δ: 7.36 (d, *J* = 8.5 Hz, 2H), 7.25 (d, *J* = 2.1 Hz, 1H), 6.98 (d, *J* = 8.5 Hz, 2H), 6.95 (d, overlap, *J* = 2.2 Hz, 2H), 6.94 (d, overlap, *J* = 8.5 Hz, 2H), 6.77 (d, *J* = 2.1 Hz, 1H), 6.74 (d, *J* = 8.5 Hz, 2H), 6.64 (t, *J* = 2.2 Hz, 1H), 5.02 (s, 2H), 4.91 (s, 2H), 3.83 (s, 3H), 3.78 (s, 6H), 3.76 (s, 3H), 3.69 (s, 3H);

¹³C NMR (175 MHz, CDCl₃, 25 °C) δ: 195.5, 166.0, 160.9, 160.2, 159.9, 159.4, 157.1, 140.2, 130.5, 129.7, 128.7, 128.3, 128.2, 125.1, 114.3, 113.9, 107.3, 106.8, 105.7, 105.3, 70.5, 55.7, 55.5, 55.4, 52.5;

HRMS (ESI): *m/z* calculated for C₃₃H₃₃O₉ [M+H]⁺: 573.2119, found 573.2120;

FTIR (neat) cm⁻¹: 1718 (s), 1700 (m), 1684 (s), 1653 (s), 1596 (s, br), 1558 (s), 1540 (s), 1515 (s), 1457 (s), 1436 (m), 1322 (m), 1300 (s), 1248 (s), 1204 (m), 1153 (s), 1032 (m).



(2R,3R)-3-(3,5-bis(benzyloxy)phenyl)-4-(3,5-di-tert-butyl-4-hydroxyphenethyl)-2-(3,5-di-tert-butyl-4-hydroxyphenyl)-2,3-dihydrobenzofuran-6-ol (3.31): A 4 dram vial equipped with a magnetic stirring bar was charged with starting bis-quinone methide **2.56** (300 mg, 0.289 mmol, 1.00 equiv) and dihydrostilbene **3.30**²⁵ (198 mg, 0.577 mmol, 2.00 equiv). The materials were dissolved/suspended in acetone (5.75 mL), and the vial was sealed tightly. The slowly stirring mixture was then heated to 100 °C for 12 h, over the course of which it becomes homogeneous and yellow-green and eventually yellow-orange. The vial was removed from the heat and allowed to cool to room temperature. The solvent was removed *in vacuo* and the crude material was purified by flash chromatography over SiO₂ (10% – 20% of a 2:1 EtOAc/CH₂Cl₂ mixture in Hexanes, followed by a flush at 100% of the 2:1 EtOAc/CH₂Cl₂) to yield dihydrobenzofuran **3.31** as a separable mixture of *trans*- (182 mg, 0.211 mmol, 74% yield), and *cis*- (23 mg, 0.027 mmol, 10% yield) isomers, the disproportionation product stilbene **2.50** (142 mg, 0.273 mmol, 94%) and recovered dihydrostilbene **3.30** (113 mg, 0.330 mmol, 58%).

Data for *trans*-dihydrobenzofuran **3.31**:

TLC (Hexanes/EtOAc, 80:20), R_F: 0.32 (UV, *p*-anisaldehyde (red));

¹H NMR (500 MHz, CDCl₃, 25 °C) δ: 7.42 – 7.27 (m, 10H), 7.10 (s, 2H), 6.75 (s, 2H), 6.51 (br s, 1H), 6.46 (s, 2H), 6.34 (s, 1H), 6.22 (s, 1H), 5.42 (d, *J* = 6.0 Hz, 1H), 5.22 (s, 1H), 5.00 (s, 1H), 4.94 (s, 4H), 4.77 (s, 1H), 4.42 (d, *J* = 6.0 Hz, 1H), 2.68 – 2.32 (m, 4H), 1.40 (s, 18H), 1.36 (s, 18H);

¹³C NMR (175 MHz, CDCl₃, 25 °C) δ: 161.5, 160.5, 156.9, 154.0, 152.1, 146.2, 140.8, 136.9, 136.2, 135.8, 132.4, 132.2, 128.8, 128.2, 127.8, 125.0, 122.7, 120.5, 108.8, 107.4, 100.5, 95.5, 94.2, 70.2, 56.5, 36.5, 35.5, 34.6, 34.4, 30.53, 30.46;

HRMS (ESI): *m/z* calculated for C₃₈H₆₉O₆ [M+H]⁺: 861.5089, found 861.5085;

FTIR (neat) cm⁻¹: 2916 (w), 1594 (w), 1435 (m), 1361 (s), 1222 (s), 1157 (m), 908 (s), 727 (s).

²⁵ Prepared by simple hydrogenation (5% Pd/C, 1 atm H₂ in EtOAc/MeOH) of the corresponding stilbene **2.50**. For preparation of **2.50**, consult: Section 2.9.

Data for *cis*-dihydrobenzofuran **3.31**:

TLC (Hexanes/EtOAc, 80:20), R_f : 0.46 (UV, *p*-anisaldehyde (red));

^1H NMR (400 MHz, CDCl_3 , 25 °C) δ : 7.44 – 7.27 (m, 10H), 7.12 (s, 2H), 7.02 (s, 2H), 6.58 (br s, 1H), 6.53 (br s, 2H), 6.45 (s, 1H), 6.30 (s, 1H), 5.42 (d, $J = 8.7$ Hz, 1H), 5.24 (s, 1H), 5.06 (s, 1H), 4.99 (s, 4H), 4.51 (d, $J = 8.7$ Hz, 1H), 4.34 (br s, 1H), 2.85 (br s, 4H), 1.44 (s, 18H), 1.42 (s, 18H);

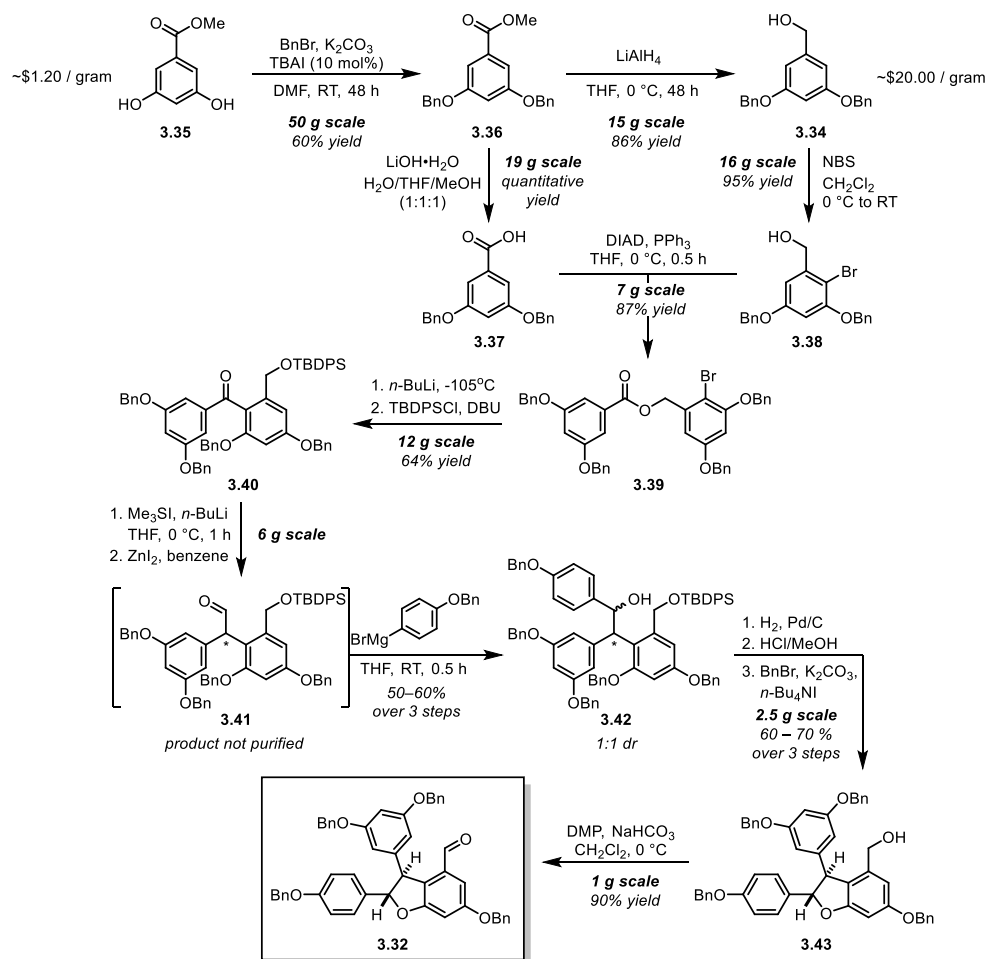
^{13}C NMR (175 MHz, CDCl_3 , 25 °C) δ : 161.5, 160.8, 154.1, 152.7, 152.2, 145.8, 142.7, 136.8, 136.2, 136.0, 132.6, 130.7, 128.8, 128.3, 127.9, 125.1, 123.1, 112.4, 109.3, 107.4, 103.0, 101.3, 94.22, 70.4, 55.6, 38.8, 38.0, 34.6, 34.5, 30.6, 30.5;

HRMS (ESI): m/z calculated for $\text{C}_{58}\text{H}_{69}\text{O}_6$ $[\text{M}+\text{H}]^+$: 861.5089, found 861.5080;

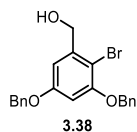
FTIR (neat) cm^{-1} : 3637 (m), 2954 (m), 2873 (m), 1593 (s), 1434 (s), 1361 (m), 1316 (m), 1233 (m), 1213 (m), 1155 (s), 1120 (m), 1056 (s), 908 (s), 726 (s), 695 (s).

Preparation of Aldehyde 3.32:

The requisite aldehyde was prepared according to the scheme depicted below using procedures described by Snyder and Wright.²⁶ Thus, synthetic protocols are not included here, but the scale and yield for each reaction as performed by us are represented in the scheme. Due to the lower cost of methyl 3,5-dihydroxybenzoate **3.35** (CAS #: 2150-44-9) versus 3,5-dibenzoyloxybenzyl alcohol **3.34** (CAS #: 24131-31-5), we elected to source the former for this synthesis. ¹H-NMR for all compounds matched the reported data and the corresponding authentic spectra are included beginning with intermediate **3.38**.

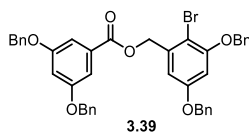


²⁶ Wright, N. E.; Snyder, S. A. *Angew. Chem.* **2014**, *126* (13), 3477–3481.



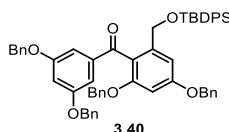
(3,5-bis(benzyloxy)-2-bromophenyl)methanol (3.38):

$^1\text{H NMR}$ (400 MHz, CDCl_3 , 25 °C) δ : 7.47 – 7.31 (m, 10H), 6.80 (d, $J = 2.7$ Hz, 1H), 6.56 (d, $J = 2.7$ Hz, 1H), 5.11 (s, 2H), 5.04 (s, 2H), 4.74 (s, 2H).



3,5-bis(benzyloxy)-2-bromobenzyl 3,5-bis(benzyloxy)benzoate (3.39):

$^1\text{H NMR}$ (500 MHz, CDCl_3 , 25 °C) δ : 7.48 – 7.28 (m, 20H), 6.82 (t, $J = 2.4$ Hz, 1H), 6.73 (d, $J = 2.7$ Hz, 1H), 6.60 (d, $J = 2.7$ Hz, 1H), 5.42 (s, 2H), 5.12 (s, 2H), 5.07 (s, 4H), 5.01 (s, 2H).



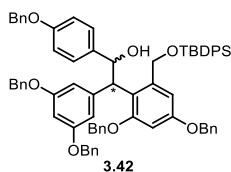
(2,4-bis(benzyloxy)-6-(((tert-butyl)diphenylsilyl)oxy)methyl)phenyl(3,5-bis(benzyloxy)phenyl)methanone (3.40):

$^1\text{H NMR}$ (500 MHz, CDCl_3 , 25 °C) δ : 7.57 – 7.55 (m, 4H), 7.45 – 7.28 (m, 24H), 7.18 (d, $J = 1.7$ Hz, 1H), 7.17 (m, overlap, 2H), 7.00 (d, $J = 2.2$ Hz, 2H), 6.93 (d, $J = 1.7$ Hz, 1H), 6.91 (d, $J = 2.7$ Hz, 1H), 6.89 (d, $J = 2.7$ Hz, 1H), 6.78 (t, $J = 2.1$ Hz, 1H), 6.50 (d, $J = 2.1$ Hz, 1H), 5.07 (s, 2H), 4.96 (s, 4H), 4.83 (s, 2H), 4.66 (s, 2H), 0.97 (s, 9H).



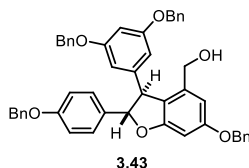
2-(2,4-bis(benzyloxy)-6-(((tert-butyl)diphenylsilyl)oxy)methyl)phenyl)-2-(3,5-bis(benzyloxy)phenyl)acetaldehyde (3.41):

$^1\text{H NMR}$ (500 MHz, CDCl_3 , 25 °C) δ : 9.80 (s, 1H), 7.64 (d, $J = 9.0$ Hz, 2H), 7.59 (d, $J = 9.0$ Hz, 2H), 7.47 – 7.20 (m, overlap, 26H), 6.78 (d, $J = 2.5$ Hz, 1H), 6.60 (d, $J = 2.5$ Hz, 1H), 6.48 (t, $J = 2.2$ Hz, 1H), 6.34 (d, $J = 2.2$ Hz, 2H), 5.02 (d, $J = 10.5$ Hz, 1H), 5.01 (d, $J = 10.5$ Hz, 1H), 4.98 (d, $J = 11.7$ Hz, 1H), 4.94 (d, $J = 11.7$ Hz, 1H), 4.85 (d, $J = 11.5$ Hz, 2H), 4.82 (d, $J = 11.5$ Hz, 2H), 4.73 (d, $J = 13.2$ Hz, 1H), 4.71 (s, 1H), 4.57 (d, $J = 13.2$ Hz, 1H), 1.02 (s, 9H).



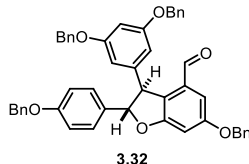
1-(4-(benzyloxy)phenyl)-2-(2,4-bis(benzyloxy)-6-(((tert-butyl)diphenylsilyloxy)methyl)phenyl)-2-(3,5-bis(benzyloxy)phenyl)ethan-1-ol (3.42):

^1H NMR (400 MHz, CDCl_3 , 25 °C) δ : Diastereomeric mixture with significant overlap so line list not included. Spectrum provided for reference.



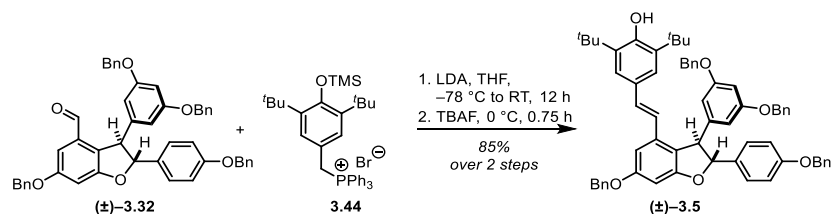
((2S,3S)-6-(benzyloxy)-2-(4-(benzyloxy)phenyl)-3-(3,5-bis(benzyloxy)phenyl)-2,3-dihydrobenzofuran-4-yl)methanol (3.43):

^1H NMR (400 MHz, CDCl_3 , 25 °C) δ : 7.47 – 7.28 (m, 20H), 7.19 (d, $J = 8.6$ Hz, 2H), 6.93 (d, $J = 8.6$ Hz, 2H), 6.60 (d, $J = 2.4$ Hz, 1H), 6.55 (d, $J = 2.4$ Hz, 1H), 6.54 (t, $J = 2.2$ Hz, 1H), 6.37 (d, $J = 2.2$ Hz, 2H), 5.47 (d, $J = 6.1$ Hz, 1H), 5.08 (s, 2H), 5.06 (s, 2H), 5.0 (d, $J = 11.7$ Hz, 2H), 4.97 (d, $J = 11.7$ Hz, 2H), 4.40 (d, $J = 6.1$ Hz, 1H), 4.16 (d, $J = 13.3$ Hz, 1H), 4.11 (d, $J = 13.3$ Hz, 1H).



(2S,3S)-6-(benzyloxy)-2-(4-(benzyloxy)phenyl)-3-(3,5-bis(benzyloxy)phenyl)-2,3-dihydrobenzofuran-4-carbaldehyde (3.32):

^1H NMR (500 MHz, CDCl_3 , 25 °C) δ : 9.71 (s, 1H), 7.48 – 7.30 (m, 20H), 7.20 (d, $J = 8.8$ Hz, 2H), 7.03 (d, $J = 2.5$ Hz, 1H), 6.95 (d, $J = 8.8$ Hz, 2H), 6.84 (d, $J = 2.5$ Hz, 1H), 6.52 (t, $J = 2.5$ Hz, 1H), 6.35 (d, $J = 2.5$ Hz, 2H), 5.55 (d, $J = 5.4$ Hz, 1H), 5.12 (s, 2H), 5.07 (s, 2H), 4.98 (d, $J = 11.5$ Hz, 2H), 4.95 (d, $J = 11.5$ Hz, 2H), 4.78 (d, $J = 5.4$ Hz, 1H).



4-((E)-2-((2R)-6-(benzyloxy)-2-(4-(benzyloxy)phenyl)-3-(3,5-bis(benzyloxy)phenyl)-2,3-dihydrobenzofuran-4-yl)vinyl)-2,6-di-tert-butylphenol (3.5): A solution of aldehyde **3.32** (500 mg, 0.690 mmol, 1.00 equiv) was prepared in anhydrous THF (14 mL) in a heart-shaped flask and maintained under inert atmosphere. To a stirring solution of diisopropylamine (freshly purified, 194 μ L, 1.380 mmol, 2.00 equiv) in anhydrous THF (9 mL) at -78 $^{\circ}$ C under inert atmosphere was added *n*-BuLi slowly (2.5 M solution in hexanes, 538 μ L, 1.345 mmol, 1.95 equiv), and the mixture was maintained at this temperature for 0.5 h. Meanwhile, a suspension of phosphonium salt **3.44** (875 mg, 1.380 mmol, 2.00 equiv) in anhydrous THF (11.5 mL) was prepared in a round bottom flask and stirred under inert atmosphere at -78 $^{\circ}$ C. At 0.5 h, the LDA was transferred dropwise to the stirring phosphonium salt by cannula, turning the suspension red, then red-brown. The mixture was stirred at -78 $^{\circ}$ C for 20 minutes, at which point the solution of aldehyde **3.32** was added slowly by cannula, turning the mixture a bright red color. The reaction was allowed to slowly warm to RT overnight. On complete consumption of the aldehyde (as determined by TLC), the solution was cooled to 0 $^{\circ}$ C and treated with TBAF (1 M solution in THF, 1.380 mL, 1.380 mmol, 2.00 equiv). After 0.75 h, the reaction was quenched by the addition of sat. aq. NH_4Cl . The mixture was diluted with Et_2O and transferred to a separatory funnel containing DI H_2O . The phases were separated and the aqueous phase extracted with additional portions of Et_2O . The combined organic layers were washed with brine, dried over Na_2SO_4 , and concentrated *in vacuo*. The crude material was purified by flash chromatography over SiO_2 (96:4 pentanes/ EtOAc) to afford the viniferin analog **3.5** (545 mg, 0.588 mmol, 85% yield) as a white foam as exclusively the (*E*)-isomer.

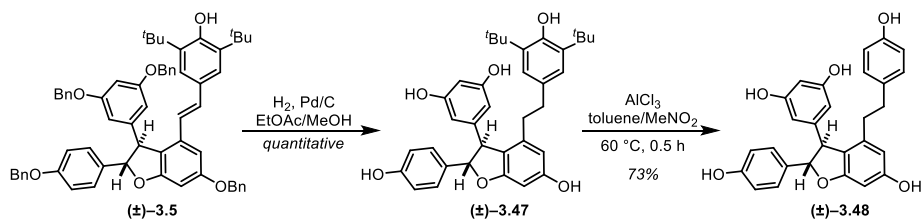
TLC (Hexanes/ EtOAc , 85:15), R_f : 0.32 (UV, *p*-anisaldehyde (purple));

^1H NMR (700 MHz, CDCl_3 , 25 $^{\circ}$ C) δ : 7.54 – 7.47 (m, 2H), 7.45 – 7.28 (m, overlap, 20H), 7.23 (d, J = 8.6 Hz, 2H), 7.05 (s, 2H), 6.94 (d, J = 8.6 Hz, 2H), 6.88 (d, J = 16.1 Hz, 1H), 6.86 (d, J = 2.1 Hz, 1H), 6.55 (d, J = 16.1 Hz, 1H), 6.52 (d, J = 2.1 Hz, 1H), 6.50 (t, J = 2.1 Hz, 1H), 6.45 (d, J = 2.1 Hz, 2H), 5.46 (d, J = 6.4 Hz, 1H), 5.22 (s, 1H), 5.12 (s, 2H), 5.07 (s, 2H), 4.94 (d, J = 11.4 Hz, 2H), 4.92 (d, J = 11.4 Hz, 2H), 4.51 (d, J = 6.4 Hz, 1H), 1.37 (s, 18H);

^{13}C NMR (125 MHz, CDCl_3 , 25 $^{\circ}$ C) δ : 161.7, 160.62, 160.57, 158.9, 154.1, 145.9, 137.2, 137.1, 136.9, 136.2, 135.9, 134.0, 130.8, 128.77, 128.75, 128.68, 128.53, 128.16, 128.14, 128.12, 127.84, 127.78, 127.6, 127.2, 123.7, 122.6, 119.7, 115.2, 107.2, 103.5, 100.6, 95.8, 93.3, 70.5, 70.20, 70.16, 57.3, 34.4, 30.4;

HRMS (ESI): m/z calculated for $\text{C}_{64}\text{H}_{63}\text{O}_6$ $[\text{M}+\text{H}]^+$: 927.4625, found 927.4604;

FTIR (neat) cm^{-1} : 3620 (m), 2957 (m), 1607 (s), 1512 (s), 1453 (s), 1374 (m), 1237 (s), 1156 (s), 1027 (m).



Dihydro-^tBu- ϵ -Viniferin (3.47): A round bottom flask was charged with starting **3.5** (40 mg, 0.043 mmol, 1.00 equiv) and Pd/C (10 wt%, 11.5 mg, 0.25 equiv). The flask was sealed with a rubber septum and flushed under N₂. EtOAc (HPLC grade, 2.1 mL), then MeOH (HPLC grade, 2.1 mL) were added, and the suspension was sparged for 25 minutes with H₂. The reaction was then stirred under H₂ (1 atm) for 5 h, at which point it was diluted with EtOAc and filtered through a pad of Celite. The filtrate was concentrated *in vacuo*, and the crude residue was purified by flash chromatography over SiO₂ (90:5:5 CH₂Cl₂/MeOH/Acetone) to afford a highly pure sample of **3.47** (18.2 mg) and a semi-pure sample (7.4 mg).

TLC (CH₂Cl₂/MeOH/Acetone, 90:5:5), R_F: 0.19 (UV, Hanessian's stain);

¹H NMR (500 MHz, Acetone-*d*₆, 25 °C) δ : 8.36 (br s, 1H), 8.20 (br s, 1H), 8.14 (br s, 2H), 7.13 (d, *J* = 8.4 Hz, 2H), 6.82 (d, *J* = 8.4 Hz, 2H), 6.77 (s, 2H), 6.30 (d, *J* = 1.8 Hz, 1H), 6.26 (t, *J* = 2.2 Hz, 1H), 6.24 (d, *J* = 1.8 Hz, 1H), 6.16 (d, *J* = 2.2 Hz, 2H), 5.75 (s, 1H), 5.27 (d, *J* = 6.6 Hz, 1H), 4.14 (d, *J* = 6.6 Hz, 1H), 2.60 – 2.38 (m, 4H), 1.36 (s, 18H);

¹³C NMR (125 MHz, Acetone-*d*₆, 25 °C) δ : 162.2, 159.8, 159.6, 158.2, 152.9, 147.3, 141.2, 137.8, 133.5, 133.3, 128.4, 125.8, 120.2, 116.2, 109.4, 107.1, 102.2, 95.5, 94.2, 57.0, 37.4, 36.1, 35.1, 30.8;

HRMS (ESI): *m/z* calculated for C₂₈H₂₅O₆ [M+H]⁺: 457.1646, found 457.1644;

FTIR (neat) cm⁻¹: 3221 (s, br), 2950 (m), 1597 (s), 1516 (m), 1433 (s), 1360 (m), 12322 (m), 1156 (s), 1120 (s), 1009 (s), 832 (s).

Dihydro- ϵ -Viniferin (3.48): A sample of **3.47** (5 mg, 0.009 mmol, 1.00 equiv) was dissolved in toluene (3 mL) and heated to 60 °C under N₂. A 0.5 M solution of AlCl₃ (67 mg in 1.0 mL) in MeNO₂ was prepared and 6 equivalents (106 μ L) were added to the stirring solution of **3.47**, turning it golden yellow. At 0.5 h, the reaction was removed from the heat and the contents poured into a separatory funnel containing 50/50 ice : 1 N HCl. The reaction flask was rinsed into the separatory funnel with EtOAc and the phases were separated. The aqueous phase was extracted with an additional portion of EtOAc. The organic layers were combined, washed with brine, dried over Na₂SO₄, and concentrated *in vacuo*. This reaction was repeated once more and the crude materials were combined and purified by preparative TLC (85:10:5 CH₂Cl₂/MeOH/Acetone) to afford **3.48** (avg. 4.0 mg, 0.0088 mmol, 72% yield). Characterization data provided on subsequent page.

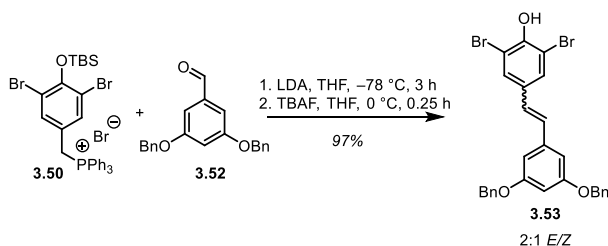
TLC (CH₂Cl₂/MeOH/Acetone, 85:10:5), R_f: 0.24 (UV, Hanessian's stain);

¹H NMR (700 MHz, Acetone-*d*₆, 25 °C) δ: 8.38 (s, 1H), 8.24 (s, 1H), 8.18 (s, 2H), 8.01 (s, 1H), 7.13 (d, *J* = 8.5 Hz, 2H), 6.82 (d, *J* = 8.5 Hz, 2H), 6.81 (d, *J* = 8.5 Hz, 2H), 6.65 (d, *J* = 8.5 Hz, 2H), 6.28 (d, *J* = 1.8 Hz, 1H), 6.26 (t, *J* = 2.1 Hz, 1H), 6.24 (d, *J* = 1.8 Hz, 1H), 6.18 (d, *J* = 2.1 Hz, 2H), 5.33 (d, *J* = 5.9 Hz, 1H), 4.18 (d, *J* = 5.9 Hz, 1H), 2.55 – 2.38 (m, 4H);

¹³C NMR (175 MHz, Acetone-*d*₆, 25 °C) δ: 162.1, 159.9, 159.6, 158.2, 156.4, 147.5, 141.1, 133.9, 133.5, 130.3, 128.2, 120.3, 116.2, 115.9, 109.4, 107.2, 102.1, 95.6, 94.1, 57.2, 36.6, 36.2;

HRMS (ESI): *m/z* calculated for C₃₆H₄₀O₆ [M+H]⁺: 569.2898, found 569.2896;

FTIR (neat) cm⁻¹: 3325 (s, br), 1599 (s), 1513 (s), 1447 (m), 1338 (m), 1229 (m), 1156 (m), 1121 (m), 1007 (m), 830 (m).



4-(3,5-bis(benzyloxy)styryl)-2,6-dibromophenol (3.53): A solution of aldehyde **3.52** (100 mg, 0.314 mmol, 1.00 equiv) was prepared in anhydrous THF (2 mL) in a heart-shaped flask and maintained under inert atmosphere. To a stirring solution of diisopropylamine (freshly purified, 88 μL , 0.628 mmol, 2.00 equiv) in anhydrous THF (2 mL) at $-78\text{ }^\circ\text{C}$ under inert atmosphere was added *n*-BuLi slowly (2.5 M solution in hexanes, 245 μL , 0.612 mmol, 1.95 equiv), and the mixture was maintained at this temperature for 0.5 h. Meanwhile, a suspension of phosphonium salt **3.50** (453 mg, 0.628 mmol, 2.00 equiv) in anhydrous THF (2 mL) was prepared in a round bottom flask and stirred under inert atmosphere at $-78\text{ }^\circ\text{C}$. At 0.5 h, the LDA was transferred dropwise to the stirring phosphonium salt by cannula, turning the suspension red-orange. The mixture was stirred at $-78\text{ }^\circ\text{C}$ for 20 minutes, at which point the solution of aldehyde **3.52** was added slowly by cannula. The reaction was allowed to slowly warm within the cooling bath over the course of 3 hours. On complete consumption of the aldehyde (as determined by TLC), the solution was cooled to $0\text{ }^\circ\text{C}$ and treated with TBAF (1 M solution in THF, 471 μL , 0.471 mmol, 1.00 equiv). After 0.25 h, the reaction was quenched by the addition of sat. aq. NH_4Cl . The mixture was diluted with Et_2O and transferred to a separatory funnel containing DI H_2O . The phases were separated and the aqueous phase extracted with additional portions of Et_2O . The combined organic layers were washed with brine, dried over Na_2SO_4 , and concentrated *in vacuo*. The crude material was purified by flash chromatography over SiO_2 (5% then 10% of a 2:1 $\text{EtOAc}/\text{CH}_2\text{Cl}_2$ mixture in hexanes) to afford the dibromo resveratrol analog **3.53** (172 mg, 0.304 mmol, 97% yield) as a white foam as a 2:1 mixture of (*E*)- and (*Z*)-isomers.²⁷

TLC (Hexanes/ $\text{EtOAc}/\text{CH}_2\text{Cl}_2$, 80:15:5), R_f : 0.63 (UV, before desilylation); 0.31 (UV, after desilylation)

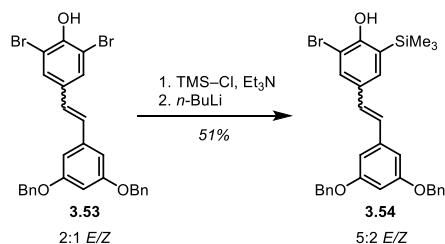
^1H NMR (500 MHz, CDCl_3 , $25\text{ }^\circ\text{C}$) δ : 7.58 (s, 2H), 7.45 – 7.30 (m, 15H), 6.88 (d, $J = 16.5\text{ Hz}$, 1H), 6.85 (d, $J = 16.5\text{ Hz}$, 1H), 6.73 (d, $J = 2.0\text{ Hz}$, 2H), 6.57 (t, $J = 2.0\text{ Hz}$, 1H), 6.50 (m, overlap, 2H), 6.50 (d, overlap, $J = 12.1\text{ Hz}$, 1H), 6.35 (d, $J = 12.1\text{ Hz}$, 1H), 5.88 (s, 1H), 5.84 (s, 1H), 5.07 (s, 4H), 4.93 (s, 4H);

^{13}C NMR (175 MHz, CDCl_3 , $25\text{ }^\circ\text{C}$) δ : 160.4, 160.2, 148.9, 148.5, 138.9, 138.3, 136.9, 132.6, 132.1, 131.2, 130.1, 129.3, 128.82, 128.76, 128.3, 128.2, 127.7, 127.6, 127.3, 126.1, 110.4, 109.6, 108.0, 106.0, 102.2, 102.1, 70.4, 70.3,

HRMS (ESI): m/z calculated for $\text{C}_{28}\text{H}_{23}\text{O}_3$ $[\text{M}+\text{H}]^+$: 565.0008, found 564.9996;

FTIR (neat) cm^{-1} : 3488 (w), 3036 (w), 1582 (s), 1476 (s), 1438 (s), 1377 (m), 1296 (m), 1152 (s), 1053 (s), 956 (m), 904 (s), 848 (m), 803 (m), 728 (s).

²⁷ All characterization data reported on a mixture of (*E*)- and (*Z*)-isomers



4-(3,5-bis(benzyloxy)styryl)-2-bromo-6-(trimethylsilyl)phenol (3.54): Starting **3.53** (100 mg, 0.177 mmol, 1.00 equiv) was dissolved in anhydrous THF (2 mL) at room temperature under inert atmosphere. To the stirring mixture was added Et₃N (37 μ L, 0.265 mmol, 1.50 equiv) then chlorotrimethylsilane (34 μ L, 0.265 mmol, 1.50 equiv) sequentially. The reaction soon became heterogeneous and was allowed to stir overnight. At 15 h, the mixture was filtered through a Celite plug and eluted with dichloromethane. The filtrate was concentrated to dryness to yield a mixture of (*E*)/(*Z*) isomers of the *O*-TMS intermediate (92% based on mass assuming 100% purity), the formation of which was confirmed by ¹H-NMR (CDCl₃ passed through basic alumina). The crude material was then suspended in THF/Et₂O (6 mL) and cooled to -78 °C. *n*-Butyllithium (1.6 M sol'n in hexanes, 105 μ L, 0.95 equiv) was then added dropwise, turning the suspension yellow. The reaction was allowed to warm slowly over 4 h, at which point it was quenched by the addition of sat. aq. NH₄Cl. The mixture was then diluted with EtOAc and transferred to a separatory funnel where the phases were separated. The aqueous phase was extracted with additional EtOAc. Combined organic layers were washed with brine, dried over Na₂SO₄, and concentrated *in vacuo*. The crude material was purified by flash chromatography over SiO₂ (5% EtOAc/hexanes) to afford **3.54** (50 mg, 0.089 mmol, 51% yield) as a clear oil.²⁸

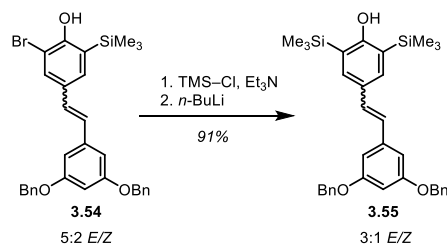
¹H NMR (500 MHz, CDCl₃, 25 °C) δ : 7.64 (d, *J* = 2.2 Hz, 1H), 7.46 – 7.30 (m, 16H), 7.23 (d, *J* = 2.2 Hz, 1H), 6.96 (d, *J* = 16.5 Hz, 1H), 6.87 (d, *J* = 16.5 Hz, 1H), 6.75 (d, *J* = 2.2 Hz, 2H), 6.55 (t, *J* = 2.2 Hz, 1H), 6.53 (d, *J* = 2.2 Hz, 2H), 6.50 (t, *J* = 2.2 Hz, 1H), 6.47 (d, *J* = 12.1 Hz, 1H), 6.43 (d, *J* = 12.1 Hz, 1H), 5.75 (s, 1H), 5.69 (s, 1H), 5.08 (s, 4H), 4.91 (s, 4H), 0.34 (s, 9H), 0.20 (s, 9H);

¹³C NMR (125 MHz, CDCl₃, 25 °C) δ : 160.4, 155.9, 139.6, 137.1, 135.8, 133.4, 131.3, 130.7, 129.7, 129.1, 128.82, 128.77, 128.24, 127.16, 127.9, 127.8, 127.7, 127.6, 127.3, 114.8, 111.2, 108.0, 105.8, 101.7, 70.34, 70.30, -0.96, -1.05;

HRMS (ESI): *m/z* calculated for C₃₁H₃₂BrO₃Si [M+H]⁺: 559.1296, found 559.1296;

FTIR (neat) cm⁻¹: 3510 (m, br), 2946 (m), 1580 (s), 1496 (w), 1434 (m), 1373 (m), 1320 (m), 1243 (s), 1144 (s), 1052 (s), 955 (m), 931 (m), 907 (m), 836 (s), 729 (s), 693 (s).

²⁸ All characterization data reported on a mixture of (*E*)- and (*Z*)-isomers



4-(3,5-bis(benzyloxy)styryl)-2,6-bis(trimethylsilyl)phenol (3.55): Starting **3.54** (48 mg, 0.086 mmol, 1.00 equiv) was dissolved in anhydrous THF (2 mL) at room temperature under inert atmosphere. To the stirring mixture was added Et₃N (18 μL, 0.129 mmol, 1.50 equiv) then chlorotrimethylsilane (16 μL, 0.129 mmol, 1.50 equiv) sequentially. The reaction soon became heterogeneous and was allowed to stir overnight. At 15 h, the mixture was filtered through a Celite plug and eluted with THF. The filtrate was concentrated to dryness to yield a mixture of (*E*)/(*Z*) isomers of the *O*-TMS intermediate (100% based on mass assuming 100% purity), the formation of which was confirmed by ¹H-NMR (CDCl₃ passed through basic alumina). The crude material was then suspended in THF (3 mL) and cooled to -78 °C. *n*-Butyllithium (1.6 M sol'n in hexanes, 54 μL, 1.00 equiv) was then added dropwise, turning the suspension yellow. The reaction was allowed to warm slowly over 4 h, at which point it was quenched by the addition of sat. aq. NH₄Cl. The mixture was then diluted with EtOAc and transferred to a separatory funnel where the phases were separated. The aqueous phase was extracted with additional EtOAc. Combined organic layers were washed with brine, dried over Na₂SO₄, and concentrated *in vacuo*. The crude material was purified by flash chromatography over SiO₂ (5% EtOAc/hexanes) to afford **3.55** (43 mg, 0.078 mmol, 91% yield) as a clear oil.²⁹

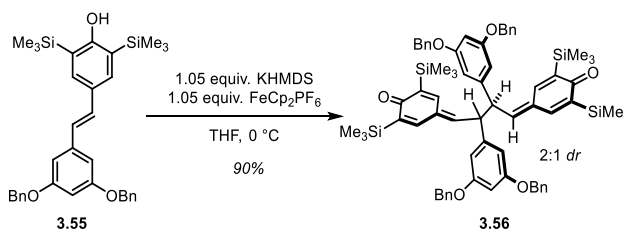
¹H NMR (500 MHz, CDCl₃, 25 °C) δ: 7.49 (s, 2H), 7.46 – 7.30 (m, 13H), 7.05 (d, *J* = 16.1 Hz, 1H), 6.88 (d, *J* = 16.1 Hz, 1H), 6.79 (d, *J* = 2.2 Hz, 2H), 6.54 (t, overlap, *J* = 2.2 Hz, 1H), 6.54 (d, overlap, *J* = 2.2 Hz, 1H), 6.51 (d, *J* = 12.1 Hz, 1H), 6.48 (t, *J* = 2.2 Hz, 1H), 6.45 (d, *J* = 12.1 Hz, 1H), 5.09 (s, 4H), 5.08 (s, 4H), 5.0 (s, 1H), 4.91 (s, 1H), 0.38 (s, 18H), 0.25 (s, 18H);

¹³C NMR (125 MHz, CDCl₃, 25 °C) δ: 165.4, 160.4, 140.2, 137.2, 135.3, 129.6, 129.5, 128.81, 128.75, 128.2, 128.1, 127.7, 127.6, 128.3, 124.7, 108.0, 105.8, 101.4, 70.4, 70.2, -0.33, -0.40;

HRMS (ESI): *m/z* calculated for C₃₄H₄₀O₃Si₂ [M+H]⁺: 553.2589, found 553.2590;

FTIR (neat) cm⁻¹: 3597 (m), 3029 (m), 2951 (m), 1582 (s), 1446 (m), 1404 (m), 1301 (m), 1244 (m), 1149 (s), 1050 (s), 955 (m), 906 (m), 833 (s), 729 (s), 690 (s).

²⁹ All characterization data reported on a mixture of (*E*)- and (*Z*)-isomers



4,4'-((2*S*,3*S*)-2,3-bis(3,5-bis(benzyloxy)phenyl)butane-1,4-diylidene)bis(2,6-bis(trimethylsilyl)cyclohexa-2,5-dien-1-one) (3.56): A solution of starting ϵ -viniferin derivative **3.55** (45 mg, 0.081 mmol, 1.00 equiv) was prepared in THF (6 mL) and cooled to 0 °C under inert atmosphere. To the stirring mixture was added potassium bis(trimethylsilyl)amide [KHMDs] (0.7 M solution in toluene, 122 μ L, 0.085 mmol, 1.05 equiv) slowly. The mixture was allowed to equilibrate for 10 minutes, at which point FeCp_2PF_6 (29 mg, 0.085 mmol, 1.05 equiv) was added in a single portion. At 3 h, TLC analysis indicated full consumption of the starting material, and the reaction was quenched by the addition of sat. aq. NH_4Cl . The mixture was then diluted with EtOAc and transferred to a separatory funnel where the phases were separated. The aqueous layer was extracted with additional portions of EtOAc. The combined organic layers were then washed with brine, dried over Na_2SO_4 and concentrated in vacuo. The desired **3.56** (40 mg, 0.036 mmol, 90% yield, 2:1 mixture of diastereomers) was isolated from the crude material as a yellow-brown oil by flash chromatography over SiO_2 (5% of a 1:1 EtOAc/ CH_2Cl_2 mixture in hexanes).³⁰

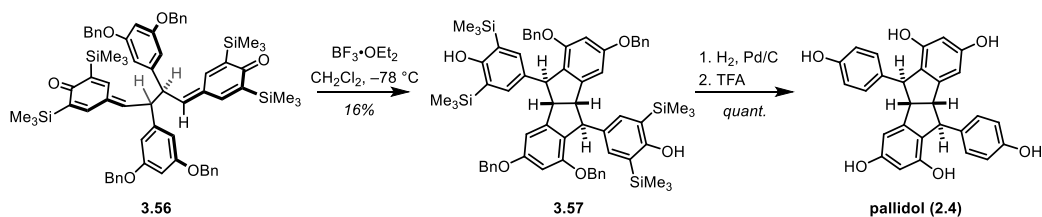
$^1\text{H NMR}$ (500 MHz, CDCl_3 , 25 °C) δ : 7.47 (d, $J = 2.5$ Hz, 2H, major), 7.45 – 7.28 (m, 32H), 7.15 (d, $J = 2.5$ Hz, 2H, minor), 7.04 (d, $J = 2.5$ Hz, 2H, major), 6.50 – 6.47 (m, overlap, 4H), 6.45 (d, $J = 2.2$ Hz, 4H, major), 6.38 (m, 4H), 6.37 (d, $J = 2.2$ Hz, 4H, minor), 5.07 (d, $J = 9.3$ Hz, 2H, minor), 4.99 (d, $J = 9.3$ Hz, 2H, minor), 4.96 (s, 8H, major/minor overlap), 4.91 (d, $J = 11.2$ Hz, 2H, major), 4.89 (d, $J = 11.2$ Hz, 2H, major), 4.36 – 4.28 (m, overlap, 4H, major/minor), 0.20 (s, 18H, minor), 0.19 (s, 18H, minor), 0.18 (s, 36H, major);

$^{13}\text{C NMR}$ (125 MHz, CDCl_3 , 25 °C) δ : 193.33, 193.28, 160.6, 160.5, 160.3, 149.2, 149.0, 146.7, 145.2, 143.8, 143.7, 142.9, 142.6, 141.9, 141.5, 140.0, 139.9, 137.2, 136.9, 136.6, 136.5, 133.8, 132.8, 131.6, 128.9, 128.8, 128.4, 128.3, 128.2, 127.85, 127.80, 127.76, 124.3, 108.12, 108.06, 107.9, 105.6, 100.65, 100.63, 70.50, 70.48, 70.34, 70.30, 51.7, 51.0, -0.34, -1.15, -1.16, -1.20;

HRMS (ESI): m/z calculated for $\text{C}_{68}\text{H}_{79}\text{O}_6\text{Si}_4$ $[\text{M}+\text{H}]^+$: 1103.4948, found 1103.4952;

FTIR (neat) cm^{-1} : 2950 (m), 1593 (s), 1452 (m), 1317 (w), 1245 (m), 1159 (s), 1059 (m), 839 (s), 734 (m), 697 (m).

³⁰ Compound **3.56** exists as a rapidly equilibrating and therefore inseparable mixture of diastereomers.



4,4'-((4*b*S,5*S*,9*b*S,10*S*)-1,3,6,8-tetrakis(benzyloxy)-4*b*,5,9*b*,10-tetrahydroindeno[2,1-*a*]indene-5,10-diyl)bis(2,6-bis(trimethylsilyl)phenol) (3.57): A solution of **3.56** (7.5 mg, 0.007 mmol, 1.00 equiv) in CH₂Cl₂ (1 mL) was cooled to -78 °C in a dry ice/acetone bath under inert atmosphere. To this, BF₃·OEt₂ (7 μL, 46.5% in diethyl ether, 4 equiv) was added dropwise, turning the reaction a brilliant magenta color. The reaction was allowed to run for 40 minutes upon which the reaction was quenched with sat. aq. NaHCO₃ at temperature and allowed to warm to room temperature under vigorous stirring. The reaction was diluted with CH₂Cl₂ and transferred to a separatory funnel. The phases were separated and the aqueous layer was extracted with portions of CH₂Cl₂. The organic layers were combined, washed with sat. aq. NaHCO₃, brine, dried over sodium sulfate and concentrated *in vacuo*. The crude material was purified by preparative TLC (7.5% EtOAc/Hexanes) to afford **3.57** (1.2 mg, 16% yield).

¹H NMR (700 MHz, CDCl₃, 25 °C) δ: 7.48 – 7.25 (m, 20H), 7.23 (br s, 4H), 7.19 (s, 4H), 7.02 (br s, 4H), 6.72 (s, 2H), 6.34 (s, 2H), 5.05 (m, 4H), 4.85 (m, 4H), 4.56 (s, 2H), 4.18 (s, 2H), 0.25 (s, 36H);

¹³C NMR (175 MHz, CDCl₃, 25 °C) δ: 163.8, 160.3, 156.0, 148.6, 137.7, 137.3, 135.9, 128.82, 128.79, 128.6, 128.2, 127.9, 127.8, 127.7, 127.1, 126.5, 123.9, 102.3, 99.6, 70.6, 69.7, 60.1, 54.9, -0.29;

HRMS (ESI): *m/z* calculated for C₆₈H₇₉O₆Si₄ [M+H]⁺: 1103.4948, found 1103.4934;

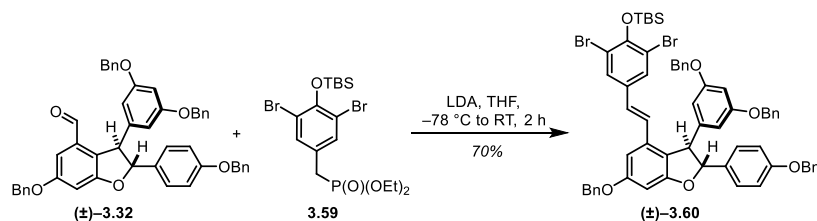
FTIR (neat) cm⁻¹: 2922 (m), 1594 (s), 1452 (m), 1401 (m), 1248 (m), 1160 (s), 838 (s), 734 (m), 696 (m);

Compound **3.57** and Pd/C (30 wt %, 2 mg) were dissolved/suspended in a 1:1 mixture of MeOH/EtOAc (2 mL, HPLC grade). The mixture was sparged with H₂ for 0.5 h then stirred under H₂ (1 atm) for 5 h. The mixture was then filtered through a pad of Celite, eluting with EtOAc. The filtrate was concentrated *in vacuo* to yield a nearly pure sample of the tetra-TMS, debenzylated pallidol derivative (not depicted).

¹H NMR (500 MHz, Acetone-*d*₆, 25 °C) δ: 7.27 (s, 4H), 6.62 (s, 2H), 6.19 (s, 2H), 4.61 (s, 2H), 3.91 (s, 2H), 0.25 (s, 36H).

This material was then dissolved in 1:1 CH₂Cl₂/MeNO₂ and treated with TFA (3 μL, 0.043 mmol, 40 equiv) at room temperature. After 1 h, the volatiles were removed *in vacuo* to afford a nearly pure sample of pallidol **2.4**.³¹

³¹ For characterization data of pallidol, consult Section 2.9



(4-((E)-2-((2R)-6-(benzyloxy)-2-(4-(benzyloxy)phenyl)-3-(3,5-bis(benzyloxy)phenyl)-2,3-dihydrobenzofuran-4-yl)vinyl)-2,6-dibromophenoxy)(tert-butyl)dimethylsilane (3.60): A solution of aldehyde **3.32** (125 mg, 0.172 mmol, 1.00 equiv) was prepared in anhydrous THF (8 mL) in a heart-shaped flask and maintained under inert atmosphere. To a stirring solution of diisopropylamine (freshly purified, 48 μ L, 0.345 mmol, 2.00 equiv) in anhydrous THF (3.5 mL) at -78 $^{\circ}$ C under inert atmosphere was added *n*-BuLi slowly (1.6 M solution in hexanes, 210 μ L, 0.336 mmol, 1.95 equiv), and the mixture was maintained at this temperature for 0.5 h. Meanwhile, a solution of phosphonate ester **3.59** (875 mg, 1.380 mmol, 2.00 equiv) in anhydrous THF (5.5 mL) was prepared in a round bottom flask and stirred under inert atmosphere at -78 $^{\circ}$ C. At 0.5 h, the LDA was transferred dropwise to the stirring phosphonate ester by cannula, turning the solution bright yellow. The mixture was stirred at -78 $^{\circ}$ C for 15 minutes, at which point the solution of aldehyde **3.32** was added slowly by cannula. The reaction was allowed to slowly warm over 2 h until TLC indicated full consumption of the aldehyde. At this point, the reaction was quenched by the addition of sat. aq. NH_4Cl . The mixture was diluted with EtOAc and transferred to a separatory funnel where the phases were separated. The aqueous layer was extracted with additional portions of EtOAc. Combined organic layers were washed with brine, dried over Na_2SO_4 , and concentrated *in vacuo*. The crude material was purified by flash chromatography over SiO_2 (95:5 Hexanes/EtOAc) to afford the desired **3.60** (131 mg, 0.121 mmol, 70% yield) as a white foam as exclusively (>20:1) the (*E*)-isomer.

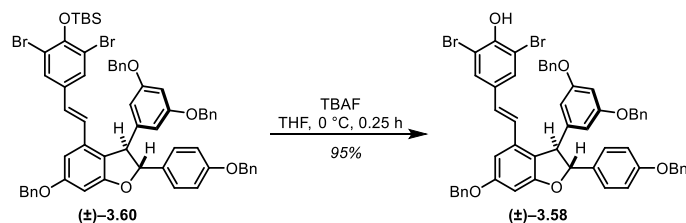
TLC (Hexanes/EtOAc, 85:15), R_f : 0.43 (UV, *p*-anisaldehyde (purple));

^1H NMR (500 MHz, CDCl_3 , 25 $^{\circ}$ C) δ : 7.50 – 7.46 (m, 2H), 7.45 – 7.28 (m, overlap, 20H), 7.24 (s, 2H), 7.22 (d, J = 8.8 Hz, 2H), 6.94 (d, J = 8.8 Hz, 2H), 6.75 (d, J = 2.2 Hz, 1H), 6.63 (d, J = 16.2 Hz, 1H), 6.57 (t, overlap, J = 1.8 Hz, 1H), 6.56 (d, overlap, J = 2.2 Hz, 1H), 6.52 (d, J = 16.2 Hz, 1H), 6.45 (d, J = 1.8 Hz, 2H), 5.52 (d, J = 6.6 Hz, 1H), 5.11 (s, 2H), 5.06 (s, 2H), 4.99 (s, 4H), 4.49 (d, J = 6.6 Hz, 1H), 1.04 (s, 9H), 0.33 (s, 6H);

^{13}C NMR (125 MHz, CDCl_3 , 25 $^{\circ}$ C) δ : 161.5, 160.53, 160.45, 158.8, 149.6, 145.3, 136.9, 136.7, 134.5, 133.6, 133.1, 130.6, 128.71, 128.65, 128.60, 128.13, 128.04, 127.71, 127.67, 127.5, 127.0, 126.7, 126.2, 120.4, 116.1, 115.1, 107.3, 104.0, 100.8, 96.6, 93.2, 70.4, 70.2, 70.1, 57.1, 26.3, 19.0, -2.01 , -2.03 ;

HRMS (ESI): m/z calculated for $\text{C}_{62}\text{H}_{59}\text{Br}_2\text{O}_6\text{Si}$ $[\text{M}+\text{H}]^+$: 1085.2442, found 1085.2440;

FTIR (neat) cm^{-1} : 3030 (w), 2925 (m), 2858 (m), 1592 (s), 1509 (m), 1462 (s), 1373 (m), 1283 (m), 1250 (m), 1151 (s), 1055 (m), 1027 (m), 959 (m), 895 (m), 824 (m), 804 (m), 733 (s), 694 (s).



4-((E)-2-((2R)-6-(benzyloxy)-2-(4-(benzyloxy)phenyl)-3-(3,5-bis(benzyloxy)phenyl)-2,3-dihydrobenzofuran-4-yl)vinyl)-2,6-dibromophenol (3.58): Starting **3.60** (125 mg, 0.115 mmol, 1.00 equiv) was dissolved in THF (11 mL) and the solution was cooled to 0 °C, stirring under inert atmosphere. To the stirring mixture was added TBAF (1 M solution in THF, 127 μL , 0.127 mmol, 1.10 equiv), turning the solution a bright yellow. At 0.25 h, TLC indicated full conversion, and the reaction mixture was worked up according to the procedure of Kaburagi and Kishi (vide infra).³² CaCO_3 (125 mg, 1 wt equiv) was added, and the mixture was stirred for several minutes before adding DOWEX-50W-8 Resin (375 mg, 3 wt equiv, 200 mesh). Finally, MeOH (11 mL) was added and the mixture was stirred under inert atmosphere for 1 h at room temperature. The mixture was then filtered over a short plug of silica, eluting with Et_2O . The filtrate was concentrated *in vacuo* to afford **3.58** (106 mg, 0.109 mmol, 95% yield) as a white foam, which did not require further purification.

TLC (Hexanes/EtOAc, 90:10), R_f : 0.13 (UV);

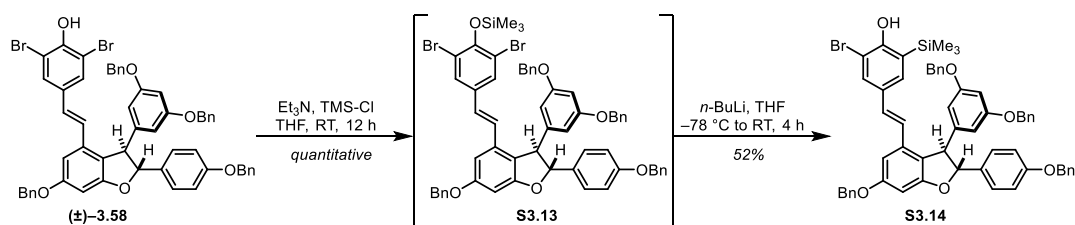
$^1\text{H NMR}$ (700 MHz, CDCl_3 , 25 °C) δ : 7.51 – 7.47 (m, 2H), 7.45 – 7.28 (m, overlap, 16H), 7.23 (d, $J = 8.3$ Hz, 2H), 7.21 (s, 2H), 6.95 (d, $J = 8.3$ Hz, 2H), 6.75 (s, 1H), 6.63 (d, $J = 16.4$ Hz, 1H), 6.57 (s, overlap, 1H), 6.57 (s, overlap 1H), 6.51 (d, $J = 16.4$ Hz, 1H), 6.46 (s, 2H), 5.80 (s, 1H), 5.53 (d, $J = 6.6$ Hz, 1H), 5.11 (s, 2H), 5.07 (s, 2H), 4.99 (s, 2H), 4.50 (d, $J = 6.6$ Hz, 1H);

$^{13}\text{C NMR}$ (175 MHz, CDCl_3 , 25 °C) δ : 161.6, 160.7, 160.6, 158.9, 148.8, 145.5, 137.0, 136.8, 134.5, 133.7, 132.7, 130.0, 128.9, 128.8, 128.7, 128.3, 128.2, 127.79, 127.78, 127.7, 127.2, 126.7, 126.2, 120.5, 115.2, 110.2, 107.4, 104.0, 100.9, 96.7, 93.3, 70.6, 70.3, 70.2, 57.3;

HRMS (ESI): m/z calculated for $\text{C}_{56}\text{H}_{45}\text{Br}_2\text{O}_6$ $[\text{M}+\text{H}]^+$: 971.1577, found 971.1562;

FTIR (neat) cm^{-1} : 3491 (m), 3028 (m), 1581 (s), 1510 (m), 1474 (m), 1452 (m), 1241 (m), 1150 (s), 1026 (m), 826 (m), 734 (s), 694 (s).

³² Kaburagi, Y.; Kishi, Y. *Org. Lett.* **2007**, 9 (4), 723–726.



4-((E)-2-((2R)-6-(benzyloxy)-2-(4-(benzyloxy)phenyl)-3-(3,5-bis(benzyloxy)phenyl)-2,3-dihydrobenzofuran-4-yl)vinyl)-2-bromo-6-(trimethylsilyl)phenol (S3.14): The following procedure was adapted from that reported by Akai and co-workers.³³ Starting dibromo-stilbene **3.58** (175 mg, 0.180 mmol, 1.00 equiv) was dissolved in anhydrous THF (2 mL) at room temperature under inert atmosphere. To the stirring mixture were added Et₃N (38 μ L, 0.270 mmol, 1.50 equiv) and TMSCl (34 μ L, 0.270 mmol, 1.50 equiv), sequentially. The reaction soon became heterogeneous and was allowed to stir overnight. At 12 h, the reaction mixture was filtered through a plug of Celite, eluting with additional THF. The filtrate was concentrated to dryness to yield the *O*-trimethylsilyl derivative **S3.13** (187 mg, quantitative yield), which was carried forward directly without further purification.

The silyl-protected phenol **S3.13** (83 mg, 0.080 mmol, 1.00 equiv) was dissolved in anhydrous THF (800 μ L) and cooled to -78 °C under inert atmosphere. To the stirring mixture, *n*-BuLi (50 μ L, 0.080 mmol, 1.00 equiv) was added dropwise, turning the solution yellow. The reaction was held at -78 °C for 15 minutes at which point the cooling bath was removed and the mixture was allowed to warm to room temperature and stir for 4 h. The reaction was quenched by the addition of sat. aq. NH₄Cl, diluted with EtOAc, and transferred to a separatory funnel where the phases were separated. The aqueous phase was extracted with additional portions of EtOAc. The organic phases were then combined, washed with brine, dried over Na₂SO₄, and concentrated *in vacuo*. The desired **S3.14** (40 mg, 0.041 mmol, 52% yield) was isolated from the crude material as a white foam by preparative TLC (85:15 Hexanes/EtOAc), along with recovered **3.58** (30 mg, 0.031 mmol, 39%).

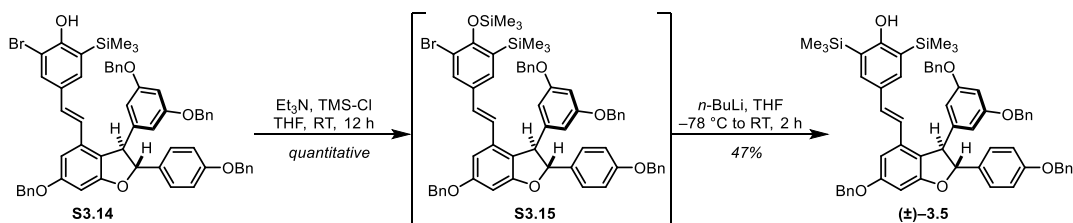
¹H NMR (500 MHz, CDCl₃, 25 °C) δ : 7.52 – 7.28 (m, overlap, 20H), 7.23 (d, *J* = 8.4 Hz, 2H), 7.11 (d, *J* = 1.7 Hz, 1H), 6.95 (d, *J* = 8.4 Hz, 2H), 6.81 (d, *J* = 1.7 Hz, 1H), 6.77 (d, *J* = 16.5 Hz, 1H), 6.55 (m, overlap, 2H), 6.53 (d, *J* = 16.5 Hz, 1H), 6.44 (d, *J* = 2.2 Hz, 2H), 5.67 (s, 1H), 5.48 (d, *J* = 6.2 Hz, 1H), 5.12 (s, 2H), 5.07 (s, 2H), 4.96 (s, 4H), 4.51 (d, *J* = 6.2 Hz, 1H), 0.25 (s, 9H);

¹³C NMR (125 MHz, CDCl₃, 25 °C) δ : 161.7, 160.6 (2C), 158.9, 155.8, 145.7, 137.15, 137.07, 136.9, 135.3, 133.9, 133.1, 131.3, 130.8, 128.82, 128.79, 128.7, 128.5, 128.24, 128.18, 128.16, 127.83, 127.79, 127.65, 127.18, 127.16, 124.4, 120.0, 115.2, 111.0, 107.2, 103.8, 100.8, 96.3, 93.3, 70.6, 70.25, 70.23, 57.2, -1.04 ;

HRMS (ESI): *m/z* calculated for C₅₉H₅₄BrO₆Si [M+H]⁺: 965.2868, found 965.2841;

FTIR (neat) cm⁻¹: 3508 (m, br), 3031 (m), 2927 (m), 1606 (s), 1583 (s), 1511 (m), 1452 (s), 1379 (m), 1329 (m), 1245 (s), 1157 (s), 1075 (m), 1058 (m), 1027 (m), 960 (w), 839 (s), 735 (s), 696 (s).

³³ Ikawa, T.; Nishiyama, T.; Nosaki, T.; Takagi, A.; Akai, S. *Org. Lett.* **2011**, *13* (7), 1730–1733.



4-((E)-2-((2R)-6-(benzyloxy)-2-(4-(benzyloxy)phenyl)-3-(3,5-bis(benzyloxy)phenyl)-2,3-dihydrobenzofuran-4-yl)vinyl)-2,6-bis(trimethylsilyl)phenol (3.5): The following procedure was adapted from that reported by Akai and co-workers.³⁴ Starting bromo-trimethylsilyl-stilbene **S3.14** (71 mg, 0.073 mmol, 1.00 equiv) was dissolved in anhydrous THF (1 mL) at room temperature under inert atmosphere. To the stirring mixture were added Et₃N (15 μ L, 0.110 mmol, 1.50 equiv) and TMSCl (14 μ L, 0.110 mmol, 1.50 equiv), sequentially. The reaction soon became heterogeneous and was allowed to stir overnight. At 12 h, the reaction mixture was filtered through a plug of Celite, eluting with additional THF. The filtrate was concentrated to dryness to yield the *O*-trimethylsilyl derivative **S3.15** (76 mg, quantitative yield), which was carried forward directly without further purification.

The silyl-protected phenol **S3.15** (76 mg, 0.073 mmol, 1.00 equiv) was dissolved in anhydrous THF (1.4 mL) and cooled to -78 °C under inert atmosphere. To the stirring mixture, *n*-BuLi (50 μ L, 0.081 mmol, 1.10 equiv) was added dropwise, turning the solution yellow. The reaction was held at -78 °C for 10 minutes at which point the cooling bath was removed and the mixture was allowed to warm to room temperature and stir for 2 h. The reaction was quenched by the addition of sat. aq. NH₄Cl, diluted with EtOAc, and transferred to a separatory funnel where the phases were separated. The aqueous phase was extracted with additional portions of EtOAc. The organic phases were then combined, washed with brine, dried over Na₂SO₄, and concentrated *in vacuo*. The desired **3.5** (33 mg, 0.034 mmol, 47% yield) was isolated from the crude material as a white foam by preparative TLC (90:7:3 Hexanes/EtOAc/CH₂Cl₂), along with recovered **S3.14** (12.5 mg, 0.013 mmol, 18%).

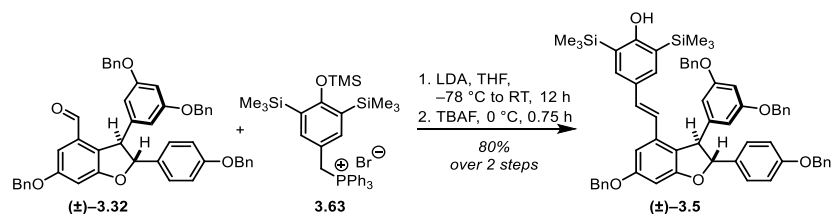
¹H NMR (500 MHz, CDCl₃, 25 °C) δ : 7.53–7.49 (m, 2H), 7.46–7.28 (m, 18H), 7.23 (d, overlap, *J* = 8.4 Hz, 2H), 7.23 (s, 2H), 6.96 (d, *J* = 8.4 Hz, 2H), 6.90 (d, *J* = 16.1 Hz, 1H), 6.88 (d, *J* = 2.0 Hz, 1H), 6.57 (d, *J* = 16.1 Hz, 1H), 6.55 (d, overlap, *J* = 2.0 Hz, 1H), 6.52 (t, *J* = 2.2 Hz, 1H), 6.43 (d, *J* = 2.2 Hz, 2H), 5.44 (d, *J* = 6.2 Hz, 1H), 5.14 (s, 2H), 5.08 (s, 2H), 5.03 (s, 1H), 4.95 (d, *J* = 11.7 Hz, 2H), 4.93 (d, *J* = 11.7 Hz, 2H), 4.53 (d, *J* = 6.2 Hz, 1H), 0.29 (s, 18H);

¹³C NMR (125 MHz, CDCl₃, 25 °C) δ : 165.3, 161.8, 160.6, 160.5, 158.9, 145.8, 137.2, 137.1, 136.9, 135.9, 135.2, 134.1, 130.1, 129.4, 128.82, 128.81, 128.7, 128.22, 128.20, 128.15, 127.9, 127.8, 127.7, 127.2, 124.5, 122.9, 119.5, 115.2, 107.0, 103.6, 100.6, 95.9, 93.3, 70.6, 70.24, 70.17, 57.2, -0.43 ;

HRMS (ESI): *m/z* calculated for C₆₂H₆₃O₆Si₂ [M+H]⁺: 959.4158, found 959.4157;

FTIR (neat) cm⁻¹: 3596 (m), 3033 (m), 2953 (m), 1606 (s), 1581 (s), 1511 (m), 1452 (m), 1414 (w), 1377 (w), 1311 (w), 1242 (m), 1221 (m), 1157 (s), 1131 (s), 1053 (m), 1027 (m), 961 (w), 908 (m), 835 (s), 732 (s), 694 (s).

³⁴ Ikawa, T.; Nishiyama, T.; Nosaki, T.; Takagi, A.; Akai, S. *Org. Lett.* **2011**, *13* (7), 1730–1733.



4-((E)-2-((2R)-6-(benzyloxy)-2-(4-(benzyloxy)phenyl)-3-(3,5-bis(benzyloxy)phenyl)-2,3-dihydrobenzofuran-4-yl)vinyl)-2,6-bis(trimethylsilyl)phenol (3.5): A solution of aldehyde **3.32** (150 mg, 0.207 mmol, 1.00 equiv) was prepared in anhydrous THF (4 mL) in a heart-shaped flask and maintained under inert atmosphere. To a stirring solution of diisopropylamine (freshly purified, 58 μ L, 0.414 mmol, 2.00 equiv) in anhydrous THF (1.5 mL) at -78 $^{\circ}$ C under inert atmosphere was added *n*-BuLi slowly (2.5 M solution in hexanes, 161 μ L, 0.404 mmol, 1.95 equiv), and the mixture was maintained at this temperature for 0.5 h. Meanwhile, a suspension of phosphonium salt **3.63** (276 mg, 0.414 mmol, 2.00 equiv) in anhydrous THF (2.5 mL) was prepared in a round bottom flask and stirred under inert atmosphere at -78 $^{\circ}$ C. At 0.5 h, the LDA was transferred dropwise to the stirring phosphonium salt by cannula, turning the suspension red, then red-brown. The mixture was stirred at -78 $^{\circ}$ C for 20 minutes, at which point the solution of aldehyde **3.32** was added slowly by cannula, turning the mixture a bright red color. The reaction was allowed to slowly warm within the cooling bath over the course of 3 hours. On complete consumption of the aldehyde (as determined by TLC), the solution was cooled to 0 $^{\circ}$ C and treated with TBAF (1 M solution in THF, 414 μ L, 0.414 mmol, 2.00 equiv). After 0.25 h, the reaction was quenched by the addition of sat. aq. NH_4Cl . The mixture was diluted with Et_2O and transferred to a separatory funnel containing DI H_2O . The phases were separated and the aqueous phase extracted with additional portions of Et_2O . The combined organic layers were washed with brine, dried over Na_2SO_4 , and concentrated *in vacuo*. The crude material was purified by flash chromatography over SiO_2 (90:5:5 hexanes/ Et_2O / CH_2Cl_2) to afford the ϵ -viniferin analog **3.5** (158 mg, 0.165 mmol, 80% yield) as a white foam as exclusively the (*E*)-isomer.

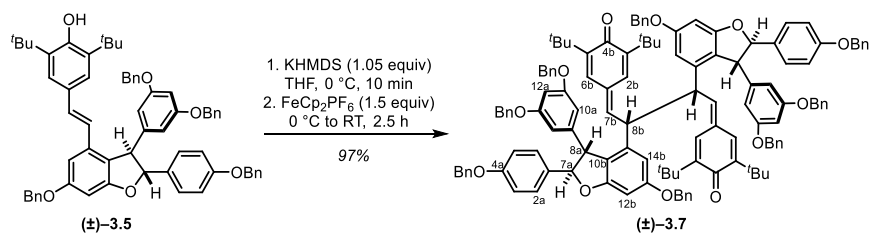
TLC (Hexanes/ EtOAc , 85:15), R_f : 0.21 (UV, *p*-anisaldehyde (purple));

^1H NMR (500 MHz, CDCl_3 , 25 $^{\circ}$ C) δ : 7.55 – 7.54 (m, 2H), 7.48 – 7.33 (m, 22H), 7.29 (s, 1H), 7.27 (d, J = 8.5 Hz, 2H), 6.99 (d, J = 8.4 Hz, 2H), 6.94 (d, J = 16.1 Hz, 1H), 6.91 (d, J = 2.0 Hz, 1H), 6.61 (d, J = 16.1 Hz, 1H), 6.58 (d, J = 2.0 Hz, 1H), 6.55 (t, J = 2.0 Hz, 1H), 6.47 (d, J = 2.0 Hz, 2H), 5.47 (d, J = 6.1 Hz, 1H), 5.17 (s, 2H), 5.11 (s, 2H), 5.06 (s, 1H, $-\text{OH}$), 4.98 (d, J = 11.7 Hz, 2H), 4.97 (d, J = 11.7 Hz, 2H), 4.56 (d, J = 6.1 Hz, 1H), 0.33 (s, 18H);

^{13}C NMR (175 MHz, CDCl_3 , 25 $^{\circ}$ C) δ : 165.3, 161.8, 160.6, 160.5, 158.9, 145.8, 137.2, 137.1, 136.9, 135.9, 135.2, 134.1, 130.1, 129.4, 128.81, 128.80, 128.7, 128.22, 128.19, 128.15, 127.9, 127.8, 127.7, 127.2, 124.5, 122.9, 119.5, 115.2, 107.0, 103.6, 100.6, 95.9, 93.3, 70.6, 70.2, 70.2, 57.2, -0.43 ;

HRMS (ESI): m/z calculated for $\text{C}_{62}\text{H}_{63}\text{O}_6\text{Si}_2$ $[\text{M}+\text{H}]^+$: 959.4158, found 959.4157;

FTIR (neat) cm^{-1} : 3596 (m), 3033 (m), 2953 (m), 1606 (s), 1581 (s), 1511 (m), 1452 (m), 1414 (m), 1377 (m), 1311 (m), 1242 (m), 1221 (m), 1157 (s), 1131 (s), 1053 (m), 1027 (m), 961 (m), 908 (m), 835 (s), 732 (s), 694 (s).



4,4'-(2,3-bis((2*S*,3*S*)-6-(benzyloxy)-2-(4-(benzyloxy)phenyl)-3-(3,5-bis(benzyloxy)phenyl)-2,3-

dihydrobenzofuran-4-yl)butane-1,4-diyldiene)bis(2,6-di-*tert*-butylcyclohexa-2,5-dien-1-one) (3.7): A solution of starting ϵ -viniferin derivative **3.5** (210 mg, 0.226 mmol, 1.00 equiv) was prepared in THF (23 mL, 0.01 M) and cooled to 0 °C under inert atmosphere. To the stirring mixture was added potassium bis(trimethylsilyl)amide [KHMDS] (0.7 M solution in toluene, 324 μ L, 0.226 mmol, 1.00 equiv) slowly, turning the solution yellow-orange. The mixture was allowed to equilibrate for 10 minutes, at which point FeCp₂PF₆ (48 mg, 0.142 mmol, 0.625 equiv) was added in a single portion. At 0.5 h, a second portion of FeCp₂PF₆ (48 mg, 0.142 mmol, 0.625 equiv) was added. At 2 h, an additional 0.25 equiv (19 mg) of FeCp₂PF₆ were added. After 30 minutes, TLC analysis indicated full consumption of the starting material, and the reaction was quenched by the addition of sat. aq. NH₄Cl. The mixture was then diluted with EtOAc and transferred to a separatory funnel where the phases were separated. The aqueous layer was extracted with additional portions of EtOAc. The combined organic layers were then washed with brine, dried over Na₂SO₄ and concentrated in vacuo. The desired **3.7** (204 mg, 0.110 mmol, 97% yield) was isolated from the crude material as an amorphous yellow solid by flash chromatography over SiO₂ (15% of a 2:1 EtOAc/CH₂Cl₂ mixture in hexanes). The product can be further purified to a yellow crystalline solid by trituration from MeNO₂.

TLC (hexanes/EtOAc, 85:15), *R_f*: 0.21 (UV, Hanessian's stain)

¹H NMR (700 MHz, CDCl₃, 50 °C) δ : 7.52 – 7.12 (m, 40H, –OCH₂C₆H₅), 7.10 (d, *J* = 8.5 Hz, 4H, C_{2a}–H), 7.01 (d, *J* = 8.5 Hz, 4H, C_{3a}–H), 6.70 (s, 2H, C_{14b}–H), 6.42 (s, 2H, C_{2/6b}–H), 6.39 (s, 2H, C_{12b}–H), 6.37 (s, 2H, C_{12a}–H), 6.23 (s, 2H, C_{2/6b}–H), 6.16 (s, 4H, C_{10a}–H), 6.11 (dd, br, *J* = 7.3, 9.2 Hz, 2H, C_{7b}–H), 5.11 (d, *J* = 8.1 Hz, 2H, C_{7a}–H), 5.04 (d, *J* = 12.5 Hz, 2H, C_{4a}–OCH₂C₆H₅), 5.02 (d, *J* = 12.5 Hz, 2H, C_{4a}–OCH₂C₆H₅), 4.83 (d, *J* = 10.8 Hz, 2H, C_{13b}–OCH₂C₆H₅), 4.77 (d, *J* = 10.8 Hz, 2H, C_{13b}–OCH₂C₆H₅), 4.62 (d, *J* = 11.1 Hz, 4H, C_{11a}–OCH₂C₆H₅), 4.56 (d, *J* = 11.1 Hz, 4H, C_{11a}–OCH₂C₆H₅), 4.06 (dd, br, *J* = 7.9, 9.2 Hz, 2H, C_{8b}–H), 3.87 (d, *J* = 8.1 Hz, 2H, C_{8a}–H), 1.17 (s, 18H, C_{3/5b}–C(CH₃)₃), 1.00 (s, 18H, C_{3/5b}–C(CH₃)₃);

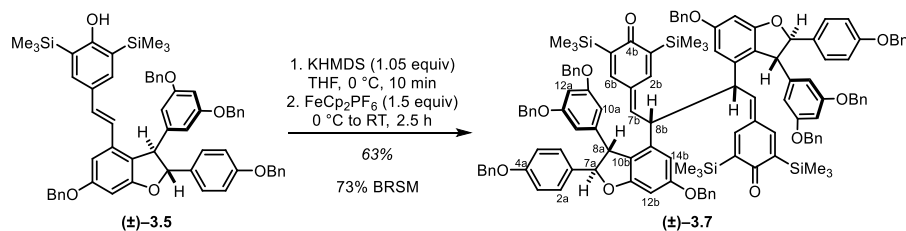
¹³C NMR (175 MHz, CDCl₃, 50 °C) δ : 186.2 (C_{4b}), 161.9 (C_{11b}), 160.8 (C_{11a}), 160.7 (C_{13b}), 159.4 (C_{4a}), 148.1 (C_{3/5b}), 147.8 (C_{3/5b}), 144.2 (C_{9a}), 143.1 (C_{7b}), 139.6 (C_{9b}), 137.2 (–OCH₂C₆H₅), 136.8 (–OCH₂C₆H₅), 136.7 (–OCH₂C₆H₅), 134.1 (C_{2/6b}), 133.5 (C_{1b}), 133.4 (C_{1a}), 128.8 (–OCH₂C₆H₅), 128.7 (–OCH₂C₆H₅), 128.4 (–OCH₂C₆H₅), 128.2 (–OCH₂C₆H₅), 128.1 (–OCH₂C₆H₅), 128.0 (C_{2a}), 127.82 (–OCH₂C₆H₅), 127.80 (–OCH₂C₆H₅), 127.7 (–OCH₂C₆H₅), 125.9 (C_{2/6b}), 121.0 (C_{10b}), 115.4 (C_{3a}), 107.5 (C_{14b}), 106.8 (C_{10a}), 101.9 (C_{12a}), 95.7 (C_{12b}), 93.7 (C_{7a}), 70.7 (C_{13b}–OCH₂C₆H₅), 70.5 (C_{4a}–OCH₂C₆H₅), 70.3 (C_{11a}–OCH₂C₆H₅), 56.9 (C_{8a}), 50.1 (C_{8b}), 35.4 (C_{3/5b}–C(CH₃)₃), 34.9 (C_{3/5b}–C(CH₃)₃), 29.8 (C_{3/5b}–C(CH₃)₃), 29.5 (C_{3/5b}–C(CH₃)₃);

HRMS (ESI):

m/z calculated for C₁₂₈H₁₂₃O₁₂ [M+H]⁺: 1851.9009, found 1851.8992;

FTIR (neat) cm^{-1} :

3034 (w), 2954 (m), 1612 (s), 1589 (s), 1517 (m), 1496 (m), 1453 (s),
1360 (m), 1331 (m), 1244 (s), 1156 (s), 1131 (s), 1080 (w), 1027 (s).



4,4'-((2R,3R)-2,3-bis((2R,3R)-6-(benzyloxy)-2-(4-(benzyloxy)phenyl)-3-(3,5-bis(benzyloxy)phenyl)-2,3-dihydrobenzofuran-4-yl)butane-1,4-diyldene)bis(2,6-bis(trimethylsilyl)cyclohexa-2,5-dien-1-one) (3.7): A solution of starting ε -viniferin derivative **3.5** (150 mg, 0.156 mmol, 1.00 equiv) was prepared in THF (6.25 mL) and cooled to 0 °C under inert atmosphere. To the stirring mixture was added potassium bis(trimethylsilyl)amide [KHMDS] (0.7 M solution in toluene, 224 μ L, 0.156 mmol, 1.00 equiv) slowly, turning the solution yellow-brown. The mixture was allowed to equilibrate for 3 minutes, at which point FeCp_2PF_6 (66 mg, 0.195 mmol, 1.25 equiv) was added in a single portion. TLC analysis at 30 minutes indicated incomplete consumption of the starting material, so an additional 0.25 equiv of FeCp_2PF_6 were added. At 90 minutes, the reaction was quenched by the addition of sat. aq. NH_4Cl . The mixture was then diluted with EtOAc and transferred to a separatory funnel where the phases were separated. The aqueous layer was extracted with additional portions of EtOAc. The combined organic layers were then washed with brine, dried over Na_2SO_4 and concentrated in vacuo. The desired **3.7** (94 mg, 0.049 mmol, 63% yield) was isolated from the crude material as an amorphous brown solid by preparative TLC (80:15:5 Hexanes/EtOAc/ CH_2Cl_2) as a single diastereomer along with recovered **3.5** (21 mg, 0.022 mmol, 14% recovery).

TLC (hexanes/EtOAc, 85:15), R_f : 0.19 (UV, *p*-anisaldehyde (faint pink))

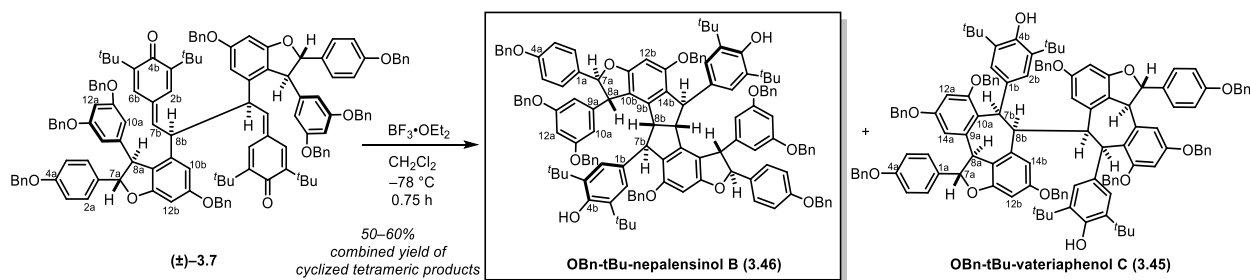
^1H NMR (500 MHz, CDCl_3 , 25 °C) δ : 7.44 – 7.10 (m, 40H, $-\text{OCH}_2\text{C}_6\text{H}_5$), 7.11 (d, $J = 8.6$ Hz, 4H, $\text{C}_{2a}\text{-H}$), 7.03 (d, $J = 8.6$ Hz, 4H, $\text{C}_{3a}\text{-H}$), 6.80 (d, $J = 2.2$ Hz, 2H, $\text{C}_{2/6b}\text{-H}$), 6.69 (s, br, 2H, $\text{C}_{14b}\text{-H}$), 6.51 (d, br, $J = 2.2$ Hz, 2H, $\text{C}_{2/6b}\text{-H}$), 6.44 (d, $J = 2.2$ Hz, 2H, $\text{C}_{12b}\text{-H}$), 6.34 (t, $J = 2.0$ Hz, 2H, $\text{C}_{12a}\text{-H}$), 6.21 (dd, $J = 7.7, 9.9$ Hz, 2H, $\text{C}_{7b}\text{-H}$), 6.15 (d, $J = 2.0$ Hz, 4H, $\text{C}_{10a}\text{-H}$), 5.14 (d, $J = 8.6$ Hz, 2H, $\text{C}_{7a}\text{-H}$), 5.01 (s, 4H, $\text{C}_{4a}\text{-OCH}_2\text{C}_6\text{H}_5$), 4.85 (d, $J = 11.0$ Hz, 2H, $\text{C}_{13b}\text{-OCH}_2\text{C}_6\text{H}_5$), 4.77 (d, $J = 11.0$ Hz, 2H, $\text{C}_{13b}\text{-OCH}_2\text{C}_6\text{H}_5$), 4.56 (d, $J = 11.0$ Hz, 4H, $\text{C}_{11a}\text{-OCH}_2\text{C}_6\text{H}_5$), 4.51 (d, $J = 11.0$ Hz, 4H, $\text{C}_{11a}\text{-OCH}_2\text{C}_6\text{H}_5$), 4.11 (dd, $J = 7.7, 9.9$ Hz, 2H, $\text{C}_{8b}\text{-H}$), 3.99 (d, $J = 8.6$ Hz, 2H, $\text{C}_{8a}\text{-H}$), 0.14 (s, 18H, $\text{C}_{3/5b}\text{-Si}(\text{CH}_3)_3$), -0.02 (s, 18H, $\text{C}_{3/5b}\text{-Si}(\text{CH}_3)_3$);

^{13}C NMR (175 MHz, CDCl_3 , 25 °C) δ : 192.8 (C_{4b}), 161.8 (C_{11b}), 160.68 (C_{11a}), 160.62 (C_{13b}), 159.3 (C_{4a}), 148.2 ($\text{C}_{2/6b}$), 144.5 (C_{7b}), 143.7 (C_{9a}), 142.5 ($\text{C}_{3/5b}$), 141.8 ($\text{C}_{3/5b}$), 139.9 ($\text{C}_{2/6b}$), 138.9 (C_{9b}), 136.95 ($-\text{OCH}_2\text{C}_6\text{H}_5$), 136.5 ($-\text{OCH}_2\text{C}_6\text{H}_5$), 136.4 ($-\text{OCH}_2\text{C}_6\text{H}_5$), 133.1 (C_{1a}), 132.8 (C_{1b}), 128.82 ($-\text{OCH}_2\text{C}_6\text{H}_5$), 128.80 ($-\text{OCH}_2\text{C}_6\text{H}_5$), 128.77 ($-\text{OCH}_2\text{C}_6\text{H}_5$), 128.72 ($-\text{OCH}_2\text{C}_6\text{H}_5$), 128.66 ($-\text{OCH}_2\text{C}_6\text{H}_5$), 128.5 ($-\text{OCH}_2\text{C}_6\text{H}_5$), 128.3 ($-\text{OCH}_2\text{C}_6\text{H}_5$), 128.1 ($-\text{OCH}_2\text{C}_6\text{H}_5$), 128.0 ($-\text{OCH}_2\text{C}_6\text{H}_5$), 127.9 (C_{2a}), 127.8 ($-\text{OCH}_2\text{C}_6\text{H}_5$), 127.72 ($-\text{OCH}_2\text{C}_6\text{H}_5$), 127.66 ($-\text{OCH}_2\text{C}_6\text{H}_5$), 120.9 (C_{10b}), 115.3 (C_{3a}), 107.1 (C_{14b}), 106.5 (C_{10a}), 101.3 (C_{12a}), 95.6 (C_{12b}), 93.6 (C_{7a}), 70.6 ($-\text{OCH}_2\text{C}_6\text{H}_5$), 70.3 ($-\text{OCH}_2\text{C}_6\text{H}_5$), 70.0 ($-\text{OCH}_2\text{C}_6\text{H}_5$), 57.0 (C_{8a}), 49.6 (C_{8b}), -1.10 ($\text{C}_{3/5b}\text{-Si}(\text{CH}_3)_3$), -1.33 ($\text{C}_{3/5b}\text{-Si}(\text{CH}_3)_3$);

HRMS (ESI): m/z calculated for $\text{C}_{124}\text{H}_{123}\text{O}_{12}\text{Si}_4$ $[\text{M}+\text{H}]^+$: 1915.8035, found 1915.8036;

FTIR (neat) cm^{-1} :

3031 (m), 2954 (m), 1591 (s), 1512 (m), 1496 (w), 1453 (m), 1377 (m),
1318 (m), 1244 (s), 1219 (m), 1156 (s), 1132 (m), 1054 (m), 1028 (m),
904 (w), 838 (s), 734 (s), 695 (s).



Cyclization of Bis-Quinone Methide (3.7): A solution of the starting bis-quinone methide **3.7** (75 mg, 0.040 mmol, 1.00 equiv) was prepared in anhydrous CH_2Cl_2 under inert atmosphere. The stirring mixture was cooled to -60°C using an immersion chiller (Neslab CC 100, ThermoScientific). To the solution was added $\text{BF}_3\cdot\text{OEt}_2$ (43 μL , 46.5% in diethyl ether, 4.00 equiv). After 5 minutes, the temperature setting was adjusted to -30°C , and the reaction/cooling bath were allowed to slowly equilibrate to this temperature over 1.25 h. The reaction was then held at this temperature for an additional 2.5 h, at which point it was quenched with sat. aq. NaHCO_3 . The reaction was lifted from the cooling bath and stirred until the ice thawed. The contents were then diluted with EtOAc and transferred to a separatory funnel, where the phases were separated. The aqueous phase was extracted with additional portions of EtOAc. The combined organic layers were washed with brine, dried over Na_2SO_4 , and concentrated *in vacuo*. $^1\text{H-NMR}$ of the crude material indicated an approximately 3.5:1 ratio of the bicyclic [3.3.0] product to the bis-7-*exo* product as the two major isomers. The crude material was subjected to purification by preparative TLC (80:15:5 Hexanes/EtOAc/ CH_2Cl_2) to afford **3.46** (33 mg, 0.018 mmol, 44% yield) and hopeaphenol derivative **3.45** (7 mg, 0.004 mmol, 9% yield). Characterization data for the nepalensinol B derivative **3.46** are provided below:

TLC (Hexanes/EtOAc/ CH_2Cl_2 , 85:10:5), R_f : 0.21 (UV, Hanessian's stain)

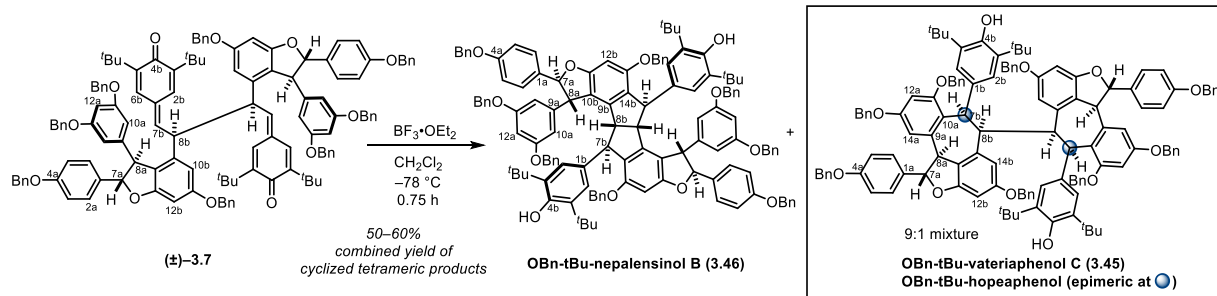
$^1\text{H NMR}$ (500 MHz, CDCl_3 , 25°C) δ :³⁵ 7.47 – 7.23 (m, 32H, $-\text{OCH}_2\text{C}_6\text{H}_5$), 7.19 (d, $J = 8.8$ Hz, 4H, $\text{C}_{2a}\text{-H}$), 7.11 – 7.04 (m, 8H, $-\text{OCH}_2\text{C}_6\text{H}_5$), 6.88 (d, $J = 8.8$ Hz, 4H, $\text{C}_{3a}\text{-H}$), 6.65 (s, 4H, $\text{C}_{2b}\text{-H}$), 6.33 (s, 2H, $\text{C}_{12b}\text{-H}$), 6.05 (t, $J < 2.0$ Hz, 2H, $\text{C}_{12a}\text{-H}$), 5.46 (s, 2H, $\text{C}_{7a}\text{-H}$), 5.05 (s, 4H, $\text{C}_{4a}\text{-OCH}_2\text{C}_6\text{H}_5$), 4.93 (s, 2H, $\text{C}_{4b}\text{-OH}$), 4.71 (s, 2H, $\text{C}_{8a}\text{-H}$), 4.64 (d, $J = 13.5$ Hz, $\text{C}_{13b}\text{-OCH}_2\text{C}_6\text{H}_5$), 4.61 (d, $J = 13.5$ Hz, $\text{C}_{13b}\text{-OCH}_2\text{C}_6\text{H}_5$), 4.51 (s, 2H, $\text{C}_{7b}\text{-H}$), 4.03 (s, 2H, $\text{C}_{8b}\text{-H}$), 1.31 (s, 36H, $\text{C}_{3/5b}\text{-C}(\text{CH}_3)_3$);

$^{13}\text{C NMR}$ (125 MHz, CDCl_3 , 50°C) δ :³⁵ 162.8 (C_{11b}), 160.9 (C_{11a}), 159.0 (C_{4a}), 156.7 (C_{13b}), 151.9 (C_{4b}), 147.8 (C_{9a}), 144.7 (C_{9b}), 137.7 ($-\text{OCH}_2\text{C}_6\text{H}_5$), 137.4 ($-\text{OCH}_2\text{C}_6\text{H}_5$), 137.2 ($-\text{OCH}_2\text{C}_6\text{H}_5$), 137.1 (C_{14b}), 135.7 ($\text{C}_{3/5b}$), 135.4 (C_{1a}), 128.84 ($-\text{OCH}_2\text{C}_6\text{H}_5$), 128.81 ($-\text{OCH}_2\text{C}_6\text{H}_5$), 128.77 ($-\text{OCH}_2\text{C}_6\text{H}_5$), 128.72 ($-\text{OCH}_2\text{C}_6\text{H}_5$), 128.65 ($-\text{OCH}_2\text{C}_6\text{H}_5$), 128.24 ($-\text{OCH}_2\text{C}_6\text{H}_5$), 128.20 ($-\text{OCH}_2\text{C}_6\text{H}_5$), 128.0 ($-\text{OCH}_2\text{C}_6\text{H}_5$), 127.8 (C_{1b}), 127.66 ($-\text{OCH}_2\text{C}_6\text{H}_5$), 127.62 ($-\text{OCH}_2\text{C}_6\text{H}_5$), 127.1 ($-\text{OCH}_2\text{C}_6\text{H}_5$), 126.8 (C_{2a}), 126.48 ($-\text{OCH}_2\text{C}_6\text{H}_5$), 124.0 ($\text{C}_{2/6b}$), 115.4 ($\text{C}_{3/5a}$), 114.9 (C_{10b}), 109.0 – 104.5 (C_{10a}), 101.1 (C_{12a}), 94.1 (C_{12b}), 93.5 (C_{7a}), 70.5 ($-\text{OCH}_2\text{C}_6\text{H}_5$), 69.8 ($-\text{OCH}_2\text{C}_6\text{H}_5$), 69.2 ($-\text{OCH}_2\text{C}_6\text{H}_5$), 59.7 (C_{8b}), 56.2 (C_{8a}), 50.1 (C_{7b}), 34.5 ($\text{C}_{3/5b}\text{-C}(\text{CH}_3)_3$), 30.7 ($\text{C}_{3/5b}\text{-C}(\text{CH}_3)_3$);

³⁵ Notably, the $\text{C}_{10a}\text{-H}$ protons are not visible due to extreme broadening in the $^1\text{H-NMR}$ spectrum. This is presumably due to hindered rotation in the highly congested bicyclic ring system. The $\text{C}_{11a}\text{-}$ and $\text{C}_{13a}\text{-}$ benzyloxy methylenes are also not visible in the $^1\text{H-NMR}$ spectrum further corroborating this property. The C_{10a} resonance in the $^{13}\text{C-NMR}$ spectrum is broadened over 4.5 ppm and is barely visible above the noise.

HRMS (ESI): m/z calculated for $C_{128}H_{123}O_{12}$ $[M+H]^+$: 1851.9009, found 1851.8947;

FTIR (neat) cm^{-1} : 3639 (m), 3028 (m), 2960 (m), 1593 (s), 1511 (m), 1452 (s), 1294 (m), 1237 (m), 1157 (s), 1108 (m), 1028 (m).



For preparation, consult previous entry. Data for the vateriaphenol C derivative **3.45** are provided below:³⁶

TLC (hexanes/EtOAc, 85:10:5), R_f : 0.21 (UV, Hanessian's stain)

$^1\text{H NMR}$ (700 MHz, CDCl_3 , 50 °C) δ :³⁷ 7.46 (d, $J = 8.5$ Hz, 4H, $\text{C}_{2/6a}\text{-H}$), 7.43 – 7.30 (m, 22H, $-\text{OCH}_2\text{C}_6\text{H}_5$), 7.27 – 7.20 (m, 5H, $-\text{OCH}_2\text{C}_6\text{H}_5$), 7.15 – 7.11 (m, 5H, $-\text{OCH}_2\text{C}_6\text{H}_5$), 7.06 (t, $J = 7.4$ Hz, 4H, $-\text{OCH}_2\text{C}_6\text{H}_5$), 6.95 (d, $J = 8.5$ Hz, 4H, $\text{C}_{3/5a}\text{-H}$), 6.87 (d, $J = 7.4$ Hz, 4H, $-\text{OCH}_2\text{C}_6\text{H}_5$), 6.47 (d, $J = 1.9$ Hz, 2H, $\text{C}_{14a}\text{-H}$), 6.44 (d, $J = 1.9$ Hz, 2H, $\text{C}_{12a}\text{-H}$), 6.10 (d, $J = 1.9$ Hz, 2H, $\text{C}_{12b}\text{-H}$), 5.96 (s, br, 2H, $\text{C}_{7b}\text{-H}$), 5.83 (d, $J = 8.2$ Hz, 2H, $\text{C}_{7a}\text{-H}$), 5.29 (d, $J = 8.2$ Hz, 2H, $\text{C}_{8a}\text{-H}$), 5.25 (d, $J = 1.9$ Hz, 2H, $\text{C}_{14b}\text{-H}$), 5.00 (s, 4H, $-\text{OCH}_2\text{C}_6\text{H}_5$), 4.99 (d, $J = 12.0$ Hz, 2H, $-\text{OCH}_2\text{C}_6\text{H}_5$), 4.90 (d, $J = 12.0$ Hz, 2H, $-\text{OCH}_2\text{C}_6\text{H}_5$), 4.74 (s, 2H, $\text{C}_{4b}\text{-OH}$), 4.60 (d, $J = 12.3$ Hz, 2H, $\text{OCH}_2\text{C}_6\text{H}_5$), 4.44 (d, $J = 12.3$ Hz, 2H, $-\text{OCH}_2\text{C}_6\text{H}_5$), 4.39 (d, $J = 11.0$ Hz, 2H, $-\text{OCH}_2\text{C}_6\text{H}_5$), 4.28 (d, $J = 11.0$ Hz, 2H, $-\text{OCH}_2\text{C}_6\text{H}_5$), 4.13 (s, 2H, $\text{C}_{8b}\text{-H}$), 1.06 (s, 36H, $\text{C}_{3/5b}\text{-C}(\text{CH}_3)_3$);

$^{13}\text{C NMR}$ (175 MHz, CDCl_3 , 50 °C) δ :³⁸ 160.2 (C_{13b}), 159.5 (C_{2a}), 159.0 (C_{11b}), 158.4 (C_{11a}), 157.9 (C_{13a}), 151.7 (C_{4b}), 140.7 (C_{9a}), 140.6 (C_{9b}), 137.5 ($-\text{OCH}_2\text{C}_6\text{H}_5$), 137.48 ($-\text{OCH}_2\text{C}_6\text{H}_5$), 137.41 ($-\text{OCH}_2\text{C}_6\text{H}_5$), 137.2 ($-\text{OCH}_2\text{C}_6\text{H}_5$), 134.7 (C_{1a}), 134.5 (br, $\text{C}_{3/5b}$), 133.0 (C_{1b}), 129.1 (C_{2a}), 128.83 ($-\text{OCH}_2\text{C}_6\text{H}_5$), 128.81 ($-\text{OCH}_2\text{C}_6\text{H}_5$), 128.7 ($-\text{OCH}_2\text{C}_6\text{H}_5$), 128.23 ($-\text{OCH}_2\text{C}_6\text{H}_5$), 128.17 ($-\text{OCH}_2\text{C}_6\text{H}_5$), 128.14 ($-\text{OCH}_2\text{C}_6\text{H}_5$), 128.05 ($-\text{OCH}_2\text{C}_6\text{H}_5$), 127.9 ($-\text{OCH}_2\text{C}_6\text{H}_5$), 127.7 ($-\text{OCH}_2\text{C}_6\text{H}_5$), 127.6 ($-\text{OCH}_2\text{C}_6\text{H}_5$), 127.2 ($-\text{OCH}_2\text{C}_6\text{H}_5$), 126.6 ($-\text{OCH}_2\text{C}_6\text{H}_5$), 125.5 (C_{10a}), 125.3 (br, $\text{C}_{2/6b}$), 118.4 (C_{10b}), 115.8 (C_{3a}), 105.7 (C_{14a}), 105.3 (C_{14b}), 99.8 (C_{12a}), 95.5 (C_{12b}), 93.1 (C_{7a}), 70.42 ($-\text{OCH}_2\text{C}_6\text{H}_5$), 70.36 ($-\text{OCH}_2\text{C}_6\text{H}_5$), 70.1 ($-\text{OCH}_2\text{C}_6\text{H}_5$), 69.6 ($-\text{OCH}_2\text{C}_6\text{H}_5$), 53.3 (C_{8a}), 44.4 (C_{8b}), 42.3 (C_{7b}), 34.1 ($\text{C}_{3/5b}\text{-C}(\text{CH}_3)_3$), 30.3 ($\text{C}_{3/5b}\text{-C}(\text{CH}_3)_3$);

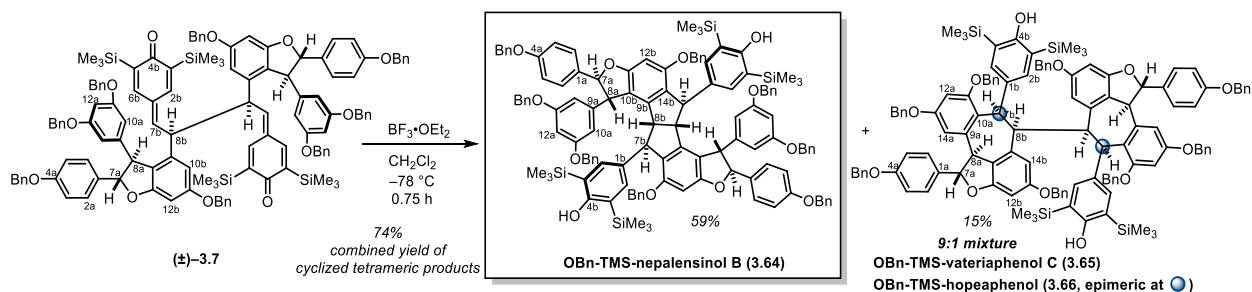
HRMS (ESI): m/z calculated for $\text{C}_{128}\text{H}_{123}\text{O}_{12}$ $[\text{M}+\text{H}]^+$: 1851.9009, found 1851.8961;

FTIR (neat) cm^{-1} : 3627 (m), 2952 (m), 1602 (s), 1582 (m), 1511 (m), 1496 (m), 1453 (m), 1433 (m), 1359 (m), 1306 (m), 1232 (m), 1170 (m), 1132 (s), 1027 (m).

³⁶ The NMR resonances of the protected hopeaphenol derivative are not well enough resolved at this stage to report

³⁷ Notably, the $\text{C}_{2/6b}\text{-H}$ protons are not visible due to extreme broadening in the $^1\text{H-NMR}$ spectrum. This is presumably due to hindered/slow rotation in a sterically encumbered environment.

³⁸ In the $^{13}\text{C-NMR}$ spectrum, observed resonances for $\text{C}_{3/5b}$ and $\text{C}_{2/6b}$ were both very broadened, further corroborating that rotation of the bulky phenol is likely hindered in this sterically congested system.



Cyclization of Bis-Quinone Methide (3.7): A solution of the starting bis-quinone methide **3.7** (110 mg, 0.057 mmol, 1.00 equiv) was prepared in anhydrous CH_2Cl_2 under inert atmosphere and cooled to $-78\text{ }^\circ\text{C}$. To the solution was added $\text{BF}_3\cdot\text{OEt}_2$ (61 μL , 46.5% in diethyl ether, 4.00 equiv) turning it a light red-brown. The reaction was then held at this temperature for 0.75 h, at which point it was quenched with sat. aq. NaHCO_3 . The reaction was lifted from the cooling bath and stirred vigorously until the ice thawed. The contents were then diluted with CH_2Cl_2 and transferred to a separatory funnel, where the phases were separated. The aqueous phase was extracted with additional portions of CH_2Cl_2 . The combined organic layers were washed with brine, dried over Na_2SO_4 , and concentrated *in vacuo*. $^1\text{H-NMR}$ of the crude material indicated an ~4:1 ratio of **3.64** to **3.65/3.66**. The crude material was subjected to purification by preparative TLC (85:10:5 Hexanes/EtOAc/ CH_2Cl_2 , plate developed 2x) to afford **3.64** (65 mg, 0.034 mmol, 59% yield) and a 9:1 mixture of vateriaphenol derivative **3.65** and hopeaphenol derivative **3.66** (16.7 mg, 0.009 mmol, 15% yield). Characterization data for nepalensinol B derivative **3.64** are provided below:

TLC (Hexanes/EtOAc/ CH_2Cl_2 , 75:20:5), R_f : 0.49 (UV, *p*-anisaldehyde (pale brown))

$^1\text{H NMR}$ (500 MHz, CDCl_3 , $50\text{ }^\circ\text{C}$) δ :³⁹

7.45 – 7.15 (m, 32H, $-\text{OCH}_2\text{C}_6\text{H}_5$), 7.22 (d, $J = 8.6\text{ Hz}$, 4H, $\text{C}_{2a}\text{-H}$), 7.11 – 7.04 (m, 8H, $-\text{OCH}_2\text{C}_6\text{H}_5$), 6.91 (d, $J = 8.6\text{ Hz}$, 4H, $\text{C}_{3a}\text{-H}$), 6.86 (s, 4H, $\text{C}_{2/6b}\text{-H}$), 6.69 (s, 2H, $\text{C}_{10a}\text{-H}$), 6.67 (s, 2H, $\text{C}_{10a}\text{-H}$), 6.35 (s, 2H, $\text{C}_{12b}\text{-H}$), 6.09 (t, $J = 2.2\text{ Hz}$, 2H, $\text{C}_{12a}\text{-H}$), 5.49 (d, $J = 1.8\text{ Hz}$, 2H, $\text{C}_{7a}\text{-H}$), 5.06 (s, 4H, $\text{C}_{4a}\text{-OCH}_2\text{C}_6\text{H}_5$), 4.73 (d, $J = 1.8\text{ Hz}$, 2H, $\text{C}_{8a}\text{-H}$), 4.68 (s, 2H, $\text{C}_{4b}\text{-OH}$), 4.65 (s, 8H $\text{C}_{13b}\text{-OCH}_2\text{C}_6\text{H}_5$), 4.56 (s, 2H, $\text{C}_{7b}\text{-H}$), 3.93 (s, 2H, $\text{C}_{8b}\text{-H}$), -0.20 (s, 36H, $\text{C}_{3/5b}\text{-Si}(\text{CH}_3)_3$);

$^{13}\text{C NMR}$ (175 MHz, CDCl_3 , $50\text{ }^\circ\text{C}$) δ :³⁹

163.7 (C_{11b}), 162.8 (C_{4a}), 160.9 (br, C_{11a}), 158.9 (C_{13b}), 156.7 (C_{4b}), 147.8 (C_{9a}), 144.6 (C_{9b}), 137.59 ($-\text{OCH}_2\text{C}_6\text{H}_5$), 137.55 ($-\text{OCH}_2\text{C}_6\text{H}_5$), 137.4 ($-\text{OCH}_2\text{C}_6\text{H}_5$), 137.1 (br, C_{14b}), 135.6 ($\text{C}_{3/5b}$), 135.4 (C_{1a}), 128.82 ($-\text{OCH}_2\text{C}_6\text{H}_5$), 128.63 ($-\text{OCH}_2\text{C}_6\text{H}_5$), 128.23 ($-\text{OCH}_2\text{C}_6\text{H}_5$), 128.17 ($-\text{OCH}_2\text{C}_6\text{H}_5$), 128.0 ($-\text{OCH}_2\text{C}_6\text{H}_5$), 127.82 (br, C_{1b}), 127.6 ($-\text{OCH}_2\text{C}_6\text{H}_5$), 127.2 ($-\text{OCH}_2\text{C}_6\text{H}_5$), 127.1 ($-\text{OCH}_2\text{C}_6\text{H}_5$), 126.7 (C_{2a}), 126.3 ($-\text{OCH}_2\text{C}_6\text{H}_5$), 123.8 ($\text{C}_{2/6b}$), 115.5 ($\text{C}_{3/5a}$), 114.8 (C_{10b}), 108.5 – 104.5 (C_{10a}), 101.1 (C_{12a}), 94.0 (C_{12b}), 93.4 (C_{7a}), 70.5 ($-\text{OCH}_2\text{C}_6\text{H}_5$), 69.8 ($-\text{OCH}_2\text{C}_6\text{H}_5$), 69.1 ($-\text{OCH}_2\text{C}_6\text{H}_5$), 59.8 (C_{8b}), 56.3 (C_{8a}), 49.1 (C_{7b}), -0.27 ($\text{C}_{3/5b}\text{-Si}(\text{CH}_3)_3$);

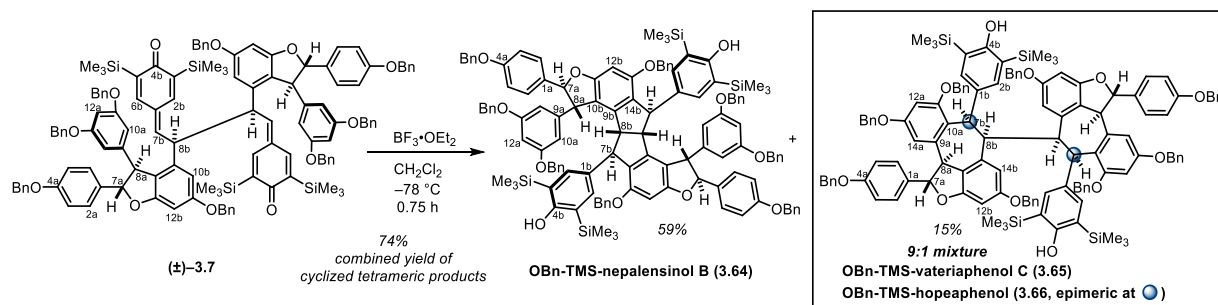
HRMS (ESI):

m/z calculated for $\text{C}_{124}\text{H}_{123}\text{O}_{12}\text{Si}_4$ $[\text{M}+\text{H}]^+$: 1915.8086, found 1933.8329 $[\text{M}+\text{NH}_4]^+$;

³⁹ Notably, the $\text{C}_{10a}\text{-H}$ protons are magnetically nonequivalent in the $^1\text{H-NMR}$ spectrum. This is presumably due to hindered rotation in the highly congested bicyclic ring system. The $\text{C}_{11a}\text{-}$ and $\text{C}_{13a}\text{-}$ benzyloxy methylenes are also not visible in the $^1\text{H-NMR}$ spectrum further corroborating this property. The C_{10a} resonance in the $^{13}\text{C-NMR}$ spectrum is broadened over 4.5 ppm and is barely visible above the noise.

FTIR (neat) cm^{-1} :

3032 (m), 2954 (m), 1593 (s), 1511 (m), 1497 (m), 1451 (s), 1402 (m), 1296 (m), 1243 (m), 1157 (s), 1112 (m), 1027 (m), 910 (w), 836 (s),m 734 (s), 695 (s).



For preparation, see previous page. Data for the major product, vateriaphenol C derivative **3.65** are provided below:⁴⁰

TLC (Hexanes/EtOAc/ CH_2Cl_2 , 75:20:5), R_f : 0.49 (UV, *p*-anisaldehyde (pale brown))

^1H NMR (700 MHz, CDCl_3 , 50°C) δ :⁴¹

7.43 (d, $J = 8.5$ Hz, 4H, $\text{C}_{2/6a}\text{-H}$), 7.45 – 7.20 (m, 27H, $-\text{OCH}_2\text{C}_6\text{H}_5$), 7.16 – 7.11 (m, 5H, $-\text{OCH}_2\text{C}_6\text{H}_5$), 7.06 (t, $J = 7.4$ Hz, 4H, $-\text{OCH}_2\text{C}_6\text{H}_5$), 6.95 (d, $J = 8.5$ Hz, 4H, $\text{C}_{3/5a}\text{-H}$), 6.85 (d, $J = 7.4$ Hz, 4H, $-\text{OCH}_2\text{C}_6\text{H}_5$), 6.49 (d, $J = 2.0$ Hz, 2H, $\text{C}_{14a}\text{-H}$), 6.45 (d, $J = 2.0$ Hz, 2H, $\text{C}_{12a}\text{-H}$), 6.09 (d, $J = 1.5$ Hz, 2H, $\text{C}_{12b}\text{-H}$), 5.93 (s, br, 2H, $\text{C}_{7b}\text{-H}$), 5.84 (d, $J = 8.2$ Hz, 2H, $\text{C}_{7a}\text{-H}$), 5.29 (d, $J = 8.2$ Hz, 2H, $\text{C}_{8a}\text{-H}$), 5.24 (d, $J = 1.5$ Hz, 2H, $\text{C}_{14b}\text{-H}$), 5.02 (d, $J = 11.7$ Hz, 2H, $-\text{OCH}_2\text{C}_6\text{H}_5$), 5.00 (d, $J = 11.7$ Hz, 2H, $-\text{OCH}_2\text{C}_6\text{H}_5$), 4.98 (d, $J = 12.1$ Hz, 2H, $-\text{OCH}_2\text{C}_6\text{H}_5$), 4.89 (d, $J = 12.1$ Hz, 2H, $-\text{OCH}_2\text{C}_6\text{H}_5$), 4.60 (d, $J = 12.3$ Hz, 2H, $-\text{OCH}_2\text{C}_6\text{H}_5$), 4.57 (s, 2H, $\text{C}_{4b}\text{-OH}$), 4.47 (d, $J = 12.3$ Hz, 2H, $-\text{OCH}_2\text{C}_6\text{H}_5$), 4.39 (d, $J = 11.1$ Hz, 2H, $-\text{OCH}_2\text{C}_6\text{H}_5$), 4.30 (d, $J = 11.1$ Hz, 2H, $-\text{OCH}_2\text{C}_6\text{H}_5$), 4.08 (s, 2H, $\text{C}_{8b}\text{-H}$), +0.07 – -0.15 (br s, 36H, $\text{C}_{3/5b}\text{-Si}(\text{CH}_3)_3$);

^{13}C NMR (175 MHz, CDCl_3 , 50°C) δ :⁴²

163.4 (C_{13b}), 160.2 (C_{2a}), 159.5 (C_{11b}), 159.0 (C_{11a}), 158.10 (C_{13a}), 158.07 (C_{4b}), 140.6 (C_{9a}), 140.3 (C_{9b}), 137.5 ($-\text{OCH}_2\text{C}_6\text{H}_5$), 137.4 ($-\text{OCH}_2\text{C}_6\text{H}_5$), 137.3 ($-\text{OCH}_2\text{C}_6\text{H}_5$), 137.2 ($-\text{OCH}_2\text{C}_6\text{H}_5$), 137.0 (br, $\text{C}_{3/5b}$), 134.6 (C_{1a}), 133.8 (C_{1b}), 129.1 (C_{2a}), 128.82 ($-\text{OCH}_2\text{C}_6\text{H}_5$), 128.81 ($-\text{OCH}_2\text{C}_6\text{H}_5$), 128.77 ($-\text{OCH}_2\text{C}_6\text{H}_5$), 128.65 ($-\text{OCH}_2\text{C}_6\text{H}_5$), 128.21 ($-\text{OCH}_2\text{C}_6\text{H}_5$), 128.15 ($-\text{OCH}_2\text{C}_6\text{H}_5$), 128.0 ($-\text{OCH}_2\text{C}_6\text{H}_5$), 127.9 ($-\text{OCH}_2\text{C}_6\text{H}_5$), 127.72 ($-\text{OCH}_2\text{C}_6\text{H}_5$), 127.66 ($-\text{OCH}_2\text{C}_6\text{H}_5$), 127.64 ($-\text{OCH}_2\text{C}_6\text{H}_5$), 127.3 ($-\text{OCH}_2\text{C}_6\text{H}_5$), 126.7 ($-\text{OCH}_2\text{C}_6\text{H}_5$), 125.2 (C_{10a}), 118.3 (C_{10b}), 115.8 (C_{3a}), 105.8 (C_{14a}), 105.7 (C_{14b}), 100.1 (C_{12a}), 95.6 (C_{12b}), 93.0 (C_{7a}), 70.5 ($-\text{OCH}_2\text{C}_6\text{H}_5$), 70.4 ($-\text{OCH}_2\text{C}_6\text{H}_5$), 70.2 ($-\text{OCH}_2\text{C}_6\text{H}_5$), 69.8 ($-\text{OCH}_2\text{C}_6\text{H}_5$), 53.1 (C_{8a}), 44.4 (C_{8b}), 41.9 (C_{7b}), -0.56 ($\text{C}_{3/5b}\text{-Si}(\text{CH}_3)_3$);

HRMS (ESI):

m/z calculated for $\text{C}_{124}\text{H}_{123}\text{O}_{12}\text{Si}_4$ $[\text{M}+\text{H}]^+$: 1915.8086, found 1915.8012;

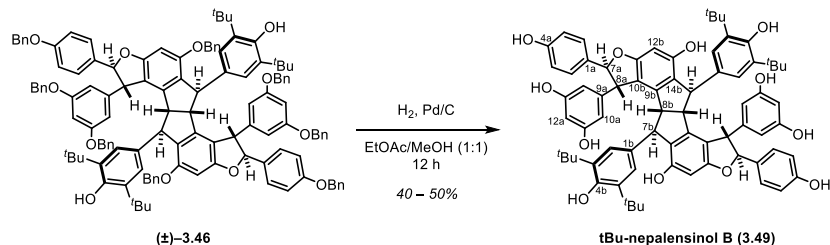
⁴⁰ The NMR resonances of the protected hopeaphenol derivative **3.66** are not well enough resolved at this stage to report

⁴¹ Notably, the $\text{C}_{2/6b}\text{-H}$ protons are not visible due to extreme broadening in the ^1H -NMR spectrum. This is presumably due to hindered/slow rotation in a sterically encumbered environment. The trimethylsilyl resonance is also very broadened, further supporting hindered rotation.

⁴² In the ^{13}C -NMR spectrum, observed resonances for $\text{C}_{3/5b}$ and $\text{C}_{2/6b}$ were both very broadened, $\text{C}_{2/6b}$ to the point that it was not visible, further corroborating that rotation of the bulky phenol is likely hindered in this sterically congested system.

FTIR (neat) cm^{-1} :

3607 (m), 3031 (m), 2952 (m), 1603 (s), 1512 (m), 1497 (m), 1454 (m), 1398 (m), 1305 (m), 1246 (s), 1171 (s), 1135 (s), 1027 (m), 835 (s), 734 (s), 696 (s).



Global Debenzoylation of (3.46): A reaction flask was charged with starting benzylated tetramer **3.46** (33 mg, 0.018 mmol, 1.00 equiv) and Pd/C (30 wt%, 33 mg, 1 wt. equiv), and the solids were placed under inert atmosphere. After several minutes of purging, EtOAc (HPLC grade, 3 mL) and MeOH (HPLC grade, 3 mL) were added sequentially. The inert gas supply was then replaced with an H₂ balloon and the mixture was sparged for 2 hours. At 90 minutes, MeOH was added to replace lost volume. At 2 h, the vent needle was removed and the balloon lifted above the reaction solution. The reaction was then allowed to stir under an H₂ atmosphere for an additional 9 – 12 h, until deemed complete by TLC. On completion, the reaction contents were filtered over a plug of Celite and eluted with EtOAc. The filtrate was concentrated *in vacuo*. The crude material was then purified by preparative TLC (85:10:5 CH₂Cl₂/MeOH/Acetone) to afford **3.49** (9 mg, 0.008 mmol, 45% yield).

TLC (CH₂Cl₂/MeOH/Acetone, 85:10:5), R_f: 0.26 (UV, Hanessian's stain)

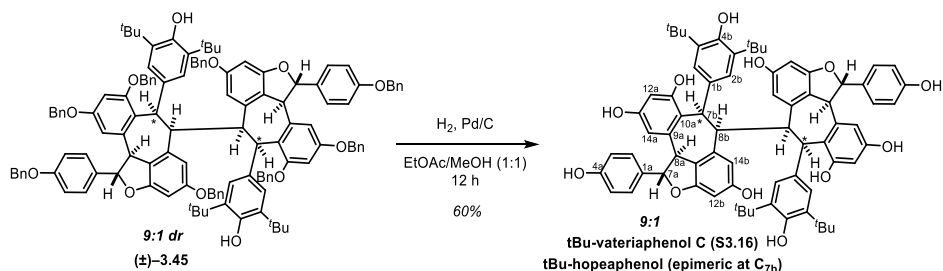
¹H NMR (500 MHz, Acetone-*d*₆, 25 °C) δ:⁴³ 8.34 (s, 2H, –OH [exchangeable, D₂O]), 8.24 (s, 4H, –OH [exchangeable, D₂O]), 7.14 (d, *J* = 8.4 Hz, 4H, C_{2a}–H), 7.05 (s, 2H, –OH [exchangeable, D₂O]), 6.77 (d, *J* = 8.4 Hz, 4H, C_{3a}–H), 6.72 (s, 4H, C_{2b}–H), 6.36 – 6.28 (br s, 4H, C_{10a}–H), 6.29 (s, 2H, C_{12a}–H), 6.25 (s, 2H, C_{12b}–H), 5.63 (s, 2H, C_{4b}–OH), 5.31 (s, 2H, C_{7a}–H), 4.47 (s, 2H, C_{8a}–H), 4.42 (s, 2H, C_{7b}–H), 3.81 (s, 2H, C_{8b}–H), 1.30 (s, 36H, C_{3/5b}–C(CH₃)₃);

¹³C NMR (175 MHz, Acetone-*d*₆, 45 °C) δ: 163.7 (C_{11b}), 160.3 (C_{11a}), 158.2 (C_{4a}), 155.8 (C_{13b}), 152.8 (C_{4b}), 148.9 (C_{9a}), 145.1 (C_{9b}), 138.3 (C_{1b}), 137.8 (C_{3/5b}), 135.1 (C_{1a}), 127.4 (C_{2a}), 126.2 (C_{14b}), 124.4 (C_{2b}), 116.6 (C_{10b}), 116.4 (C_{3a}), 106.7 (C_{10a}), 102.6 (C_{12a}), 97.1 (C_{12b}), 94.3 (C_{7a}), 61.0 (C_{8b}), 57.4 (C_{8a}), 50.3 (C_{7b}), 35.2 (C_{3/5b}–C(CH₃)₃), 31.1 (C_{3/5b}–C(CH₃)₃);

HRMS (ESI): *m/z* calculated for C₇₂H₇₅O₁₂ [M+H]⁺: 1131.5253, found 1131.5230;

FTIR (neat) cm⁻¹: 3349 (s, br), 2926 (s), 1600 (s), 1559 (m), 1516 (m), 1436 (s), 1364 (m), 1232 (s), 1158 (s), 1083 (m), 998 (m), 835 (m).

⁴³ As was observed for the benzylated precursor, the C_{10a}–H protons are broadened in the ¹H-NMR spectrum, indicating that rotation of the resorcinol remains hindered even after debenzoylation.



Global Debenzoylation of 3.45: A reaction flask was charged with starting benzylated tetramer **3.45** (6 mg, 0.003 mmol, 1.00 equiv) and Pd/C (30 wt%, 6 mg, 1 wt. equiv), and the solids were placed under inert atmosphere. After several minutes of purging, EtOAc (HPLC grade, 1 mL) and MeOH (HPLC grade, 1 mL) were added sequentially. The inert gas supply was then replaced with an H₂ balloon and the mixture was sparged for 2 hours. At 90 minutes, MeOH was added to replace lost volume. At 2 h, the vent needle was removed and the balloon lifted above the reaction solution. The reaction was then allowed to stir under an H₂ atmosphere for an additional 9 – 12 h, until deemed complete by TLC. On completion, the reaction contents were filtered over a plug of Celite and eluted with EtOAc. The filtrate was concentrated *in vacuo*. The crude material was then purified by preparative TLC (85:10:5 CH₂Cl₂/MeOH/Acetone) to afford a 9:1 mixture of vateriaphenol and hopeaphenol derivatives **S3.16** (2.2 mg, 0.002 mmol, 60% yield). Data for the vateriaphenol C derivative are provided below.

TLC (CH₂Cl₂/MeOH/Acetone, 85:10:5), R_F: 0.26 (UV, Hanessian's stain)

¹H NMR (500 MHz, Acetone-*d*₆, 45 °C) δ:⁴⁴ 7.51 (d, *J* = 8.4 Hz, 4H, C_{2a}-H), 6.96 (d, *J* = 8.4 Hz, 4H, C_{3a}-H), 6.73 – 6.45 (br s, 4H, C_{2/6b}-H), 6.38 (d, *J* = 2.2 Hz, 2H, C_{14a}-H), 6.32 (d, *J* = 2.2 Hz, 2H, C_{12a}-H), 6.01 (s, 2H, C_{7b}-H), 5.88 (d, *J* = 1.8 Hz, 2H, C_{12b}-H), 5.82 (d, *J* = 8.4 Hz, 2H, C_{7a}-H), 5.31 (s, br, overlap, 2H, C_{4b}-OH, [exchangeable, D₂O]), 5.30 (d, overlap, *J* = 8.5 Hz, 2H, C_{8a}-H), 5.28 (d, *J* = 1.8 Hz, 2H, C_{14b}-H), 3.99 (s, 2H, C_{8b}-H), 1.12 (s, 36H, C_{3/5b}-C(CH₃)₃);

¹³C NMR (175 MHz, Acetone-*d*₆, 45 °C) δ: 159.9 (C_{11b}), 158.69 (C_{13b}), 158.65 (C_{4a}), 158.0 (C_{11a}), 157.1 (C_{13a}), 152.5 (C_{4b}), 142.3 (C_{9a}), 142.0 (C_{9b}), 136.2 (C_{3/5b}), 134.6 (C_{1a}), 134.5 (C_{1b}), 130.4 (C_{2a}), 126.6 (C_{2/6b}), 123.2 (C_{10a}), 118.0 (C_{10b}), 116.7 (C_{3a}), 108.0 (C_{14b}), 107.1 (C_{14a}), 102.5 (C_{12a}), 95.0 (C_{12b}), 94.2 (C_{7a}), 53.1 (C_{8a}), 45.1 (C_{8b}), 42.9 (C_{7b}), 35.0 (C_{3/5b}-C(CH₃)₃), 30.9 (C_{3/5b}-C(CH₃)₃);

HRMS (ESI): *m/z* calculated for C₇₂H₇₅O₁₂ [M+H]⁺: 1131.5253, found 1131.5242;

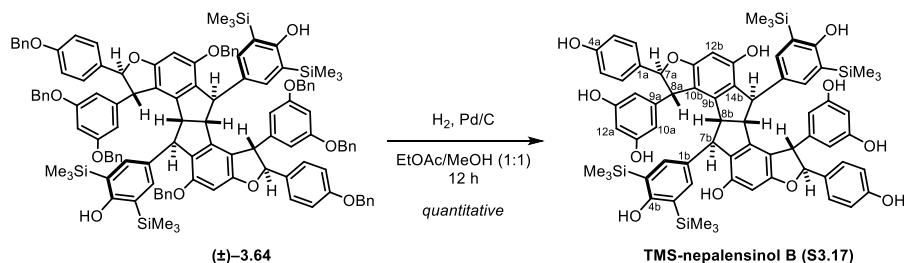
FTIR (neat) cm⁻¹: 3329 (s, br), 2924 (s), 1611 (s), 1559 (m), 1519 (m), 1436 (s), 1362 (s), 1231 (s), 1173 (s), 1128 (s), 1039 (m), 1003 (m), 893 (m), 835 (s).

Observable ¹H-NMR resonances for the hopeaphenol derivative are provided below.⁴⁵

¹H NMR (500 MHz, Acetone-*d*₆, 45 °C) δ: 7.55 (d, *J* = 8.5 Hz, 4H), 7.38 (d, *J* = 8.5 Hz, 4H), 6.98 (d, *J* = 8.4 Hz, 4H), 6.31 (d, *J* = 3.3 Hz, 2H), 5.94 (d, *J* = 1.8 Hz, 2H), 5.92 (d, *J* = 5.1 Hz, 2H), 5.77 (d, *J* = 1.8 Hz, 2H), 5.74 (br s, 2H), 5.55 (br s, 2H), 5.07 (s, 2H), 3.98 (s, 2H).

⁴⁴ As was observed for the benzylated precursor, the C_{2/6b}-H protons are extremely broadened in the ¹H-NMR spectrum, indicating that rotation of the bulky phenol remains hindered even after debenzoylation.

⁴⁵ Signal intensity for the hopeaphenol isomer was too low to observe in the ¹³C-NMR spectrum



Global Debzoylation of (3.64): A 4 dram vial was charged with starting benzylated tetramer **3.64** (65 mg, 0.034 mmol, 1.00 equiv) and Pd/C (30 wt%, 96 mg, 1.5 wt. equiv), and the solids were placed under inert atmosphere. After several minutes of purging, EtOAc (HPLC grade, 3.5 mL) and MeOH (HPLC grade, 3.5 mL) were added sequentially. The solvent line was marked on the side of the vial. The inert gas supply was then replaced with an H₂ balloon and the mixture was sparged for 2.5 hours. At 2 hours, MeOH was added to replace lost volume. At 2.5 h, the vent needle was removed and the H₂ inlet lifted above the reaction solution. The reaction was then allowed to stir vigorously under an H₂ atmosphere for an additional 9 – 12 h, until deemed complete by TLC. On completion, the reaction contents were filtered over a plug of Celite and eluted with EtOAc. The filtrate was concentrated *in vacuo* to a white/off white solid film. ¹H-NMR and ¹³C-NMR of the crude material indicate that it consists almost exclusively of the desired product **S3.17** (41.6 mg, 0.035 mmol, 103% yield), and therefore it was carried on directly without further purification. At pilot scale, the product was isolated by preparative TLC (85:10:5 CH₂Cl₂/MeOH/Acetone) to afford a pure sample for analysis.

TLC (CH₂Cl₂/MeOH/Acetone, 85:10:5), R_f: 0.16 (UV, Hanessian's stain, streaks)

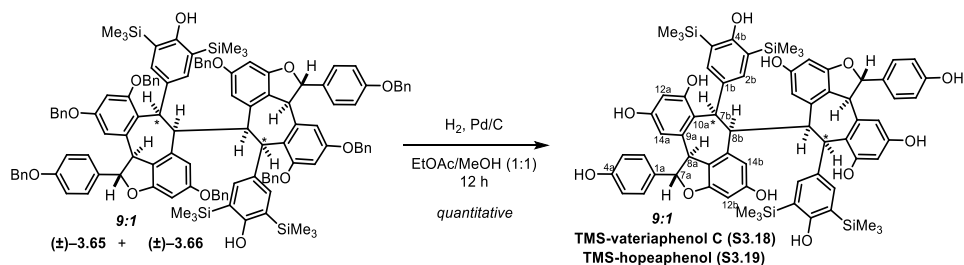
¹H NMR (500 MHz, Acetone-*d*₆, 25 °C) δ:⁴⁶ 8.33 (s, 2H, –OH [exchangeable, D₂O]), 8.22 (s, 4H, –OH [exchangeable, D₂O]), 7.29 (s, 2H, –OH [exchangeable, D₂O]), 7.15 (d, *J* = 8.4 Hz, 4H, C_{2a}–H), 6.95 (s, 4H, C_{2b}–H), 6.77 (d, *J* = 8.4 Hz, 4H, C_{3a}–H), 6.34 – 6.27 (br s, 4H, C_{10a}–H), 5.99 (s, 2H, C_{12a}–H), 5.74 (s, 2H, C_{12b}–H), 5.32 (br s, 2H, C_{7a}–H), 5.11 (s, 2H, C_{4b}–OH), 4.46 (s, overlap, 2H, C_{8a}–H), 4.46 (s, overlap, 2H, C_{7b}–H), 3.80 (s, 2H, C_{8b}–H), 0.19 (s, 36H, C_{3/5b}–Si(CH₃)₃);

¹³C NMR (175 MHz, Acetone-*d*₆, 45 °C) δ: 164.6 (C_{11b}), 163.6 (C_{11a}), 160.2 (C_{4a}), 158.1 (C_{13b}), 155.9 (C_{4b}), 148.9 (C_{9a}), 144.8 (C_{9b}), 138.8 (C_{1b}), 136.2 (C_{3/5b}), 135.0 (C_{1a}), 127.3 (C_{2a}), 126.2 (C_{14b}), 125.7 (C_{2b}), 116.4 (C_{3a}), 116.3 (C_{10b}), 106.6 (C_{10a}), 102.6 (C_{12a}), 97.0 (C_{12b}), 94.2 (C_{7a}), 61.1 (C_{8b}), 57.5 (C_{8a}), 49.6 (C_{7b}), –0.02 (C_{3/5b}–Si(CH₃)₃);

HRMS (ESI): *m/z* calculated for C₆₈H₇₅O₁₂Si₄ [M+H]⁺: 1195.4330, found 1195.4299;

FTIR (neat) cm^{–1}: 3356 (s, br), 2947 (m), 1604 (s), 1515 (m), 1448 (m), 1402 (m), 1246 (s), 1162 (s), 1084 (m), 998 (m), 838 (s).

⁴⁶ As was observed for the benzylated precursor, the C_{10a}–H protons are broadened in the ¹H-NMR spectrum, indicating that rotation of the resorcinol remains hindered even after debenzoylation.



Global Debenzylation of (3.65/3.66): A 4 dram vial was charged with starting benzylated tetramer **3.65/3.66** (16.7 mg, 0.009 mmol, 1.00 equiv) and Pd/C (30 wt%, 25 mg, 1.5 wt. equiv), and the solids were placed under inert atmosphere. After several minutes of purging, EtOAc (HPLC grade, 1.0 mL) and MeOH (HPLC grade, 1.0 mL) were added sequentially. The solvent line was marked on the side of the vial. The inert gas supply was then replaced with an H₂ balloon and the mixture was sparged for 2.5 hours. At 2 hours, MeOH was added to replace lost volume. At 2.5 h, the vent needle was removed and the H₂ inlet lifted above the reaction solution. The reaction was then allowed to stir vigorously under an H₂ atmosphere for an additional 9 – 12 h, until deemed complete by TLC. On completion, the reaction contents were filtered over a plug of Celite and eluted with EtOAc. The filtrate was concentrated *in vacuo* to a white/off white solid film. ¹H-NMR and ¹³C-NMR of the crude material indicate that it is a nearly pure sample of vateriaphenol C derivative **S3.18** and hopeaphenol derivative **S3.19** in an approximately 9:1 mixture (11.6 mg, 0.009 mmol, 111% yield), and therefore it was carried on directly without further purification. At pilot scale, the products were isolated by preparative TLC (85:10:5 CH₂Cl₂/MeOH/Acetone) to afford a pure sample for analysis. The resolution and signal/noise ratio in the ¹H-NMR spectrum was not high enough to accurately report the data for minor hopeaphenol component **S3.19** at this stage, and therefore only the data for **S3.18** is reported.

TLC (CH₂Cl₂/MeOH/Acetone, 85:10:5), R_f: 0.18 (UV, Hanessian's stain)

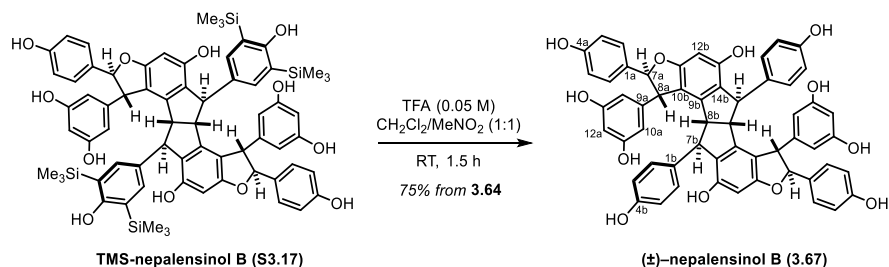
¹H NMR (500 MHz, Acetone-*d*₆, 25 °C) δ:⁴⁷ 8.56 (s, 2H, -OH, [exchangeable, D₂O]), 8.05 (s, 4H, -OH, [exchangeable, D₂O]), 7.51 (d, *J* = 8.4 Hz, 4H, C_{2a}-H), 7.50 (s, 2H, -OH, [exchangeable, D₂O]), 6.96 (d, *J* = 8.4 Hz, 4H, C_{3a}-H), 6.35 (br s, 2H, C_{14a}-H), 6.33 (br s, 2H, C_{12a}-H), 6.03 (s, 2H, C_{7b}-H), 5.90 (d, *J* = 1.8 Hz, 2H, C_{12b}-H), 5.85 (d, *J* = 8.1 Hz, 2H, C_{7a}-H), 5.78 (s, 2H, C_{4b}-OH), 5.27 (s, overlap, 2H, C_{14b}-H), 5.27 (d, overlap, *J* = 8.1 Hz, 2H, C_{8a}-H), 3.89 (s, 2H, C_{8b}-H), 0.02 (s, 36H, C_{3/5b}-Si(CH₃)₃);

¹³C NMR (125 MHz, Acetone-*d*₆, 45 °C) δ:⁴⁷ 164.4 (C_{11b}), 160.0 (C_{13b}), 158.6 (C_{4a}), 158.5 (C_{11a}), 157.8 (C_{13a}), 157.1 (C_{4b}), 142.0 (C_{9a}), 141.8 (C_{9b}), 138.6 (C_{3/5b}), 135.4 (C_{1a}), 134.6 (C_{1b}), 130.3 (C_{2a}), 124.7 – 124.4 (br, C_{2/6b}) 123.1 (C_{10a}), 118.1 (C_{10b}), 116.6 (C_{3a}), 108.2 (C_{14b}), 106.8 (C_{14a}), 102.4 (C_{12a}), 95.0 (C_{12b}), 94.0 (C_{7a}), 52.8 (C_{8a}), 44.8 (C_{8b}), 42.3 (C_{7b}), -0.13 (C_{3/5b}-Si(CH₃)₃);

HRMS (ESI): *m/z* calculated for C₆₈H₇₅O₁₂Si₄ [M+H]⁺: 1195.4330, found 1195.4331;

FTIR (neat) cm⁻¹: 3397 (br, s), 2952 (m), 1612 (s), 1514 (m), 1462 (m), 1446 (m), 1249 (s), 1173 (s), 1131 (s), 1004 (w), 836 (s).

⁴⁷ As was observed for the benzylated precursor, the C_{2/6b}-H and C_{2/6b} resonances are extremely broadened in the ¹H-NMR and ¹³C-NMR spectra — indicating that rotation of the bulky phenol remains hindered even after debenylation.



(±)-Nepalensinol B (3.67): A flask containing starting crude **S3.17** was equipped with a stir bar and placed under inert atmosphere. The material was then dissolved in a 1:1 (v/v) mixture of $\text{CH}_2\text{Cl}_2/\text{MeNO}_2$ (8 mL). To the stirring solution at room temperature was added TFA (30 μL , 0.398 mmol, 12 equiv, 0.05 M), which immediately caused the solution to become yellow. The solution was stirred at room temperature for 1.5 h, at which point TLC indicated full conversion and it was concentrated directly. Nepalensinol B (**3.67**) was isolated by preparative TLC (83:12:5 $\text{CH}_2\text{Cl}_2/\text{MeOH}/\text{Acetone}$) as a white solid (22 mg). From the benzylated precursor **3.64**, this represents a 75% yield over two steps (hydrogenolysis and protodesilylation) when accounting for the 5% aliquot of intermediate **S3.17** that was removed for characterization purposes.

TLC ($\text{CH}_2\text{Cl}_2/\text{MeOH}/\text{Acetone}$, 85:10:5), R_f : 0.10 (UV, Hanessian's stain)

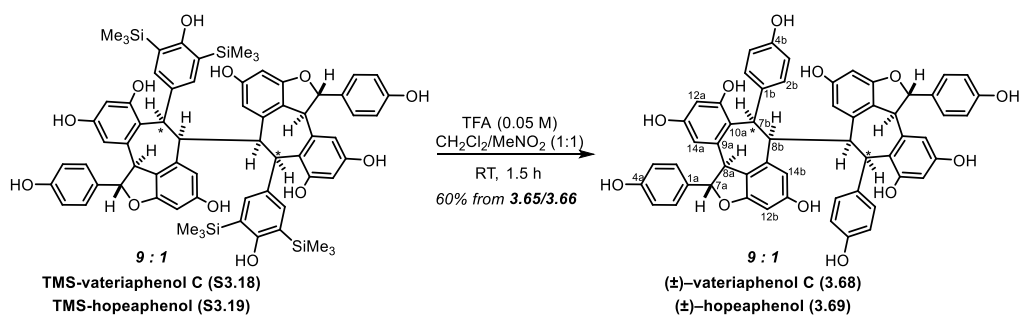
^1H NMR (500 MHz, Acetone- d_6 , 25 °C) δ :⁴⁸ 8.31 (s, 1H, $-\text{OH}$), 8.29 (s, 2H, $-\text{OH}$), 7.89 (s, 1H, $-\text{OH}$), 7.29 (s, 1H, $-\text{OH}$), 7.10 (d, $J = 8.4$ Hz, 4H, $\text{C}_{2/6a}\text{-H}$), 6.75 (d, overlap, $J = 8.4$ Hz, 8H, $\text{C}_{3/5a}\text{-H}$ and $\text{C}_{2/6b}\text{-H}$), 6.56 (d, $J = 8.4$ Hz, 4H, $\text{C}_{3/5b}\text{-H}$), 6.31 (t, $J = 2.2$ Hz, 2H, $\text{C}_{12a}\text{-H}$), 6.32 – 6.25 (br s, 4H, $\text{C}_{10a}\text{-H}$), 6.20 (s, 2H, $\text{C}_{12b}\text{-H}$), 5.30 (d, $J = 1.7$ Hz, 2H, $\text{C}_{7a}\text{-H}$), 5.11 (s, 2H, $-\text{OH}$), 4.31 (d, $J = 1.7$ Hz, $\text{C}_{8a}\text{-H}$), 4.29 (s, 2H, $\text{C}_{7b}\text{-H}$), 3.97 (s, 2H, $\text{C}_{8b}\text{-H}$);

^{13}C NMR (175 MHz, Acetone- d_6 , 25 °C) δ :⁴⁸ 163.3 (C_{11b}), 160.2 ($\text{C}_{11/13a}$), 158.0 (C_{4a}), 156.0 (C_{4b}), 155.6 (C_{13b}), 148.7 (C_{9a}), 144.6 (C_{9b}), 138.6 (C_{1b}), 134.8 (C_{1a}), 129.4 ($\text{C}_{2/6b}$), 127.3 ($\text{C}_{2/6a}$), 126.6 (C_{14b}), 116.3 (C_{10b}), 116.1 ($\text{C}_{3/5a}$), 115.5 ($\text{C}_{3/5b}$), 106.7 (br, C_{10a}), 102.2 (C_{12a}), 96.8 (C_{12b}), 93.9 (C_{7a}), 60.6 (C_{8b}), 57.2 (C_{8a}), 50.3 (C_{7b});

HRMS (ESI): m/z calculated for $\text{C}_{56}\text{H}_{42}\text{O}_{12}$ $[\text{M}+\text{H}]^+$: 907.2749, found 907.2736;

FTIR (neat) cm^{-1} : 3362 (s, br), 2923 (s), 2851 (m), 1620 (m), 1603 (s), 1512 (m), 1480 (m), 1462 (m), 1444 (m), 1248 (s, br), 1161 (s, br), 1084 (m), 1006 (m), 837 (m).

⁴⁸ As was true of its precursors, the natural product itself exhibits restricted rotation of the resorcinol substituents at the C_3 positions of each dihydrobenzofuran moiety. This is evidenced by extreme broadening of the $\text{C}_{10a}\text{-H}$ resonance in the ^1H -NMR and the C_{10a} resonance in the ^{13}C -NMR spectra.



(±)-Vateriaphenol C (**3.68**) and (±)-Hopeaphenol (**3.69**): A vial containing starting crude **S3.18/S3.19** was equipped with a stir bar and placed under inert atmosphere. The material was then dissolved in a 1:1 (v/v) mixture of $\text{CH}_2\text{Cl}_2/\text{MeNO}_2$ (2.5 mL). To the stirring solution at room temperature was added TFA (8 μL , 0.110 mmol, 12 equiv, 0.05 M), which immediately caused the solution to become yellow. The solution was stirred at room temperature for 1 h, at which point TLC indicated full conversion and it was concentrated directly. A 9:1 mixture of the natural products vateriaphenol C **3.68** and hopeaphenol **3.69** was isolated by preparative TLC (83:12:5 $\text{CH}_2\text{Cl}_2/\text{MeOH}/\text{Acetone}$) as a white solid (4.5 mg). From the benzylated precursors **3.65/3.66**, this represents a 60% yield over two steps (hydrogenolysis and protodesilylation) when accounting for the 5% aliquot of intermediates **S3.18/S3.19** that was removed for characterization purposes.

TLC ($\text{CH}_2\text{Cl}_2/\text{MeOH}/\text{Acetone}$, 85:10:5), R_f : 0.10 (UV, Hanessian's stain)

HRMS (ESI): m/z calculated for $\text{C}_{56}\text{H}_{42}\text{O}_{12}$ $[\text{M}+\text{H}]^+$: 907.2749, found 907.2736;

FTIR (neat) cm^{-1} : 3307 (s, br), 2920 (s), 2851 (m), 1613 (s), 1511 (s), 1457 (s), 1359 (m), 1243 (s), 1174 (s), 1128 (s), 1038 (w), 1007 (w), 836 (m).

NMR data for Vateriaphenol C (**3.68**) is reported below:

^1H NMR (500 MHz, Acetone- d_6 , 25 °C) δ : 8.52 (s, 2H, $-\text{OH}$), 8.11 (s, 2H, $-\text{OH}$), 8.10 (s, 2H, $-\text{OH}$), 7.73 (s, 2H, $-\text{OH}$), 7.53 (d, $J = 8.4$ Hz, 4H, $\text{C}_{2/6a}\text{-H}$), 7.49 (s, 2H, $-\text{OH}$), 6.95 (d, $J = 8.4$ Hz, 4H, $\text{C}_{3/5a}\text{-H}$), 6.51 (d, $J = 8.4$ Hz, 4H, $\text{C}_{2/6b}\text{-H}$), 6.37 (br s, 2H, $\text{C}_{14a}\text{-H}$), 6.34 (br s, 2H, $\text{C}_{12a}\text{-H}$), 6.30 (d, $J = 8.4$ Hz, 4H, $\text{C}_{3/5b}\text{-H}$), 5.98 (br s, 2H, $\text{C}_{7b}\text{-H}$), 5.89 (d, $J = 0.8$ Hz, 2H, $\text{C}_{12b}\text{-H}$), 5.82 (d, $J = 8.4$ Hz, 2H, $\text{C}_{7a}\text{-H}$), 5.45 (d, $J = 0.8$ Hz, 2H, $\text{C}_{14b}\text{-H}$), 5.33 (d, $J = 8.4$ Hz, 2H, $\text{C}_{8a}\text{-H}$), 5.11 (s, 2H, $-\text{OH}$), 3.99 (s, 2H, $\text{C}_{8b}\text{-H}$);

^{13}C NMR (175 MHz, Acetone- d_6 , 25 °C) δ : 159.2 (C_{11b}), 158.61 (C_{13b}), 158.59 (C_{4a}), 156.9 (C_{11a}), 155.7 (C_{13a}), 155.5 (C_{4b}), 142.0 (C_{9b}), 141.6 (C_{9a}), 134.8 (C_{1b}), 134.3 (C_{1a}), 131.0 ($\text{C}_{2/6b}$), 130.5 ($\text{C}_{2/6a}$), 123.1 (C_{10a}), 118.0 (C_{10b}), 116.6 ($\text{C}_{3/5a}$), 114.5 ($\text{C}_{3/5b}$), 108.0 (C_{14b}), 106.9 (C_{14a}), 102.1 (C_{12a}), 94.8 (C_{12b}), 93.8 (C_{7a}), 52.7 (C_{8a}), 45.0 (C_{8b}), 42.1 (C_{7b});

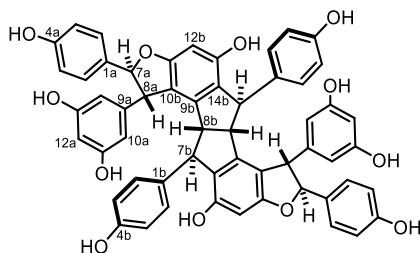
NMR data for observable resonances of Hopeaphenol (**3.69**) is reported below:⁴⁹

¹H NMR (500 MHz, Acetone-*d*₆, 25 °C) δ: 8.41 (s, 2H, -OH), 8.17 (s, 2H, -OH), 7.94 (s, 2H, -OH), 7.39 (s, 2H, -OH), 7.14 (d, *J* = 8.4 Hz, 4H, C_{2/6a}-H), 6.91 (d, *J* = 8.4 Hz, 4H, C_{2/6b}-H), 6.79 (d, *J* = 8.4 Hz, 4H, C_{3/5a}-H), 6.56 (d, overlap, *J* = 8.4 Hz, 4H, C_{3/5b}-H), 6.55 (d, overlap, C_{12a}-H), 5.76 (d, *J* = 12.1 Hz, 2H, C_{7a}-H), 5.73 (d, *J* = 1.8 Hz, 2H, C_{12b}-H), 5.17 (d, *J* = 1.8 Hz, 2H, C_{14b}-H), 5.11 (s, 2H, -OH), 4.24 (d, *J* = 12.1 Hz, 2H, C_{8a}-H), 3.93 (br s, 2H, C_{8b}-H);

¹³C NMR (175 MHz, Acetone-*d*₆, 25 °C) δ: 159.4 (C_{11b}), 158.9 (C_{11a}), 158.5 (C_{4a}), 157.33 (C_{13a}), 157.25 (C_{13b}), 155.7 (C_{4b}), 142.5 (C_{9a}), 140.6 (C_{9b}), 135.4 (C_{1b}), 131.1 (C_{1a}), 130.4 (C_{2/6a}), 129.4 (C_{2/6b}), 121.3 (C_{10a}), 118.7 (C_{10b}), 116.1 (C_{3/5a}), 115.3 (C_{3/5b}), 111.4 (C_{14b}), 106.5 (C_{14a}), 101.2 (C_{12a}), 95.3 (C_{12b}), 88.3 (C_{7a}), 49.9 (C_{8a}), 48.3 (C_{8b}), 41.3 (C_{7b}).

⁴⁹ The ¹H-NMR resonances for C_{7b}-H and C_{14a}-H of hopeaphenol are obfuscated due to overlap with resonances from the major product, vateriaphenol C.

Table 3.3 Comparison of ^1H -NMR Spectrum of 3.67 with Reported Literature Data



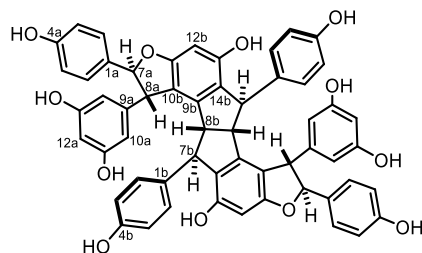
(±)-nepalensinol B (3.67)

Assignment	^1H Literature ⁵⁰		^1H Observed	
	Chemical Shift	Multiplicity and Integration	Chemical Shift	Multiplicity and Integration
$\text{C}_{2/6a}\text{-H}$	7.11	d, $J = 8.5$ Hz, 4H	7.10	d, $J = 8.4$ Hz, 4H
$\text{C}_{3/5a}\text{-H}$ and $\text{C}_{2/6b}\text{-H}$	6.75	d, $J = 8.5$ Hz, 8H	6.75	d, $J = 8.4$ Hz, 8H
$\text{C}_{3/5b}\text{-H}$	6.56	d, $J = 8.5$ Hz, 4H	6.56	d, $J = 8.4$ Hz, 4H
$\text{C}_{12a}\text{-H}$	6.31	t, $J = 2.0$ Hz, 2H	6.31	t, $J = 2.2$ Hz, 2H
$\text{C}_{10a}\text{-H}$	6.29	br s, 4H	6.32–6.25	br s, 4H
$\text{C}_{12b}\text{-H}$	6.20	s, 2H	6.20	s, 2H
$\text{C}_{7a}\text{-H}$	5.31	d, $J = 1.7$ Hz, 2H	5.30	d, $J = 1.7$ Hz, 2H
$\text{C}_{8a}\text{-H}$	4.31	d, $J = 1.7$ Hz, 2H	4.31	d, $J = 1.7$ Hz, 2H
$\text{C}_{7b}\text{-H}$	4.29	s, 2H	4.29	s, 2H
$\text{C}_{8b}\text{-H}$	3.97	s, 2H	3.97	s, 2H

Experiments conducted in Acetone- d_6

⁵⁰ Yamada, M.; Hayashi, K.; Hayashi, H.; Ikeda, S.; Hoshino, T.; Tsutsui, K.; Tsutsui, K.; Inuma, M.; Nozaki, H. *Phytochemistry* **2006**, 67 (3), 307–313.

Table 3.4 Comparison of ^{13}C -NMR Spectrum of 3.67 with Literature Reported Data



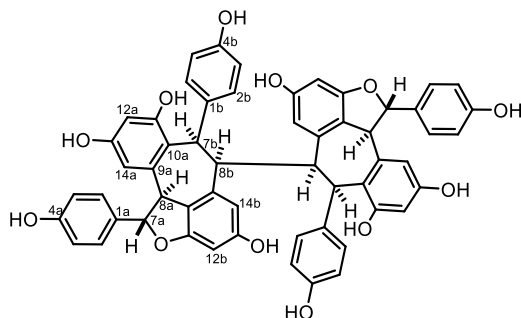
(±)-nepalensinol B (3.67)

Assignment	^{13}C Literature ⁵¹		^{13}C Observed
	Reported Chemical Shift	Recalibrated Chemical Shift	Chemical Shift
$\underline{\text{C}}_{11\text{b}}$	162.6	163.3	163.3
$\underline{\text{C}}_{11/13\text{a}}$	159.5	160.2	160.2
$\underline{\text{C}}_{4\text{a}}$	157.3	158.0	158.0
$\underline{\text{C}}_{4\text{b}}$	155.3	156.0	156.0
$\underline{\text{C}}_{13\text{b}}$	154.9	155.6	155.6
$\underline{\text{C}}_{9\text{a}}$	148.0	148.7	148.7
$\underline{\text{C}}_{9\text{b}}$	143.9	144.6	144.6
$\underline{\text{C}}_{1\text{b}}$	137.9	138.6	138.6
$\underline{\text{C}}_{1\text{a}}$	134.0	134.7	134.8
$\underline{\text{C}}_{2/6\text{b}}$	128.6	129.3	129.4
$\underline{\text{C}}_{2/6\text{a}}$	126.6	127.3	127.3
$\underline{\text{C}}_{14\text{b}}$	125.9	126.6	126.6
$\underline{\text{C}}_{10\text{b}}$	115.6	116.3	116.3
$\underline{\text{C}}_{3/5\text{a}}$	115.4	116.1	116.1
$\underline{\text{C}}_{3/5\text{b}}$	114.8	115.5	115.5
$\underline{\text{C}}_{10\text{a}}$	106.0	106.7	106.7
$\underline{\text{C}}_{12\text{a}}$	101.6	102.3	102.2
$\underline{\text{C}}_{12\text{b}}$	96.1	96.8	96.8
$\underline{\text{C}}_{7\text{a}}$	93.2	93.9	93.9
$\underline{\text{C}}_{8\text{b}}$	59.9	60.6	60.6
$\underline{\text{C}}_{8\text{a}}$	56.4	57.1	57.2
$\underline{\text{C}}_{7\text{b}}$	49.6	50.3	50.3

Experiments conducted in Acetone- d_6

⁵¹ Yamada, M.; Hayashi, K.; Hayashi, H.; Ikeda, S.; Hoshino, T.; Tsutsui, K.; Tsutsui, K.; Inuma, M.; Nozaki, H. *Phytochemistry* **2006**, 67 (3), 307–313.

Table 3.5 Comparison of ^1H -NMR Spectrum of 3.68 with Literature Reported Data



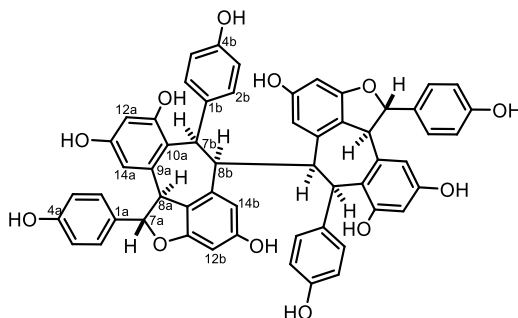
(±)-vateriaphenol C (3.68)

^1H Literature ⁵²			^1H Observed	
Assignment	Chemical Shift	Multiplicity and Integration	Chemical Shift	Multiplicity and Integration
$\text{C}_{2/6a}\text{-H}$	7.53	d, $J = 8.4$ Hz, 4H	7.53	d, $J = 8.4$ Hz, 4H
$\text{C}_{3/5a}\text{-H}$	6.95	d, $J = 8.4$ Hz, 4H	6.95	d, $J = 8.4$ Hz, 4H
$\text{C}_{2/6b}\text{-H}$	6.51	d, $J = 8.6$ Hz, 4H	6.51	d, $J = 8.4$ Hz, 4H
$\text{C}_{14a}\text{-H}$	6.37	br s, 2H	6.37	br s, 2H
$\text{C}_{12a}\text{-H}$	6.35	br s, 2H	6.34	br s, 2H
$\text{C}_{3/5b}\text{-H}$	6.30	d, $J = 8.6$ Hz, 4H	6.30	d, $J = 8.4$ Hz, 4H
$\text{C}_{7b}\text{-H}$	5.97	br s, 2H	5.98	br s, 2H
$\text{C}_{12b}\text{-H}$	5.89	d, $J = 1.8$ Hz, 2H	5.89	d, $J = 0.8$ Hz, 2H
$\text{C}_{7a}\text{-H}$	5.83	d, $J = 8.3$ Hz, 2H	5.82	d, $J = 8.4$ Hz, 2H
$\text{C}_{14b}\text{-H}$	5.45	d, $J = 1.8$ Hz, 2H	5.45	d, $J = 0.8$ Hz, 2H
$\text{C}_{8a}\text{-H}$	5.32	br d, $J = 8.3$ Hz, 2H	5.33	d, $J = 8.4$ Hz, 2H
$\text{C}_{8b}\text{-H}$	3.99	s, 2H	3.99	s, 2H

Experiments conducted in Acetone- d_6

⁵² Ito, T.; Abe, N.; Oyama, M.; Iinuma, M. *Helv. Chim. Acta* **2008**, *91* (10), 1989–1998.

Table 3.6 Comparison of ^{13}C -NMR Spectrum of 3.68 with Literature Reported Data



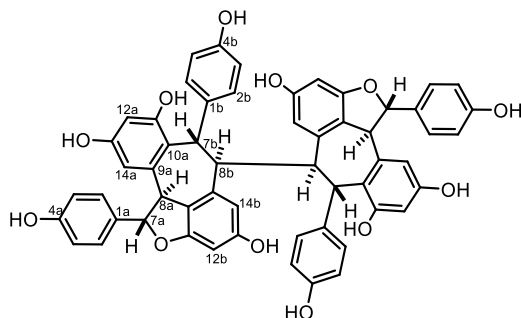
(±)-vateriaphenol C (3.68)

Assignment	^{13}C Literature ⁵³		^{13}C Observed
	Reported Chemical Shift	Recalibrated Chemical Shift	Chemical Shift
$\underline{\text{C}}_{11\text{b}}$	159.4	159.8	159.2
$\underline{\text{C}}_{13\text{b}}$	158.2	158.6	158.6
$\underline{\text{C}}_{4\text{a}}$	158.2	158.6	158.6
$\underline{\text{C}}_{11\text{a}}$	157.3	157.7	156.9
$\underline{\text{C}}_{13\text{a}}$	156.5	156.9	155.7
$\underline{\text{C}}_{4\text{b}}$	155.3	155.7	155.5
$\underline{\text{C}}_{9\text{b}}$	141.6	142.0	142.0
$\underline{\text{C}}_{9\text{a}}$	141.2	141.6	141.6
$\underline{\text{C}}_{1\text{b}}$	134.4	134.8	134.8
$\underline{\text{C}}_{1\text{a}}$	133.8	134.2	134.3
$\underline{\text{C}}_{2/6\text{b}}$	130.6	131.0	131.0
$\underline{\text{C}}_{2/6\text{a}}$	130.0	130.4	130.5
$\underline{\text{C}}_{10\text{a}}$	122.6	123.0	123.1
$\underline{\text{C}}_{10\text{b}}$	117.6	118.0	118.0
$\underline{\text{C}}_{3/5\text{a}}$	116.1	116.5	116.6
$\underline{\text{C}}_{3/5\text{b}}$	114.1	114.5	114.5
$\underline{\text{C}}_{14\text{b}}$	107.6	108.0	108.0
$\underline{\text{C}}_{14\text{a}}$	106.4	106.8	106.9
$\underline{\text{C}}_{12\text{a}}$	101.7	102.1	102.1
$\underline{\text{C}}_{12\text{b}}$	94.4	94.8	94.8
$\underline{\text{C}}_{7\text{a}}$	93.4	93.8	93.8
$\underline{\text{C}}_{8\text{a}}$	52.3	52.7	52.7
$\underline{\text{C}}_{8\text{b}}$	44.5	44.9	45.0
$\underline{\text{C}}_{7\text{b}}$	41.6	42.0	42.1

Experiments conducted in Acetone- d_6

⁵³ Ito, T.; Abe, N.; Oyama, M.; Iinuma, M. *Helv. Chim. Acta* **2008**, *91* (10), 1989–1998.

Table 3.7 Comparison of ^1H -NMR Spectrum of 3.69 with Literature Reported Data



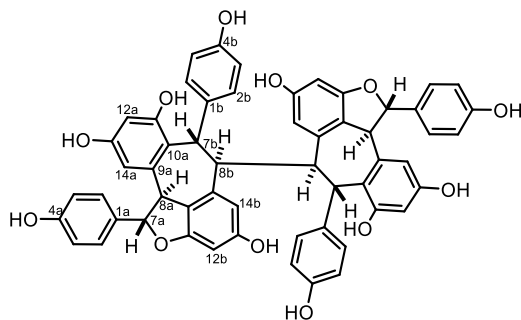
(±)-hopeaphenol (3.69)

^1H Literature ⁵⁴			^1H Observed	
Assignment	Chemical Shift	Multiplicity and Integration	Chemical Shift	Multiplicity and Integration
$\text{C}_{2/6a}\text{-H}$	7.15	d, $J = 8.6$ Hz, 4H	7.14	d, $J = 8.4$ Hz, 4H
$\text{C}_{2/6b}\text{-H}$	6.92	d, $J = 8.4$ Hz, 4H	6.91	d, $J = 8.4$ Hz, 4H
$\text{C}_{3/5a}\text{-H}$	6.80	d, $J = 8.6$ Hz, 4H	6.79	d, $J = 8.4$ Hz, 4H
$\text{C}_{3/5b}\text{-H}$	6.58	d, $J = 8.4$ Hz, 4H	6.56	d, $J = 8.4$ Hz, 4H
$\text{C}_{12a}\text{-H}$	6.56	d, $J = 1.7$ Hz, 2H	6.55	d, overlap, 2H
$\text{C}_{14a}\text{-H}$	6.31	d, $J = 1.7$ Hz, 2H	Not observed due to overlap with 3.68	
$\text{C}_{7b}\text{-H}$	5.81	s, 2H		
$\text{C}_{7a}\text{-H}$	5.78	d, $J = 12.1$ Hz, 2H	5.76	d, $J = 12.1$ Hz, 2H
$\text{C}_{12b}\text{-H}$	5.75	d, $J = 2.1$ Hz, 2H	5.73	d, $J = 1.8$ Hz, 2H
$\text{C}_{14b}\text{-H}$	5.18	d, $J = 2.1$ Hz, 2H	5.17	d, $J = 1.8$ Hz, 2H
$\text{C}_{8a}\text{-H}$	4.25	d, $J = 12.1$ Hz, 2H	4.24	d, $J = 12.1$ Hz, 2H
$\text{C}_{8b}\text{-H}$	3.96	s, 2H	3.93	br s, 2H

Experiments conducted in Acetone- d_6

⁵⁴ Kawabata, J.; Fukushi, E.; Hara, M.; Mizutani, J. *Magn. Reson. Chem.* **1992**, *30* (1), 6–10.

Table 3.8 Comparison of ^{13}C -NMR Spectrum of 3.69 with Literature Reported Data

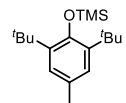


(±)-hopeaphenol (3.69)

Assignment	^{13}C Literature ⁵⁵		^{13}C Observed
	Reported Chemical Shift	Recalibrated Chemical Shift	Chemical Shift
$\underline{\text{C}}_{11\text{b}}$	159.2	159.4	159.4
$\underline{\text{C}}_{11\text{a}}$	158.7	158.9	158.9
$\underline{\text{C}}_{4\text{a}}$	158.4	158.6	158.5
$\underline{\text{C}}_{13\text{a}}$	157.2	157.4	157.3
$\underline{\text{C}}_{13\text{b}}$	157.1	157.3	157.3
$\underline{\text{C}}_{4\text{b}}$	155.5	155.7	155.7
$\underline{\text{C}}_{9\text{a}}$	142.3	142.5	142.5
$\underline{\text{C}}_{9\text{b}}$	140.4	140.6	140.6
$\underline{\text{C}}_{1\text{b}}$	135.2	135.4	135.4
$\underline{\text{C}}_{1\text{a}}$	130.9	131.1	131.1
$\underline{\text{C}}_{2/6\text{a}}$	130.2	130.4	130.1
$\underline{\text{C}}_{2/6\text{b}}$	129.2	129.4	129.4
$\underline{\text{C}}_{10\text{a}}$	121.1	121.3	121.3
$\underline{\text{C}}_{10\text{b}}$	118.5	118.7	118.7
$\underline{\text{C}}_{3/5\text{a}}$	115.2	115.4	116.1
$\underline{\text{C}}_{3/5\text{b}}$	115.2	115.4	115.3
$\underline{\text{C}}_{14\text{b}}$	111.2	111.4	111.4
$\underline{\text{C}}_{14\text{a}}$	106.3	106.5	106.5
$\underline{\text{C}}_{12\text{a}}$	101.1	101.3	101.2
$\underline{\text{C}}_{12\text{b}}$	95.2	95.4	95.3
$\underline{\text{C}}_{7\text{a}}$	88.2	88.4	88.3
$\underline{\text{C}}_{8\text{a}}$	49.7	49.9	49.9
$\underline{\text{C}}_{8\text{b}}$	48.2	48.4	48.3
$\underline{\text{C}}_{7\text{b}}$	41.2	41.4	41.3

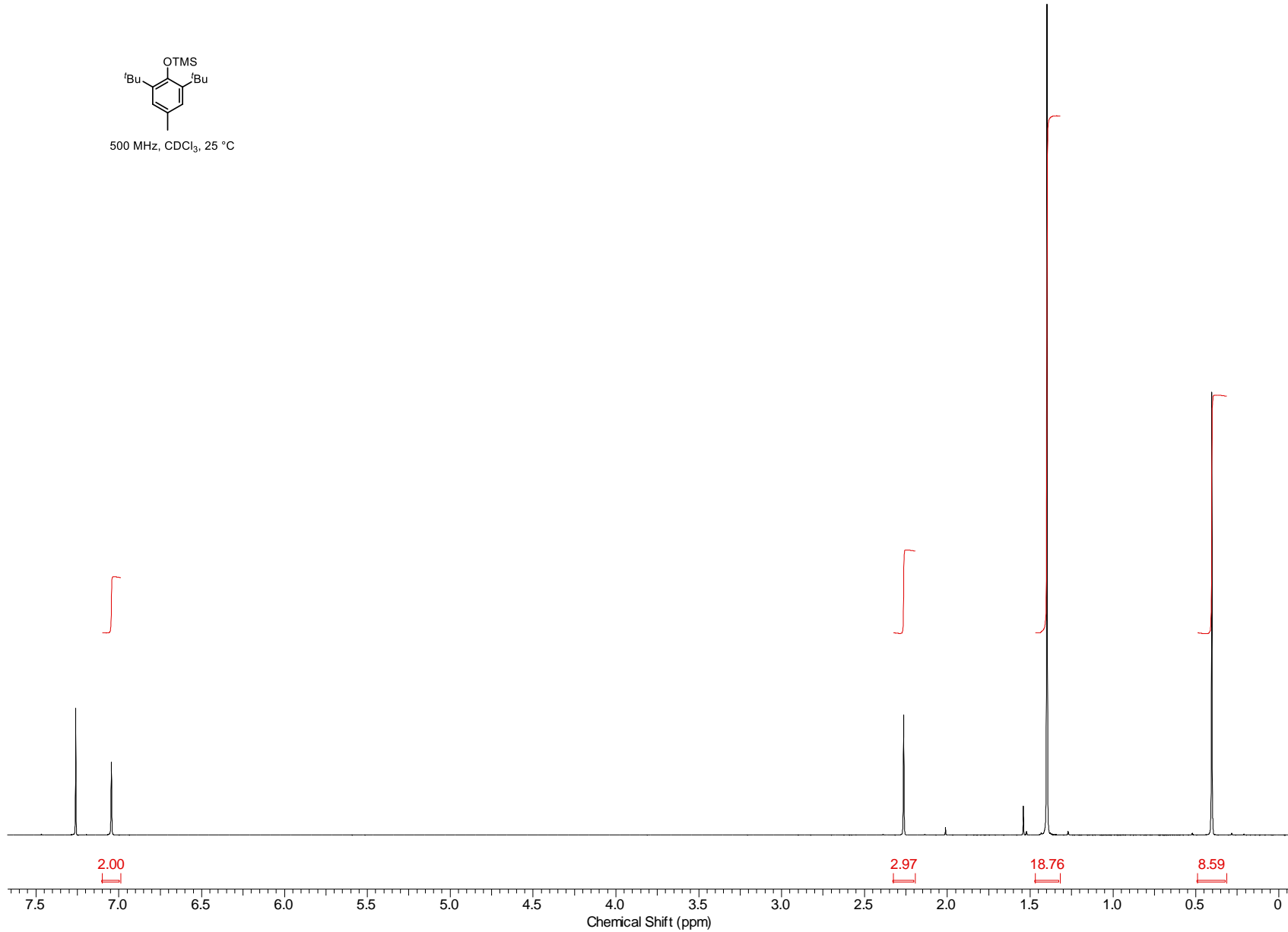
Experiments conducted in Acetone- d_6

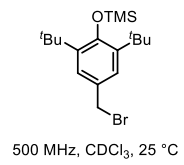
⁵⁵ Kawabata, J.; Fukushi, E.; Hara, M.; Mizutani, J. *Magn. Reson. Chem.* **1992**, *30* (1), 6–10.



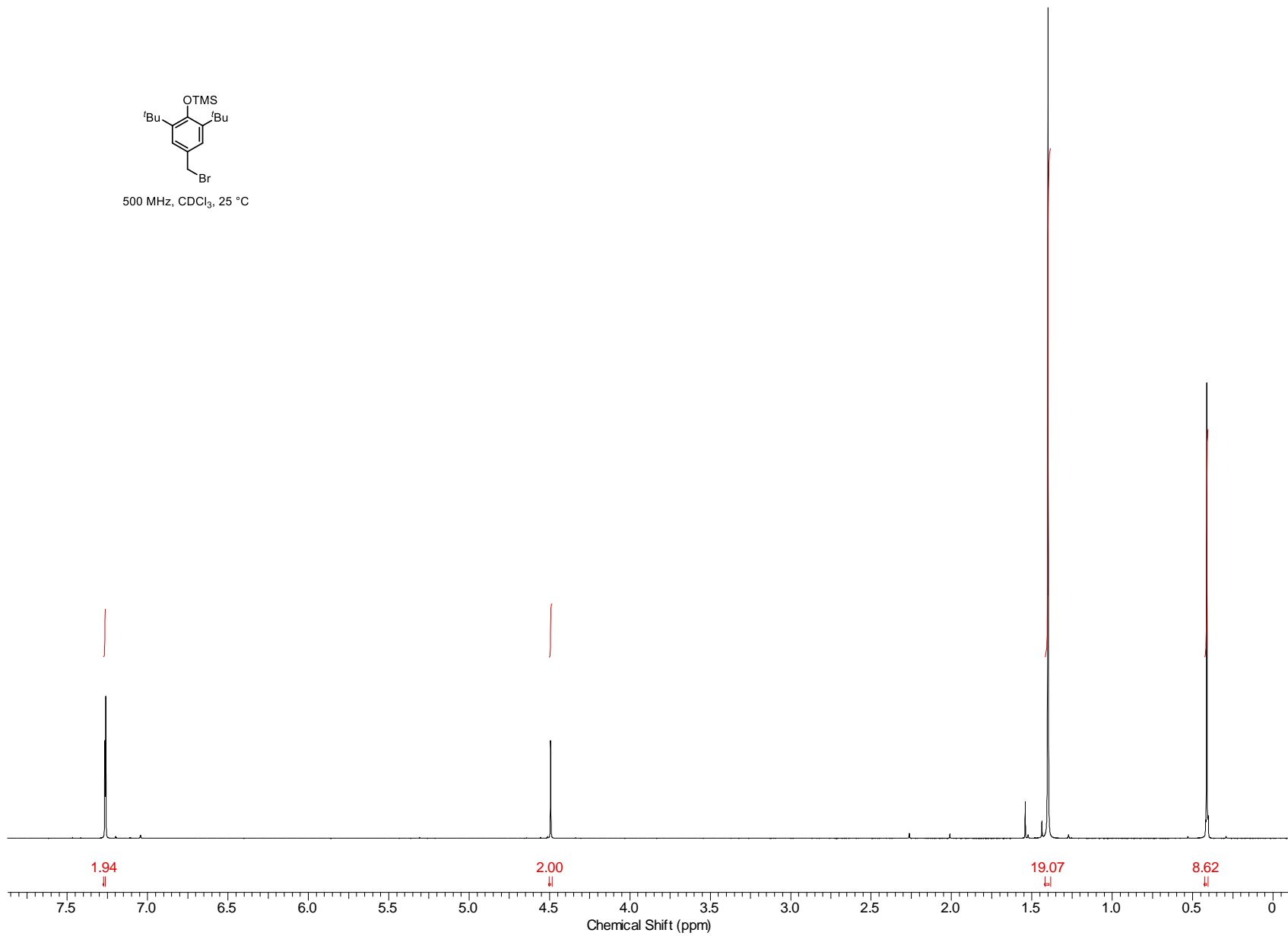
500 MHz, CDCl₃, 25 °C

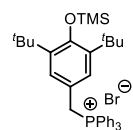
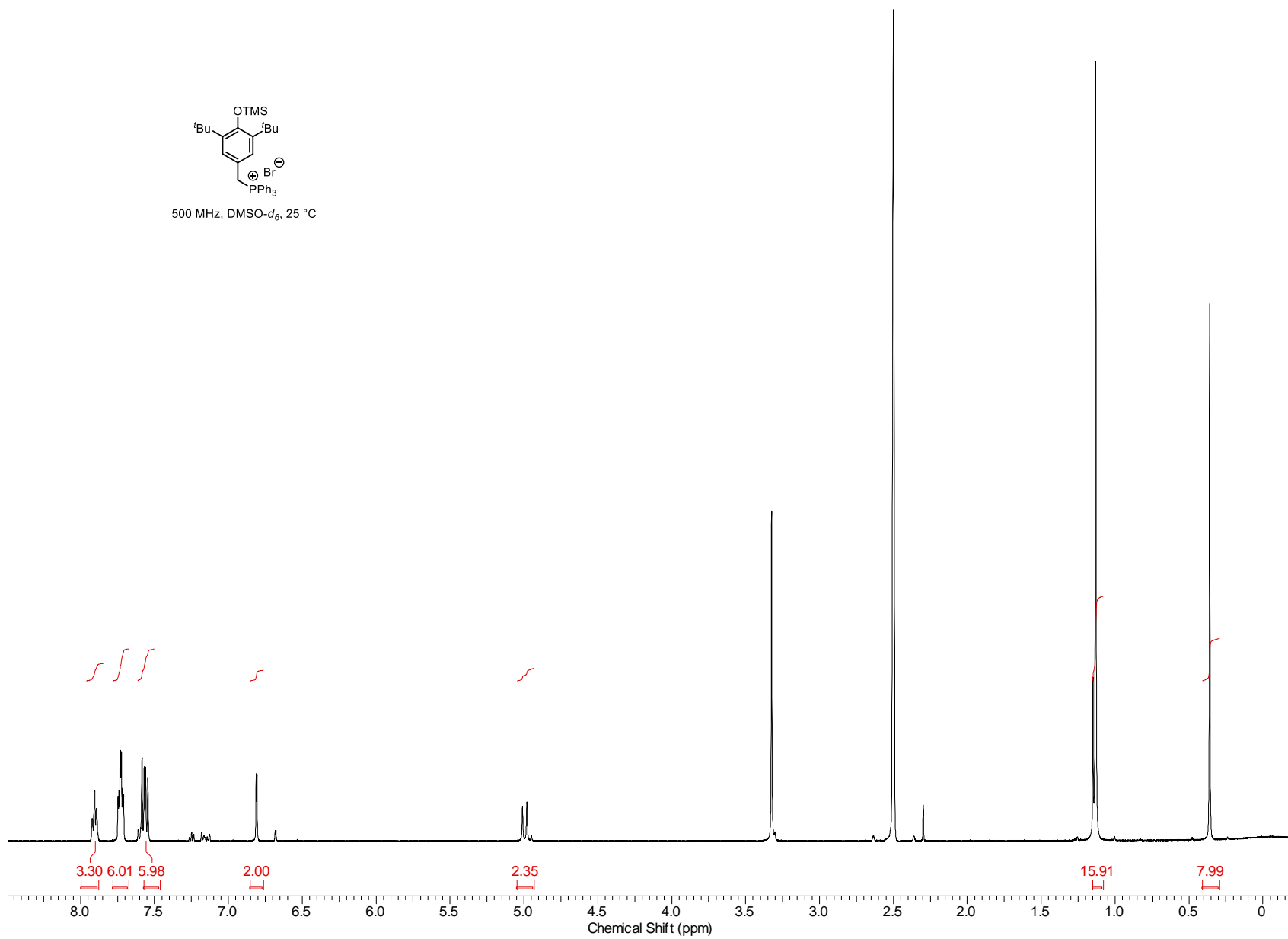
217

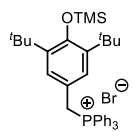




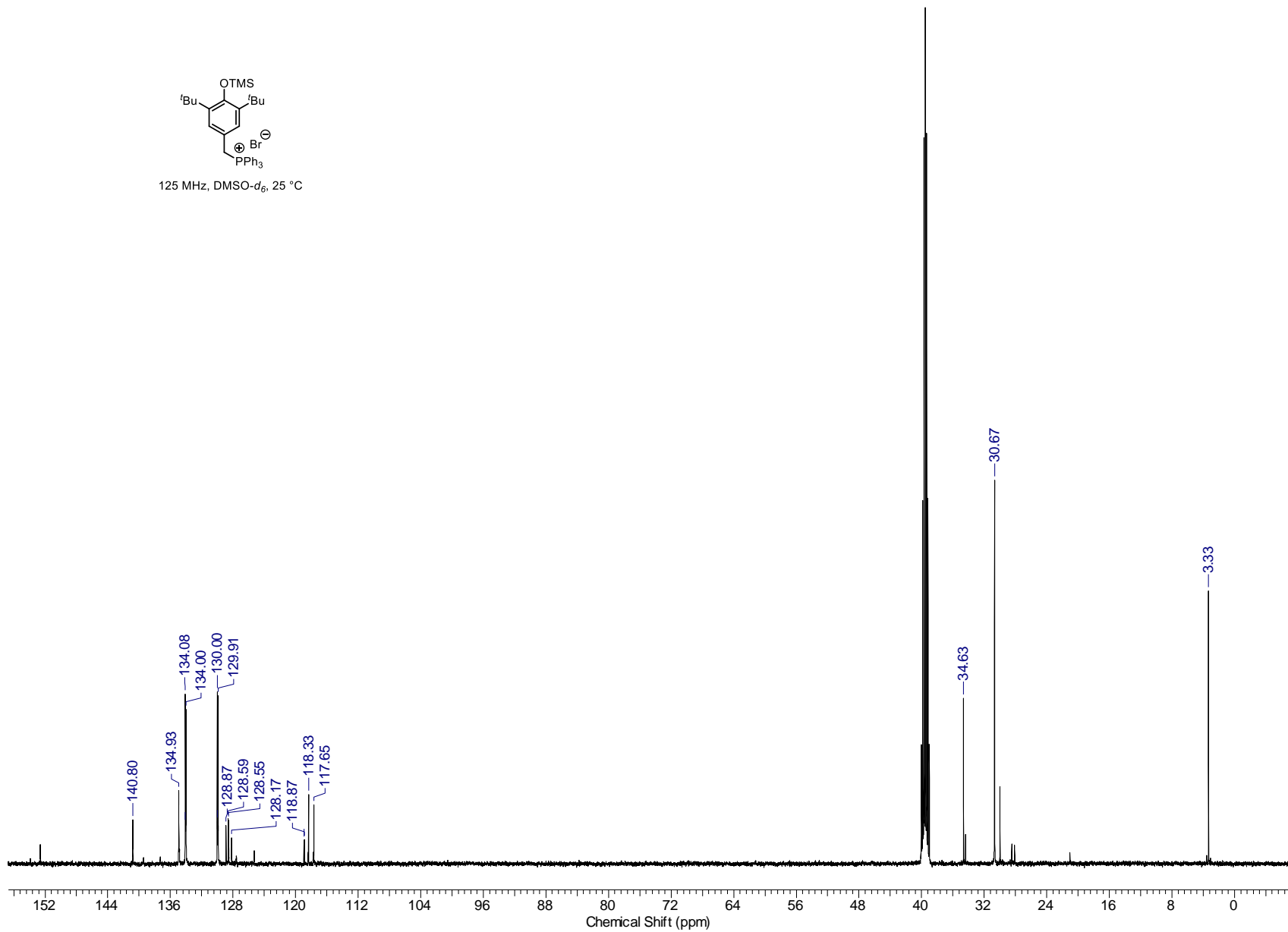
218

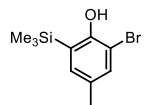


500 MHz, DMSO-*d*₆, 25 °C



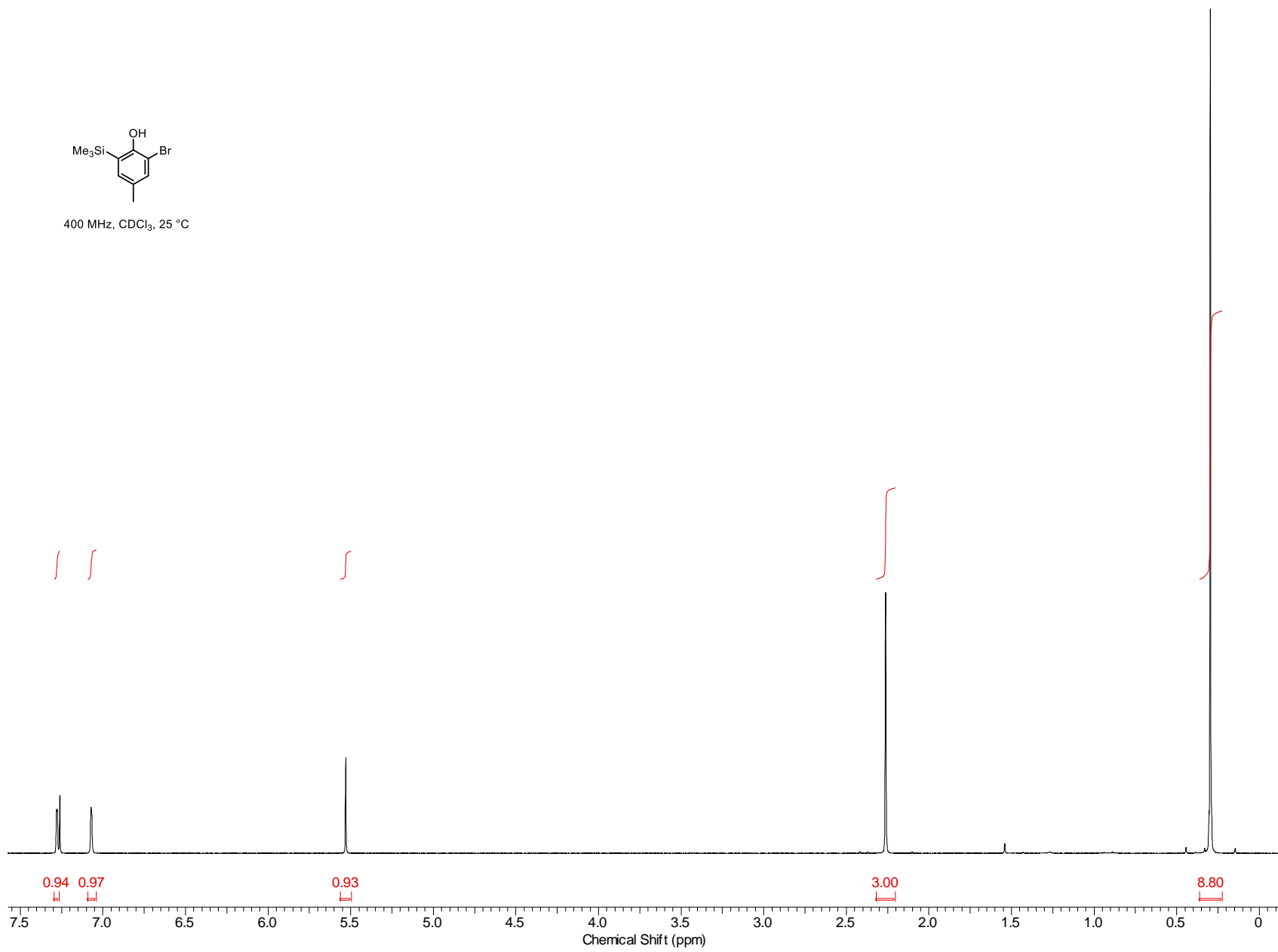
125 MHz, DMSO-*d*₆, 25 °C

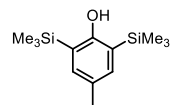




400 MHz, CDCl₃, 25 °C

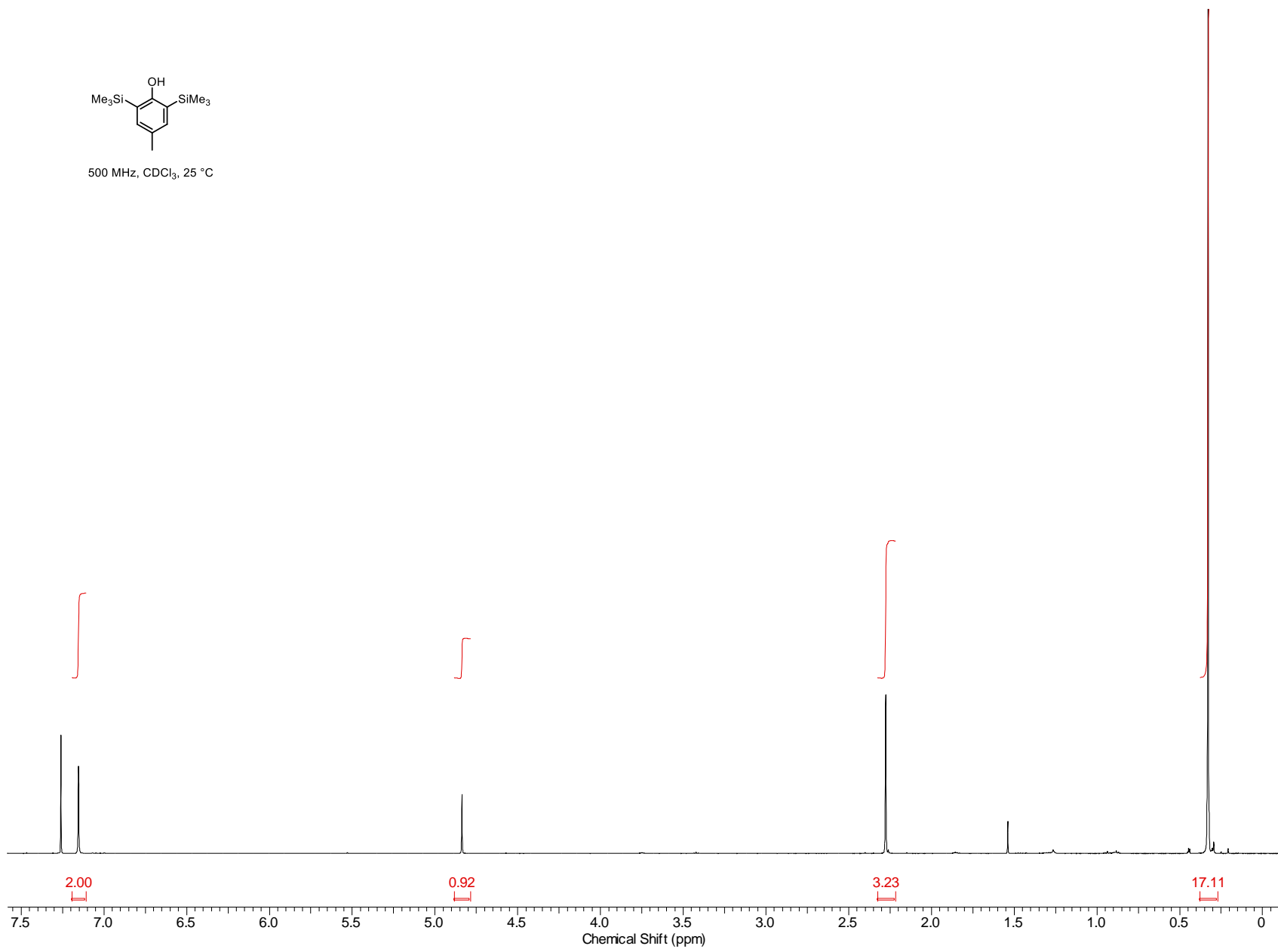
221

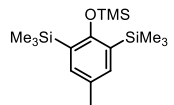




500 MHz, CDCl₃, 25 °C

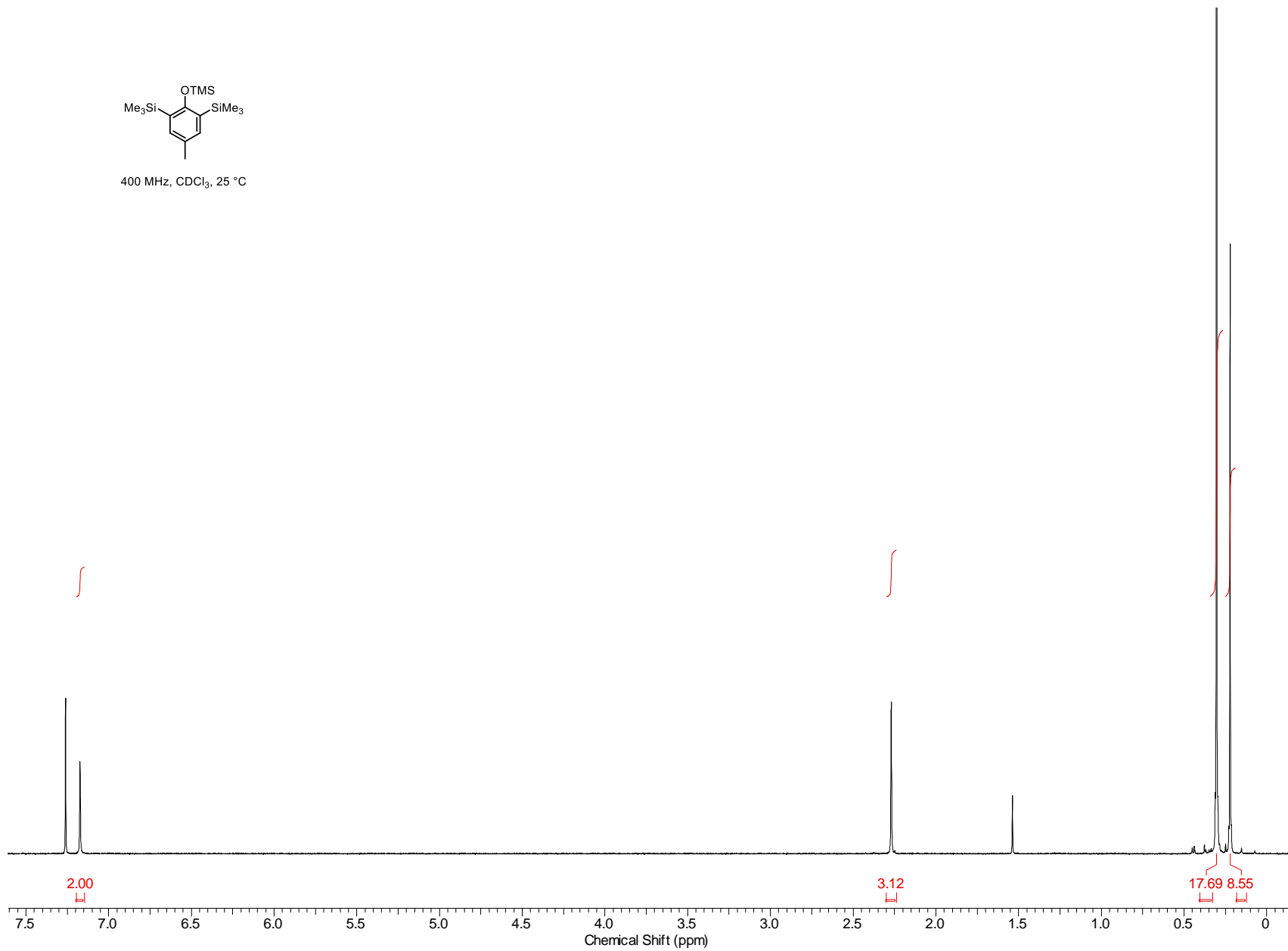
222

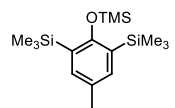




400 MHz, CDCl₃, 25 °C

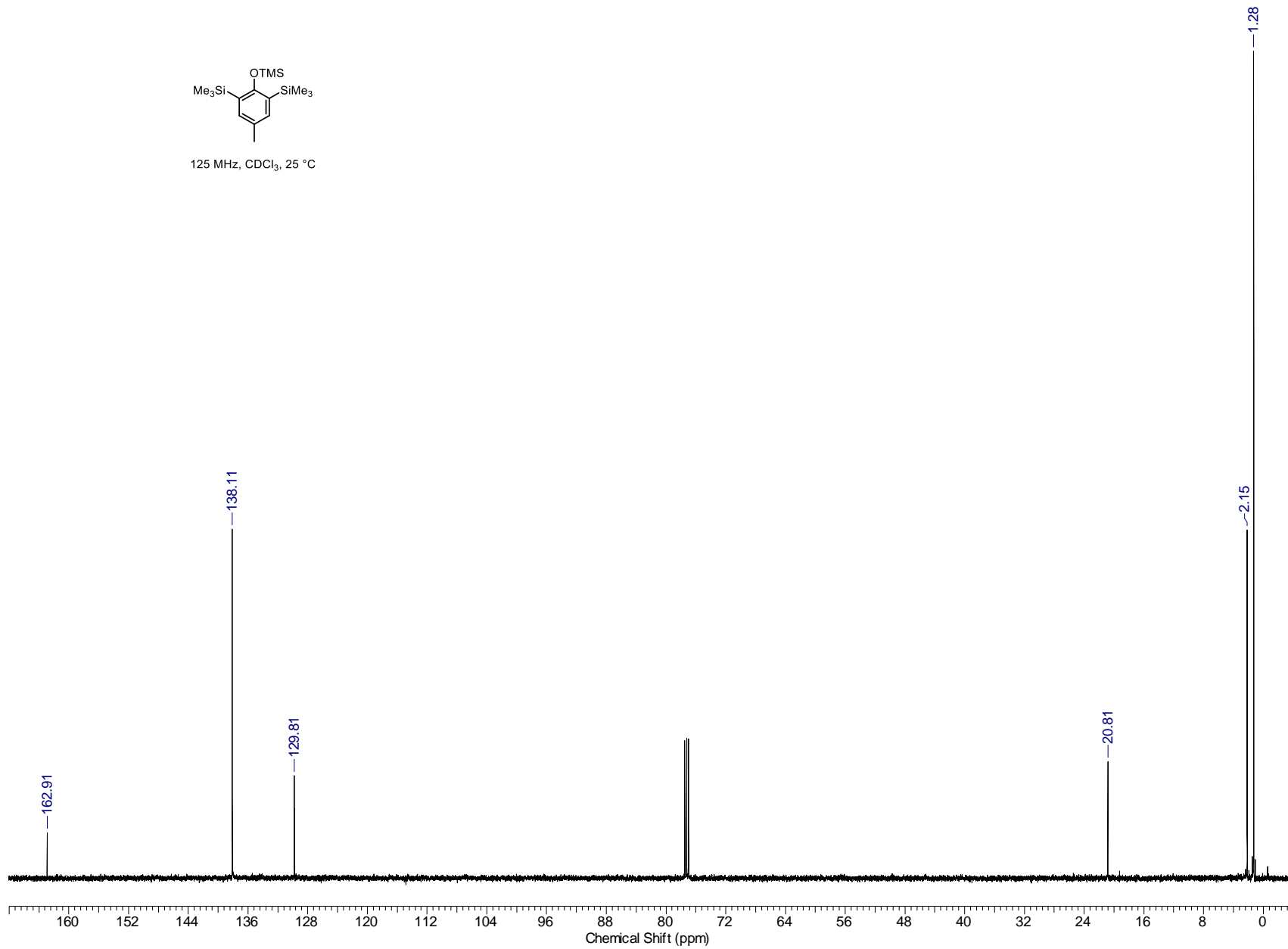
223

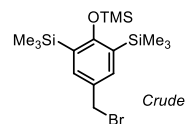




125 MHz, CDCl₃, 25 °C

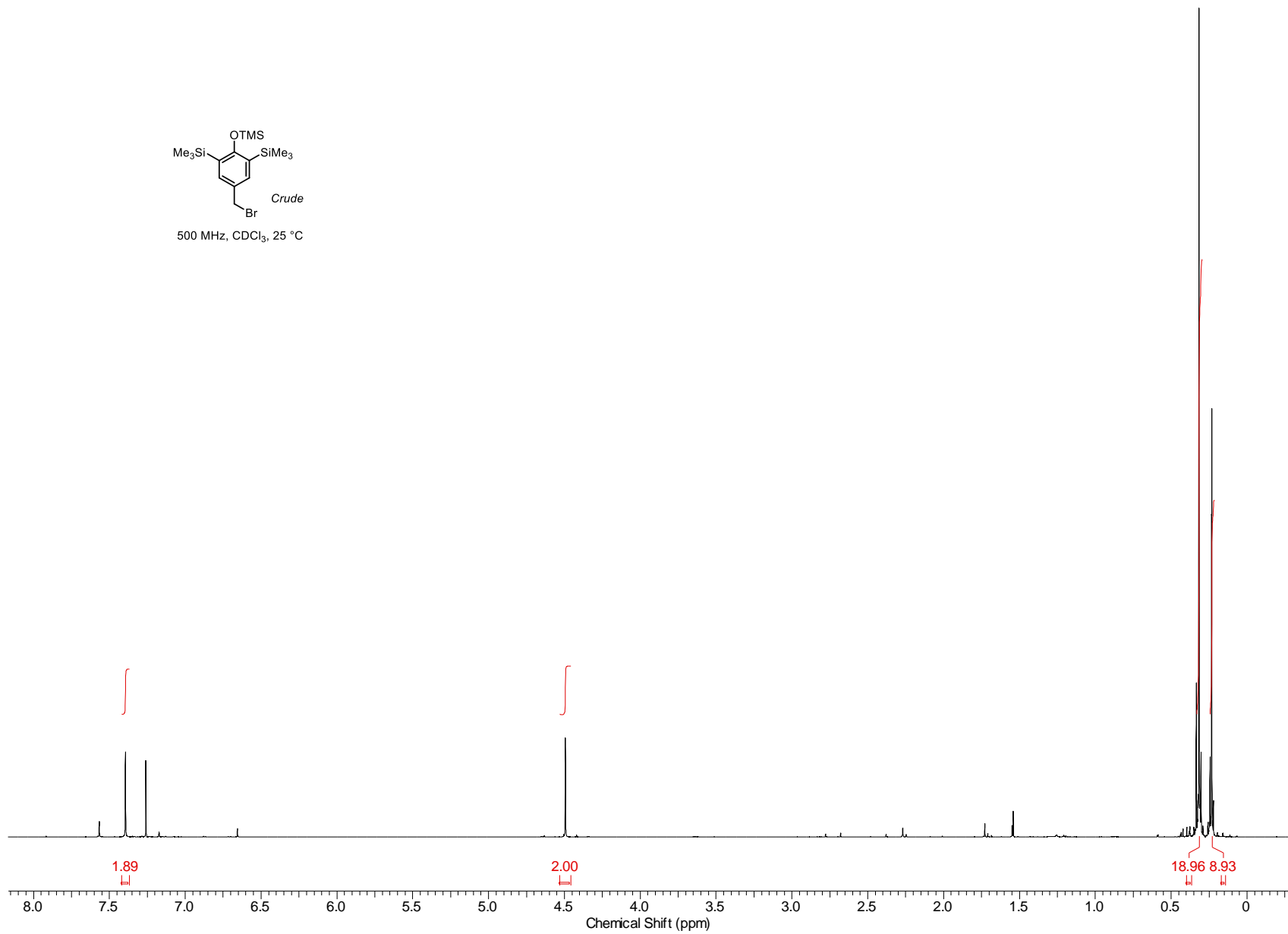
224

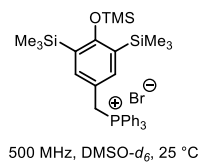




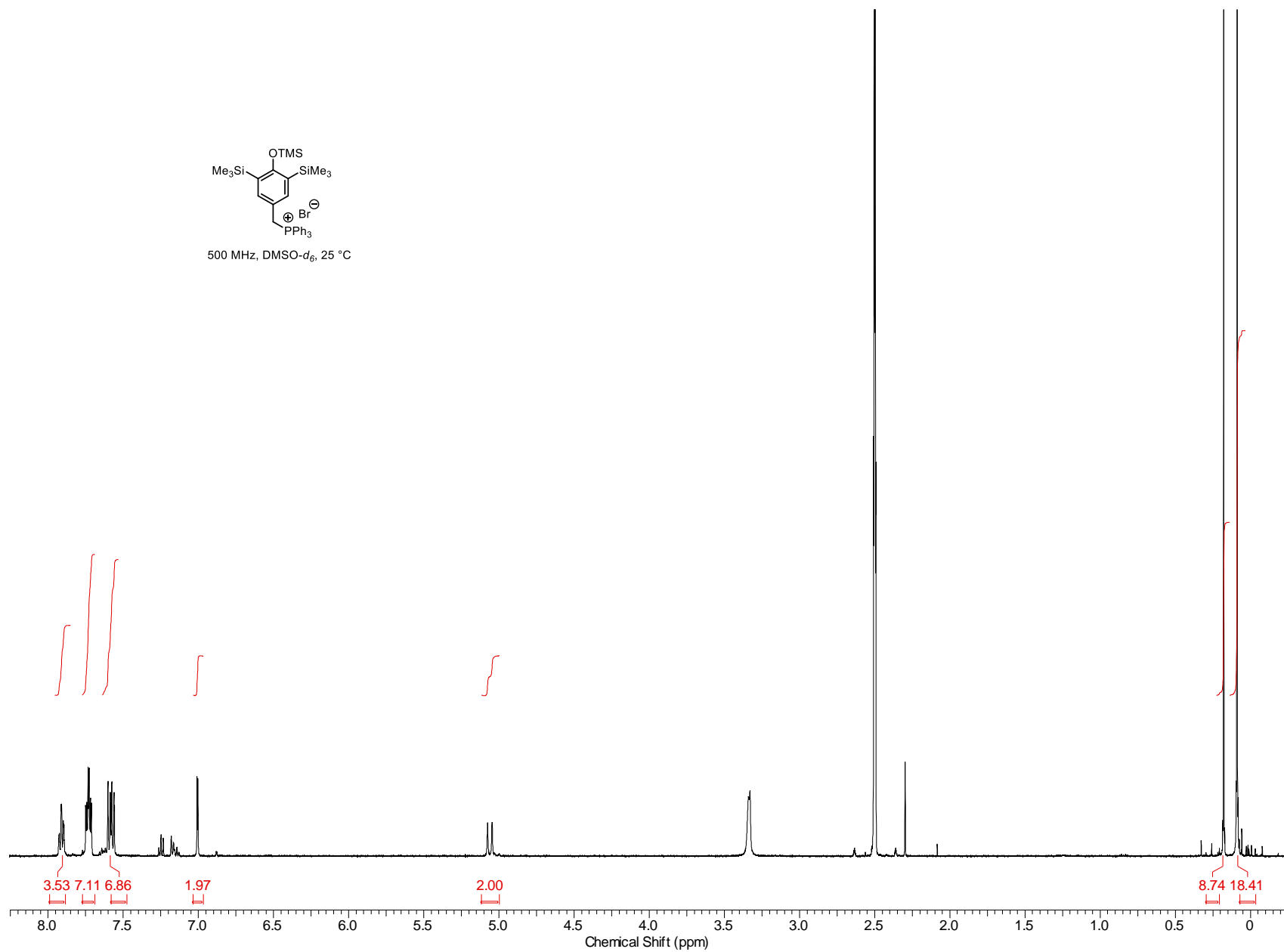
500 MHz, CDCl₃, 25 °C

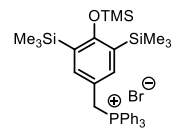
225



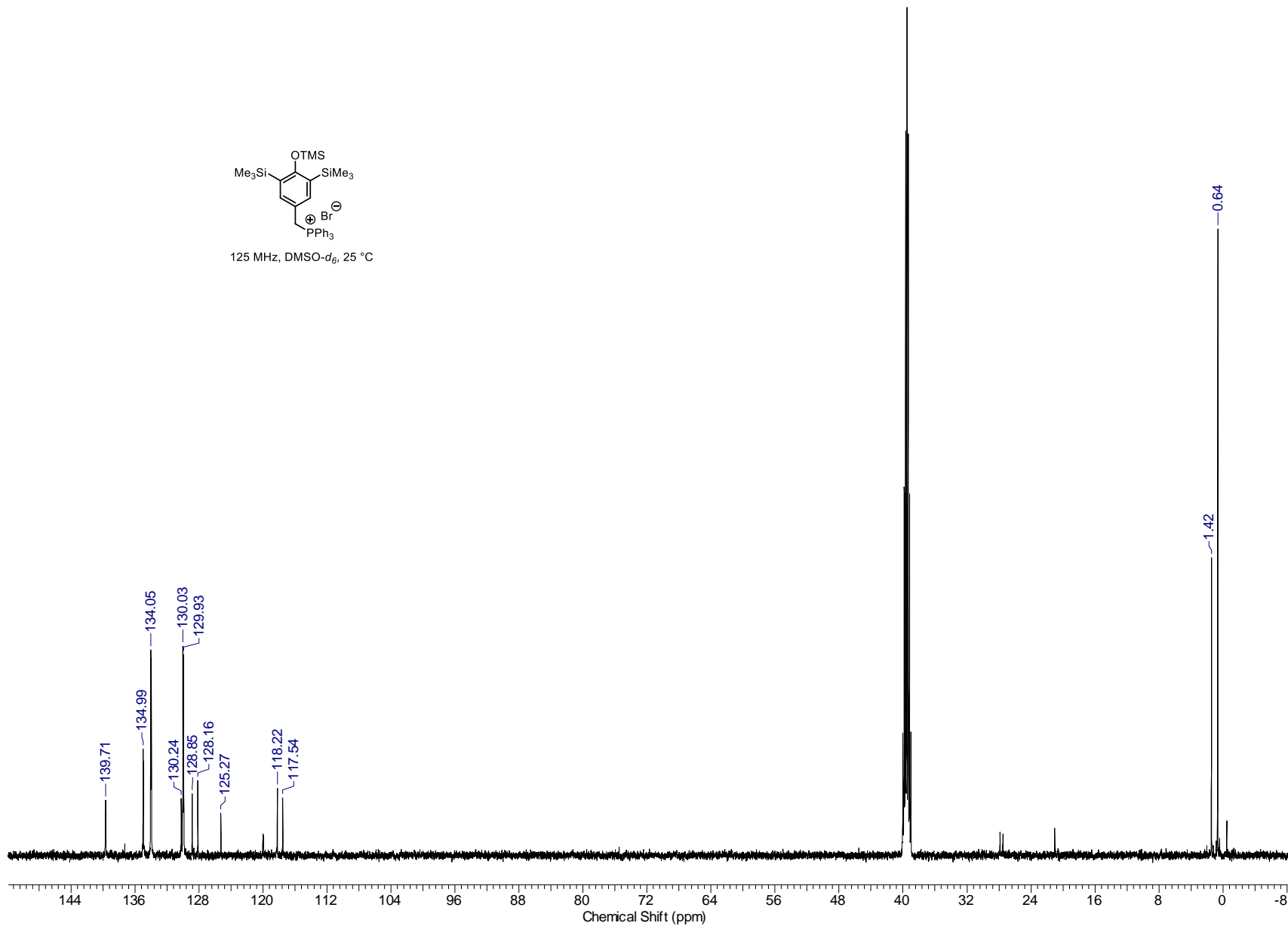


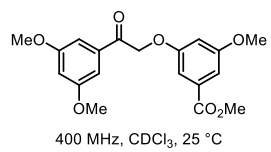
226



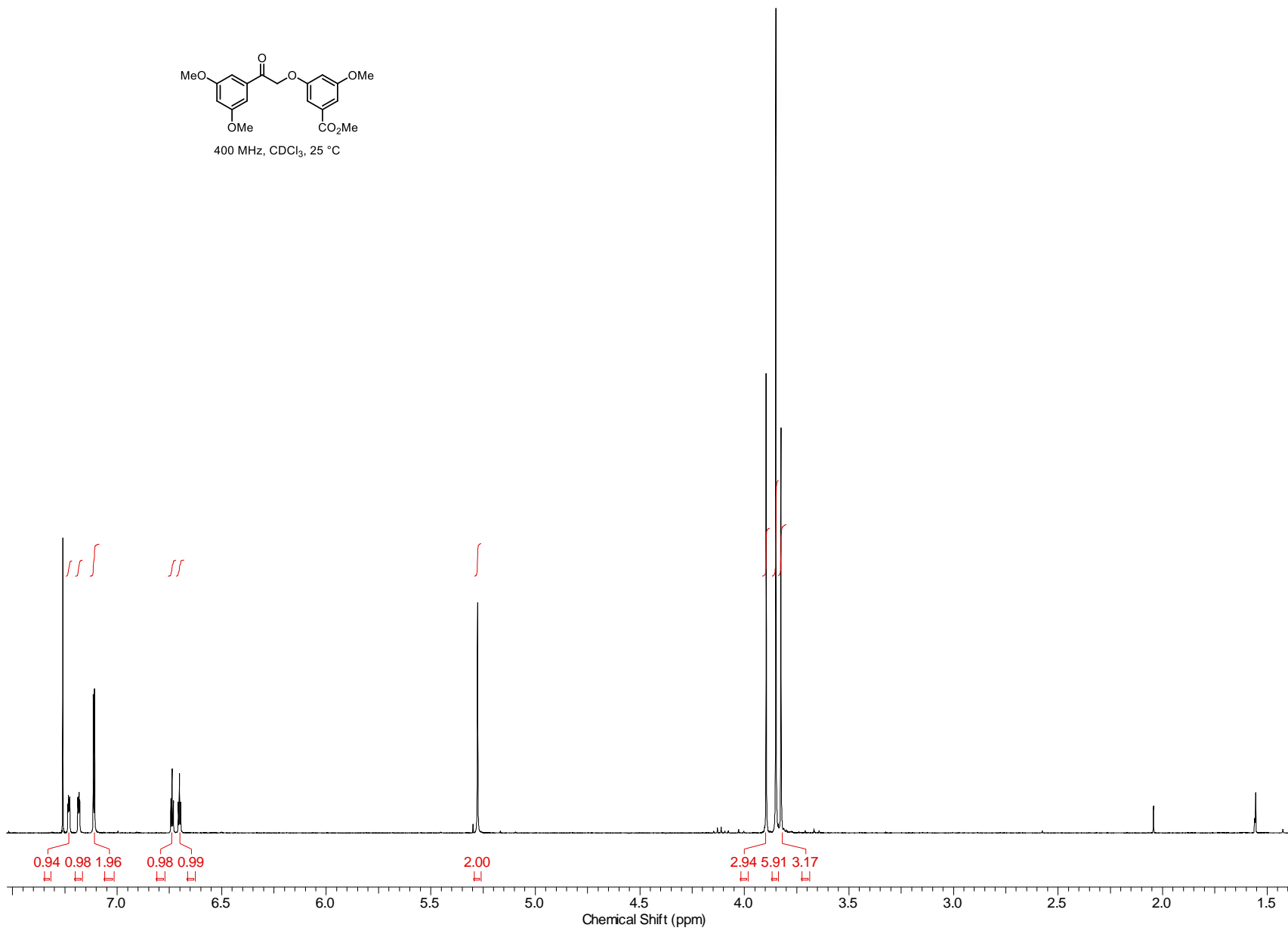


125 MHz, DMSO-*d*₆, 25 °C

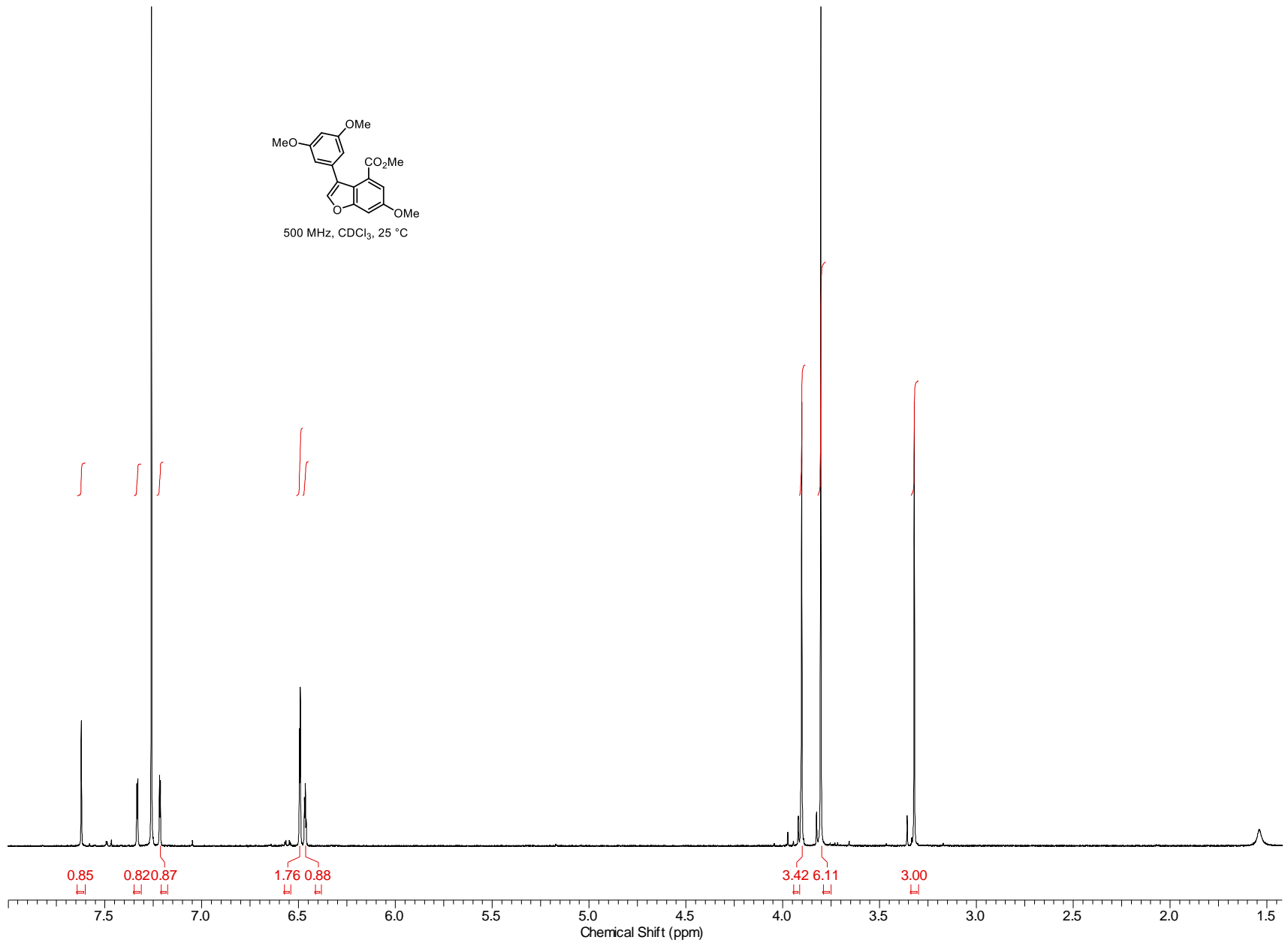
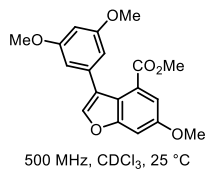


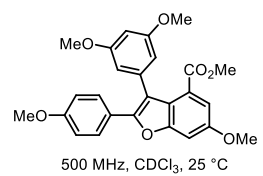


228

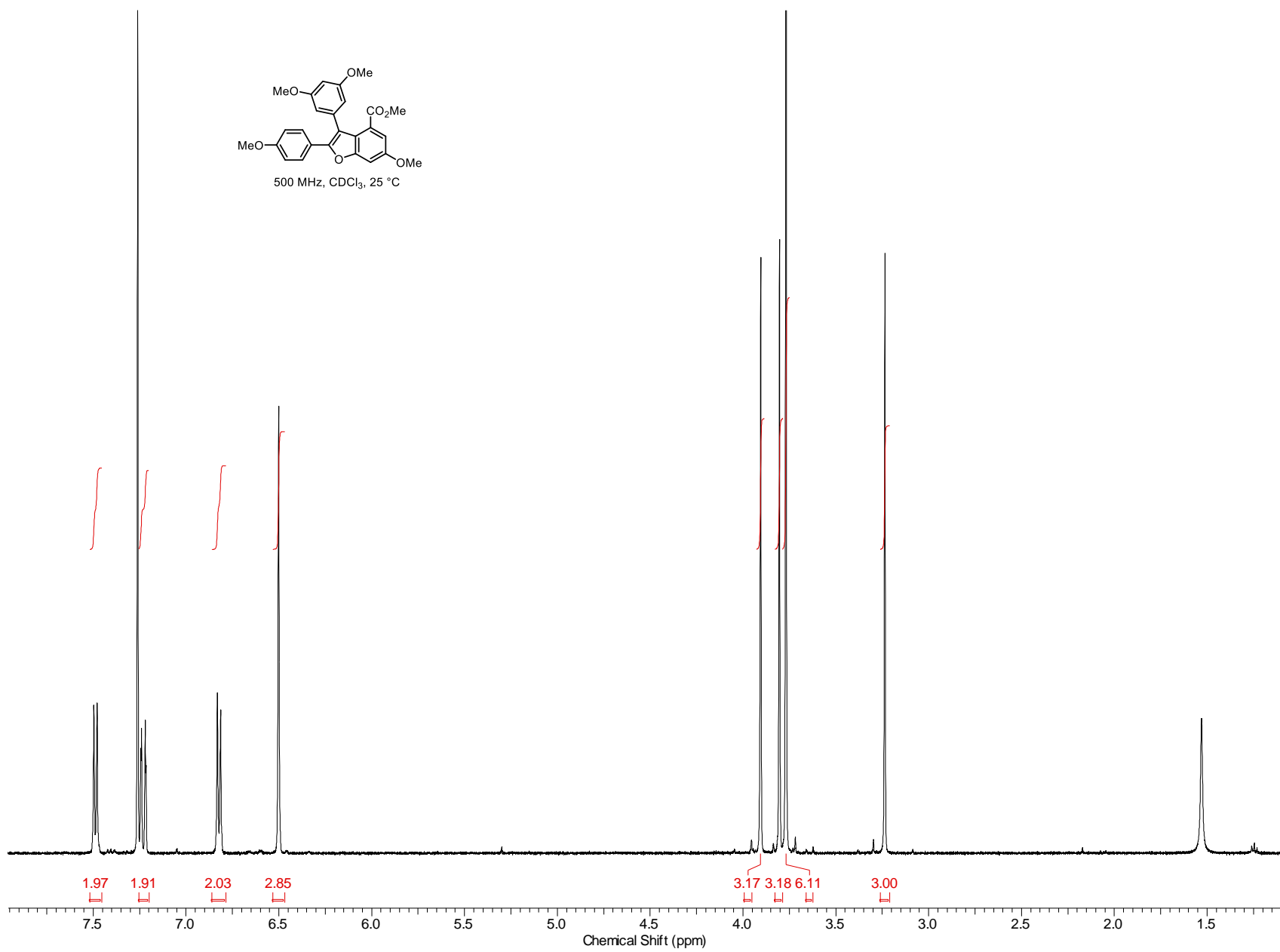


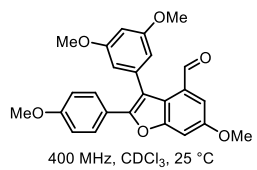
229



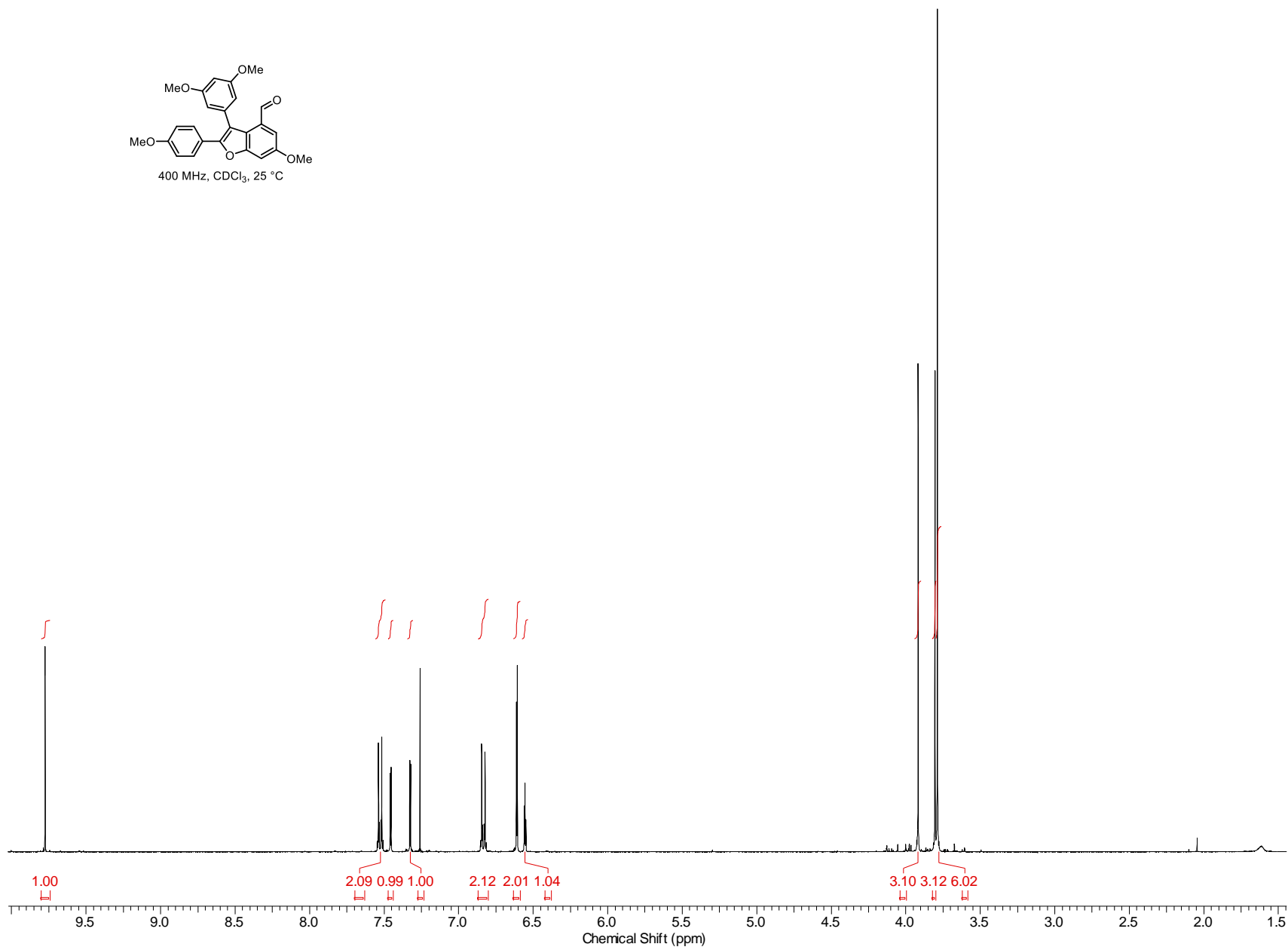


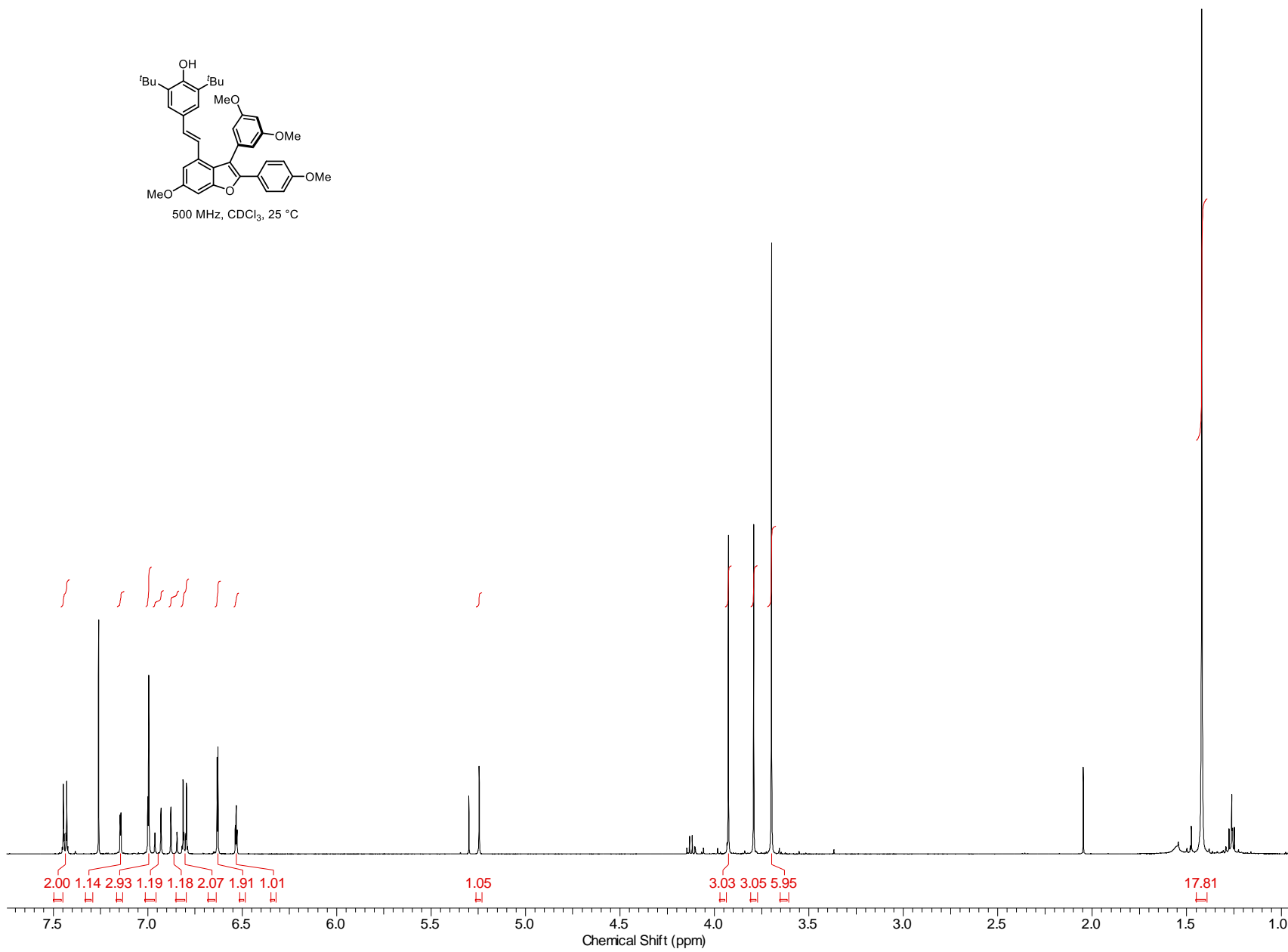
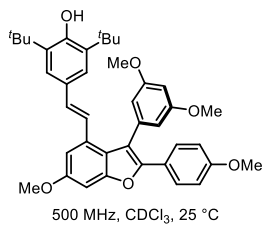
230

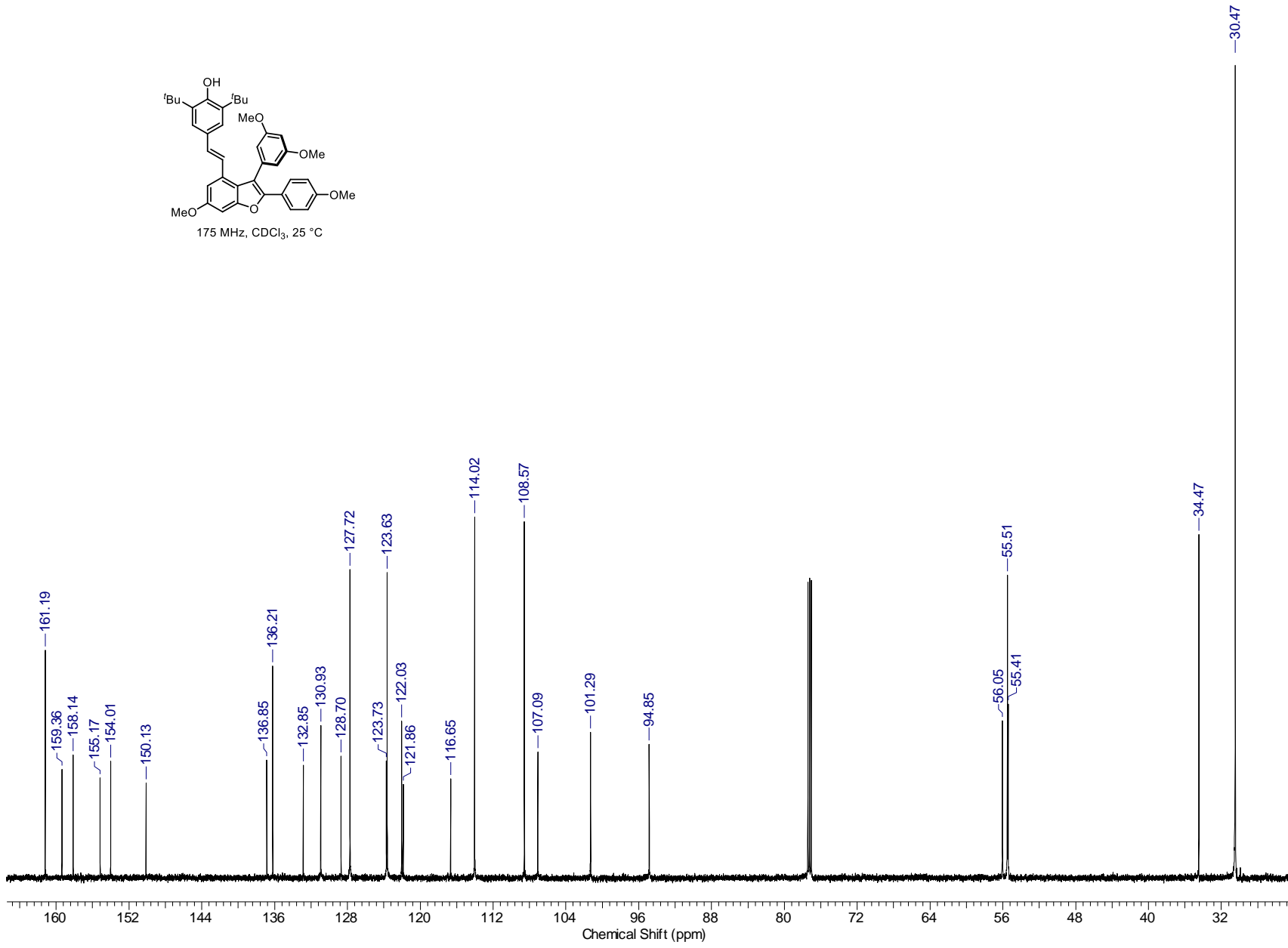
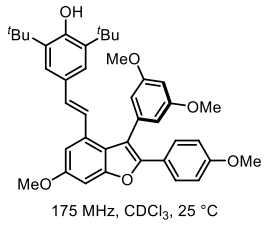


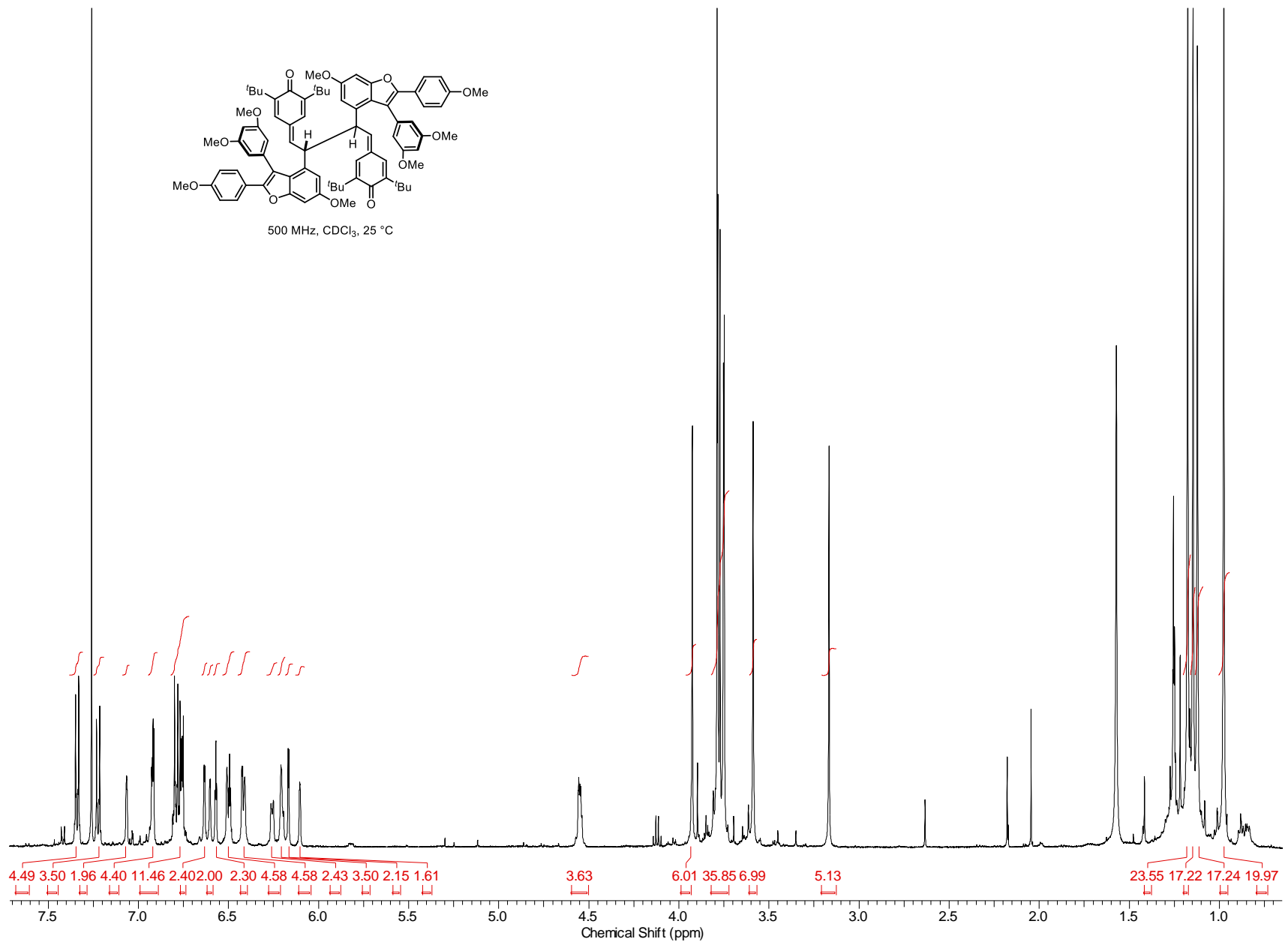


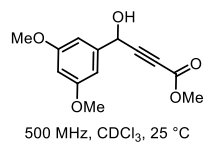
231



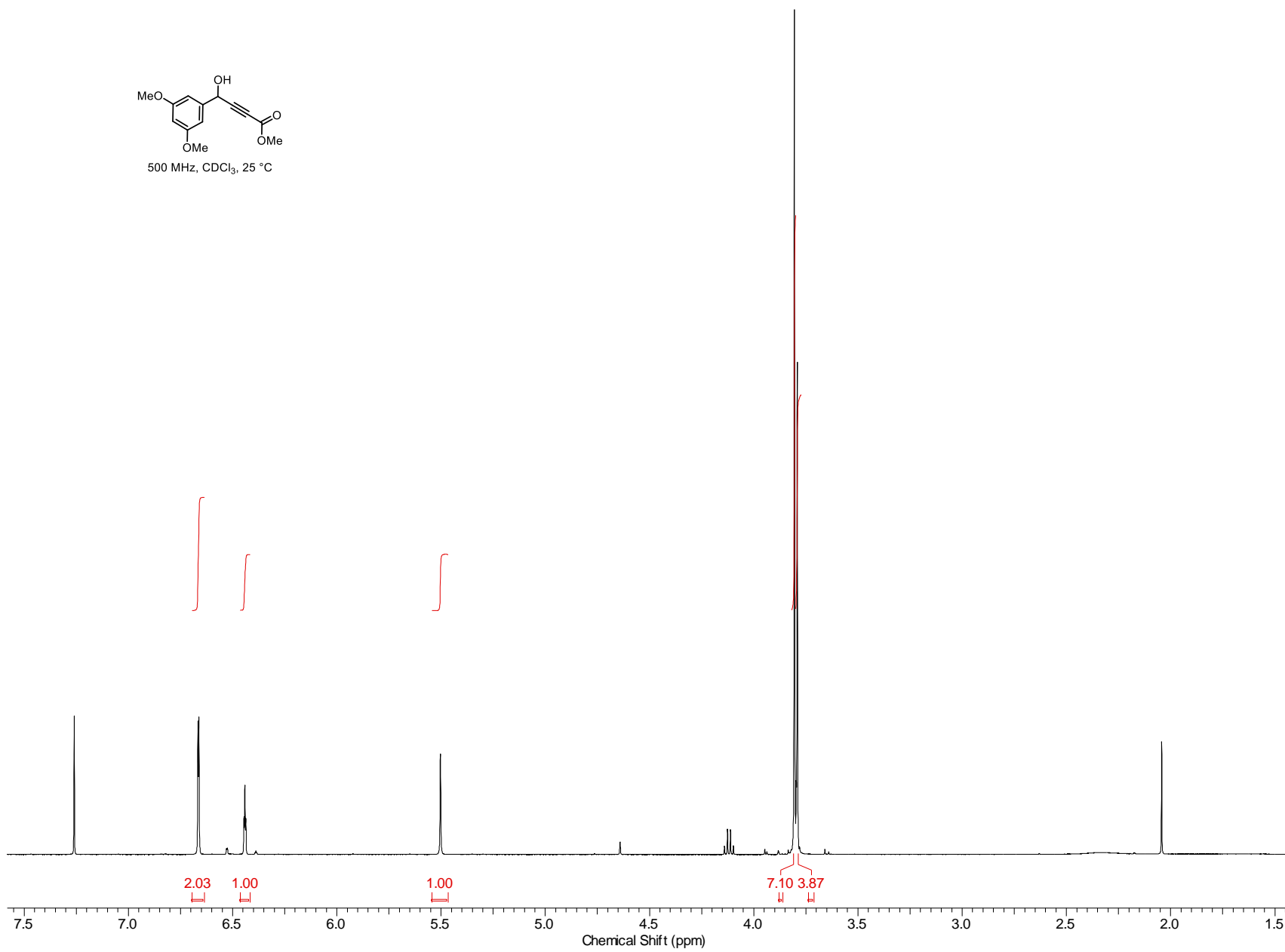




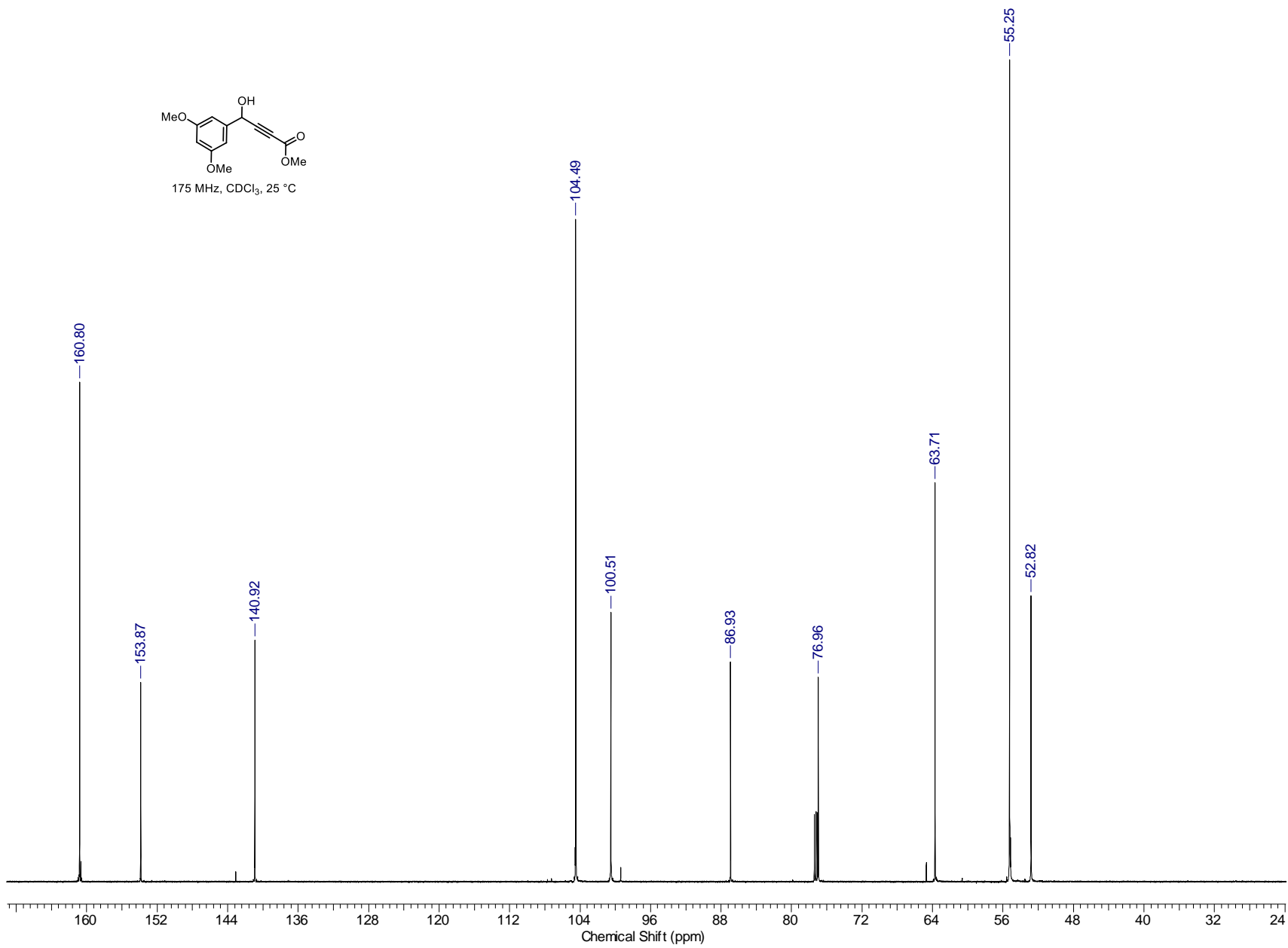
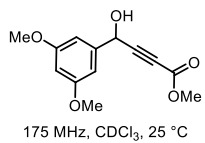


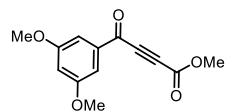


235



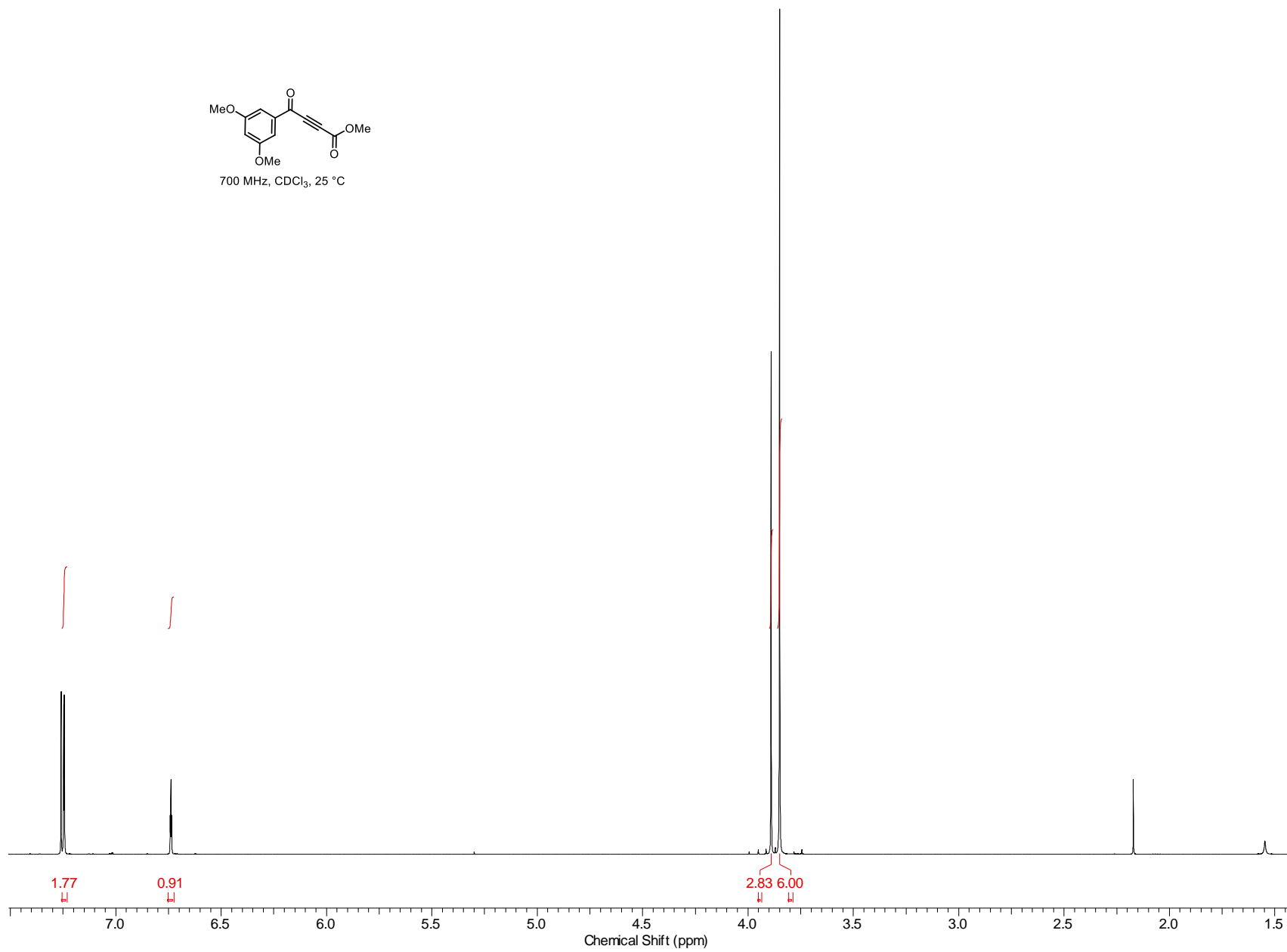
236



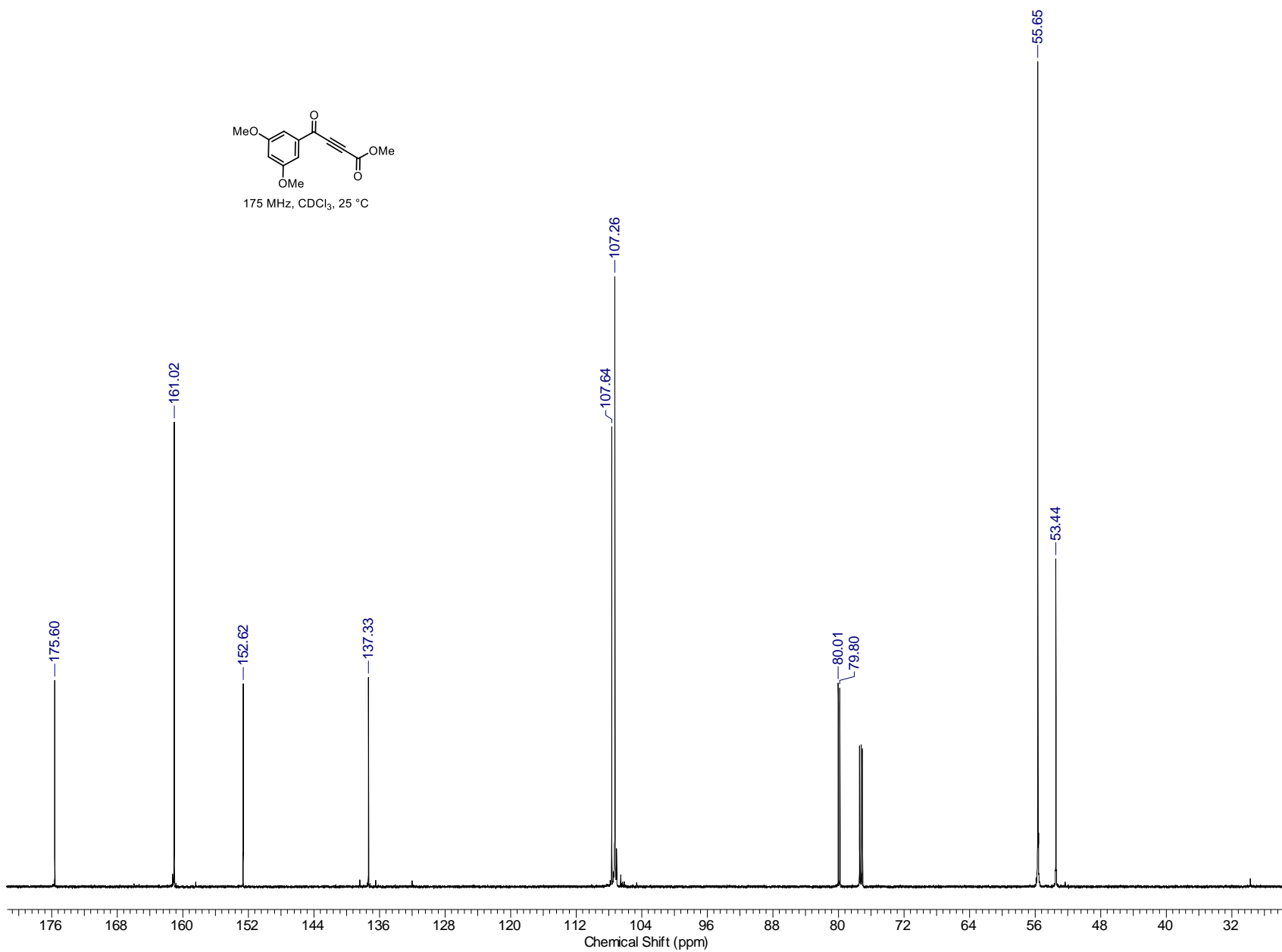
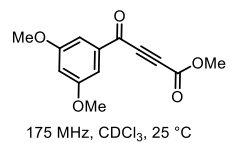


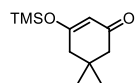
700 MHz, CDCl₃, 25 °C

237



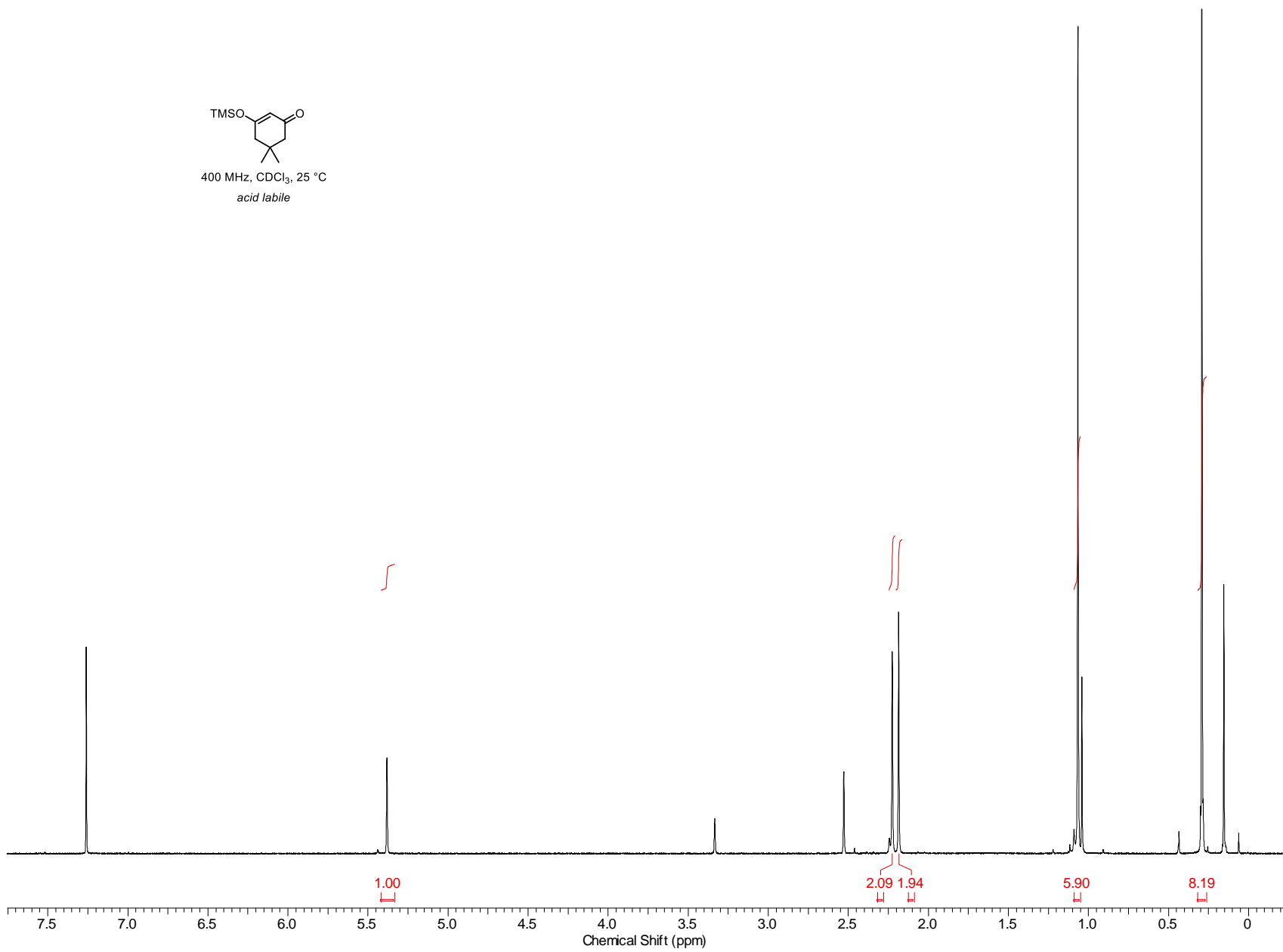
238

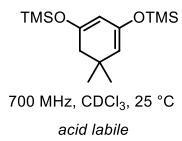




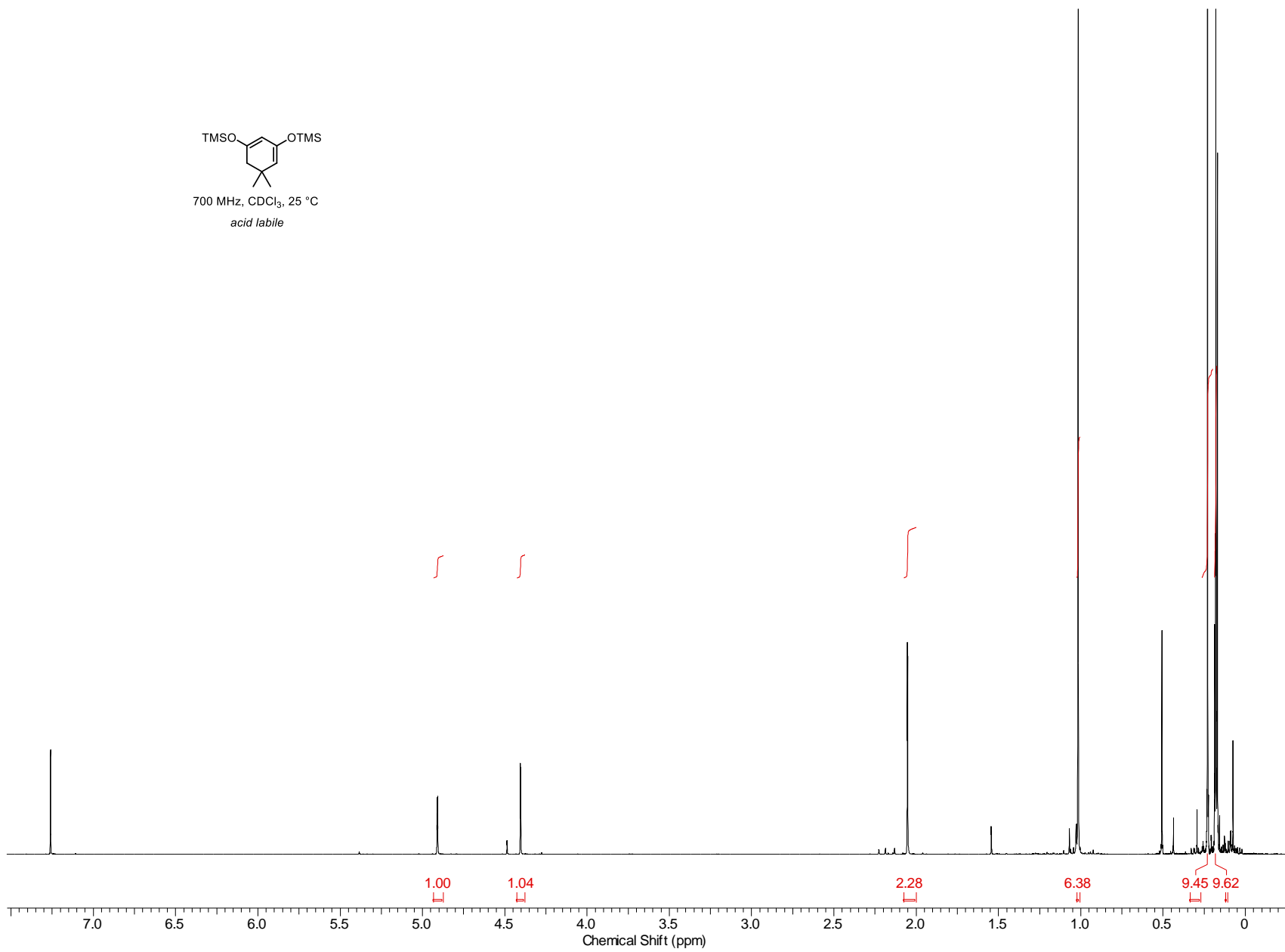
400 MHz, CDCl₃, 25 °C
acid labile

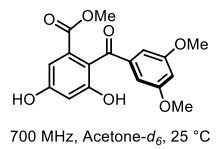
239



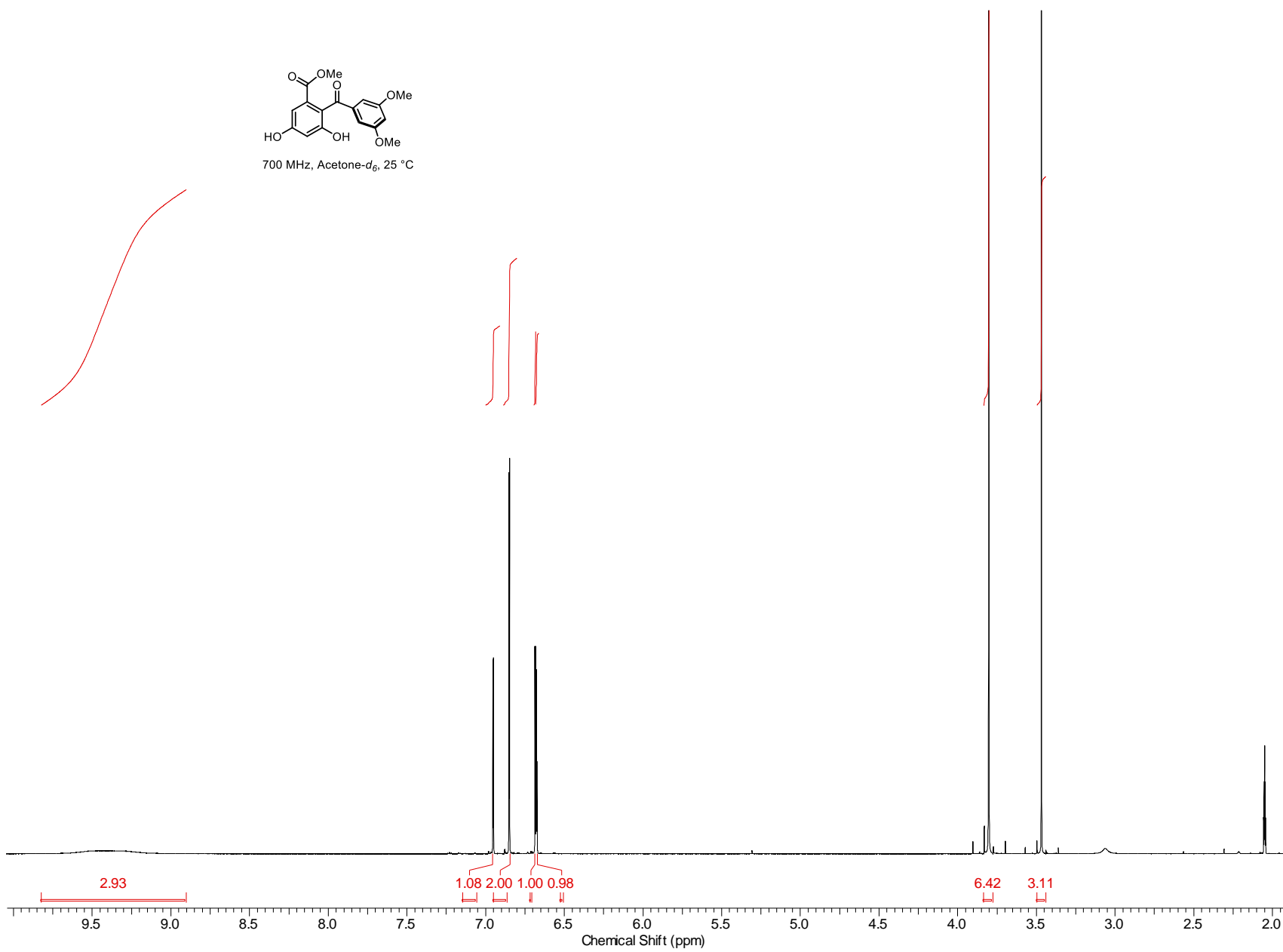


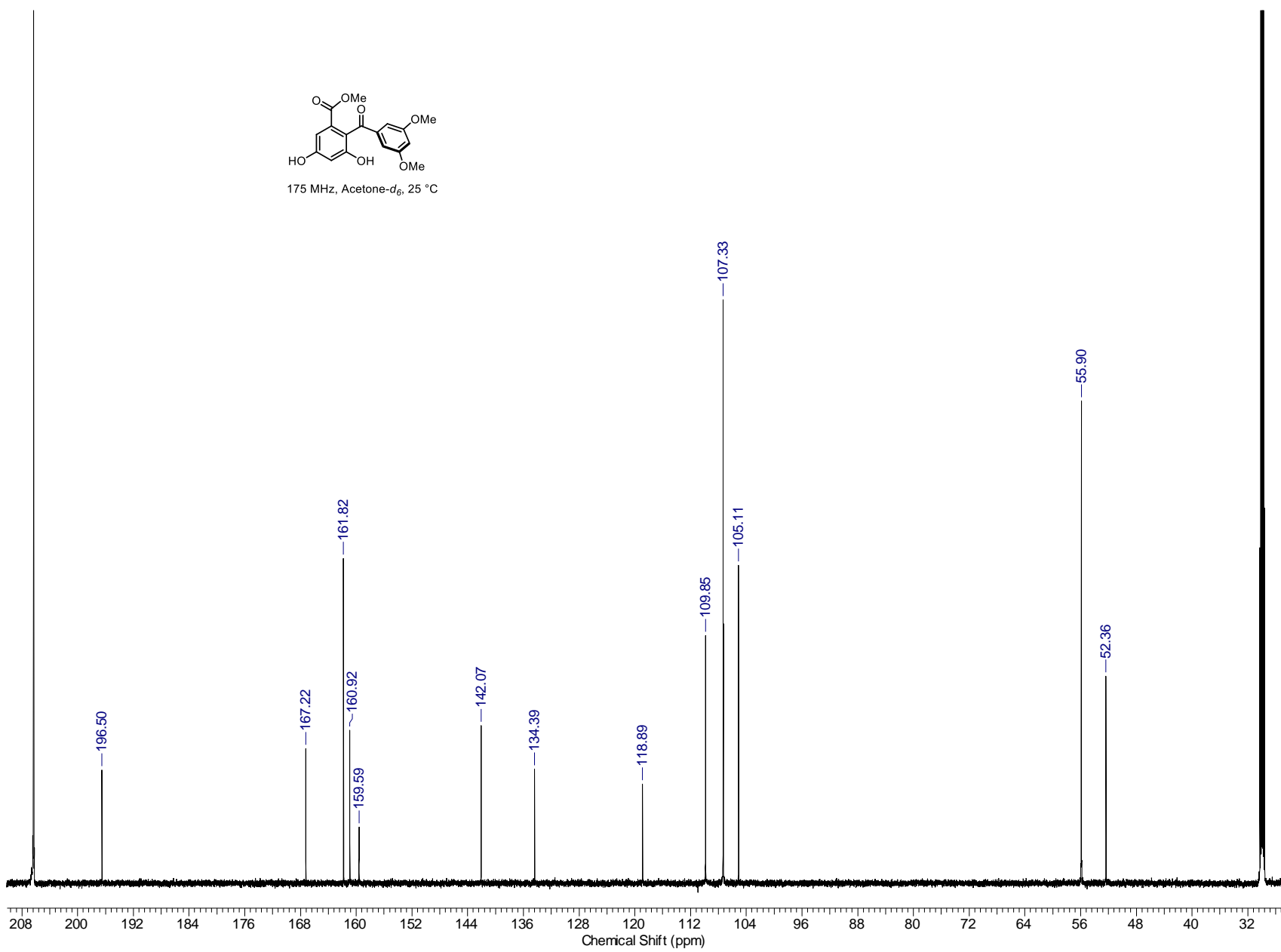
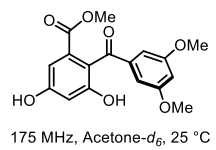
240

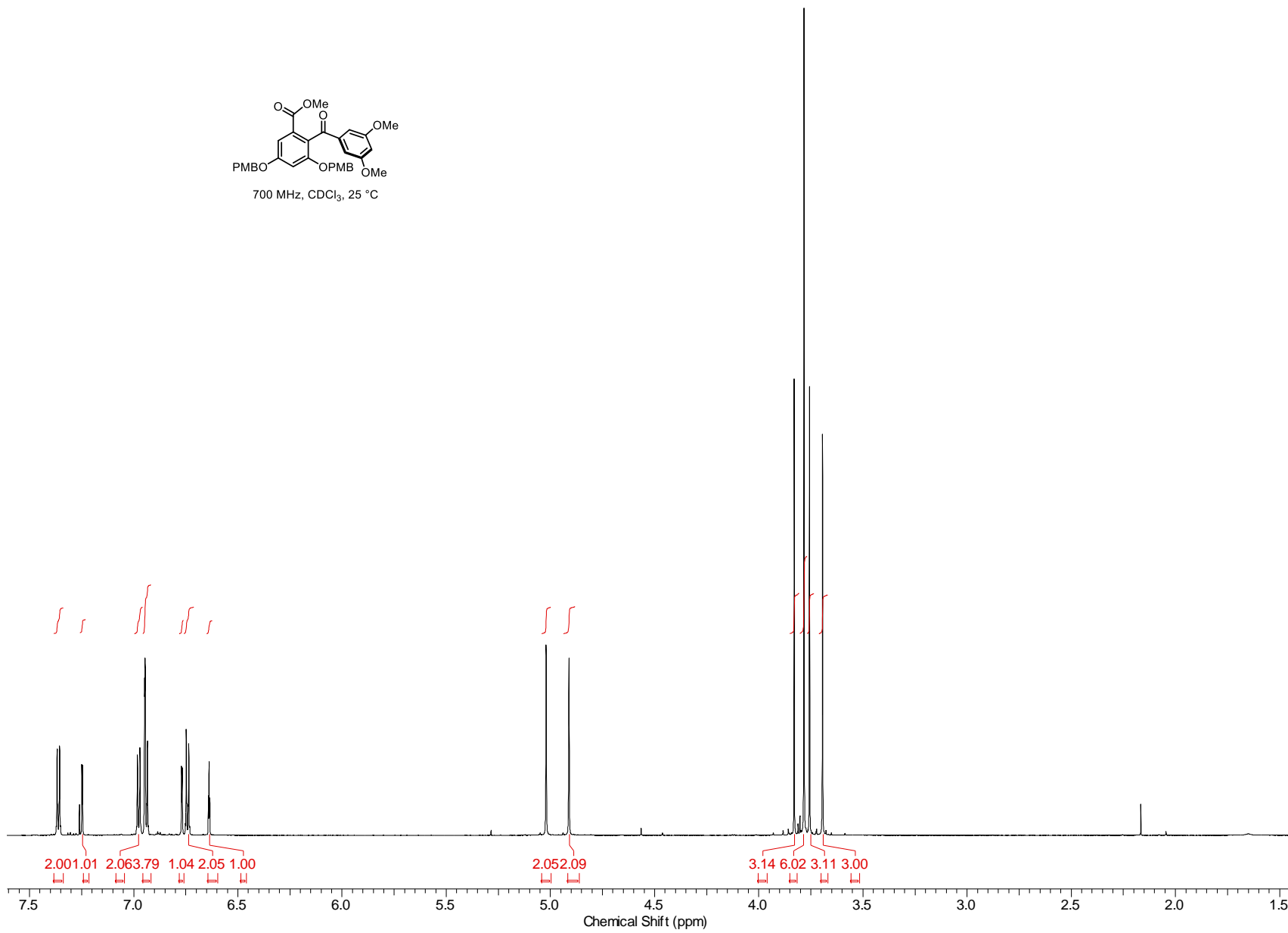
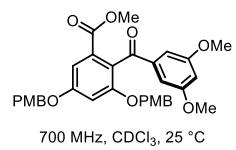


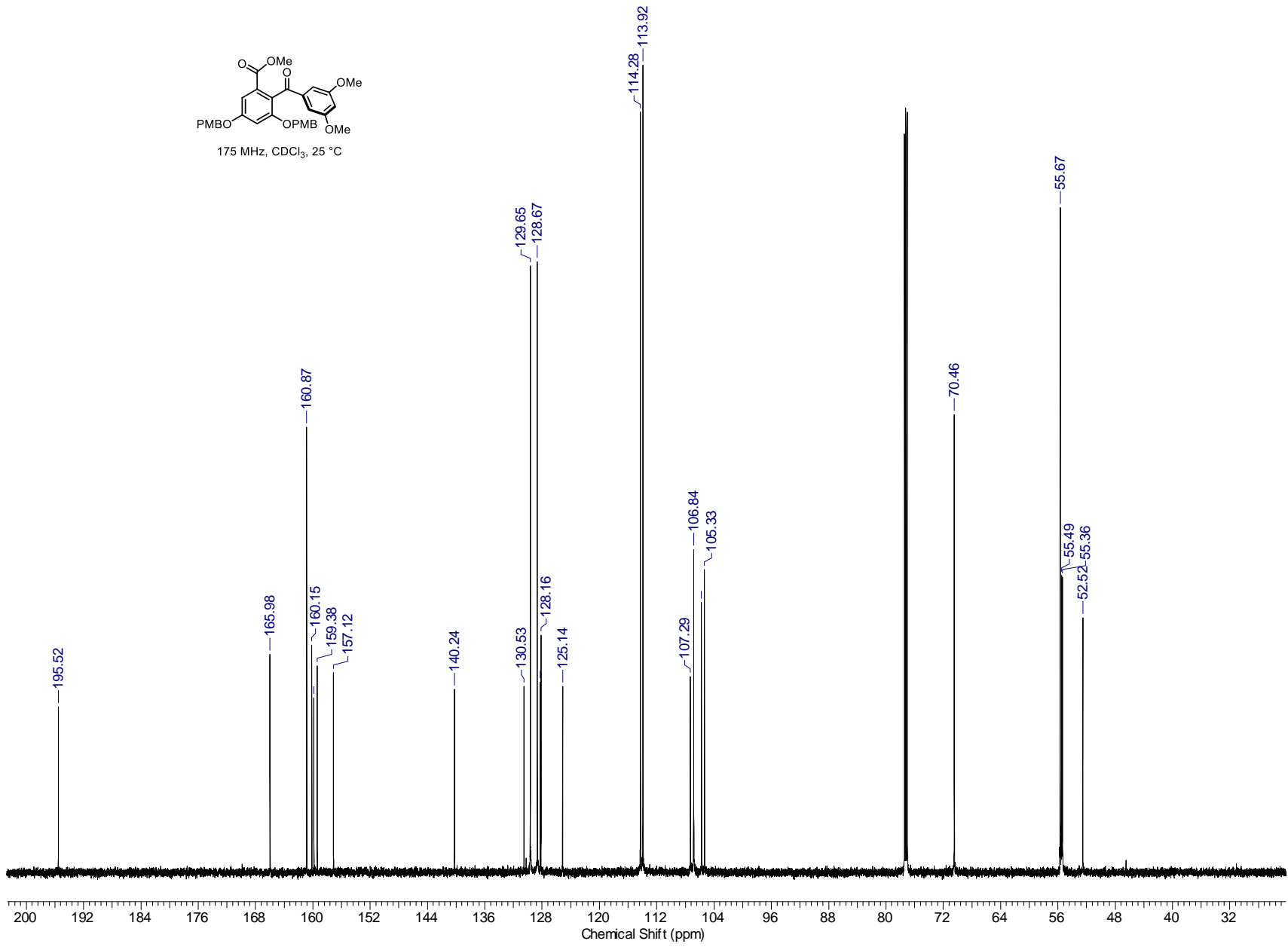
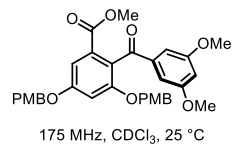


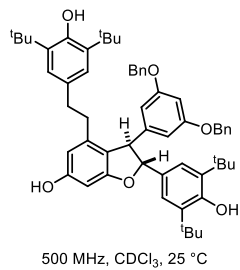
241



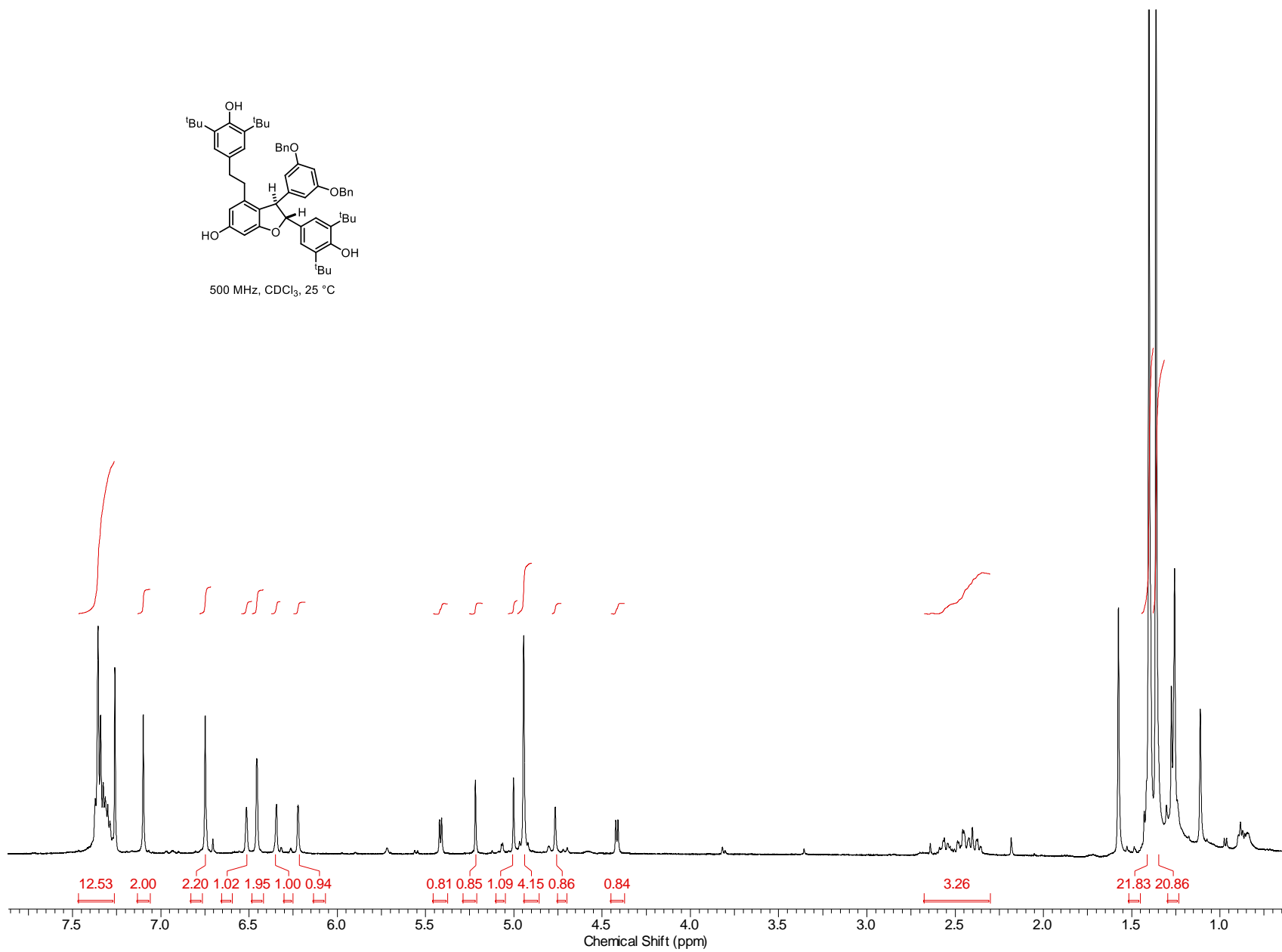


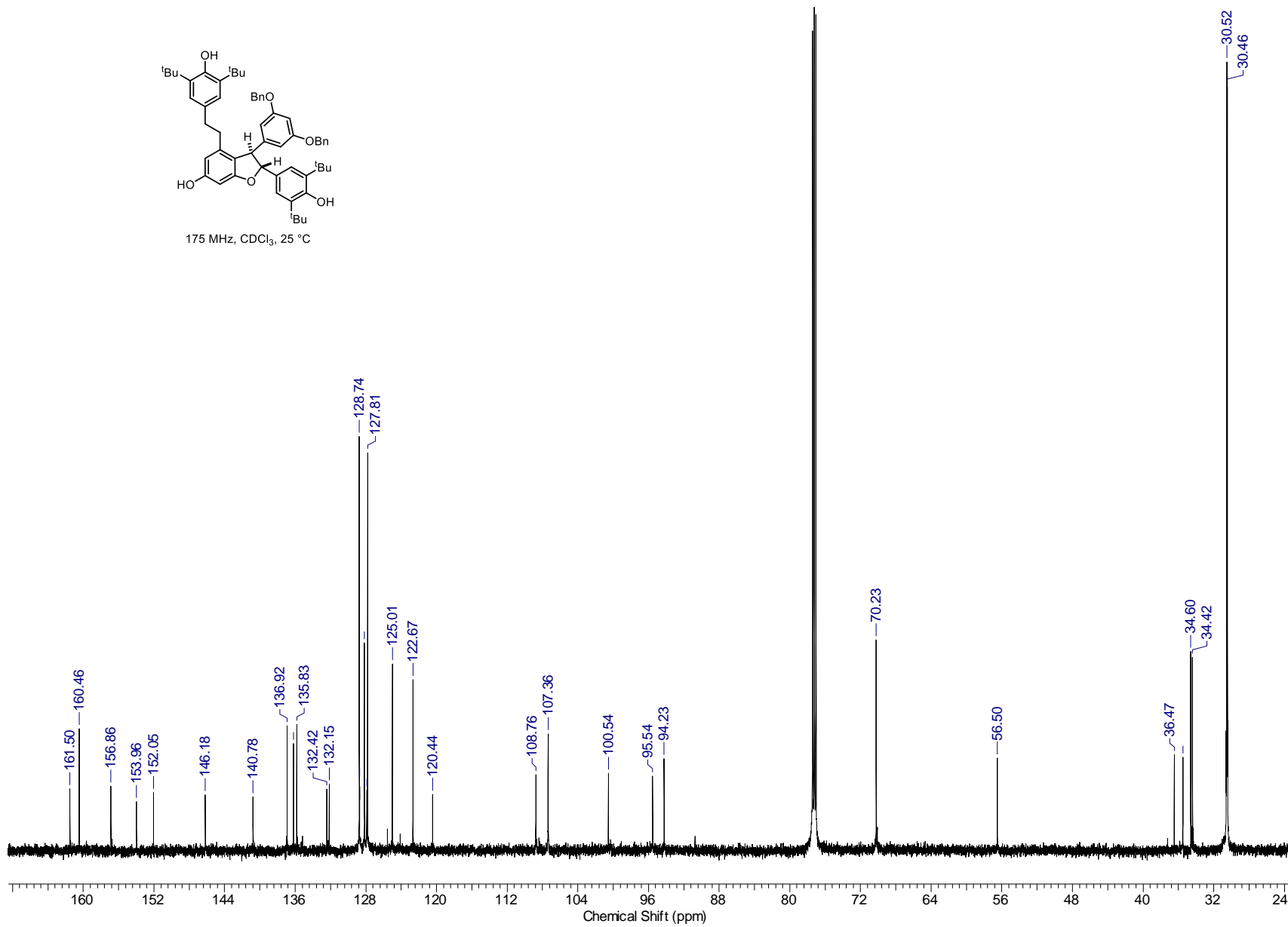
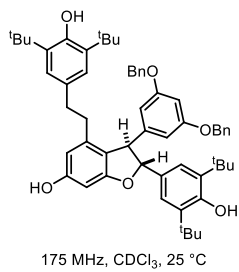


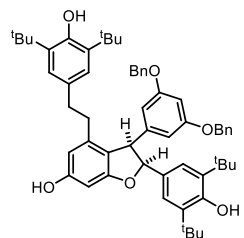




245

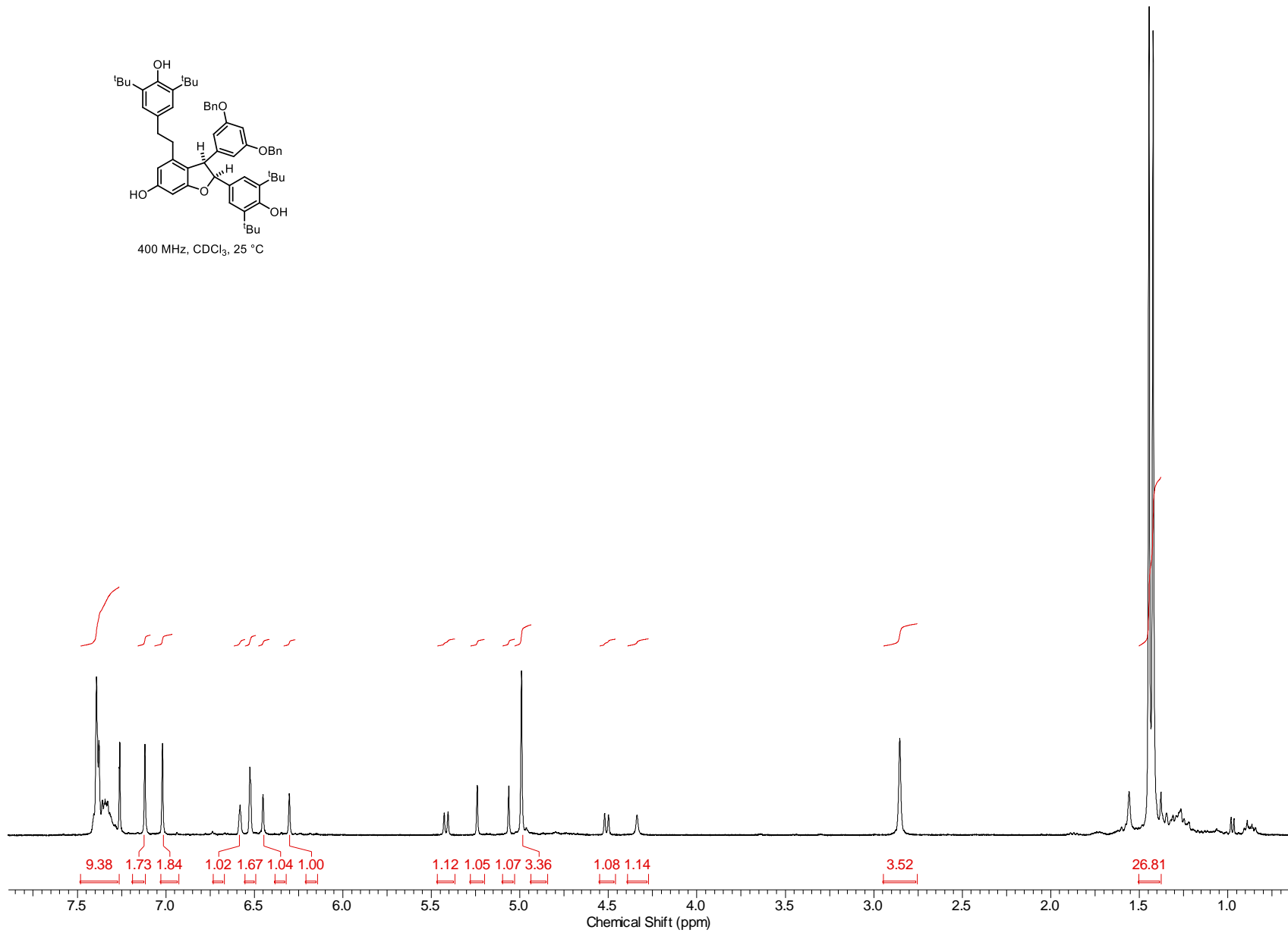


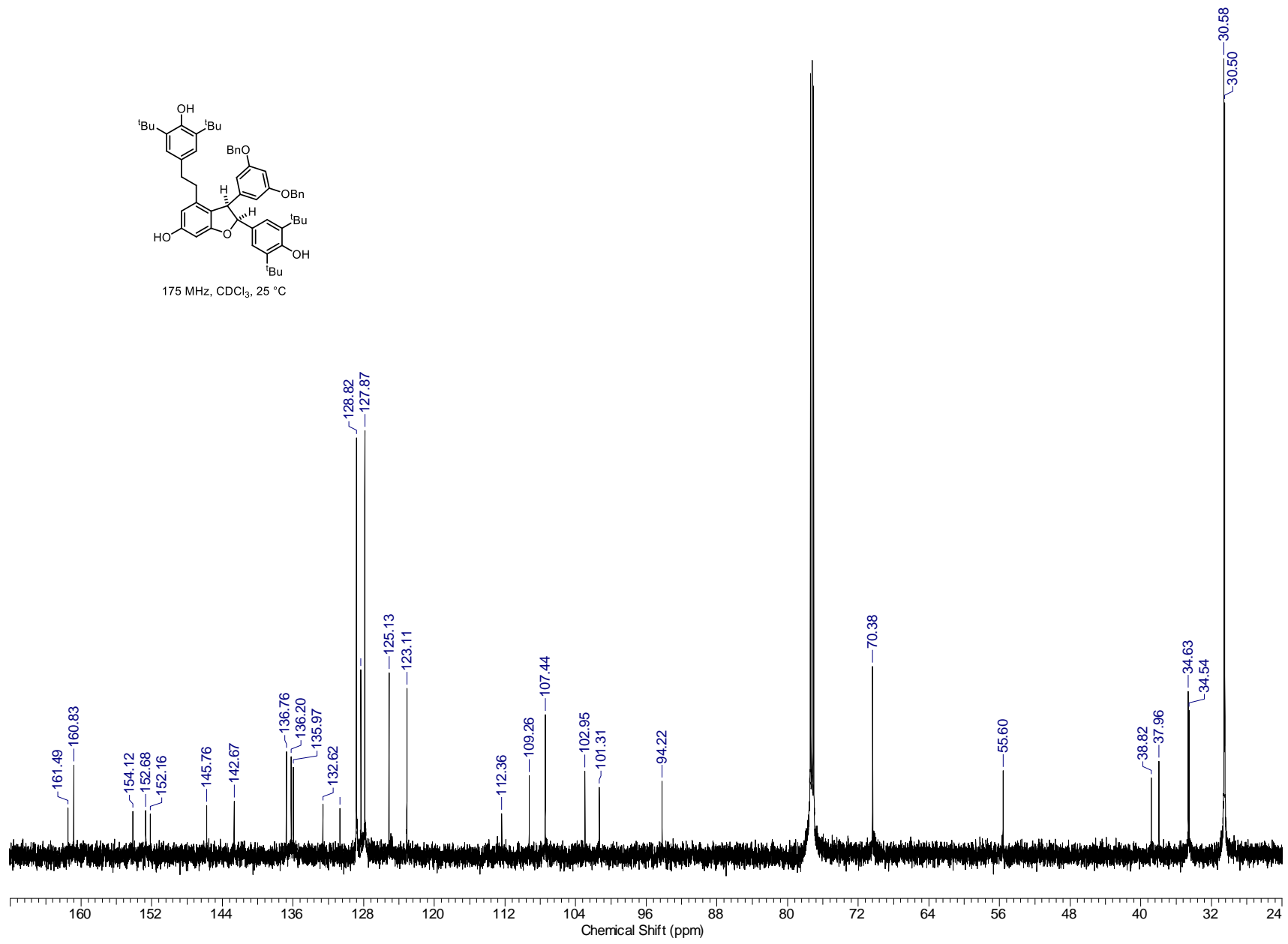
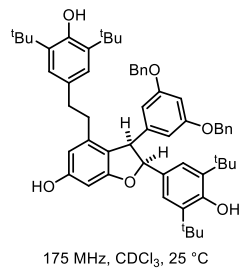


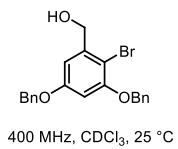


400 MHz, CDCl₃, 25 °C

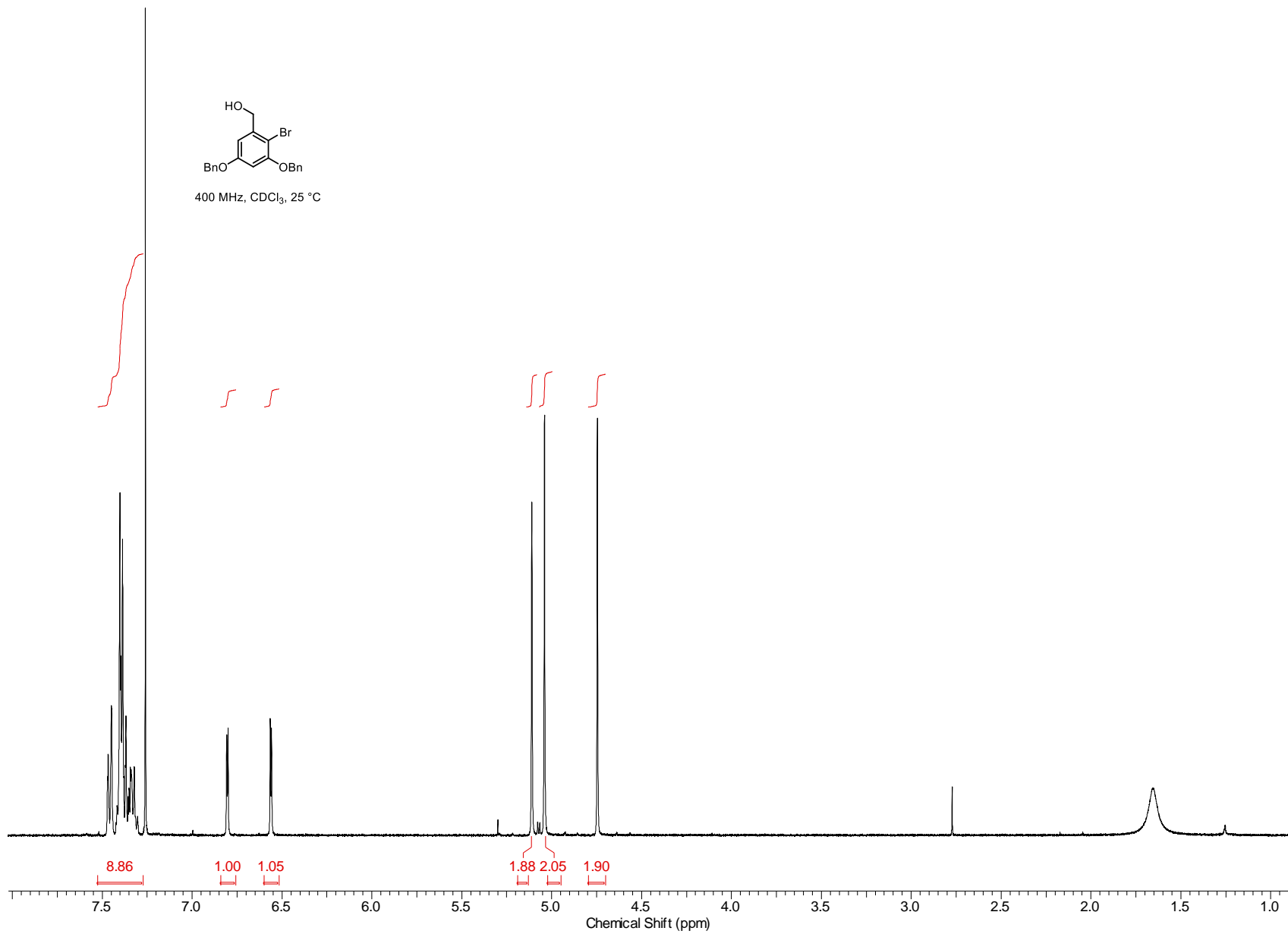
247



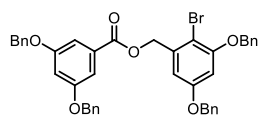




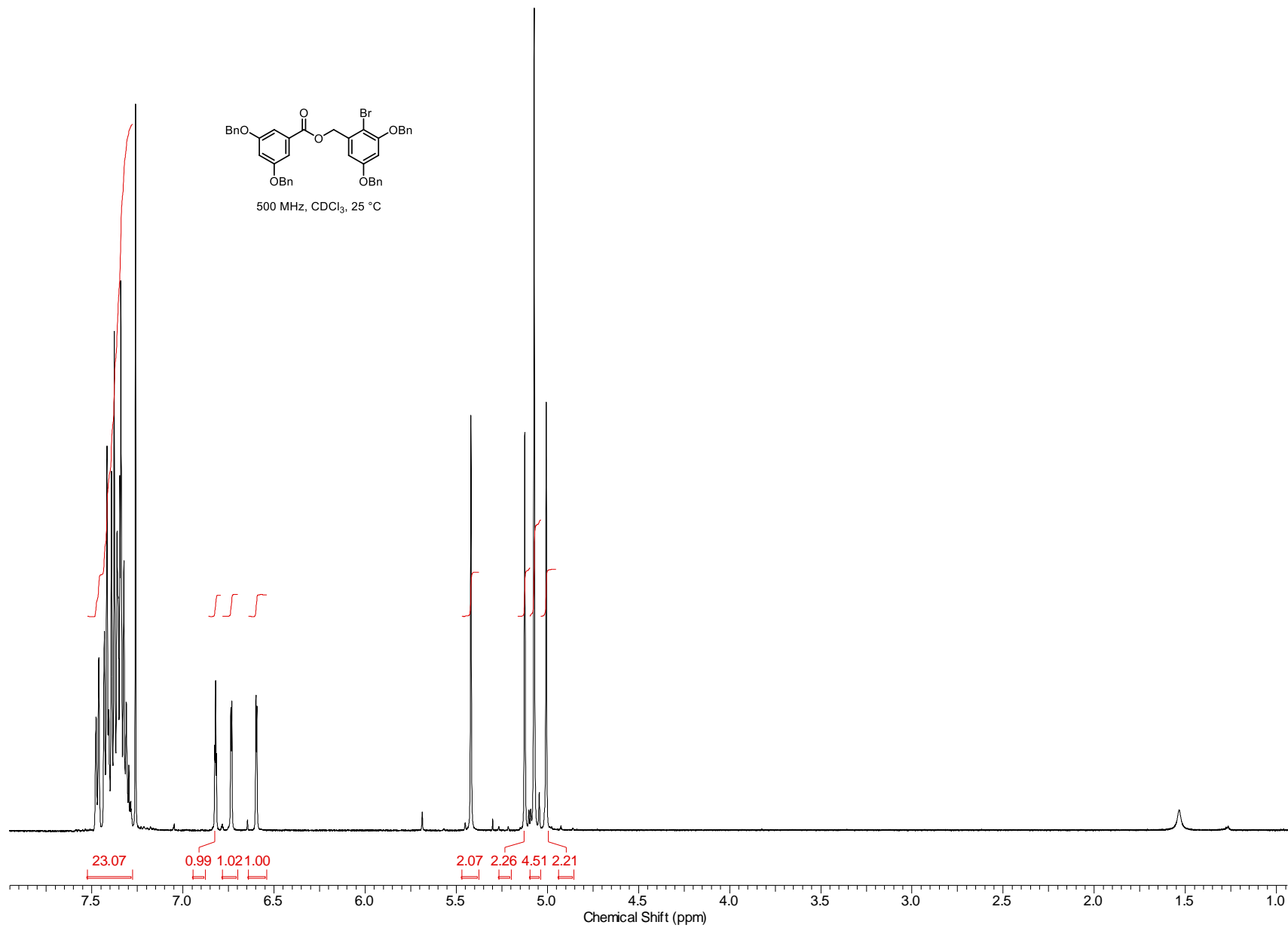
249

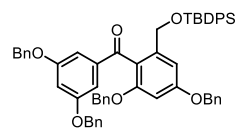


250



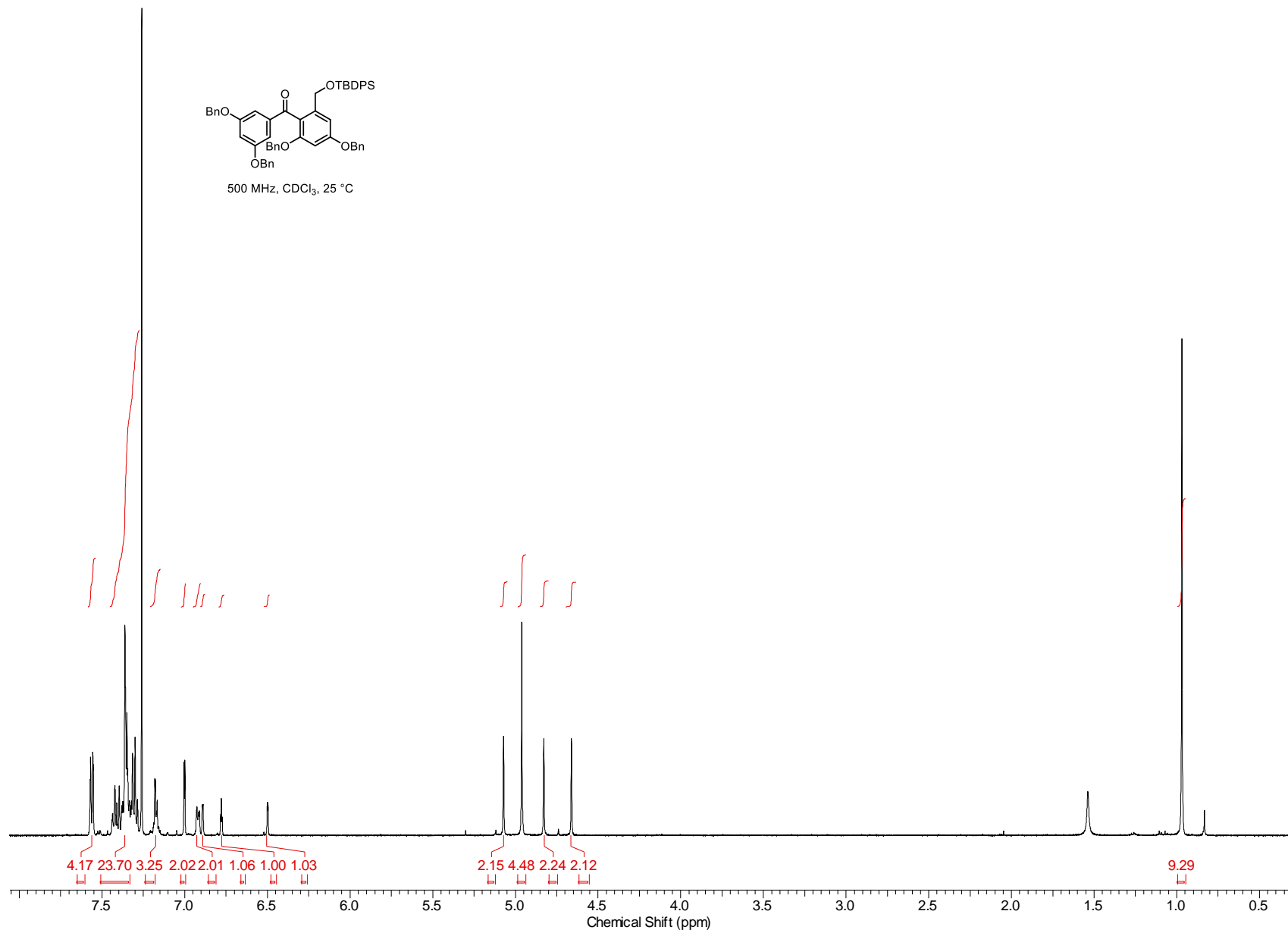
500 MHz, CDCl₃, 25 °C

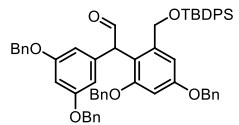




500 MHz, CDCl₃, 25 °C

251

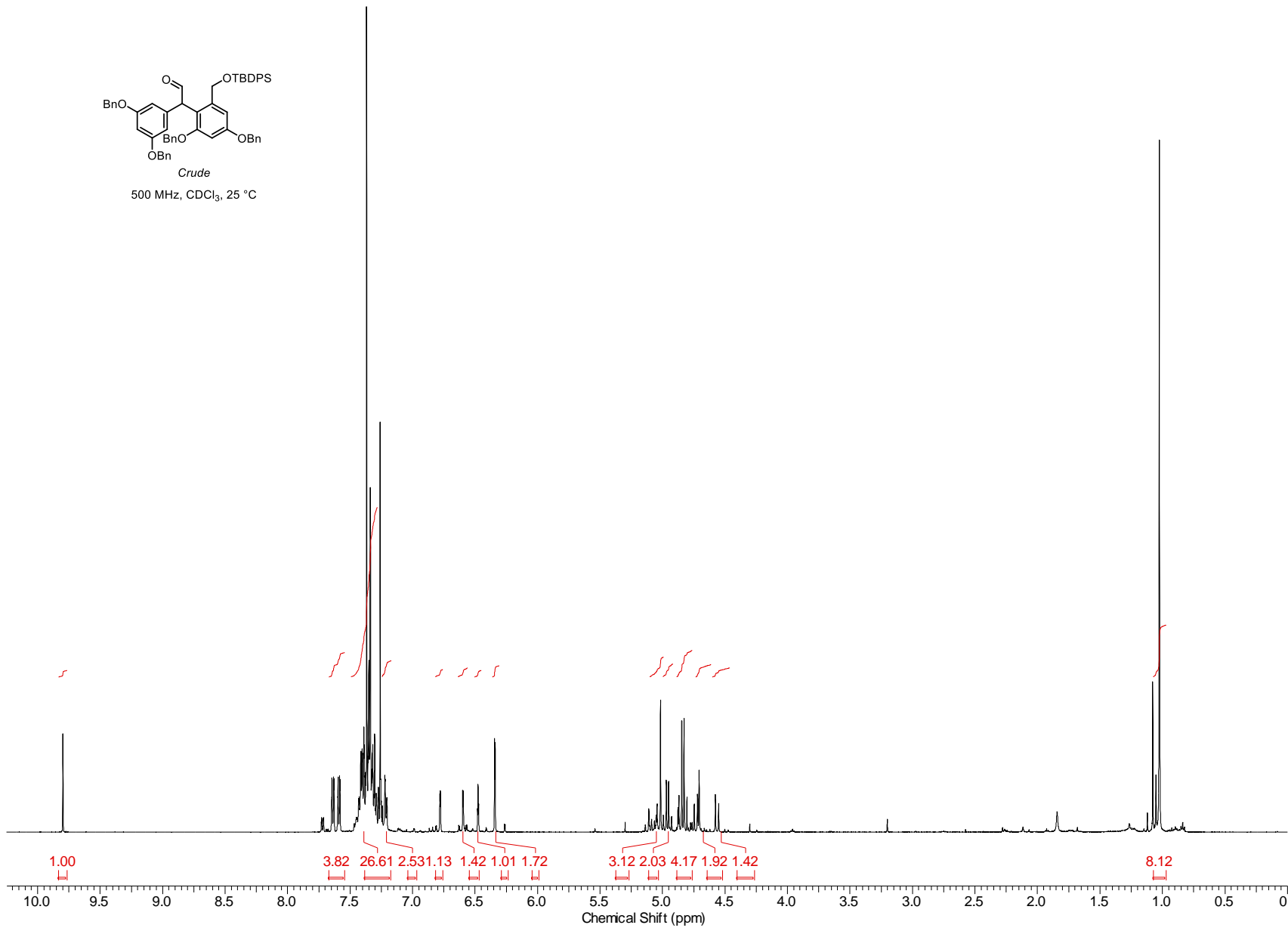


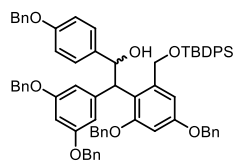


Crude

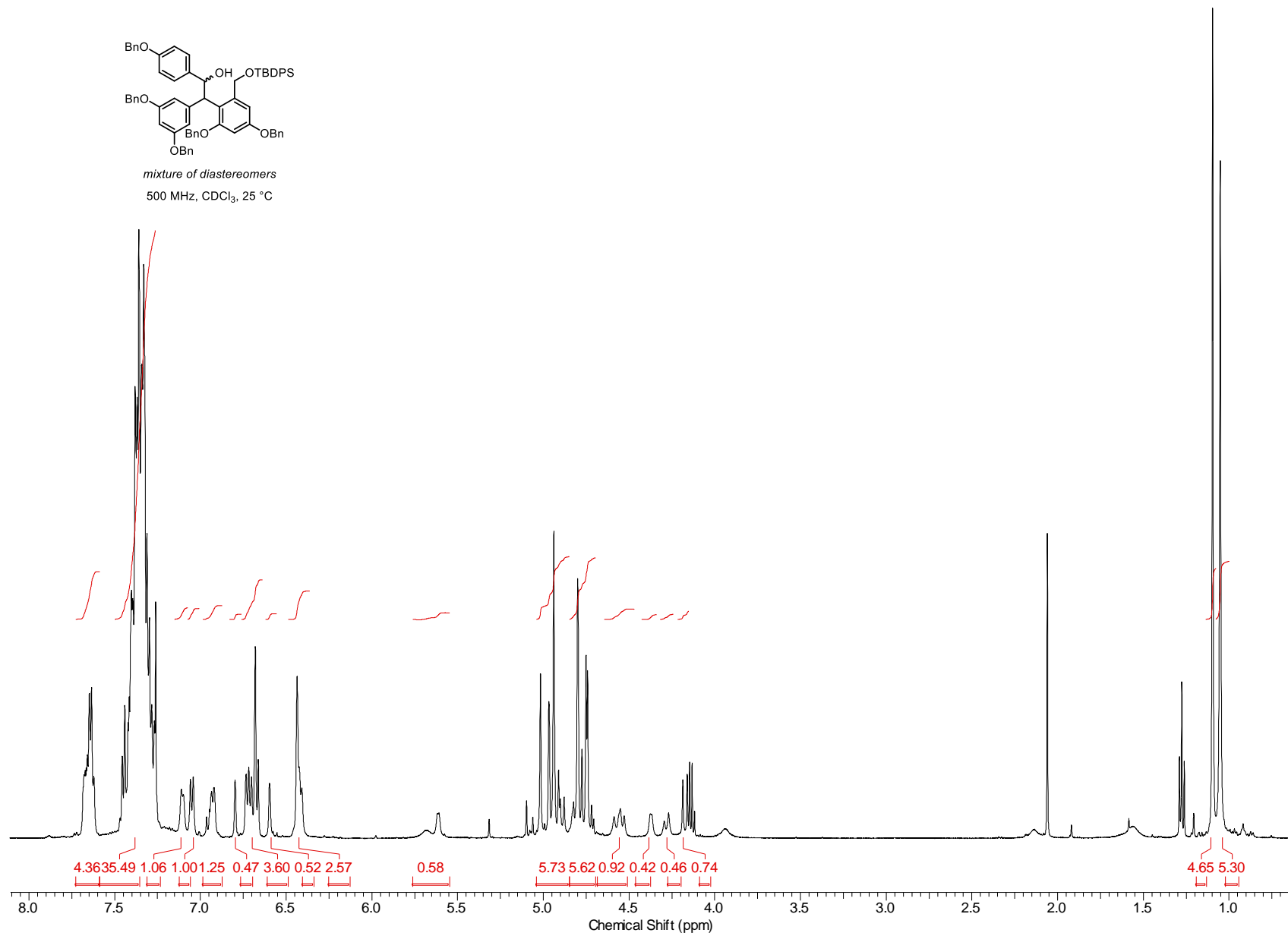
500 MHz, CDCl₃, 25 °C

252

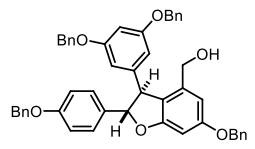




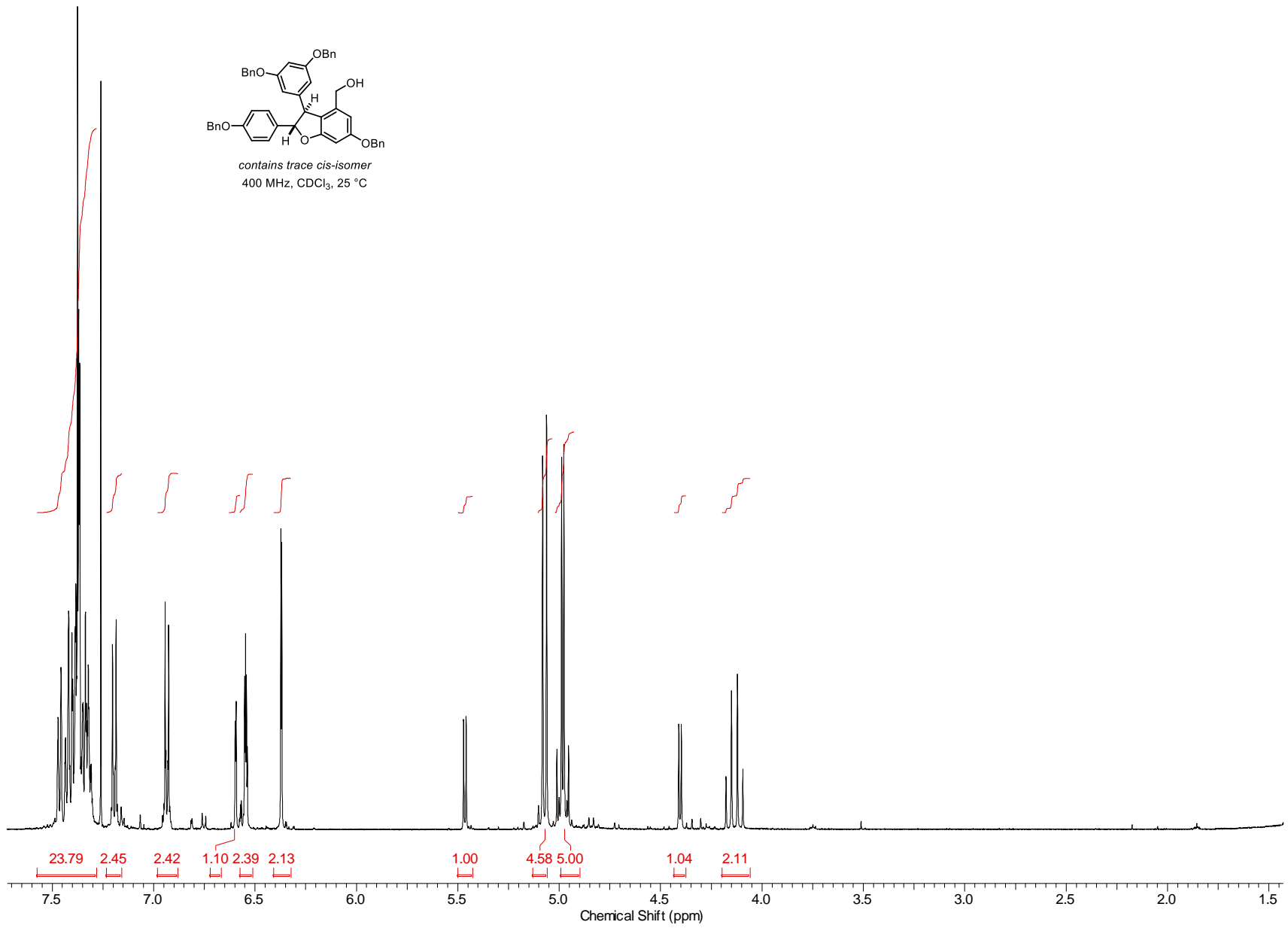
mixture of diastereomers
500 MHz, CDCl₃, 25 °C

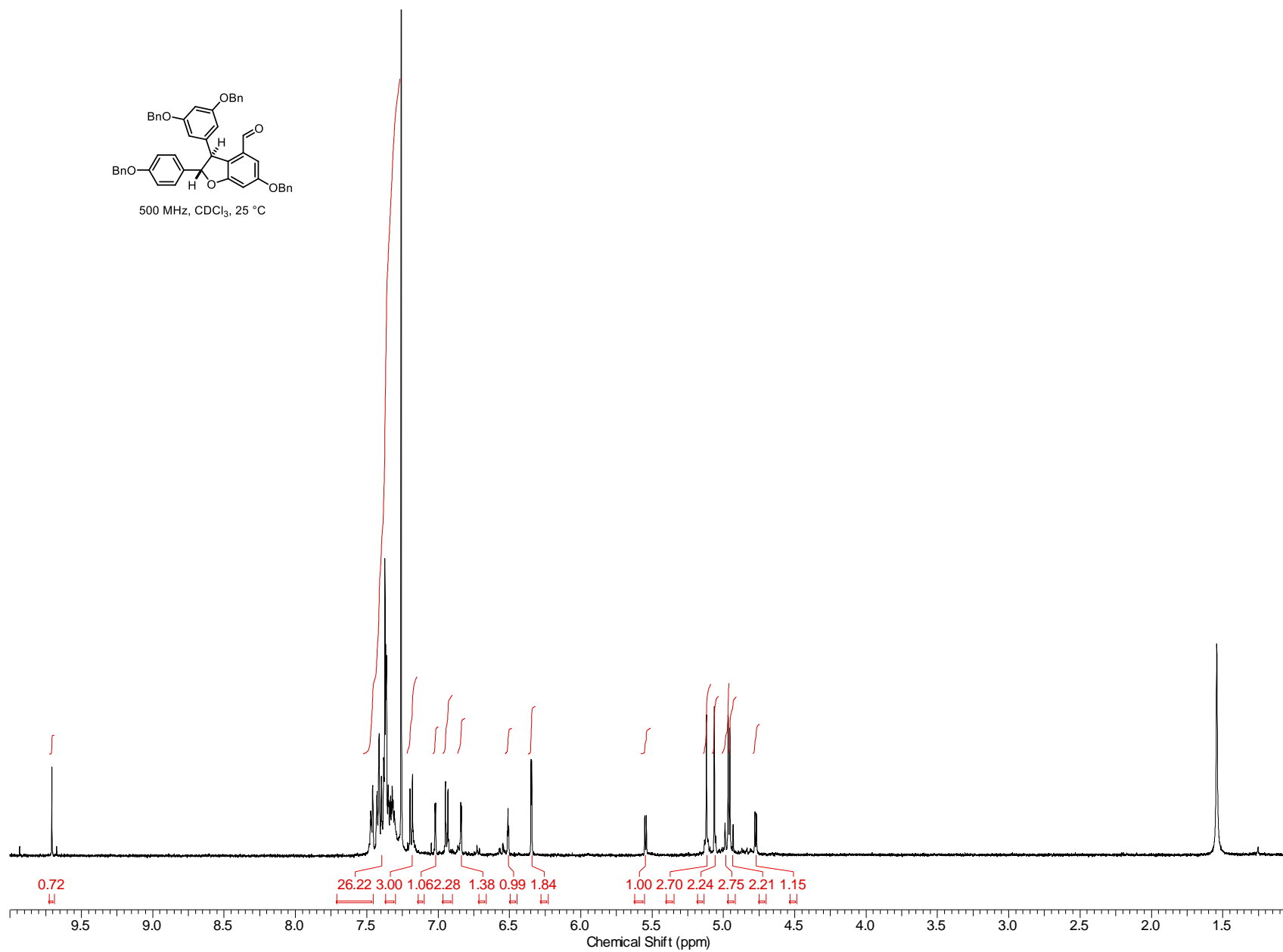
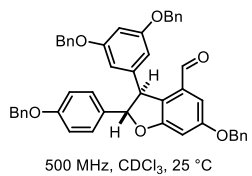


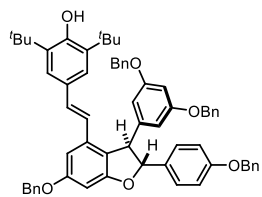
254



contains trace cis-isomer
400 MHz, CDCl₃, 25 °C

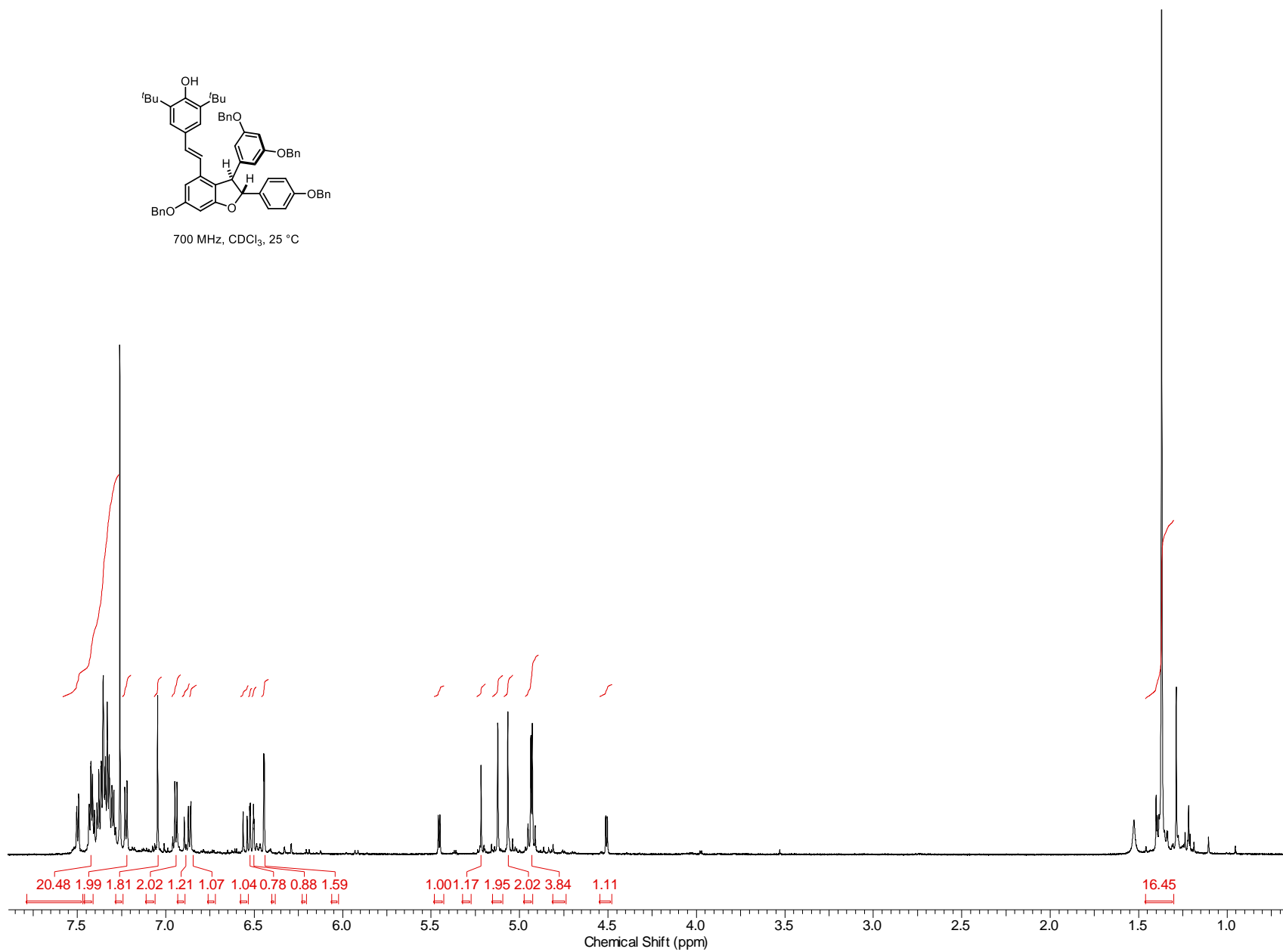


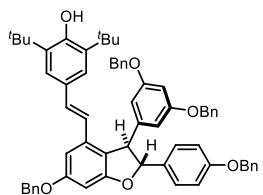




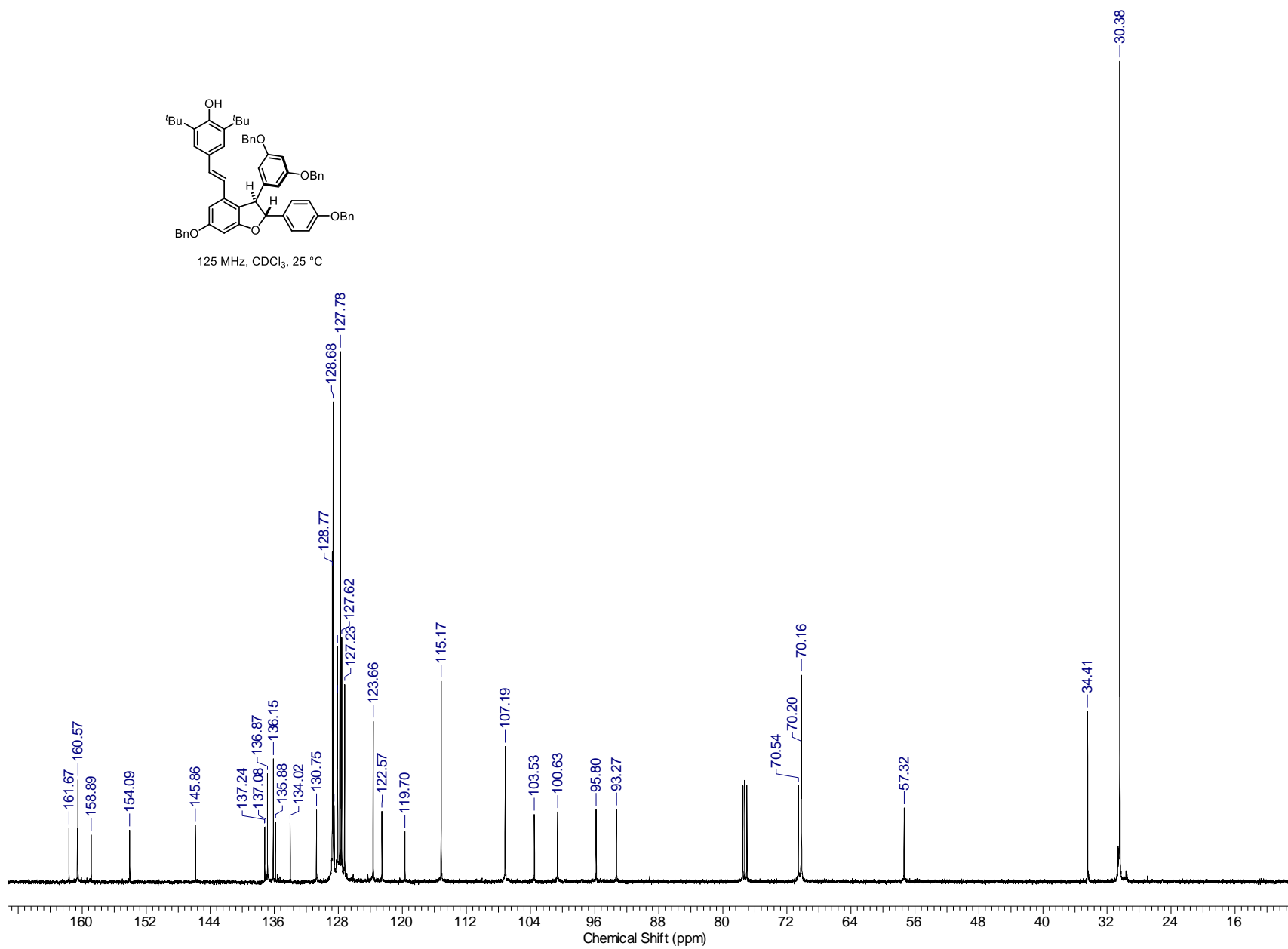
700 MHz, CDCl₃, 25 °C

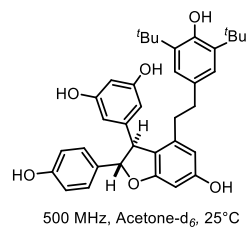
256



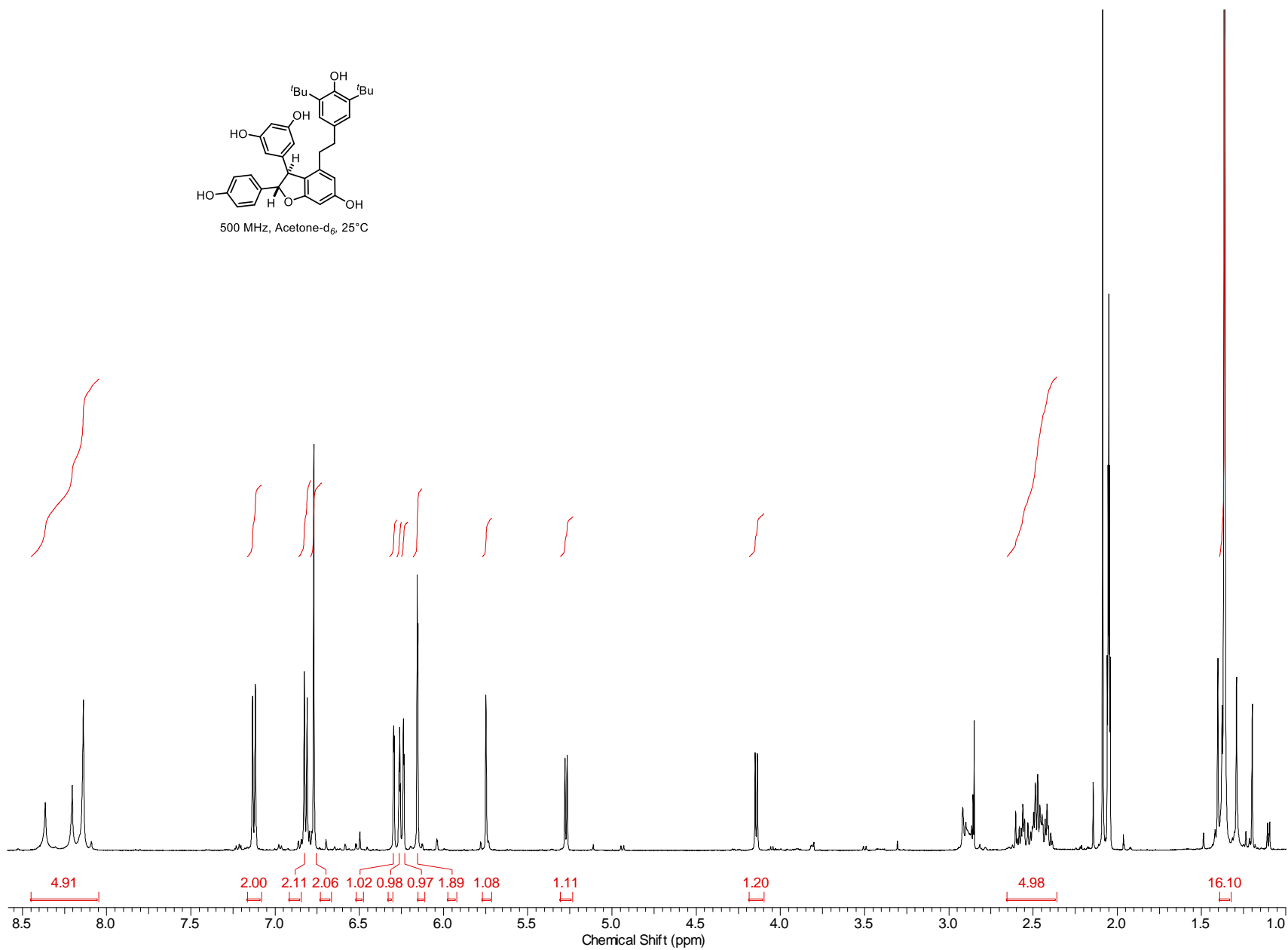


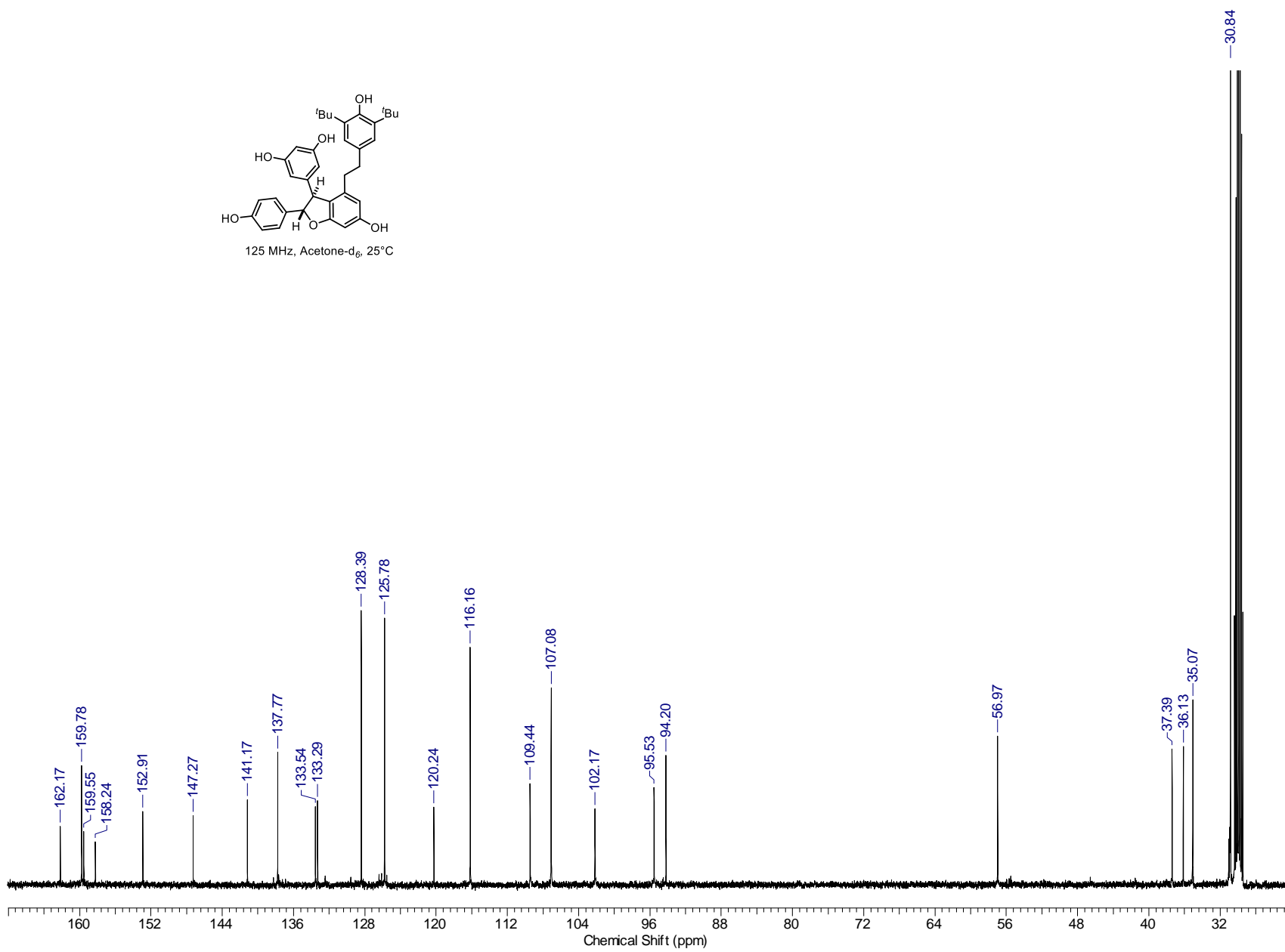
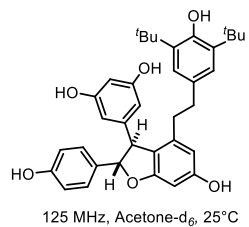
125 MHz, CDCl₃, 25 °C

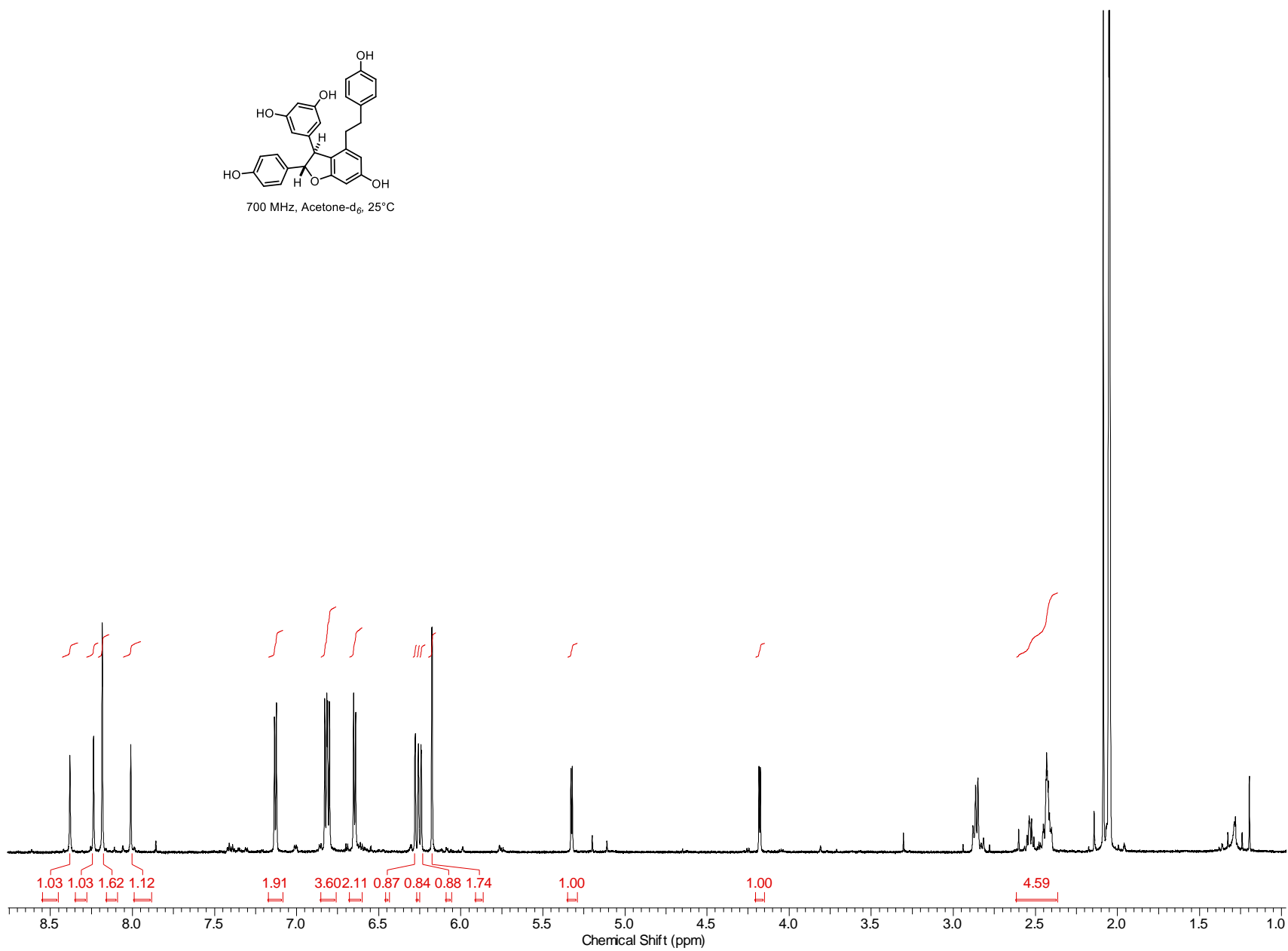
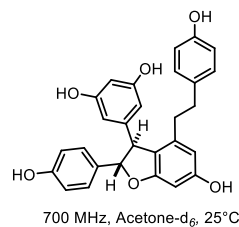


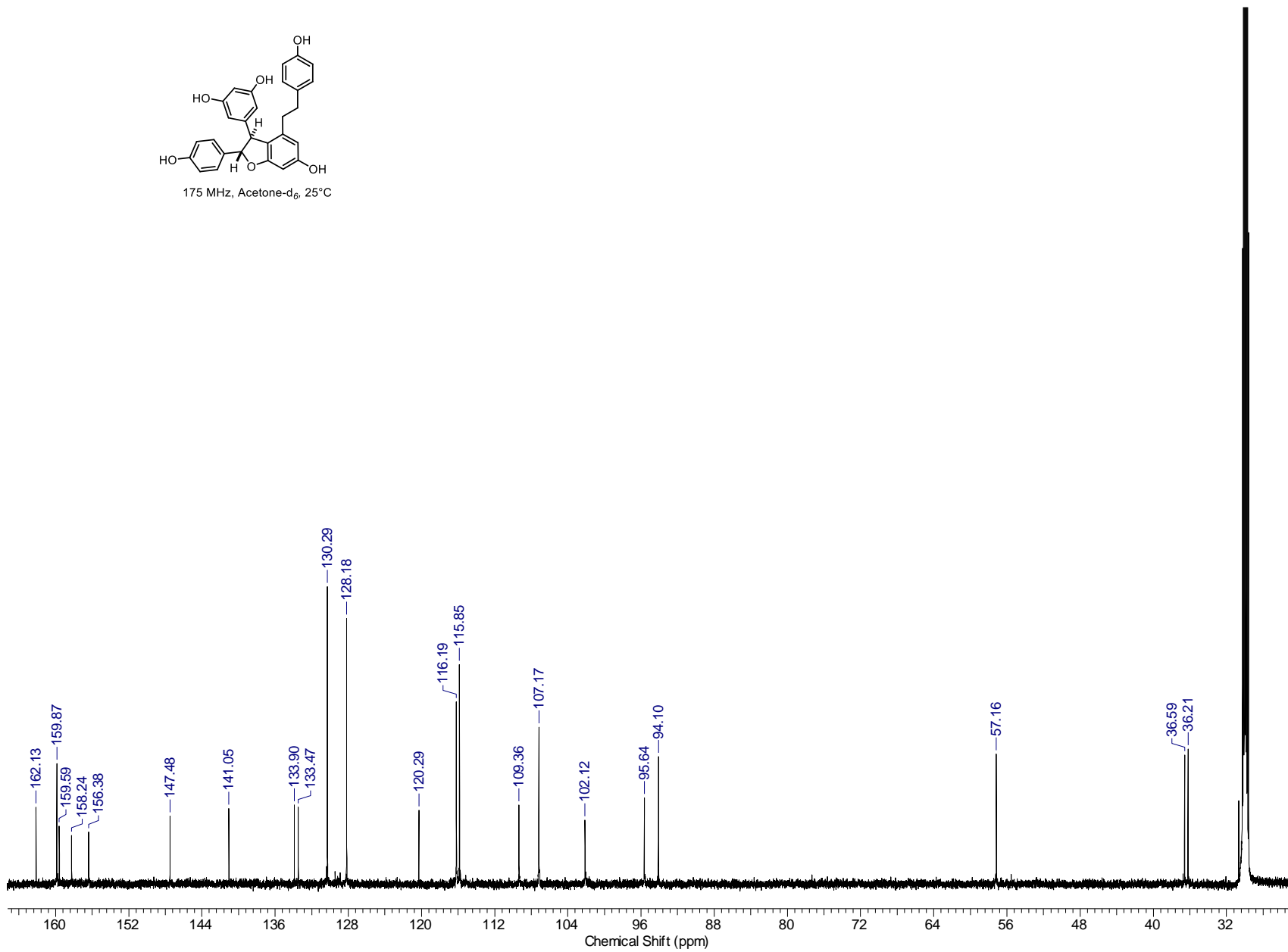
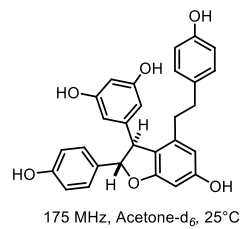


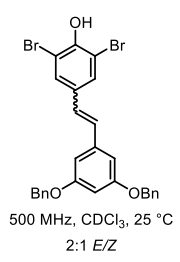
258



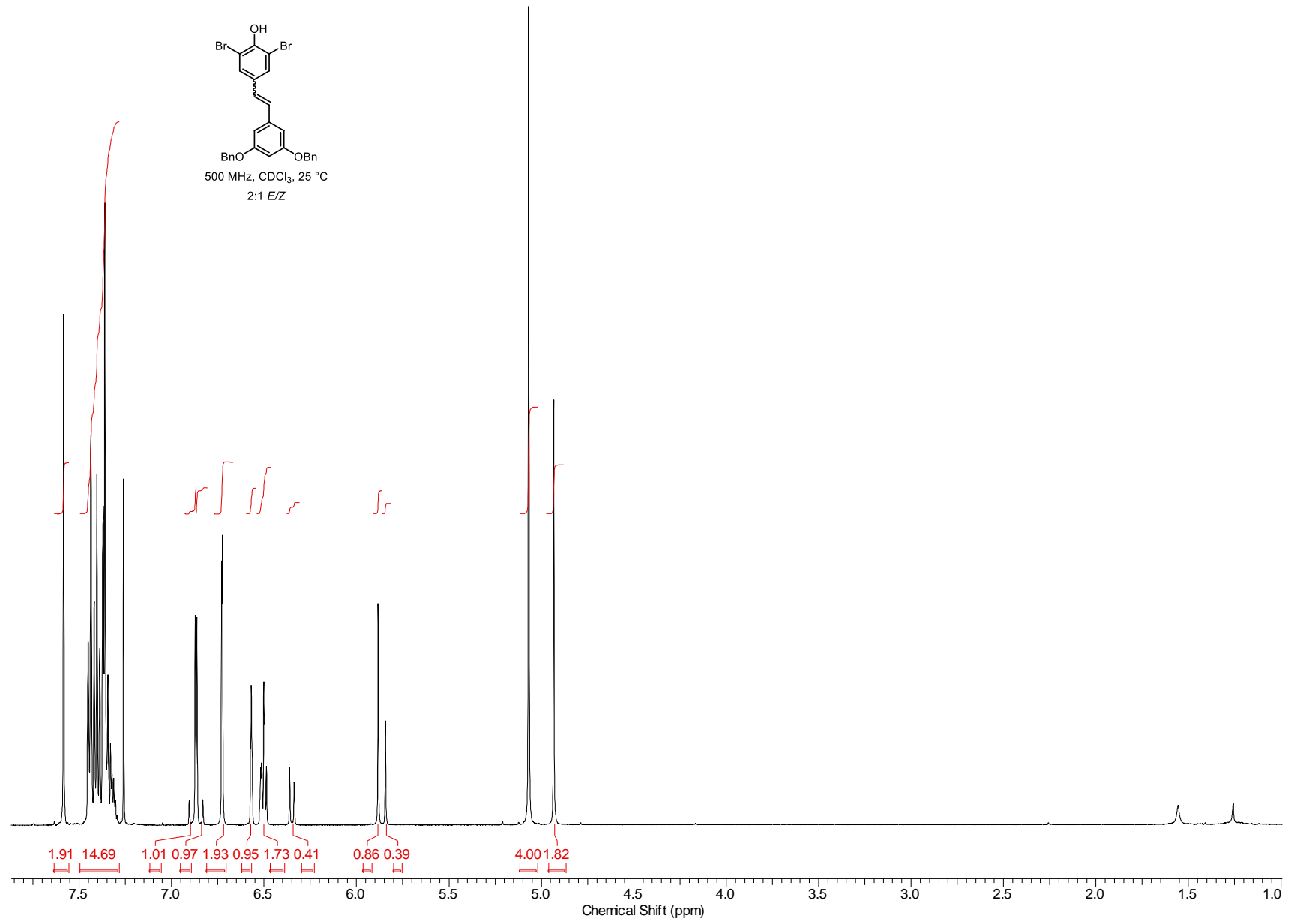


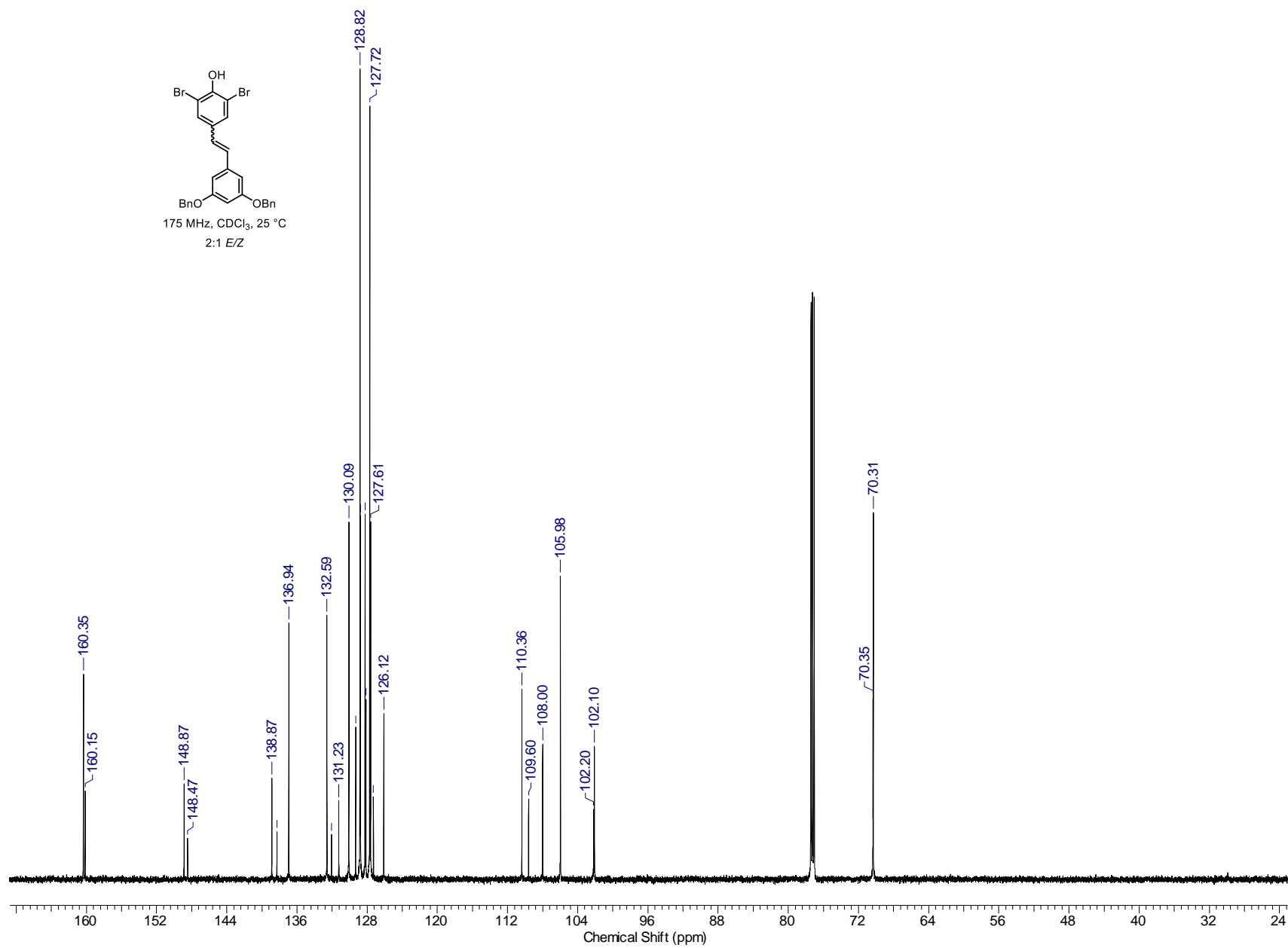


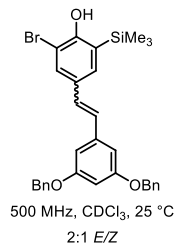




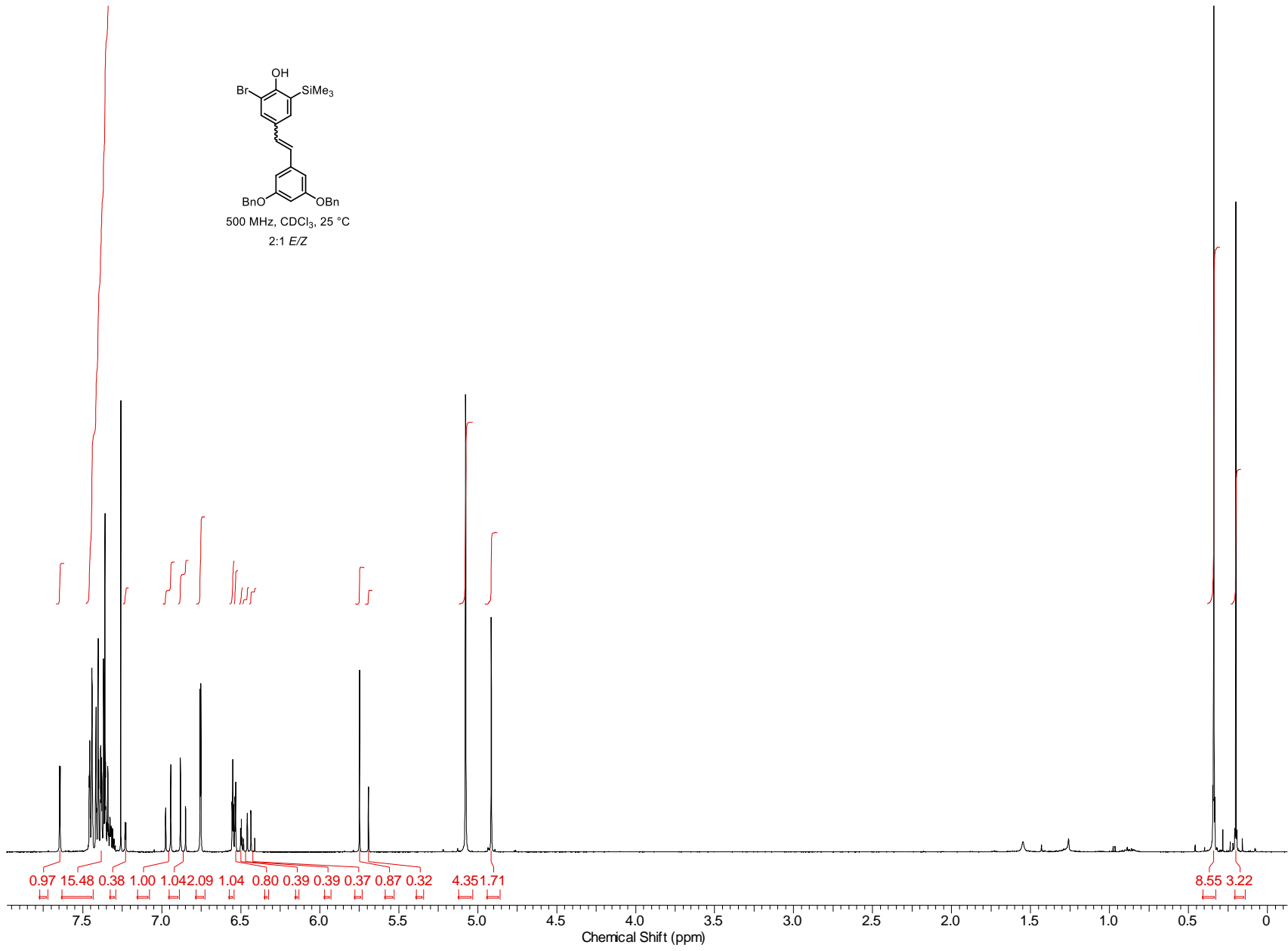
262

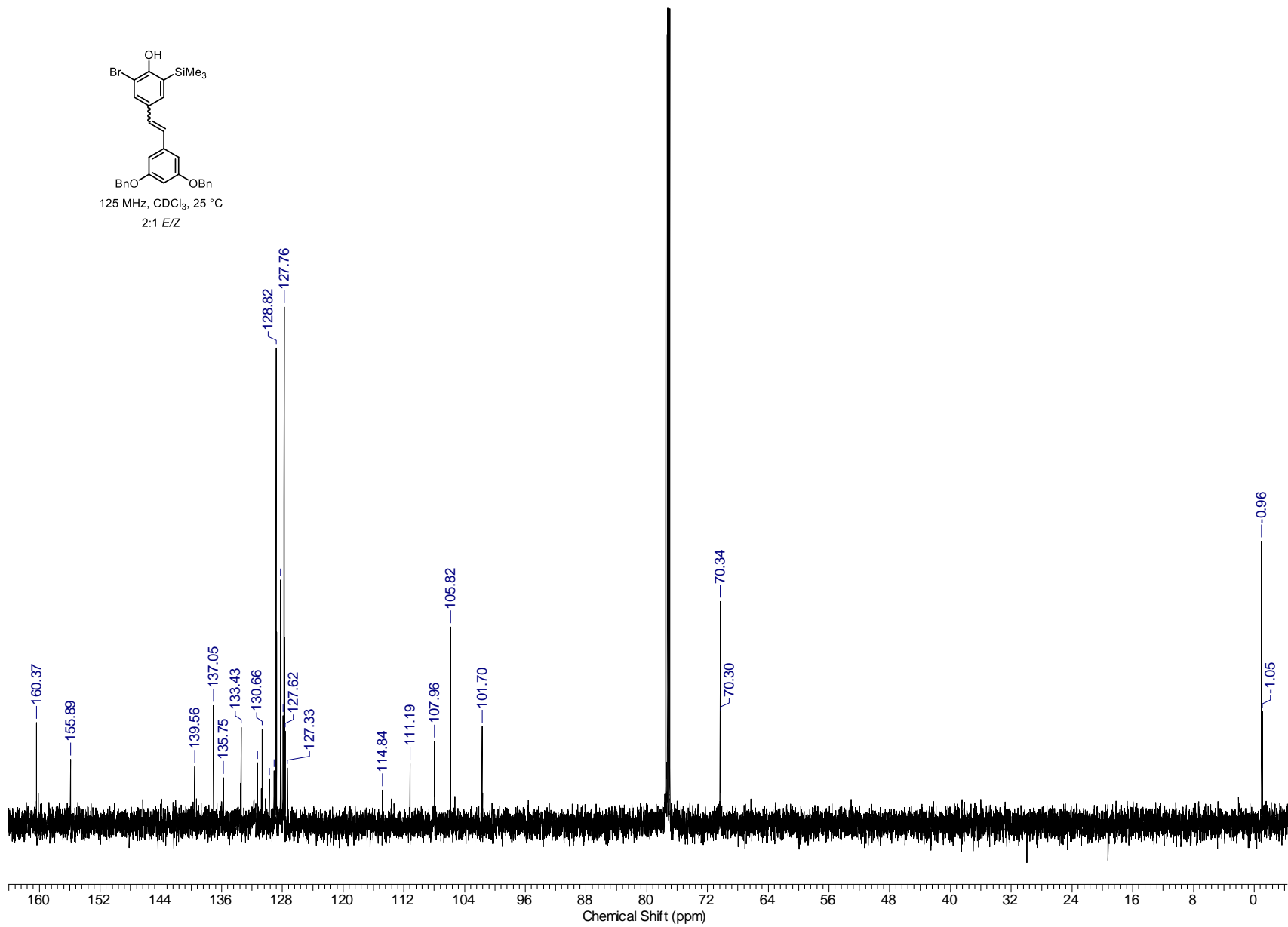
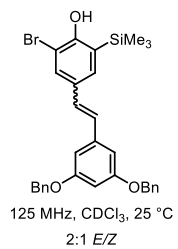




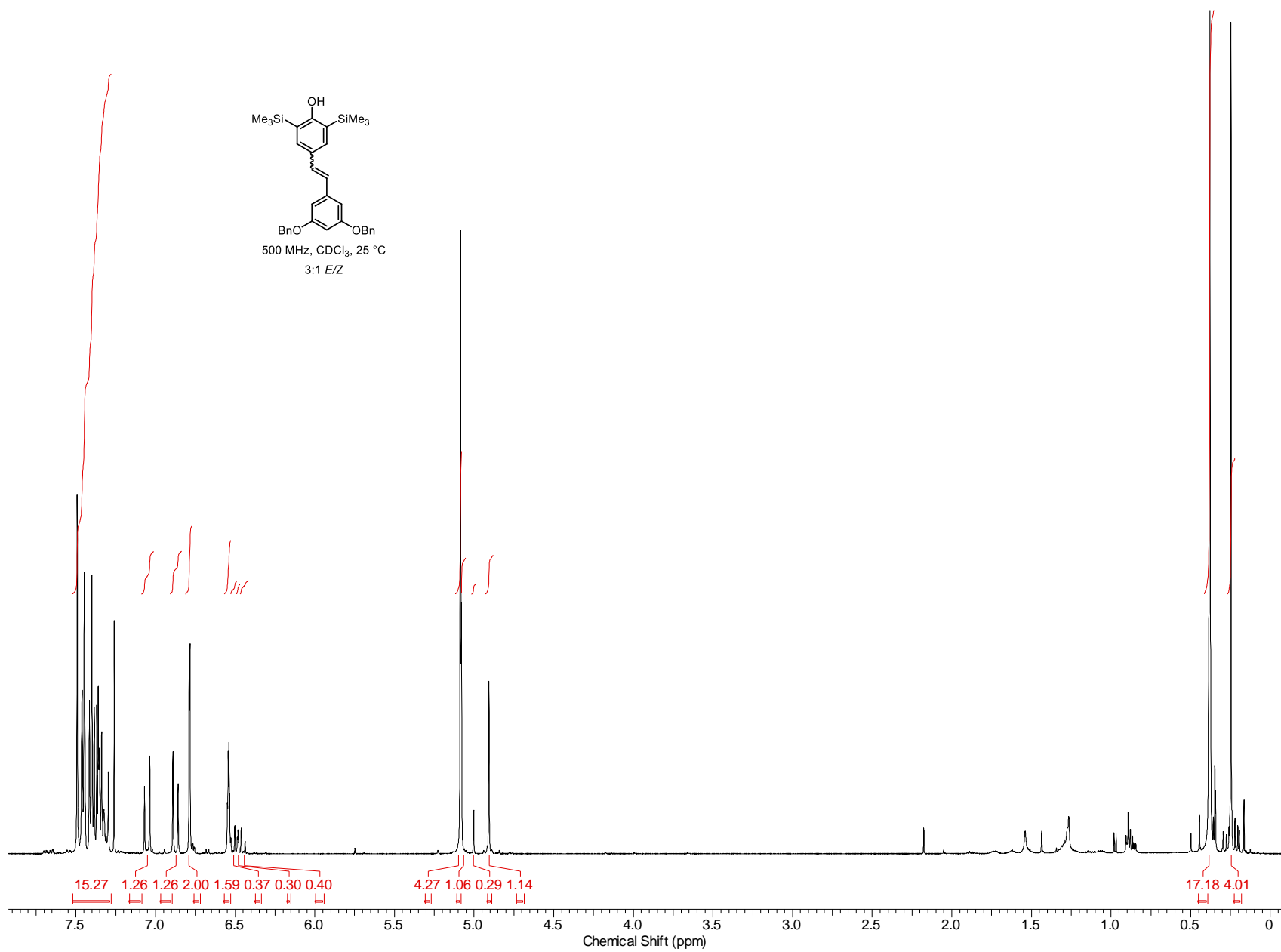
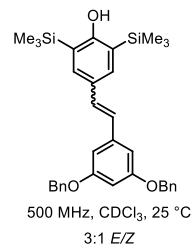


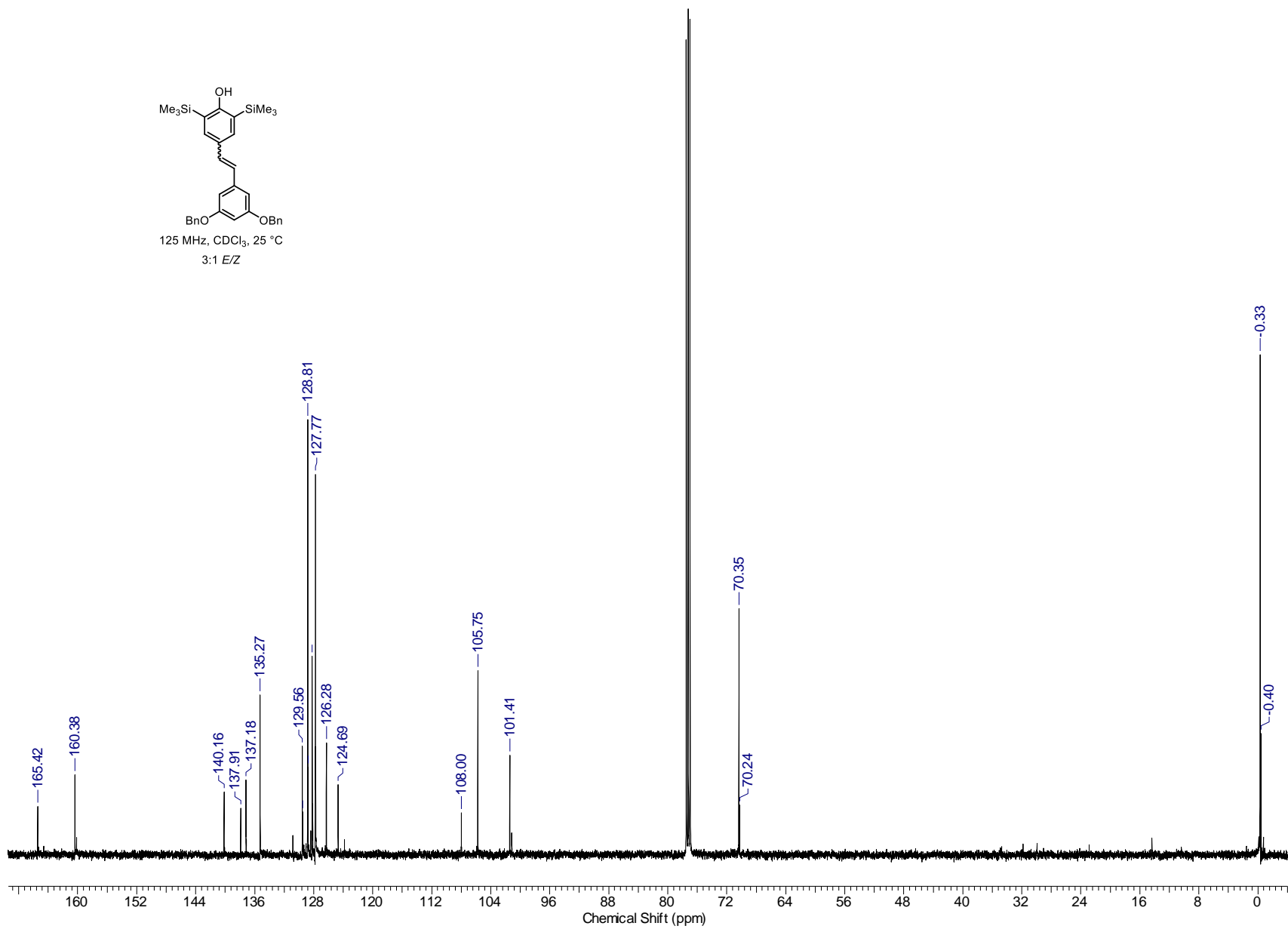
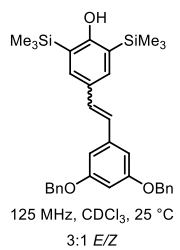
264

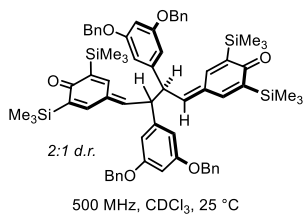




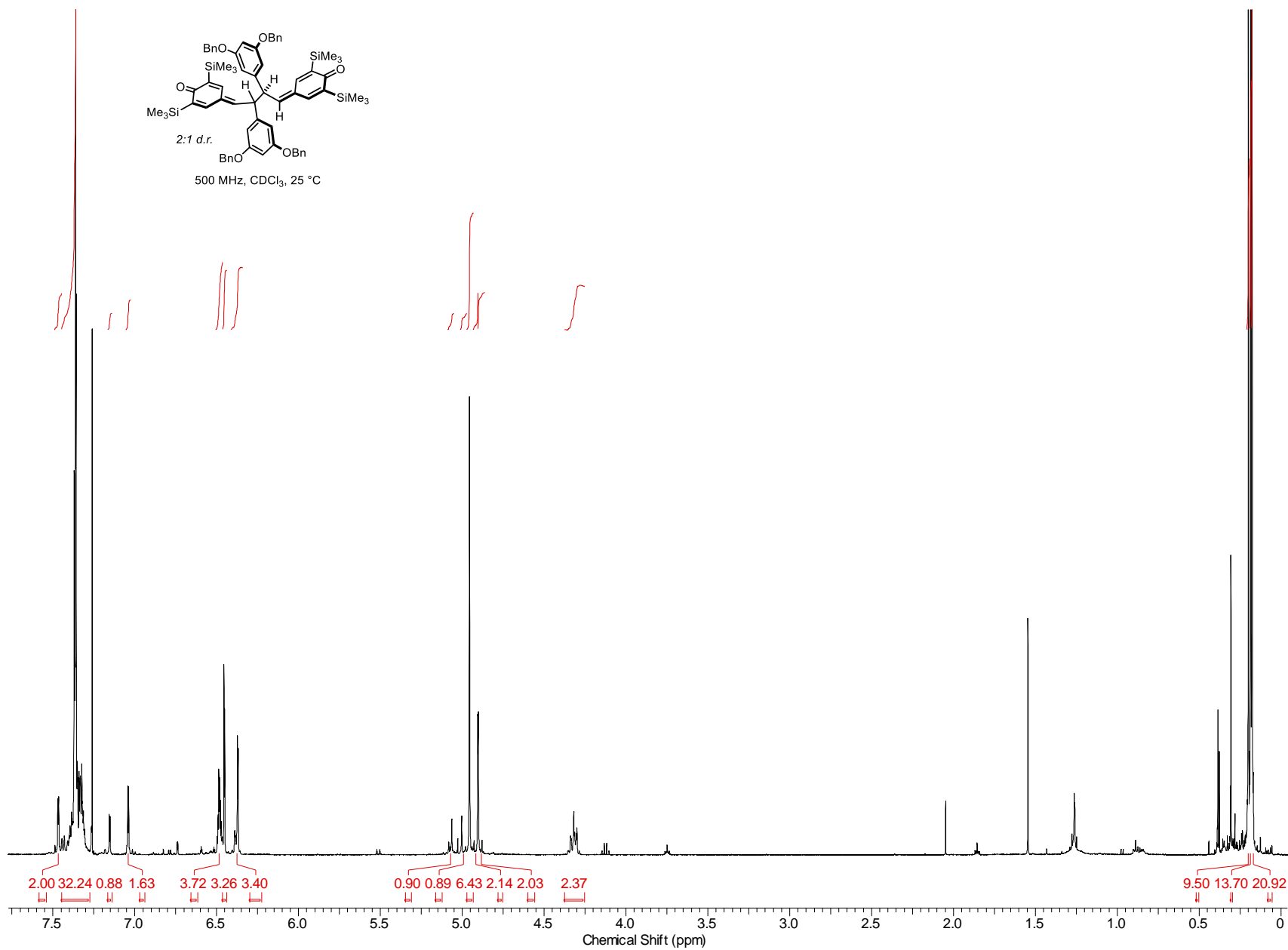
266

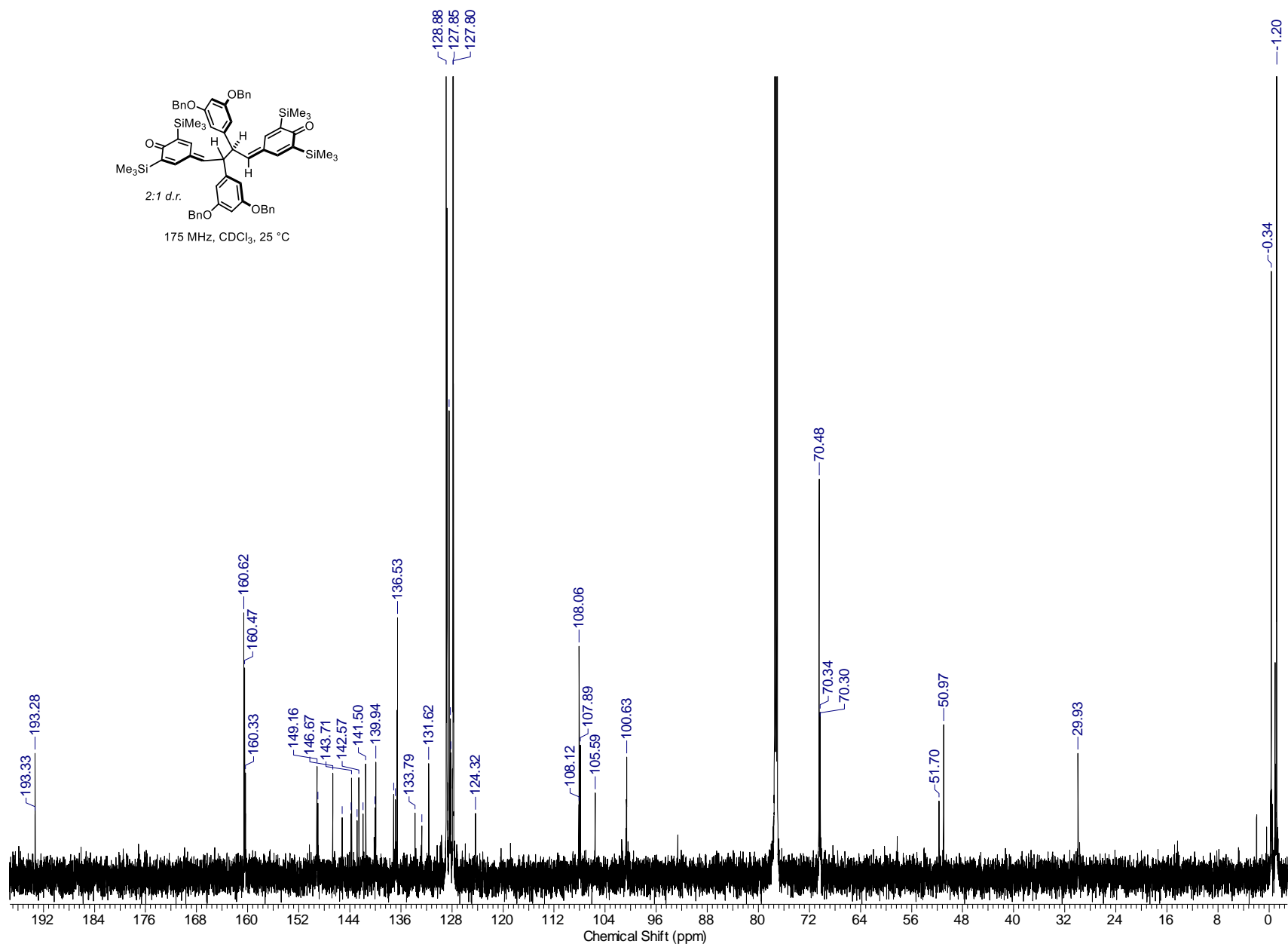


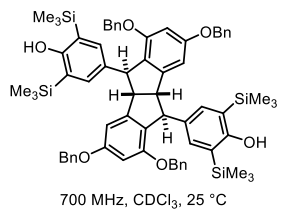




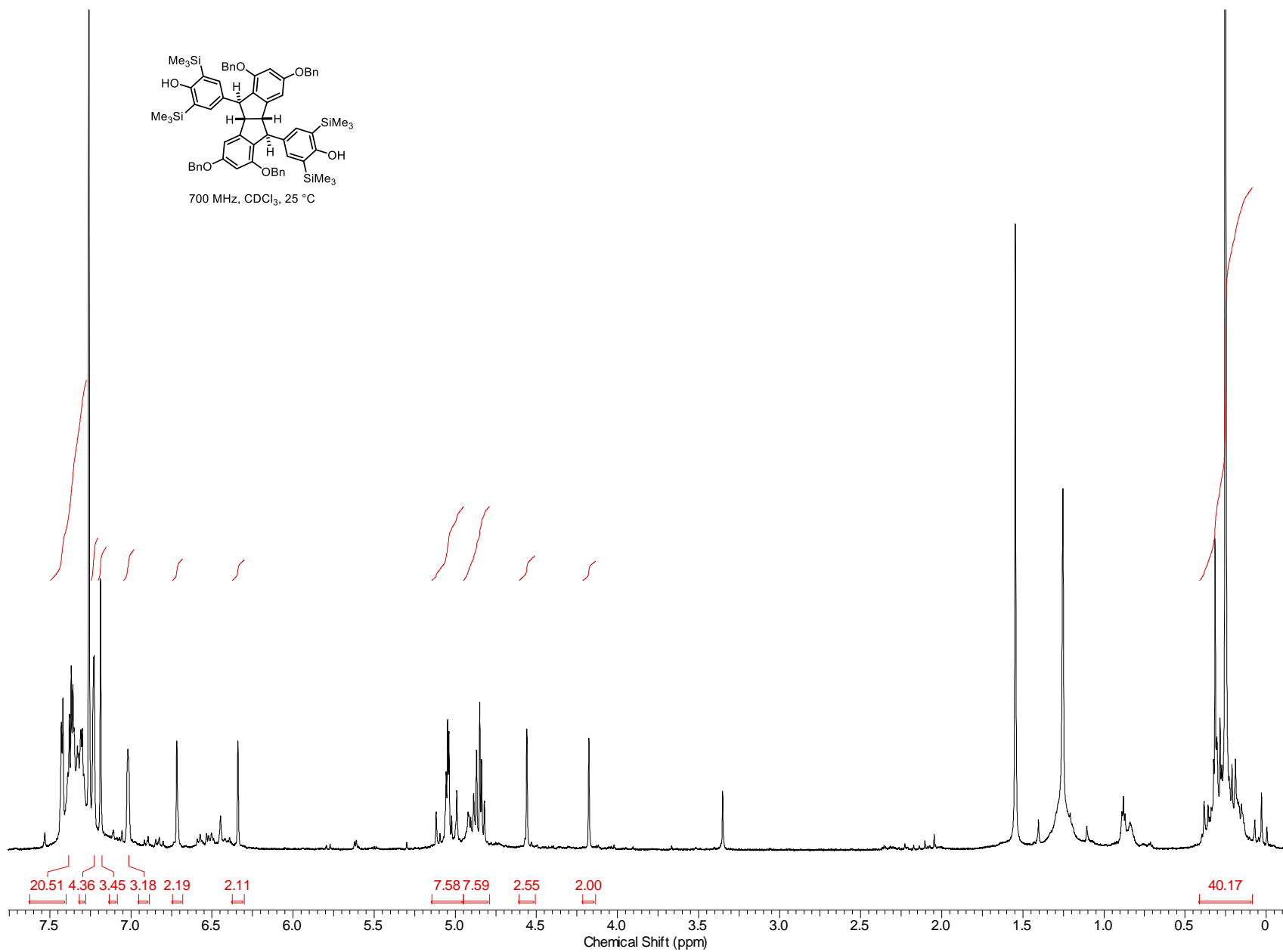
268



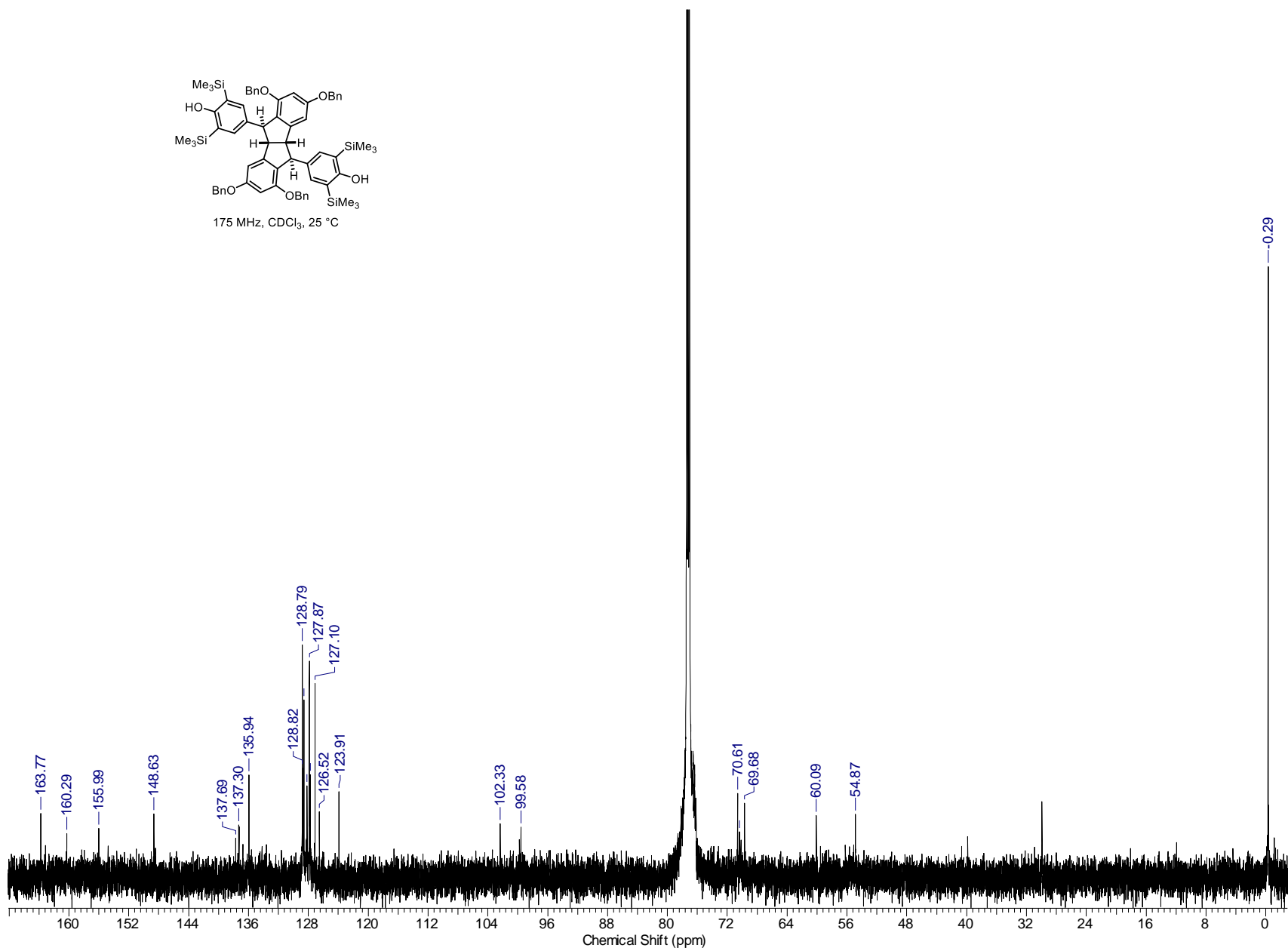
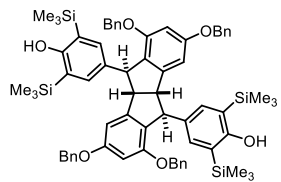




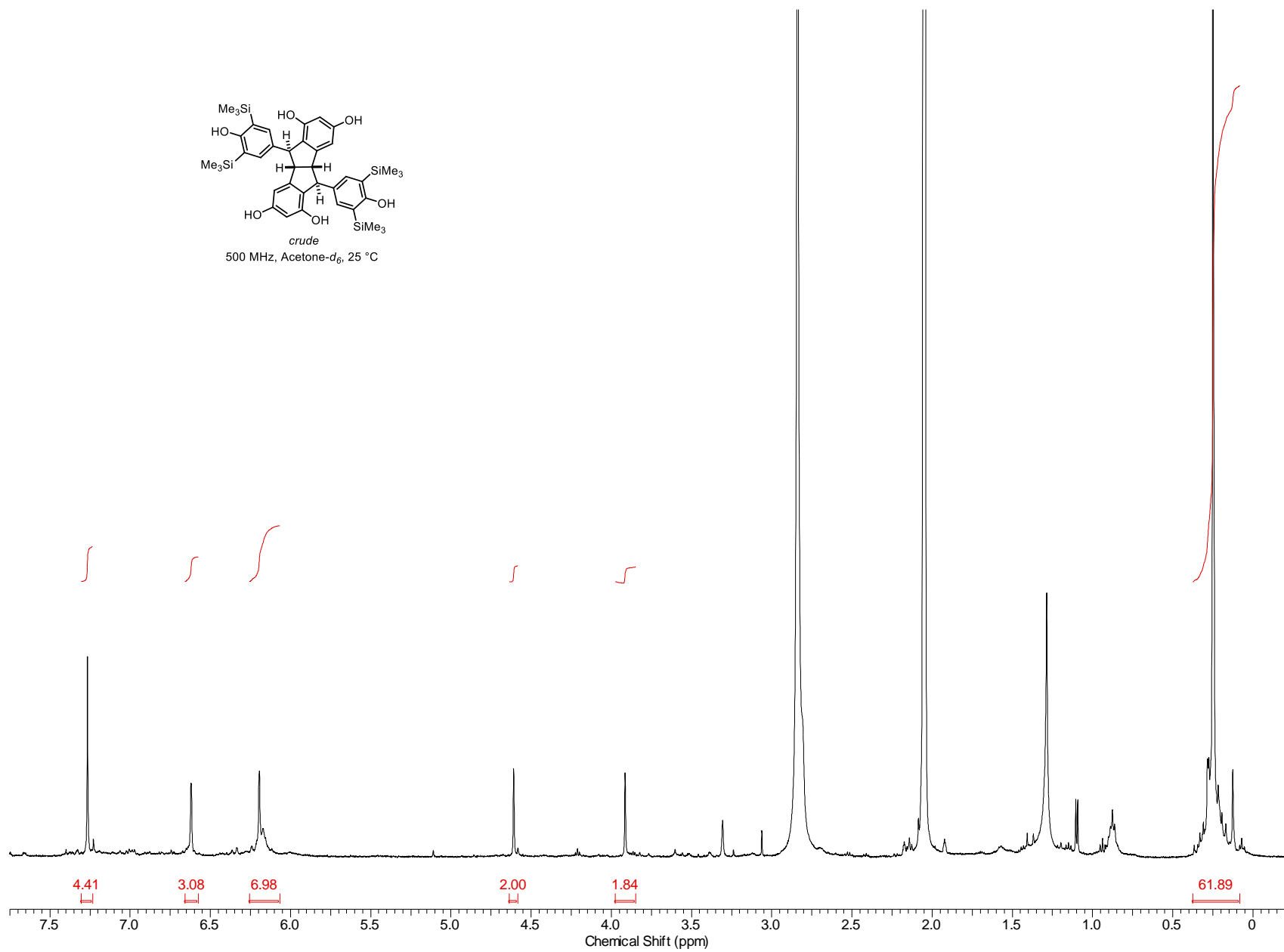
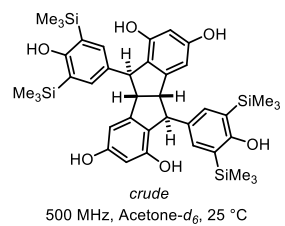
270

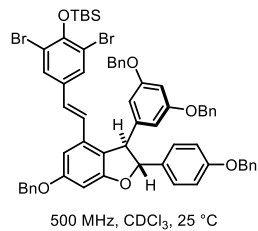


271

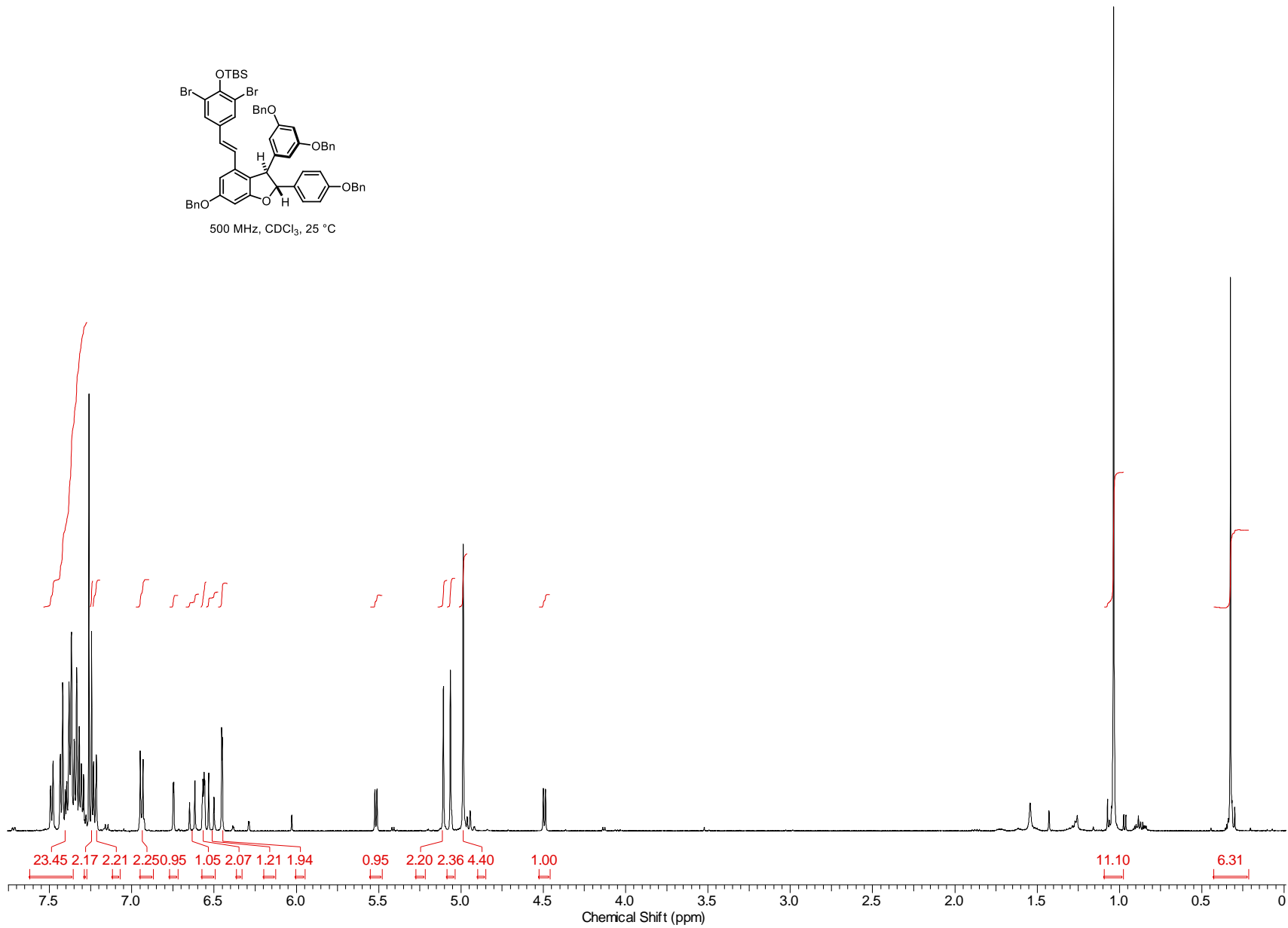


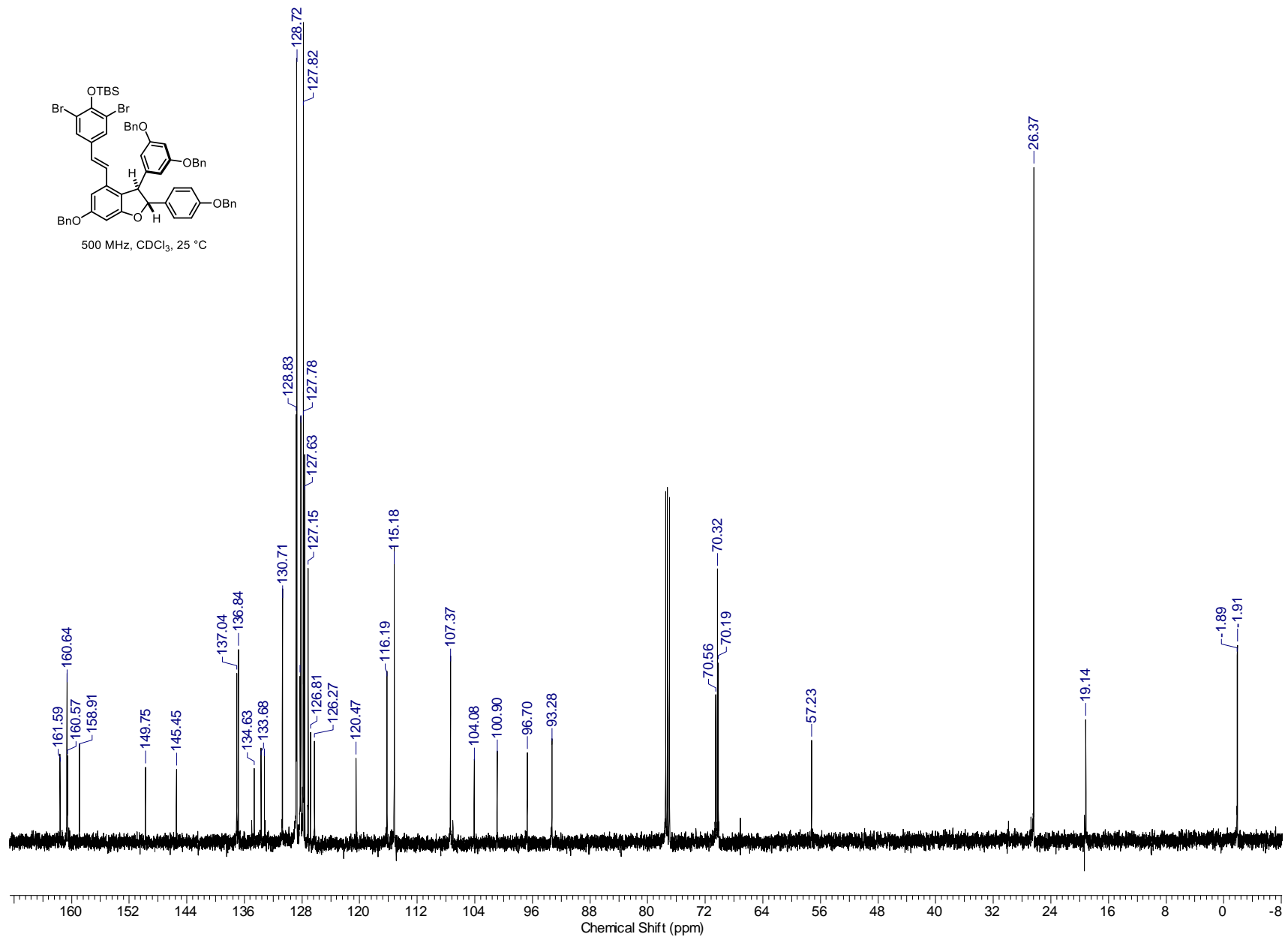
272



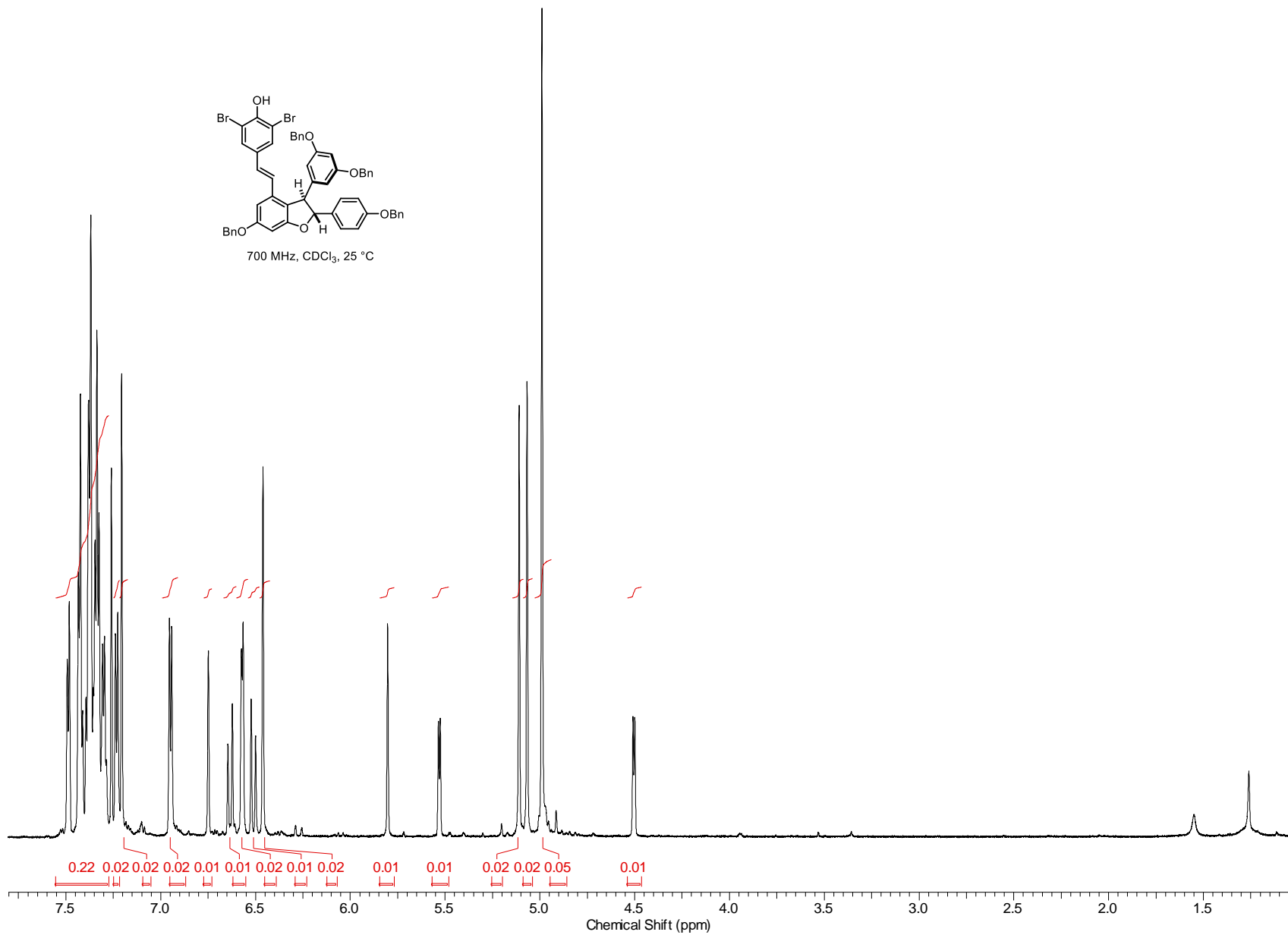
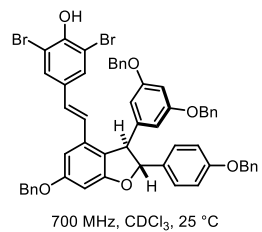


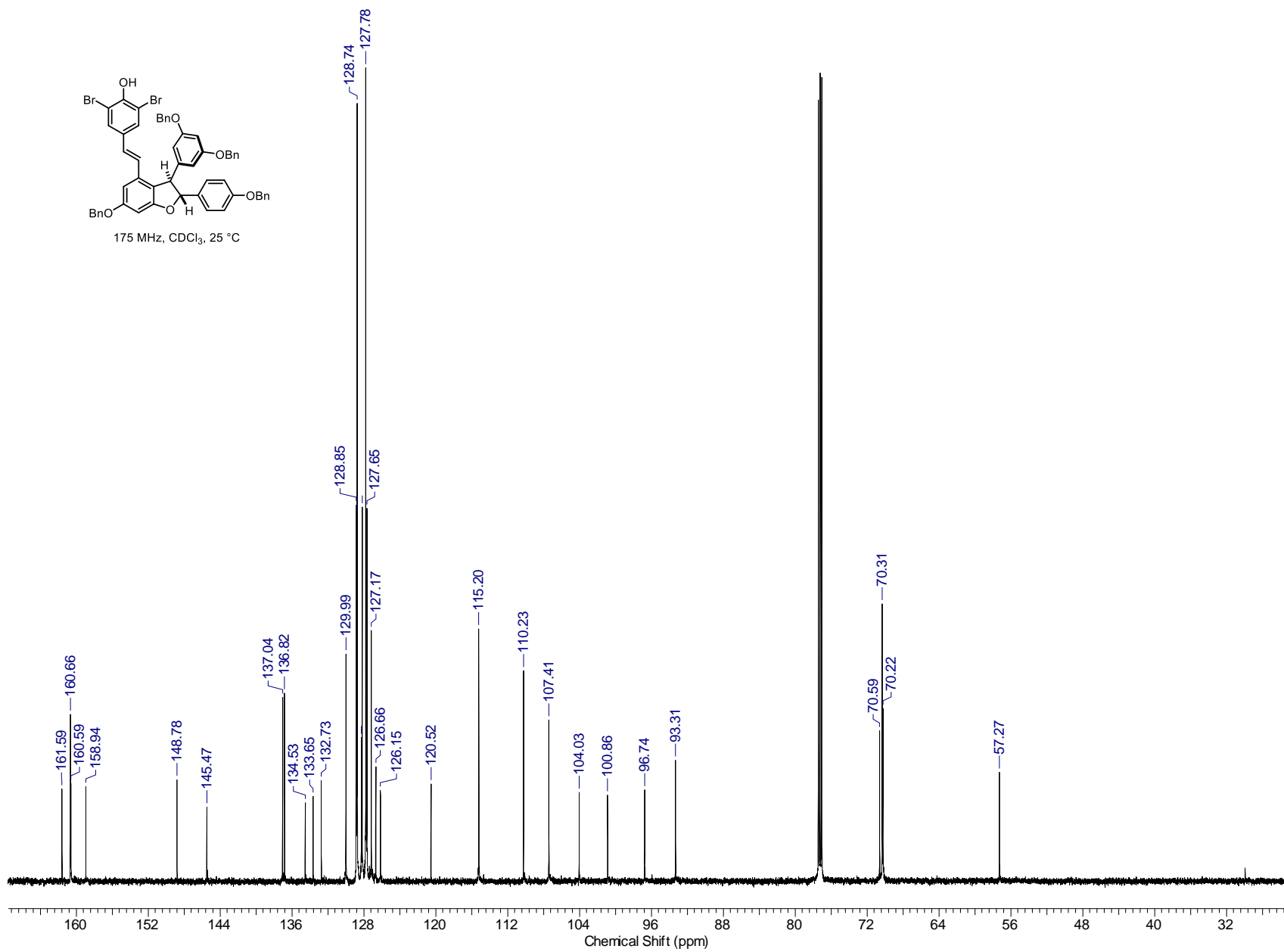
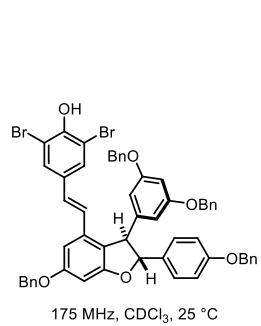
273

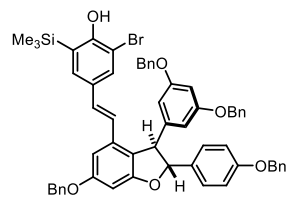




275

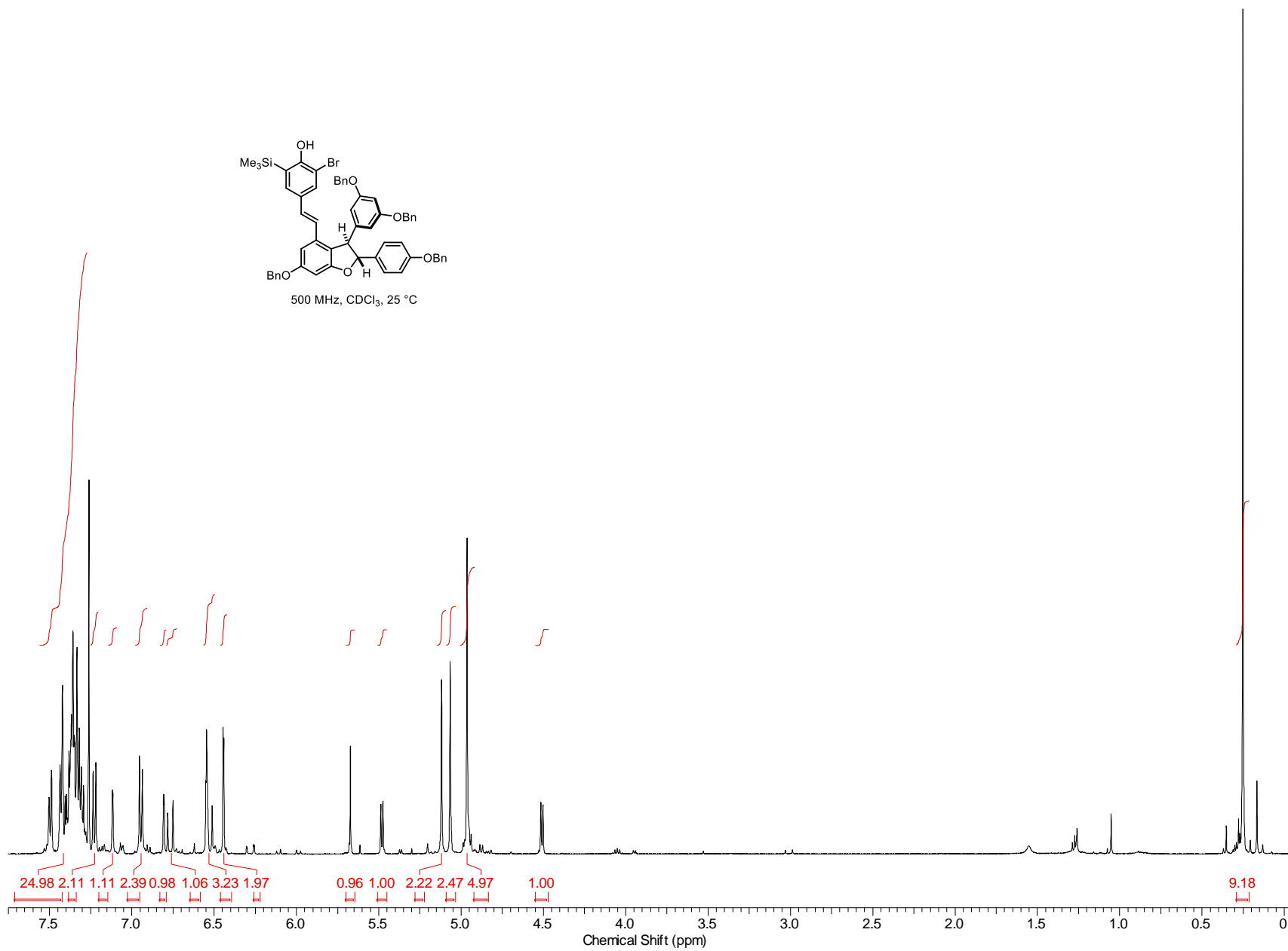


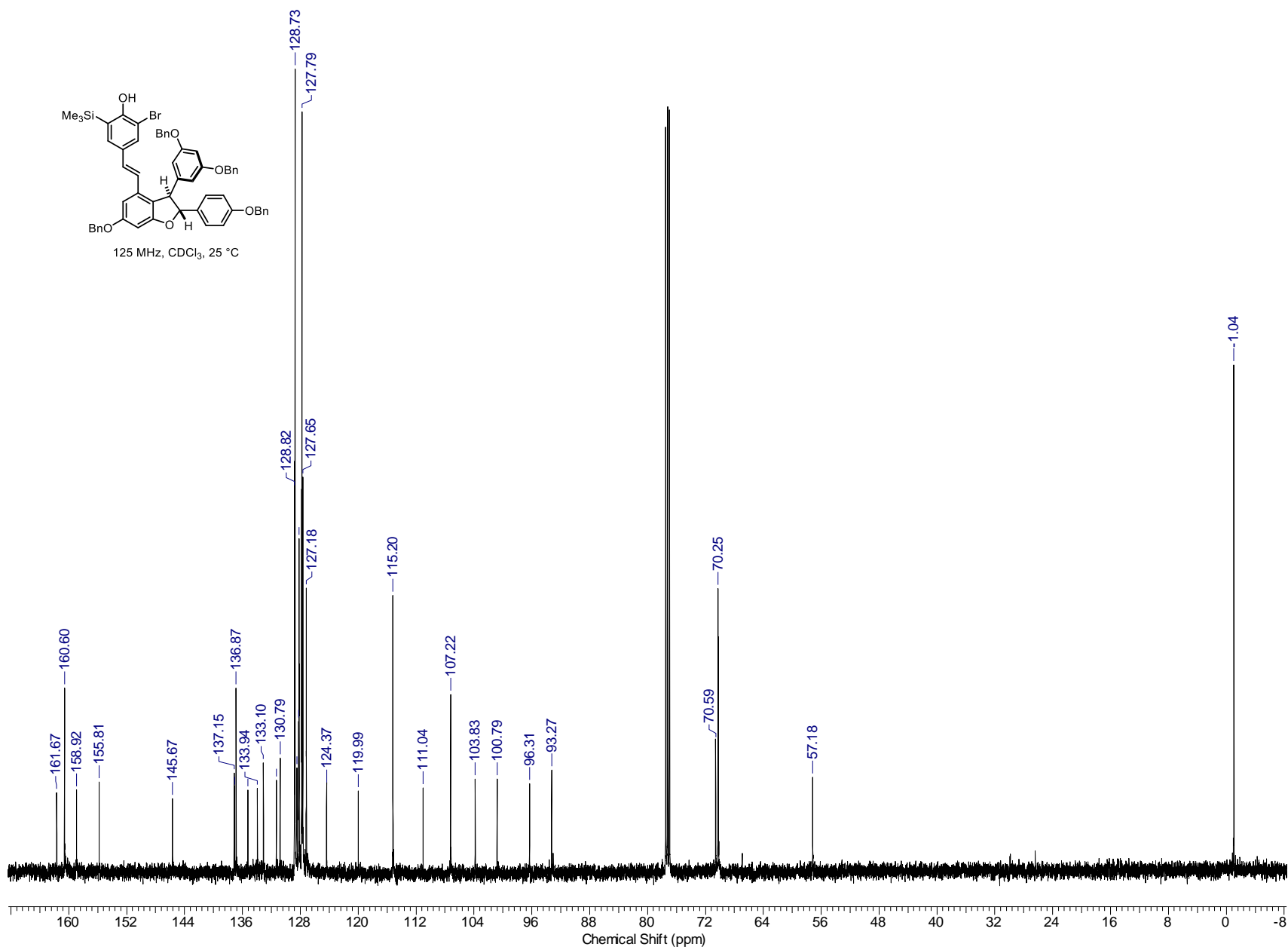




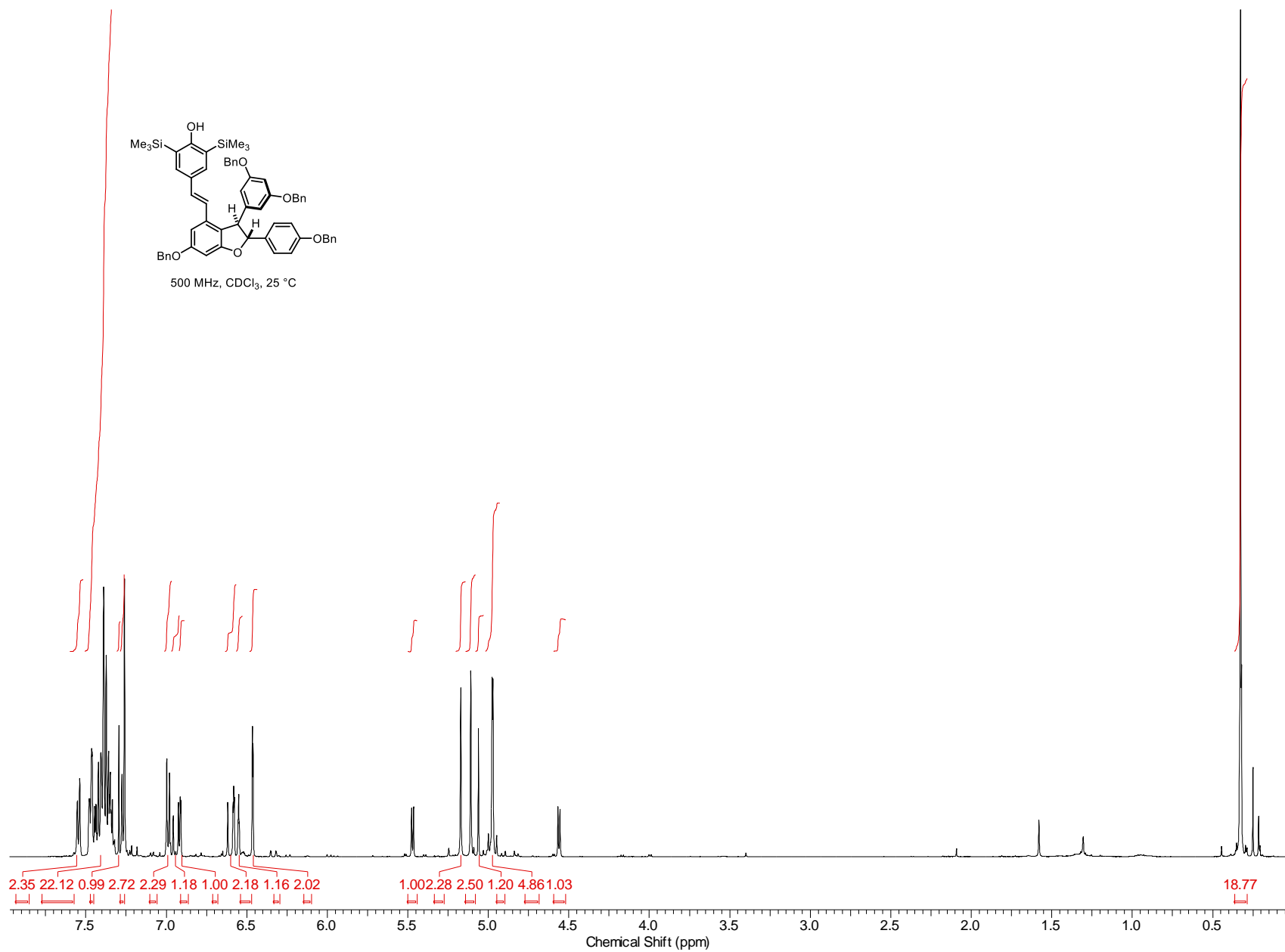
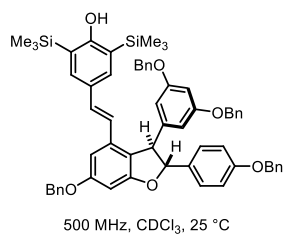
500 MHz, CDCl₃, 25 °C

277

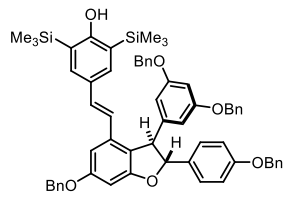




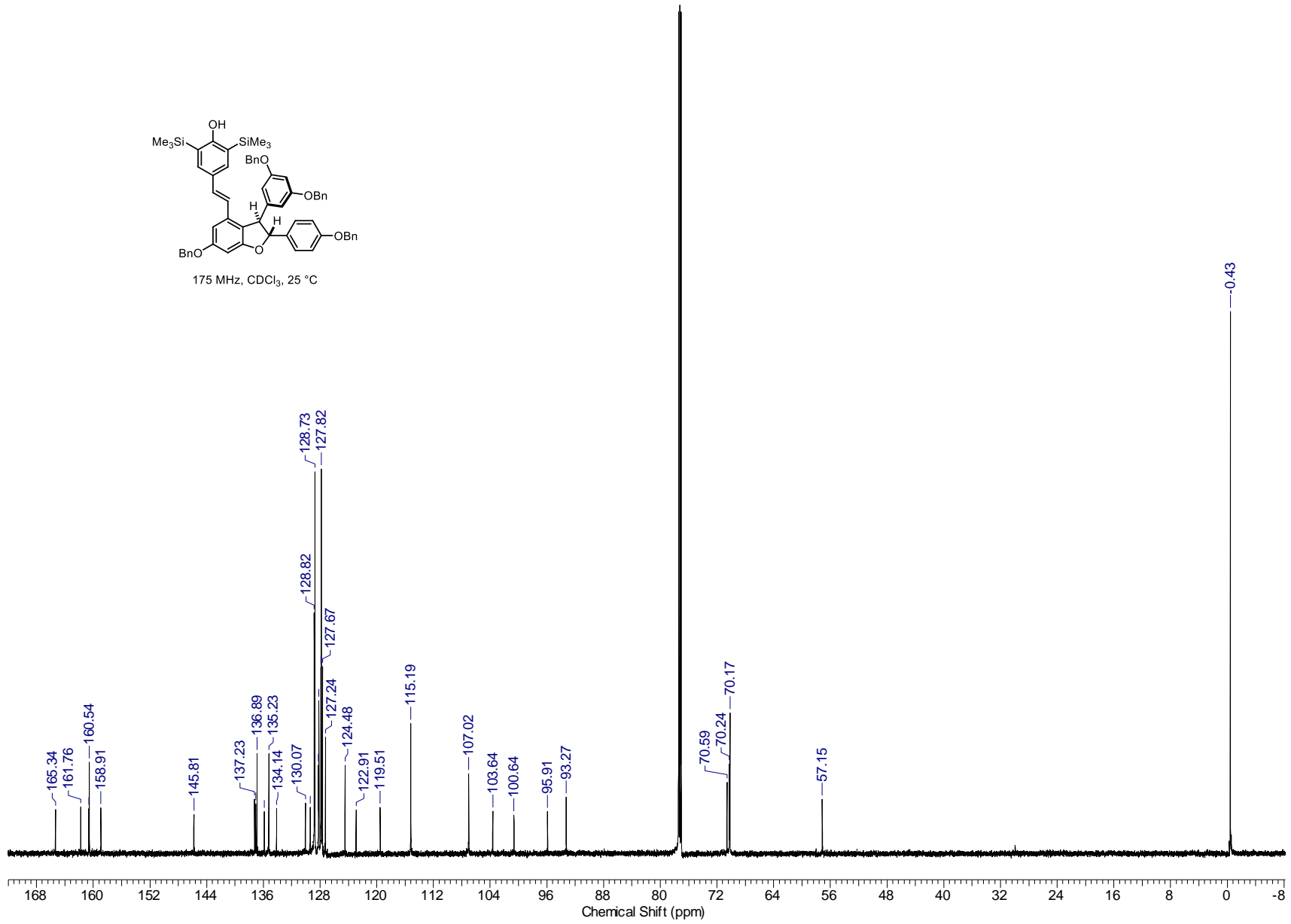
279

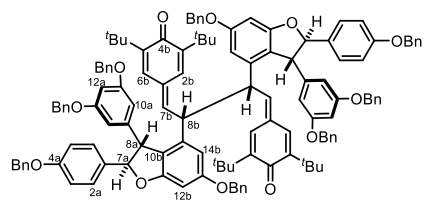


280



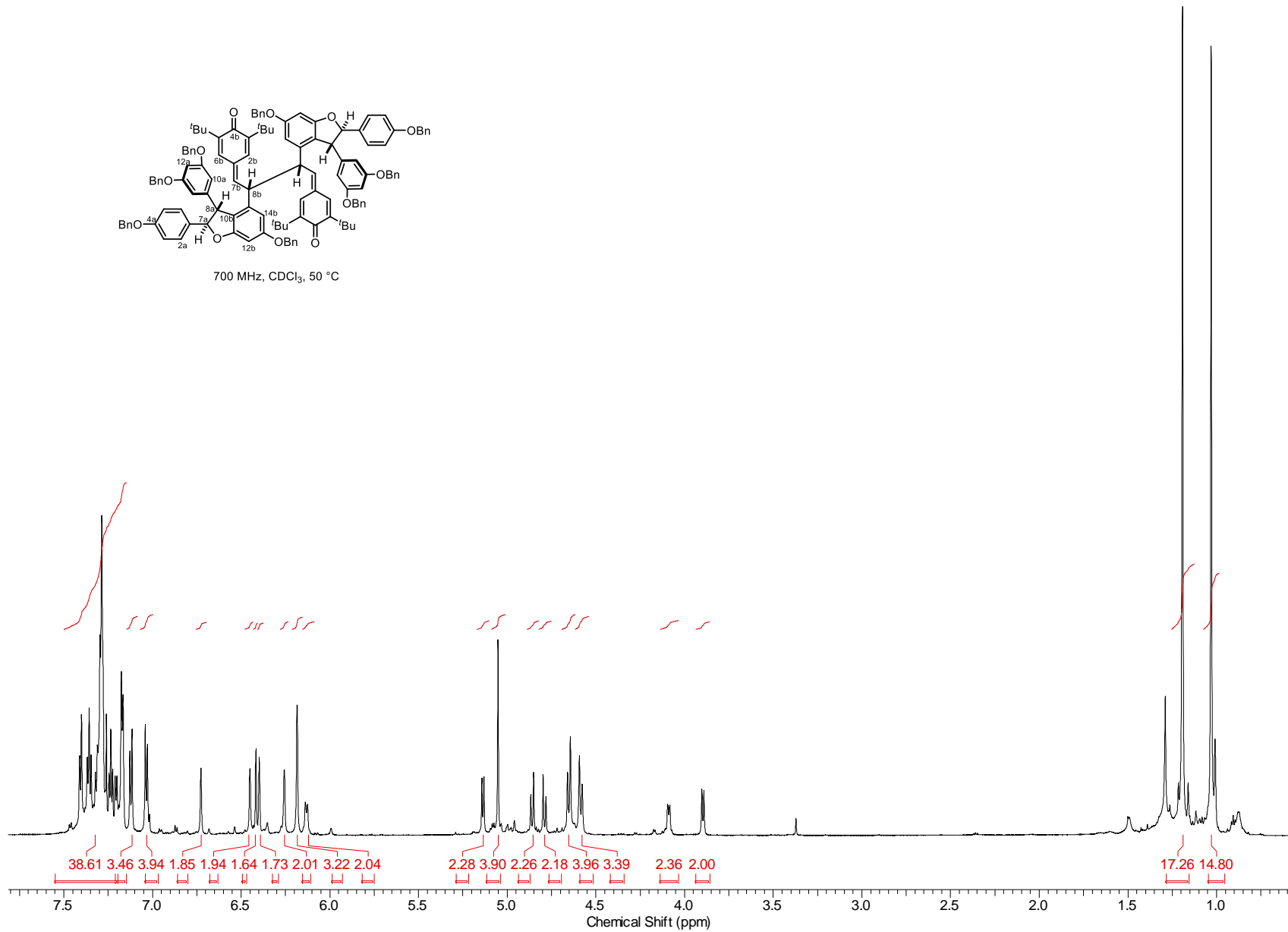
175 MHz, CDCl₃, 25 °C

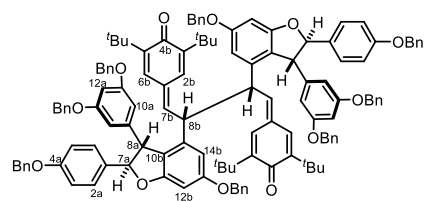




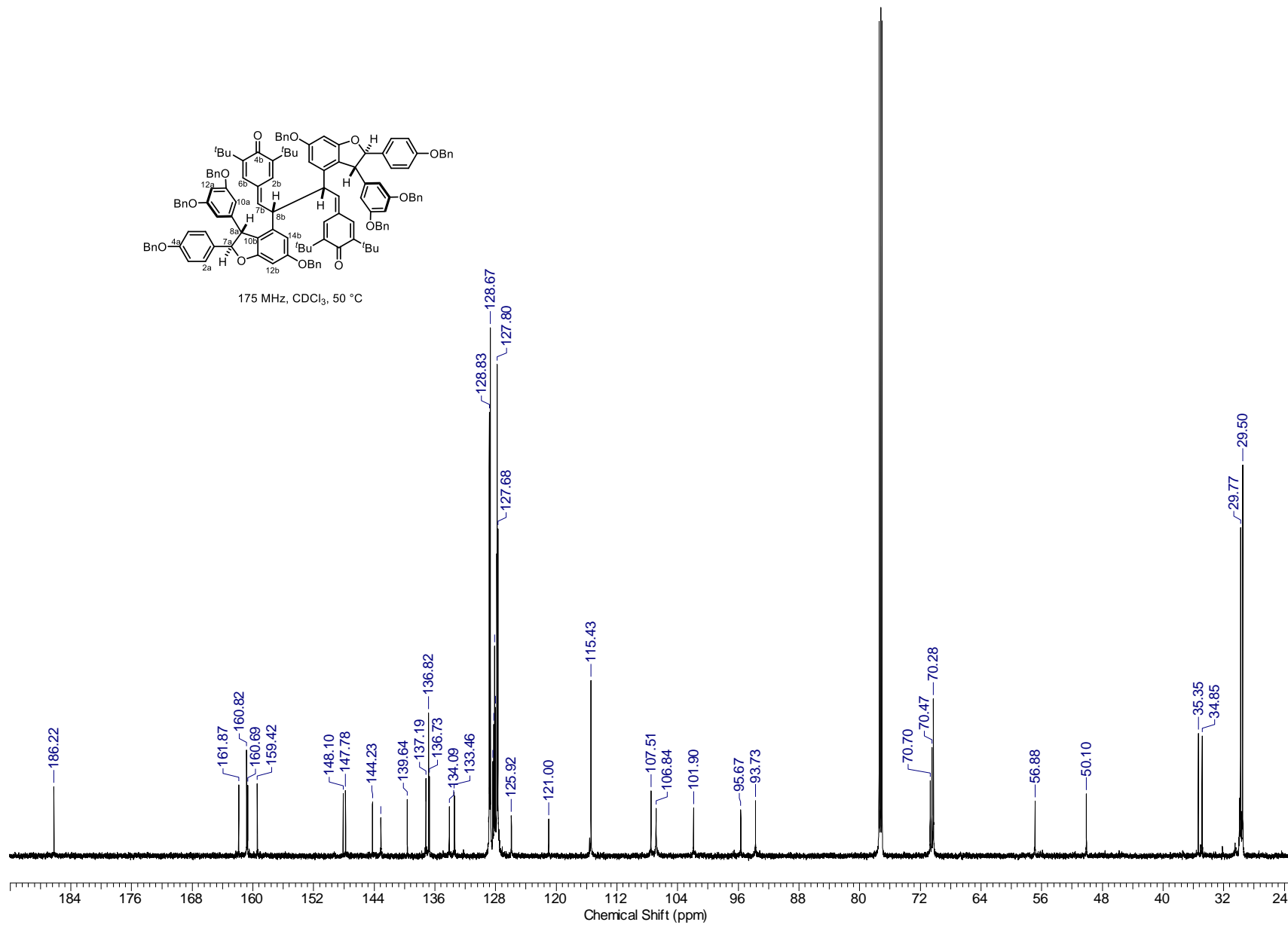
700 MHz, CDCl₃, 50 °C

281

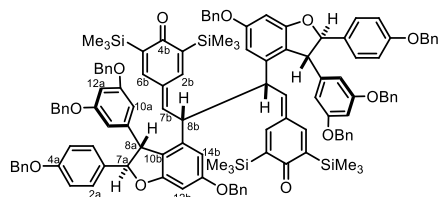




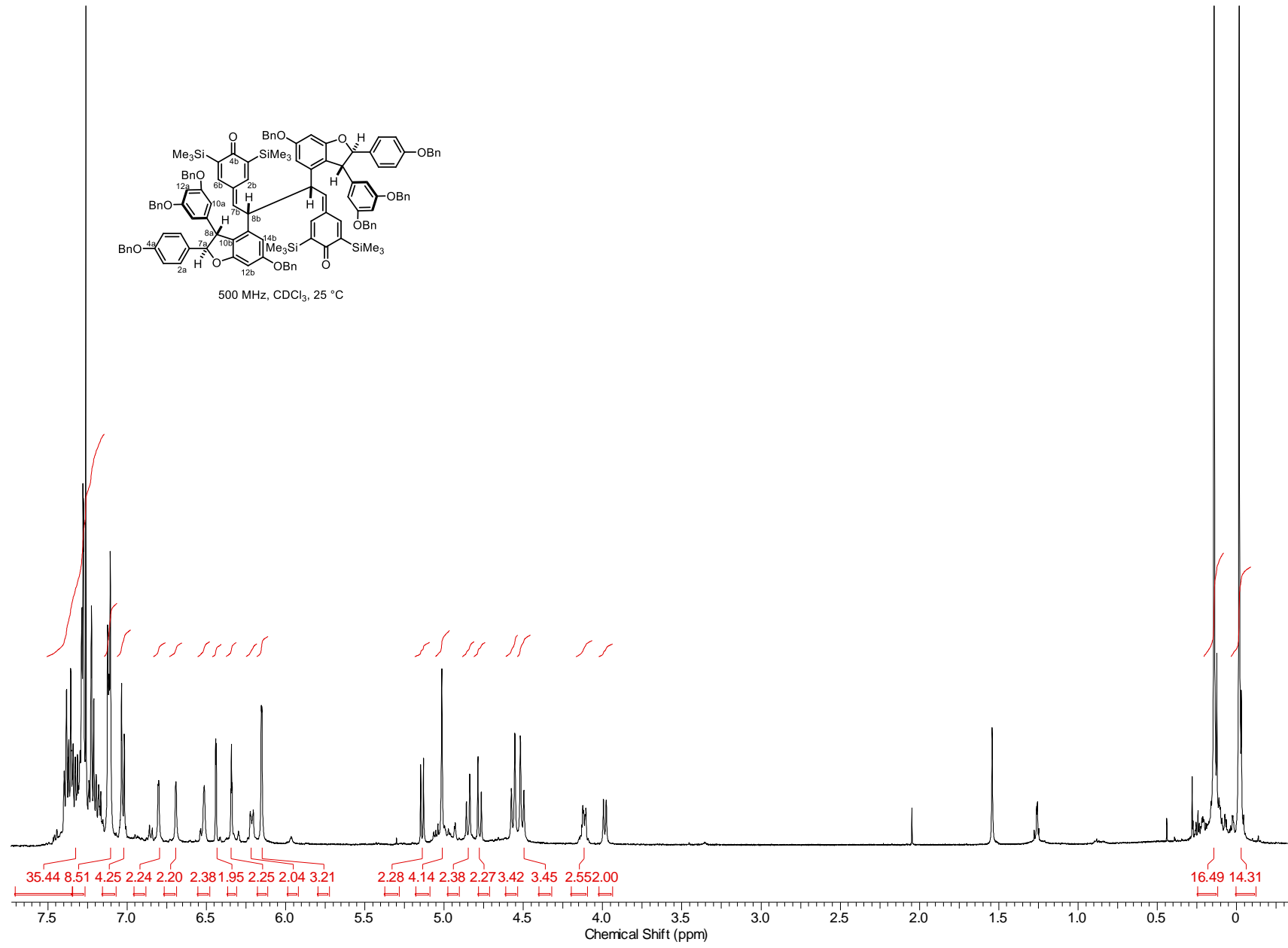
175 MHz, CDCl₃, 50 °C

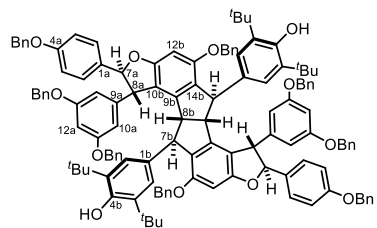


283



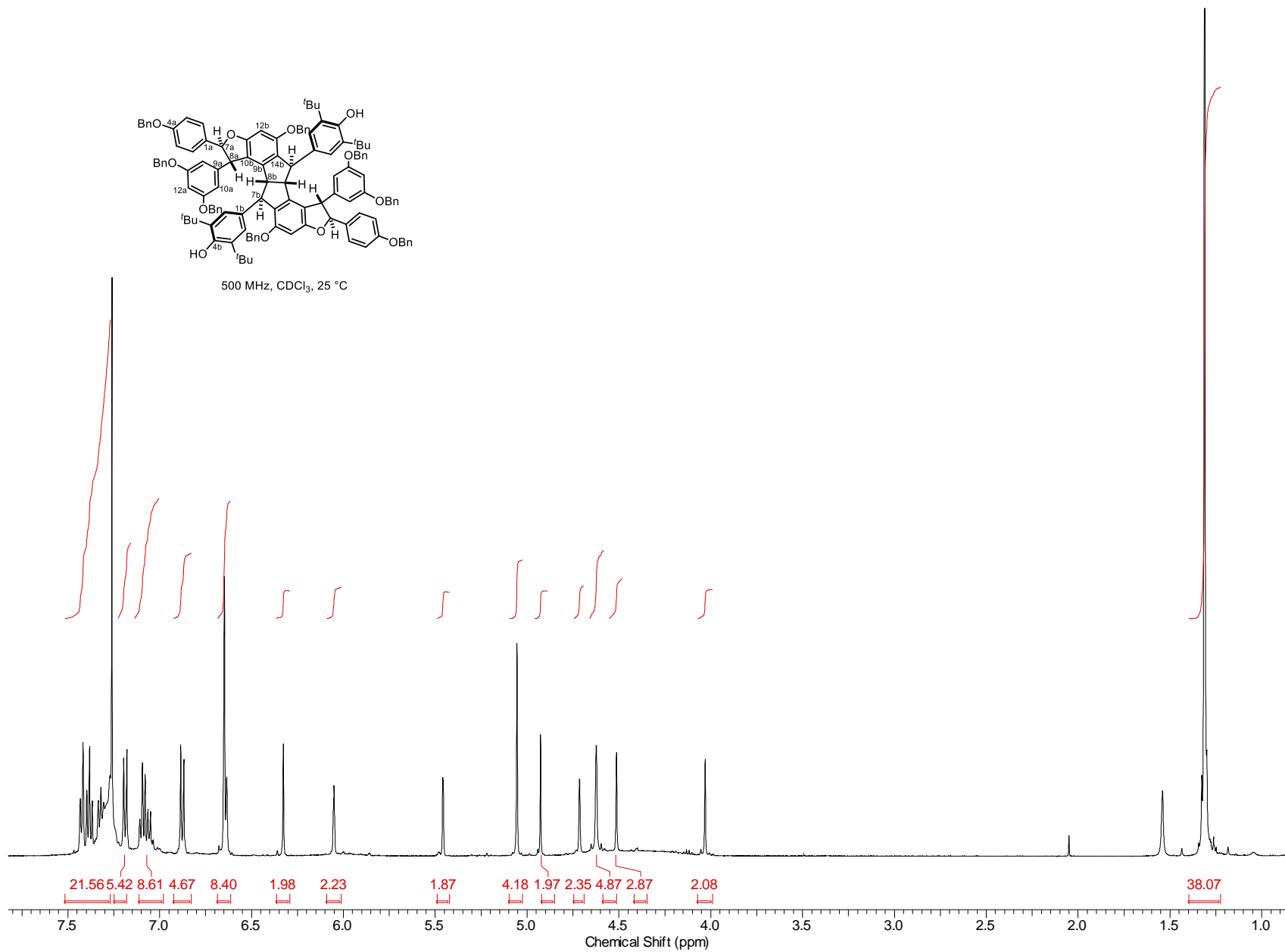
500 MHz, CDCl₃, 25 °C

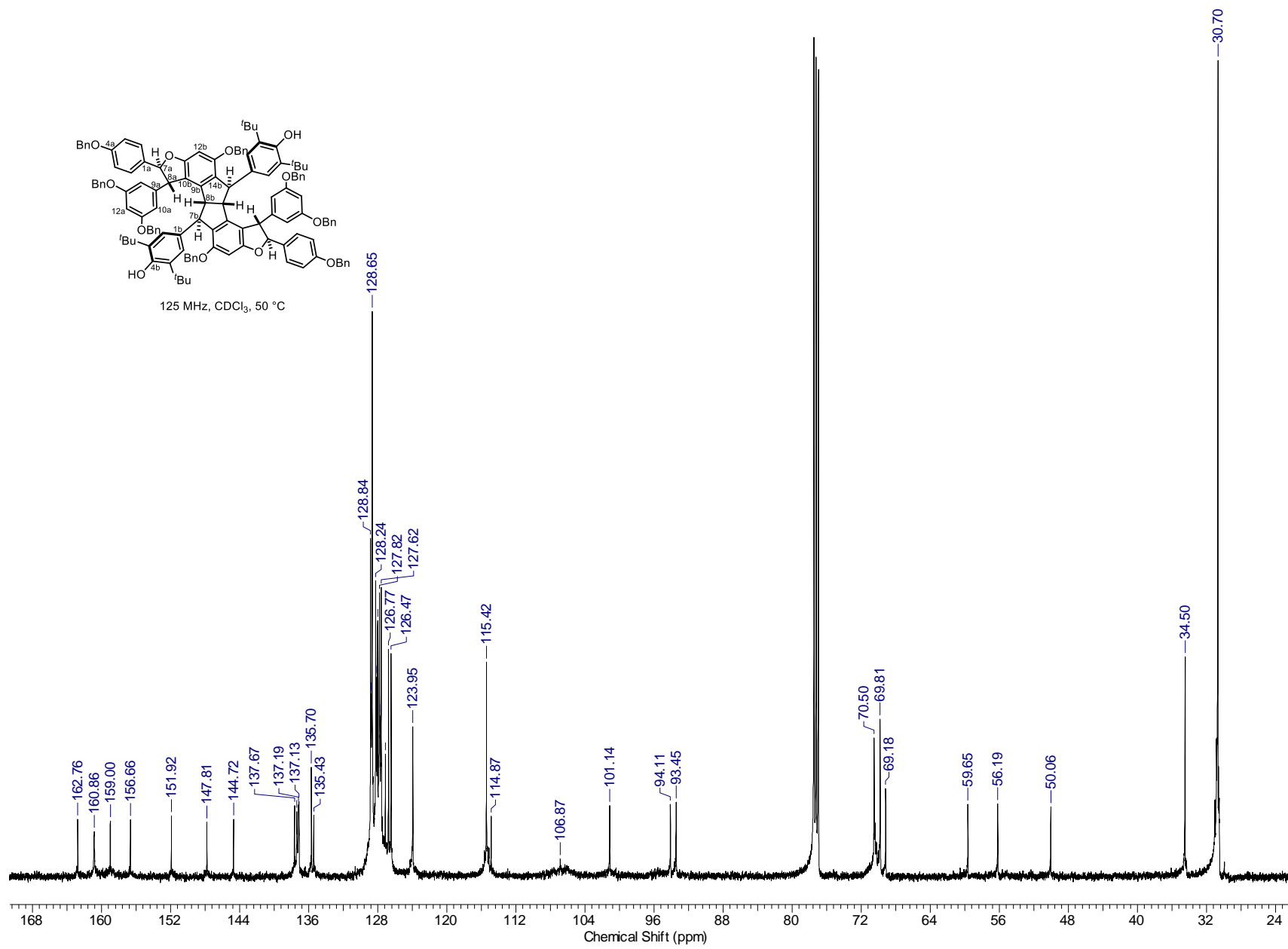


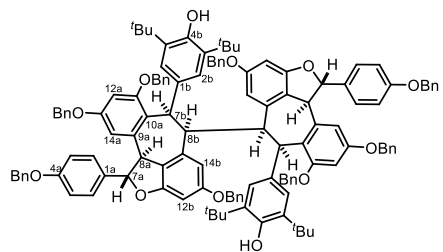


500 MHz, CDCl₃, 25 °C

285

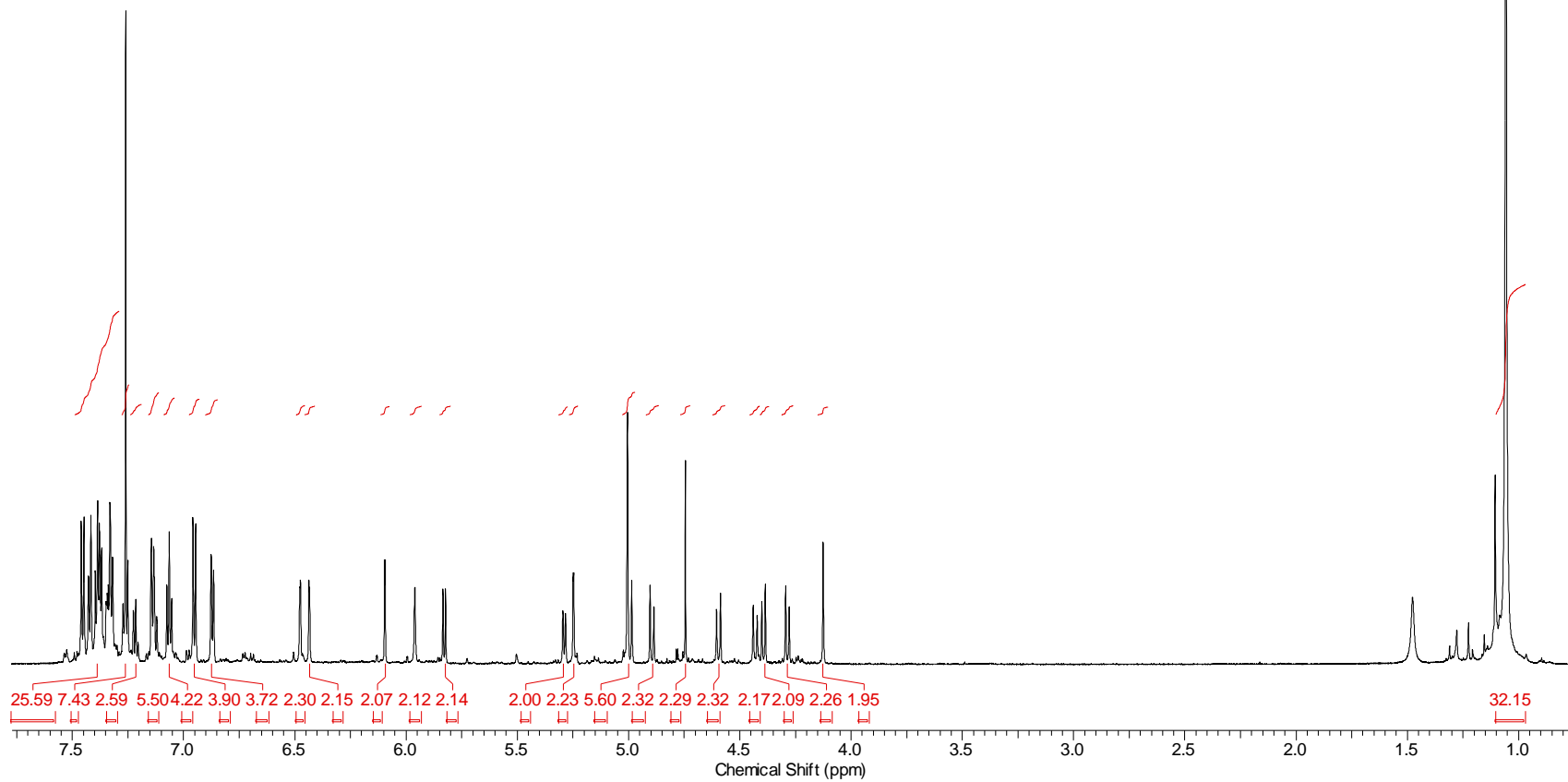


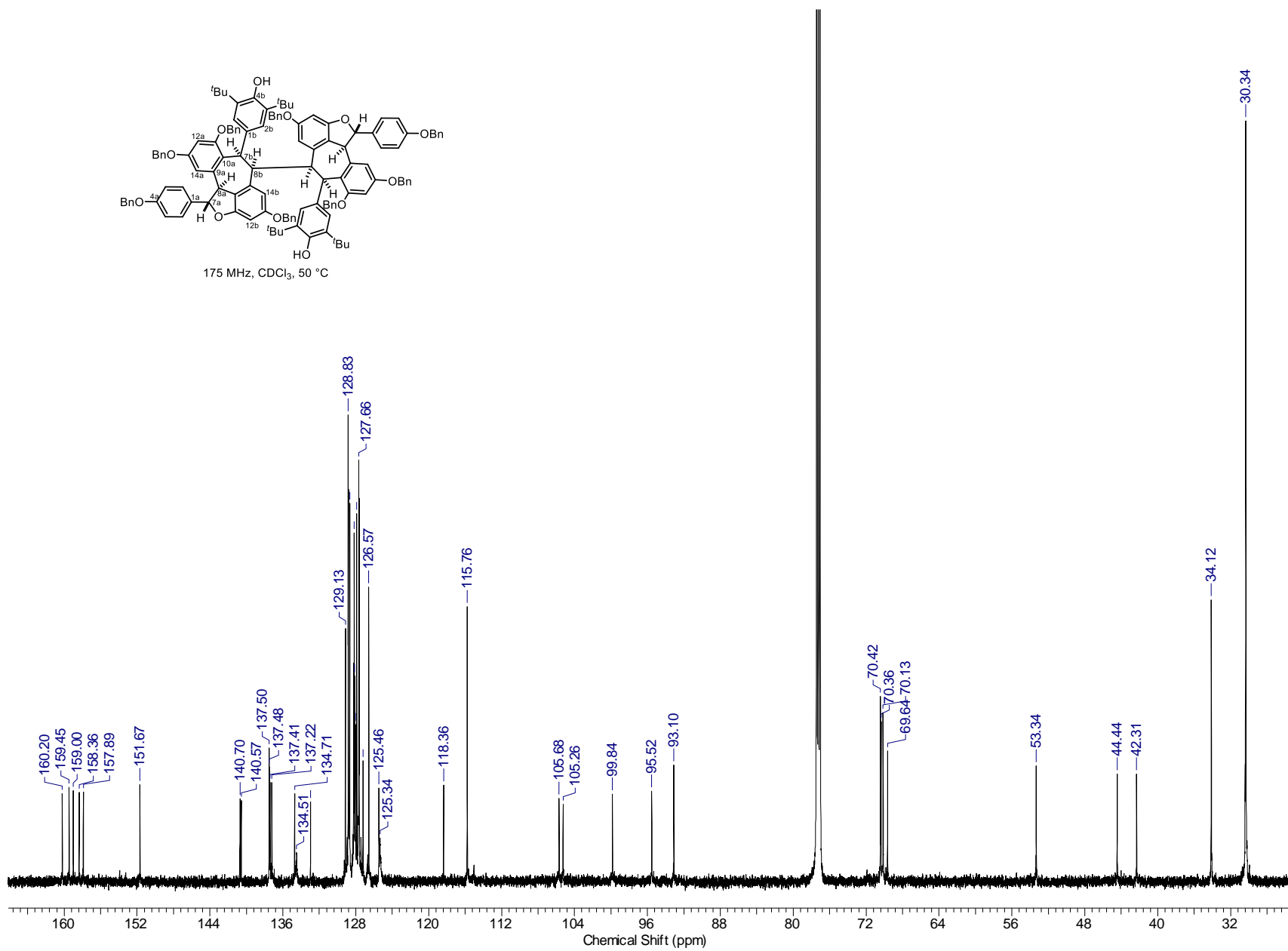
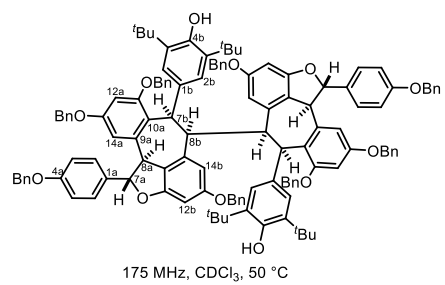


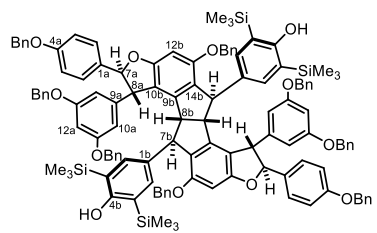


700 MHz, CDCl₃, 50 °C

287

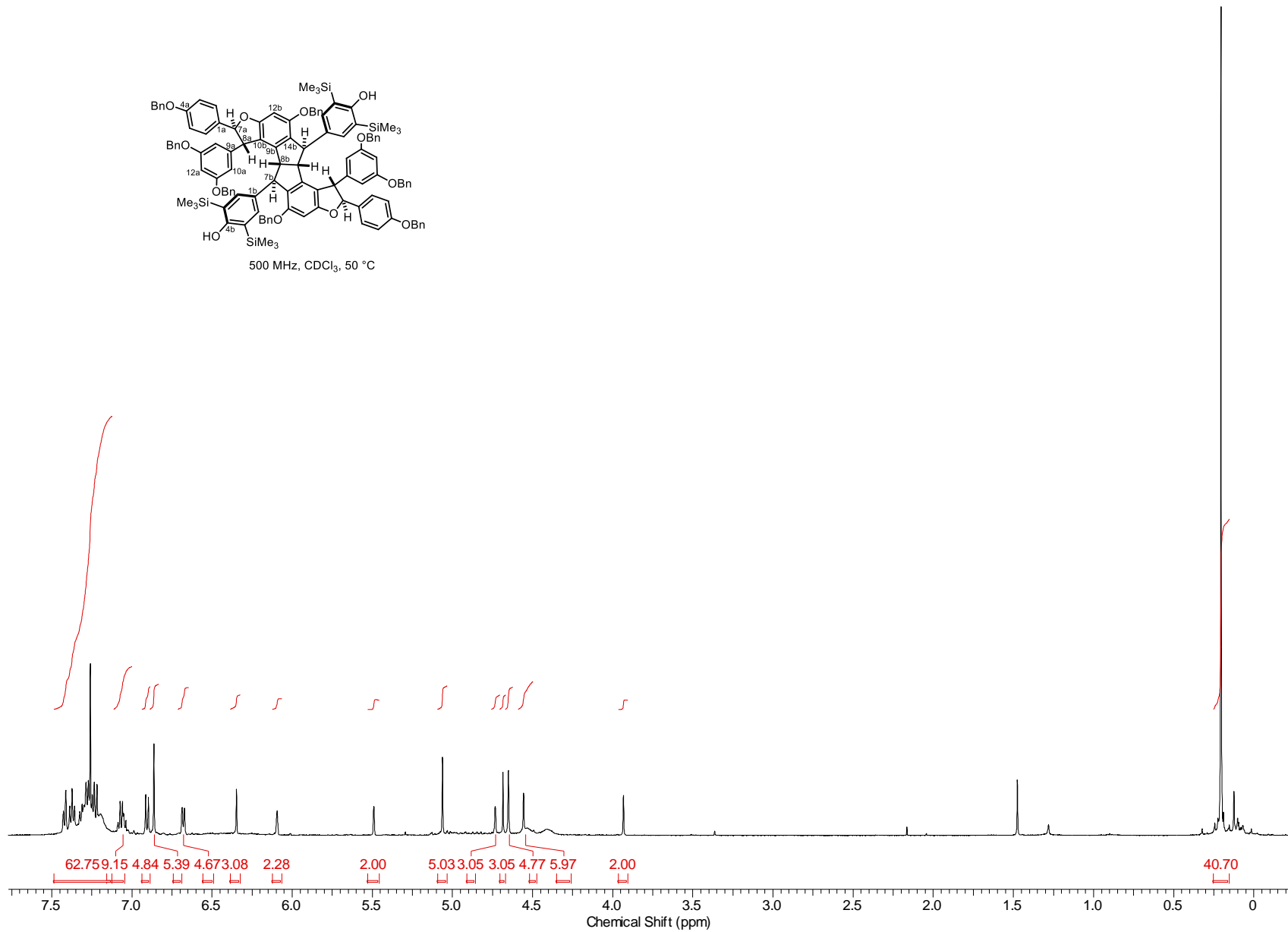


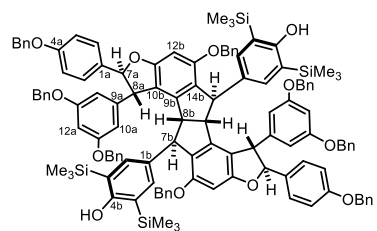
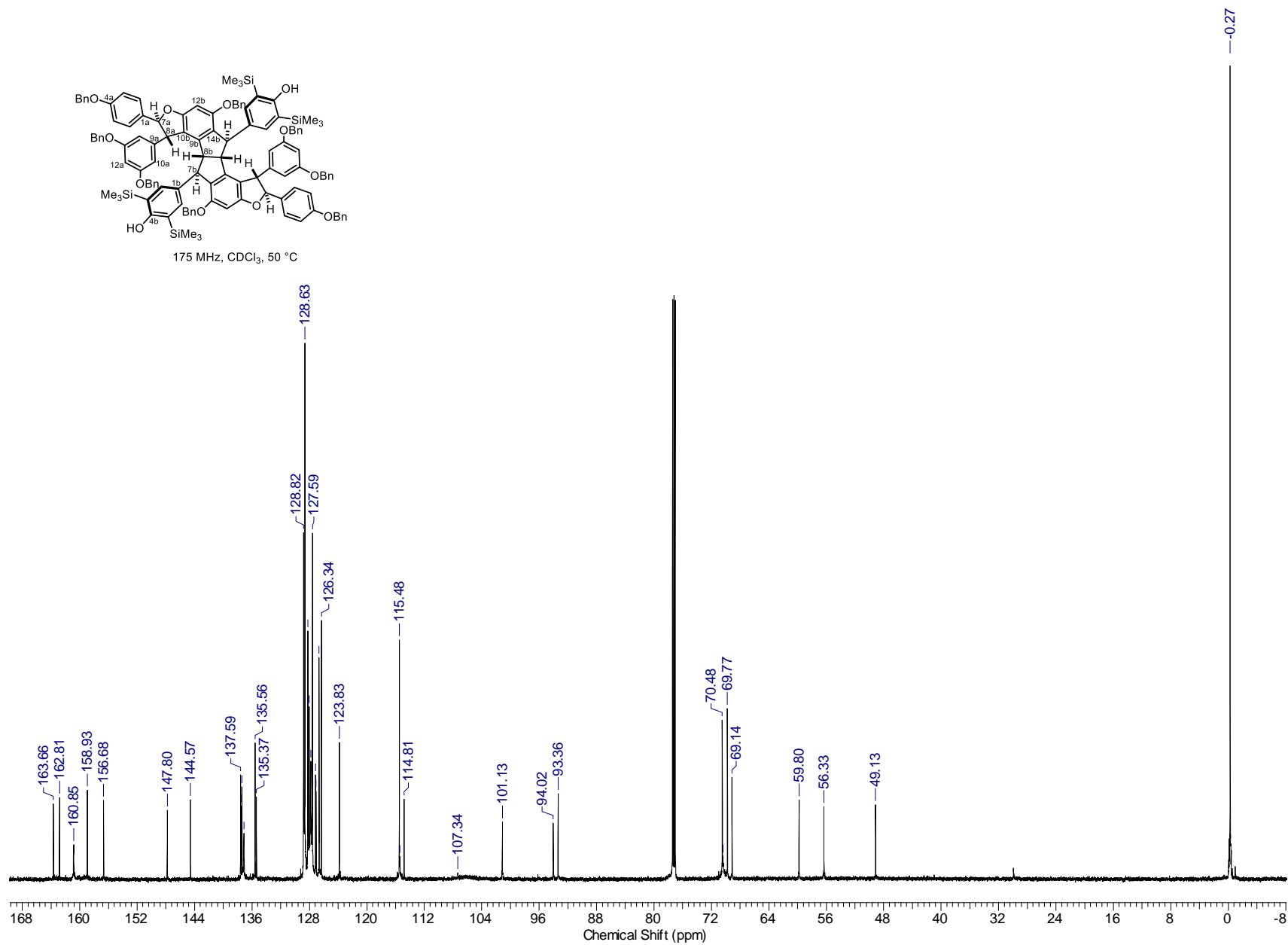


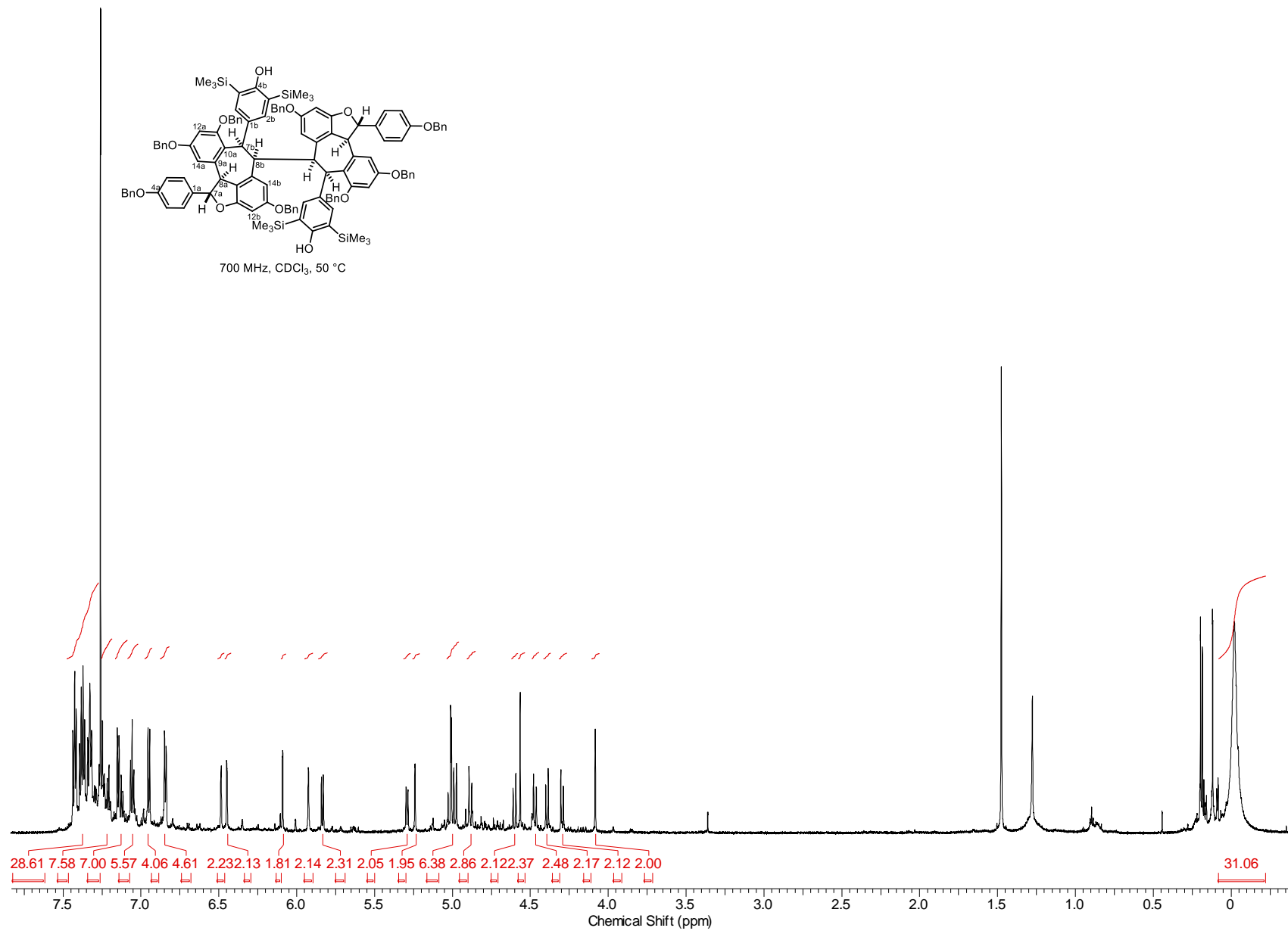


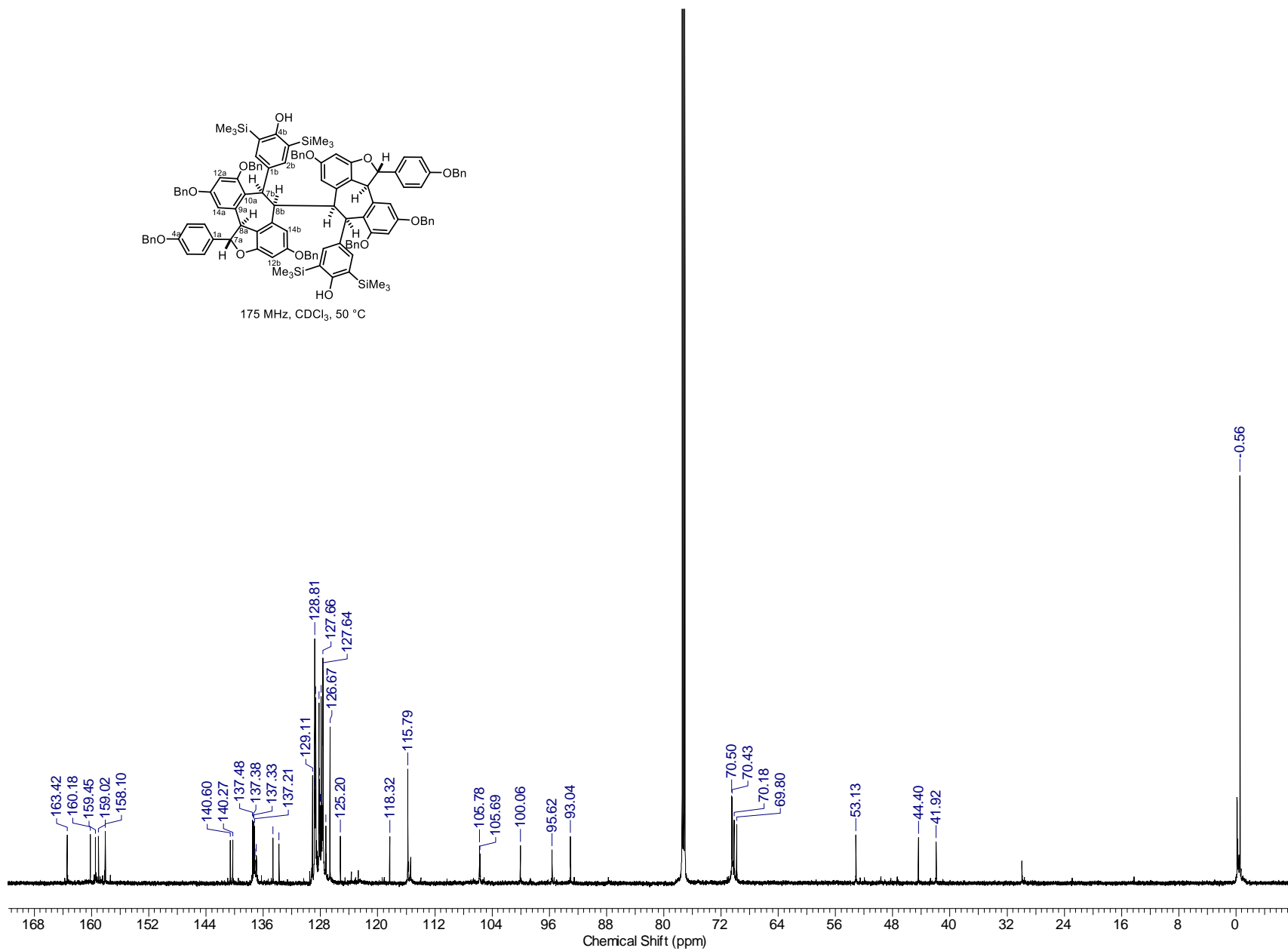
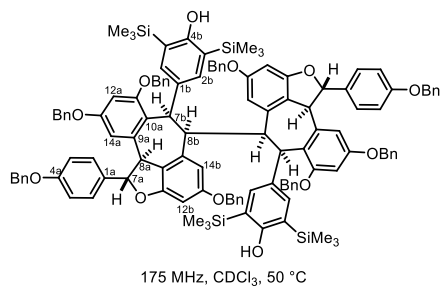
500 MHz, CDCl₃, 50 °C

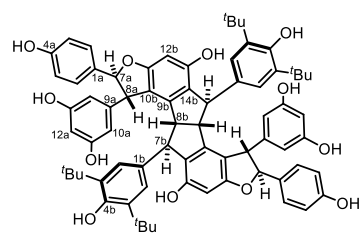
289



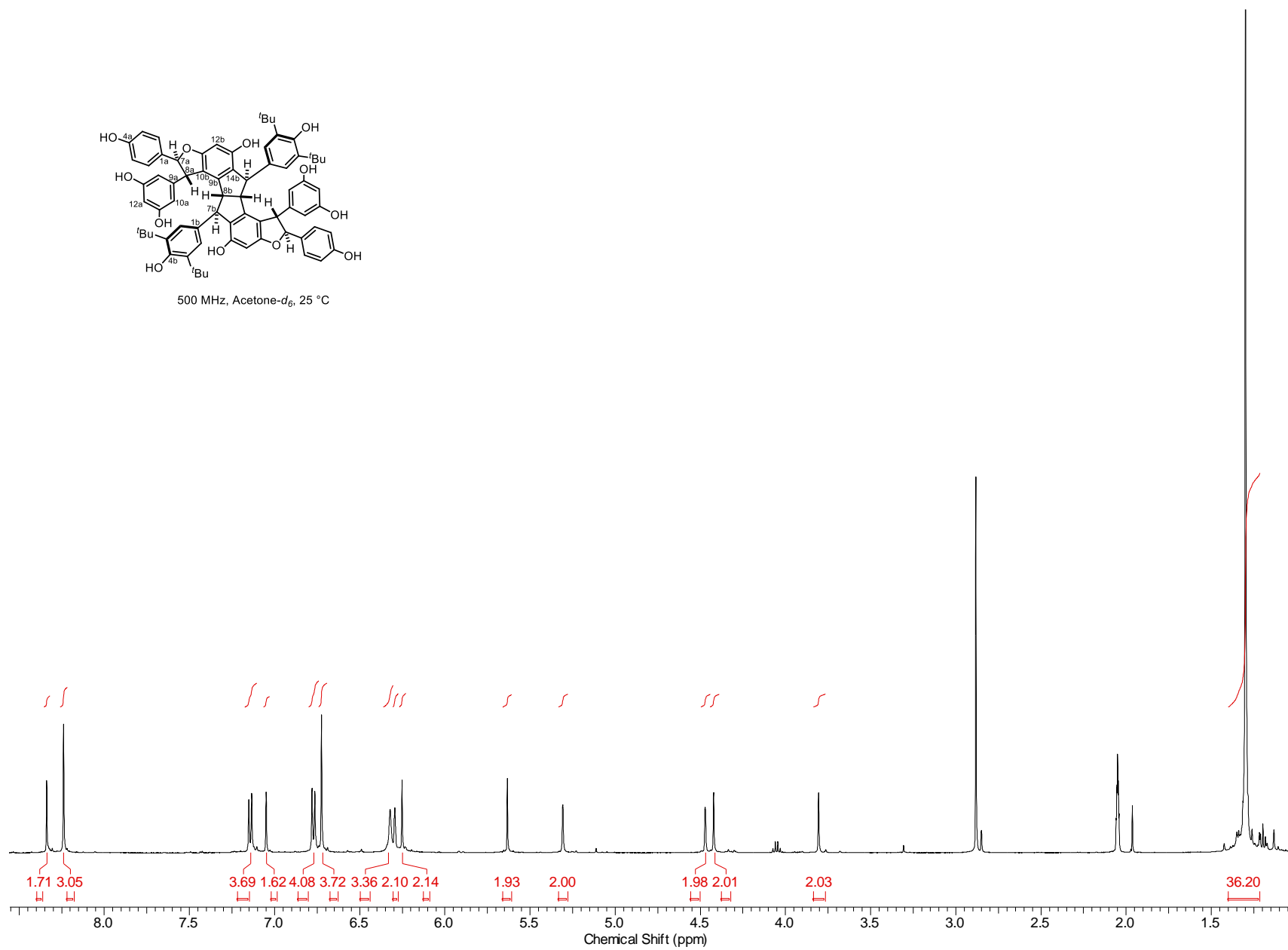
175 MHz, CDCl₃, 50 °C

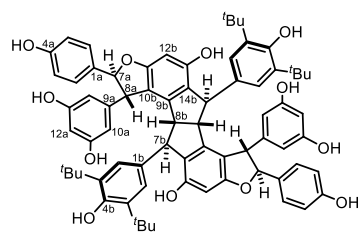




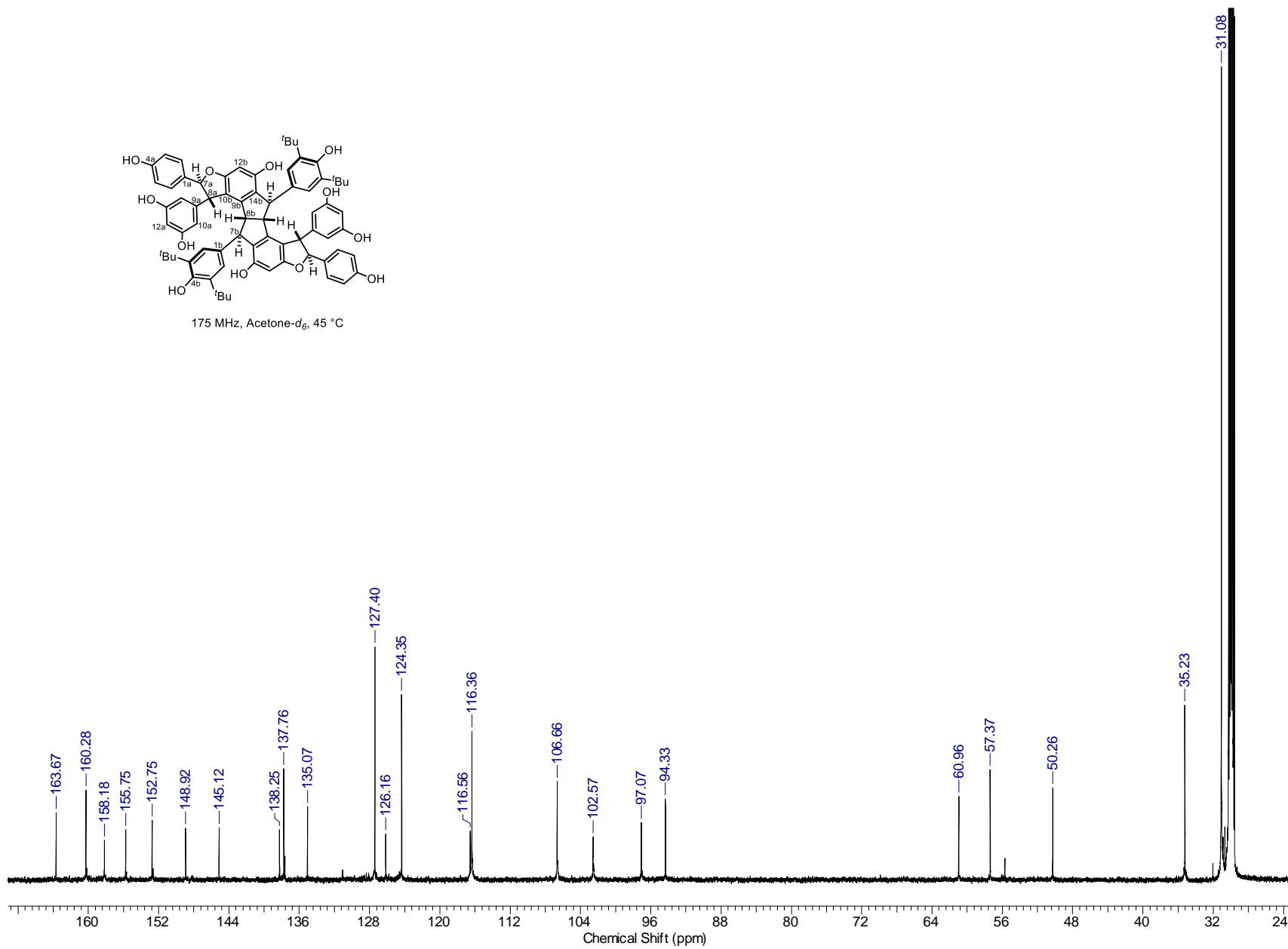


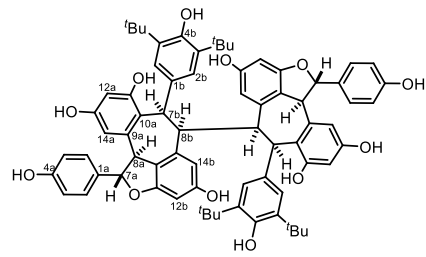
500 MHz, Acetone- d_6 , 25 °C



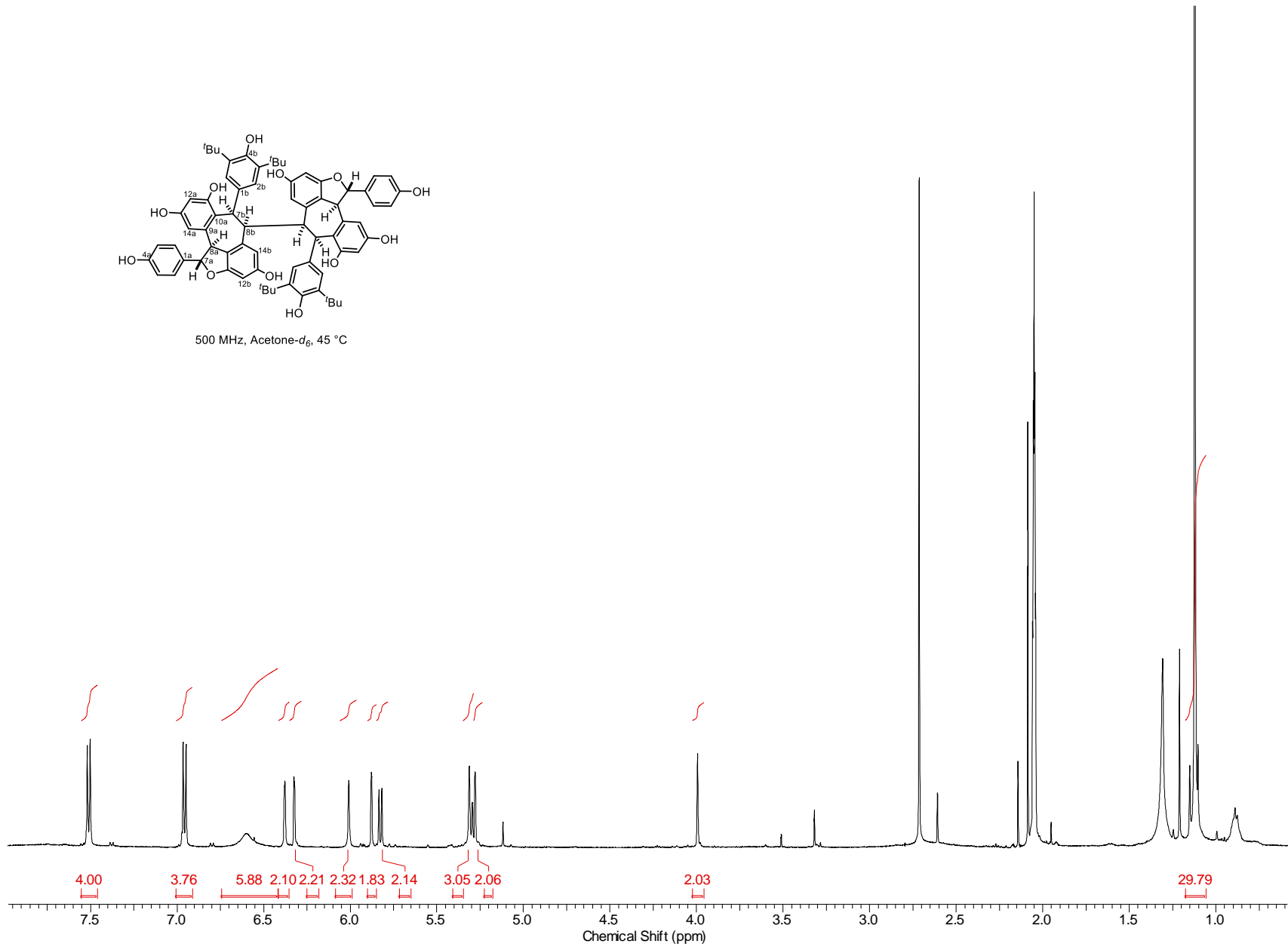


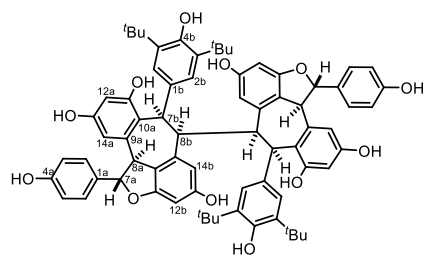
175 MHz, Acetone- d_6 , 45 °C



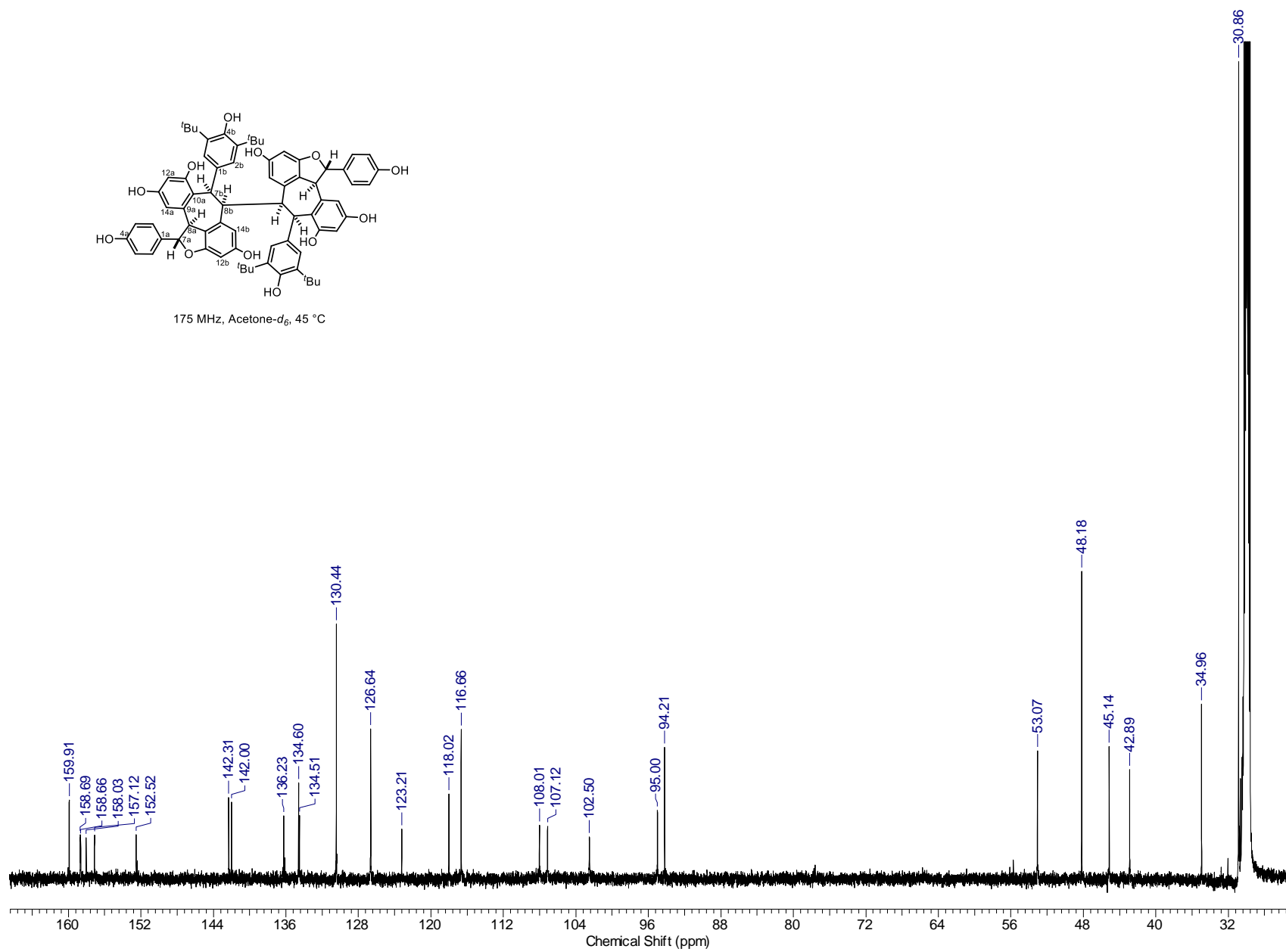


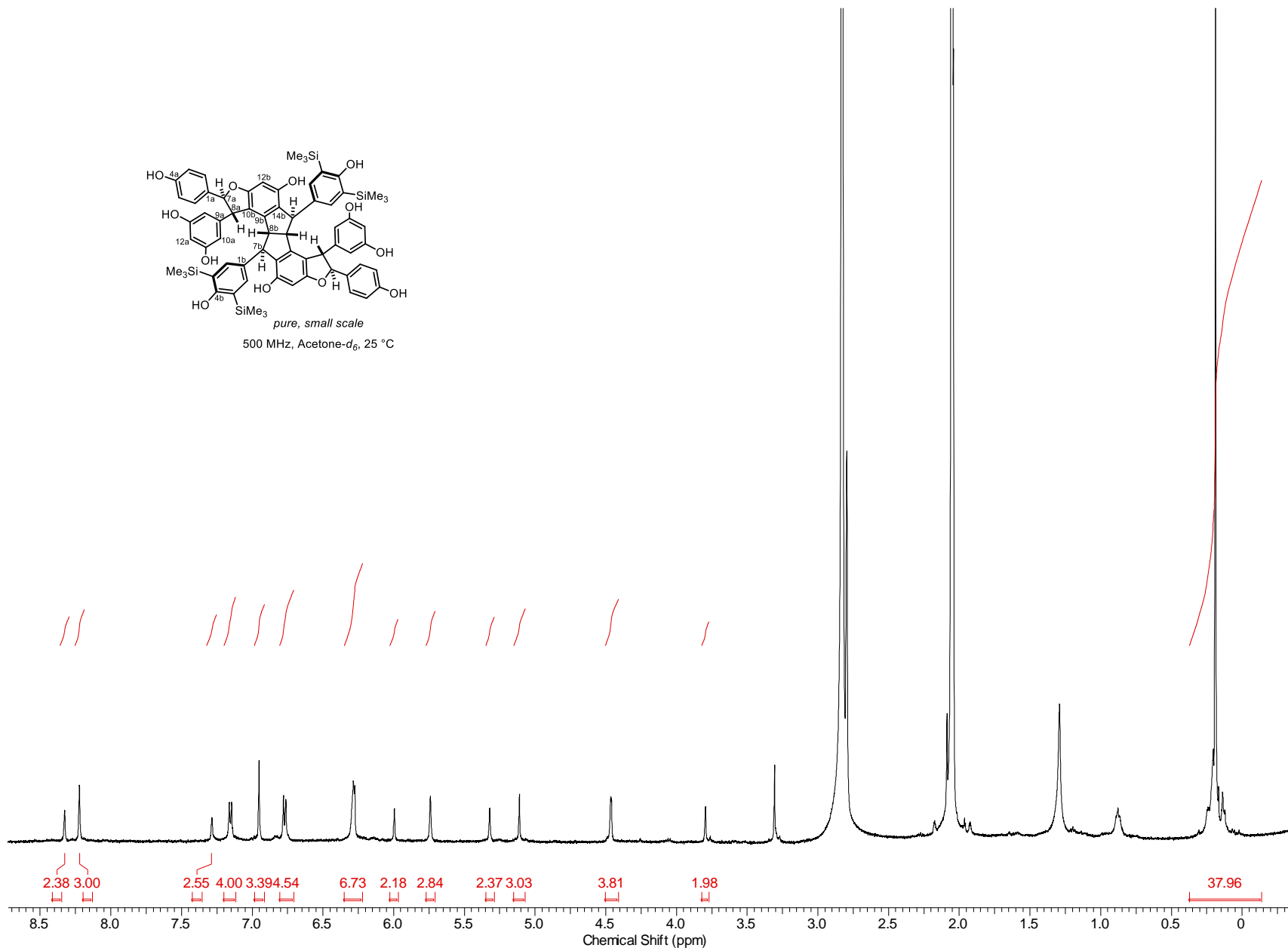
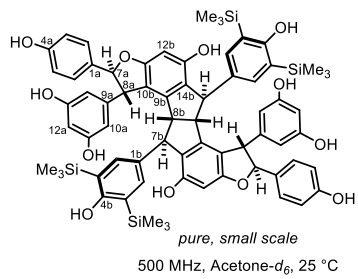
500 MHz, Acetone-*d*₆, 45 °C

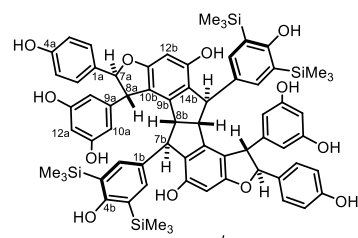




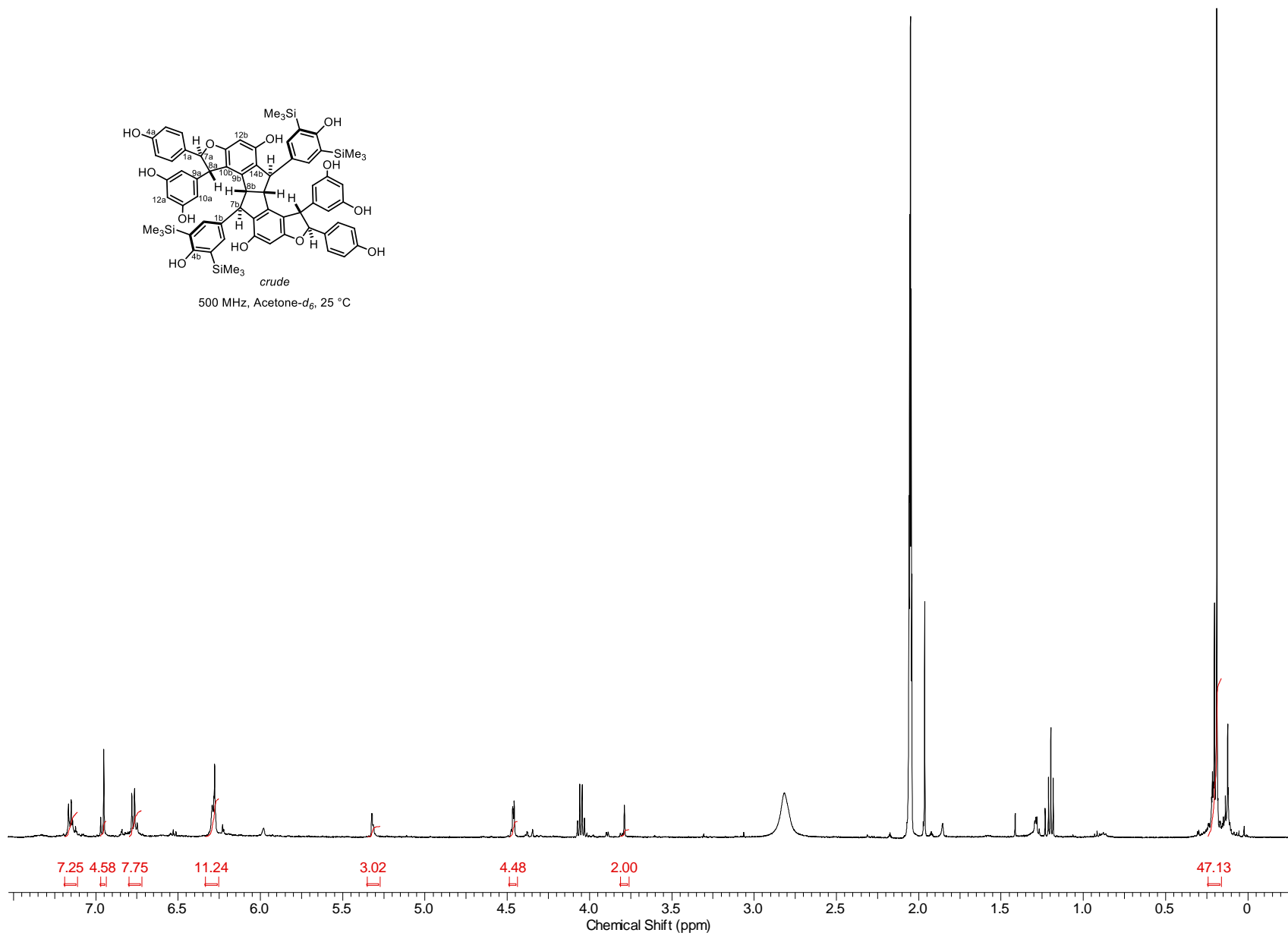
175 MHz, Acetone- d_6 , 45 °C

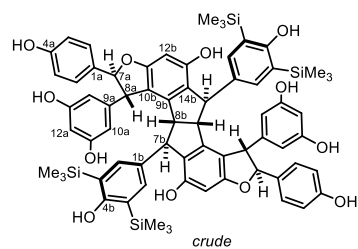




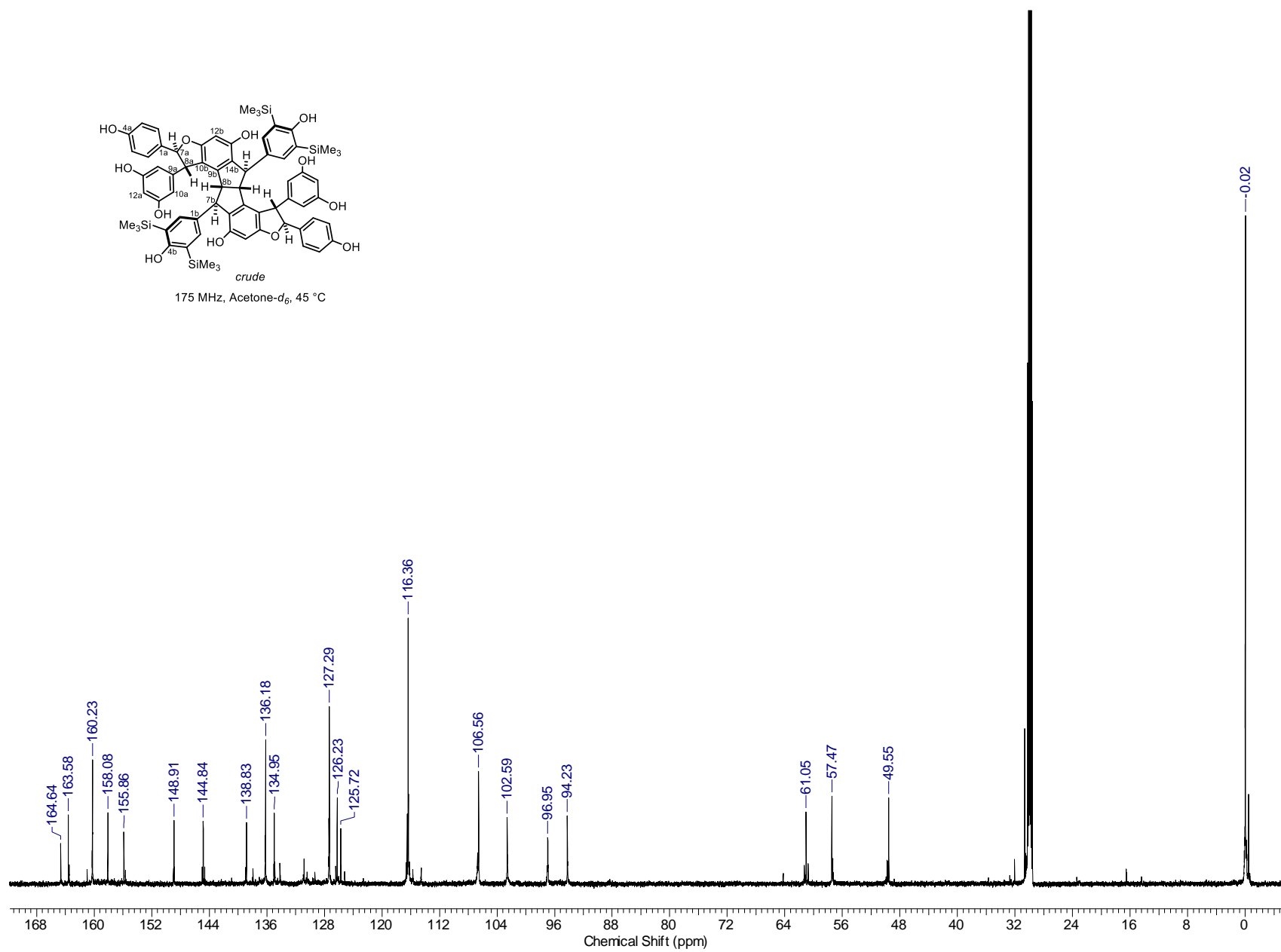


500 MHz, Acetone- d_6 , 25 °C

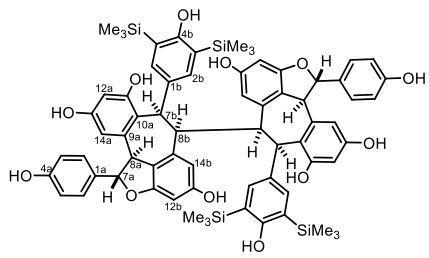




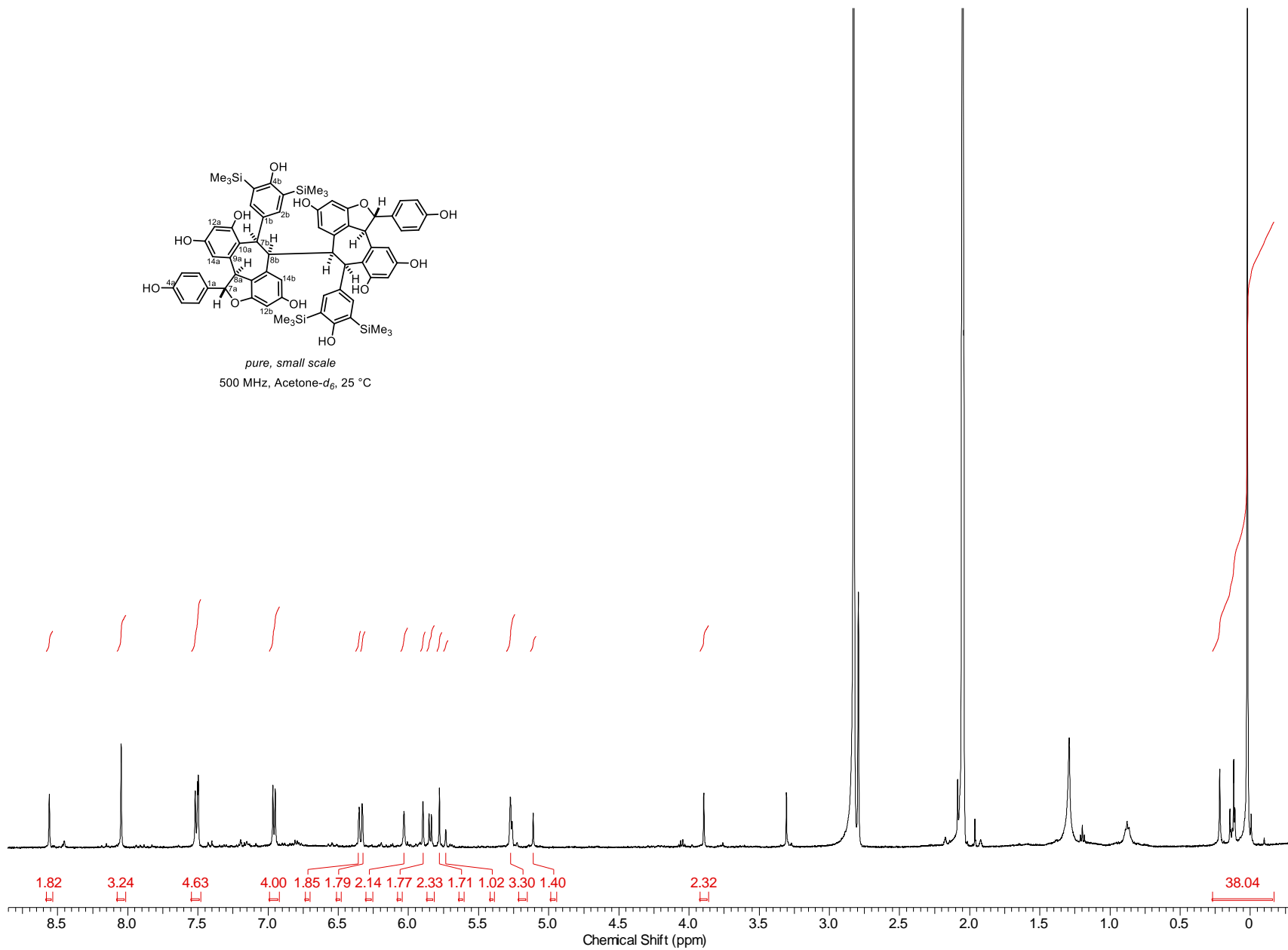
175 MHz, Acetone- d_6 , 45 °C

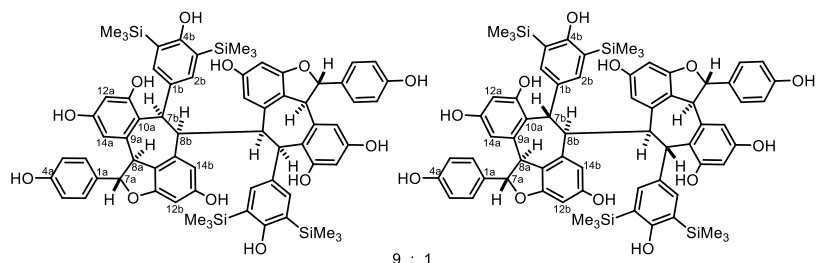
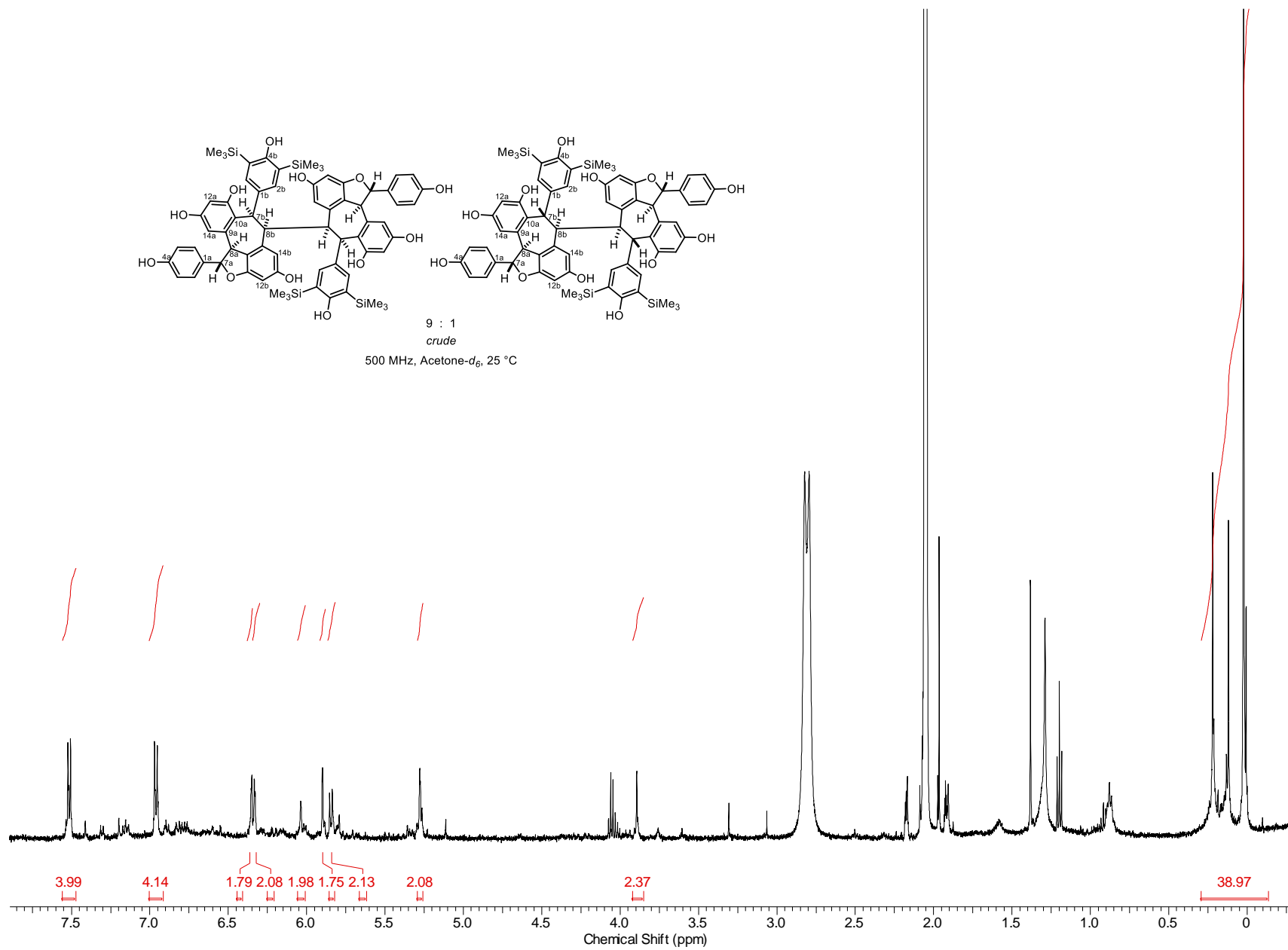


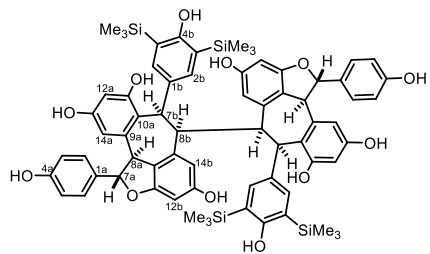
300



pure, small scale
500 MHz, Acetone-*d*₆, 25 °C

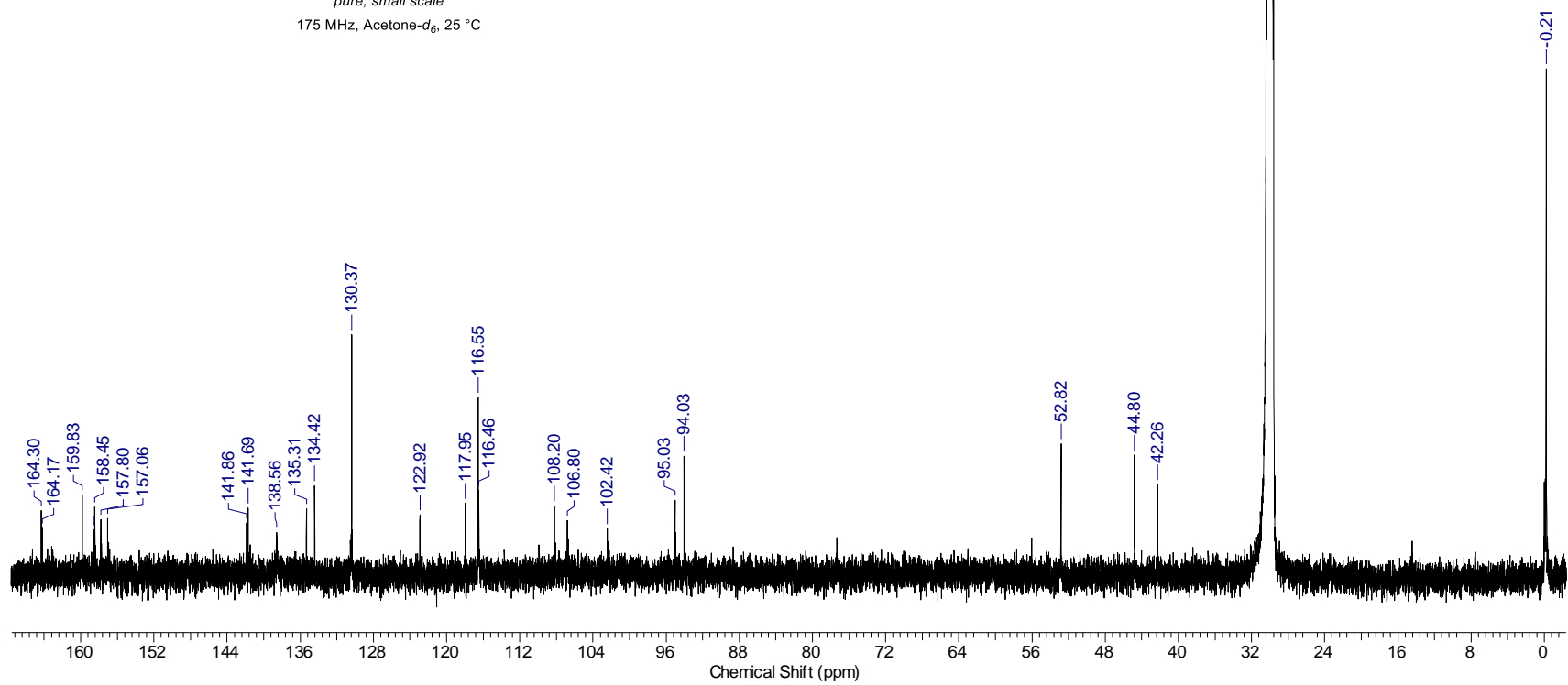


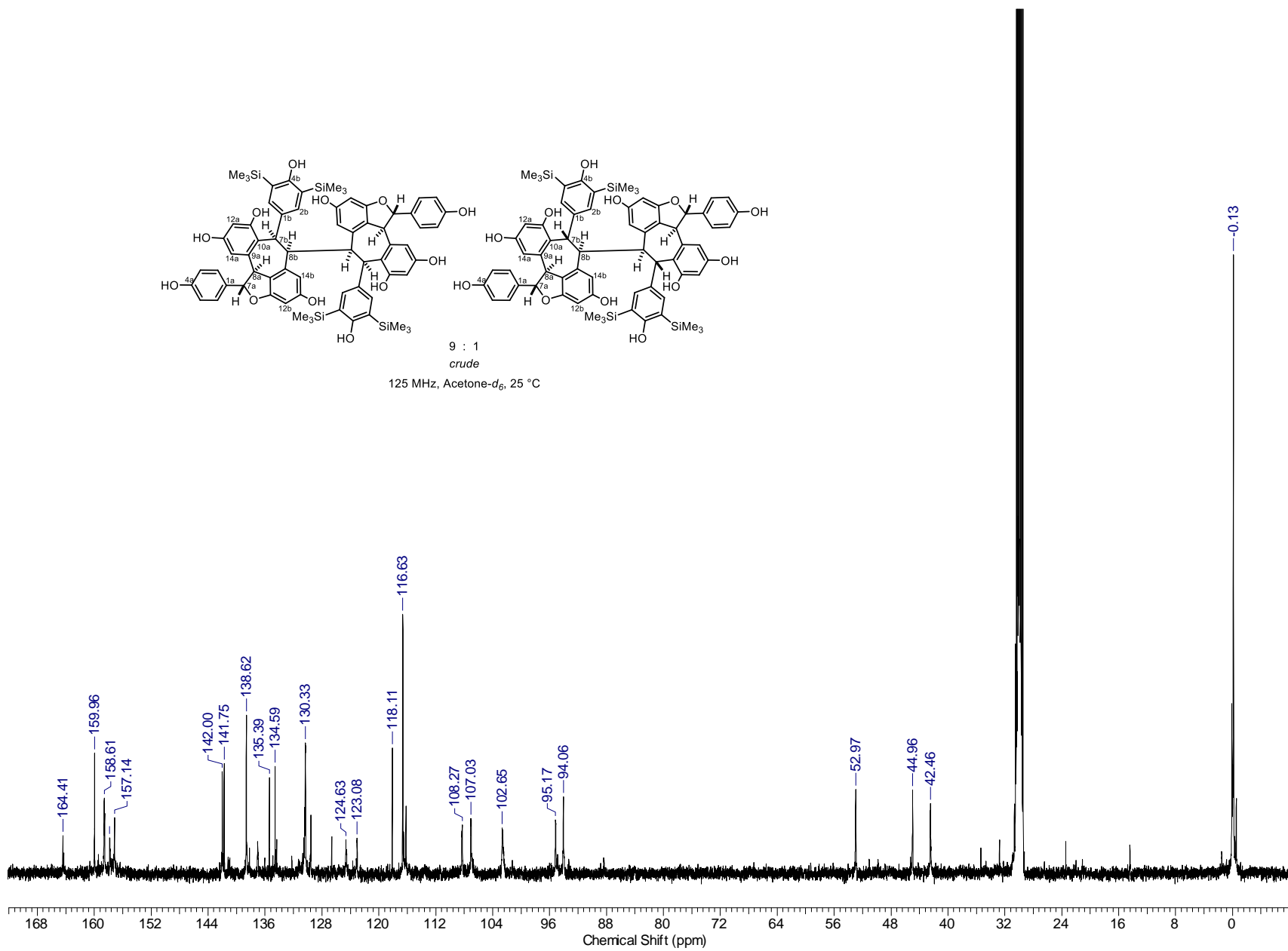
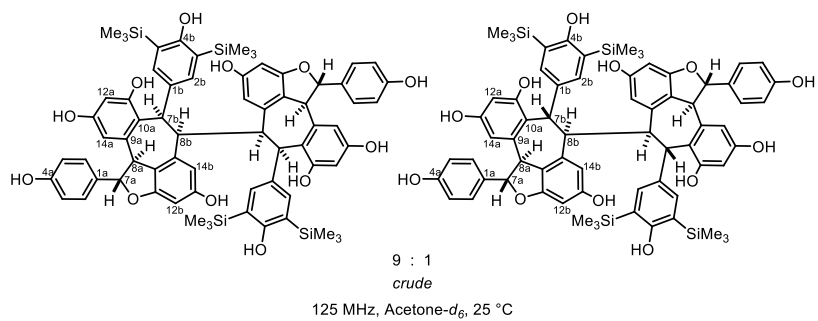
500 MHz, Acetone- d_6 , 25 °C

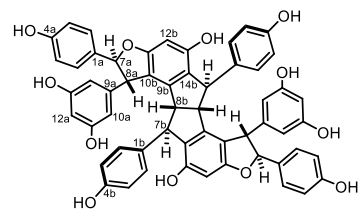


pure, small scale

175 MHz, Acetone- d_6 , 25 °C

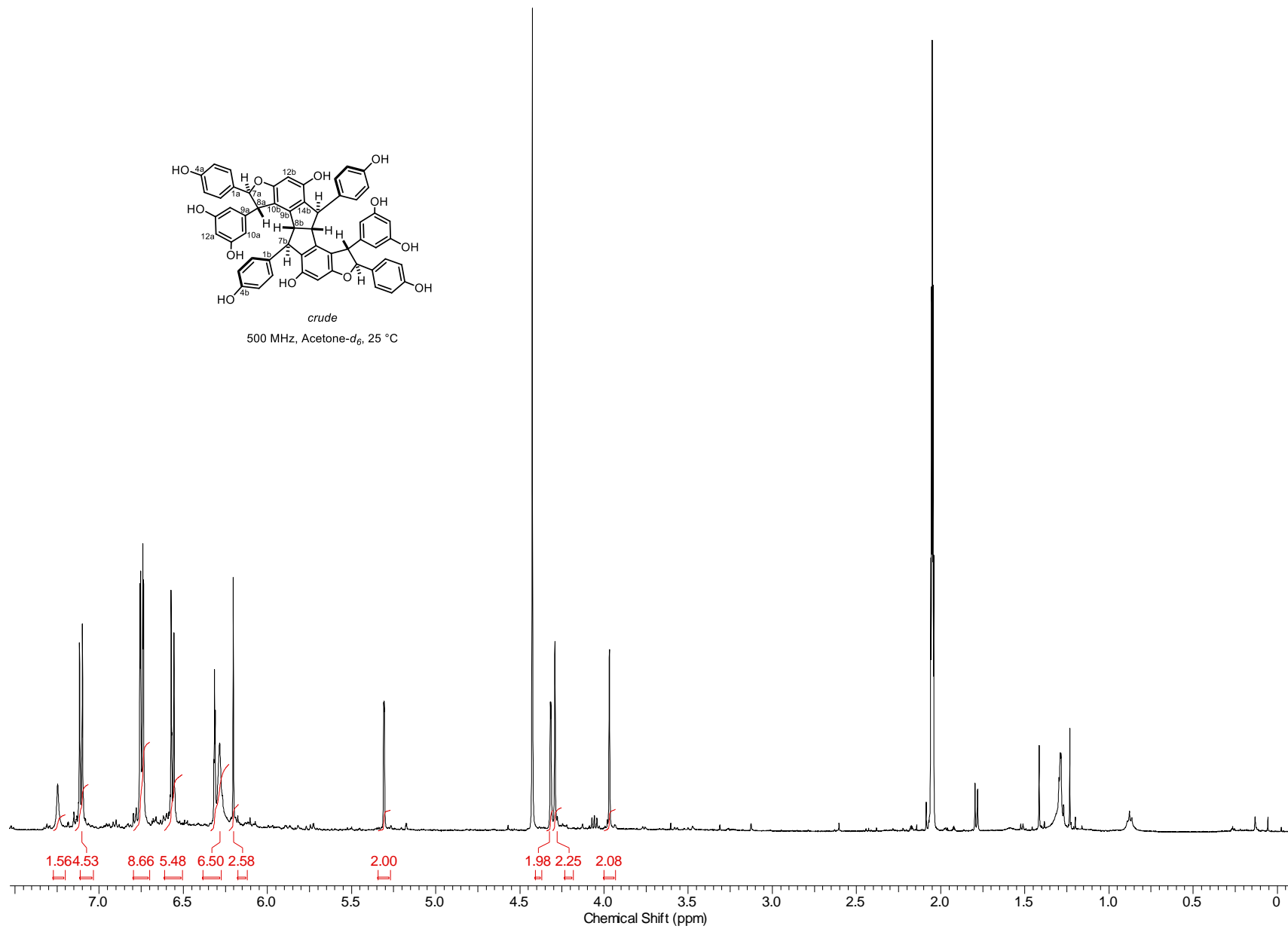


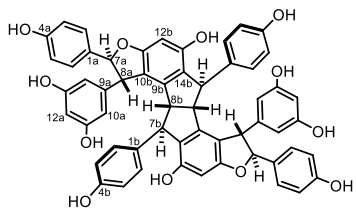




crude

500 MHz, Acetone- d_6 , 25 °C



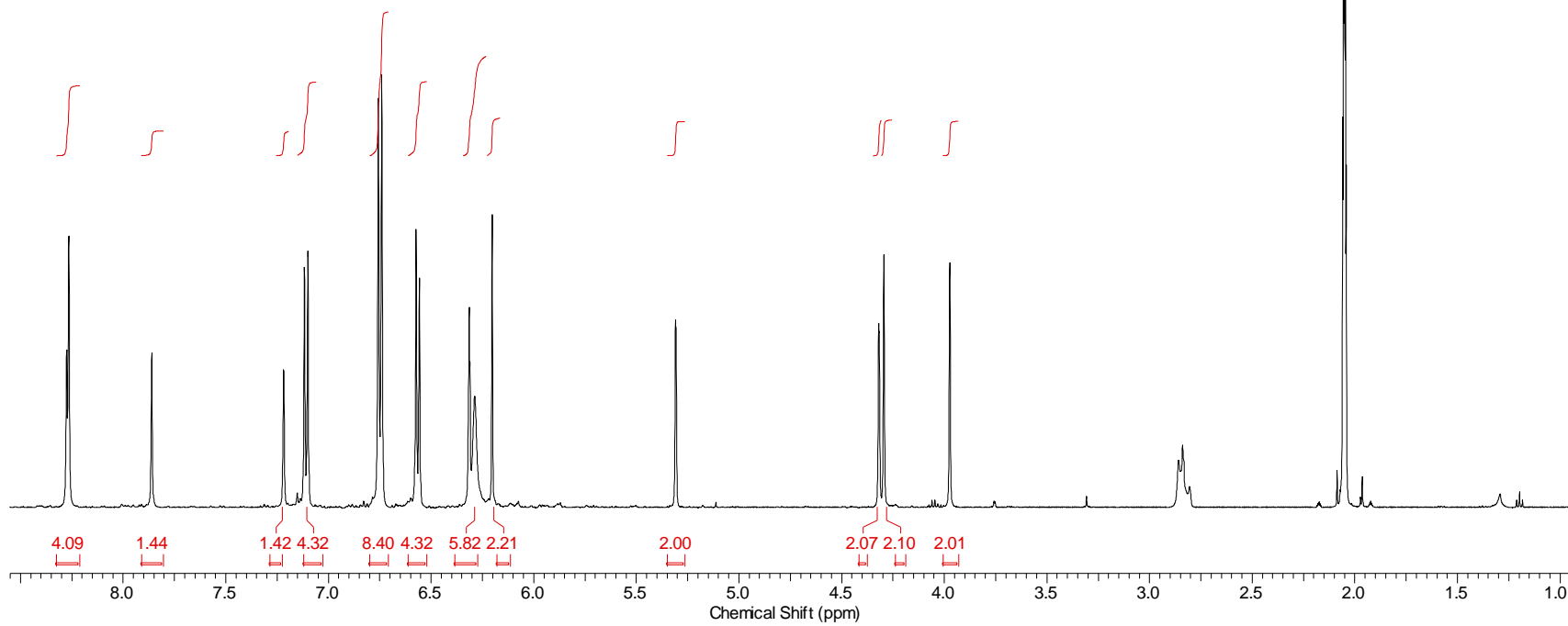


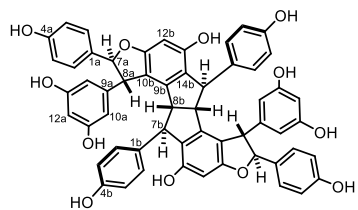
nepalensinol B

pure

500 MHz, Acetone- d_6 , 25 °C

305



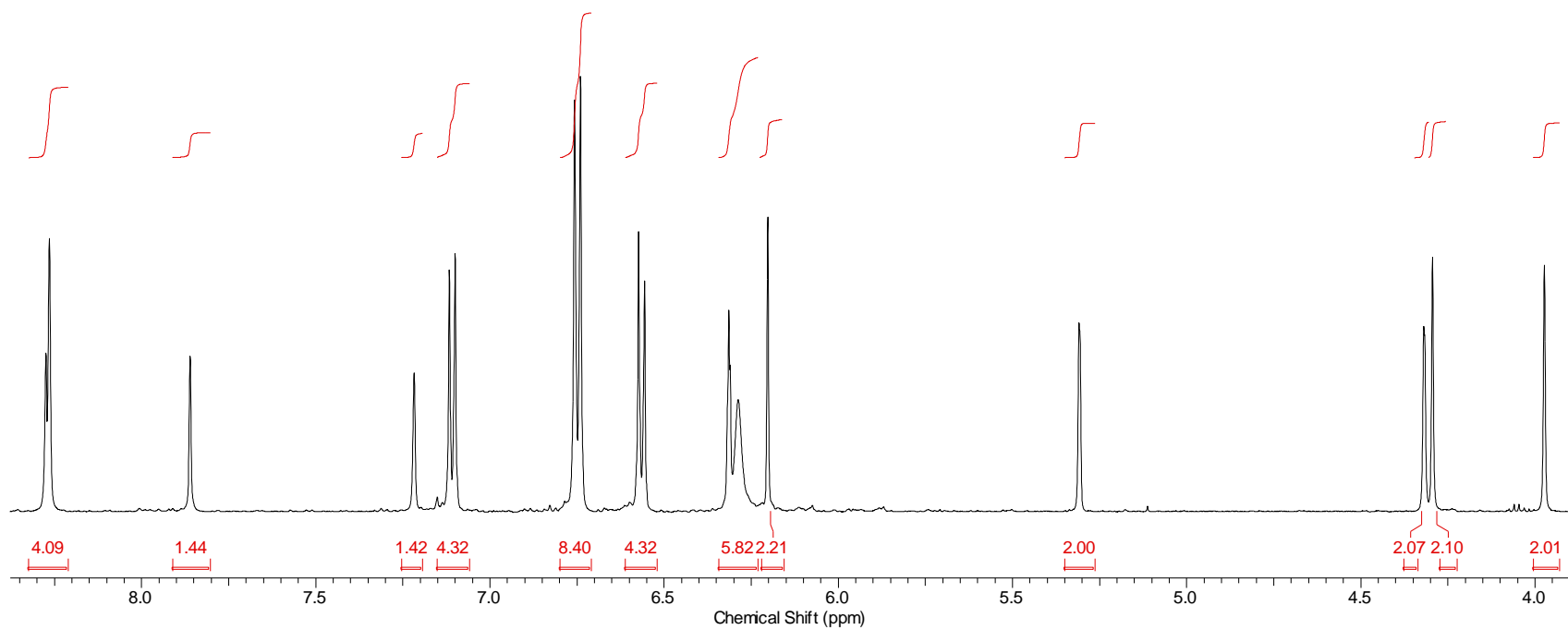


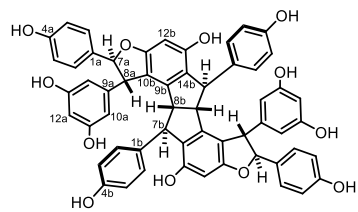
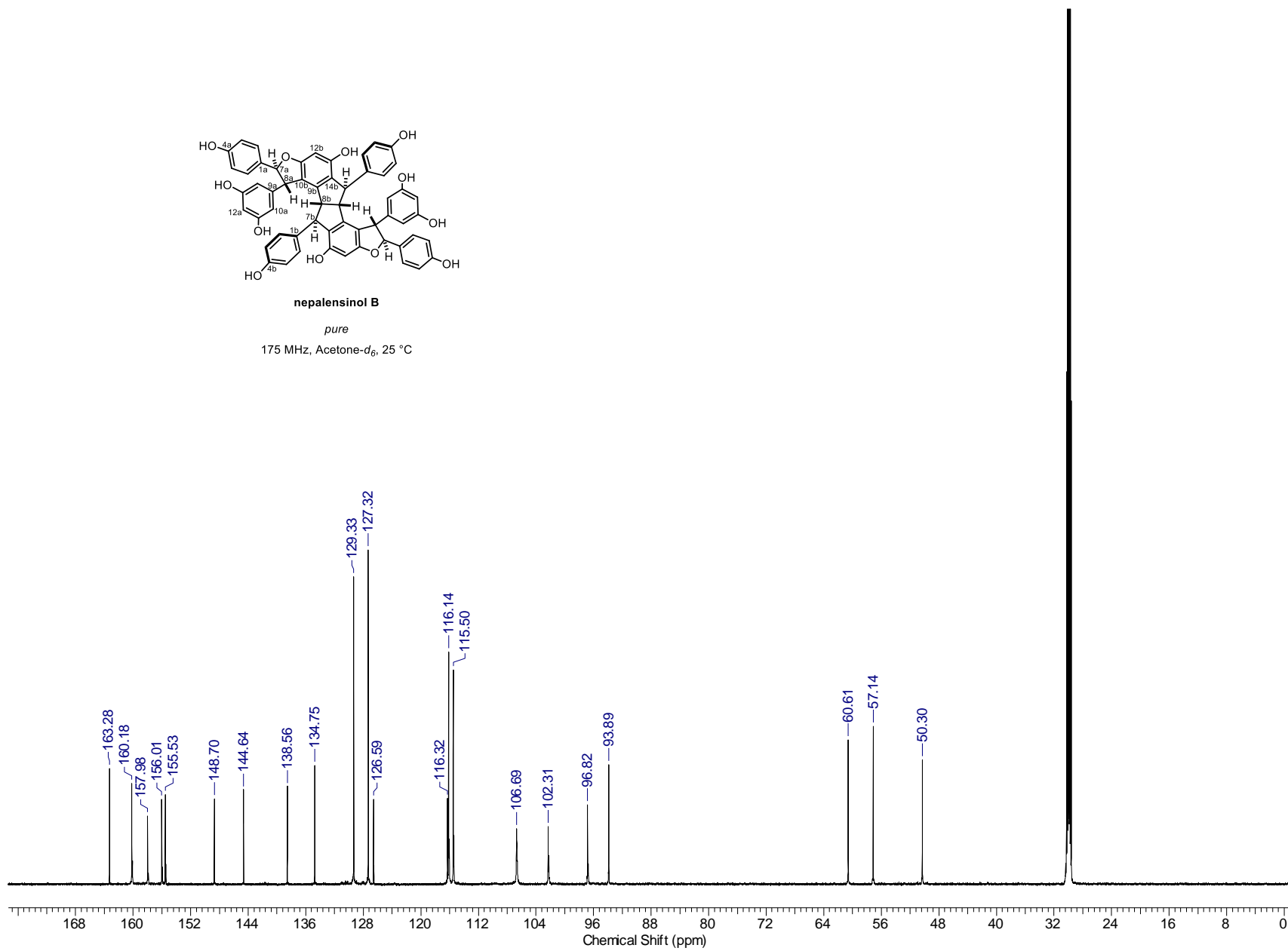
nepalensinol B

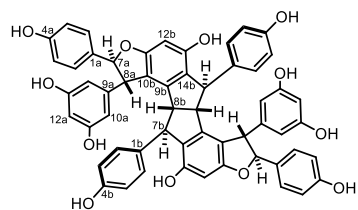
pure

500 MHz, Acetone- d_6 , 25 °C

306



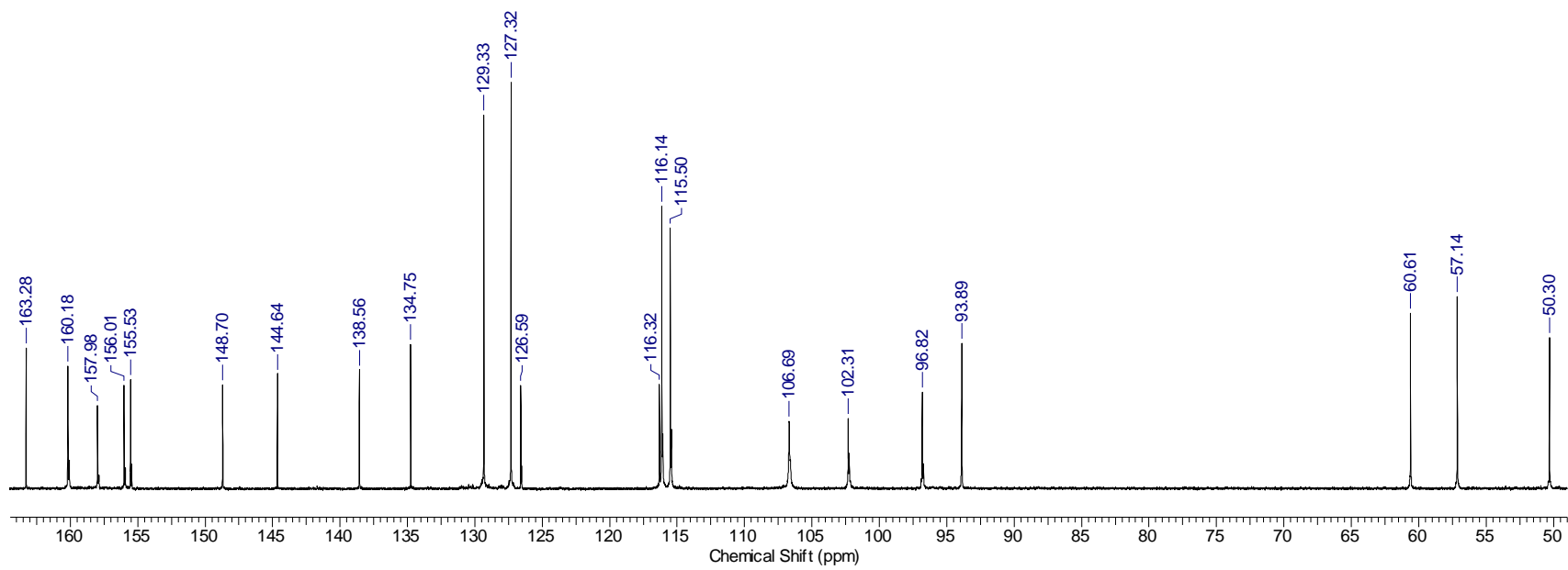
**nepalensinol B***pure*175 MHz, Acetone- d_6 , 25 °C

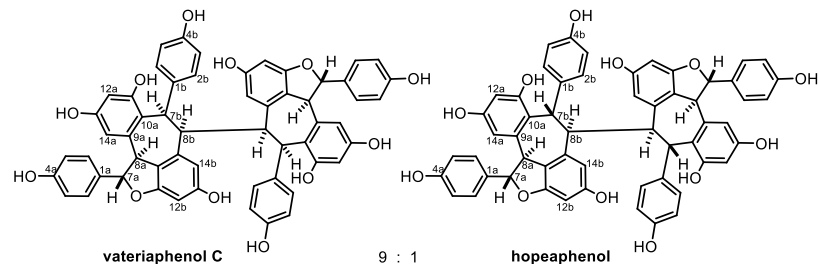


nepalensinol B

pure

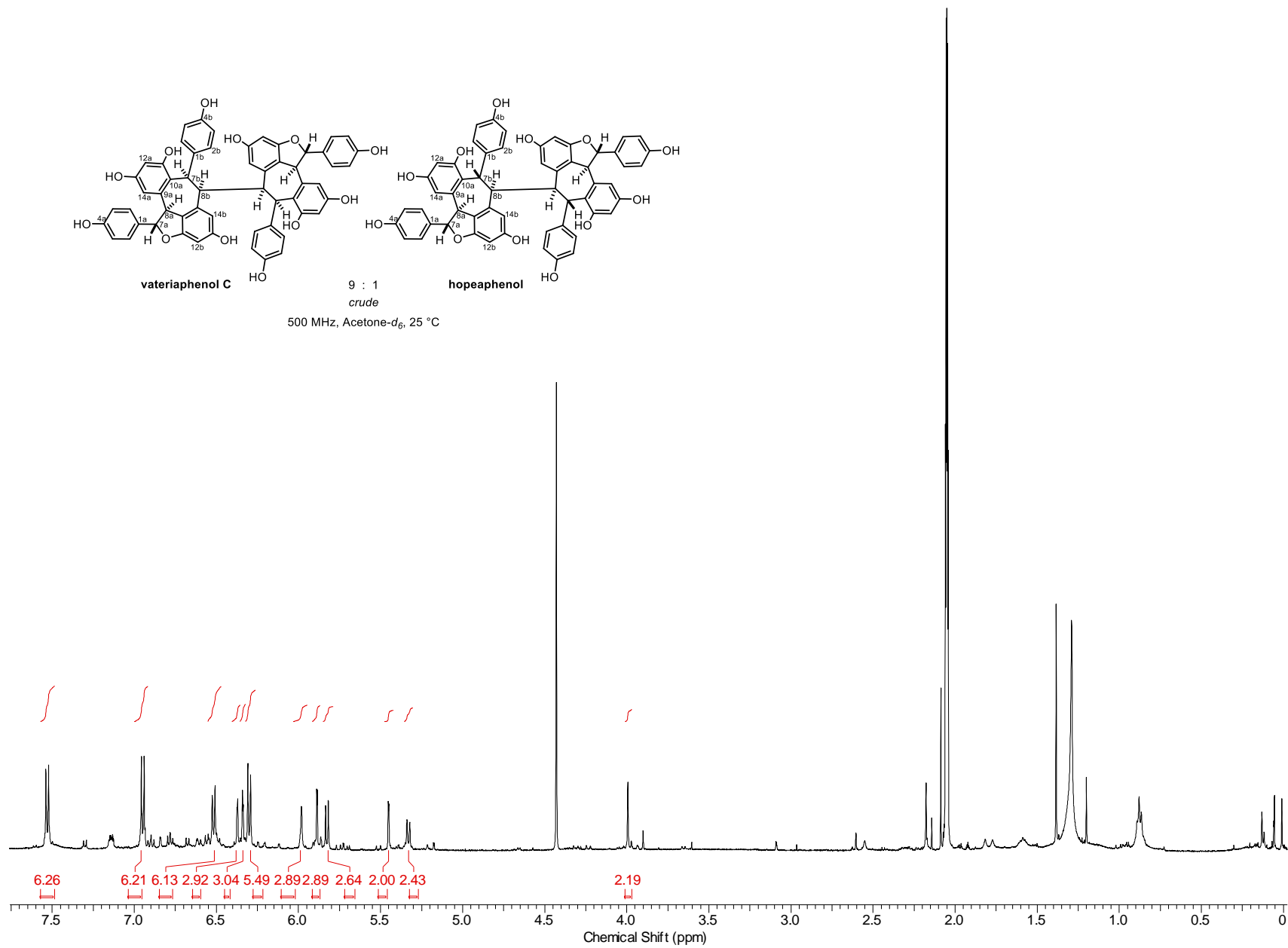
175 MHz, Acetone- d_6 , 25 °C

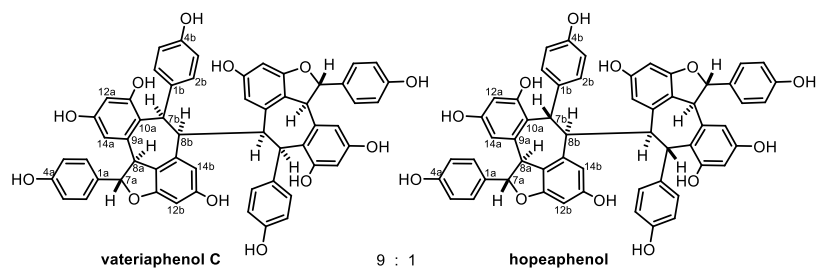




9 : 1
crude

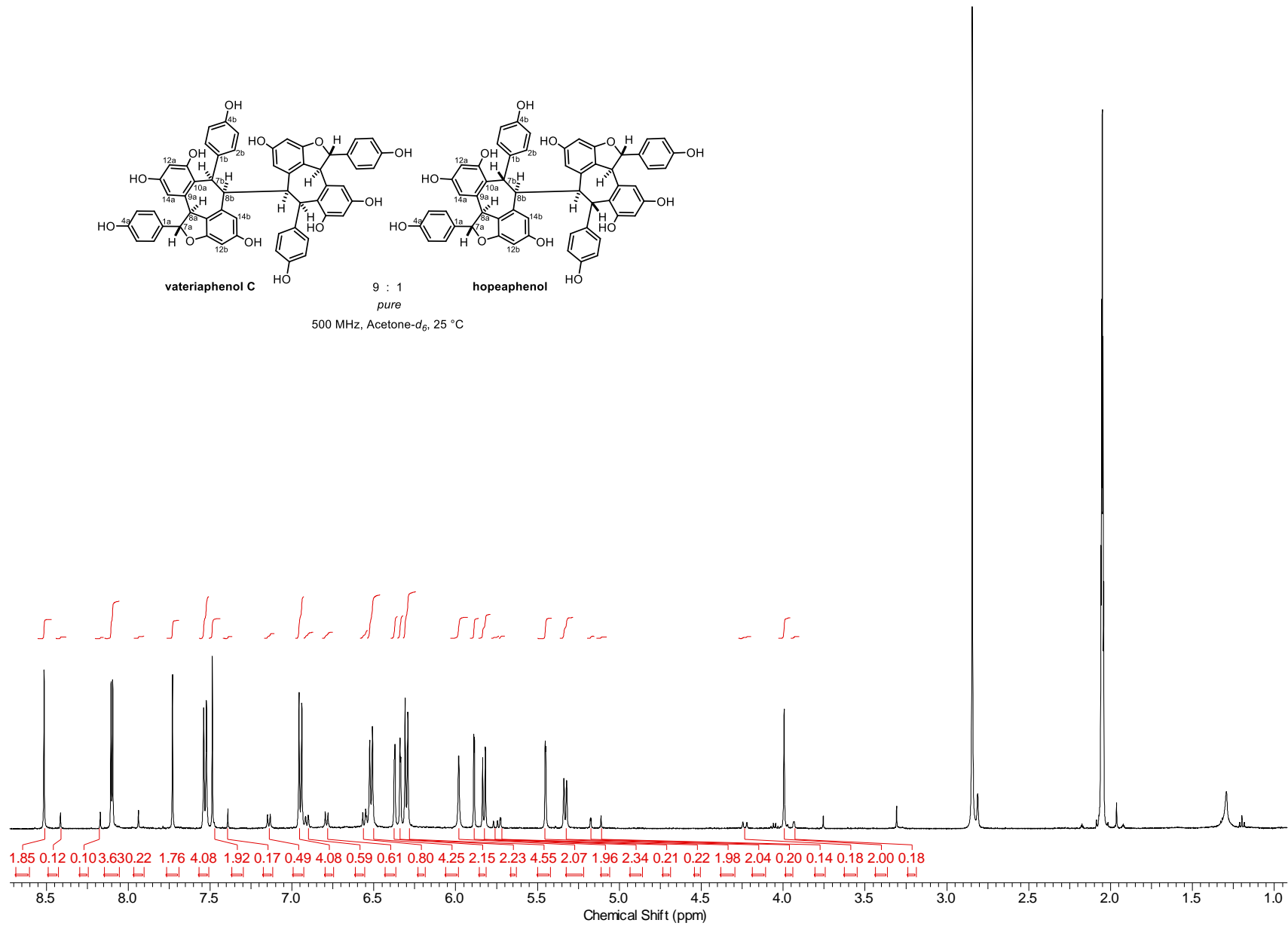
500 MHz, Acetone- d_6 , 25 °C

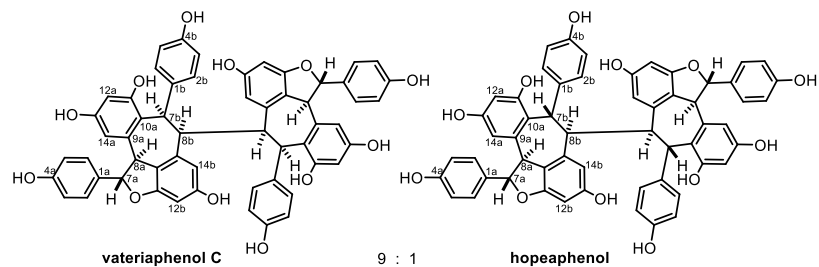




9 : 1
pure

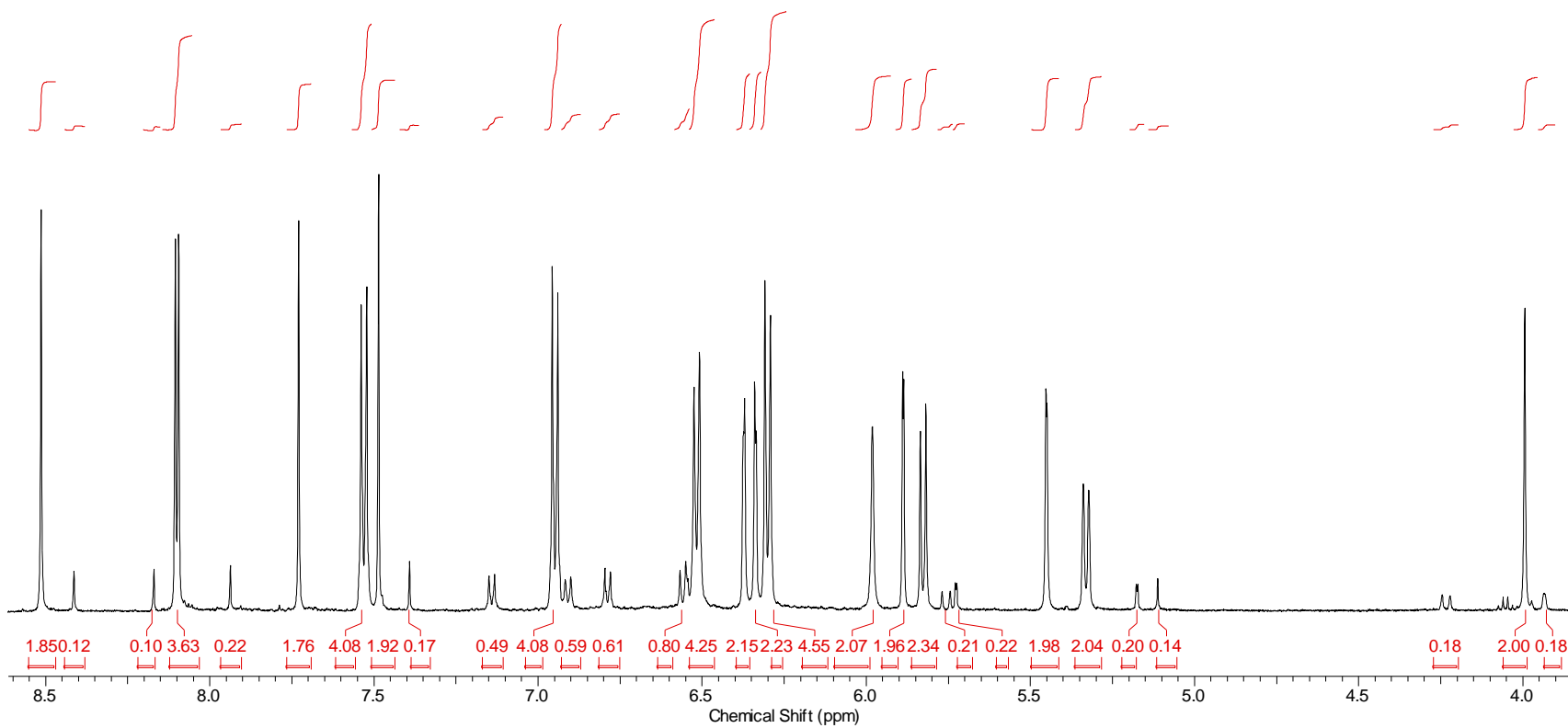
500 MHz, Acetone- d_6 , 25 °C

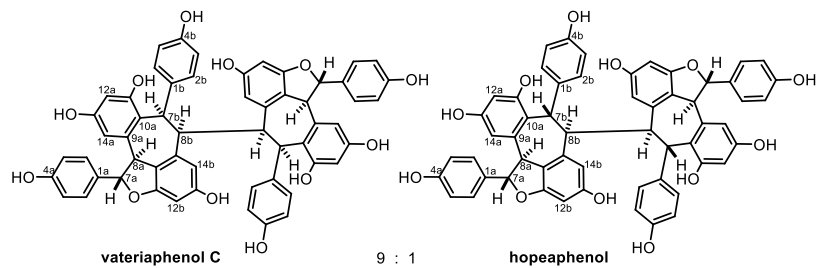




9 : 1
pure

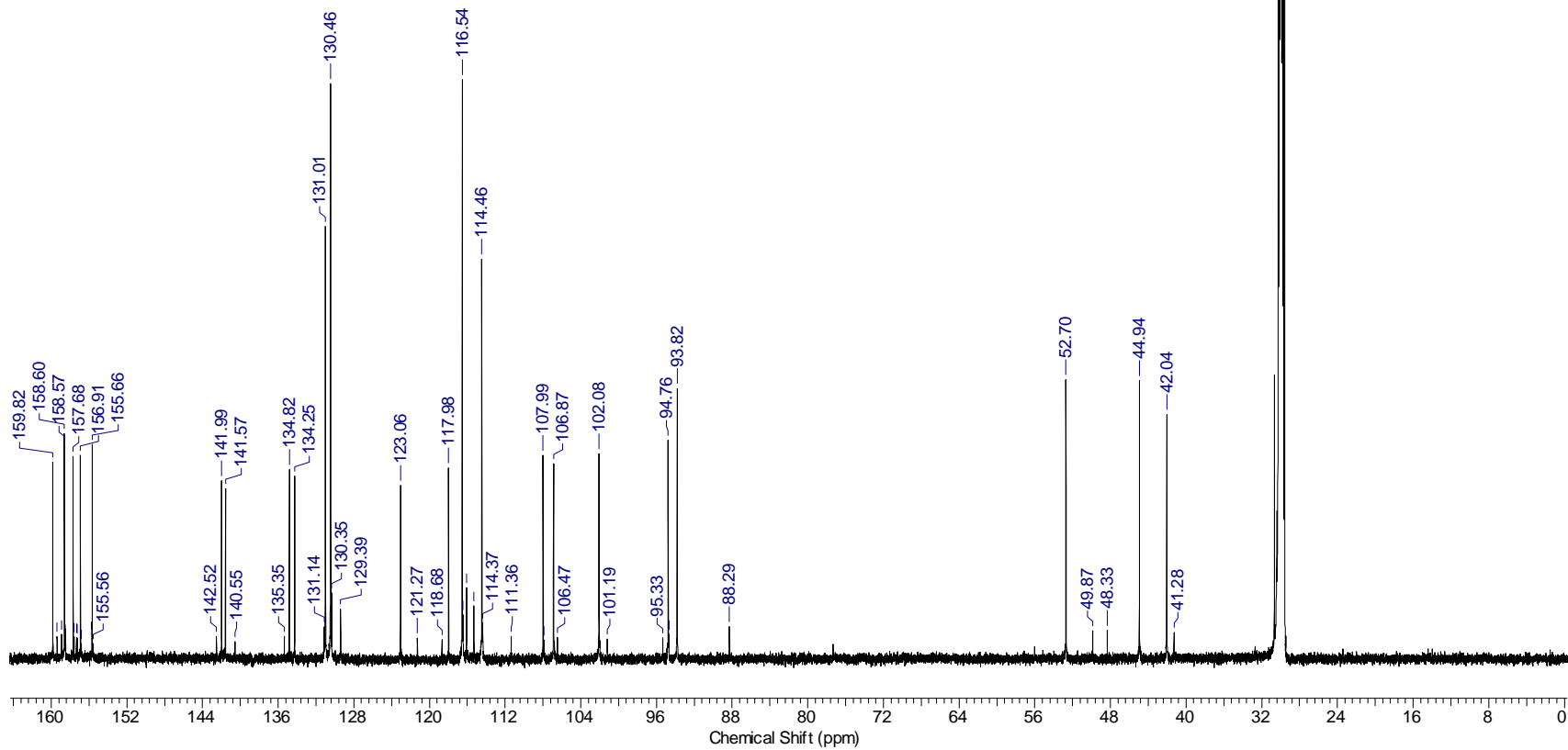
500 MHz, Acetone-*d*₆, 25 °C

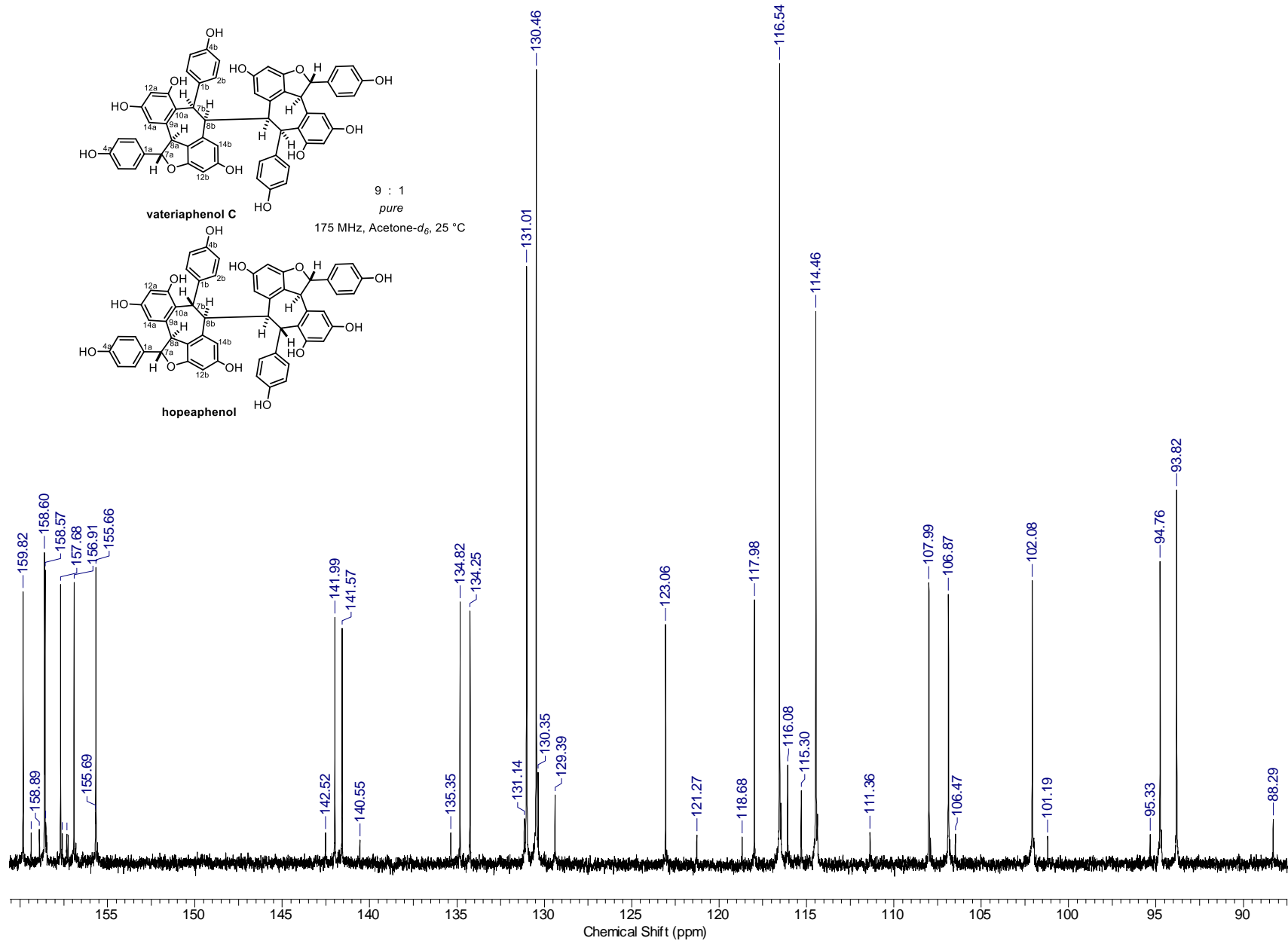




9 : 1
pure

175 MHz, Acetone- d_6 , 25 °C





CHAPTER 4: EFFORTS TOWARD THE TOTAL SYNTHESIS OF TRIMERIC RESVERATROL NATURAL PRODUCTS

4.1 Introduction

In the previous two chapters, we shared the story of our biomimetic syntheses of resveratrol dimers and tetramers. These approaches are conceptually similar and presented in a way that makes this extension of our preliminary findings appear obvious — hindsight is 20/20. In reality, this is not the chronological order in which the research unfolded, and a substantial amount of the interim from completion of the dimer synthesis to that of the tetramers was invested in pursuit of the synthesis of resveratrol trimers. Although it may seem counterintuitive given the greater degree of complexity present in the resveratrol tetramers, many are more synthetically accessible than the trimers by virtue of their symmetry, which renders them amenable to convergent synthesis (cf. Section 3.3). By contrast, the vast majority of trimers break symmetry, a subtle difference that profoundly increases the difficulty of their synthesis due to the presence of multiple identical functional groups within the same molecule.

As was true of the resveratrol tetramers (cf. Section 3.2), the total synthesis of resveratrol trimers has only been accomplished by one group thus far – Snyder and co-workers. In their initial approach to higher oligomers containing [3.2.1] and [3.3.0] bicyclooctane cores (Figure 3.4), a *de novo* approach was executed through a series of reagent-controlled brominations followed by iterative homologation reactions to forge the 2,3-diaryl-dihydrobenzofuran rings.¹³⁸

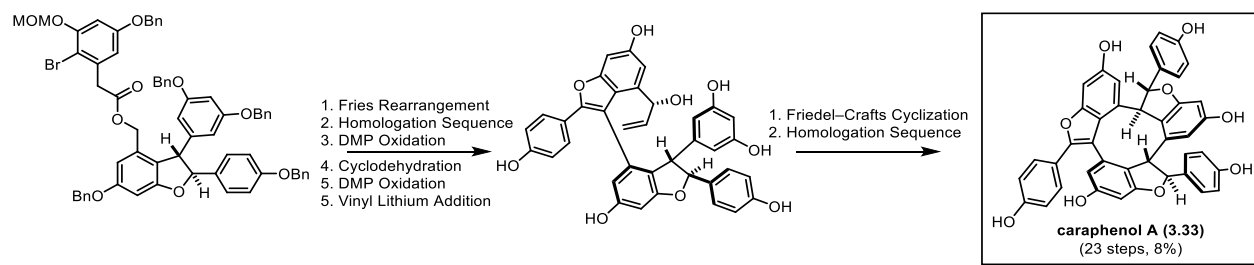


Figure 4.1 Synthesis of Caraphenol A by Snyder and Wright

Using this strategy, the synthesis of three resveratrol trimers, carasiphenols B and C,^{41,279} and ampelopsin G,²⁸⁰ was achieved, each in 20 steps and 0.5–3% overall yield. Since this initial report, this group has completed the syntheses of two additional trimeric natural products — vaticanol A (**4.1**) and caraphenol A (**3.33**).^{260,281} The first segment of the caraphenol A synthesis is shown in Figure 3.19. This cyclotrimeric scaffold is architecturally distinct from the various indane-derived cores previously targeted by this group. They again leveraged their iterative homologation chemistry for the synthesis of each dihydrobenzofuran (Figure 3.3), and the 8–10' linkages were formed using anionic Fries-rearrangements and an eventual Friedel–Crafts cyclization for 9-membered ring formation (Figure 4.1).¹⁴² This *de novo* synthetic sequence proved to be robust, delivering over 600 mg of the final target.

More closely related to our work in this area is the synthesis of vaticanol A (**4.1**), an indane-derived resveratrol trimer containing a fused [7,5]-carbocyclic core.¹⁴³ Starting from permethyl pauciflorol F (**2.36**), the dibromoampelopsin D derivative **4.2** was prepared through a six-step sequence previously developed for the synthesis of caraphenols B and C.¹⁴⁰ A double lithium-halogen exchange with subsequent addition of 3,5-dimethoxybenzaldehyde gave the monoalkylated product **4.3** without formation of its regioisomer or the doubly alkylated product. Oxidation to **4.4** followed by debenzoylation afforded **4.5**, which was subjected to DDQ to dehydrogenate the exposed phenol to its corresponding quinone methide. This promoted *in situ*

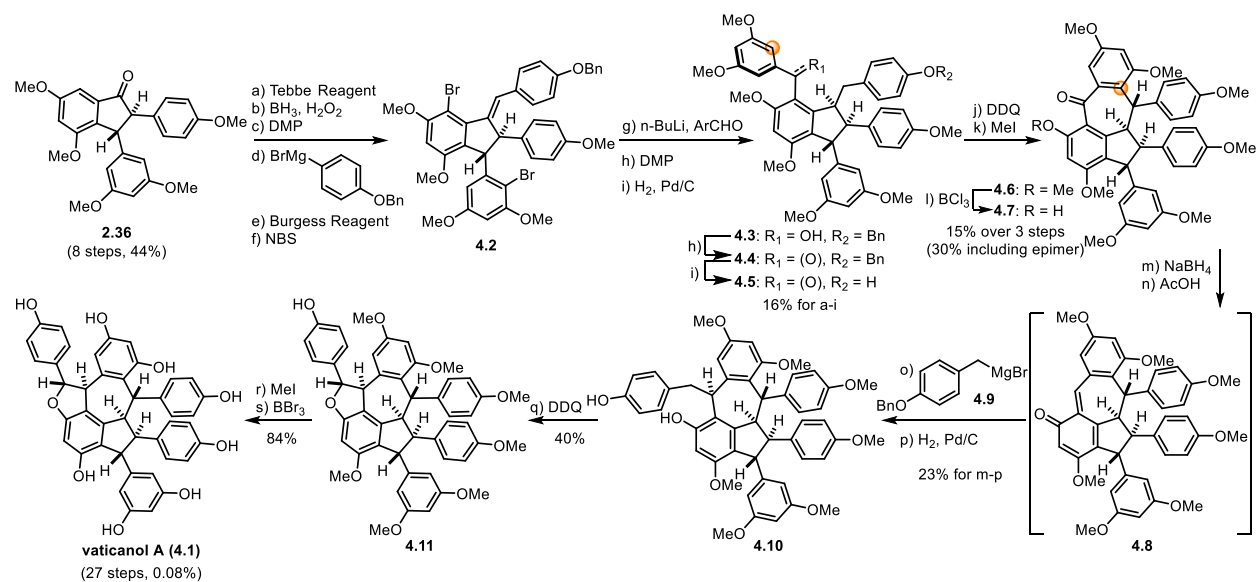


Figure 4.2 Synthesis of Vaticanol A by Snyder and Co-workers

cyclization to **4.6** as a 1:1 mixture of diastereomers, which was then demethylated to **4.7**. Here, rather than their usual homologation protocol for construction of the dihydrobenzofuran, an alternate sequence was employed. Reduction of the benzophenone followed by treatment with acetic acid promoted generation of quinone methide **4.8**. Alkylation of this intermediate with Grignard reagent **4.9** and subsequent debenzoylation afforded intermediate **4.10**. A second DDQ-mediated dehydrogenation promoted cyclization to dihydrofuran **4.11**, albeit in moderate yield. Attempts to directly deprotect dihydrofuran **4.11** with BBR_3 were unsuccessful, necessitating methylation of the free phenol prior to exposure to this reagent, which yielded a sample containing vaticanol A (**4.1**, 0.9 mg).¹⁴³

4.2 Toward the Synthesis of Indane-Derived Resveratrol Trimers

The total synthesis of vaticanol A is an impressive feat, although it is shadowed by its long linear sequence (27 steps) and provides only 0.08% overall yield of the target structure. In order to facilitate rigorous investigation of the biological activities of structures such as **4.1**, new

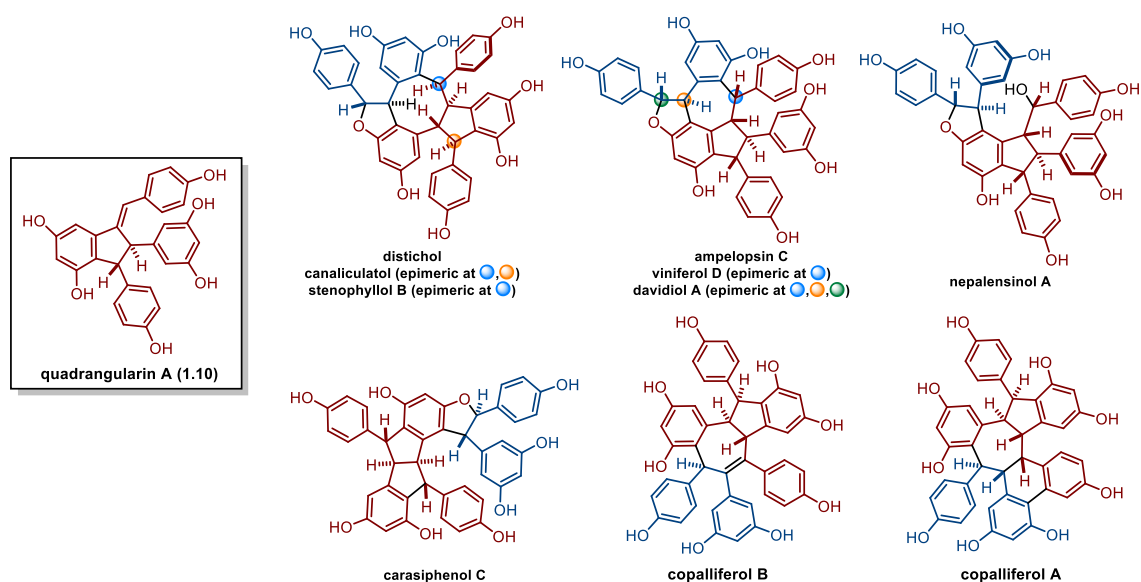


Figure 4.3 Trimeric Structures based on the Core of Quadrangularin A

synthetic strategies must be developed. Just as vaticanol A is built upon the core of ampelopsin D (2.30), there are number of resveratrol trimers built upon the framework of the regioisomeric dimer, quadrangularin A (1.10) (Figure 4.3). These natural products are characterized by the presence of an indane, dihydrobenzofuran, or medium (seven- or eight-membered) ring, or some combination of all three of these structural motifs. These polycyclic cores are densely functionalized, containing up to six-stereogenic centers which, despite their sp^3 -character, are conformationally rigidified by their positioning within a fused ring system. Though difficult to appreciate in a planar drawing, the variances in relative configuration about the core confer vastly different three-dimensional presentations and biological properties, rendering them attractive targets for chemical synthesis.

Recall that during our studies toward the synthesis of resveratrol dimers (Section 2.6), we discovered that a diastereomeric mixture of *meso*- and *D/L*-bis-quinone methide dimers 2.55/2.56 could undergo dynamic epimerization and desymmetrization to afford the indane quinone

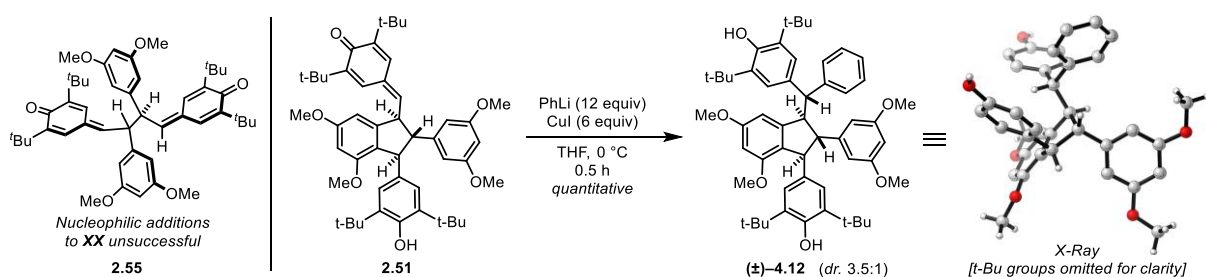


Figure 4.4 Probing the Feasibility of Intermolecular Quinone Methide Functionalization

methides **2.51/2.52** (Table 3.1). We hypothesized that **2.51/2.52** could serve as a progenitor to resveratrol trimers such as those depicted in Figure 4.3 via arylation of the electrophilic quinone methide moiety. To probe the validity of the proposed strategy, we first attempted the conjugate addition of a variety of nucleophiles (Grignard reagents, organocuprates, water, Al-salen promoted oxime additions,²⁸² trimethylsilylanolate, thiols, amines, cyanide, aryl- and alkyl-halide derived radicals, hydrides, enamines, Rh-mediated boronic acid conjugate additions,²⁸³ copper phosphoramidite-mediated alane conjugate additions,²⁸⁴ etc.) to both **2.55/2.56** and **2.51** (Figure 4.4).

The linear bis *p*-quinone methide **2.55** proved to be poorly suited to this task, giving either no reactivity, simple isomerization, or complex mixtures. This can be accounted for by its high steric demand and the previously described homolytic dissociation equilibrium (Section 3.4). Conversely, the addition of various nucleophiles to **2.51** proved to be highly efficient and proceeded with moderate levels of diastereoselectivity. Our first major success in this area came with the addition of the Gilman reagent derived from phenyl lithium,²⁸⁵ which proceeded in quantitative yield to afford the corresponding phenyl adduct **4.12** as a 3.5:1 mixture of diastereomers (Figure 4.4). Notably, an excess of the nucleophile is utilized in these conditions to overcome potential quenching by the free phenol of the electrophile. Crystals of the major diastereomer suitable for X-ray diffraction studies were obtained by slow cooling from

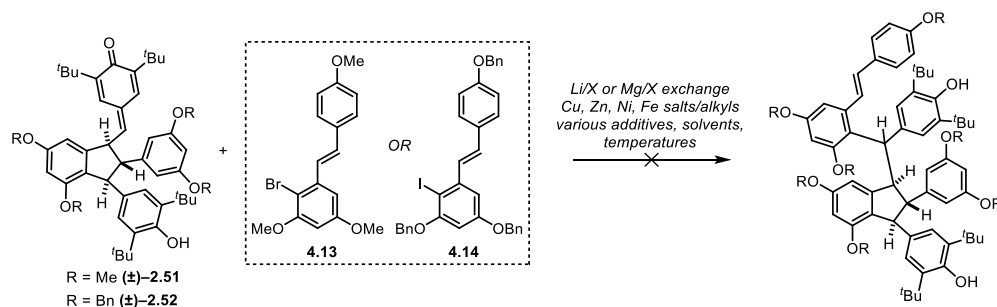


Figure 4.5 Attempted Regioselective 1,6 Additions to Quinone Methide

EtOH. This confirmed the *trans,trans*- relative configuration about the indane core and indicated a preference for addition to the *re* face of prochiral **2.51**, yielding a product whose relative configuration is consistent with that of ampelopsin C, and stenophyllol B (Figure 4.3).

Based on these findings, we were excited by the prospect of performing a similar reaction from a halo-resveratrol derivative to access trimeric materials through organometallic quinone methide functionalization (Figure 4.5). From known bromopermethyl resveratrol **4.13**,¹⁴¹ attempts were made to generate the corresponding Gilman reagent through a lithium halogen exchange and transmetalation to copper. However, addition of a solution of **2.51** to this mixture did not lead to formation of the desired product, returning **2.51** and the hydrodehalogenated product. Later efforts using iodoperbenzyl resveratrol **4.14** with the corresponding benzyl-protected quinone methide intermediate **2.52** were also unsuccessful. A wide variety of conditions were investigated for this purpose, including both lithium-halogen and magnesium-halogen (using Knochel's "turbo" Grignard)²⁸⁶ exchange reactions followed by either direct addition to **2.52** or transmetalation to various copper, zinc,²⁸⁷ iron²⁸⁸ and nickel²⁸⁹ reagents prior to addition to **2.52** in the presence or absence of various additives such as TMS-Cl,^{290,291} BF₃·OEt₂,²⁹² or HMPA. Disappointingly, none of the conditions employed delivered any of the desired 1,6-addition product. Adding to the difficulty, we had not yet at the time of these studies discovered a scalable preparation of **2.51/2.52**, so material attrition was a continuous challenge.

Using 4-iodoanisole as a model system, it was found that Mg/I-exchange followed by addition to **2.52** in the presence of CuBr•Me₂S afforded a 1:1 mixture of starting material to the corresponding adduct. This ratio could be improved to 9:1 in favor of product by the use of CuCN instead. Nevertheless, application of these conditions to **4.14** led only to recovery of **2.52**, leading us to finally conclude that the desired transformation is too sterically demanding.

For each of the aforementioned organometallic nucleophiles, the carbanion resides in the sp²-orbital of an aromatic carbon, therefore requiring a “head-on” approach to the electrophilic quinone methide. Based on our hypothesis that our many reaction failures could be attributed to unfavorable steric interactions during the approach of the two reaction partners, particularly given the known propensity of organometallics to form aggregates in solution, we considered that perhaps an inversion in reaction conditions to acidic, therefore favoring a Friedel–Crafts mechanism, would be more feasible. Not only would the geometry of this “side-on” approach via a Wheland intermediate be more conducive to the desired reactivity, but it is also known that the electrophilicity of quinone methides is greatly enhanced on protonation and/or Lewis acid complexation of the quinone oxygen.¹⁸³ The decision to pursue this approach demanded the consideration of a number of new challenges, such as controlling the regio- and stereochemical outcome of the reaction, as well as preventing oligomerization of the electrophile with itself.

We were pleased to find that upon exposure of *p*-quinone methide **2.52** to BF₃•OEt₂ in the presence of perbenzyl resveratrol **4.15**, the desired Friedel–Crafts addition occurred cleanly, affording only intermolecular addition products in high yield (Figure 4.6). Although a mixture of desired (**4.16**) and undesired (**4.17**) regioisomers was obtained, each was isolated as a *single diastereomer* (configuration at the newly formed stereogenic center undefined). The connectivity

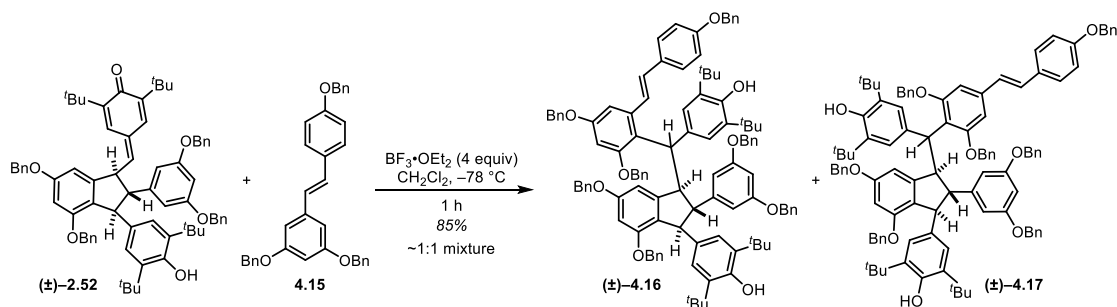
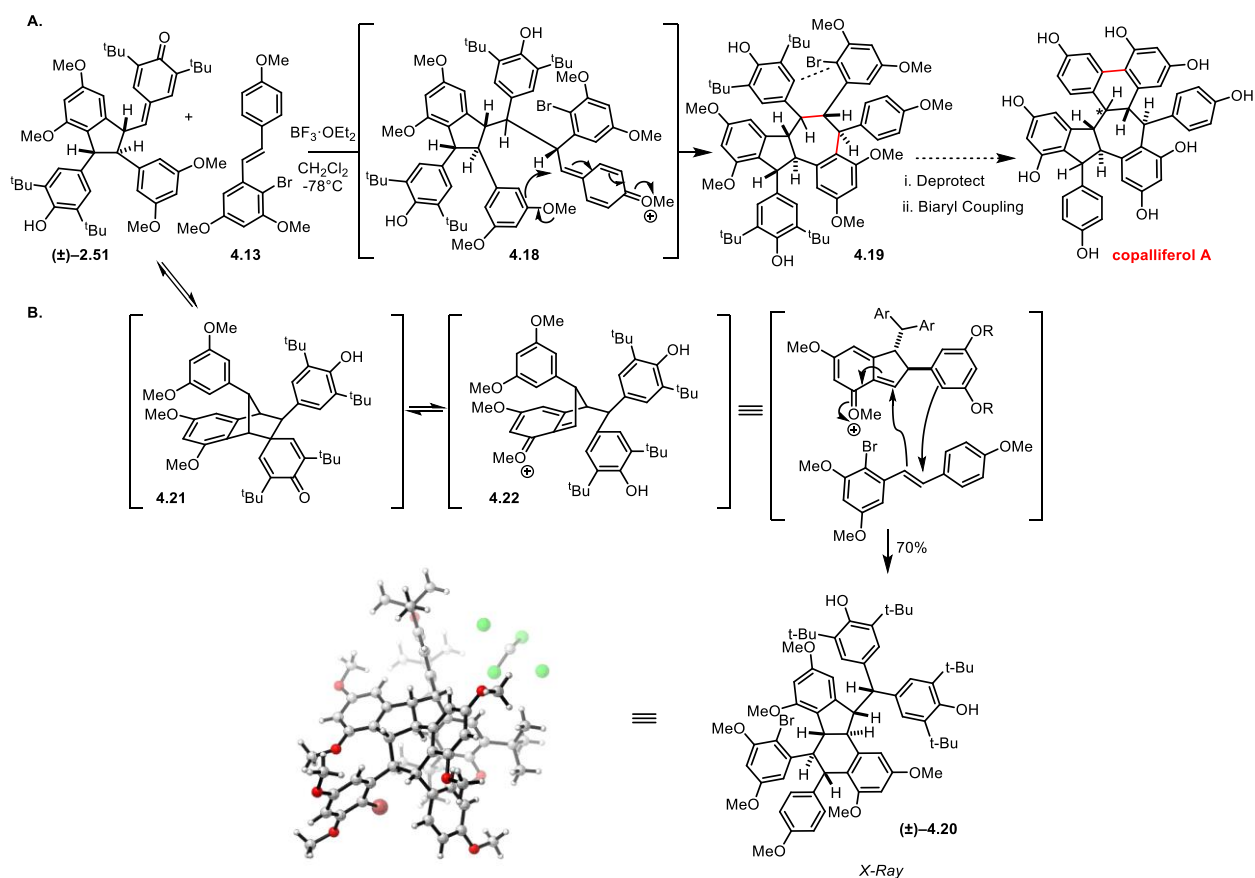


Figure 4.6 Friedel–Crafts Trimerization Reaction

of each trimer was deduced through heteronuclear 2D NMR experiments on the corresponding debenzylated compounds.⁵⁶ While the diastereoselectivity of this reaction could be rationalized on steric grounds, we have since discovered an unanticipated mode of intramolecular reactivity that may also contribute to this outcome (vide infra).

My colleague Dr. Bryan Matsuura postulated that the use of bromopermethyl resveratrol **4.13** for this reaction — wherein the resorcinol is both sterically and electronically deactivated — could perhaps direct the Friedel–Crafts reaction to occur vinylogously through the 4-benzyloxystyrene functionality. This in turn would generate a cationic *para*-quinone methide **4.18**, which, upon trapping by the pendant resorcinol, would result in a one-pot formal (5+2) cycloaddition to produce the [7,5]-fused ring system **4.19** which represents the core of the natural product copalliferol A (Figure 4.7 A). It was found that the bromo-derivative did in fact exhibit attenuated reactivity as compared to permethyl resveratrol, and that it reacted nucleophilically through the styrene; however, the reaction was kinetically too slow to compete with an unanticipated skeletal rearrangement, and instead the [6,5] annulated product **4.20** was obtained. Bryan was able to obtain crystals of **4.20** suitable for X-ray diffraction studies by slow evaporation from THF. The formation of this product can be accounted for by the mechanism depicted in (Figure 4.7 B). Namely, in lieu of rapid trapping of the quinone methide cation, the

⁵⁶ See supporting information for details



disposes the quinone methide-derived phenol in the pseudo equatorial position (depicted) or the pseudoaxial position. Regardless, provided that one of these configurations is preferred, the existence of an equilibrium between **2.51** and **4.21** could account for the facial selectivity observed during attack of the quinone methide by the incipient resveratrol nucleophile.

4.3 Concept for Biomimetic Trimer Synthesis and Efforts Toward this End

The Friedel–Crafts reaction described above (Figure 4.6) afforded a mixture of trimeric regioisomers **4.16** and **4.17**. Although the R_F values of these compounds were essentially identical, it was possible to achieve partial separation through assiduous column chromatography. Although the configuration at the newly formed stereocenter could not be assigned, for the purpose of discussion we will assume that diastereoselectivity mirrors that observed previously for addition of the phenyl Gilman reagent (cf. Figure 4.4). From the desired **4.16**, we envisioned a biomimetic synthesis of trimers such as stenophyllol B and ampelopsin C, whereby medium-ring *and* dihydrobenzofuran synthesis would be achieved in a single process through an intramolecular oxidative (3+2) annulation from the corresponding deprotected compound **4.23** (Figure 4.8). In this scenario, access to both the seven-membered and eight-membered ring series would in principle be possible from a common intermediate by rotational isomerism and regioisomeric annulation of the two resorcinol moieties present

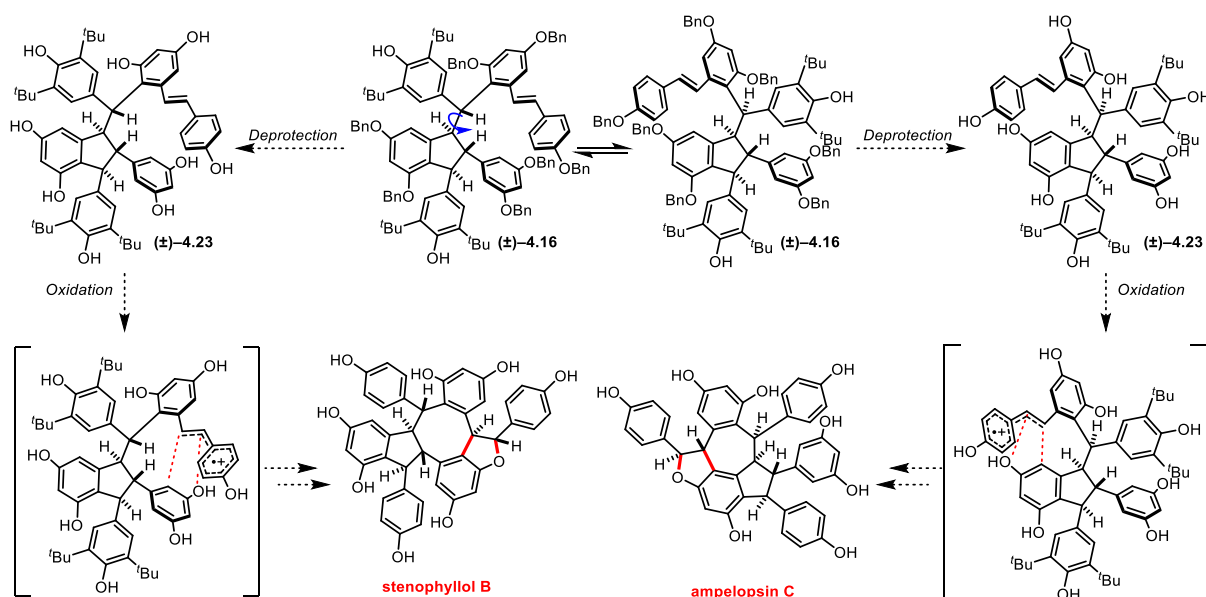


Figure 4.8 Proposed Biomimetic Oxidative (3+2) Annulation for Trimer Synthesis

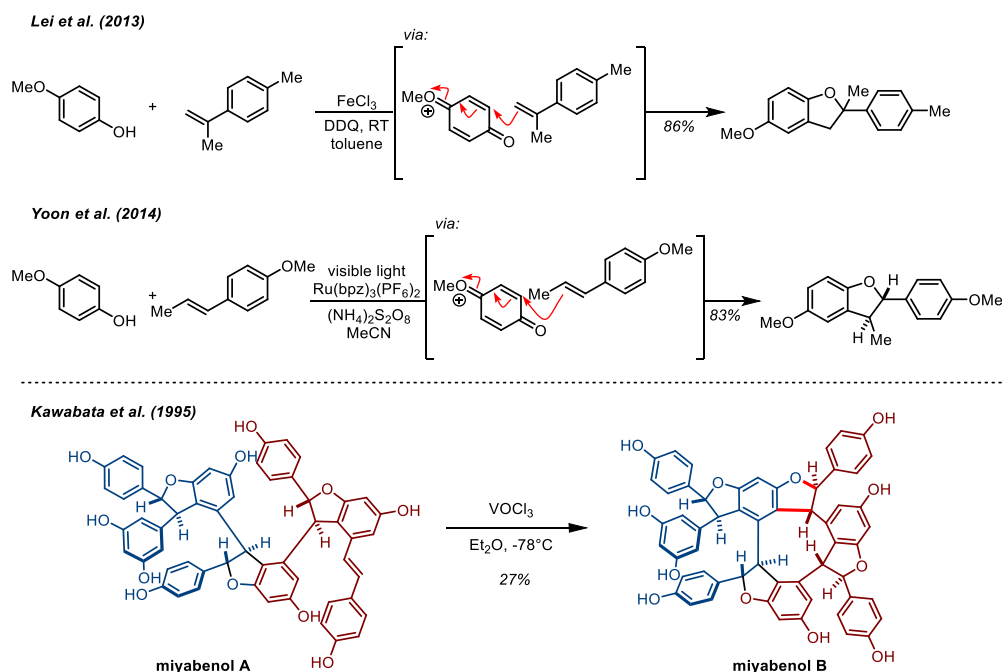


Figure 4.9 Dihydrobenzofuran Synthesis through Formal Oxidative (3+2) Cycloadditions in the quadrangularin A core.

The oxidative (3+2) cycloaddition between a phenol and olefin is a well-precedented reaction for the synthesis of dihydrobenzofurans, and has traditionally been accomplished either electrochemically or by the use of hypervalent iodine-based reagents.^{293,294} More recently, Lei and Yoon have accomplished this transformation using iron trichloride and ruthenium-trisbipyrazine catalysts in combination with DDQ and persulfate as terminal oxidants, respectively (Figure 4.9, top).^{295,296} Almost uniformly, however, reported methods for the (3+2) phenol–olefin cycloaddition require the use of *p*-hydroquinone monomethyl ether (above) or other hydroquinone derived substrates which generate electrophilic quinonium intermediates upon two-electron oxidation. Only with rare exception,²⁹⁷ including those methods described for the synthesis of ϵ - and/or δ -viniferin (Table 2.1),^{27,156} have phenols been used for this transformation which do not have the ability to form quinonium intermediates. However, the proposed intramolecular cycloaddition is not without precedent. In fact, Kawabata and co-

workers have similarly applied oxidative conditions for the conversion of miyabenol A to miyabenol B using VOCl_3 (Figure 4.9, bottom),²⁹⁸ simultaneously achieving 9-membered ring formation and DHB synthesis in a single operation. Though low-yielding, this result lends credence to the feasibility of the proposed cycloaddition for the synthesis of medium-sized rings.

With **4.16** in hand, we began our efforts to reveal the phenols while preserving the unsaturation of the stilbene. Given the incompatibility of palladium-mediated hydrogenolysis in the presence of the stilbene, a series of Lewis acid-mediated deprotections were investigated. The conditions attempted include BBr_3 , AlCl_3 , and various TMS-I sources (commercial, prepared from NaI/TMSCl in MeCN , prepared from LiI/TMSCl in CHCl_3 , prepared ‘salt-free’ from HMDS/I_2), each at various temperatures and in the presence or absence of cation scavengers such as 1,3-dimethoxybenzene and *N,N*-dimethylaniline. Unfortunately, all conditions explored led to significant and/or complete decomposition of the valuable starting material **4.16**, presumably due to the instability of the electron-rich styrene under these conditions combined with indiscriminate *O*- to *C*-transfer of benzyl cations. Ironically, this research was ongoing concurrently with our dimer synthesis (Section 2.6), and it was actually through these trials and tribulations that we came upon the uniquely effective combination of BCl_3 /pentamethyl benzene for debenylation developed by Yoshino and Fukuyama which we ultimately employed in our synthesis of quadrangularin A.^{185,186}

Thus, the free phenolic compound **4.23** was obtained using $\text{BCl}_3/\text{Me}_5\text{-benzene}$ (Figure 4.10 A), and from here we were able to investigate the proposed oxidative (3+2) cycloaddition. Each of the oxidants reported for the synthesis of ϵ - and δ -viniferin were attempted,^{15,27} including AgOAc , FeCl_3 , $\text{Tl}(\text{NO}_3)_3$, and $\text{K}_3[\text{Fe}(\text{CN})_6]$, but in each case only decomposition of **4.23** was observed (Figure 4.10 B). We posit that either the molecule cannot adopt a

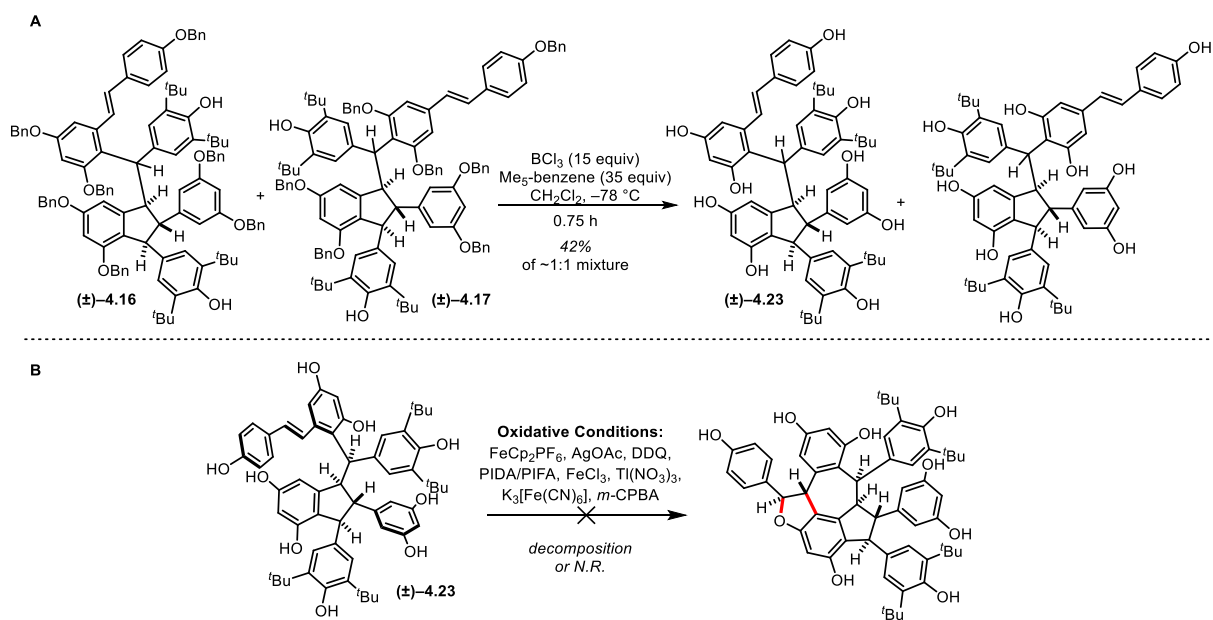


Figure 4.10 A) $\text{BCl}_3/\text{Me}_5\text{-Benzene}$ Mediated Debzoylation of Trimers; B) Failed Attempts at Intramolecular Oxidative (3+2) Annulation

conformation that enables the intended reaction partners to come within proximity of one another, or that oxidation of the *tert*-butyl phenols was taking place in preference to the 4-hydroxy stilbene.

In an effort to overcome this decomposition, we performed the Friedel–Crafts trimerization using *tert*-butyl resveratrol derivatives **2.49/2.50** (Figure 4.11 A), reasoning that the 4-hydroxystilbene motif in the product trimer **4.24** would be readily oxidized under mild conditions. Once again, a mixture of regioisomers **4.24** and **4.25** was obtained, which could be partially separated by column chromatography. For access to the corresponding free phenolic compound, we considered the possibility of performing a global hydrogenolysis — sacrificing the unsaturation of the stilbene in the process — and later selectively dehydrogenating at the dihydrostilbene. Hydrogenolysis to **4.26** proceeded as it had for previous analogues (Figure 4.11 B), and attempts were made to dehydrogenate using Pd, Rh, or Pt, with neohexene as an H_2 -acceptor or aerobically in the presence of base. Although these reactions were not successful, it

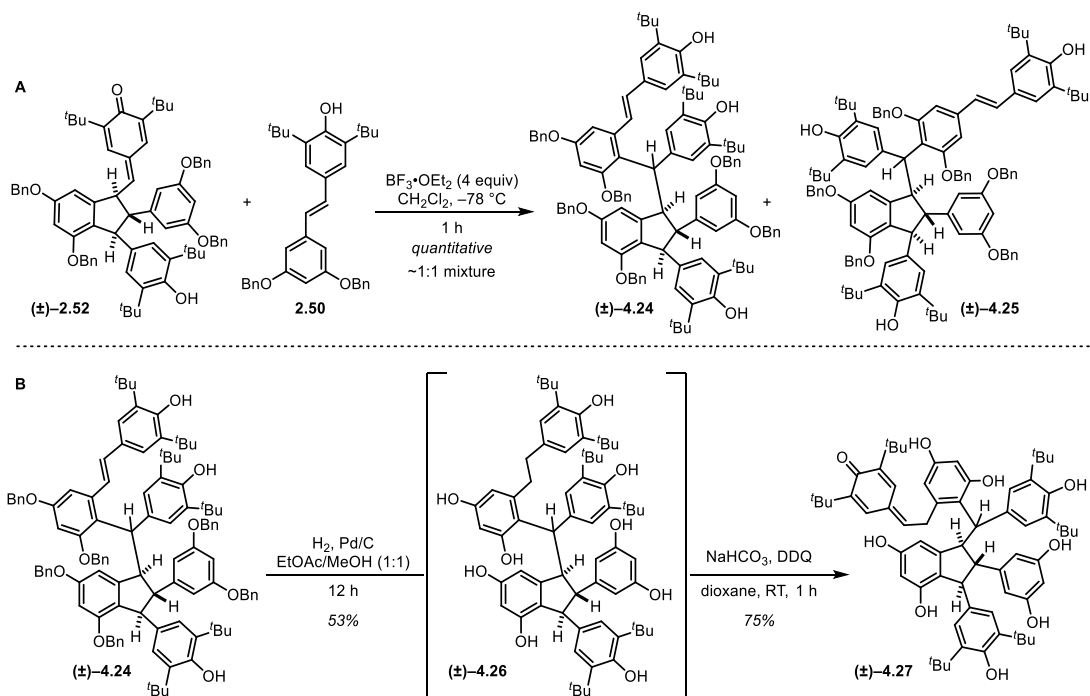


Figure 4.11 A) Friedel–Crafts Trimerization of *t*Bu Resveratrol Derivative; B) Deprotection and Chemoselective Dehydrogenation of *t*Bu Trimer

was found that DDQ had the remarkable ability to chemoselectively dehydrogenate **4.26** to the corresponding quinone methide **4.27** in a buffered solution of dioxane (Figure 4.11 B). Compound **4.27** was found to partially isomerize to the corresponding stilbene on purification over SiO₂. Unfortunately, as was observed for **4.23**, all efforts to effect the intramolecular oxidative annulation of **4.27** were unsuccessful, leading predominantly to decomposition.

We next attempted to perform the oxidation at the protected stage with the aim of improving chemoselectivity and mitigating indiscriminate oxidative decomposition. It had been observed previously that the quinone methides of the *tert*-butyl phenols are stable enough to isolate, so a two-step annulation was envisioned in which oxidative C–C bond formation occurs first to form a medium-sized ring with dihydrobenzofuran closure and deprotection taking place in subsequent steps (Figure 4.12, top). Indeed, upon exposure of **4.24** to AgOAc, clean conversion was observed. However, the ¹H-NMR spectrum of the product formed **4.28** was

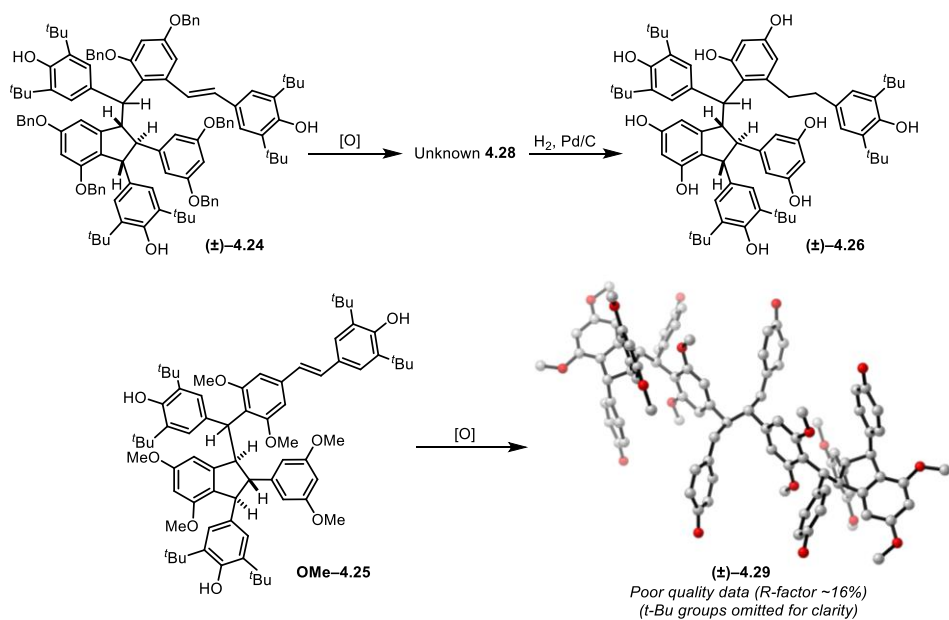


Figure 4.12 Hexamer Formation Occurs in Preference to Intramolecular Cyclization

remarkably complex. In an effort to deconvolute the spectrum, we subjected the unknown to debenzoylation. Incredibly, ¹H-NMR of the crude material obtained upon hydrogenolysis of the unknown revealed its identity as **4.26**. During the course of these studies, we often first treated the undesired regioisomer **4.25** with each oxidant to determine the likelihood of decomposition of **4.24**. It was found that AgOAc, FeCp₂PF₆, or aerobic oxidation of OMe-**4.25** also led to the clean formation of a new product with a highly complex ¹H-NMR spectrum. Although the data quality is poor, X-ray analysis of crystals of this product revealed its identity as the hexameric bis-quinone methide **4.29** (Figure 4.12, bottom). Thus, upon oxidation, trimers **4.24** and **4.25** each react through intermolecular dimerization in preference to intramolecular trapping of the phenoxyl radical. The isolation of **4.26** upon hydrogenolysis of **4.28** can be accounted for by spontaneous homolysis of the weak C–C bond of the hexameric bis-quinone methide and reduction of the resultant phenoxyl radicals. Indeed, Becker observed a similar outcome on subjecting dimeric bis-quinone methides to hydrogenation using a Pd/C catalyst, suggesting that the rate of reduction of the phenoxyl radical is far greater than that of the bis-quinone methide.¹⁶³

4.4 Future Directions: Applications of Persistent Radical Chemistry to Trimer Synthesis

It became clear that the proposed intramolecular oxidative annulation strategy (cf. Figure 4.8) was not going to be successful. Extensive efforts had revealed that oxidation of compound **4.23** could not be accomplished chemoselectively, and that oxidation of **4.24**, while chemoselective, promoted hexamer formation instead of intramolecular cyclization. Based on our success with the use of persistent phenoxyl radicals for the annulation of simple phenols to the corresponding dihydrobenzofurans (see Section 3.7), we sought to extend this to more complex phenols, such as the quadrangularin A core.

To access the required substrate, indane quinone methide **2.52** was reduced to **4.30** using sodium borohydride, and subsequent benzyl group removal was achieved under Lewis acidic conditions (Figure 4.13). It was unclear whether or not the dihydrobenzofuran synthesis would tolerate a more complex substrate such as **4.31**, and if so, what the regio- and stereochemical outcome would be. In practice, subjection of compound **4.31** to our standard conditions (acetone, 100 °C) in the presence of bis-quinone methide dimer **2.56** yielded 28% of dihydrobenzofuran product **4.32** as a single regioisomer in which annulation had taken place on the resorcinol that comprises the indane backbone (Figure 4.13). The product was obtained as a ~2:1 mixture of separable diastereomers. Although the relative configuration could not be conclusively assigned by NOESY, NMR data are consistent with each of the stereoisomers as *trans*-diaryl dihydrobenzofurans, and correlations suggest that the major isomer places the C₃-methine of the dihydrobenzofuran *cisoid* to the C₃ methine of the indane core, which would be consistent with the relative configuration of davidiol A (cf. Figure 4.3). Based on the observed chemoselectivity for benzylic methylene dehydrogenation on exposure of **4.26** to DDQ, we anticipated that it may be possible to effect selective oxidation of **4.32** in order to promote an intramolecular 7-*exo*

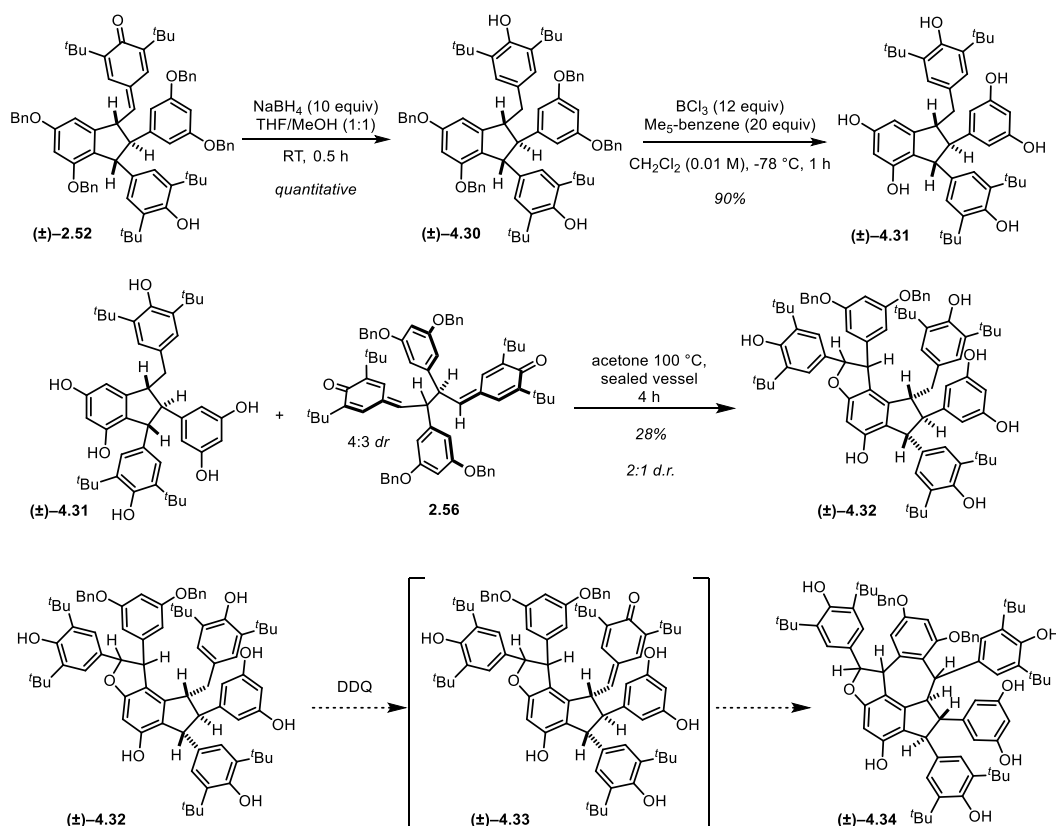


Figure 4.13 Late-Stage Dihydrobenzofuran Synthesis using Persistent Phenoxy Radicals

Friedel–Crafts cyclization (presumably via the intermediacy of quinone methide **4.33**) to generate the [7,5] fused core **4.34**. Treatment of **4.32** with DDQ in a buffered solution of dioxane gave only trace conversion to quinone methide **4.33**, and none of the cyclized product **4.34** was observed. Alternatively, performing the oxidation in dichloromethane in the absence of buffer¹⁴³ led to rapid conversion to a complex mixture from which the major products isolated are not consistent with **4.34**, and are instead suggestive of a skeletal rearrangement similar to that observed in Figure 4.7B.

We then decided to reverse the order of operations, and perform the oxidation prior to dihydrobenzofuran formation. We were fortunate to have the assistance of a talented visiting graduate student from Spain, Mariia Kirillova, who helped us to execute the route shown in Figure 4.14. Thus, **4.31** was subjected to our standard conditions for dehydrogenation and the

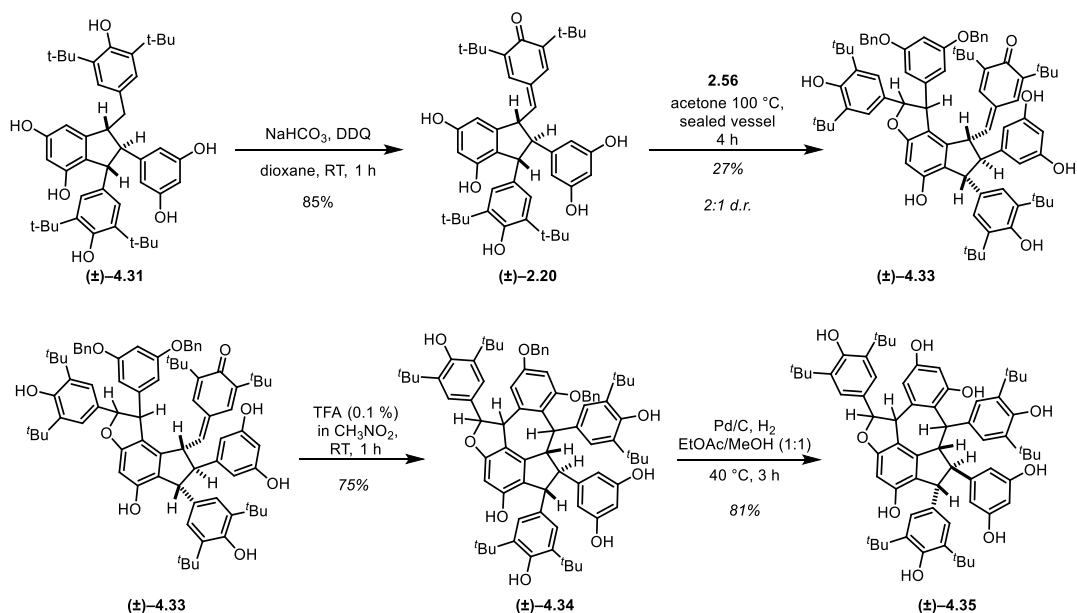


Figure 4.14 Access to *tert*-Butylated Natural Product Cores

product quinone methide **2.20** was isolated in 85% yield. Compound **2.20** is ambiphilic, possessing both electron-rich resorcinols which are competent nucleophiles for oxidative dihydrobenzofuran formation, and a quinone methide whose electrophilicity can be engaged for subsequent medium-ring formation. Compound **2.20** does not react unto itself (e.g. Friedel–Crafts cyclization) due to the fact that the resorcinol and quinone methide moieties are *trans*-configured and the formation of *trans*-fused [3.3.0] bicyclic ring systems is thermodynamically disfavored.¹⁸⁴ However, the compound is not very stable and must be handled minimally. We were pleased to find that **2.20** was competent for DHB synthesis, affording an ~2:1 mixture of diastereomers of **4.33** as a single regioisomer in 27% yield. While the connectivity of each diastereomer was rigorously assigned by 2D NMR, we were not able to determine the relative configuration. Subsequent treatment with TFA promoted an intramolecular 7-*exo* Friedel–Crafts cyclization in good yield to generate the desired natural product core **4.34**. Hydrogenolysis proceeded smoothly to yield the *tert*-butyl derivative **4.35**. Unfortunately, as was observed for the *tert*-butylated tetramers (Section 3.8), attempted dealkylation through a retro-Friedel–Crafts

reaction led to complete decomposition of the material. Current work to repeat this route utilizing the corresponding trimethylsilyl derivatives is underway, and is expected to enable the concise synthesis of two or more resveratrol trimers.

The synthetic strategy described above relies on late-stage formation of the dihydrobenzofuran moiety onto an indane scaffold. The reverse approach — in which the dihydrobenzofuran is present prior to a convergent trimerization event during which the indane is formed — is also possible and likely represents the biosynthetic order of operations.¹⁹ In this case, oxidative cross coupling of a resveratrol monomer with the dimeric natural product, ϵ -viniferin (**1.11**) would lead to structures such as ampelopsin C (Figure 4.15, A). Since this represents an 8–8' coupling of the two 4-hydroxy stilbene moieties, we were excited at the prospect of applying our dimerization conditions to accomplish the radical cross coupling of resveratrol derivative **2.50** with the corresponding *tert*-butylated ϵ -viniferin analog **3.5**. At the time of conception of this idea, we did not yet have synthetic access to **3.5**, and so the experiment was attempted using the corresponding viniferifuran analogue, **3.16**. However, upon subjecting a 5:1 mixture of **2.50** and **3.16** to our optimized dimerization conditions, we observed exclusively the formation of homocoupled products **2.56** and **3.17** (Figure 4.15, B).

Although direct cross coupling appears not to be favored, we hypothesize that it will be possible to exploit the propensity of the linear bis-*para*-quinone methide intermediates **2.56** and **3.7** to dissociate into their respective monomeric phenoxyl radicals to effect the *formal* cross-coupling of resveratrol and ϵ -viniferin derivatives from their corresponding dimers (Figure 4.15, C). Thus, thermally induced homolysis of a mixture of **2.56** and **3.7** to the free radicals will produce a statistical distribution (1:1:2) of the recombined starting materials and crossover product **4.36**. The regioisomeric cyclization pathways of **4.36** will provide access to two or more

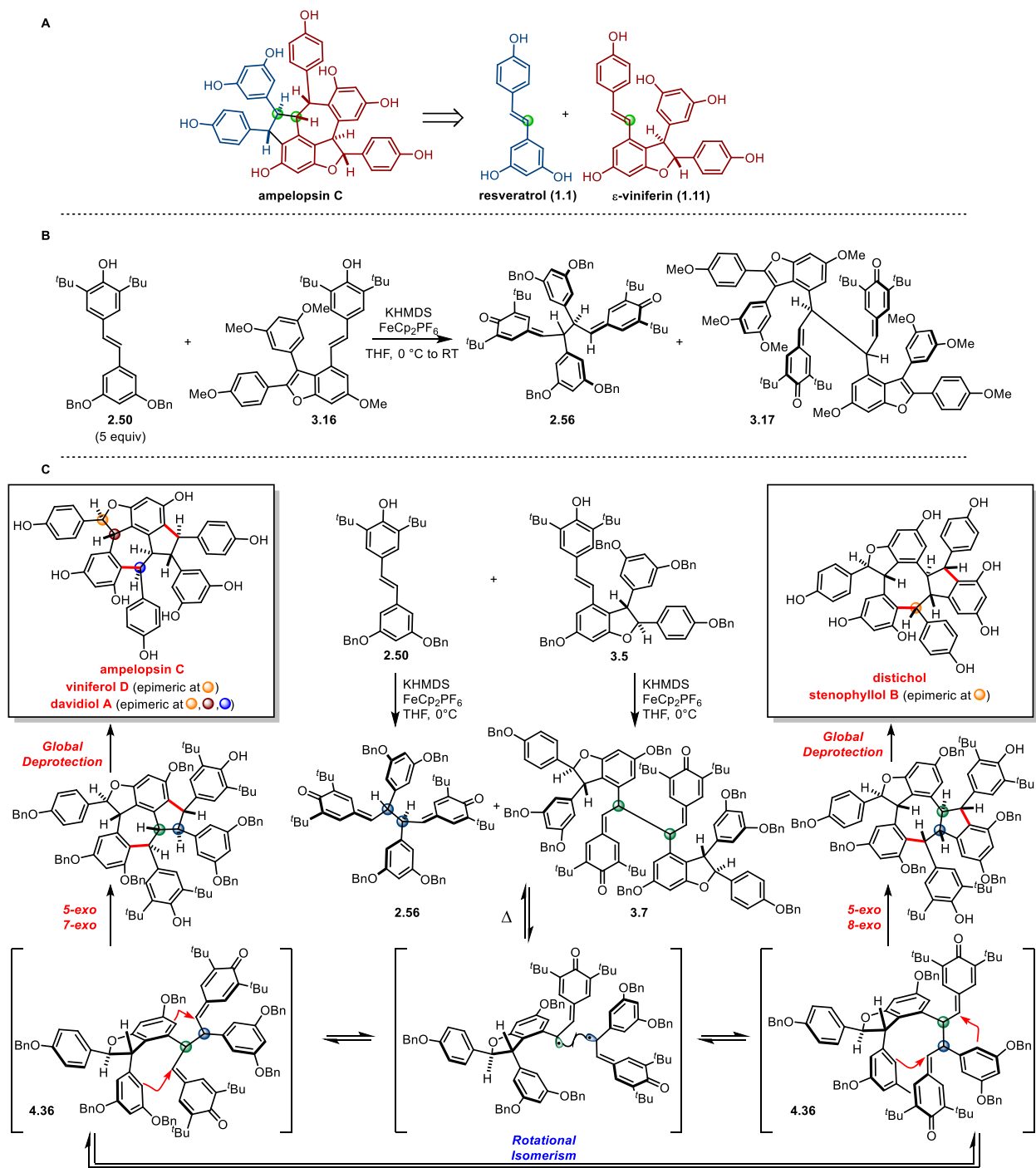


Figure 4.15 A) Likely Biogenesis of Resveratrol Trimers; B) Cross Coupling Attempt Leads to only Homocoupled Products; C) Formal Cross Coupling of Resveratrol and Viniferin through Thermal Radical Crossover

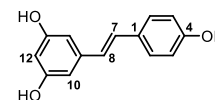
medium-ring fused natural products, such as ampelopsin C (davidiol A, viniferol D) or distichol (stenophyllol B), depending on the stereochemical outcome.

4.5 Experimental Procedures and Spectral Data

General Procedures: Glassware was dried in a 150 °C oven or flame-dried under vacuum (~0.5 Torr) prior to use. Reaction vessels were equipped with Teflon/PTFE-coated magnetic stir bars and fitted with rubber septa, and reaction mixtures were maintained under a positive pressure of dry nitrogen unless otherwise noted. Air- and/or moisture-sensitive liquids were transferred using stainless steel needles or cannulae. Reaction progress was monitored by analytical thin-layer chromatography (TLC) using glass-backed plates pre-coated with 230–400 mesh silica gel (250 μm, Indicator F-254), available from Silicycle, Inc (cat #: TLG-R10011B-323). Thin layer chromatography plates were visualized by exposure to a dual short-wave/long-wave UV lamp and/or by exposure to ethanolic solutions of *p*-anisaldehyde or vanillin, or an aqueous solution of ceric ammonium molybdate (Hanessian's stain), and the stained plates were developed by warming with a heat gun. Flash column chromatography was performed according to the procedure described by Still et al.⁵⁷ either manually using 43-60 μm (230–400 mesh) silica gel or utilizing RediSep®R_F Gold silica columns with a Teledyne Isco CombiFlash R_F automated purification system. Upon reaction quenching and work up, organic solutions were dried over Na₂SO₄ or MgSO₄ and concentrated on Büchi rotary evaporators at ~10 Torr/35 °C, then at ~0.5 Torr/25 °C using a Welch vacuum pump.

Materials: Commercially available starting materials were used as received without further purification unless otherwise noted. Organic solvents (acetonitrile, dichloromethane, diethyl ether, dimethylformamide, dimethyl sulfoxide, methanol, tetrahydrofuran, toluene) and amine bases (triethylamine, pyridine, *N,N*-diisopropylethylamine, and diisopropylamine) were purified immediately prior to use by the method of Grubbs et al.⁵⁸ using a Phoenix Solvent Drying System (JC-Meyer Solvent Systems) or PureSolv Micro amine drying columns (Innovative Technology/Inert), respectively, and maintained under positive argon pressure. Solutions of organolithium reagents (*n*-BuLi, *t*-BuLi) and Grignard reagents were purchased from Acros Organics unless otherwise noted and titrated prior to use (1,10-phenanthroline/menthol) according to the method of Paquette.⁵⁹

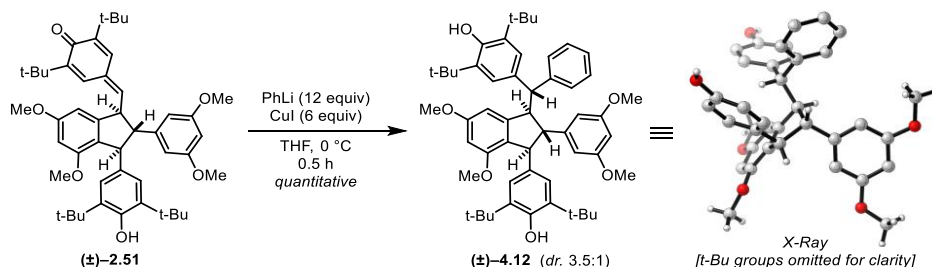
Product Analysis: Product names were generated using ChemDraw Ultra 14.0 (PerkinElmer). ¹H and ¹³C NMR spectra were recorded at the indicated temperature at 117 kG and 176 kG (¹H 500 MHz, 700 MHz; ¹³C 125 MHz and 175 MHz) using an internal deuterium lock on Varian Inova 500 or Varian VNMR 500 and 700 spectrometers. ¹H chemical shifts are expressed in parts per million (ppm) relative to the residual protio solvent resonance in CDCl₃ using δ 7.26 as standard for residual CHCl₃ or using the center line of the solvent signal as internal reference for acetone-*d*₆: δ 2.05, and DMSO-*d*₆: δ 2.50. Multiplicity is reported as follows: (br = broad, s = singlet, d = doublet, t = triplet, dd = doublet of doublets, ddd = doublet of doublet of doublets, m = multiplet), and the corresponding coupling constants are indicated as *J*-values in units of Hz. ¹³C NMR spectra were completely ¹H-decoupled (broadband) and the center line of the solvent signal was used as internal reference: CDCl₃ δ 77.23; acetone-*d*₆ δ 29.92; DMSO-*d*₆ δ 39.51. ¹³C chemical shifts are expressed in parts per million (ppm) to a single decimal place; in instances where multiple resonances approximate the same chemical shift value, two decimal places are used. For ¹H and ¹³C assignments, the following resveratrol numbering scheme was used, and each successive resveratrol equivalent was denoted with (a, b, c, etc.). Diastereotopic protons are denoted with ('), and protons found to exchange in the presence of D₂O are indicated with "exchangeable [D₂O]". Infrared data were obtained on a Perkin-Elmer Spectrum BX FT-IR spectrophotometer using an ATR mount with a ZnSe crystal and are reported as follows: [frequency of absorption (cm⁻¹), intensity of absorption (s = strong, m = medium, w = weak, br = broad)]. High-resolution mass spectra (HRMS) were obtained on a Micromass AutoSpec Ultima Magnetic Sector mass spectrometer using electrospray ionization (ESI), positive ion mode—we thank James Windak and Paul Lennon at the University of Michigan Department of Chemistry instrumentation facility for conducting these experiments. X-ray crystallographic data were collected on a Rigaku AFC10K Saturn 944+ CCD-based X-ray diffractometer—we thank Dr. Jeff W. Kampf for conducting these experiments.



⁵⁷ Still, W. C.; Kahn, M.; Mitra, A. *J. Org. Chem.* **1978**, *43* (14), 2923–2925.

⁵⁸ Pangborn, A. B.; Giardello, M. A.; Grubbs, R. H.; Rosen, R. K.; Timmers, F. J. *Organometallics* **1996**, *15* (5), 1518–1520.

⁵⁹ Lin, H.S.; Paquette, L. A. *Synth. Commun.* **1994**, *24* (17), 2503–2506; Watson, S. C.; Eastham, J. F. *J. Organomet. Chem.* **1967**, *9* (1), 165–68.



2,6-di-tert-butyl-4-((1S,2S,3R)-3-((S)-(3,5-di-tert-butyl-4-hydroxyphenyl)(phenyl)methyl)-2-(3,5-dimethoxyphenyl)-5,7-dimethoxy-2,3-dihydro-1H-inden-1-yl)phenol (4.12):

To a round bottom flask was added copper iodide (143 mg, 0.751 mmol, 6.00 equiv) and the vessel was flame-dried under vacuum. The salt was suspended in THF (1.00 mL) and cooled to 0 °C under inert atmosphere. To the stirring suspension at was added PhLi (1.9 M in cyclohexane/ether (7:3), 834 μL , 12.00 equiv), and the mixture was stirred at this temperature for 0.5 h. A separate, heart-shaped flask was charged with the starting **2.51** (92 mg, 0.125 mmol, 1.00 equiv) and the substrate was dissolved in THF (0.75 mL) and cooled to 0 °C. After 30 minutes of cuprate formation, the solution of substrate was transferred dropwise into the stirring suspension at 0 °C. Reaction progress was monitored by TLC and at 30 minutes, the reaction was quenched by the addition of sat. aq. NH_4Cl . The mixture was diluted with EtOAc and transferred to a separatory funnel. The phases were separated and the aqueous layer was extracted with portions of EtOAc. The organic layers were combined, washed with sat. aq. NH_4Cl , brine, dried over sodium sulfate and concentrated *in vacuo*. The crude material was purified by column chromatography over SiO_2 (90:5:5 Hexanes/EtOAc/ CH_2Cl_2) to afford **4.12** (101 mg, 0.124 mmol, 99% yield, 3.5:1 *dr*) as a white amorphous solid. Crystals of the major diastereomer suitable for X-ray diffraction studies were obtained by slow cooling from EtOH.

TLC (Hexanes/EtOAc, 90:10), R_f : 0.16 (UV, *p*-anisaldehyde (gray));

$^1\text{H NMR}$ (500 MHz, CDCl_3 , 25 °C) δ : 7.28 – 7.22 (m, 1H), 7.18 – 7.15 (m, 2H), 7.13 – 7.10 (m, 1H), 6.90 – 6.87 (m, overlap, 5H), 6.79 (minor, s, 1H), 6.33 (major, d, $J = 2.2$ Hz, 1H), 6.29 (major, t, $J = 2.2$ Hz, 1H), 6.26 (minor, m, 1H), 6.04 (major, d, $J = 2.2$ Hz, 2H), 5.95 (minor, d, $J = 2.2$ Hz, 2H), 5.20 (minor, d, $J = 2.2$ Hz, 1H), 5.15 (major, d, $J = 2.2$ Hz, 1H), 5.05 (major, s, 1H), 5.02 (major, s, 1H), 5.01 (minor, s, 1H), 4.94 (minor, s, 1H), 4.40 (major, s, 1H), 4.28 (minor, d, $J = 2.2$ Hz, 1H), 3.92 (minor, dd, $J = 2.2, 11.7$ Hz, 1H), 3.78 (minor, d, $J = 11.7$ Hz, 1H), 3.71 (major, s, 3H), 3.68 (major, s, 6H), 3.69 (major, dd, overlap, $J = 2.0, 12.0$ Hz, 1H), 3.66 (minor, s, 6H), 3.59 (minor, s, 3H), 3.46 (major, d, $J = 12.0$ Hz, 1H), 3.37 (major, s, 3H), 3.34 (minor, s, 3H), 3.15 (major, br t, $J = 2.0$ Hz, 1H), 2.97 (minor, t, $J = 2.2$, 1H), 1.42 (minor, s, 18H), 1.41 (major, s, 18H), 1.36 (major, s, 18H), 1.26 (minor, s, 18H);

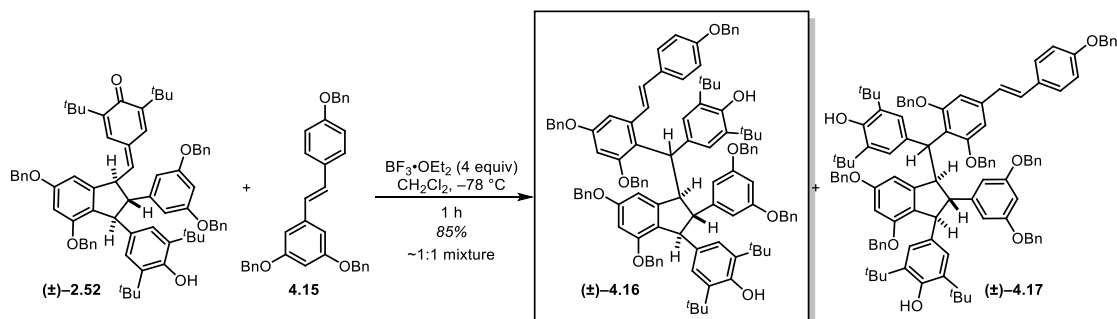
$^{13}\text{C NMR}$ (125 MHz, CDCl_3 , 25 °C) δ :⁶⁰ 160.8, 159.9, 157.1, 152.4, 151.9, 151.1, 148.0, 144.8, 136.1, 135.7, 135.5, 134.7, 128.6, 128.4, 126.2, 125.4, 124.6, 124.2, 105.0, 101.9, 98.0, 97.5, 60.4, 59.9, 58.7, 55.4, 55.3, 55.0, 53.9, 34.6, 34.5, 30.8*, 30.7, 30.6, 30.4*;

HRMS (ESI): m/z calculated for $\text{C}_{54}\text{H}_{69}\text{O}_6$ $[\text{M}+\text{H}]^+$: 813.5094, found 813.5061;

⁶⁰ With the exception of two *t*Bu signals at 30.8 and 30.4 ppm, only the resonances for the major diastereomer were observable.

FTIR (neat) cm^{-1} : 3640 (m), 2956 (s), 1598 (s), 1464 (m), 1435 (m), 1203 (m), 1146 (s), 1070 (w);

X-Ray: For coordinates, see Appendix A.



4-((R)-((1R,2S,3S)-4,6-bis(benzyloxy)-2-(3,5-bis(benzyloxy)phenyl)-3-(3,5-di-tert-butyl-4-hydroxyphenyl)-2,3-dihydro-1H-inden-1-yl)(2,4-bis(benzyloxy)-6-((E)-4-(benzyloxy)styryl)phenyl)methyl)-2,6-di-tert-butylphenol (4.16): A round bottom flask was charged with the starting **2.52** (514 mg, 0.495 mmol, 1.00 equiv) and perbenzyl resveratrol **4.15**⁶¹ (284 mg, 0.569 mmol, 1.15 equiv). The materials were dissolved in CH₂Cl₂ (4.8 mL) under inert atmosphere and the solution cooled to -78 °C. To this, BF₃·OEt₂ (244 μL, 46.5% in diethyl ether, 4.00 equiv) was added dropwise, turning the reaction a brilliant magenta color. Reaction progress was monitored by TLC in 90:10 Hexanes/EtOAc, and the reaction was quenched at 1 h by the addition of sat. aq. NaHCO₃. The solution was removed from the cooling bath and allowed to stir while the ice thawed. The mixture was diluted with EtOAc and transferred to a separatory funnel. The phases were separated and the aqueous layer was extracted with portions of EtOAc. The organic layers were combined, washed with brine, dried over sodium sulfate and concentrated *in vacuo*. Purification by column chromatography SiO₂ (95:5 to 85:15 Hexanes/EtOAc) afford **4.16** and **4.17** as a mixture of regioisomers – each as a single diastereomer (relative configuration at C₇ undefined) – (647 mg, 0.421 mmol, 85% yield) as a white amorphous solid. Samples of each regioisomer for ¹H-NMR analysis could be isolated by preparative TLC on a fraction of the material in 90:10 Hexanes/EtOAc. Otherwise, isolation and full assignment was performed *after* global debenzylation (*vide infra*). Data for **4.16**:

TLC (Hexanes/EtOAc, 90:10), R_F: 0.10 (UV, *p*-anisaldehyde (pale red));

¹H NMR (500 MHz, CDCl₃, 25 °C) δ: 7.46 – 7.27 (m, overlap, 16H), 7.30 (d, *J* = 8.7 Hz, 2H), 7.22 – 7.02 (m, overlap, 19H), 6.97 (s, 2H), 6.93 (d, *J* = 8.7 Hz, 2H), 6.78 (m, overlap, 2H), 6.75 (s, 2H), 6.63 (br s, 1H), 6.54 (br s, 1H), 6.48 (d, *J* = 2.0 Hz, 1H), 6.36 (t, *J* = 2.0 Hz, 1H), 6.07 (d, *J* = 2.0 Hz, 2H), 5.71 (d, *J* = 2.0 Hz, 1H), 5.18 (d, *J* = 13.9 Hz, 1H), 5.13 (d, *J* = 13.9 Hz, 1H), 5.09 (br s, 2H), 5.02 (d, *J* = 12.0 Hz, 1H), 5.00 (br s, 2H), 4.97 (d, *J* = 12.0 Hz, 1H), 4.97 (s, 1H), 4.94 (d, *J* = 12.2 Hz, 1H), 4.88 (d, *J* = 12.2 Hz, 1H), 4.84 (s, 1H), 4.81 (br s, 4H), 4.35 (d, *J* = 12.3 Hz, 1H), 4.30 (d, *J* = 4.7 Hz, 1H), 4.16 (d, *J* = 12.3 Hz, 1H), 3.12 (m, 1H), 1.31 (s, 18H), 1.12 (s, 18H);

¹³C NMR (125 MHz, CDCl₃, 25 °C) δ:

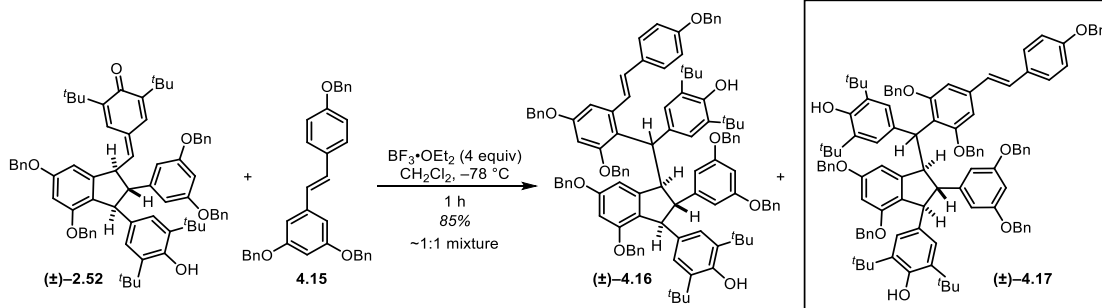
HRMS (ESI):

FTIR (neat) cm⁻¹:

Consult next page⁶²

⁶¹ Prepared by alkylation of resveratrol (TCI America) with BnBr (6 equiv) in the presence of Cs₂CO₃ (3.3 equiv) and TBAI (0.5 equiv) in DMF (0.2 M). Data for isolated **XX** (86% yield) consistent with that reported in: Orsini, F.; Verotta, L.; Lecchi, M.; Restano, R.; Curia, G.; Redaelli, E.; Wanke, E. *J. Nat. Prod.* **2004**, *67* (3), 421–426.

⁶² Reported on the regioisomeric mixture



4-((R)-((1R,2S,3S)-4,6-bis(benzyloxy)-2-(3,5-bis(benzyloxy)phenyl)-3-(3,5-di-tert-butyl-4-hydroxyphenyl)-2,3-dihydro-1H-inden-1-yl)(2,6-bis(benzyloxy)-4-((E)-4-(benzyloxy)styryl)phenyl)methyl)-2,6-di-tert-butylphenol (4.17): Data for 4.17:

TLC (Hexanes/EtOAc, 90:10), R_f : 0.12 (UV, *p*-anisaldehyde (pale red));

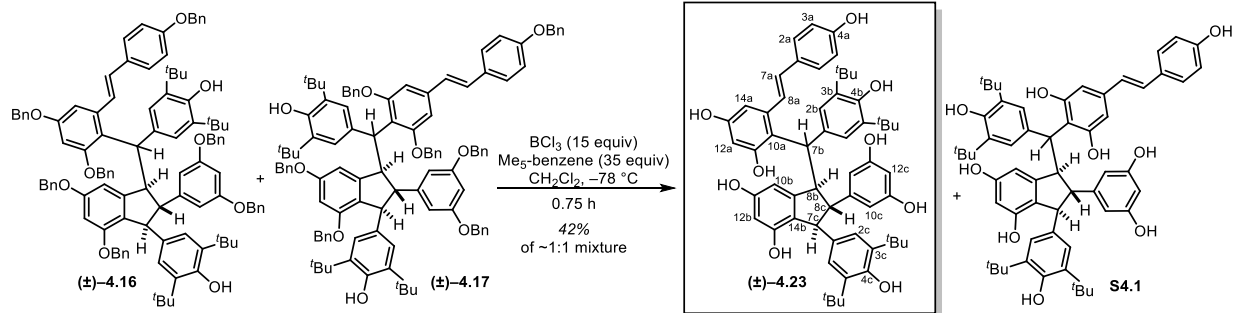
^1H NMR (500 MHz, CDCl_3 , 25°C) δ : 7.60 – 7.27 (m, overlap, 14H), 7.24 – 7.00 (m, overlap, 21H), 6.87 (d, $J = 8.8$ Hz, 2H), 6.79 (s, 2H), 6.68 (br s, 1H), 6.66 (d, $J = 2.0$ Hz, 1H), 6.61 (d, $J = 16.1$ Hz, 1H), 6.56 (d, $J = 16.1$ Hz, 1H), 6.51 (d, $J = 2.0$ Hz, 1H), 6.32 (t, $J = 2.2$ Hz, 1H), 5.95 (br s, 2H), 5.80 (d, $J = 2.0$ Hz, 1H), 5.09 (s, 2H), 5.05 (s, 2H), 5.04 (s, 1H), 4.99 (s, 1H), 4.90 (d, $J = 12.0$ Hz, 1H), 4.83 (d, $J = 12.0$ Hz, 1H), 4.82 (m, overlap, 1H), 4.54 (d, $J = 11.0$ Hz, 2H), 4.54 (d, $J = 7.8$ Hz, 1H), 4.48 (d, $J = 11.0$ Hz, 2H), 4.43 (d, $J = 7.8$ Hz, 1H), 4.43 (overlap, 1H), 2.94 (t, $J = 6.4$ Hz, 1H), 1.32 (br s, 18H), 1.28 (s, 18H);

^{13}C NMR (125 MHz, CDCl_3 , 25°C) δ :⁶³ 159.5, 159.4, 158.6, 158.5, 158.3, 157.3, 155.8, 155.6, 152.1, 152.0, 151.9, 151.81, 151.76, 150.0, 149.30, 148.9, 137.8, 137.7, 137.6, 137.5, 137.4, 137.34, 137.28, 137.2, 137.14, 137.08, 136.9, 136.8, 136.5, 136.4, 135.3, 135.2, 135.1, 134.6, 134.57, 133.5, 130.42, 130.41, 128.8, 128.74, 128.66, 128.6, 128.5, 128.4, 128.32, 128.25, 128.22, 128.19, 128.01, 127.95, 127.92, 127.88, 127.84, 127.82, 127.71, 127.66, 127.62, 127.58, 127.48, 127.46, 127.4, 127.22, 127.17, 127.15, 127.0, 126.9, 126.6, 126.34, 126.29, 126.2, 125.3, 124.4, 124.0, 121.8, 120.5, 115.23, 115.15, 107.2, 106.6, 104.5, 103.8, 103.7, 102.6, 102.0, 100.0, 99.8, 99.6, 98.9, 70.5, 70.3, 70.2, 70.1, 69.9, 69.8, 69.7, 69.5, 69.3, 69.2, 64.4, 61.9, 59.6, 58.9, 53.6, 53.1, 49.6, 48.9, 34.48, 34.46, 34.2, 30.8, 30.7, 30.6, 30.4;

HRMS (ESI):⁶³ m/z calculated for $\text{C}_{107}\text{H}_{109}\text{O}_9$ $[\text{M}+\text{H}]^+$: 1536.7993, found 1559.7828 $[\text{M}+\text{Na}]$;

FTIR (neat) cm^{-1} :⁶³ 3639 (m), 3064 (w), 3032 (w), 2953 (m), 2907 (w), 2873 (w), 1596 (s), 1509 (w), 1453 (w), 1434 (m), 1375 (w), 1298 (w), 1233 (w), 1148 (s), 1100 (m), 909 (m).

⁶³ Reported on the regioisomeric mixture



(1R,2S,3S)-3-(3,5-di-tert-butyl-4-hydroxyphenyl)-1-((R)-(3,5-di-tert-butyl-4-hydroxyphenyl)(2,4-dihydroxy-6-((E)-4-hydroxystyryl)phenyl)methyl)-2-(3,5-dihydroxyphenyl)-2,3-dihydro-1H-indene-4,6-diol (4.23): A round bottom flask was charged with starting mixture of trimers **4.16/4.17** (75 mg, 0.488 mmol, 1.00 equiv) and pentamethylbenzene (200 mg, 1.71 mmol, 35 equiv). The vessel was purged with inert gas and the solids dissolved in anhydrous CH_2Cl_2 (9.75 mL, 0.005 M). The solution was cooled to $-78\text{ }^\circ\text{C}$ and BCl_3 (731 μL , 1.0 M soln. in CH_2Cl_2 , 15 equiv) was added dropwise turning the solution a brilliant magenta color. Reaction was maintained at $-78\text{ }^\circ\text{C}$ until deemed complete by TLC (ca. 0.75 h). At this point, the reaction was quenched with a 4:1 THF/sat. aq. NaHCO_3 mixture at $-78\text{ }^\circ\text{C}$ and allowed to warm to room temperature while stirring vigorously. Upon thawing, the reaction was diluted with ethyl acetate and transferred to a separatory funnel containing additional sat. aq. NaHCO_3 . The phases were separated and the aqueous layer extracted with additional EtOAc (2x). The organic layers were combined and washed with brine, dried over Na_2SO_4 , and concentrated *in vacuo*. The crude residue was purified by flash chromatography over SiO_2 (90:5:5 $\text{CH}_2\text{Cl}_2/\text{MeOH}/\text{Acetone}$) to afford a mixture of **4.23** and the undesired regioisomer **S4.1** (23 mg, 0.213 mmol, 42% yield) as a white amorphous solid. The regioisomers were separated by preparative TLC (85:10:5 $\text{CHCl}_3/\text{MeOH}/\text{Acetone}$) to afford ~10 mg of each. The connectivity of each was rigorously assigned by 2D NMR, although relative configuration at C_{7b} could not be assigned. Data for **4.23**:

TLC ($\text{CHCl}_3/\text{MeOH}/\text{Acetone}$, 85:10:5), R_f : 0.23 (UV, *p*-anisaldehyde (maroon));

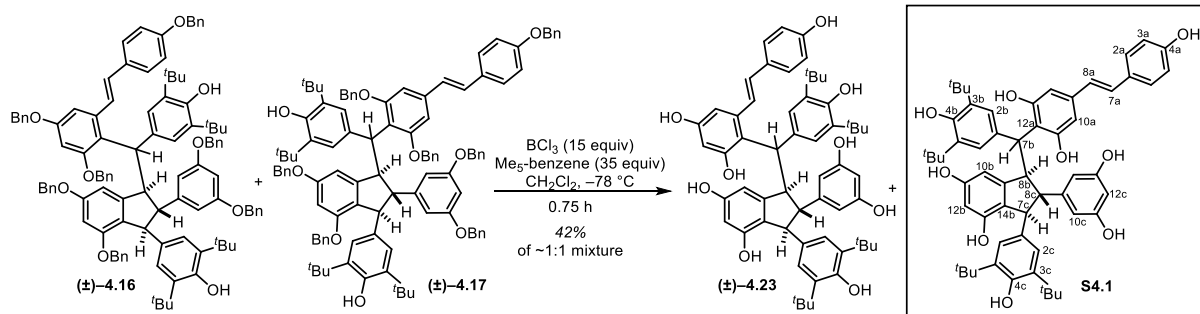
^1H NMR (700 MHz, acetone- d_6 , $25\text{ }^\circ\text{C}$) δ : 8.26 (br s, 1H, OH), 7.93 (br s, 1H, OH), 7.90 (br s, 2H, OH), 7.76 (br s, 1H, OH), 7.36 (d, $J = 8.7\text{ Hz}$, 2H, $\text{C}_{2a}\text{-H}$), 7.25 (br s, 1H, OH), 7.18 (br s, 2H, $\text{C}_{2b}\text{-H}$), 7.01 (s, 2H, $\text{C}_{2c}\text{-H}$), 6.87 (d, $J = 16.2\text{ Hz}$, 1H, $\text{C}_{7a}\text{-H}$), 6.81 (d, $J = 8.7\text{ Hz}$, 2H, $\text{C}_{3a}\text{-H}$), 6.77 (d, $J = 16.2\text{ Hz}$, 1H, $\text{C}_{8a}\text{-H}$), 6.54 (br s, 1H, $\text{C}_{12a}\text{-H}$), 6.49 (br s, 1H, $\text{C}_{14s}\text{-H}$), 6.21 (d, $J = 2.0\text{ Hz}$, 1H, $\text{C}_{12b}\text{-H}$), 6.13 (t, $J = 2.0\text{ Hz}$, 1H, $\text{C}_{12c}\text{-H}$), 6.03 (d, $J = 2.0\text{ Hz}$, 1H, $\text{C}_{10b}\text{-H}$), 5.88 (d, $J = 2.0\text{ Hz}$, 2H, $\text{C}_{10c}\text{-H}$), 5.66 (s, 1H, OH), 5.48 (s, 1H, OH), 4.84 (d, $J = 1.5, 12.6\text{ Hz}$, 1H, $\text{C}_{8b}\text{-H}$), 4.62 (d, $J = 12.6\text{ Hz}$, 1H, $\text{C}_{7b}\text{-H}$), 4.23 (d, $J = 1.5\text{ Hz}$, $\text{C}_{7c}\text{-H}$), 2.93 (t, $J = 1.5\text{ Hz}$, 1H, $\text{C}_{8c}\text{-H}$), 1.41 (s, 18H, $-\text{C}(\text{CH}_3)_3$), 1.25 (s, 18H, $-\text{C}(\text{CH}_3)_3$);

^{13}C NMR (175 MHz, acetone- d_6 , $25\text{ }^\circ\text{C}$) δ : 159.3 (C_{11c}), 158.7 (C_{11b}), 158.1 (C_{4a}), 157.8 (C_{11a}), 157.3 (C_{13a}), 154.9 (C_{13b}), 154.2 (C_{9c}), 152.7 (C_{4c}), 152.3 (C_{4b}), 152.0 (C_{9b}), 138.8 (C_{1c}), 137.3 (C_{3c}), 137.1 (C_{9a}), 136.9 (C_{1b}), 136.5 (C_{3b}), 130.2 (C_{1a}), 128.6 (C_{2a}), 128.0 (C_{7a}), 127.1 (C_{2b}), 127.0 (C_{8a}), 124.7 (C_{2c}), 122.8 (C_{14b}), 119.1 (C_{10a}), 116.5 (C_{3a}), 106.8 (C_{12a}), 106.0 (C_{14a}), 105.7 (C_{10c}), 105.6 (C_{10b}), 101.8 (C_{12b}), 100.8 (C_{12c}), 61.1 (C_{8c}), 57.3 (C_{7c}), 55.0 (C_{8b}), 49.3 (C_{7b}), 35.2 ($-\text{C}(\text{CH}_3)_3$), 35.0 ($-\text{C}(\text{CH}_3)_3$), 31.1 ($-\text{C}(\text{CH}_3)_3$), 30.9 ($-\text{C}(\text{CH}_3)_3$);

HRMS (ESI): m/z calculated for $\text{C}_{58}\text{H}_{67}\text{O}_9$ $[\text{M}+\text{H}]^+$: 907.4707, found 907.4762;

FTIR (neat) cm^{-1} :

3272 (s, br), 2961 (m), 1623 (s), 1512 (w), 1434 (m), 1339 (m), 1236 (m), 1156 (m), 1016 (m).



(1R,2S,3S)-3-(3,5-di-tert-butyl-4-hydroxyphenyl)-1-((R)-(3,5-di-tert-butyl-4-hydroxyphenyl)(2,6-dihydroxy-4-((E)-4-hydroxystyryl)phenyl)methyl)-2-(3,5-dihydroxyphenyl)-2,3-dihydro-1H-indene-4,6-diol (XX): For preparation, consult previous page. Data for **S4.1**:

TLC ($\text{CHCl}_3/\text{MeOH}/\text{Acetone}$, 85:10:5), R_f : 0.32 (UV, *p*-anisaldehyde (maroon));

^1H NMR (700 MHz, acetone- d_6 , 25 °C) δ : 7.91 (br s, 2H, OH), 7.58 (br s, 1H, OH), 7.38 (br s, 2H, OH), 7.35 (d, $J = 8.5$ Hz, 2H, C_{2a}-H), 7.32 (br s, 1H, OH), 7.00 (s, 2H, C_{2c}-H), 6.83 (d, $J = 16.2$ Hz, 1H, C_{7a}-H), 6.81 (d, $J = 8.5$ Hz, 2H, C_{3a}-H), 6.75 (d, $J = 16.2$ Hz, 1H, C_{8a}-H), 6.44 (s, 2H, C_{10a}-H), 6.24 (d, $J = 2.2$ Hz, 1H, C_{12b}-H), 6.10 (t, $J = 2.2$ Hz, 1H, C_{12c}-H), 6.03 (d, $J = 2.2$ Hz, 2H, C_{10c}-H), 5.63 (s, 1H, OH), 5.61 (s, 1H, OH), 5.28 (d, $J = 2.2$ Hz, 1H, C_{10b}-H), 4.56 (d, $J = 12.1$ Hz, 1H, C_{8b}-H), 4.23 (d, $J = 12.1$ Hz, 1H, C_{7b}-H), 4.20 (d, $J < 1.5$ Hz, 1H, C_{7c}-H), 3.13 (t, $J < 1.5$ Hz, 1H, C_{8c}-H), 1.41 (s, 18H, $-\text{C}(\text{CH}_3)_3$), 1.38 (s, 18H, $-\text{C}(\text{CH}_3)_3$);

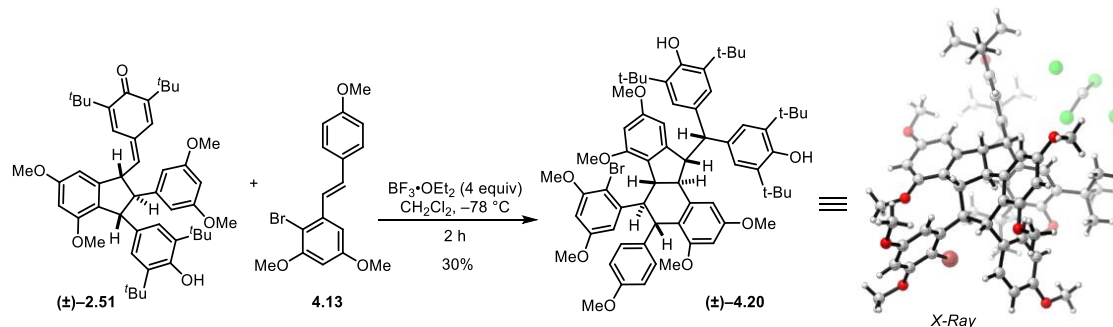
^{13}C NMR (175 MHz, acetone- d_6 , 25 °C) δ : 159.1 (C_{11c}), 158.0 (C_{4a}), 157.9 (C_{11b}), 157.6 (C_{11a}), 155.0 (C_{13b}), 153.5 (C_{9c}), 152.69 (C_{4b}), 152.68 (C_{4c}), 151.7 (C_{9b}), 138.0 (C_{1c}), 137.7 (C_{3c}), 137.0 (C_{9a}), 136.82 (C_{1b}), 136.78 (C_{3b}), 130.2 (C_{1a}), 128.6 (C_{2a}), 128.0 (C_{7a}), 127.4 (C_{2b}), 127.0 (C_{8a}), 125.0 (C_{2c}), 122.5 (C_{14b}), 119.0 (C_{12a}), 116.5 (C_{3a}), 107.0 (C_{10b}), 106.3 (C_{10a}), 105.9 (C_{10c}), 101.7 (C_{12b}), 100.7 (C_{12c}), 61.2 (C_{8c}), 57.0 (C_{8b}), 56.8 (C_{7c}), 49.8 (C_{7b}), 35.3 ($-\text{C}(\text{CH}_3)_3$), 35.2 ($-\text{C}(\text{CH}_3)_3$), 31.1 ($-\text{C}(\text{CH}_3)_3$), 31.0 ($-\text{C}(\text{CH}_3)_3$);

HRMS (ESI):

m/z calculated for $\text{C}_{58}\text{H}_{67}\text{O}_9$ $[\text{M}+\text{H}]^+$: 907.4707, found 907.4757;

FTIR (neat) cm^{-1} :

3372 (s, br), 2957 (m), 2925 (m), 1604 (s), 1512 (w), 1435 (s), 1337 (m), 1236 (m), 1156 (m).



4,4'-(((5S,6S,6aR,11S,11aR)-6-(2-bromo-3,5-dimethoxyphenyl)-2,4,7,9-tetramethoxy-5-(4-methoxyphenyl)-6,6a,11,11a-tetrahydro-5H-benzo[a]fluoren-11-yl)methylene)bis(2,6-di-tert-butylphenol) (4.20): A round bottom flask was charged with the starting **2.51** (500 mg, 0.680 mmol, 1.00 equiv) and bromo permethyl resveratrol **4.13**⁶⁴ (518 mg, 1.361 mmol, 2.00 equiv). The materials were dissolved in CH_2Cl_2 (10.0 mL) under inert atmosphere and the solution cooled to -78°C . To this, $\text{BF}_3 \cdot \text{OEt}_2$ (342 μL , 46.5% in diethyl ether, 4.00 equiv) was added dropwise, turning the reaction a brilliant magenta color. Reaction progress was monitored by TLC in 90:10 Hexanes/EtOAc, and the reaction was allowed to slowly warm (dry ice not replaced). At 2 h, the reaction was quenched by the addition of sat. aq. NaHCO_3 . The solution was removed from the cooling bath and allowed to stir while the ice thawed. The mixture was diluted with EtOAc and transferred to a separatory funnel. The phases were separated and the aqueous layer was extracted with portions of EtOAc. The organic layers were combined, washed with brine, dried over sodium sulfate and concentrated *in vacuo*. Purification by column chromatography SiO_2 (95:5 to 90:10 Hexanes/EtOAc) afforded **4.20** as a single diastereomer (220 mg, 0.203 mmol, 30% yield) as a white amorphous solid. Crystals of **4.20** suitable for X-ray diffraction studies were obtained by slow evaporation from THF.

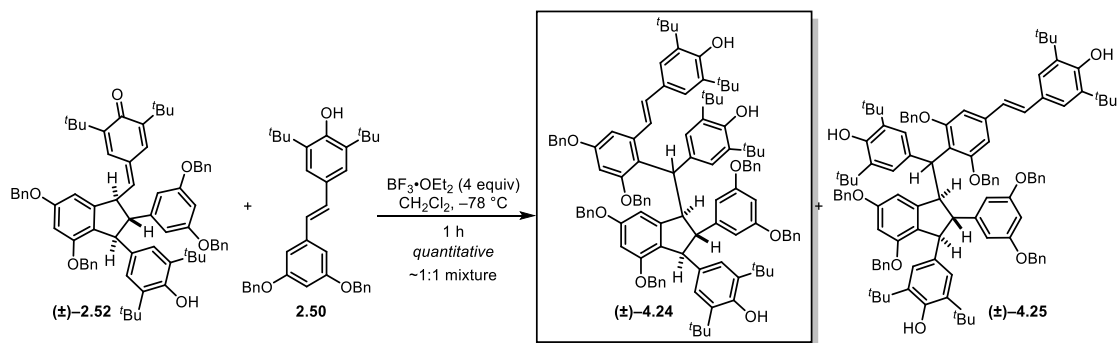
TLC (Hex/EtOAc, 90:10), R_F : 0.15 (UV);

^1H NMR (500 MHz, CDCl_3 , 25°C) δ : 7.11 (br s, 2H), 6.86 (br s, 2H), 6.74 (d, $J < 1.5$ Hz, 1H), 6.72 (s, 1H), 6.70 (s, 1H), 6.48 (d, $J < 1.5$ Hz, 1H), 6.46 (s, 1H), 6.35 (s, 1H), 6.33 (s, 1H), 6.17 (s, 1H), 6.02 (s, 1H), 5.66 (s, 1H), 5.07 (s, 1H), 5.01 (s, 1H), 4.85 (d, $J = 4.4$ Hz, 1H), 4.47 (s, 1H), 4.28 – 4.24 (m, overlap, 2H), 3.89 (s, 3H), 3.83 (s, 3H), 3.70 (t, $J = 11.0$ Hz, 1H), 3.66 (s, 3H), 3.59 (s, 6H), 3.34 (s, 3H), 3.20 (s, 3H), 3.15 (t, $J = 11.0$ Hz, 1H), 1.35 (s, 18 H), 1.20 (s, 18H);

^{13}C NMR (175 MHz, CDCl_3 , 25°C) δ : 159.9, 159.33, 159.2, 157.8, 157.1, 156.0, 152.5, 151.9, 151.8, 148.6, 144.0, 137.7, 135.51, 135.49, 135.4, 131.7, 128.6, 126.8, 125.6, 124.0, 120.8, 113.3, 105.7, 103.9, 101.17, 101.15, 100.6, 97.0, 96.9, 96.0, 56.4, 55.7, 55.3, 55.2, 55.1, 55.0, 54.9, 54.3, 51.9, 51.6, 50.6, 49.7, 48.1, 34.4, 34.2, 30.3, 30.2;

X-Ray: For coordinates, see Appendix A.

⁶⁴ Prepared according to: Snyder, S. A.; Thomas, S. B.; Mayer, A. C.; Breazzano, S. P. *Angew. Chem. Int. Ed.* **2012**, *51* (17), 4080–4084.



4-((E)-3,5-bis(benzyloxy)-2-((R)-((1R,2S,3S)-4,6-bis(benzyloxy)-2-(3,5-bis(benzyloxy)phenyl)-3-(3,5-di-tert-butyl-4-hydroxyphenyl)-2,3-dihydro-1H-inden-1-yl)(3,5-di-tert-butyl-4-hydroxyphenyl)methyl)styryl)-2,6-di-tert-butylphenol (4.24**):** A round bottom flask was charged with the starting **2.52** (975 mg, 0.938 mmol, 1.00 equiv) and resveratrol derivative **2.50** (977 mg, 1.87 mmol, 2.00 equiv). The materials were dissolved in CH_2Cl_2 (10 mL) under inert atmosphere and the solution cooled to -78°C . To this, $\text{BF}_3 \cdot \text{OEt}_2$ (463 μL , 46.5% in diethyl ether, 4.00 equiv) was added dropwise, turning the reaction a brilliant magenta color. Reaction progress was monitored by TLC in 85:10:5 Hexanes/EtOAc/ CH_2Cl_2 , and the reaction was quenched at 0.5 h by the addition of sat. aq. NaHCO_3 . The solution was removed from the cooling bath and allowed to stir while the ice thawed. The mixture was diluted with EtOAc and transferred to a separatory funnel. The phases were separated and the aqueous layer was extracted with portions of EtOAc. The organic layers were combined, washed with brine, dried over sodium sulfate and concentrated *in vacuo*. Purification by column chromatography over SiO_2 (90:5 to 85:15 Hexanes/EtOAc) afforded **4.24** and **4.25** as a mixture of regioisomers – each as a single diastereomer (relative configuration at C_{7b} undefined) – (1.454 g, 0.932 mmol, 99% yield) as a white amorphous solid. Samples of each regioisomer could be isolated by preparative TLC on a fraction of the material in 90:10 Hexanes/EtOAc. Data for **4.24**:

TLC (Hex/EtOAc/ CH_2Cl_2 , 85:10:5), R_f : 0.19 (UV, *p*-anisaldehyde (pale red));

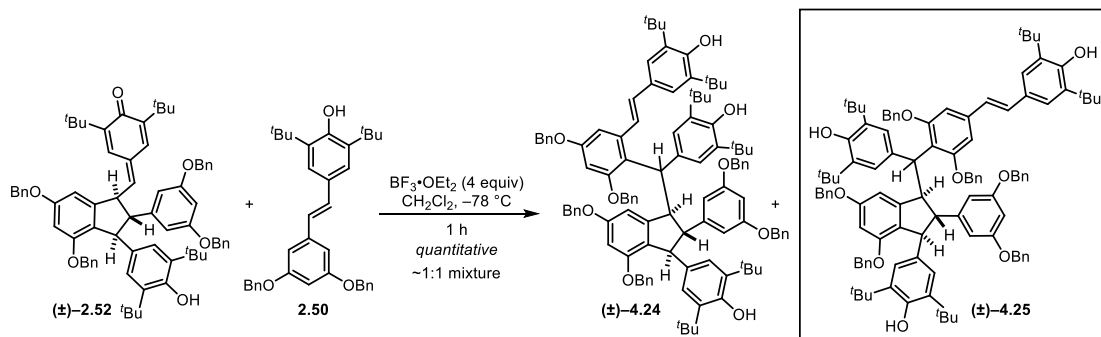
^1H NMR (500 MHz, CDCl_3 , 25°C) δ : 7.36 – 7.28 (m, overlap, 12H), 7.22 (s, 2H), 7.21 – 7.04 (m, overlap, 25H), 6.95 (s, 2H), 6.79 (d, $J = 16.2$ Hz, 1H), 6.76 (m, overlap, 2H), 6.73 (d, $J = 16.2$ Hz, 1H), 6.65 (s, 1H), 6.58 (s, 1H), 6.49 (d, $J = 1.8$ Hz, 1H), 6.35 (t, $J = 2.2$ Hz, 1H), 6.04 (d, $J = 2.2$ Hz, 2H), 5.76 (d, $J = 1.5$ Hz, 1H), 5.27 (s, 1H), 5.18 (d, $J = 13.9$ Hz, 1H), 5.14 (d, $J = 13.9$ Hz, 1H), 5.03 – 4.94 (m, overlap, 6H), 4.94 (d, $J = 12.5$ Hz, 1H), 4.87 (d, $J = 12.5$ Hz, 1H), 4.83 (s, 1H), 4.80 (d, $J = 11.9$ Hz, 2H), 4.78 (d, $J = 11.9$ Hz, 2H), 4.38 (d, $J = 12.5$ Hz, 1H), 4.28 (d, $J = 4.6$ Hz, 1H), 4.23 (d, $J = 12.5$ Hz, 1H), 3.09 (t, $J = 4.6$ Hz, 1H), 1.46 (s, 18H), 1.30 (s, 18H), 1.10 (s, 18H);

^{13}C NMR (175 MHz, CDCl_3 , 25°C) δ : 159.8, 159.6, 158.4, 157.3, 155.8, 154.0, 151.84, 151.80, 151.75, 149.4, 137.8, 137.7, 137.5, 137.4, 137.2, 136.9, 136.3, 135.3, 134.6, 133.7, 129.8, 128.8, 128.71, 128.66, 128.5, 128.4, 128.3, 128.0, 127.9, 127.7, 127.45, 127.43, 127.35, 127.2, 126.9, 126.6, 126.3, 126.2, 126.1, 124.4, 123.6, 121.5, 106.7, 104.4, 103.8, 102.1, 100.0, 98.9, 70.6, 70.1, 69.8, 69.5, 69.3, 62.2, 59.5, 53.7, 49.7, 34.6, 34.5, 34.2, 30.8, 30.5, 30.4;

HRMS (ESI): m/z calculated for $\text{C}_{108}\text{H}_{119}\text{O}_9$ $[\text{M}+\text{H}]^+$: 1559.8849, found 1559.8801;

FTIR (neat) cm^{-1} :

3631 (m), 2954 (m), 1594 (s), 1433 (s), 1366 (m), 1312 (m), 1232 (m), 1209 (m), 1146 (s), 1098 (m), 1048 (m), 1028 (m).



4-((R)-((1R,2S,3S)-4,6-bis(benzyloxy)-2-(3,5-bis(benzyloxy)phenyl)-3-(3,5-di-tert-butyl-4-hydroxyphenyl)-2,3-dihydro-1H-inden-1-yl)(2,6-bis(benzyloxy)-4-(E)-3,5-di-tert-butyl-4-hydroxystyryl)phenyl)methyl)-2,6-di-tert-butylphenol (4.25): For preparation, consult previous page. Samples of each regioisomer could be isolated by preparative TLC on a fraction of the material in 90:10 Hexanes/EtOAc. Data for **4.25**:

TLC (Hex/EtOAc/ CH_2Cl_2 , 85:10:5), R_f : 0.20 (UV, *p*-anisaldehyde (pale red));

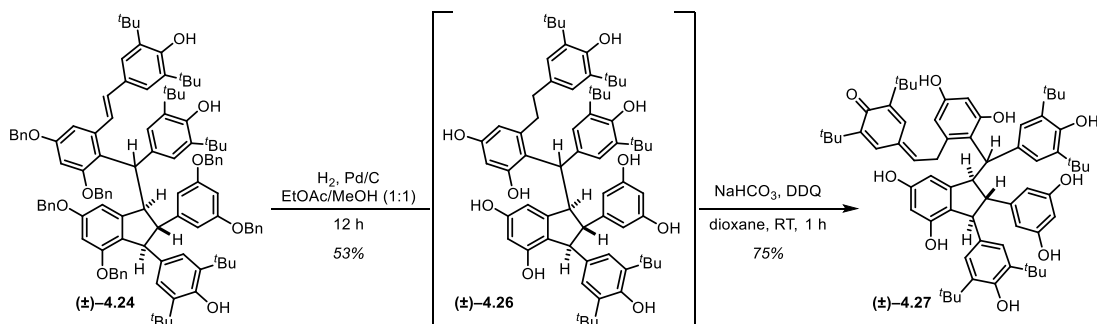
^1H NMR (500 MHz, CDCl_3 , 25 °C) δ : 7.37 – 7.28 (m, overlap, 7H), 7.22 – 7.04 (m, overlap, 27H), 6.79 (s, 2H), 6.68 (s, 1H), 6.66 (d, $J = 1.6$ Hz, 1H), 6.66 (d, $J = 16.1$ Hz, 1H), 6.50 (d, $J = 1.6$ Hz, 1H), 6.33 (t, $J = 1.5$ Hz, 1H), 5.97 (br s, 2H), 5.73 (d, $J < 1.5$ Hz, 1H), 5.24 (s, 1H), 5.05 – 5.01 (m, overlap, 4H), 4.98 (s, 1H), 4.89 (d, $J = 11.9$ Hz, 1H), 4.82 (d, $J = 11.9$ Hz, 1H), 4.56 (d, $J = 11.0$ Hz, 2H), 4.53 (d, overlap, $J = 11.0$ Hz, 1H), 4.52 (d, overlap, $J = 11.0$ Hz, 2H), 4.51 (d, overlap, $J = 6.8$ Hz, 1H), 4.42 (d, overlap, $J = 6.8$ Hz, 1H), 4.41 (d, overlap, $J = 11.0$ Hz, 1H), 2.93 (m, 1H), 1.43 (s, 18H), 1.30 (br s, 18H), 1.27 (s, 18H);

^{13}C NMR (175 MHz, CDCl_3 , 25 °C) δ : 159.46, 159.45, 155.6, 153.9, 152.1, 151.9, 150.0, 149.3, 137.8 (br), 137.29, 137.26, 137.2, 137.0, 136.6, 136.2, 135.24, 135.16, 134.7, 129.5, 128.8, 128.63, 128.59, 128.5, 128.3, 127.9, 127.8, 127.7, 127.6, 127.2, 127.1, 126.4, 125.9, 125.4, 124.0, 123.6, 120.2, 107.1, 103.7 (br), 102.6, 99.8, 99.7, 69.9, 69.7, 69.3, 64.3, 58.9, 53.5, 49.1, 34.51, 34.47, 34.46, 30.7, 30.6, 30.5;

HRMS (ESI): m/z calculated for $\text{C}_{108}\text{H}_{119}\text{O}_9$ $[\text{M}+\text{H}]^+$: 1559.8849, found 1559.8818;

FTIR (neat) cm^{-1} :

3632 (m), 2955 (m), 1594 (s), 1434 (s), 1312 (m), 1233 (m), 1209 (m), 1146 (s), 1098 (m), 1028 (m).



2,6-di-tert-butyl-4-(2-(2-((R)-(3,5-di-tert-butyl-4-hydroxyphenyl)((1R,2S,3S)-3-(3,5-di-tert-butyl-4-hydroxyphenyl)-2-(3,5-dihydroxyphenyl)-4,6-dihydroxy-2,3-dihydro-1H-inden-1-yl)methyl)-3,5-dihydroxyphenyl)ethylidene)cyclohexa-2,5-dien-1-one (4.27): A round bottom flask was charged with starting **4.24** (500 mg, 0.320 mmol, 1.00 equiv) and Pd/C (30 wt%, 35 mg) and the flask was sealed and purged with N₂. EtOAc (HPLC grade, 3 mL) and MeOH (HPLC grade, 3 mL) were sequentially added and N₂ inlet was replaced with a H₂ balloon. The mixture was gently sparged with H₂ for 30 minutes at room temperature, at which point the vent needle was removed and the reaction was stirred at room temperature under H₂ (1 atm). Every 3 h, reaction progress was monitored by TLC (90:5:5 CH₂Cl₂/Acetone/MeOH) and the reaction mixture was re-sparged with H₂. Evaporated solvent was replaced with MeOH and the reaction was continued until full conversion was achieved (24 h). Upon completion, the reaction contents were filtered through a short plug of Celite, eluting with 1:1 EtOAc/MeOH. The filtrate was concentrated to dryness *in vacuo* and the resulting residue was purified by flash chromatography over SiO₂ (90:5:5 CH₂Cl₂/Acetone) to afford **4.26** (173 mg, 0.169 mmol, 53% yield) as a white amorphous solid. Partial characterization for **4.26** is provided below, but it was otherwise carried on directly.

TLC (Hexanes/EtOAc, 85:15), R_F: 0.23 (UV);

¹H NMR (500 MHz, acetone-*d*₆, 25 °C) δ: 8.06 (s, 1H), 7.88 (s, 2H), 7.72 (s, 1H), 7.64 (s, 1H), 7.21 (s, 1H), 7.19 (s, 1H), 7.00 (s, 2H), 6.99 (s, 1H), 6.28 (s, 1H), 6.22 (s, 2H), 6.13 (s, 1H), 6.01 (s, 1H), 5.86 (s, 2H), 5.77 (s, 1H), 5.65 (s, 1H), 5.45 (s, 1H), 4.83 (d, *J* = 12.2 Hz, 1H), 4.59 (d, *J* = 12.2 Hz, 1H), 4.22 (s, 1H), 2.91 (s, 1H), 2.71 (m, 2H), 2.62 (m, 2H), 1.41 (s, 18H), 1.39 (s, 18H), 1.26 (s, 18H).

Intermediate **4.26** (83 mg, 0.081 mmol, 1.00 equiv) and NaHCO₃ (41 mg, 0.488 mmol, 6 equiv) were stirred in dioxane (14.5 mL) at 23 °C under inert atmosphere. In separate vessel, a solution of DDQ (21 mg, 0.093 mmol, 1.15 equiv) in dioxane (1.8 mL) was prepared. The solution of DDQ was added dropwise to the reaction mixture. Reaction progress was monitored by TLC and the reaction was quenched at 1 h with 10% aq. Na₂S₂O₃. The mixture was diluted with ethyl acetate and transferred to a separatory funnel containing sat. aq. Na₂CO₃. The aqueous phase was extracted with ethyl acetate (2x). Combined organic layers were washed with sat. aq. Na₂CO₃ (2x), dried over Na₂SO₄, and concentrated *in vacuo*. ¹H-NMR of the crude material showed **4.27** as essentially the exclusive product. Attempted isolation by flash chromatography over SiO₂ (96:2:2 DCM/MeOH/Acetone) afforded a mixture of **4.27** and its *E*-stilbene tautomer (62 mg, 0.060 mmol, 75% yield). (NOTE: **4.27** is not stable in solution at room temperature and should be stored at -20 °C under inert atmosphere or used immediately).

For full characterization, consult the next page:

TLC (Hexanes/EtOAc, 85:15), R_f : 0.35 (UV, *p*-anisaldehyde (maroon));

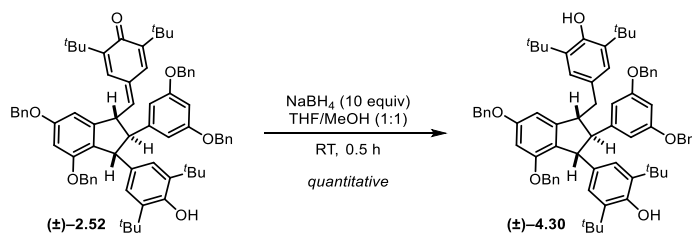
^1H NMR (500 MHz, acetone- d_6 , 25 °C) δ :⁶⁵ 7.87 (s, 2H), 7.56 (s, 1H), 7.50 (d, $J = 2.0$ Hz, 1H), 7.38 (br s, 3H), 7.24 (s, 1H), 7.02 – 7.00 (m, overlap 2H), 6.98 (s, 2H), 6.50 (t, $J = 8.3$ Hz, 1H), 6.23 (d, $J = 2.0$ Hz, 1H), 6.10 (t, $J = 2.5$ Hz, 1H), 6.09 (br s, 2H), 6.01 (d, $J = 2.5$ Hz, 2H), 5.61 (s, 1H), 5.59 (s, 1H), 5.30 (d, $J = 2.0$ Hz, 1H), 4.57 (dd, $J = 1.5, 12.0$ Hz, 1H), 4.22 (d, $J = 12.0$ Hz, 1H), 4.17 (d, $J = 1.5$ Hz, 1H), 3.65 (dd, $J = 8.3, 15.7$ Hz, 1H), 3.60 (dd, $J = 8.3, 15.7$ Hz, 1H), 3.12 (t, $J = 1.5$ Hz, 1H), 1.38 (s, 18H), 1.37 (s, 18H), 1.31 (s, 9H), 1.28 (s, 9H);

^{13}C NMR (125 MHz, acetone- d_6 , 25 °C) δ :⁶⁶ 187.2, 159.0, 158.91, 158.88, 157.9, 157.8, 157.6, 157.5, 157.2, 153.4, 154.94, 154.93, 154.90, 154.68, 153.47, 153.4, 153.1, 152.9, 152.8, 152.64, 152.62, 152.59, 152.56, 151.8, 151.7, 149.0, 147.9, 147.0, 141.5, 138.4, 138.1, 137.89, 137.86, 137.8, 137.68, 137.66, 137.63, 137.59, 137.5, 137.2, 137.0, 136.84, 136.78, 136.75, 136.7, 136.4, 134.0, 132.1, 130.0, 129.7, 129.3, 128.5, 127.39, 127.35, 127.3, 126.8, 125.4, 125.01, 124.96, 124.9, 124.5, 124.0, 122.48, 122.46, 122.38, 118.9, 117.6, 116.8, 114.8, 108.6, 108.3, 107.0, 106.9, 106.8, 106.3, 106.13, 106.06, 105.9, 103.5, 102.5, 101.7, 101.6, 100.71, 100.68, 61.2, 61.1, 57.0, 56.8, 56.5, 49.8, 49.4, 36.0, 35.4, 35.22, 35.20, 35.16, 35.14, 35.13, 31.07, 31.04, 30.95, 30.8, 30.7, 29.9, 29.8;

HRMS (ESI): m/z calculated for $\text{C}_{66}\text{H}_{81}\text{O}_6$ [M–H][–]: 1017.5886, found 1017.5844.

⁶⁵ Reported on exclusively the *p*-quinone methide tautomer of **4.27**

⁶⁶ Reported on a mixture of *p*-quinone methide and stilbene tautomers of **4.27**



4-((1*R*,2*R*,3*R*)-5,7-bis(benzyloxy)-2-(3,5-bis(benzyloxy)phenyl)-3-(3,5-di-*tert*-butyl-4-hydroxybenzyl)-2,3-dihydro-1*H*-inden-1-yl)-2,6-di-*tert*-butylphenol (4.30): The reaction vessel was charged with starting quinone methide **2.52** (290 mg, 0.279 mmol, 1.00 equiv) and NaBH₄ (106 mg, 2.79 mmol, 10.00 equiv). The mixture was taken up in THF (5.5 mL) at room temperature under inert atmosphere. To the faint yellow stirring solution was carefully added MeOH (5.5 mL), causing it to immediately become colorless with concomitant H₂-evolution. While the starting material and product have nearly identical R_F values, reaction progress can be monitored by the use of *p*-anisaldehyde stain, the action of which turns the starting material yellow-orange and the product pink. TLC analysis at 0.5 h indicated full conversion to **4.30**, and the excess reductant was quenched by careful addition of sat. aq. NH₄Cl. MeOH was then removed from the heterogeneous mixture by rotary evaporation. The crude material was then dissolved into a mixture of EtOAc/H₂O, and transferred to a separatory funnel where the phases were separated. The aqueous layer was further extracted with additional portions of EtOAc. The organic layers were combined, washed with brine, dried over Na₂SO₄ and concentrated in vacuo to yield the desired **4.30** (290 mg, 0.278 mmol, quantitative yield) as a white foam, which was carried on without further purification.

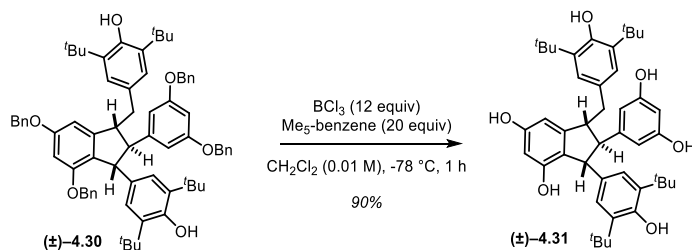
TLC (Hexanes/EtOAc, 85:15), R_F: 0.41 (UV, *p*-anisaldehyde (pink));

¹H NMR (500 MHz, CDCl₃, 25 °C) δ: 7.47 – 7.28 (m, 15H), 7.14 – 7.09 (m, 3H), 6.89 (s, 2H), 6.79 (s, 2H), 6.73 (m, 2H), 6.50 (d, *J* = 1.3 Hz, 1H), 6.41 (t, *J* = 2.0 Hz, 1H), 6.33 (d, *J* = 1.3 Hz, 1H), 6.19 (d, *J* = 2.0 Hz, 2H), 5.01 (d, *J* = 10.0 Hz, 1H), 4.99 (d, *J* = 10.0 Hz, 1H), 4.97 (d, *J* = 11.5 Hz, 1H), 4.95 (d, *J* = 11.5 Hz, 1H), 4.90 (d, *J* = 12.0 Hz, 1H), 4.88 (d, *J* = 11.7 Hz, 1H), 4.86 (d, *J* = 11.7 Hz, 1H), 4.82 (d, *J* = 12.0 Hz, 1H), 4.30 (d, *J* = 6.0 Hz, 1H), 3.59 (ddd [apparent quartet], *J* = 6.4, 7.3, 7.8 Hz, 1H), 3.02 (dd, *J* = 7.3, 13.9 Hz, 1H), 3.00 (dd [apparent triplet], *J* = 6.0, 6.4 Hz, 1H), 2.94 (dd, *J* = 7.8, 13.9 Hz, 1H), 1.35 (s, 18H), 1.33 (s, 18H);

¹³C NMR (125 MHz, CDCl₃, 25 °C) δ: 160.0, 159.9, 156.0, 152.1, 152.0, 149.1, 148.6, 137.3, 137.18, 137.16, 136.15, 135.7, 135.4, 130.7, 128.8, 128.7, 128.3, 128.2, 128.1, 127.9, 127.8, 127.4, 126.5, 126.2, 125.2, 124.2, 106.8, 102.1, 99.8, 99.6, 70.4, 70.1, 69.5, 62.5, 57.5, 54.3, 41.9, 34.5, 34.4, 30.7, 30.6;

HRMS (ESI): *m/z* calculated for C₇₂H₈₁O₆ [M+H]⁺: 1041.6028, found 1041.6022;

FTIR (neat) cm⁻¹: 3629 (w), 2953 (m), 1593 (s), 1434 (s), 1374 (m), 1313 (m), 1232 (m), 1145 (s), 1047 (m).



(1*R*,2*R*,3*R*)-1-(3,5-di-*tert*-butyl-4-hydroxybenzyl)-3-(3,5-di-*tert*-butyl-4-hydroxyphenyl)-2-(3,5-

dihydroxyphenyl)-2,3-dihydro-1*H*-indene-4,6-diol (4.31): A solution of starting indane **4.30** (100 mg, 0.096 mmol, 1.00 equiv) and pentamethylbenzene (285 mg, 1.92 mmol, 20.00 equiv) was prepared in CH₂Cl₂ (9.0 mL, 0.01 M) under inert atmosphere. The solution was cooled to -78 °C and BCl₃ (1.0 M in CH₂Cl₂, 1.15 mL, 12.00 equiv) was added slowly, turning the solution a red-orange color. TLC analysis at 1 h revealed full conversion to the desired product, and the reaction was quenched by the addition sat. aq. NaHCO₃/THF (3:1 (v/v), 4 mL) at -78 °C. The dry ice bath was removed and the mixture was allowed to stir for ~20 minutes at RT before diluting with EtOAc and transferring to a separatory funnel containing sat. aq. NaHCO₃. The phases were separated and the aqueous layer was extracted with portions of EtOAc. The organic layers were combined, washed with brine, dried over Na₂SO₄ and concentrated in vacuo. The desired **4.31** (59 mg, 0.086 mmol, 90% yield) was isolated from the crude material as a white foam by flash chromatography using an isocratic mobile phase of 2% MeOH in CH₂Cl₂.

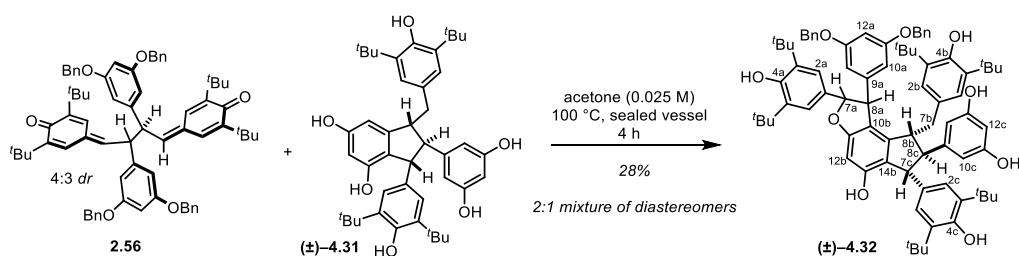
TLC (CH₂Cl₂/MeOH, 95:5), R_F: 0.17 (UV, *p*-anisaldehyde (red));

¹H NMR (500 MHz, acetone-*d*₆, 25 °C) δ: 8.00 (s, br, 1H, exchangeable [D₂O]), 7.97 (s, br, 1H, exchangeable [D₂O]), 7.21 (s, br, 1H, exchangeable [D₂O]), 6.90 (s, br, 2H), 6.82 (s, br, 2H), 6.29 (d, br, *J* = 1.5 Hz, 1H), 6.24 (d, br, *J* = 1.5 Hz, 1H), 6.15 (t, br, *J* = 1.5 Hz, 1H), 6.01 (d, br, *J* = 1.5 Hz, 2H), 5.79 (s, br, 1H, exchangeable [D₂O]), 5.72 (s, br, 1H, exchangeable [D₂O]), 4.25 (d, *J* = 3.9 Hz, 1H), 3.37 (ddd, *J* = 4.2, 6.6, 8.1 Hz, 1H), 2.91 (dd [apparent triplet], *J* = 3.9, 4.2 Hz, 1H), 2.86 (dd, *J* = 6.6, 13.7 Hz, 1H), 2.79 (s, br, 1H, exchangeable [D₂O]), 2.77 (dd, *J* = 8.1, 13.7 Hz, 1H), 1.37 (s, 18H), 1.34 (s, 18H);

¹³C NMR (175 MHz, acetone-*d*₆, 25 °C) δ: 159.3, 159.1, 155.3, 152.94, 152.86, 150.8, 150.5, 137.71, 137.69, 137.1, 131.8, 126.6, 124.7, 121.7, 106.3, 104.2, 102.2, 101.2, 61.8, 57.0, 55.6, 42.7, 35.2, 35.1, 30.90, 30.86;

HRMS (ESI): *m/z* calculated for C₄₄H₅₇O₆ [M+H]⁺: 681.4150, found 681.4148;

FTIR (neat) cm⁻¹: 3322 (m, br), 2957 (m), 1600 (s), 1434 (s), 1360 (s), 1230 (s), 1156 (m), 1134 (m), 1006 (w).



5-((1*S*,2*S*,6*R*,7*R*,8*R*)-1-(3,5-bis(benzyloxy)phenyl)-8-(3,5-di-*tert*-butyl-4-hydroxybenzyl)-2,6-bis(3,5-di-*tert*-butyl-4-hydroxyphenyl)-5-hydroxy-1,6,7,8-tetrahydro-2*H*-indeno[5,4-*b*]furan-7-yl)benzene-1,3-diol (4.32): A suspension of starting bis-*para*-quinone methide **2.56** (39 mg, 0.038 mmol, 1.00 equiv) and starting indane **4.31** (51 mg, 0.075 mmol, 2.00 equiv) was prepared in acetone (1.52 mL, 0.025 M) at room temperature in a 2 dram vial. The vessel was tightly sealed and the slowly stirring mixture heated to 100 °C. At 4 h, the reaction was removed from the heat and allowed to cool to room temperature over the course of 0.5 h. TLC confirmed full consumption of **2.56**. Column chromatography using 20%, then 30% of a 3:1 EtOAc/acetone mixture in hexanes afforded the disproportionation product **2.50** (24 mg, 0.046 mmol, 123% yield),⁶⁷ four products of intermediate *R_f* (30 mg collectively), and recovered **4.31** (30 mg, 0.044 mmol, 59% recovery). The mixture of ≥ 4 compounds was further purified by preparative thin layer chromatography (plate developed 3x using 1% EtOH in CH₂Cl₂) and the desired product **4.32** was isolated as a tan amorphous solid (8.0 mg, 0.0067 mmol, 18% yield) along with an impure sample containing mostly a diastereomer of **4.32** (4.7 mg, 10% yield). Characterization data for the major diastereomer is provided below:

TLC (CH₂Cl₂/Acetone, 95:5), *R_f*: 0.22 (UV, *p*-anisaldehyde (red));

¹H NMR (500 MHz, CDCl₃, 25 °C) δ : 7.42 – 7.28 (m, 10H, –OCH₂C₆H₅), 7.13 (s, 2H, C_{2a}–H), 6.92 (s, 2H, C_{2c}–H), 6.56 (s, br, overlap, 2H, C_{10a}–H), 6.55 (s, overlap, 1H, C_{12b}–H), 6.45 (s, br, 1H, C_{12a}–H), 6.43 (s, 2H, C_{2b}–H), 6.02 (s, C_{12c}–H), 5.57 (s, 2H, C_{10c}–H), 5.51 (d, *J* = 2.9 Hz, 1H, C_{7a}–H), 5.22 (s, 1H, –OH, exchangeable [D₂O]), 5.10 (s, 1H, –OH, exchangeable [D₂O]), 4.95 (d, *J* = 11.5 Hz, 2H, –OCH₂C₆H₅), 4.92 (d, *J* = 11.5 Hz, 2H, –OCH₂C₆H₅), 4.56 (s, br, 1H, –OH, exchangeable [D₂O]), 4.48 (d, *J* = 2.9 Hz, 1H, C_{8a}–H), 4.40 (s, br, 1H, –OH, exchangeable [D₂O]), 4.25 (d, *J* = 2.0 Hz, 1H, C_{7c}–H), 3.19 (ddd, br, *J* = 2.7, 3.4, 11.7 Hz, 1H, C_{8b}–H), 2.90 (dd [apparent triplet], *J* = 2.0, 2.7 Hz, 1H, C_{8c}–H), 2.47 (dd, *J* = 3.4, 13.5 Hz, 1H, C_{7b}–H), 1.98 (dd, *J* = 11.7, 13.5 Hz, 1H, C_{7b}–H), 1.42 (s, 18H, C_{3a}–C(CH₃)₃), 1.34 (s, 18H, C_{3c}–C(CH₃)₃), 1.25 (s, 18H, C_{3b}–C(CH₃)₃);

¹³C NMR (125 MHz, CDCl₃, 25 °C) δ : 162.8 (C_{11b}), 160.7 (br, C_{11a}), 156.6 (C_{11c}), 153.9 (C_{4a}), 153.5 (C_{13b}), 153.0 (C_{4c}), 151.8 (C_{4b}), 150.9 (C_{9c}), 148.0 (C_{9a}), 145.1 (C_{9b}), 136.9 (–OCH₂C₆H₅), 136.5 (C_{3c}), 136.3 (C_{3a}), 135.7 (C_{3b}), 134.1 (C_{1c}), 133.2 (C_{1a}), 131.2 (C_{1b}), 128.7 (–OCH₂C₆H₅), 128.2 (–OCH₂C₆H₅), 127.9 (–OCH₂C₆H₅), 125.8 (C_{2b}), 124.2 (C_{2c}), 122.7 (C_{14b}), 122.2 (C_{2a}), 117.7 (C_{10b}), 107.0 (br, C_{10a}), 106.1 (C_{10c}), 100.6 (C_{12a}), 100.3 (C_{12c}), 96.8 (C_{12b}), 94.1 (C_{7a}), 70.2 (–OCH₂C₆H₅), 59.2 (C_{8c}), 56.4 (C_{8a}), 56.2 (C_{8b}),

⁶⁷ Full disproportionation can generate 2 equiv. of **2.50** relative to the starting indane, but only 1 equiv. is theoretically needed, hence the yield >100%

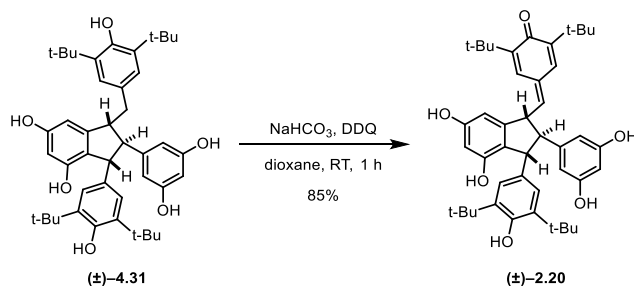
55.1 (\underline{C}_{7c}), 41.1 (\underline{C}_{7b}), 34.62 ($\underline{C}_{3a}-\underline{C}(\underline{CH}_3)_3$), 34.58 ($\underline{C}_{3c}-\underline{C}(\underline{CH}_3)_3$), 34.3 ($\underline{C}_{3b}-\underline{C}(\underline{CH}_3)_3$), 30.54 ($\underline{C}_{3c}-\underline{C}(\underline{CH}_3)_3$), 30.52 ($\underline{C}_{3b}-\underline{C}(\underline{CH}_3)_3$), 30.44 ($\underline{C}_{3a}-\underline{C}(\underline{CH}_3)_3$);

HRMS (ESI):

m/z calculated for $C_{44}H_{57}O_6$ $[M+H]^+$: 1199.6971, found 1199.6970;

FTIR (neat) cm^{-1} :

3638 (w), 2956 (m), 1594 (s), 1434 (s), 1365 (m), 1316 (m), 1234 (m), 1153 (s), 1082 (w), 1052 (m).



2,6-di-tert-butyl-4-(((1R,2R,3R)-3-(3,5-di-tert-butyl-4-hydroxyphenyl)-2-(3,5-dihydroxyphenyl)-4,6-dihydroxy-2,3-dihydro-1H-inden-1-yl)methylene)cyclohexa-2,5-dien-1-one (2.20): Starting **4.31** (37 mg, 0.055 mmol, 1.00 equiv) and NaHCO_3 (46 mg, 0.55 mmol, 10 equiv) were stirred in dioxane (1.0 mL) at 23 °C under inert atmosphere. In separate vessel, a solution of DDQ (14 mg, 0.061 mmol, 1.1 equiv) in dioxane (1.7 mL) was prepared. The solution of DDQ was added dropwise to the reaction mixture. Reaction progress was monitored by TLC and the reaction was quenched at 1 h with 10% aq. $\text{Na}_2\text{S}_2\text{O}_3$. The mixture was diluted with ethyl acetate and transferred to a separatory funnel containing sat. aq. Na_2CO_3 . The aqueous phase was extracted with ethyl acetate (2x). Combined organic layers were washed with sat. aq. Na_2CO_3 (2x), dried over Na_2SO_4 , and concentrated *in vacuo*. (NOTE: Do not expose material to alcoholic/nucleophilic solvents [e.g. *i*PrOH, MeOH, etc.], as the corresponding ether adduct forms readily). The resulting residue was purified by preparative TLC using 8% acetone in CH_2Cl_2 mobile phase to give **2.20** as a yellow-orange amorphous solid (31 mg, 0.046 mmol, 85% yield). (NOTE: **2.20** is not stable to prolonged storage in solution and should be stored at -20 °C under inert atmosphere or used immediately).

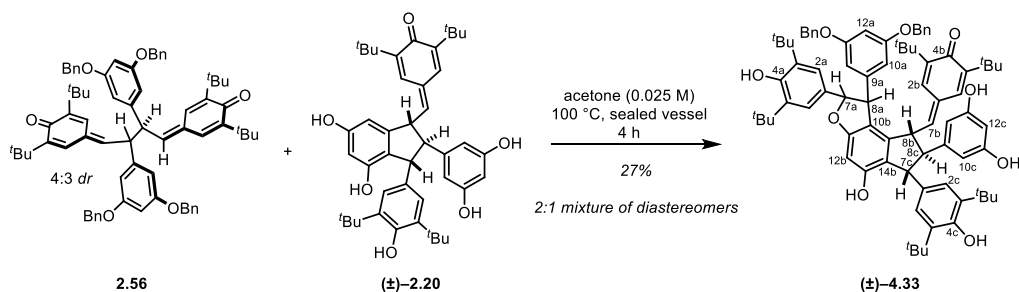
TLC (Hexanes/EtOAc, 4:1), R_f : 0.57 (UV, *p*-anisaldehyde (yellow-orange));

^1H NMR (500 MHz, acetone- d_6 , 25 °C) δ : 8.12 (br s, 3H), 7.28 (d, $J = 2.2$ Hz, 1H), 7.20 (br s, 1H), 7.03 (d, $J = 2.2$ Hz, 1H), 6.89 (s, 2H), 6.53 (d, $J = 9.5$ Hz, 1H), 6.33 (d, $J = 2.0$ Hz, 1H), 6.24 (d, $J = 2.0$ Hz, 1H), 6.23 (d, $J = 2.0$ Hz, 1H), 6.17 (d, $J = 2.0$ Hz, 1H), 5.83 (s, 1H), 4.63 (t, $J = 9.5$ Hz, 1H), 4.42 (d, $J = 8.2$ Hz, 1H), 3.02 (dd [apparent triplet], $J = 8.2$ Hz, 1H), 1.34 (s, 18 H), 1.26 (s, 9H), 1.22 (s, 9H);

^{13}C NMR (125 MHz, acetone- d_6 , 25 °C) δ : 187.1, 159.7, 159.5, 155.6, 153.3, 150.3, 148.9, 148.1, 147.2, 145.5, 137.8, 135.9, 134.7, 133.3, 128.2, 124.9, 121.4, 107.5, 104.1, 103.2, 102.0, 66.4, 57.4, 52.9, 35.9, 35.5, 35.2, 30.8, 29.9, 29.8;

All characterization data consistent with that reported.⁶⁸

⁶⁸ Li, W.; Li, H.; Li, Y.; Hou, Z. *Angew. Chem. Int. Ed.* **2006**, *45* (45), 7609–7611.

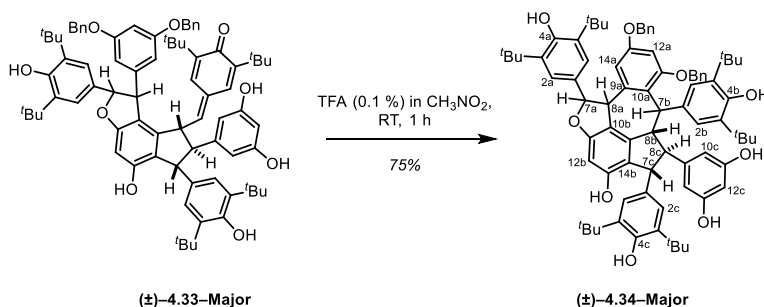


4-(((1S,2S,6R,7R,8R)-1-(3,5-bis(benzyloxy)phenyl)-2,6-bis(3,5-di-tert-butyl-4-hydroxyphenyl)-7-(3,5-dihydroxyphenyl)-5-hydroxy-1,6,7,8-tetrahydro-2H-indeno[5,4-b]furan-8-yl)methylene)-2,6-di-tert-butylcyclohexa-2,5-dien-1-one (4.33): A suspension of starting bis-*para*-quinone methide **2.56** (95 mg, 0.092 mmol, 2.00 equiv) and starting indane **2.20** (31 mg, 0.046 mmol, 1.00 equiv) was prepared in acetone (400 μ L) at room temperature in a 1 dram vial. The vessel was tightly sealed and the slowly stirring mixture heated to 100 $^{\circ}$ C. At 4 h, the reaction was removed from the heat and allowed to cool to room temperature over the course of 0.5 h. The solvent was removed *in vacuo* and the resultant residue was purified by preparative TLC (96:4 CH_2Cl_2 /Acetone) to afford **4.33** as a pale pink amorphous solid (8.0 mg, 0.0067 mmol, 18% yield) as well an impure sample containing mostly a diastereomer of **4.33** (4.0 mg, 0.0034 mmol, 9% yield). (NOTE: these intermediates are not stable to prolonged storage in solution and should be stored at -20 $^{\circ}$ C under inert atmosphere or used immediately). Partial characterization data for the major diastereomer is provided below, but otherwise complete characterization was performed after the subsequent step (consult next page).

TLC (CH_2Cl_2 /Acetone, 95:5), R_f : 0.48 (UV, vanillin (pale red));

^1H NMR (500 MHz, CDCl_3 , 25 $^{\circ}$ C) δ : 7.41 – 7.29 (m, overlap, 6H), 7.09 (s, 2H), 6.89 (s, 2H), 6.75 (d, J = 2.0 Hz, 1H), 6.54 (s, 1H), 6.51 (t, J = 2.2 Hz, 1H), 6.32 (d, J = 2.2 Hz, 2H), 6.16 (t, J = 2.2 Hz, 1H), 6.11 (d, J = 2.2 Hz, 2H), 5.98 (d, J = 2.0 Hz, 1H), 5.64 (d, J = 10.5 Hz, 1H), 5.40 (d, J = 3.9 Hz, 1H), 5.21 (s, 1H), 5.17 (s, 1H), 4.91 (m br, 2H), 4.70 (m, br, 2H), 4.45 (dd, J = 8.3, 10.5 Hz, 1H), 4.33 (d, J = 8.3 Hz, 1H), 4.25 (d, J = 3.9 Hz, 1H), 2.88 (dd [apparent triplet], J = 8.3 Hz, 1H), 1.40 (s, 18H), 1.34 (s, 18H), 1.15 (s, 9H), 1.09 (s, 9H);

^{13}C NMR (125 MHz, CDCl_3 , 25 $^{\circ}$ C) δ : 186.9, 163.0, 160.4, 157.0, 154.0, 153.8, 153.6, 148.1, 147.8, 147.4, 146.1, 144.7, 141.5, 136.9, 136.8, 136.3, 135.0, 132.8, 131.4, 131.1, 128.8, 128.3, 127.9, 126.4, 124.2, 122.1, 117.8, 107.8, 106.8, 101.6, 101.2, 97.8, 94.0, 70.1, 65.2, 56.4, 56.3, 54.0, 52.0, 35.3, 34.8, 34.62, 34.60, 30.45, 30.43, 29.6, 29.5.



5-((3R,4R,4aS)-6,8-bis(benzyloxy)-3,5,10-tris(3,5-di-tert-butyl-4-hydroxyphenyl)-2-hydroxy-3,4,4a,5,9b,10-hexahydrobenzo[5,6]azuleno[7,8,1-cde]benzofuran-4-yl)benzene-1,3-diol (4.34): The quinone methide intermediate **4.33** (8 mg, 0.0067 mmol, 1.00 equiv) was dissolved in 0.1% TFA in CH₃NO₂ (500 μL) and stirred at RT under inert atmosphere. After 1 hour, TLC showed full consumption of the starting material. A drop of Et₃N was added to quench the reaction and the solvent was removed *in vacuo*. The resulting residue was purified by preparative TLC (97:3 CH₂Cl₂/Acetone) to yield the cyclized product **4.34** (6 mg, 0.005 mmol, 75% yield) as a pale pink amorphous solid, determined to be a single diastereomer. The connectivity was rigorously assigned by 2D NMR, though the relative configuration at C_{7a}, C_{8a}, and C_{7b} could not be determined.

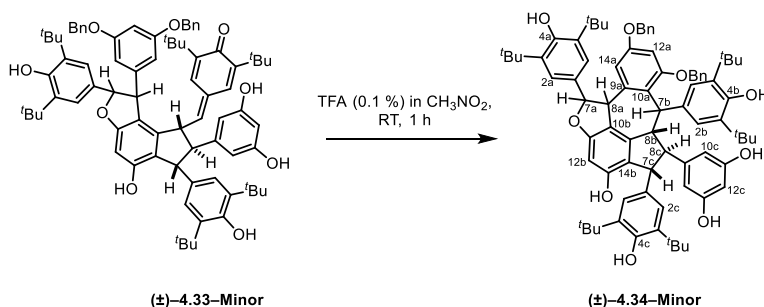
TLC (CH₂Cl₂/Acetone, 95:5), R_F: 0.22 (UV, vanillin (pale red));

¹H NMR (500 MHz, acetone-*d*₆, 25 °C) δ: 7.47 – 7.28 (m, 10H), 7.07 (s, 2H, C_{2a}-H), 6.90 (s, 1H, C_{14a}-H), 6.81 (s, 2H, C_{2c}-H), 6.73 (s, 2H, C_{2b}-H), 6.63 (s, 1H, C_{12a}-H), 6.17 (d, *J* = 3.4 Hz, 1H, C_{7a}-H), 6.16 (s, 1H, C_{12b}-H), 6.12 (t, *J* < 1.5 Hz, 1H, C_{12c}-H), 6.09 (d, *J* < 1.5 Hz, 2H, C_{10c}-H), 5.37 (s, 1H, C_{7b}-H), 5.13 (d, *J* = 11.7 Hz, 1H, -OCH₂C₆H₅), 5.12 (s, 1H, -OH), 5.09 (d, *J* = 11.7 Hz, 1H, -OCH₂C₆H₅), 4.99 (d, *J* = 11.3 Hz, 1H, -OCH₂C₆H₅), 4.95 (d, *J* = 11.3 Hz, 1H, -OCH₂C₆H₅), 4.87 (s, 1H, -OH), 4.43 (d, overlap, *J* = 3.4 Hz, 1H, C_{8a}-H), 4.40 (d, *J* = 10.7 Hz, 1H, C_{7c}-H), 4.14 (br s, 2H, -OH), 4.01 (d, *J* = 11.2 Hz, 1H, C_{8b}-H), 2.97 (dd [apparent triplet], *J* = 10.7, 11.2 Hz, 1H, C_{8c}-H), 1.34 (s, 18H, C_{3a}-C(CH₃)₃), 1.32 (s, 18H, C_{3c}-C(CH₃)₃), 1.13 (s, 18H, C_{3b}-C(CH₃)₃);

¹³C NMR (125 MHz, acetone-*d*₆, 25 °C) δ: 159.4 (C_{11b}), 159.3 (C_{11a}), 157.9 (C_{13a}), 156.7 (C_{11c}), 153.8 (C_{4a}), 153.5 (C_{13b}), 153.4 (C_{4c}), 151.5 (C_{4b}), 147.0 (C_{9a}), 143.4 (C_{9c}), 141.1 (C_{9b}), 137.4 (-OCH₂C₆H₅), 137.0 (-OCH₂C₆H₅), 136.6 (C_{3c}), 136.1 (C_{3a}), 135.1 (C_{3b}), 135.0 (C_{1b}), 132.9 (C_{1a}), 130.4 (C_{1c}), 128.90 (-OCH₂C₆H₅), 128.87(-OCH₂C₆H₅), 128.43 (-OCH₂C₆H₅), 128.37 (-OCH₂C₆H₅), 128.3 (-OCH₂C₆H₅), 127.9 (-OCH₂C₆H₅), 124.7 (C_{2c}), 124.5 (C_{2b}), 122.3 (C_{2a}), 120.2 (C_{10a}), 120.0 (C_{10b}), 118.8 (C_{14b}), 108.6 (C_{10c}), 104.3 (C_{14a}), 101.3 (C_{12c}), 98.4 (C_{12a}), 95.9 (C_{12b}), 86.7 (C_{7a}), 71.5 (-OCH₂C₆H₅), 70.4 (-OCH₂C₆H₅), 66.0 (C_{8c}), 55.3 (C_{7c}), 54.2 (C_{8b}), 51.3 (C_{8a}), 37.0 (C_{7b}), 34.6 (C-C(CH₃)₃), 34.5 (C-C(CH₃)₃), 34.4 (C-C(CH₃)₃), 30.51 (C-C(CH₃)₃), 30.47 (C-C(CH₃)₃), 30.4 (C-C(CH₃)₃);

HRMS (ESI): *m/z* calculated for C₈₀H₉₃O₆ [M+H]⁺: 1197.6814, found 1197.6783;

FTIR (neat) cm⁻¹: 3178 (br), 2922 (s), 2855 (s), 1602 (s), 1452 (s), 1359 (m), 1211 (m), 1155 (s).



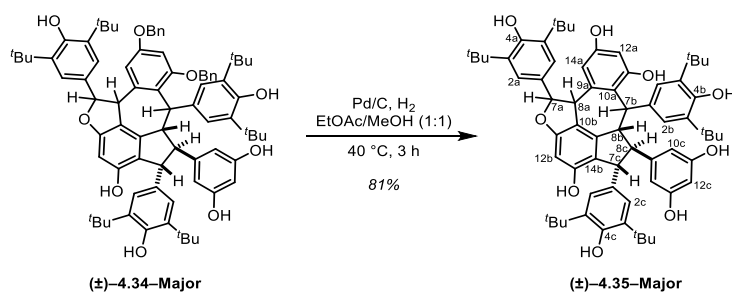
5-((3R,4R,4aS)-6,8-bis(benzyloxy)-3,5,10-tris(3,5-di-tert-butyl-4-hydroxyphenyl)-2-hydroxy-3,4,4a,5,9b,10-hexahydrobenzo[5,6]azuleno[7,8,1-cde]benzofuran-4-yl)benzene-1,3-diol (4.34): Using the impure sample containing predominantly the minor diastereomer of quinone methide intermediate **4.33** (~5 mg), the acid-mediated 7-*exo* Friedel–Crafts cyclization was performed as described in the previous entry. Isolation of the desired product was achieved by preparative TLC (97:3 CH₂Cl₂/Acetone) to yield the cyclized product **4.34** (~4 mg), determined to be a single diastereomer. The connectivity was rigorously assigned by 2D NMR, though the relative configuration at C_{7a}, C_{8a}, and C_{7b} could not be determined.

TLC (CH₂Cl₂/Acetone, 95:5), R_F: 0.22 (UV, vanillin (pale red));

¹H NMR (500 MHz, CDCl₃, 25 °C) δ: 7.37 – 7.27 (m, overlap, 8H, –OCH₂C₆H₅), 7.30 (s, 2H, C_{2a}–H), 7.21–7.19 (m, overlap, 2H, –OCH₂C₆H₅), 7.08 (s, 2H, C_{2b}–H), 6.92 (br s, 2H, C_{2c}–H), 6.54 (d, *J* = 2.2 Hz, 1H, C_{12a}–H), 6.38 (d, *J* = 2.2 Hz, 1H, C_{14a}–H), 6.30 (s, 1H, C_{12b}–H), 6.21 (t, *J* = 2.2 Hz, 1H, C_{12c}–H), 6.13 (d, *J* = 2.2 Hz, 2H, C_{10c}–H), 5.86 (d, *J* = 12.1 Hz, 1H, C_{7a}–H), 5.47 (d, *J* = 3.9 Hz, 1H, C_{7b}–H), 5.25 (s, 1H, C_{4a}–OH), 5.14 (s, 1H, C_{4c}–OH), 5.09 (d, *J* = 12.0 Hz, 1H, –OCH₂C₆H₅), 4.93 (d, *J* = 12.0 Hz, 1H, –OCH₂C₆H₅), 4.93 (s, 1H, C_{4b}–OH), 4.87 (d, *J* = 11.0 Hz, 1H, –OCH₂C₆H₅), 4.76 (d, *J* = 11.0 Hz, 1H, –OCH₂C₆H₅), 4.73 (br d, *J* = 12.1 Hz, 1H, C_{8a}–H), 4.67 (s, 1H, –OH), 4.22 (d, *J* = 10.3 Hz, 1H, C_{7c}–H), 3.80 (br dd, *J* = 3.9, 11.5 Hz, 1H, C_{8b}–H), 3.37 (dd, *J* = 10.3, 11.5 Hz, 1H, C_{8c}–H), 1.36 (s, 18H, C_{3a}–C(CH₃)₃), 1.34 (s, 18H, C_{3c}–C(CH₃)₃), 1.21 (s, 18H, C_{3b}–C(CH₃)₃);

¹³C NMR (125 MHz, CDCl₃, 25 °C) δ: 159.2 (C_{11b}), 157.7 (C_{13a}), 156.7 (C_{11a}), 156.6 (C_{11c}), 154.8 (C_{4a}), 153.5 (C_{4c}), 153.4 (C_{13b}), 151.8 (C_{4b}), 143.3 (C_{9c}), 142.6 (C_{9b}), 140.9 (C_{9a}), 137.2 (–OCH₂C₆H₅), 136.8 (–OCH₂C₆H₅), 136.7 (C_{3c}), 136.4 (C_{3a}), 135.3 (C_{3b}), 131.7 (C_{1b}), 129.7 (C_{1c}), 128.77 (–OCH₂C₆H₅), 128.75 (–OCH₂C₆H₅), 128.34 (–OCH₂C₆H₅), 128.31 (–OCH₂C₆H₅), 128.0 (–OCH₂C₆H₅), 127.8 (C_{10a}), 127.7 (–OCH₂C₆H₅), 126.7 (–OCH₂C₆H₅), 125.7 (C_{2b}), 125.3 (C_{2a}), 124.7 (C_{2c}—see footnote⁶⁹), 118.0 (C_{14b}), 116.3 (C_{10b}), 108.5 (C_{10c}), 105.7 (C_{14a}), 101.4 (C_{12c}), 99.5 (C_{12a}), 96.5 (C_{12b}), 92.6 (C_{7a}), 70.7 (–OCH₂C₆H₅), 70.2 (–OCH₂C₆H₅), 62.3 (C_{8c}), 56.4 (C_{7c}), 50.7 (C_{8b}), 47.7 (C_{8a}), 37.9 (C_{7b}), 34.59 (C_{3c}–C(CH₃)₃), 34.55 (C_{3a}–C(CH₃)₃), 34.4 (C_{3b}–C(CH₃)₃), 30.6 (C_{3c}–C(CH₃)₃), 30.55 (C_{3c}–C(CH₃)₃), 30.45 (C_{3a}–C(CH₃)₃).

⁶⁹ Resonance for C_{2c} is broadened (presumably due to restricted rotation) to the point that it is not visible above the noise. This is consistent with broadening of C_{2c}–H in the ¹H-NMR spectrum. The existence of the ¹³C–resonance at this frequency was confirmed by correlations in both the HSQC and HMBC spectra



(3R,4R,4aS)-3,5,10-tris(3,5-di-tert-butyl-4-hydroxyphenyl)-4-(3,5-dihydroxyphenyl)-3,4,4a,5,9b,10-

hexahydrobenzo[5,6]azuleno[7,8,1-cde]benzofuran-2,6,8-triol (4.35): A round bottom flask was charged with the major diastereomer of dibenzylated trimer **4.34** (6 mg, 0.005 mmol, 1.00 equiv) and Pd/C (30 wt%, 1 mg) and the flask was sealed and purged with N₂. EtOAc (HPLC grade, 500 μL) and MeOH (HPLC grade, 500 μL) were sequentially added and N₂ inlet was replaced with a H₂ balloon. The mixture was gently sparged with H₂ for 10 minutes at room temperature, at which point the vent needle was removed and the reaction mixture was warmed to 40 °C under H₂ (1 atm). After 3 h, the reaction was removed from the heat source, cooled to room temperature, and the contents filtered through a short plug of Celite, eluting with 1:1 EtOAc/MeOH. The filtrate was concentrated to dryness *in vacuo* and the resulting residue was purified by preparative TLC (90:10 CH₂Cl₂/Acetone) to afford **4.35** (4.1 mg, 0.004 mmol, 81% yield) as a single diastereomer. The connectivity was rigorously assigned by 2D NMR, though the relative configuration at C_{7a}, C_{8a}, and C_{7b} could not be determined.

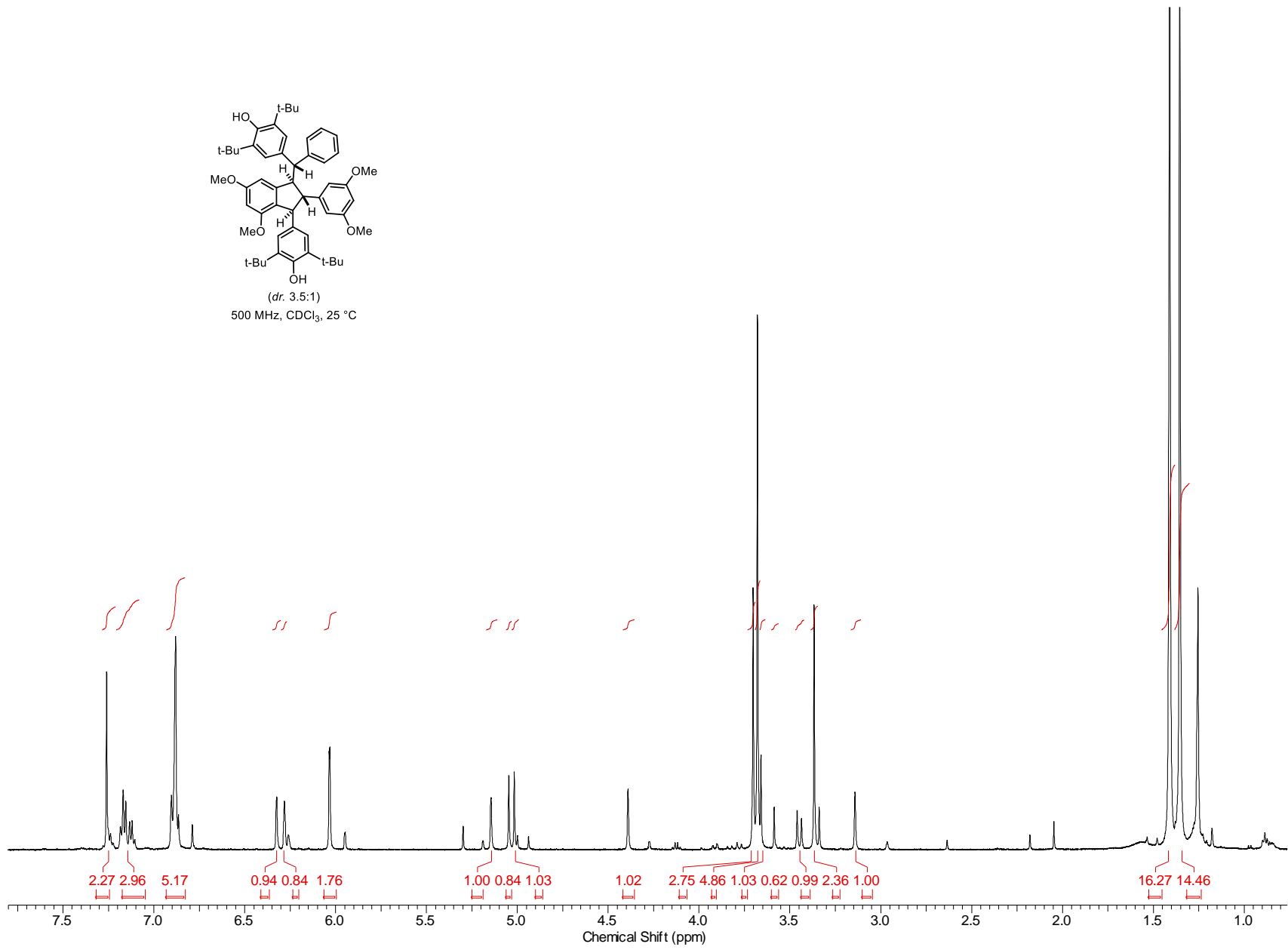
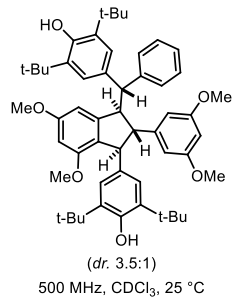
TLC (CH₂Cl₂/Acetone, 95:5), R_F: 0.15 (UV, vanillin (pale red));

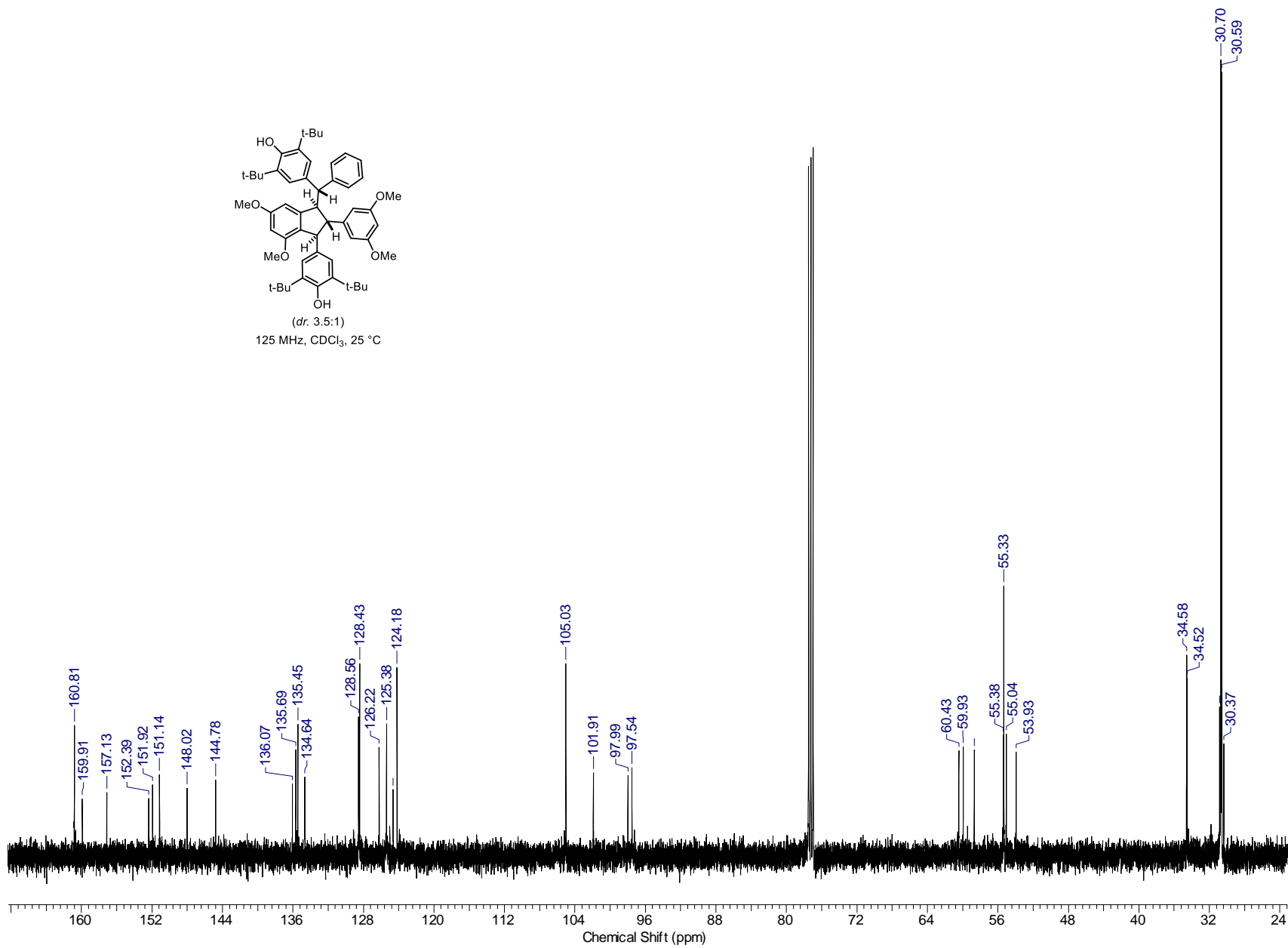
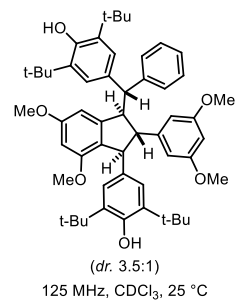
¹H NMR (500 MHz, CDCl₃, 25 °C) δ: 8.26 (br s, 1H), 8.11 (br s, 1H), 8.03 (br s, 1H), 7.16 (s, 2H, C_{2a}-H), 6.91 (s, 2H, C_{2b}-H), 6.81 (s, 2H, C_{2c}-H), 6.73 (d, *J* = 1.7 Hz, 1H, C_{14a}-H), 6.59 (br s, 1H), 6.53 (d, *J* = 2.0 Hz, 2H, C_{10c}-H), 6.42 (d, *J* = 1.7 Hz, 1H, C_{12a}-H), 6.24 (t, overlap *J* = 2.0 Hz, 1H, C_{12c}-H), 6.23 (d, overlap, *J* = 2.0 Hz, 1H, C_{7a}-H), 6.10 (s, 1H, C_{12b}-H), 5.95 (s, 1H, C_{4a}-OH), 5.74 (s, 1H, C_{4c}-OH), 5.58 (s, 1H, C_{4b}-OH), 5.34 (s, 1H, C_{7b}-H), 4.48 (d, *J* = 10.0 Hz, 1H, C_{7c}-H), 4.42 (d, *J* = 2.0 Hz, 1H, C_{8a}-H), 4.16 (d, *J* = 11.7 Hz, 1H, C_{8b}-H), 2.96 (dd [apparent triplet], *J* = 10.0, 11.7 Hz, 1H, C_{8c}-H), 1.35 (s, 18H, C_{3a}-C(CH₃)₃), 1.28 (s, 18H, C_{3c}-C(CH₃)₃), 1.16 (s, 18H, C_{3b}-C(CH₃)₃);

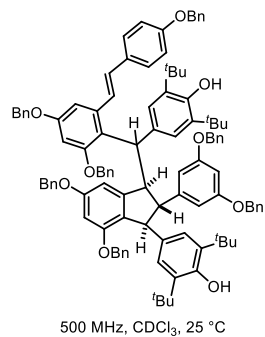
¹³C NMR (125 MHz, CDCl₃, 25 °C) δ: 160.0 (C_{11b}), 159.3 (C_{11c}), 158.5 (C_{11a}), 156.9 (C_{13a}), 154.9 (C_{13b}), 154.6 (C_{4a}), 154.4 (C_{4a}), 153.2 (C_{4c}), 152.2 (C_{4b}), 147.8 (C_{9a}), 144.6 (C_{9c}), 143.4 (C_{9b}), 138.1 (C_{3a})⁷⁰, 137.4 (C_{3c})⁷⁰, 137.1 (C_{3b})⁷⁰, 136.6 (C_{1b}), 135.0 (C_{1a}), 133.3 (C_{1c}), 125.4 (C_{2c}), 125.0 (C_{2b}), 122.8 (C_{2a}), 121.1 (C_{14b}), 119.0 (C_{10b}), 116.9 (C_{10a}), 109.9 (C_{10c}), 104.2 (C_{14a}), 101.9 (C_{12c}), 101.6 (C_{12a}), 95.6 (C_{12b}), 86.8 (C_{7a}), 67.6 (C_{8c}), 56.7 (C_{7c}), 55.0 (C_{8b}), 52.3 (C_{8a}), 37.4 (C_{7b}), 35.2 (C-C(CH₃)₃), 35.1 (C-C(CH₃)₃), 30.9 (C-C(CH₃)₃), 30.78 (C-C(CH₃)₃), 30.75 (C-C(CH₃)₃).

⁷⁰ Each of the resonances for ^tBu-bearing carbons (C_{3a}, C_{3b}, C_{3c}) had an accompanying minor resonance (approx. one-half the intensity) 0.1 ppm upfield of the major resonance, indicating restricted rotation of these sterically encumbered phenols

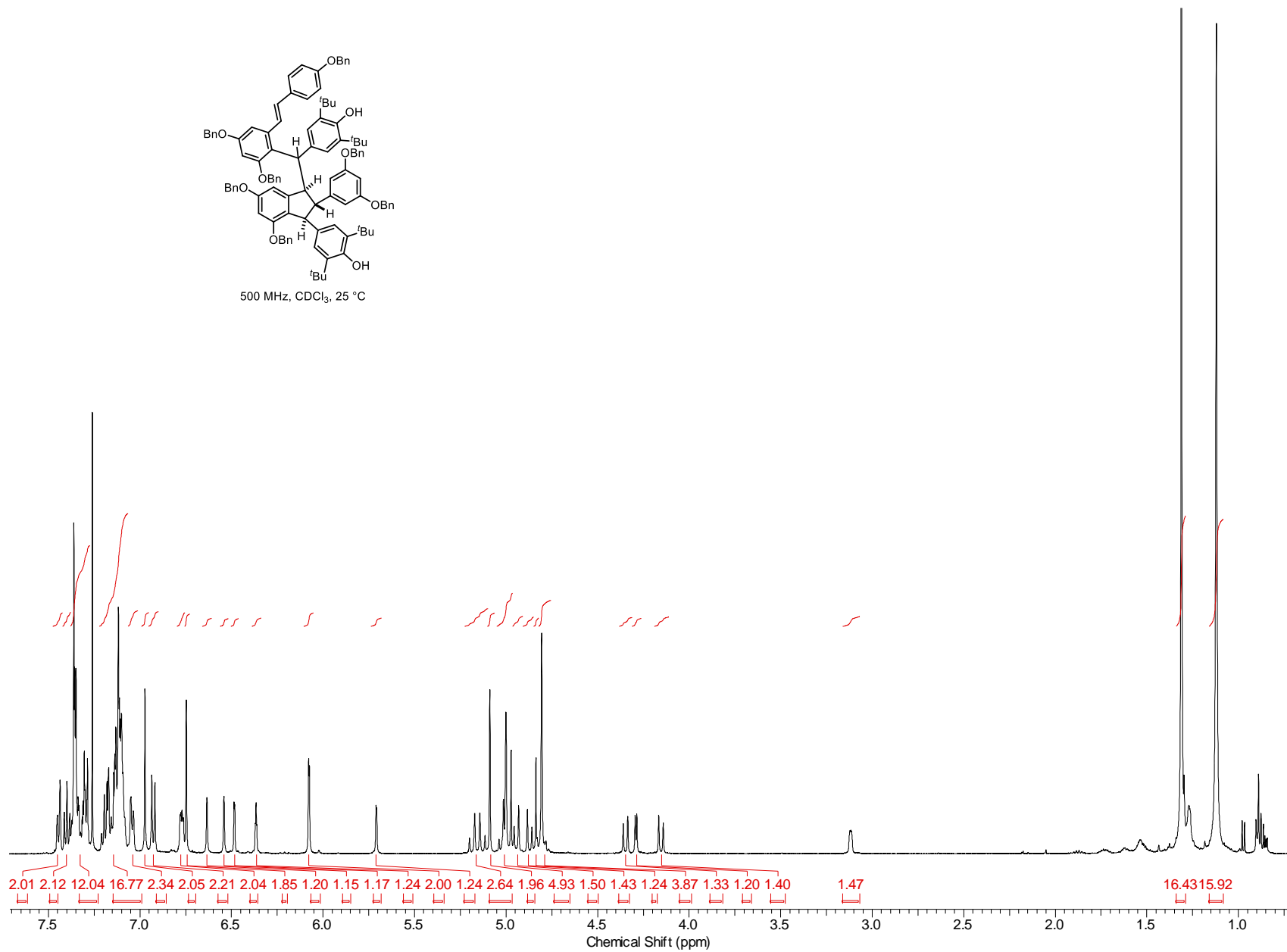
356

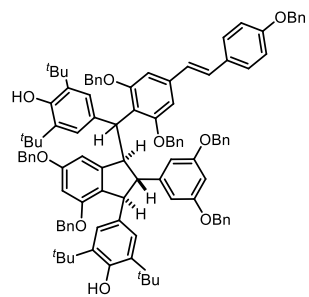






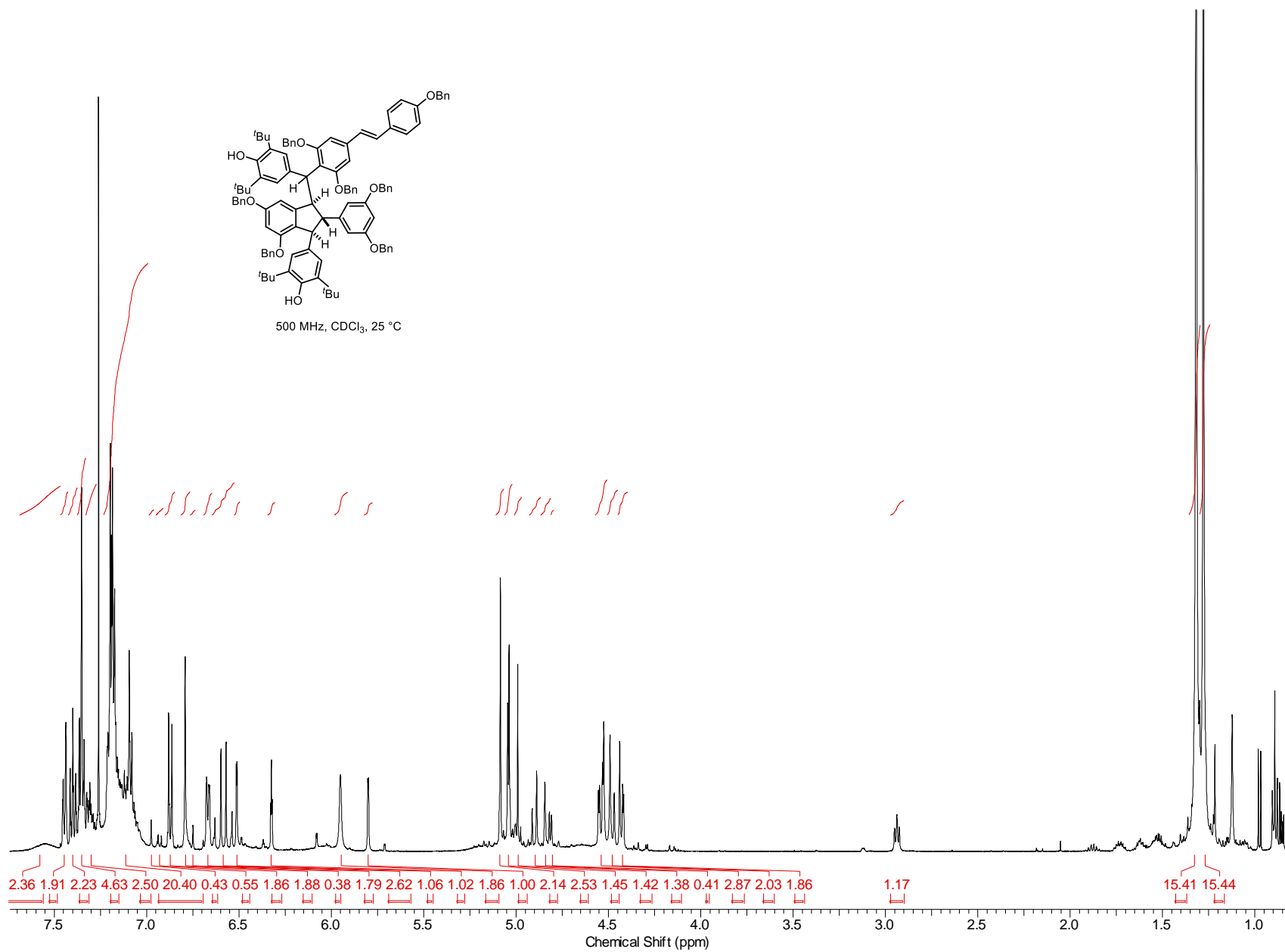
358

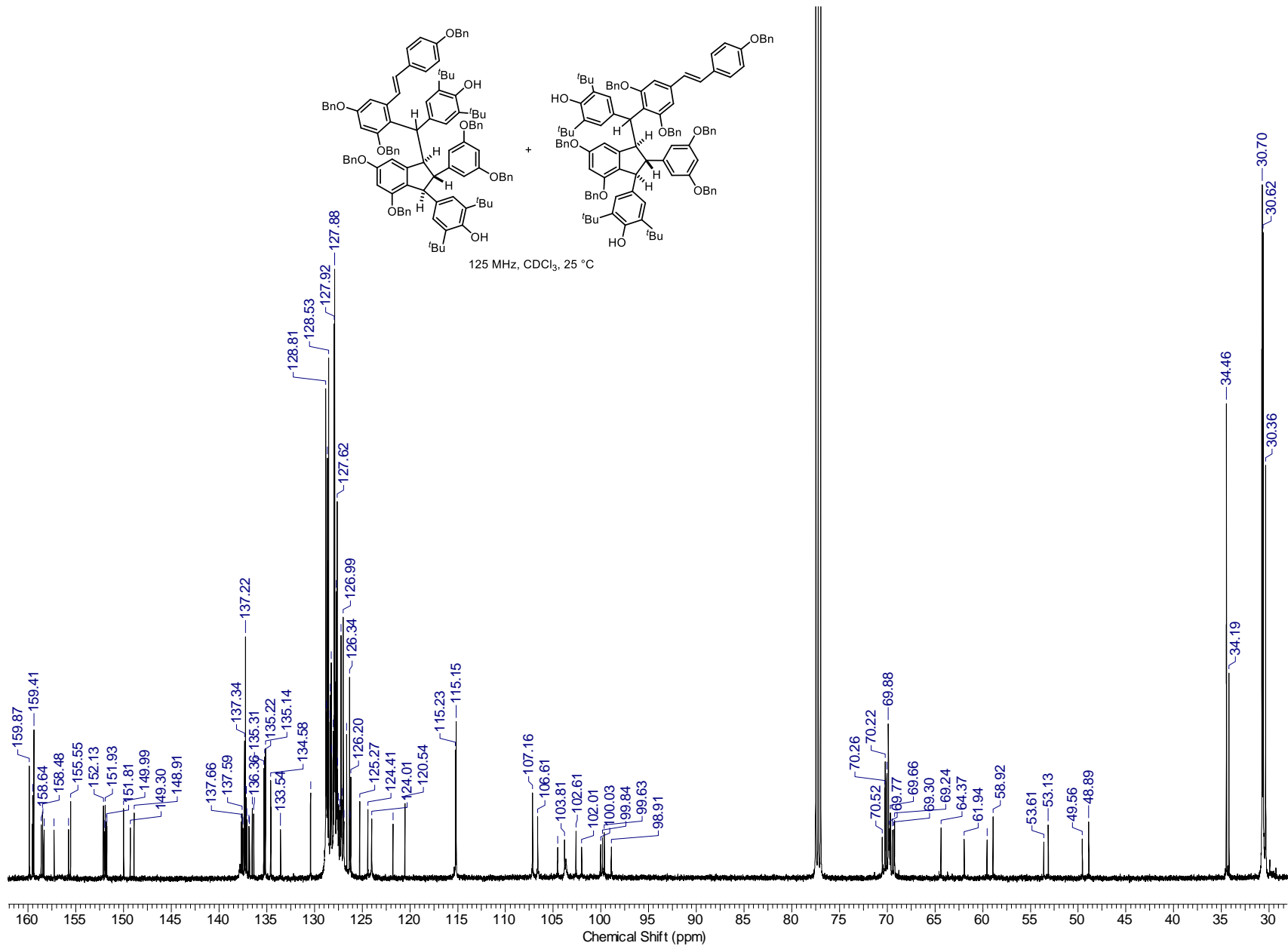


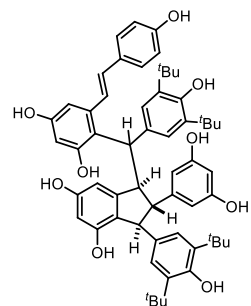


500 MHz, CDCl₃, 25 °C

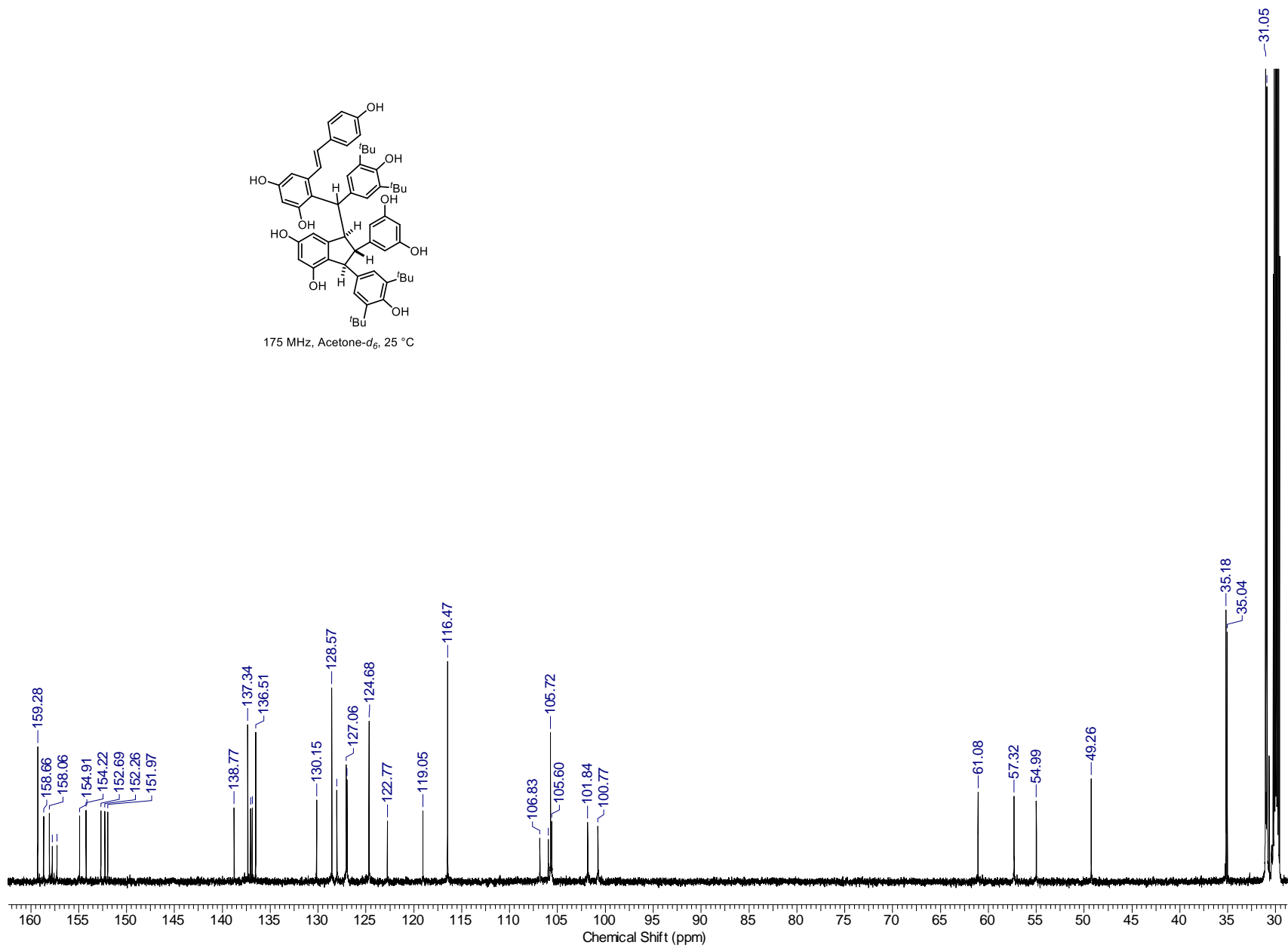
359

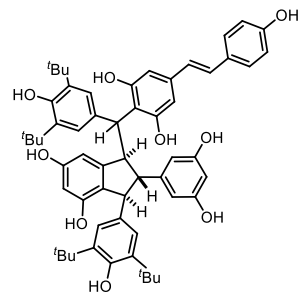




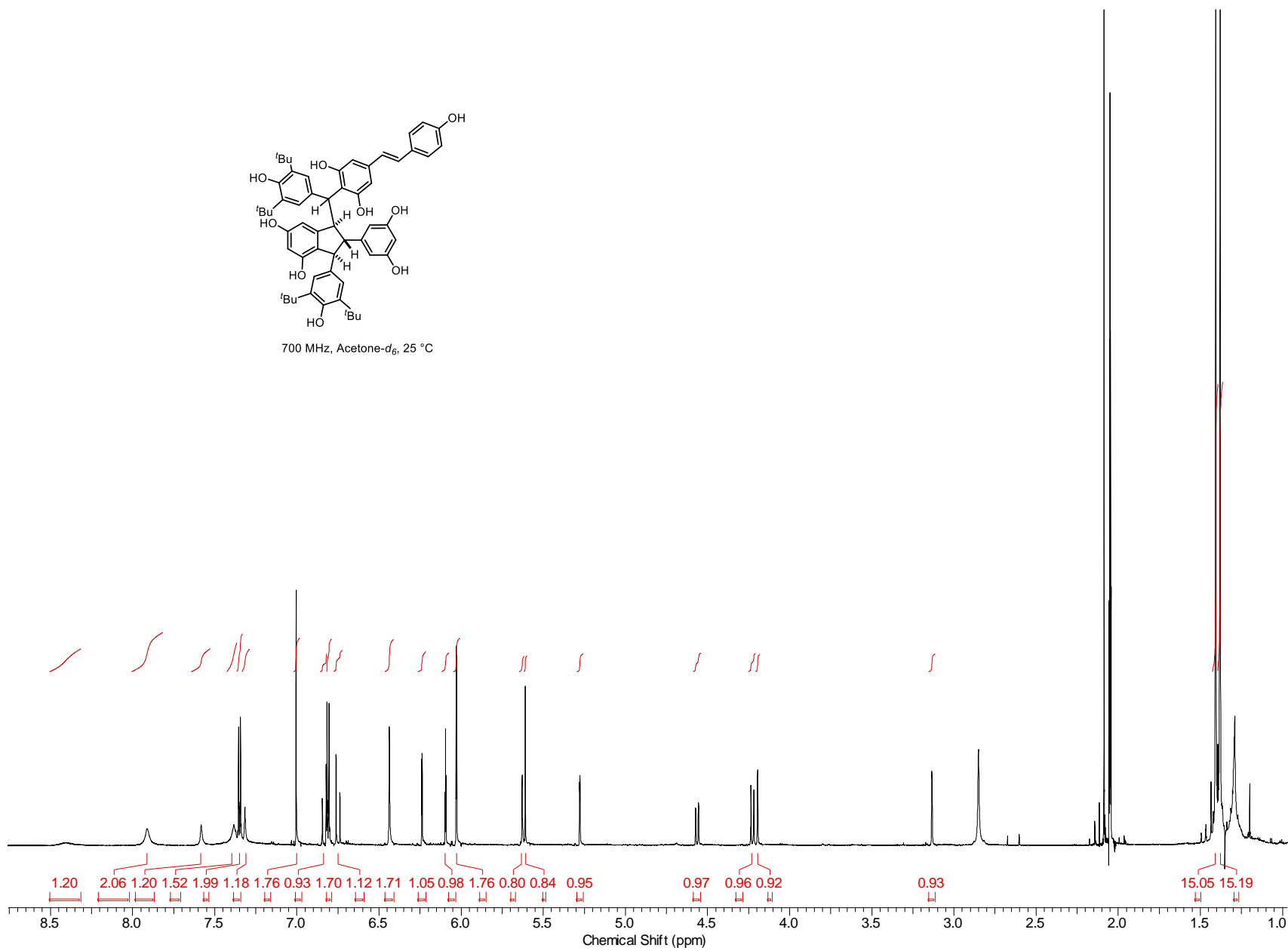


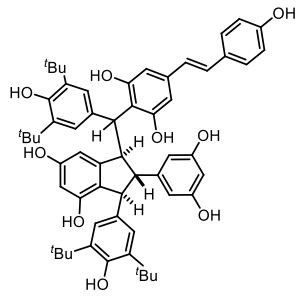
175 MHz, Acetone- d_6 , 25 °C



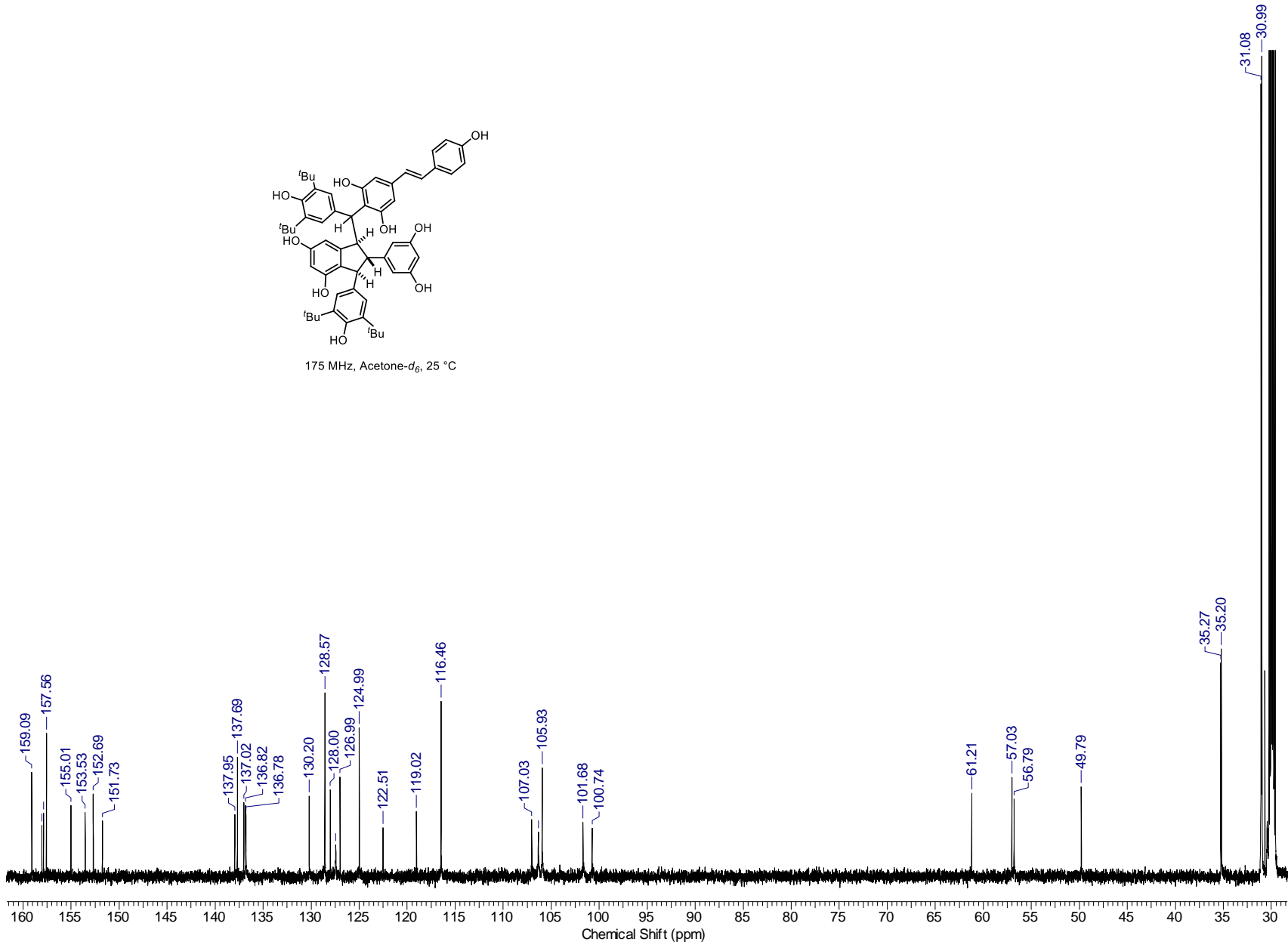


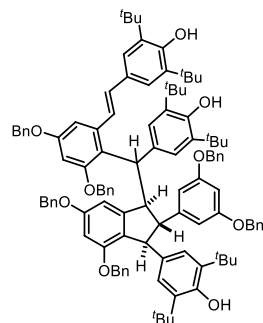
700 MHz, Acetone- d_6 , 25 °C





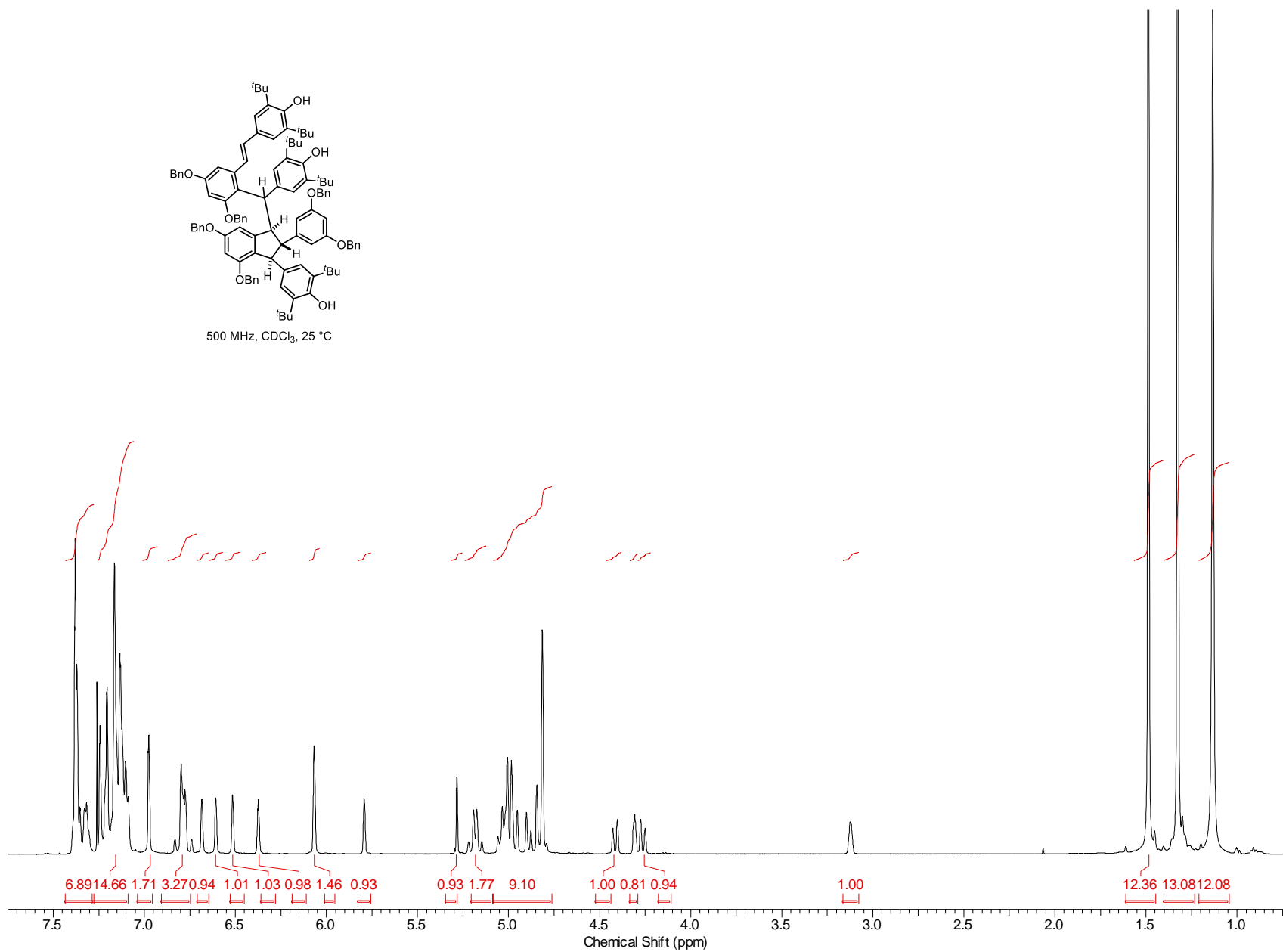
175 MHz, Acetone- d_6 , 25 °C

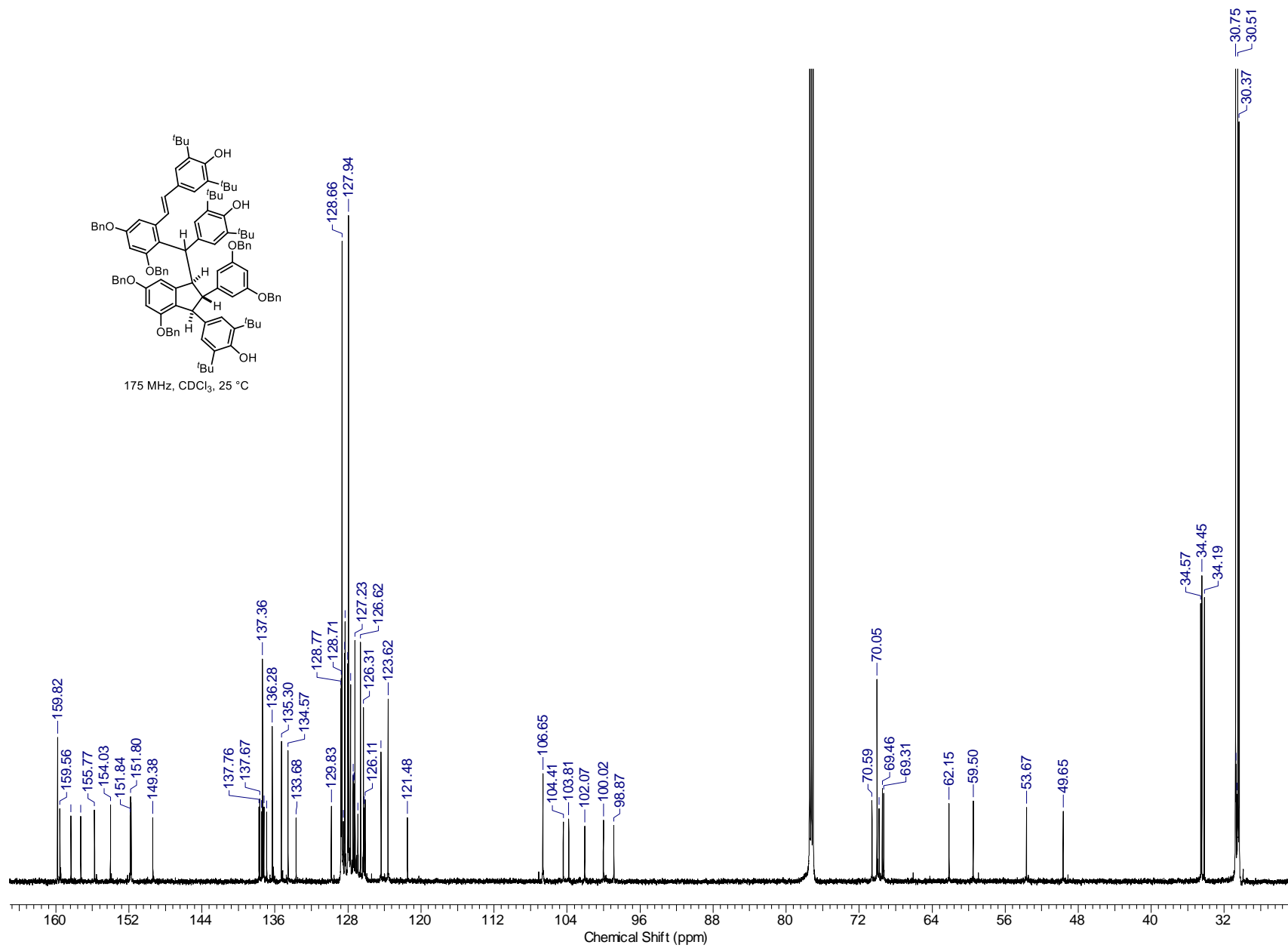




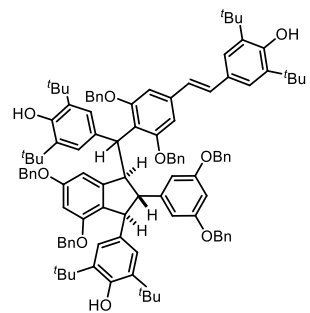
500 MHz, CDCl₃, 25 °C

365

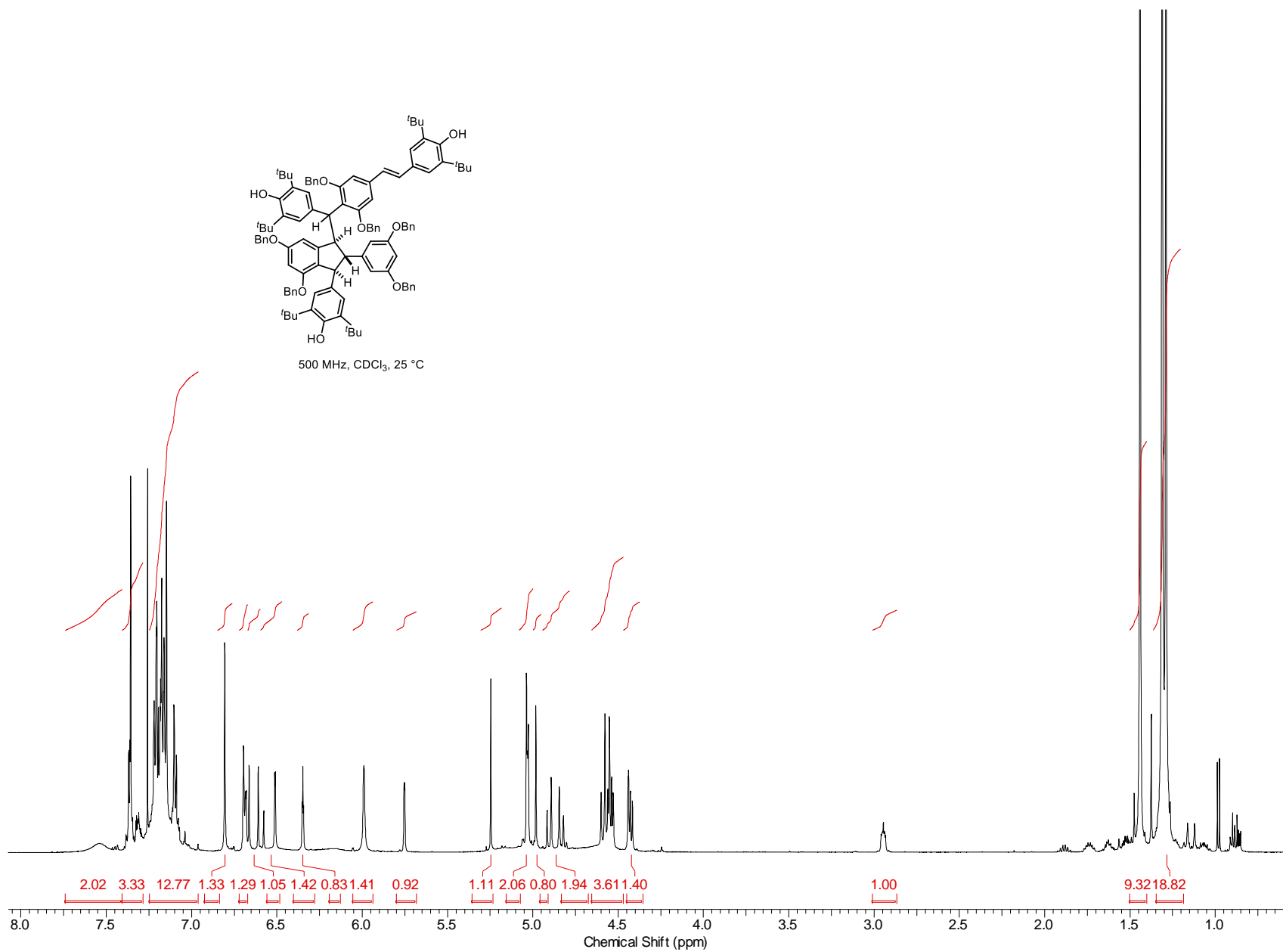


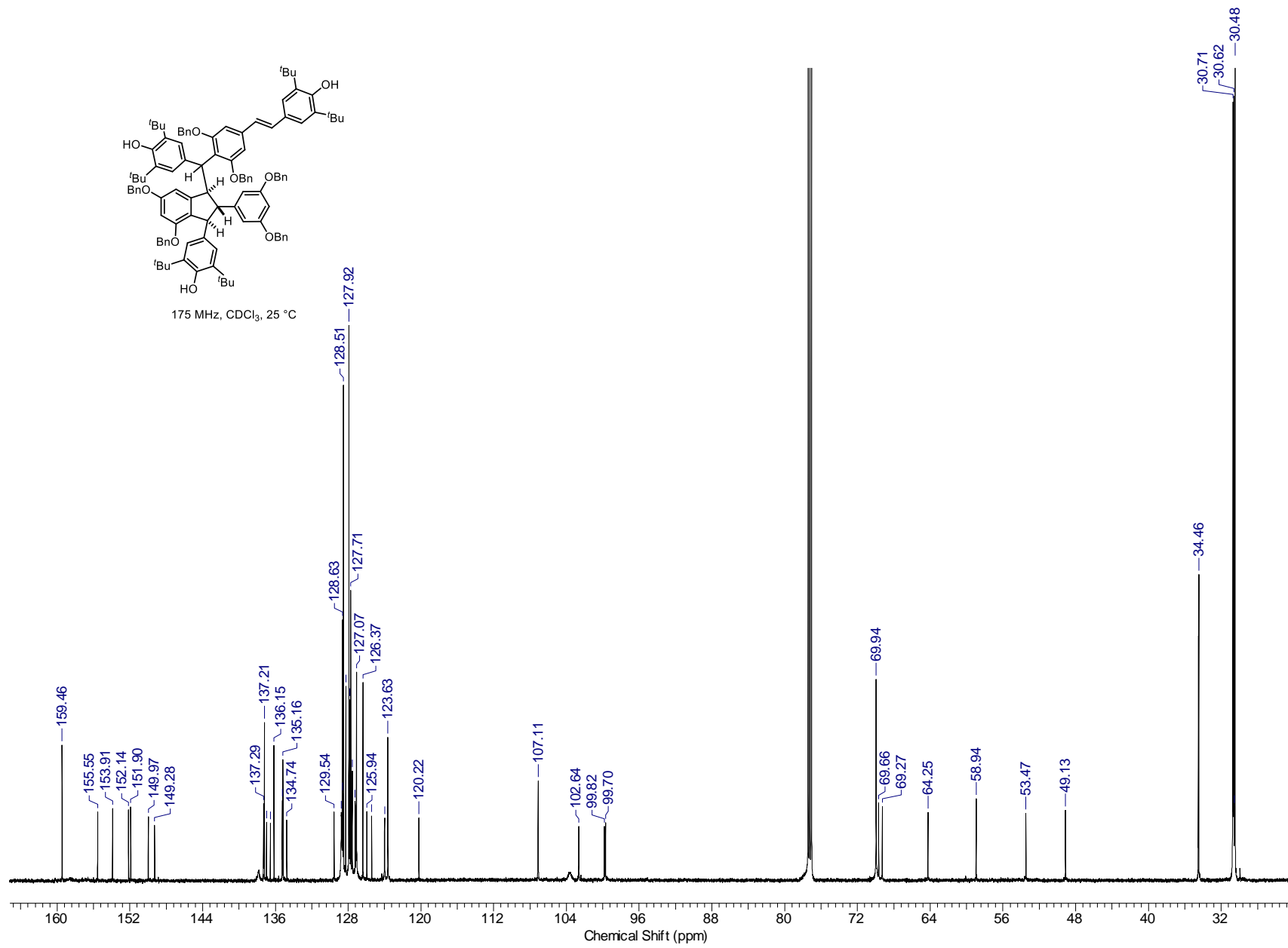


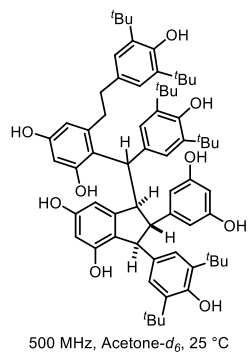
367



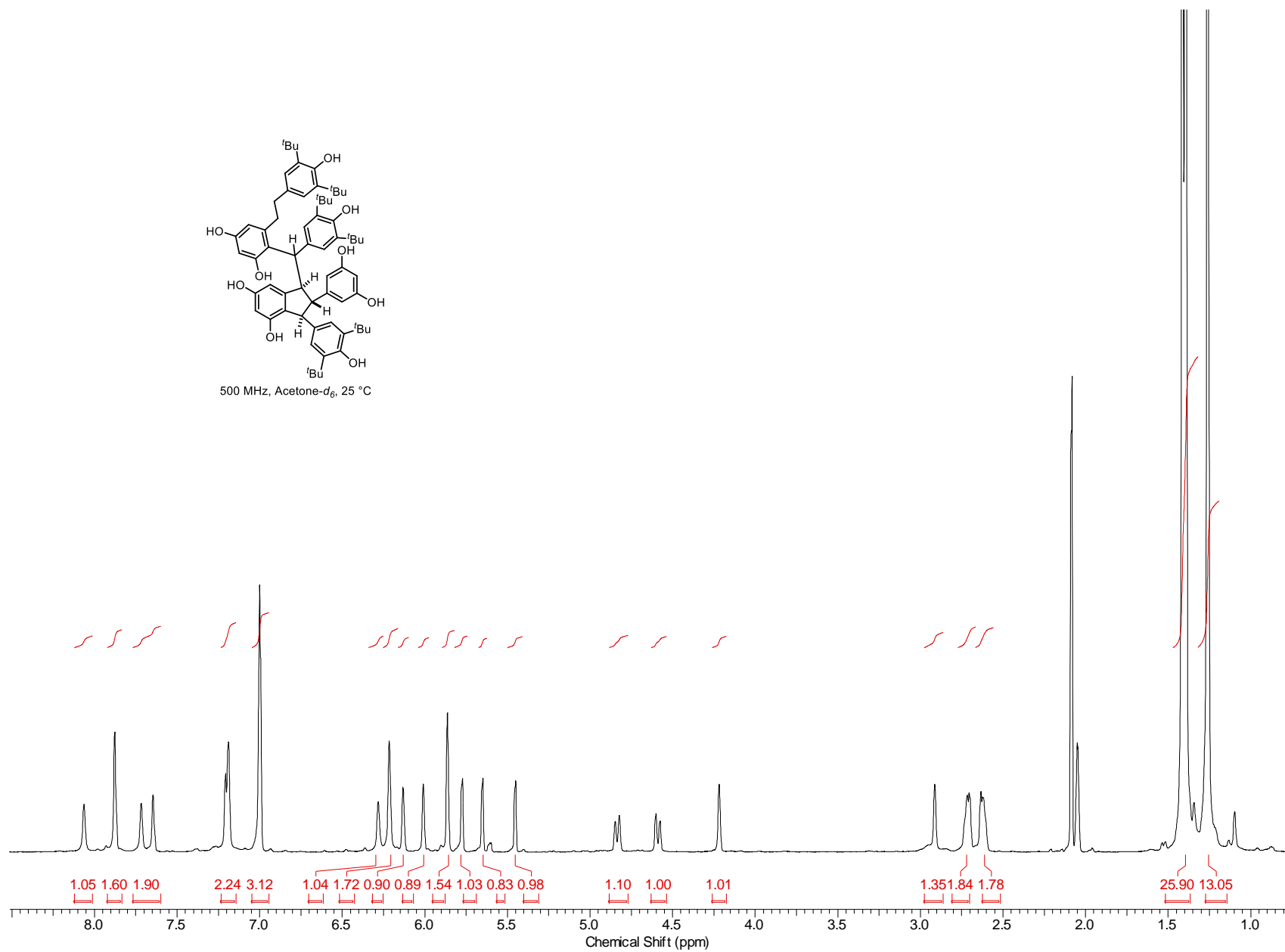
500 MHz, CDCl₃, 25 °C

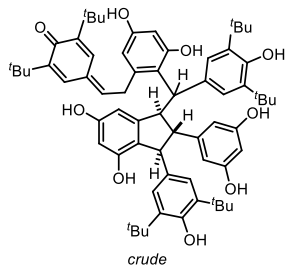






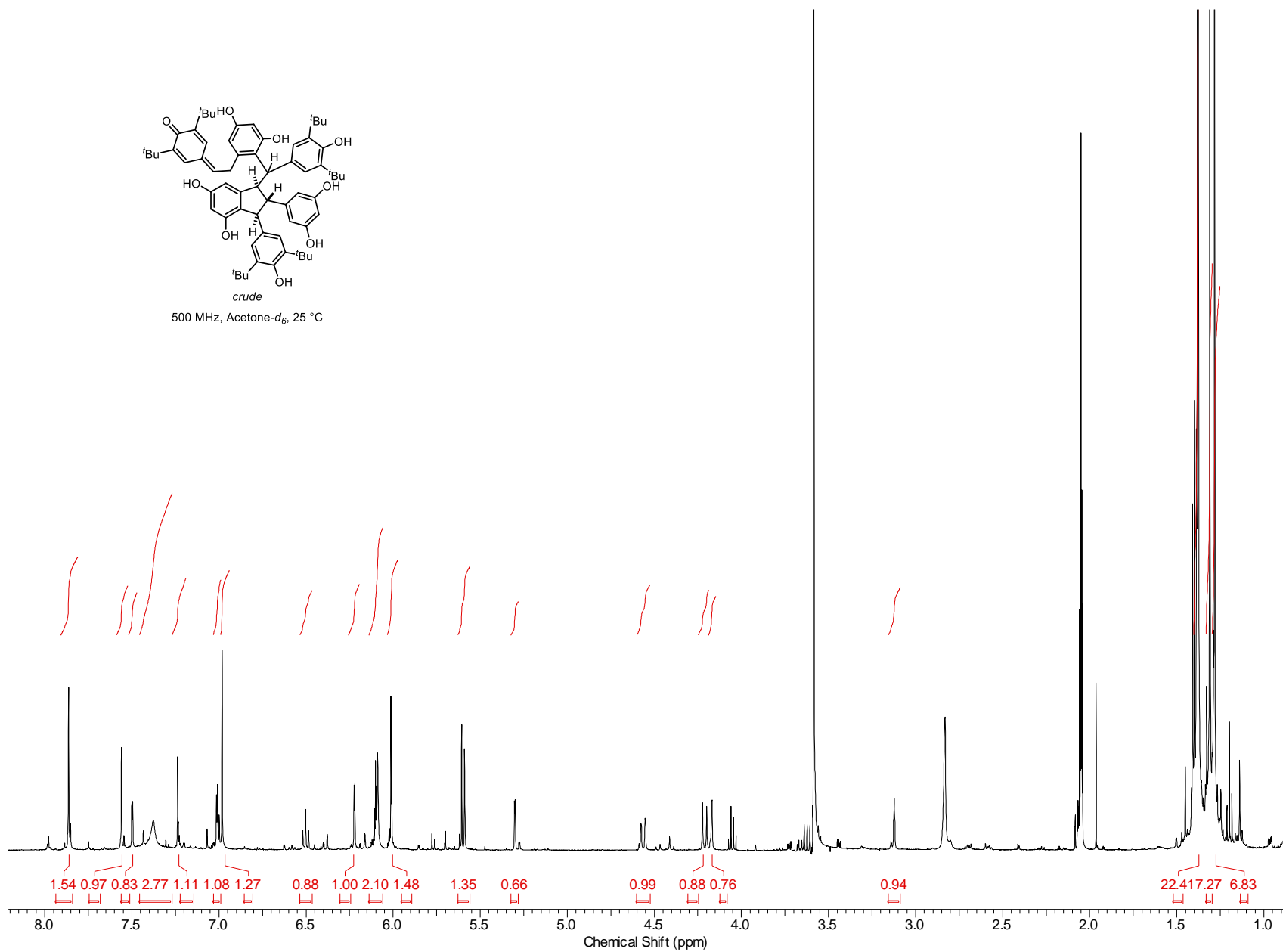
369

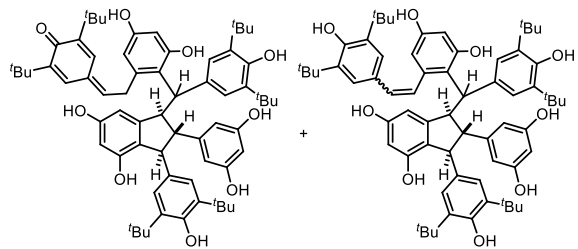
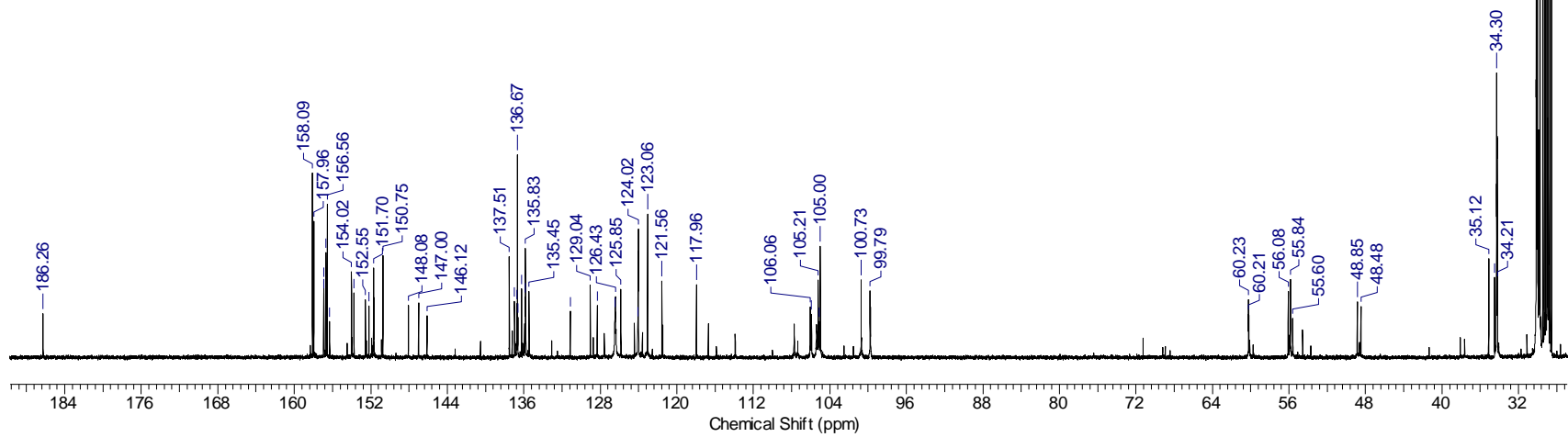


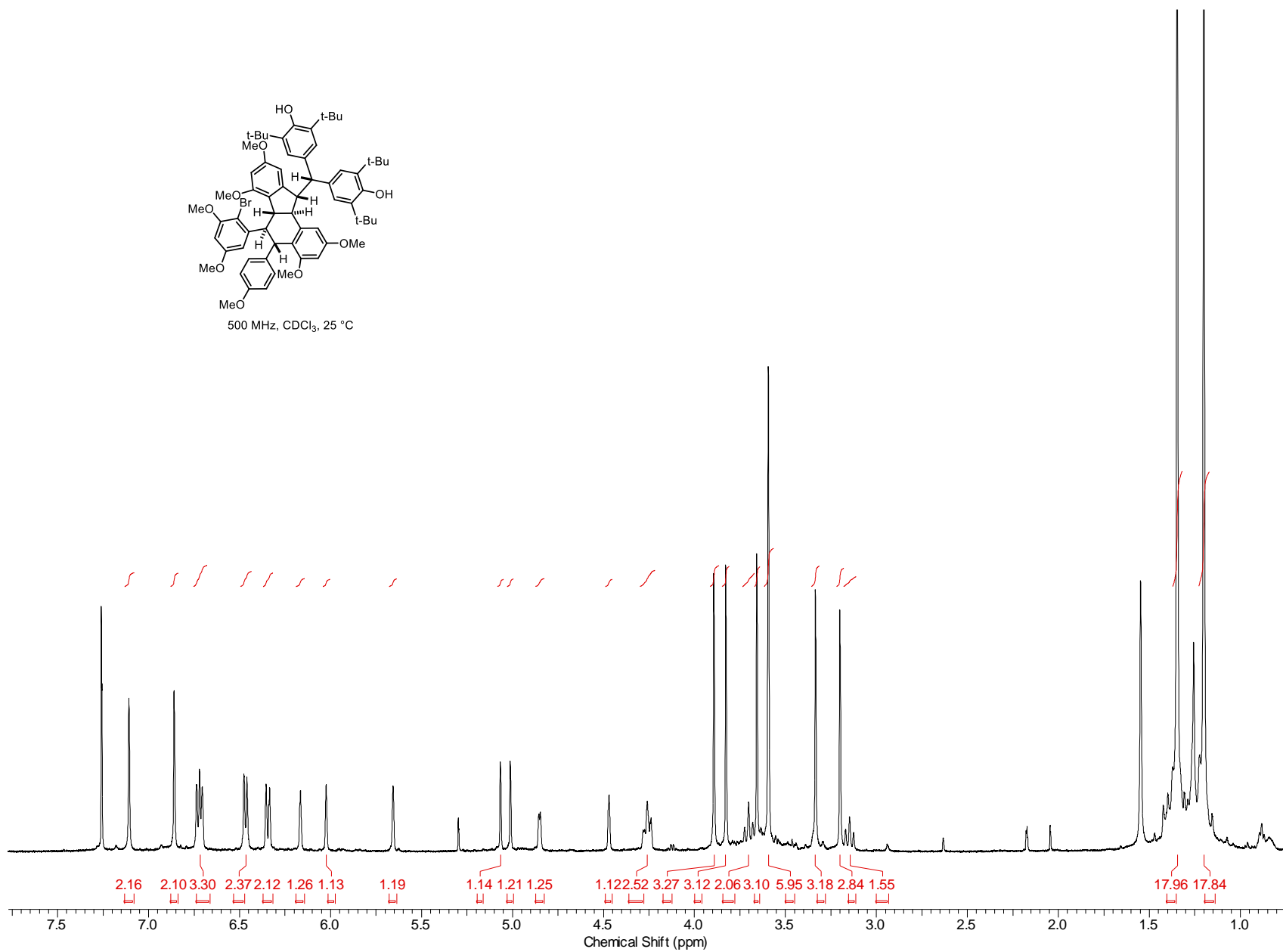
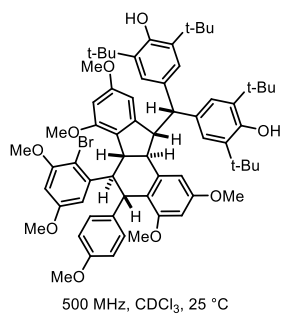


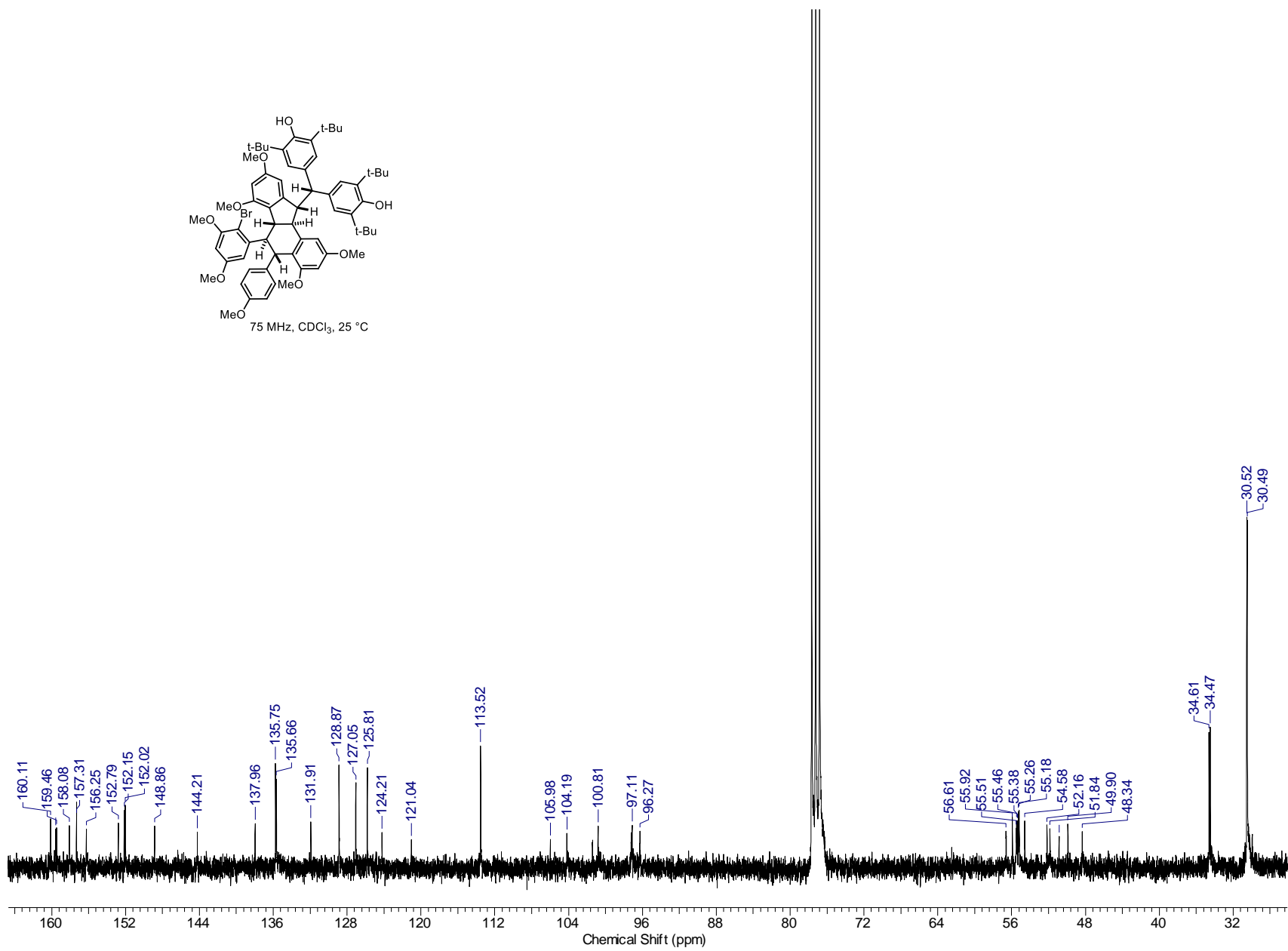
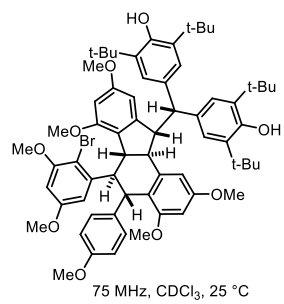
500 MHz, Acetone- d_6 , 25 °C

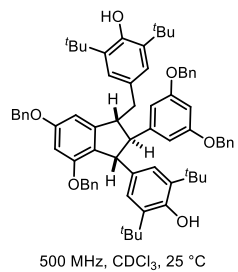
370



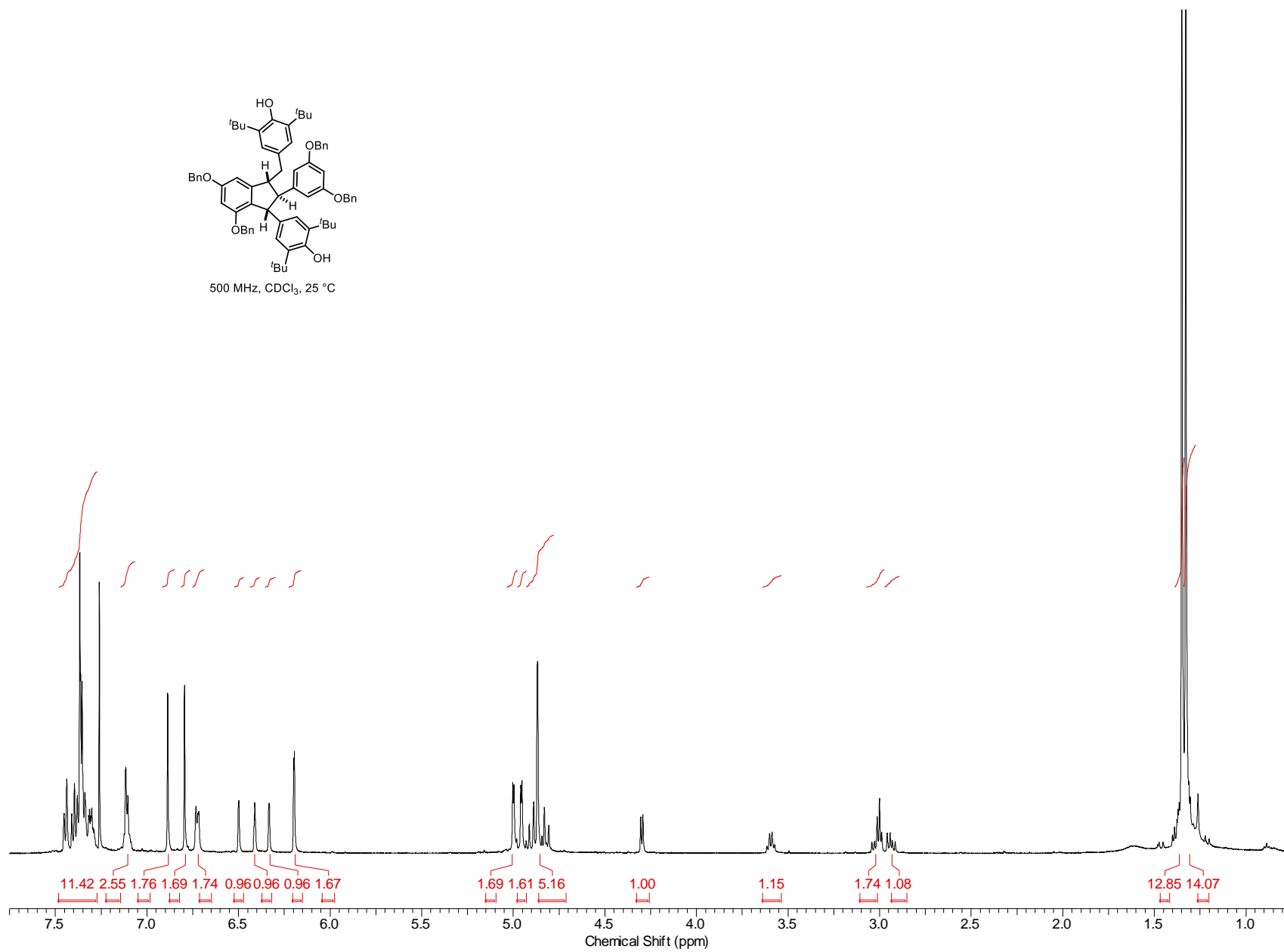
125 MHz, Acetone- d_6 , 25 °C

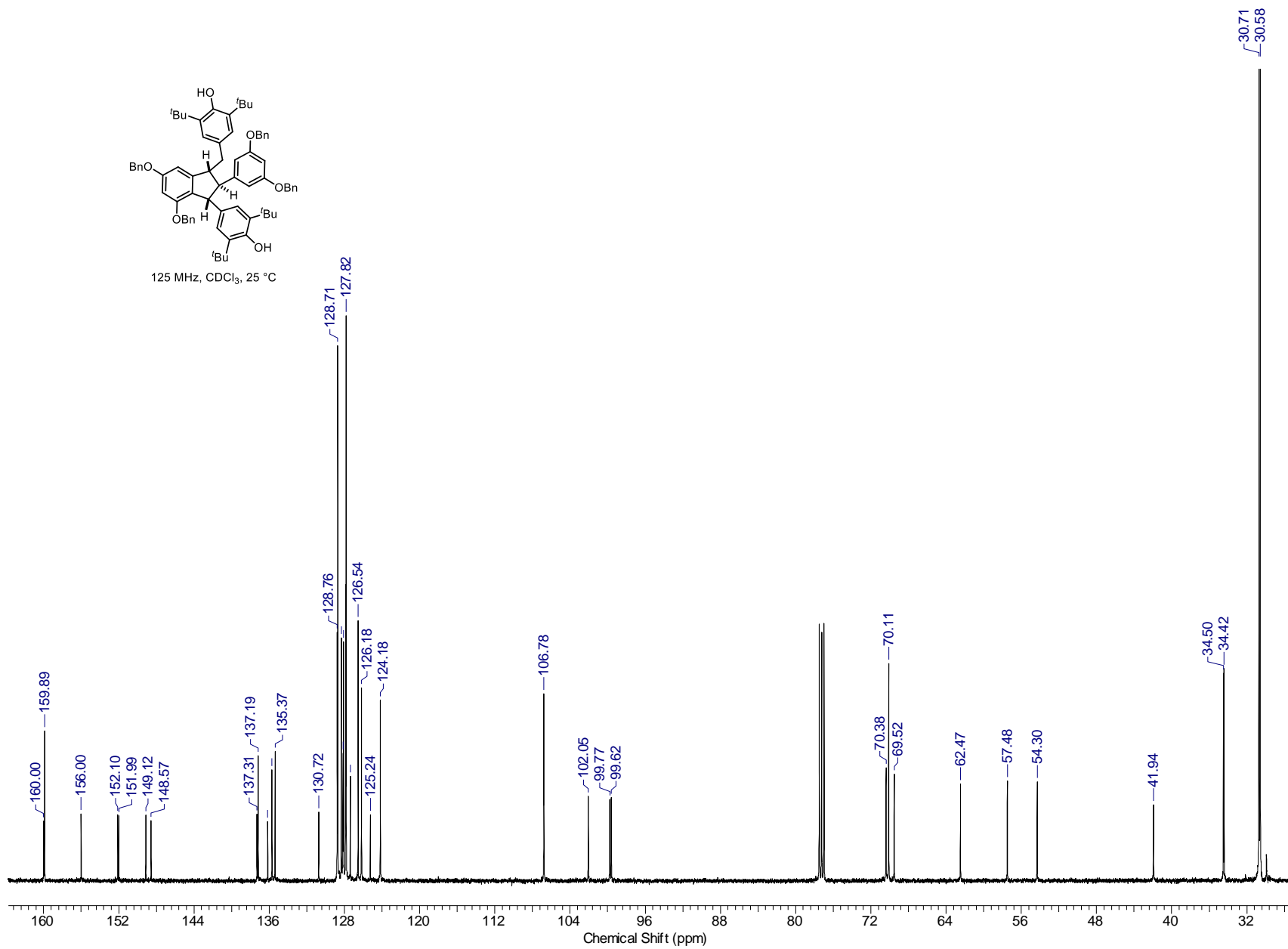
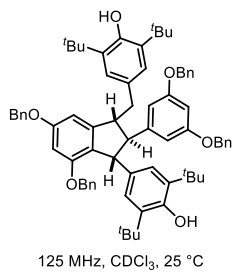


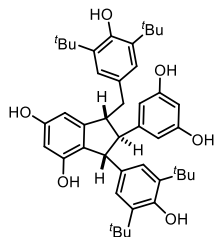




374

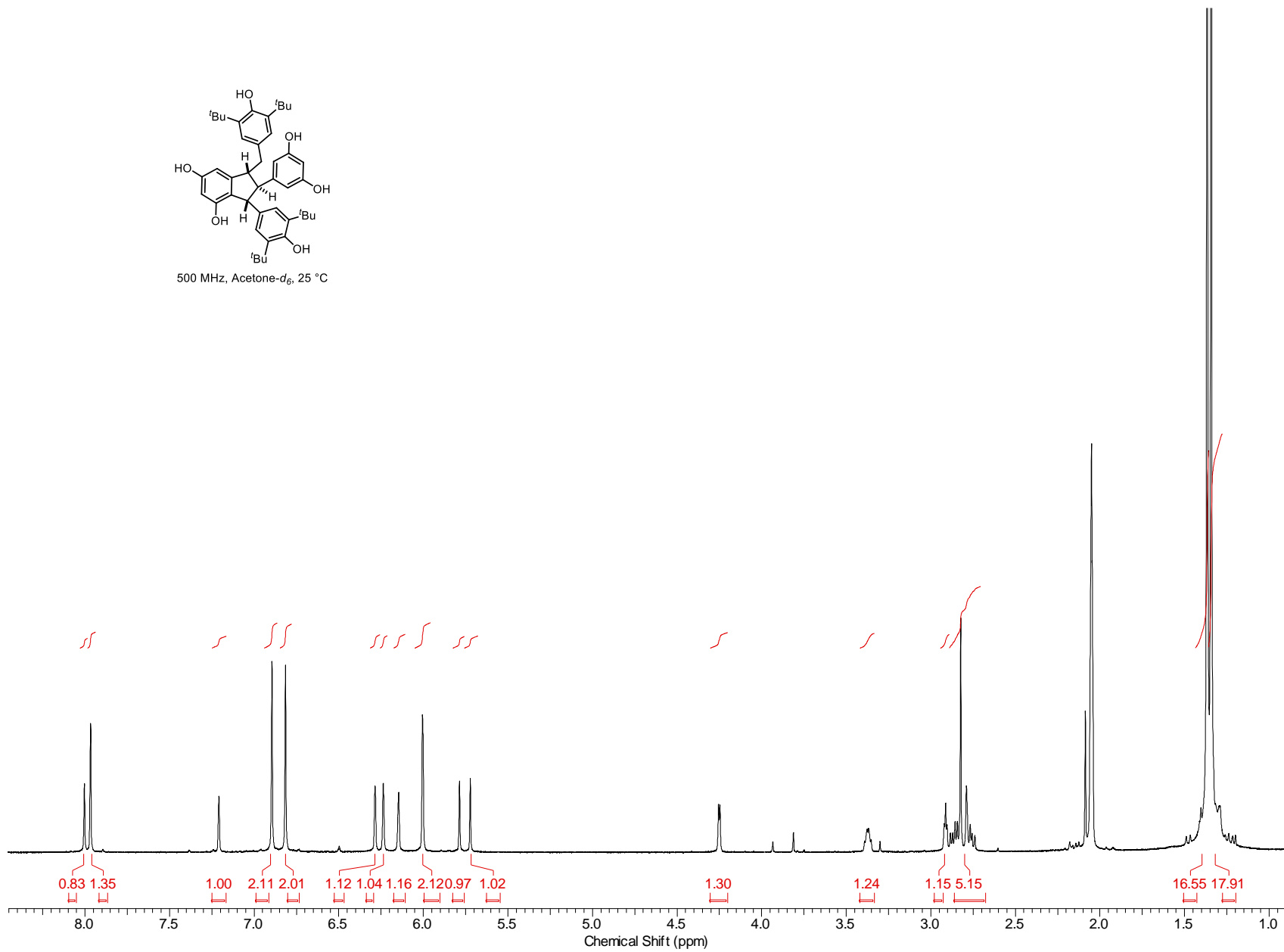


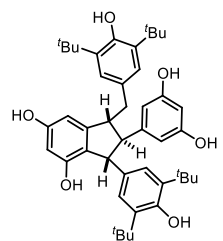




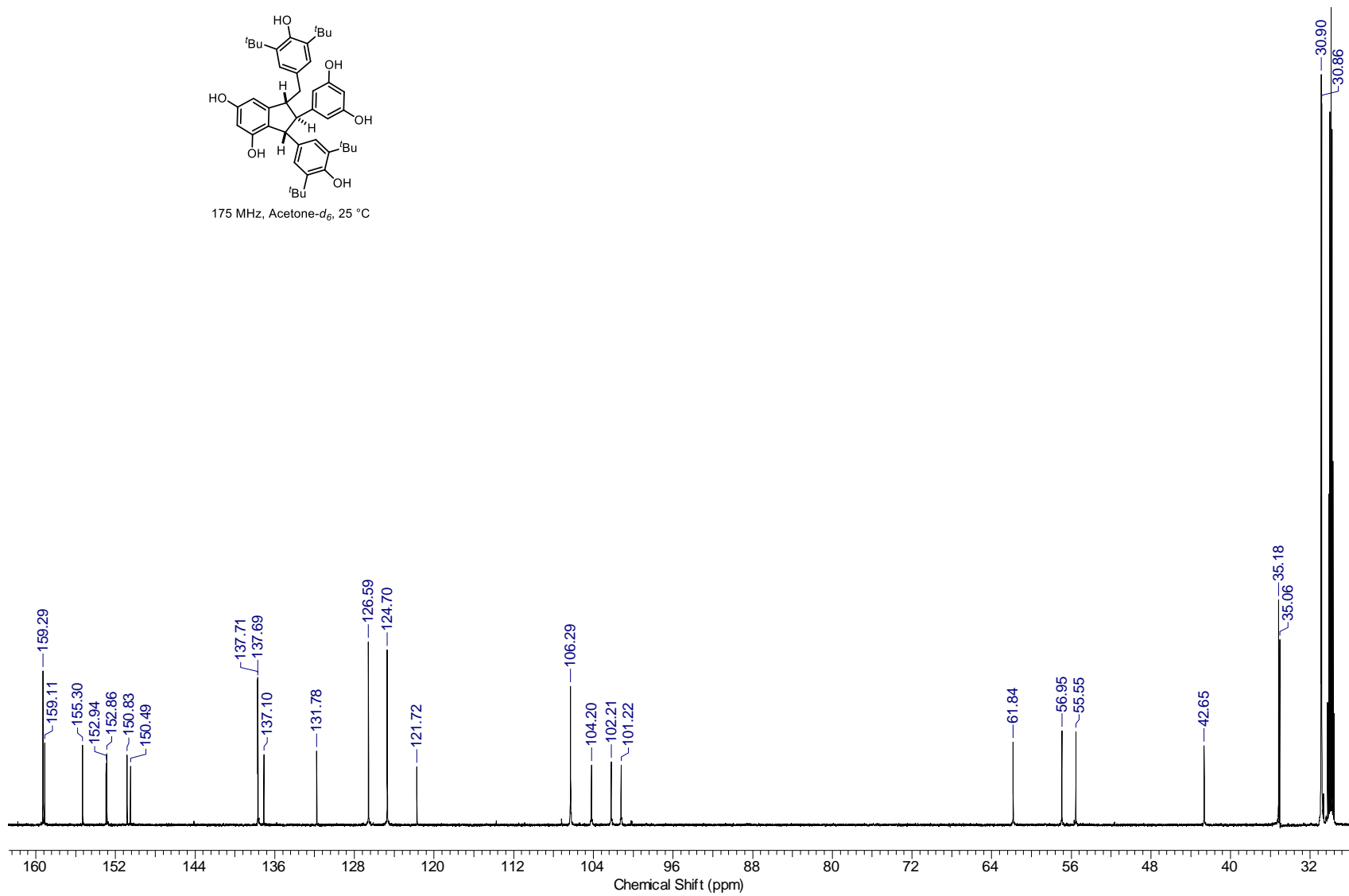
500 MHz, Acetone-d₆, 25 °C

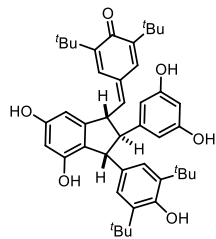
376





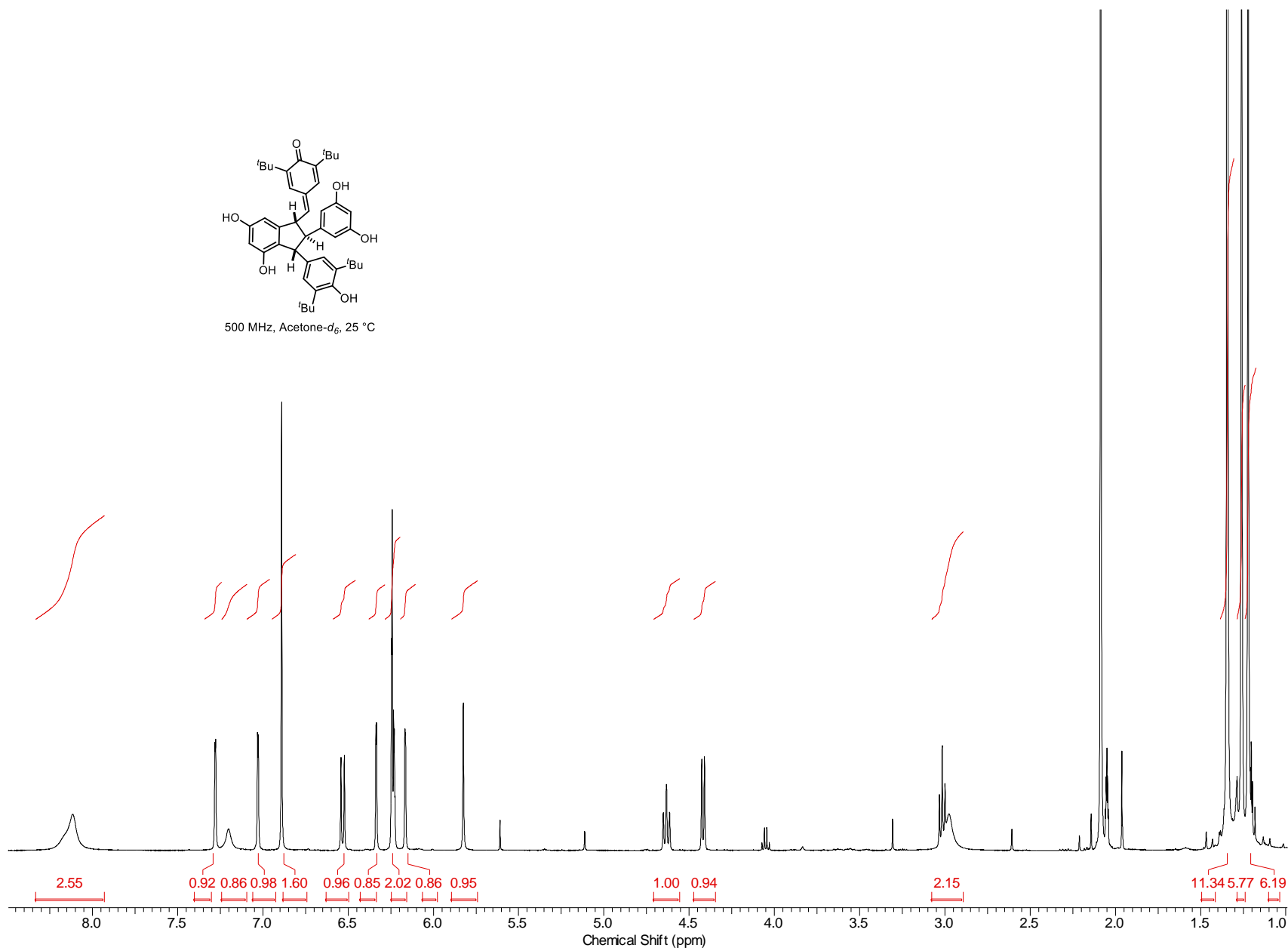
175 MHz, Acetone- d_6 , 25 °C

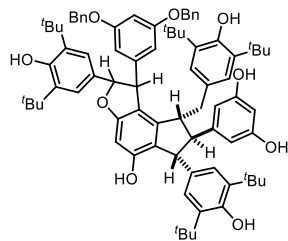




500 MHz, Acetone- d_6 , 25 °C

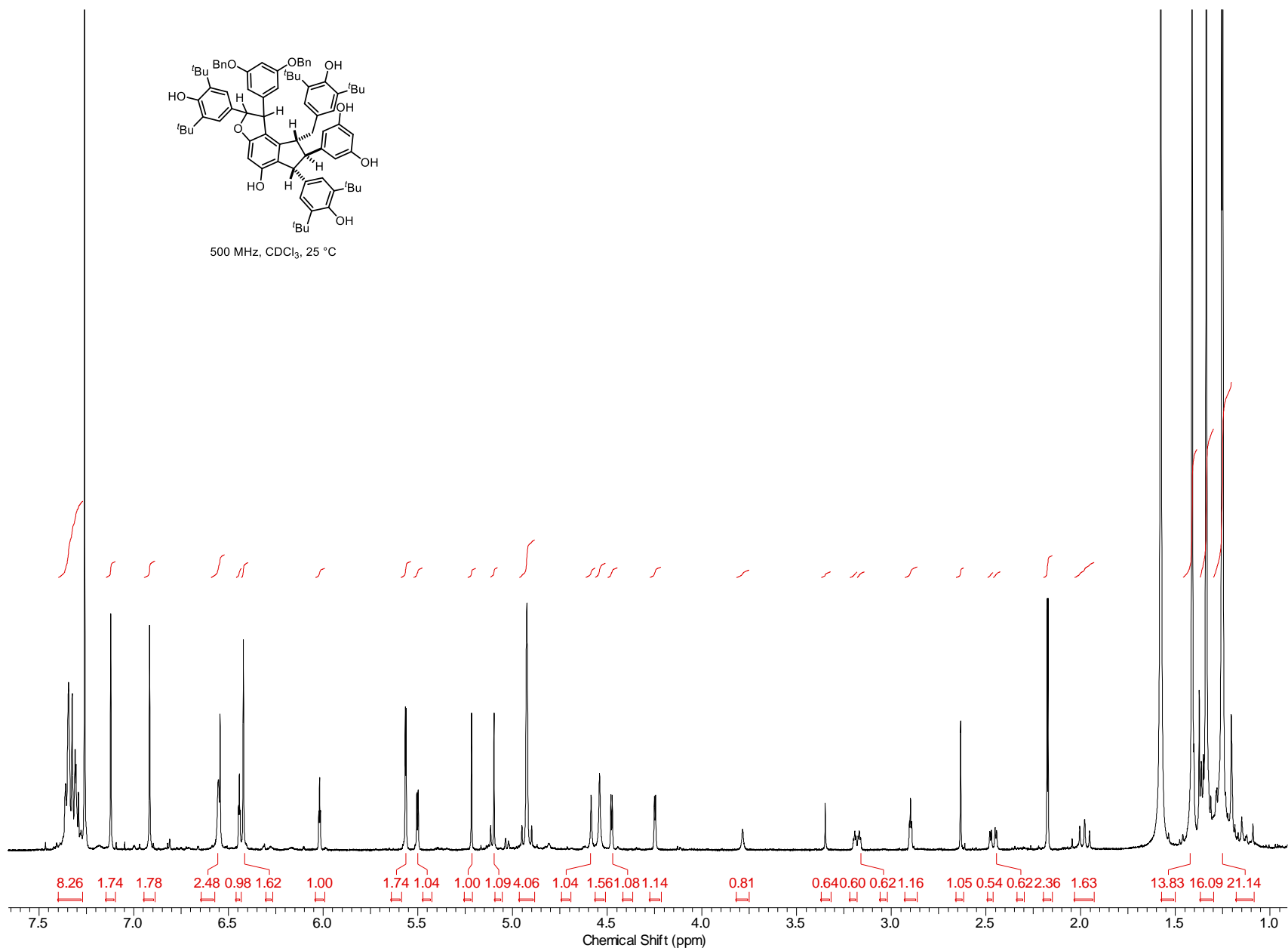
378

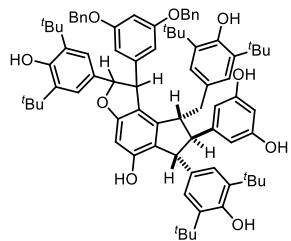
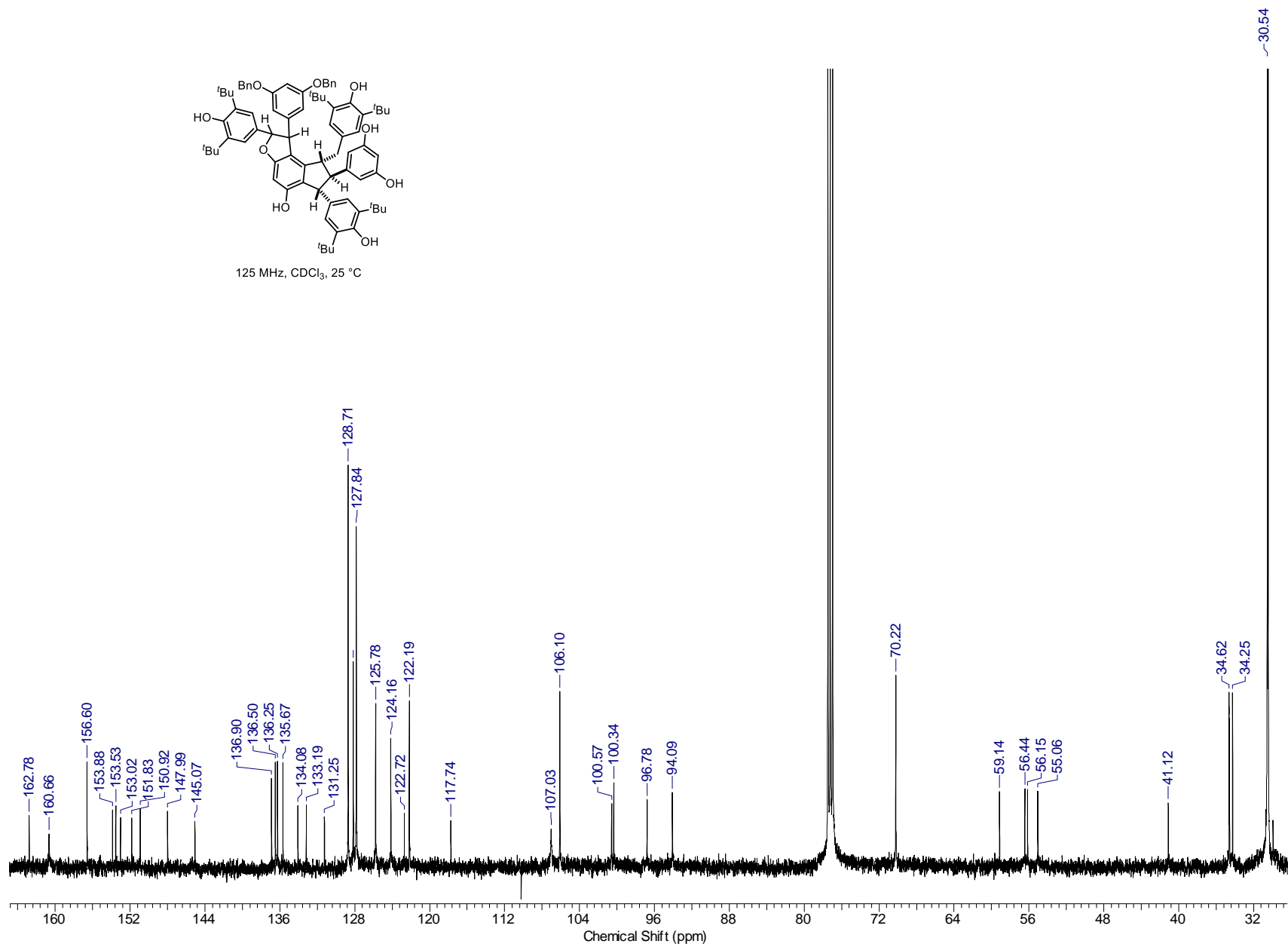




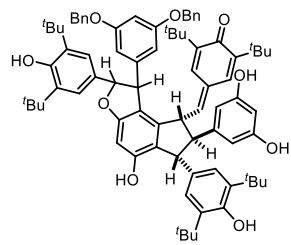
500 MHz, CDCl₃, 25 °C

379

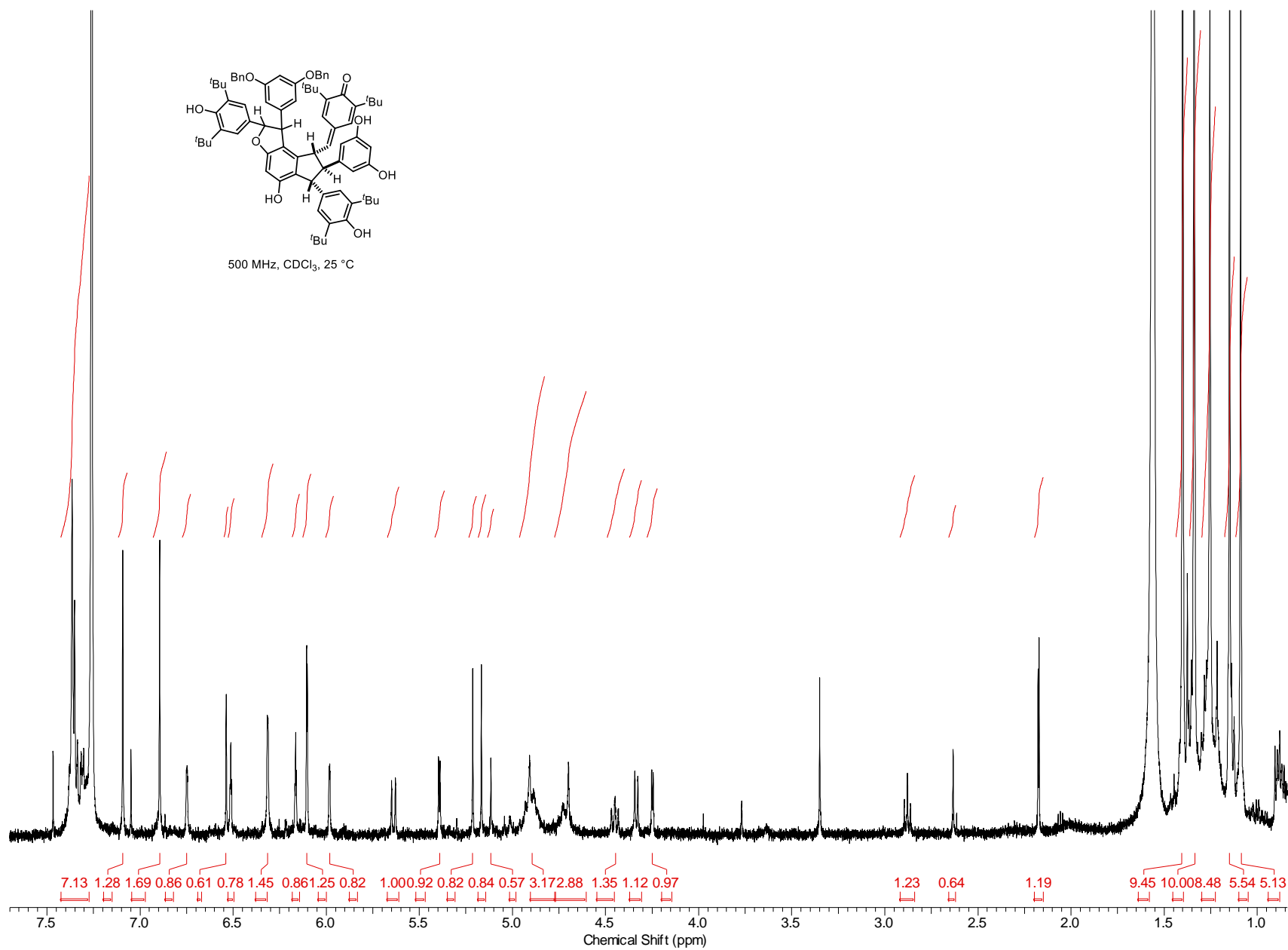


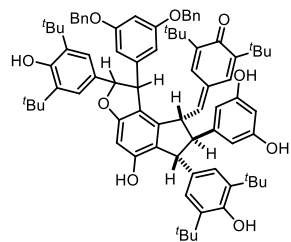
125 MHz, CDCl₃, 25 °C

381

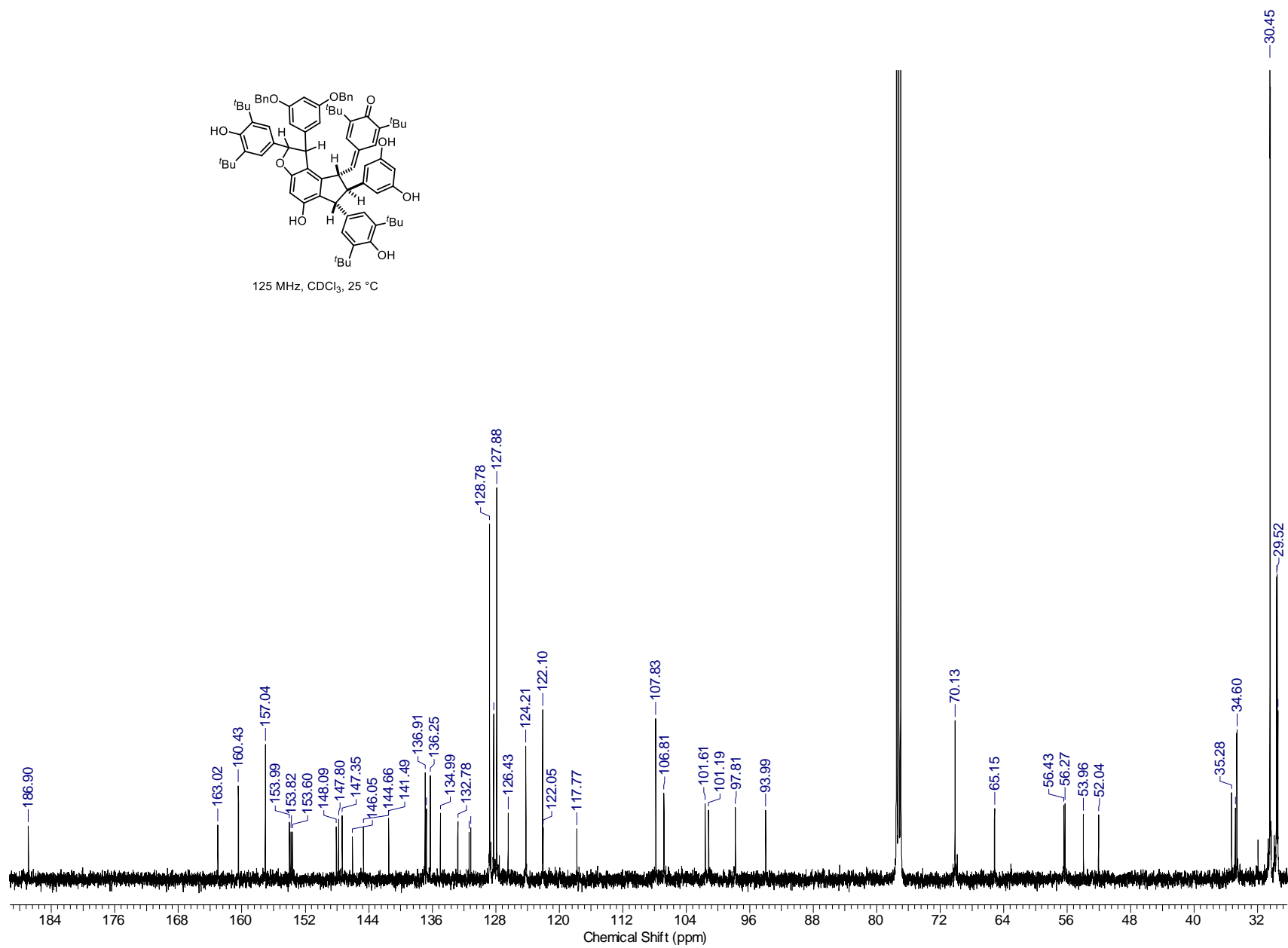


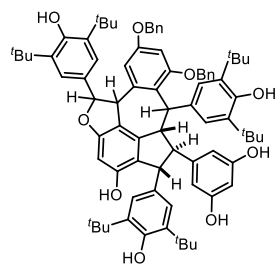
500 MHz, CDCl₃, 25 °C





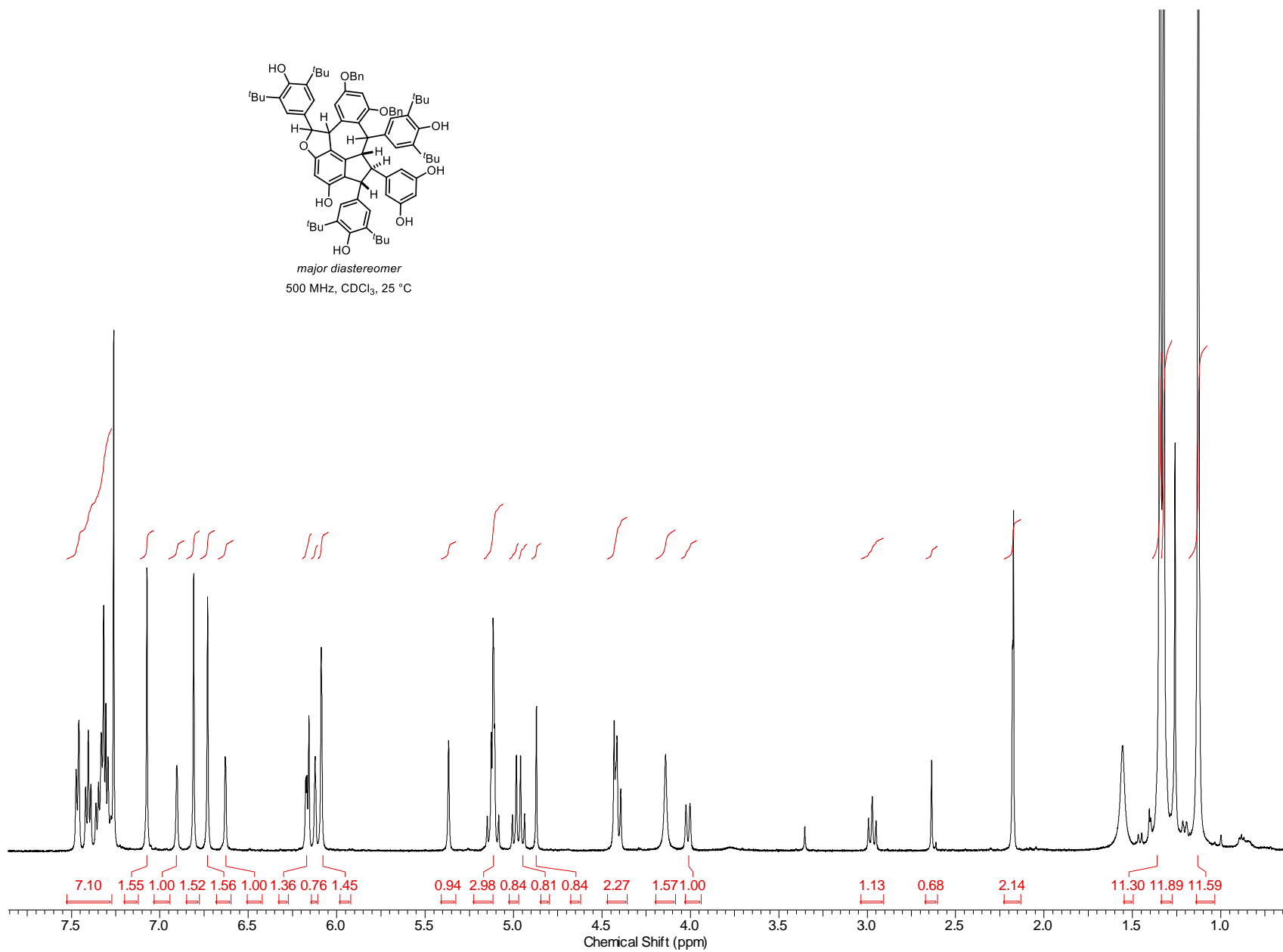
125 MHz, CDCl₃, 25 °C

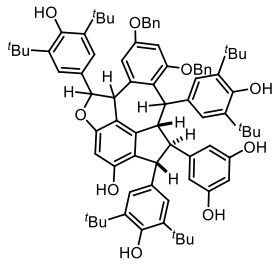




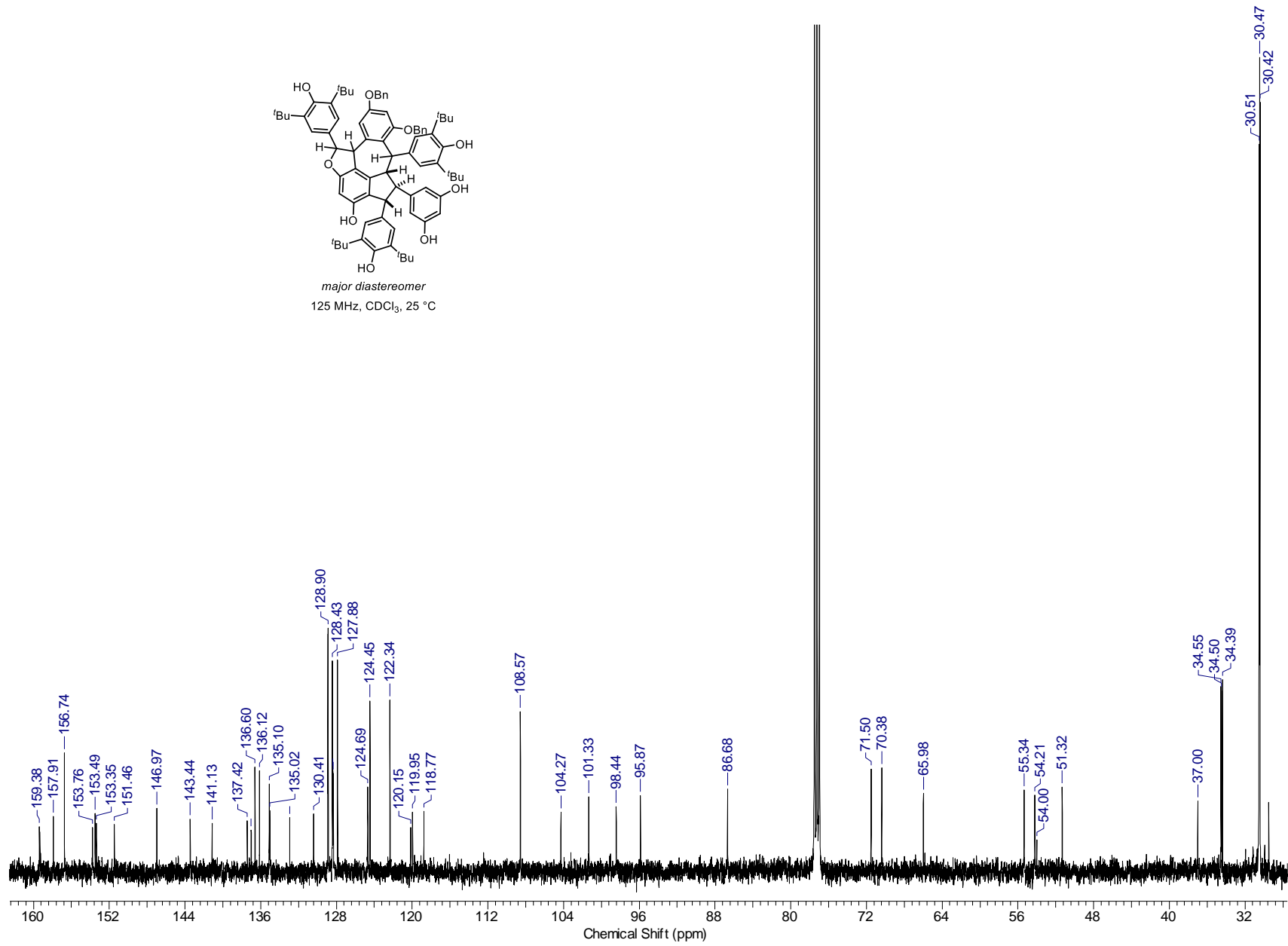
major diastereomer
500 MHz, CDCl₃, 25 °C

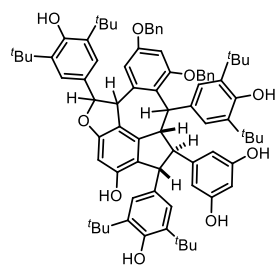
383





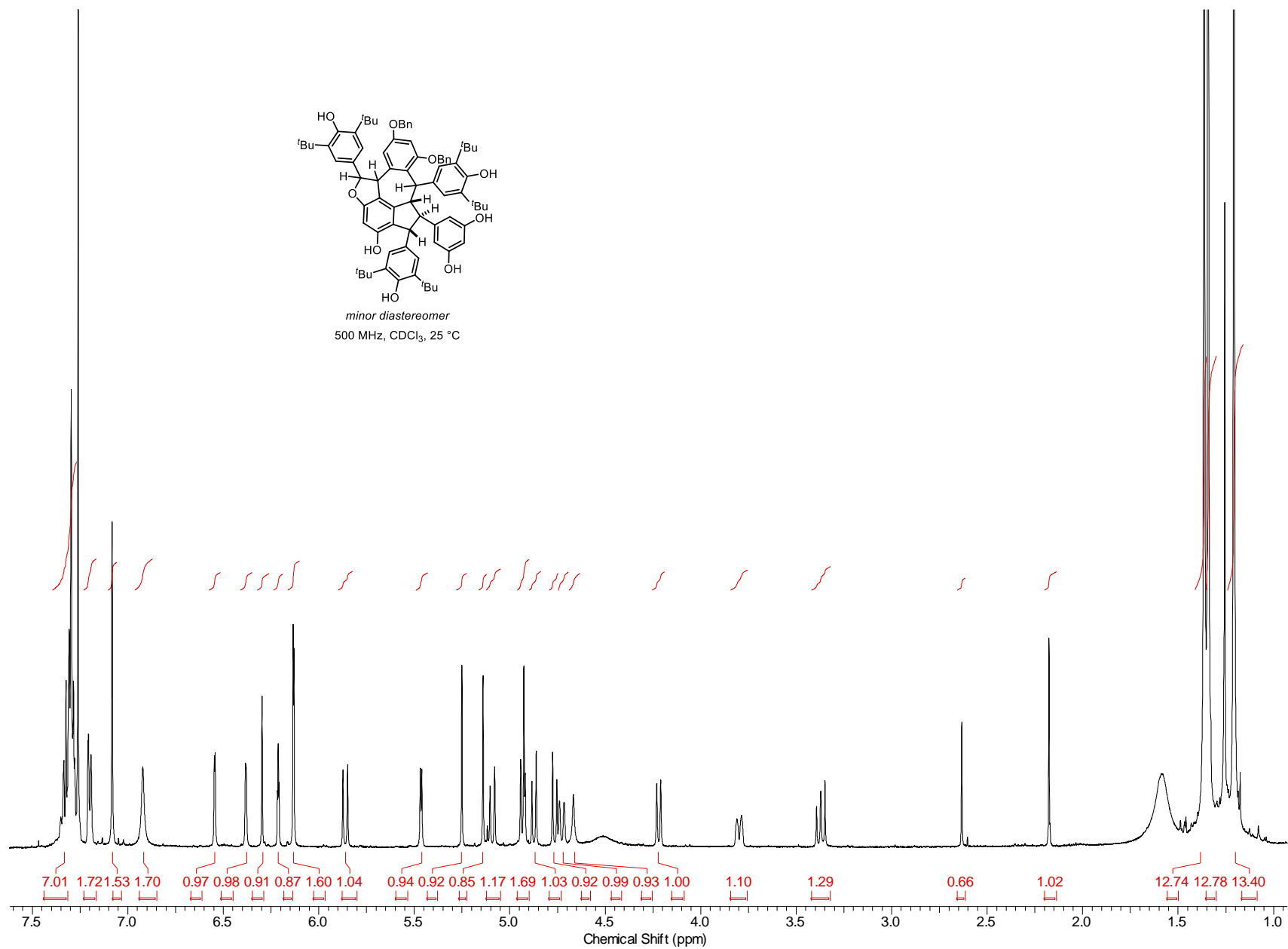
major diastereomer
125 MHz, CDCl₃, 25 °C

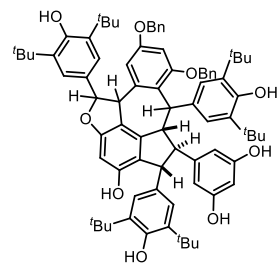




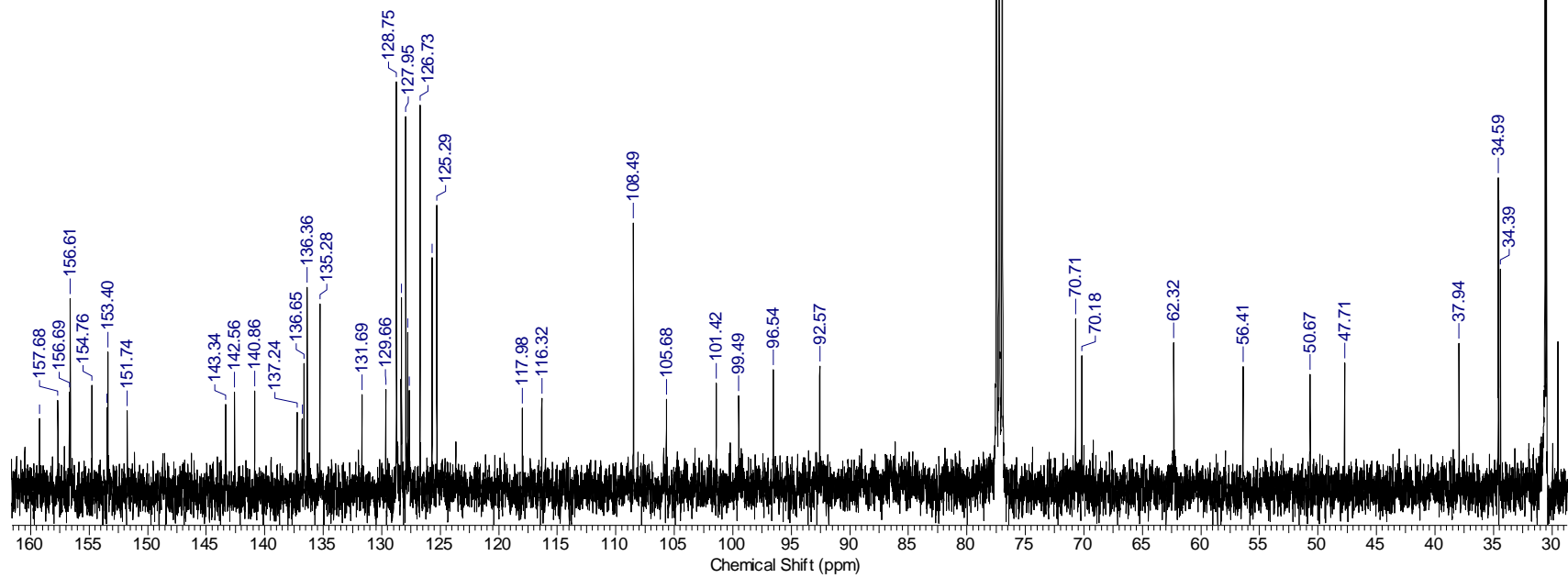
minor diastereomer
500 MHz, CDCl₃, 25 °C

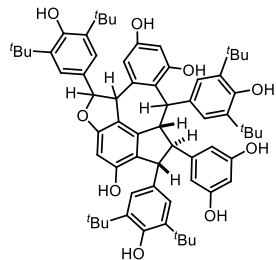
385





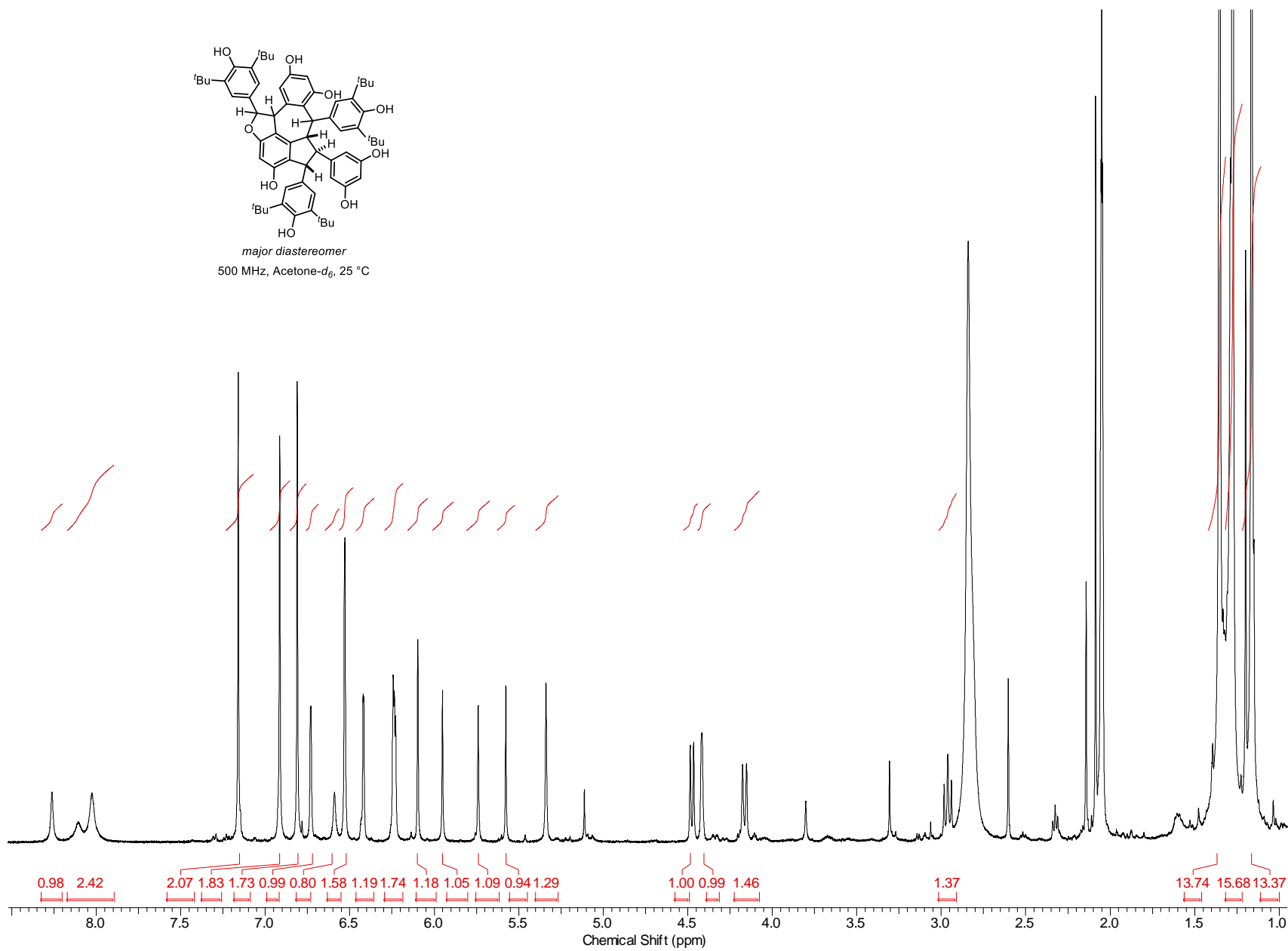
minor diastereomer
125 MHz, CDCl₃, 25 °C

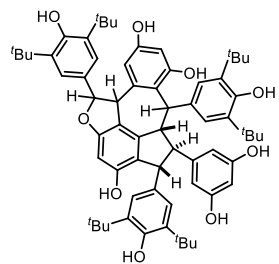




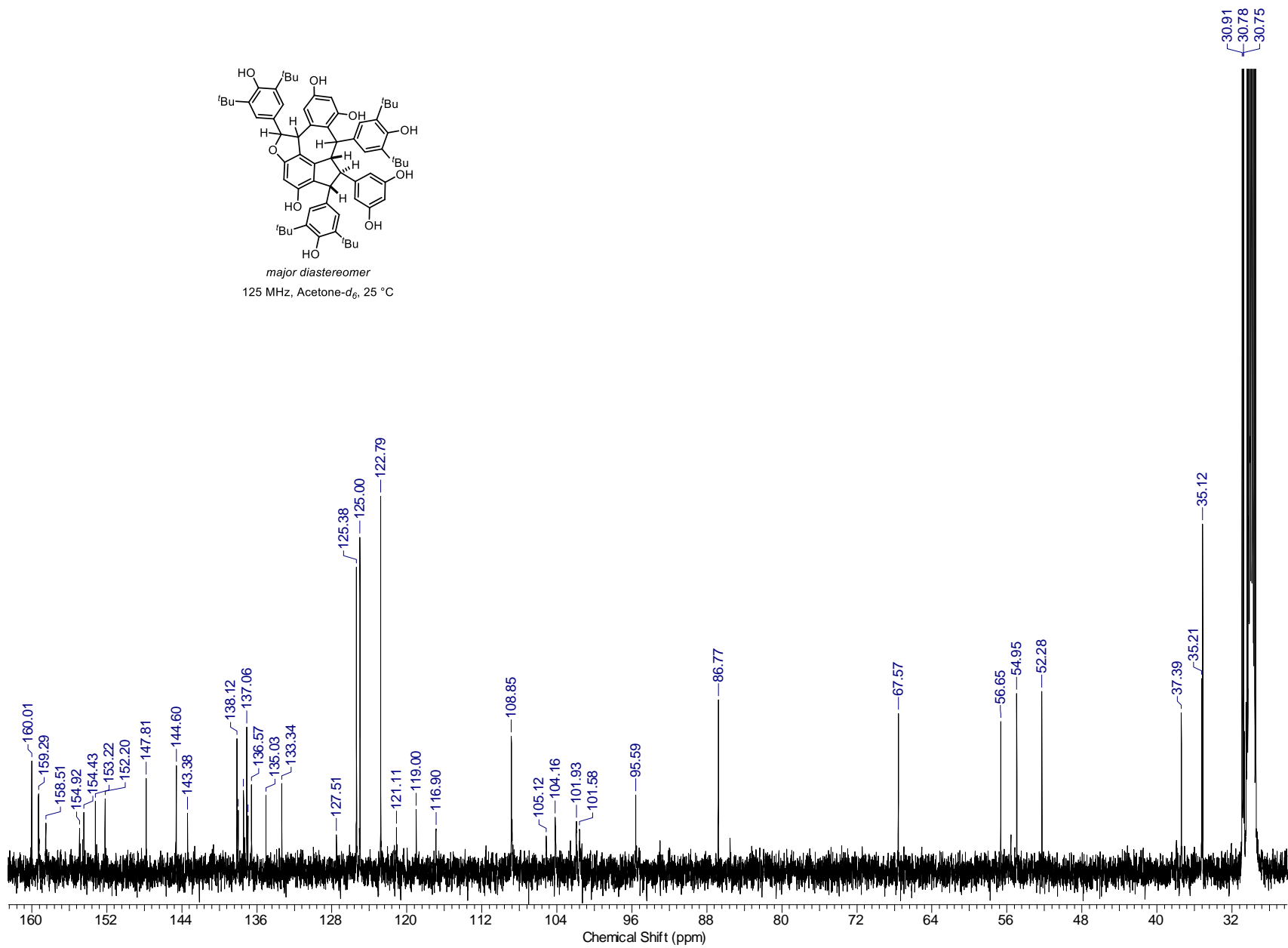
major diastereomer
500 MHz, Acetone- d_6 , 25 °C

387





major diastereomer
125 MHz, Acetone- d_6 , 25 °C



**APPENDIX A:
X-RAY CRYSTALLOGRAPHIC DATA**

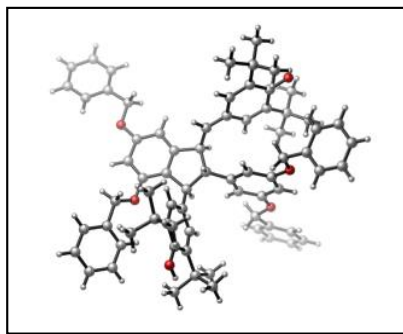
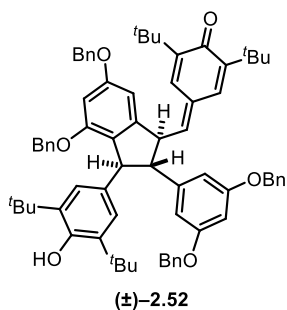


Table A.1 Crystal Data and Structural Refinement for 2.52

Empirical Formula	C ₇₂ H ₇₈ O ₆
Formula Weight	1039.34
Temperature	85(2) K
Wavelength	1.54178 Å
Crystal System	Triclinic
Space Group	P-1
Unit Cell Dimensions	a = 10.3118(2) Å α = 93.895(7)° b = 15.2757(3) Å β = 103.590(7)° c = 18.4170(13) Å γ = 93.108(7)°
Volume	2805.9(2) Å ³
Z	2
Calculated Density	1.230 Mg/m ³
Absorption Coefficient	0.595 mm ⁻¹
F (000)	1116
Crystal Size	0.150 x 0.050 x 0.010 mm
Theta Range for Data Collection	2.477 to 68.211°
Limiting Indices	-12 ≤ h ≤ 12, -18 ≤ k ≤ 18, -19 ≤ l ≤ 21
Reflections Collected	43095
Independent Reflections	10082 [R(int) = 0.0627]
Completeness to Theta	98.2%
Absorption Correction	Semi-empirical from equivalents
Max and Min Transmission	0.994 to 0.751
Refinement Method	Full-matrix least-squares on F ²
Data / Restraints / Parameters	10082 / 0 / 720
Goodness-of-Fit on F ²	1.11
Final R Indices [I > 2σ(I)]	R1 = 0.0587, wR2 = 0.1598
R Indices (all data)	R1 = 0.0679, wR2 = 0.1675
Largest Difference Peak and Hole	0.512 and -0.406 (e Å ⁻³)

Table A.2 Atomic coordinates ($\times 10^4$) and equivalent isotropic displacement parameters ($\text{\AA}^2 \times 10^3$) for 2.52

U(eq) is defined as one third of the trace of the orthogonalized Uij tensor				
	x	y	z	U(eq)
O(1)	3771(1)	5162(1)	5537(1)	29(1)
O(2)	7675(1)	6293(1)	7226(1)	28(1)
O(3)	6619(2)	7065(1)	9871(1)	33(1)
O(4)	3791(2)	408(1)	8977(1)	29(1)
O(5)	5582(1)	331(1)	6834(1)	24(1)
O(6)	9708(2)	1284(1)	5396(1)	31(1)
C(1)	6169(2)	3213(1)	7398(1)	20(1)
C(2)	5775(2)	2328(1)	6909(1)	19(1)
C(3)	5401(2)	1728(1)	7462(1)	19(1)
C(4)	5235(2)	809(1)	7416(1)	22(1)
C(5)	4704(2)	399(1)	7940(1)	25(1)
C(6)	4346(2)	894(1)	8516(1)	24(1)
C(7)	4545(2)	1808(1)	8591(1)	22(1)
C(8)	5079(2)	2202(1)	8060(1)	20(1)
C(9)	5364(2)	3185(1)	8025(1)	19(1)
C(10)	6021(2)	4053(1)	7007(1)	21(1)
C(11)	4924(2)	4159(1)	6416(1)	22(1)
C(12)	4800(2)	4971(1)	6113(1)	24(1)
C(13)	5735(2)	5673(1)	6394(1)	24(1)
C(14)	6812(2)	5558(1)	6981(1)	23(1)
C(15)	6969(2)	4752(1)	7290(1)	22(1)
C(16)	2814(2)	4471(1)	5176(1)	27(1)
C(17)	1753(2)	4845(1)	4595(1)	26(1)
C(18)	526(2)	4372(1)	4341(1)	30(1)
C(19)	-499(2)	4681(1)	3811(1)	33(1)
C(20)	-305(2)	5488(1)	3532(1)	31(1)
C(21)	920(2)	5967(1)	3783(1)	31(1)
C(22)	1944(2)	5644(1)	4305(1)	28(1)
C(23)	8840(2)	6200(1)	7814(1)	28(1)
C(24)	9614(2)	7081(1)	7973(1)	27(1)
C(25)	10324(2)	7376(1)	7478(1)	28(1)
C(26)	10993(2)	8200(1)	7601(1)	31(1)
C(27)	10985(2)	8733(1)	8231(1)	33(1)
C(28)	10288(2)	8444(1)	8738(1)	34(1)
C(29)	9594(2)	7620(1)	8604(1)	32(1)
C(30)	6193(2)	3635(1)	8744(1)	21(1)
C(31)	6251(2)	4494(1)	9011(1)	20(1)

C(32)	5394(2)	5132(1)	8647(1)	21(1)
C(33)	5482(2)	5986(1)	8909(1)	21(1)
C(34)	6513(2)	6286(1)	9606(1)	24(1)
C(35)	7422(2)	5643(1)	9986(1)	22(1)
C(36)	7249(2)	4803(1)	9690(1)	22(1)
C(37)	4553(2)	6653(1)	8514(1)	24(1)
C(38)	3568(2)	6218(1)	7811(1)	28(1)
C(39)	5370(2)	7404(1)	8276(1)	31(1)
C(40)	3726(2)	7022(1)	9047(1)	28(1)
C(41)	8494(2)	5959(1)	10702(1)	24(1)
C(42)	9452(2)	6690(1)	10544(1)	28(1)
C(43)	7822(2)	6296(1)	11319(1)	29(1)
C(44)	9338(2)	5205(1)	11001(1)	28(1)
C(45)	3401(2)	861(1)	9585(1)	28(1)
C(46)	2864(2)	182(1)	10018(1)	29(1)
C(47)	2143(3)	446(2)	10526(2)	38(1)
C(48)	1637(3)	-162(2)	10934(2)	40(1)
C(49)	1857(2)	-1034(2)	10842(1)	36(1)
C(50)	2586(2)	-1303(2)	10343(1)	36(1)
C(51)	3094(2)	-699(1)	9933(1)	32(1)
C(52)	6535(3)	-292(2)	7070(1)	46(1)
C(53)	6854(2)	-800(1)	6416(1)	29(1)
C(54)	7433(2)	-1598(1)	6539(1)	31(1)
C(55)	7752(2)	-2092(1)	5955(1)	31(1)
C(56)	7500(2)	-1793(1)	5243(1)	35(1)
C(57)	6940(3)	-993(1)	5125(2)	37(1)
C(58)	6622(2)	-498(1)	5712(1)	30(1)
C(59)	6833(2)	2057(1)	6512(1)	20(1)
C(60)	8056(2)	1790(1)	6896(1)	21(1)
C(61)	9039(2)	1538(1)	6532(1)	22(1)
C(62)	8741(2)	1565(1)	5746(1)	23(1)
C(63)	7541(2)	1865(1)	5337(1)	22(1)
C(64)	6604(2)	2097(1)	5741(1)	22(1)
C(65)	10388(2)	1246(1)	6963(1)	25(1)
C(66)	10494(2)	1287(2)	7809(1)	29(1)
C(67)	10556(2)	287(2)	6711(1)	36(1)
C(68)	11549(2)	1854(2)	6847(1)	34(1)
C(69)	7253(2)	1938(1)	4486(1)	26(1)
C(70)	7072(2)	1016(1)	4066(1)	29(1)
C(71)	8366(2)	2512(2)	4282(1)	34(1)
C(72)	5963(2)	2390(1)	4207(1)	30(1)

Table A.3 Bond Lengths [Å] and Angles [°] for 2.52

O(1)-C(12)	1.373(2)
O(1)-C(16)	1.419(2)
O(2)-C(14)	1.375(2)
O(2)-C(23)	1.436(2)
O(3)-C(34)	1.245(2)
O(4)-C(6)	1.368(2)
O(4)-C(45)	1.424(2)
O(5)-C(4)	1.381(2)
O(5)-C(52)	1.421(3)
O(6)-C(62)	1.379(2)
O(6)-H(6)	0.88(4)
C(1)-C(10)	1.512(3)
C(1)-C(2)	1.552(3)
C(1)-C(9)	1.573(3)
C(1)-H(1)	1
C(2)-C(59)	1.510(3)
C(2)-C(3)	1.516(3)
C(2)-H(2)	1
C(3)-C(8)	1.391(3)
C(3)-C(4)	1.400(3)
C(4)-C(5)	1.385(3)
C(5)-C(6)	1.392(3)
C(5)-H(5)	0.95
C(6)-C(7)	1.392(3)
C(7)-C(8)	1.386(3)
C(7)-H(7)	0.95
C(8)-C(9)	1.523(2)
C(9)-C(30)	1.496(3)
C(9)-H(9)	1
C(10)-C(15)	1.394(3)
C(10)-C(11)	1.399(3)
C(11)-C(12)	1.395(3)
C(11)-H(11)	0.95
C(12)-C(13)	1.388(3)
C(13)-C(14)	1.385(3)
C(13)-H(13)	0.95
C(14)-C(15)	1.391(3)
C(15)-H(15)	0.95
C(16)-C(17)	1.506(3)
C(16)-H(16A)	0.99

C(16)-H(16B)	0.99
C(17)-C(18)	1.385(3)
C(17)-C(22)	1.387(3)
C(18)-C(19)	1.387(3)
C(18)-H(18)	0.95
C(19)-C(20)	1.389(3)
C(19)-H(19)	0.95
C(20)-C(21)	1.387(3)
C(20)-H(20)	0.95
C(21)-C(22)	1.389(3)
C(21)-H(21)	0.95
C(22)-H(22)	0.95
C(23)-C(24)	1.501(3)
C(23)-H(23A)	0.99
C(23)-H(23B)	0.99
C(24)-C(25)	1.381(3)
C(24)-C(29)	1.383(3)
C(25)-C(26)	1.380(3)
C(25)-H(25)	0.95
C(26)-C(27)	1.374(3)
C(26)-H(26)	0.95
C(27)-C(28)	1.386(3)
C(27)-H(27)	0.95
C(28)-C(29)	1.390(3)
C(28)-H(28)	0.95
C(29)-H(29)	0.95
C(30)-C(31)	1.363(3)
C(30)-H(30)	0.95
C(31)-C(32)	1.444(3)
C(31)-C(36)	1.451(3)
C(32)-C(33)	1.349(3)
C(32)-H(32)	0.95
C(33)-C(34)	1.488(3)
C(33)-C(37)	1.538(3)
C(34)-C(35)	1.489(3)
C(35)-C(36)	1.346(3)
C(35)-C(41)	1.537(3)
C(36)-H(36)	0.95
C(37)-C(38)	1.531(3)
C(37)-C(39)	1.535(3)
C(37)-C(40)	1.543(3)

C(38)-H(38A)	0.98
C(38)-H(38B)	0.98
C(38)-H(38C)	0.98
C(39)-H(39A)	0.98
C(39)-H(39B)	0.98
C(39)-H(39C)	0.98
C(40)-H(40A)	0.98
C(40)-H(40B)	0.98
C(40)-H(40C)	0.98
C(41)-C(44)	1.536(3)
C(41)-C(43)	1.538(3)
C(41)-C(42)	1.538(3)
C(42)-H(42A)	0.98
C(42)-H(42B)	0.98
C(42)-H(42C)	0.98
C(43)-H(43A)	0.98
C(43)-H(43B)	0.98
C(43)-H(43C)	0.98
C(44)-H(44A)	0.98
C(44)-H(44B)	0.98
C(44)-H(44C)	0.98
C(45)-C(46)	1.510(3)
C(45)-H(45A)	0.99
C(45)-H(45B)	0.99
C(46)-C(47)	1.377(3)
C(46)-C(51)	1.384(3)
C(47)-C(48)	1.389(3)
C(47)-H(47)	0.95
C(48)-C(49)	1.370(3)
C(48)-H(48)	0.95
C(49)-C(50)	1.373(3)
C(49)-H(49)	0.95
C(50)-C(51)	1.388(3)
C(50)-H(50)	0.95
C(51)-H(51)	0.95
C(52)-C(53)	1.499(3)
C(52)-H(52A)	0.99
C(52)-H(52B)	0.99
C(53)-C(58)	1.378(3)
C(53)-C(54)	1.396(3)
C(54)-C(55)	1.386(3)

C(54)-H(54)	0.95
C(55)-C(56)	1.389(4)
C(55)-H(55)	0.95
C(56)-C(57)	1.389(3)
C(56)-H(56)	0.95
C(57)-C(58)	1.390(3)
C(57)-H(57)	0.95
C(58)-H(58)	0.95
C(59)-C(64)	1.389(3)
C(59)-C(60)	1.390(3)
C(60)-C(61)	1.398(3)
C(60)-H(60)	0.95
C(61)-C(62)	1.412(3)
C(61)-C(65)	1.537(3)
C(62)-C(63)	1.407(3)
C(63)-C(64)	1.397(3)
C(63)-C(69)	1.538(3)
C(64)-H(64)	0.95
C(65)-C(66)	1.532(3)
C(65)-C(67)	1.537(3)
C(65)-C(68)	1.540(3)
C(66)-H(66A)	0.98
C(66)-H(66B)	0.98
C(66)-H(66C)	0.98
C(67)-H(67A)	0.98
C(67)-H(67B)	0.98
C(67)-H(67C)	0.98
C(68)-H(68A)	0.98
C(68)-H(68B)	0.98
C(68)-H(68C)	0.98
C(69)-C(72)	1.528(3)
C(69)-C(71)	1.538(3)
C(69)-C(70)	1.540(3)
C(70)-H(70A)	0.98
C(70)-H(70B)	0.98
C(70)-H(70C)	0.98
C(71)-H(71A)	0.98
C(71)-H(71B)	0.98
C(71)-H(71C)	0.98
C(72)-H(72A)	0.98
C(72)-H(72B)	0.98

C(72)-H(72C)	0.98
C(12)-O(1)-C(16)	118.34(15)
C(14)-O(2)-C(23)	117.08(15)
C(6)-O(4)-C(45)	118.11(15)
C(4)-O(5)-C(52)	114.11(16)
C(62)-O(6)-H(6)	104(2)
C(10)-C(1)-C(2)	117.79(16)
C(10)-C(1)-C(9)	112.37(15)
C(2)-C(1)-C(9)	105.93(15)
C(10)-C(1)-H(1)	106.7
C(2)-C(1)-H(1)	106.7
C(9)-C(1)-H(1)	106.7
C(59)-C(2)-C(3)	118.36(15)
C(59)-C(2)-C(1)	112.96(15)
C(3)-C(2)-C(1)	101.79(15)
C(59)-C(2)-H(2)	107.7
C(3)-C(2)-H(2)	107.7
C(1)-C(2)-H(2)	107.7
C(8)-C(3)-C(4)	118.43(18)
C(8)-C(3)-C(2)	111.76(15)
C(4)-C(3)-C(2)	129.56(17)
O(5)-C(4)-C(5)	121.48(17)
O(5)-C(4)-C(3)	118.87(17)
C(5)-C(4)-C(3)	119.64(18)
C(4)-C(5)-C(6)	120.44(18)
C(4)-C(5)-H(5)	119.8
C(6)-C(5)-H(5)	119.8
O(4)-C(6)-C(7)	124.61(18)
O(4)-C(6)-C(5)	114.31(17)
C(7)-C(6)-C(5)	121.08(19)
C(8)-C(7)-C(6)	117.35(18)
C(8)-C(7)-H(7)	121.3
C(6)-C(7)-H(7)	121.3
C(7)-C(8)-C(3)	122.97(17)
C(7)-C(8)-C(9)	126.42(17)
C(3)-C(8)-C(9)	110.59(16)
C(30)-C(9)-C(8)	113.50(16)
C(30)-C(9)-C(1)	109.84(15)
C(8)-C(9)-C(1)	102.62(14)
C(30)-C(9)-H(9)	110.2

C(8)-C(9)-H(9)	110.2
C(1)-C(9)-H(9)	110.2
C(15)-C(10)-C(11)	120.25(17)
C(15)-C(10)-C(1)	117.67(17)
C(11)-C(10)-C(1)	121.92(17)
C(12)-C(11)-C(10)	119.03(18)
C(12)-C(11)-H(11)	120.5
C(10)-C(11)-H(11)	120.5
O(1)-C(12)-C(13)	114.05(17)
O(1)-C(12)-C(11)	124.80(18)
C(13)-C(12)-C(11)	121.14(19)
C(14)-C(13)-C(12)	119.05(18)
C(14)-C(13)-H(13)	120.5
C(12)-C(13)-H(13)	120.5
O(2)-C(14)-C(13)	114.77(17)
O(2)-C(14)-C(15)	124.15(18)
C(13)-C(14)-C(15)	121.08(18)
C(14)-C(15)-C(10)	119.44(18)
C(14)-C(15)-H(15)	120.3
C(10)-C(15)-H(15)	120.3
O(1)-C(16)-C(17)	108.73(16)
O(1)-C(16)-H(16A)	109.9
C(17)-C(16)-H(16A)	109.9
O(1)-C(16)-H(16B)	109.9
C(17)-C(16)-H(16B)	109.9
H(16A)-C(16)-H(16B)	108.3
C(18)-C(17)-C(22)	118.45(19)
C(18)-C(17)-C(16)	118.50(18)
C(22)-C(17)-C(16)	123.05(19)
C(17)-C(18)-C(19)	121.5(2)
C(17)-C(18)-H(18)	119.3
C(19)-C(18)-H(18)	119.3
C(18)-C(19)-C(20)	119.7(2)
C(18)-C(19)-H(19)	120.1
C(20)-C(19)-H(19)	120.1
C(21)-C(20)-C(19)	119.3(2)
C(21)-C(20)-H(20)	120.3
C(19)-C(20)-H(20)	120.3
C(20)-C(21)-C(22)	120.4(2)
C(20)-C(21)-H(21)	119.8
C(22)-C(21)-H(21)	119.8

C(17)-C(22)-C(21)	120.6(2)
C(17)-C(22)-H(22)	119.7
C(21)-C(22)-H(22)	119.7
O(2)-C(23)-C(24)	106.80(16)
O(2)-C(23)-H(23A)	110.4
C(24)-C(23)-H(23A)	110.4
O(2)-C(23)-H(23B)	110.4
C(24)-C(23)-H(23B)	110.4
H(23A)-C(23)-H(23B)	108.6
C(25)-C(24)-C(29)	118.94(19)
C(25)-C(24)-C(23)	120.3(2)
C(29)-C(24)-C(23)	120.7(2)
C(26)-C(25)-C(24)	120.9(2)
C(26)-C(25)-H(25)	119.6
C(24)-C(25)-H(25)	119.6
C(27)-C(26)-C(25)	120.2(2)
C(27)-C(26)-H(26)	119.9
C(25)-C(26)-H(26)	119.9
C(26)-C(27)-C(28)	119.6(2)
C(26)-C(27)-H(27)	120.2
C(28)-C(27)-H(27)	120.2
C(27)-C(28)-C(29)	119.9(2)
C(27)-C(28)-H(28)	120
C(29)-C(28)-H(28)	120
C(24)-C(29)-C(28)	120.4(2)
C(24)-C(29)-H(29)	119.8
C(28)-C(29)-H(29)	119.8
C(31)-C(30)-C(9)	129.04(18)
C(31)-C(30)-H(30)	115.5
C(9)-C(30)-H(30)	115.5
C(30)-C(31)-C(32)	123.76(18)
C(30)-C(31)-C(36)	118.91(17)
C(32)-C(31)-C(36)	117.31(16)
C(33)-C(32)-C(31)	123.13(18)
C(33)-C(32)-H(32)	118.4
C(31)-C(32)-H(32)	118.4
C(32)-C(33)-C(34)	118.56(17)
C(32)-C(33)-C(37)	122.30(18)
C(34)-C(33)-C(37)	119.14(16)
O(3)-C(34)-C(33)	120.61(17)
O(3)-C(34)-C(35)	120.07(18)

C(33)-C(34)-C(35)	119.32(16)
C(36)-C(35)-C(34)	118.02(18)
C(36)-C(35)-C(41)	122.89(17)
C(34)-C(35)-C(41)	119.08(16)
C(35)-C(36)-C(31)	123.64(18)
C(35)-C(36)-H(36)	118.2
C(31)-C(36)-H(36)	118.2
C(38)-C(37)-C(39)	107.94(17)
C(38)-C(37)-C(33)	111.15(15)
C(39)-C(37)-C(33)	110.53(16)
C(38)-C(37)-C(40)	107.53(17)
C(39)-C(37)-C(40)	110.21(16)
C(33)-C(37)-C(40)	109.42(17)
C(37)-C(38)-H(38A)	109.5
C(37)-C(38)-H(38B)	109.5
H(38A)-C(38)-H(38B)	109.5
C(37)-C(38)-H(38C)	109.5
H(38A)-C(38)-H(38C)	109.5
H(38B)-C(38)-H(38C)	109.5
C(37)-C(39)-H(39A)	109.5
C(37)-C(39)-H(39B)	109.5
H(39A)-C(39)-H(39B)	109.5
C(37)-C(39)-H(39C)	109.5
H(39A)-C(39)-H(39C)	109.5
H(39B)-C(39)-H(39C)	109.5
C(37)-C(40)-H(40A)	109.5
C(37)-C(40)-H(40B)	109.5
H(40A)-C(40)-H(40B)	109.5
C(37)-C(40)-H(40C)	109.5
H(40A)-C(40)-H(40C)	109.5
H(40B)-C(40)-H(40C)	109.5
C(44)-C(41)-C(35)	111.13(16)
C(44)-C(41)-C(43)	107.49(17)
C(35)-C(41)-C(43)	109.92(16)
C(44)-C(41)-C(42)	107.50(16)
C(35)-C(41)-C(42)	110.61(17)
C(43)-C(41)-C(42)	110.12(16)
C(41)-C(42)-H(42A)	109.5
C(41)-C(42)-H(42B)	109.5
H(42A)-C(42)-H(42B)	109.5
C(41)-C(42)-H(42C)	109.5

H(42A)-C(42)-H(42C)	109.5
H(42B)-C(42)-H(42C)	109.5
C(41)-C(43)-H(43A)	109.5
C(41)-C(43)-H(43B)	109.5
H(43A)-C(43)-H(43B)	109.5
C(41)-C(43)-H(43C)	109.5
H(43A)-C(43)-H(43C)	109.5
H(43B)-C(43)-H(43C)	109.5
C(41)-C(44)-H(44A)	109.5
C(41)-C(44)-H(44B)	109.5
H(44A)-C(44)-H(44B)	109.5
C(41)-C(44)-H(44C)	109.5
H(44A)-C(44)-H(44C)	109.5
H(44B)-C(44)-H(44C)	109.5
O(4)-C(45)-C(46)	107.81(16)
O(4)-C(45)-H(45A)	110.1
C(46)-C(45)-H(45A)	110.1
O(4)-C(45)-H(45B)	110.1
C(46)-C(45)-H(45B)	110.1
H(45A)-C(45)-H(45B)	108.5
C(47)-C(46)-C(51)	118.8(2)
C(47)-C(46)-C(45)	119.20(19)
C(51)-C(46)-C(45)	122.0(2)
C(46)-C(47)-C(48)	120.6(2)
C(46)-C(47)-H(47)	119.7
C(48)-C(47)-H(47)	119.7
C(49)-C(48)-C(47)	120.3(2)
C(49)-C(48)-H(48)	119.8
C(47)-C(48)-H(48)	119.8
C(48)-C(49)-C(50)	119.5(2)
C(48)-C(49)-H(49)	120.3
C(50)-C(49)-H(49)	120.3
C(49)-C(50)-C(51)	120.5(2)
C(49)-C(50)-H(50)	119.8
C(51)-C(50)-H(50)	119.8
C(46)-C(51)-C(50)	120.3(2)
C(46)-C(51)-H(51)	119.8
C(50)-C(51)-H(51)	119.8
O(5)-C(52)-C(53)	111.7(2)
O(5)-C(52)-H(52A)	109.3
C(53)-C(52)-H(52A)	109.3

O(5)-C(52)-H(52B)	109.3
C(53)-C(52)-H(52B)	109.3
H(52A)-C(52)-H(52B)	108
C(58)-C(53)-C(54)	119.6(2)
C(58)-C(53)-C(52)	122.49(19)
C(54)-C(53)-C(52)	117.9(2)
C(55)-C(54)-C(53)	120.3(2)
C(55)-C(54)-H(54)	119.8
C(53)-C(54)-H(54)	119.8
C(54)-C(55)-C(56)	120.0(2)
C(54)-C(55)-H(55)	120
C(56)-C(55)-H(55)	120
C(55)-C(56)-C(57)	119.5(2)
C(55)-C(56)-H(56)	120.2
C(57)-C(56)-H(56)	120.2
C(56)-C(57)-C(58)	120.3(2)
C(56)-C(57)-H(57)	119.8
C(58)-C(57)-H(57)	119.8
C(53)-C(58)-C(57)	120.2(2)
C(53)-C(58)-H(58)	119.9
C(57)-C(58)-H(58)	119.9
C(64)-C(59)-C(60)	118.41(17)
C(64)-C(59)-C(2)	119.53(17)
C(60)-C(59)-C(2)	122.04(17)
C(59)-C(60)-C(61)	122.35(18)
C(59)-C(60)-H(60)	118.8
C(61)-C(60)-H(60)	118.8
C(60)-C(61)-C(62)	116.95(18)
C(60)-C(61)-C(65)	121.87(18)
C(62)-C(61)-C(65)	121.18(17)
O(6)-C(62)-C(63)	121.43(18)
O(6)-C(62)-C(61)	115.85(17)
C(63)-C(62)-C(61)	122.71(18)
C(64)-C(63)-C(62)	116.74(18)
C(64)-C(63)-C(69)	120.80(17)
C(62)-C(63)-C(69)	122.46(17)
C(59)-C(64)-C(63)	122.75(18)
C(59)-C(64)-H(64)	118.6
C(63)-C(64)-H(64)	118.6
C(66)-C(65)-C(61)	111.76(16)
C(66)-C(65)-C(67)	106.86(17)

C(61)-C(65)-C(67)	110.39(17)
C(66)-C(65)-C(68)	106.89(17)
C(61)-C(65)-C(68)	110.53(17)
C(67)-C(65)-C(68)	110.29(17)
C(65)-C(66)-H(66A)	109.5
C(65)-C(66)-H(66B)	109.5
H(66A)-C(66)-H(66B)	109.5
C(65)-C(66)-H(66C)	109.5
H(66A)-C(66)-H(66C)	109.5
H(66B)-C(66)-H(66C)	109.5
C(65)-C(67)-H(67A)	109.5
C(65)-C(67)-H(67B)	109.5
H(67A)-C(67)-H(67B)	109.5
C(65)-C(67)-H(67C)	109.5
H(67A)-C(67)-H(67C)	109.5
H(67B)-C(67)-H(67C)	109.5
C(65)-C(68)-H(68A)	109.5
C(65)-C(68)-H(68B)	109.5
H(68A)-C(68)-H(68B)	109.5
C(65)-C(68)-H(68C)	109.5
H(68A)-C(68)-H(68C)	109.5
H(68B)-C(68)-H(68C)	109.5
C(72)-C(69)-C(63)	111.11(17)
C(72)-C(69)-C(71)	105.80(17)
C(63)-C(69)-C(71)	110.86(17)
C(72)-C(69)-C(70)	107.29(17)
C(63)-C(69)-C(70)	110.35(17)
C(71)-C(69)-C(70)	111.30(17)
C(69)-C(70)-H(70A)	109.5
C(69)-C(70)-H(70B)	109.5
H(70A)-C(70)-H(70B)	109.5
C(69)-C(70)-H(70C)	109.5
H(70A)-C(70)-H(70C)	109.5
H(70B)-C(70)-H(70C)	109.5
C(69)-C(71)-H(71A)	109.5
C(69)-C(71)-H(71B)	109.5
H(71A)-C(71)-H(71B)	109.5
C(69)-C(71)-H(71C)	109.5
H(71A)-C(71)-H(71C)	109.5
H(71B)-C(71)-H(71C)	109.5
C(69)-C(72)-H(72A)	109.5

C(69)-C(72)-H(72B)	109.5
H(72A)-C(72)-H(72B)	109.5
C(69)-C(72)-H(72C)	109.5
H(72A)-C(72)-H(72C)	109.5
H(72B)-C(72)-H(72C)	109.5

Table A.4 Anisotropic Displacement Parameters ($\text{Å}^2 \times 10^3$) for 2.52

	U11	U22	U33	U23	U13	U12
O(1)	28(1)	25(1)	28(1)	5(1)	-5(1)	1(1)
O(2)	29(1)	20(1)	30(1)	4(1)	0(1)	-3(1)
O(3)	39(1)	20(1)	32(1)	-6(1)	-4(1)	6(1)
O(4)	41(1)	21(1)	29(1)	0(1)	21(1)	-4(1)
O(5)	32(1)	17(1)	25(1)	-2(1)	11(1)	5(1)
O(6)	30(1)	43(1)	24(1)	1(1)	13(1)	10(1)
C(1)	22(1)	18(1)	19(1)	1(1)	5(1)	2(1)
C(2)	22(1)	17(1)	18(1)	0(1)	4(1)	3(1)
C(3)	20(1)	16(1)	20(1)	-1(1)	4(1)	0(1)
C(4)	22(1)	21(1)	21(1)	-2(1)	5(1)	2(1)
C(5)	30(1)	18(1)	28(1)	-1(1)	10(1)	0(1)
C(6)	27(1)	22(1)	25(1)	3(1)	10(1)	-1(1)
C(7)	26(1)	20(1)	22(1)	-1(1)	8(1)	1(1)
C(8)	20(1)	19(1)	20(1)	1(1)	5(1)	2(1)
C(9)	23(1)	17(1)	18(1)	1(1)	7(1)	2(1)
C(10)	23(1)	19(1)	21(1)	1(1)	7(1)	4(1)
C(11)	24(1)	20(1)	22(1)	2(1)	6(1)	3(1)
C(12)	26(1)	24(1)	21(1)	4(1)	5(1)	5(1)
C(13)	29(1)	21(1)	24(1)	5(1)	6(1)	5(1)
C(14)	24(1)	20(1)	25(1)	2(1)	7(1)	1(1)
C(15)	23(1)	20(1)	22(1)	2(1)	4(1)	4(1)
C(16)	30(1)	22(1)	28(1)	1(1)	4(1)	1(1)
C(17)	30(1)	26(1)	21(1)	-1(1)	5(1)	4(1)
C(18)	36(1)	23(1)	28(1)	2(1)	4(1)	2(1)
C(19)	31(1)	30(1)	34(1)	-4(1)	1(1)	0(1)
C(20)	34(1)	33(1)	25(1)	1(1)	3(1)	7(1)
C(21)	35(1)	30(1)	28(1)	4(1)	7(1)	4(1)
C(22)	31(1)	28(1)	23(1)	1(1)	5(1)	2(1)
C(23)	28(1)	25(1)	29(1)	6(1)	1(1)	0(1)
C(24)	28(1)	24(1)	27(1)	6(1)	2(1)	2(1)
C(25)	30(1)	25(1)	28(1)	1(1)	4(1)	2(1)

C(26)	33(1)	28(1)	34(1)	6(1)	9(1)	0(1)
C(27)	35(1)	26(1)	36(1)	3(1)	6(1)	-2(1)
C(28)	39(1)	30(1)	32(1)	-2(1)	8(1)	0(1)
C(29)	36(1)	32(1)	27(1)	5(1)	7(1)	0(1)
C(30)	26(1)	19(1)	18(1)	2(1)	6(1)	3(1)
C(31)	24(1)	19(1)	17(1)	2(1)	5(1)	1(1)
C(32)	23(1)	21(1)	21(1)	1(1)	6(1)	3(1)
C(33)	26(1)	20(1)	19(1)	0(1)	5(1)	4(1)
C(34)	27(1)	20(1)	23(1)	-2(1)	4(1)	2(1)
C(35)	23(1)	21(1)	19(1)	-1(1)	3(1)	1(1)
C(36)	25(1)	21(1)	20(1)	1(1)	6(1)	2(1)
C(37)	29(1)	21(1)	21(1)	1(1)	4(1)	7(1)
C(38)	32(1)	26(1)	24(1)	-1(1)	1(1)	9(1)
C(39)	38(1)	25(1)	31(1)	6(1)	7(1)	5(1)
C(40)	32(1)	27(1)	26(1)	0(1)	6(1)	10(1)
C(41)	28(1)	22(1)	21(1)	-1(1)	3(1)	2(1)
C(42)	28(1)	24(1)	29(1)	-1(1)	3(1)	-2(1)
C(43)	34(1)	30(1)	23(1)	-4(1)	9(1)	3(1)
C(44)	30(1)	26(1)	24(1)	1(1)	1(1)	5(1)
C(45)	37(1)	26(1)	26(1)	0(1)	14(1)	1(1)
C(46)	32(1)	29(1)	26(1)	0(1)	8(1)	-2(1)
C(47)	48(1)	32(1)	40(2)	4(1)	20(1)	2(1)
C(48)	48(1)	41(1)	39(2)	8(1)	22(1)	3(1)
C(49)	43(1)	37(1)	32(1)	9(1)	14(1)	-1(1)
C(50)	44(1)	30(1)	34(1)	8(1)	11(1)	4(1)
C(51)	34(1)	30(1)	34(1)	5(1)	10(1)	3(1)
C(52)	57(2)	50(2)	29(1)	-2(1)	4(1)	31(1)
C(53)	31(1)	26(1)	30(1)	-2(1)	7(1)	5(1)
C(54)	31(1)	31(1)	29(1)	1(1)	5(1)	7(1)
C(55)	33(1)	26(1)	36(1)	-1(1)	10(1)	6(1)
C(56)	44(1)	29(1)	40(1)	-3(1)	24(1)	5(1)
C(57)	54(1)	28(1)	36(1)	6(1)	24(1)	6(1)
C(58)	39(1)	21(1)	34(1)	0(1)	15(1)	4(1)
C(59)	23(1)	16(1)	21(1)	1(1)	6(1)	0(1)
C(60)	25(1)	19(1)	18(1)	1(1)	6(1)	2(1)
C(61)	25(1)	20(1)	21(1)	2(1)	8(1)	2(1)
C(62)	26(1)	23(1)	21(1)	0(1)	8(1)	4(1)
C(63)	29(1)	21(1)	17(1)	1(1)	6(1)	1(1)
C(64)	24(1)	18(1)	22(1)	0(1)	5(1)	4(1)
C(65)	25(1)	27(1)	23(1)	2(1)	6(1)	6(1)
C(66)	28(1)	37(1)	23(1)	4(1)	5(1)	7(1)

C(67)	41(1)	34(1)	34(1)	1(1)	9(1)	17(1)
C(68)	24(1)	49(1)	28(1)	4(1)	7(1)	2(1)
C(69)	33(1)	27(1)	18(1)	1(1)	6(1)	4(1)
C(70)	34(1)	31(1)	22(1)	-2(1)	6(1)	3(1)
C(71)	43(1)	36(1)	23(1)	5(1)	11(1)	-1(1)
C(72)	38(1)	32(1)	21(1)	3(1)	5(1)	7(1)

Table A.5 Hydrogen Coordinates ($\times 10^4$) and Isotropic Displacement Parameters ($\text{\AA}^2 \times 10^3$) for 2.52

	x	y	z	U(eq)
H(1)	7136	3206	7657	24
H(2)	4943	2403	6518	23
H(5)	4584	-225	7907	30
H(7)	4323	2147	8990	27
H(9)	4507	3475	7867	23
H(11)	4272	3684	6224	26
H(13)	5638	6225	6186	29
H(15)	7717	4680	7689	26
H(16A)	2404	4198	5548	32
H(16B)	3254	4014	4934	32
H(18)	383	3823	4534	36
H(19)	-1329	4343	3640	40
H(20)	-1004	5709	3174	38
H(21)	1059	6520	3595	37
H(22)	2784	5973	4466	33
H(23A)	9389	5748	7652	34
H(23B)	8576	6021	8268	34
H(25)	10352	7008	7046	34
H(26)	11461	8399	7249	37
H(27)	11456	9297	8319	40
H(28)	10283	8808	9176	41
H(29)	9103	7427	8947	38
H(30)	6758	3272	9058	25
H(32)	4736	4943	8201	25
H(36)	7812	4388	9939	26
H(38A)	2987	6656	7572	43
H(38B)	3021	5743	7950	43
H(38C)	4065	5976	7460	43
H(39A)	5985	7709	8720	47
H(39B)	4764	7821	8022	47

H(39C)	5883	7163	7933	47
H(40A)	4329	7334	9492	42
H(40B)	3216	6537	9199	42
H(40C)	3109	7430	8789	42
H(42A)	9862	6472	10144	42
H(42B)	10152	6863	10999	42
H(42C)	8952	7200	10387	42
H(43A)	7327	6807	11159	43
H(43B)	8508	6467	11781	43
H(43C)	7203	5829	11409	43
H(44A)	8755	4729	11111	42
H(44B)	10003	5422	11460	42
H(44C)	9794	4983	10623	42
H(45A)	2703	1264	9392	34
H(45B)	4179	1213	9914	34
H(47)	1991	1051	10597	46
H(48)	1135	28	11280	48
H(49)	1509	-1450	11121	44
H(50)	2743	-1907	10278	43
H(51)	3603	-891	9591	39
H(52A)	6179	-706	7379	55
H(52B)	7366	18	7386	55
H(54)	7609	-1803	7026	37
H(55)	8144	-2636	6041	37
H(56)	7710	-2133	4840	43
H(57)	6772	-783	4640	44
H(58)	6244	51	5628	36
H(60)	8228	1778	7425	25
H(64)	5776	2289	5478	26
H(66A)	10399	1891	7994	44
H(66B)	11367	1101	8065	44
H(66C)	9783	894	7908	44
H(67A)	9832	-96	6807	54
H(67B)	11419	110	6991	54
H(67C)	10524	236	6173	54
H(68A)	11569	1805	6316	50
H(68B)	12397	1682	7150	50
H(68C)	11421	2464	7000	50
H(70A)	7883	706	4232	43
H(70B)	6909	1072	3525	43
H(70C)	6308	683	4173	43

H(71A)	8520	3071	4594	50
H(71B)	8096	2626	3752	50
H(71C)	9192	2204	4370	50
H(72A)	5211	2046	4316	46
H(72B)	5805	2431	3665	46
H(72C)	6046	2982	4462	46
H(6)	9370(30)	1350(20)	4920(20)	61(10)

Table A.6 Torsion Angles [°] for 2.52

C(10)-C(1)-C(2)-C(59)	78.5(2)
C(9)-C(1)-C(2)-C(59)	-154.77(15)
C(10)-C(1)-C(2)-C(3)	-153.49(16)
C(9)-C(1)-C(2)-C(3)	-26.78(18)
C(59)-C(2)-C(3)-C(8)	145.74(17)
C(1)-C(2)-C(3)-C(8)	21.3(2)
C(59)-C(2)-C(3)-C(4)	-40.2(3)
C(1)-C(2)-C(3)-C(4)	-164.65(19)
C(52)-O(5)-C(4)-C(5)	-57.8(3)
C(52)-O(5)-C(4)-C(3)	123.6(2)
C(8)-C(3)-C(4)-O(5)	-178.45(17)
C(2)-C(3)-C(4)-O(5)	7.8(3)
C(8)-C(3)-C(4)-C(5)	2.9(3)
C(2)-C(3)-C(4)-C(5)	-170.85(19)
O(5)-C(4)-C(5)-C(6)	-179.15(18)
C(3)-C(4)-C(5)-C(6)	-0.5(3)
C(45)-O(4)-C(6)-C(7)	-0.8(3)
C(45)-O(4)-C(6)-C(5)	179.62(18)
C(4)-C(5)-C(6)-O(4)	177.76(18)
C(4)-C(5)-C(6)-C(7)	-1.8(3)
O(4)-C(6)-C(7)-C(8)	-177.88(18)
C(5)-C(6)-C(7)-C(8)	1.7(3)
C(6)-C(7)-C(8)-C(3)	0.8(3)
C(6)-C(7)-C(8)-C(9)	179.16(18)
C(4)-C(3)-C(8)-C(7)	-3.1(3)
C(2)-C(3)-C(8)-C(7)	171.71(18)
C(4)-C(3)-C(8)-C(9)	178.34(17)
C(2)-C(3)-C(8)-C(9)	-6.9(2)
C(7)-C(8)-C(9)-C(30)	52.5(3)
C(3)-C(8)-C(9)-C(30)	-129.01(17)

C(7)-C(8)-C(9)-C(1)	170.91(18)
C(3)-C(8)-C(9)-C(1)	-10.6(2)
C(10)-C(1)-C(9)-C(30)	-85.75(19)
C(2)-C(1)-C(9)-C(30)	144.33(15)
C(10)-C(1)-C(9)-C(8)	153.24(16)
C(2)-C(1)-C(9)-C(8)	23.32(18)
C(2)-C(1)-C(10)-C(15)	-144.42(18)
C(9)-C(1)-C(10)-C(15)	92.1(2)
C(2)-C(1)-C(10)-C(11)	40.2(3)
C(9)-C(1)-C(10)-C(11)	-83.3(2)
C(15)-C(10)-C(11)-C(12)	0.4(3)
C(1)-C(10)-C(11)-C(12)	175.62(18)
C(16)-O(1)-C(12)-C(13)	175.61(18)
C(16)-O(1)-C(12)-C(11)	-5.6(3)
C(10)-C(11)-C(12)-O(1)	-179.56(18)
C(10)-C(11)-C(12)-C(13)	-0.8(3)
O(1)-C(12)-C(13)-C(14)	179.38(18)
C(11)-C(12)-C(13)-C(14)	0.5(3)
C(23)-O(2)-C(14)-C(13)	-177.42(18)
C(23)-O(2)-C(14)-C(15)	3.1(3)
C(12)-C(13)-C(14)-O(2)	-179.31(18)
C(12)-C(13)-C(14)-C(15)	0.2(3)
O(2)-C(14)-C(15)-C(10)	178.85(18)
C(13)-C(14)-C(15)-C(10)	-0.6(3)
C(11)-C(10)-C(15)-C(14)	0.3(3)
C(1)-C(10)-C(15)-C(14)	-175.11(17)
C(12)-O(1)-C(16)-C(17)	177.19(17)
O(1)-C(16)-C(17)-C(18)	-160.09(19)
O(1)-C(16)-C(17)-C(22)	19.5(3)
C(22)-C(17)-C(18)-C(19)	-0.2(3)
C(16)-C(17)-C(18)-C(19)	179.5(2)
C(17)-C(18)-C(19)-C(20)	-0.8(3)
C(18)-C(19)-C(20)-C(21)	0.8(3)
C(19)-C(20)-C(21)-C(22)	0.1(3)
C(18)-C(17)-C(22)-C(21)	1.1(3)
C(16)-C(17)-C(22)-C(21)	-178.5(2)
C(20)-C(21)-C(22)-C(17)	-1.1(3)
C(14)-O(2)-C(23)-C(24)	179.51(17)
O(2)-C(23)-C(24)-C(25)	-73.8(2)
O(2)-C(23)-C(24)-C(29)	104.0(2)
C(29)-C(24)-C(25)-C(26)	-0.7(3)

C(23)-C(24)-C(25)-C(26)	177.2(2)
C(24)-C(25)-C(26)-C(27)	1.4(3)
C(25)-C(26)-C(27)-C(28)	-0.8(3)
C(26)-C(27)-C(28)-C(29)	-0.4(3)
C(25)-C(24)-C(29)-C(28)	-0.6(3)
C(23)-C(24)-C(29)-C(28)	-178.4(2)
C(27)-C(28)-C(29)-C(24)	1.1(3)
C(8)-C(9)-C(30)-C(31)	-154.2(2)
C(1)-C(9)-C(30)-C(31)	91.6(2)
C(9)-C(30)-C(31)-C(32)	5.1(3)
C(9)-C(30)-C(31)-C(36)	-173.08(18)
C(30)-C(31)-C(32)-C(33)	-178.46(19)
C(36)-C(31)-C(32)-C(33)	-0.2(3)
C(31)-C(32)-C(33)-C(34)	0.1(3)
C(31)-C(32)-C(33)-C(37)	-179.64(18)
C(32)-C(33)-C(34)-O(3)	-179.3(2)
C(37)-C(33)-C(34)-O(3)	0.5(3)
C(32)-C(33)-C(34)-C(35)	0.8(3)
C(37)-C(33)-C(34)-C(35)	-179.40(18)
O(3)-C(34)-C(35)-C(36)	178.4(2)
C(33)-C(34)-C(35)-C(36)	-1.7(3)
O(3)-C(34)-C(35)-C(41)	-0.5(3)
C(33)-C(34)-C(35)-C(41)	179.43(18)
C(34)-C(35)-C(36)-C(31)	1.7(3)
C(41)-C(35)-C(36)-C(31)	-179.49(18)
C(30)-C(31)-C(36)-C(35)	177.55(19)
C(32)-C(31)-C(36)-C(35)	-0.8(3)
C(32)-C(33)-C(37)-C(38)	-0.2(3)
C(34)-C(33)-C(37)-C(38)	180.00(18)
C(32)-C(33)-C(37)-C(39)	-120.1(2)
C(34)-C(33)-C(37)-C(39)	60.2(2)
C(32)-C(33)-C(37)-C(40)	118.4(2)
C(34)-C(33)-C(37)-C(40)	-61.4(2)
C(36)-C(35)-C(41)-C(44)	1.9(3)
C(34)-C(35)-C(41)-C(44)	-179.27(18)
C(36)-C(35)-C(41)-C(43)	-116.9(2)
C(34)-C(35)-C(41)-C(43)	61.9(2)
C(36)-C(35)-C(41)-C(42)	121.3(2)
C(34)-C(35)-C(41)-C(42)	-59.9(2)
C(6)-O(4)-C(45)-C(46)	-178.27(17)
O(4)-C(45)-C(46)-C(47)	-165.3(2)

O(4)-C(45)-C(46)-C(51)	16.0(3)
C(51)-C(46)-C(47)-C(48)	-1.1(4)
C(45)-C(46)-C(47)-C(48)	-179.9(2)
C(46)-C(47)-C(48)-C(49)	0.5(4)
C(47)-C(48)-C(49)-C(50)	0.1(4)
C(48)-C(49)-C(50)-C(51)	-0.1(4)
C(47)-C(46)-C(51)-C(50)	1.1(4)
C(45)-C(46)-C(51)-C(50)	179.8(2)
C(49)-C(50)-C(51)-C(46)	-0.5(4)
C(4)-O(5)-C(52)-C(53)	179.03(19)
O(5)-C(52)-C(53)-C(58)	20.7(3)
O(5)-C(52)-C(53)-C(54)	-160.7(2)
C(58)-C(53)-C(54)-C(55)	-1.1(3)
C(52)-C(53)-C(54)-C(55)	-179.8(2)
C(53)-C(54)-C(55)-C(56)	0.2(3)
C(54)-C(55)-C(56)-C(57)	0.6(3)
C(55)-C(56)-C(57)-C(58)	-0.5(4)
C(54)-C(53)-C(58)-C(57)	1.2(3)
C(52)-C(53)-C(58)-C(57)	179.8(2)
C(56)-C(57)-C(58)-C(53)	-0.4(4)
C(3)-C(2)-C(59)-C(64)	132.64(18)
C(1)-C(2)-C(59)-C(64)	-108.62(19)
C(3)-C(2)-C(59)-C(60)	-49.1(2)
C(1)-C(2)-C(59)-C(60)	69.6(2)
C(64)-C(59)-C(60)-C(61)	-1.8(3)
C(2)-C(59)-C(60)-C(61)	179.90(17)
C(59)-C(60)-C(61)-C(62)	0.0(3)
C(59)-C(60)-C(61)-C(65)	179.80(17)
C(60)-C(61)-C(62)-O(6)	-177.82(16)
C(65)-C(61)-C(62)-O(6)	2.4(3)
C(60)-C(61)-C(62)-C(63)	2.7(3)
C(65)-C(61)-C(62)-C(63)	-177.10(18)
O(6)-C(62)-C(63)-C(64)	177.16(17)
C(61)-C(62)-C(63)-C(64)	-3.4(3)
O(6)-C(62)-C(63)-C(69)	-2.6(3)
C(61)-C(62)-C(63)-C(69)	176.84(18)
C(60)-C(59)-C(64)-C(63)	1.1(3)
C(2)-C(59)-C(64)-C(63)	179.40(17)
C(62)-C(63)-C(64)-C(59)	1.4(3)
C(69)-C(63)-C(64)-C(59)	-178.78(17)
C(60)-C(61)-C(65)-C(66)	-0.9(3)

C(62)-C(61)-C(65)-C(66)	178.86(18)
C(60)-C(61)-C(65)-C(67)	117.9(2)
C(62)-C(61)-C(65)-C(67)	-62.4(2)
C(60)-C(61)-C(65)-C(68)	-119.8(2)
C(62)-C(61)-C(65)-C(68)	59.9(2)
C(64)-C(63)-C(69)-C(72)	7.4(3)
C(62)-C(63)-C(69)-C(72)	-172.79(18)
C(64)-C(63)-C(69)-C(71)	124.78(19)
C(62)-C(63)-C(69)-C(71)	-55.4(2)
C(64)-C(63)-C(69)-C(70)	-111.5(2)
C(62)-C(63)-C(69)-C(70)	68.3(2)

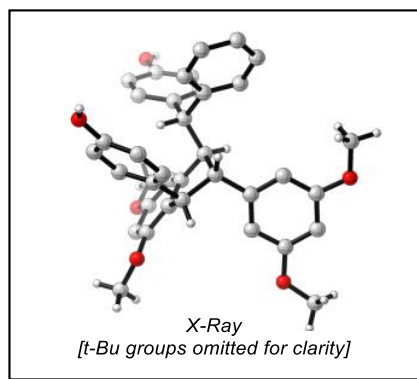
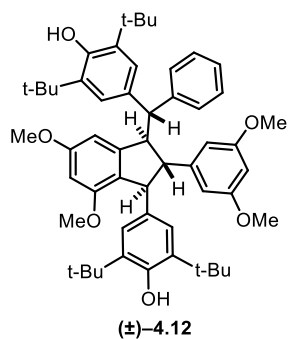


Table A.7 Crystal Data and Structural Refinement for 4.12

Empirical Formula	$C_{56}H_{74}O_7$
Formula Weight	859.15
Temperature	100 (2) K
Wavelength	1.54178 Å
Crystal System	Monoclinic
Space Group	P21/c
Unit Cell Dimensions	$a = 14.8708(3)$ Å $\alpha = 90^\circ$ $b = 18.8848(3)$ Å $\beta = 106.9550(10)^\circ$ $c = 18.2858(3)$ Å $\gamma = 90^\circ$
Volume	$4912.03(15)$ Å ³
Z	4
Calculated Density	1.162 Mg/m ³
Absorption Coefficient	0.587 mm ⁻¹
F (000)	1864
Crystal Size	0.22 x 0.16 x 0.14 mm
Theta Range for Data Collection	3.11 to 66.26°
Limiting Indices	$-17 \leq h \leq 17, -22 \leq k \leq 20, -21 \leq l \leq 20$
Reflections Collected	66856
Independent Reflections	8502 [R(int) = 0.0412]
Completeness to Theta	98.5 %
Absorption Correction	Semi-empirical from equivalents
Max and Min Transmission	0.9223 to 0.8817
Refinement Method	Full-matrix least-squares on F ²
Data / Restraints / Parameters	8502 / 8 / 585
Goodness-of-Fit on F ²	1.035
Final R Indices [$I > 2\sigma(I)$]	R1 = 0.0450, wR2 = 0.1182
R Indices (all data)	R1 = 0.0510, wR2 = 0.1234
Largest Difference Peak and Hole	0.595 and -0.492 (e Å ⁻³)

Table A.8 Atomic coordinates ($\times 10^4$) and equivalent isotropic displacement parameters ($\text{\AA}^2 \times 10^3$) for 4.12

U(eq) is defined as one third of the trace of the orthogonalized Uij tensor				
	x	y	z	U(eq)
C(1)	3102(1)	3036(1)	8752(1)	24(1)
C(2)	4063(1)	3055(1)	8852(1)	28(1)
C(3)	4522(1)	3709(1)	8903(1)	30(1)
C(4)	4038(1)	4343(1)	8859(1)	27(1)
C(5)	3068(1)	4308(1)	8740(1)	22(1)
C(6)	2384(1)	4921(1)	8644(1)	21(1)
C(7)	1510(1)	4556(1)	8790(1)	20(1)
C(8)	1549(1)	3774(1)	8523(1)	21(1)
C(9)	2595(1)	3669(1)	8681(1)	21(1)
C(10)	3097(1)	1785(1)	8949(1)	30(1)
C(11)	5980(1)	4313(1)	9073(2)	50(1)
C(12)	2183(1)	5254(1)	7832(1)	21(1)
C(13)	3072(1)	5581(1)	7719(1)	21(1)
C(14)	3546(1)	6125(1)	8186(1)	23(1)
C(15)	4372(1)	6423(1)	8114(1)	24(1)
C(16)	4728(1)	6145(1)	7539(1)	25(1)
C(17)	4262(1)	5610(1)	7036(1)	24(1)
C(18)	3441(1)	5334(1)	7150(1)	22(1)
C(19)	4865(1)	7028(1)	8649(1)	28(1)
C(20)	4301(1)	7254(1)	9189(1)	40(1)
C(21)	4960(1)	7691(1)	8182(1)	42(1)
C(22)	5830(1)	6780(1)	9162(1)	31(1)
C(23)	4623(1)	5356(1)	6370(1)	29(1)
C(24)	4596(1)	5978(1)	5821(1)	36(1)
C(25)	5619(1)	5045(1)	6667(1)	39(1)
C(26)	4000(1)	4771(1)	5903(1)	39(1)
C(27)	1369(1)	5777(1)	7640(1)	22(1)
C(28)	685(1)	5723(1)	6936(1)	29(1)
C(29)	-42(1)	6212(1)	6718(1)	34(1)
C(30)	-103(1)	6761(1)	7196(1)	34(1)
C(31)	559(1)	6814(1)	7908(1)	33(1)
C(32)	1287(1)	6325(1)	8127(1)	27(1)
C(33)	1552(1)	4622(1)	9628(1)	22(1)
C(34)	1937(1)	4100(1)	10162(1)	23(1)
C(35)	1916(1)	4179(1)	10917(1)	24(1)
C(36)	1544(1)	4779(1)	11148(1)	28(1)
C(37)	1188(1)	5311(1)	10615(1)	26(1)

C(38)	1178(1)	5236(1)	9856(1)	24(1)
C(39)	464(1)	6447(1)	10386(1)	32(1)
C(40)	2007(1)	3583(1)	12081(1)	36(1)
C(41)	990(1)	3676(1)	7683(1)	21(1)
C(42)	1430(1)	3537(1)	7127(1)	21(1)
C(43)	947(1)	3532(1)	6349(1)	22(1)
C(44)	-26(1)	3660(1)	6136(1)	23(1)
C(45)	-514(1)	3752(1)	6684(1)	24(1)
C(46)	22(1)	3766(1)	7452(1)	23(1)
C(47)	1486(1)	3447(1)	5752(1)	24(1)
C(48)	1450(1)	4157(1)	5331(1)	28(1)
C(49)	2523(1)	3264(1)	6128(1)	26(1)
C(50)	1084(1)	2846(1)	5185(1)	30(1)
C(51)	-1591(1)	3858(1)	6452(1)	30(1)
C(52)	-1850(1)	4561(1)	6026(2)	50(1)
C(53)	-2103(1)	3238(1)	5949(1)	44(1)
C(54)	-1962(1)	3848(2)	7147(1)	50(1)
O(1)	2586(1)	2428(1)	8728(1)	26(1)
O(2)	5473(1)	3663(1)	9008(1)	40(1)
O(3)	5550(1)	6400(1)	7432(1)	33(1)
O(4)	843(1)	5886(1)	10901(1)	33(1)
O(5)	2270(1)	3620(1)	11397(1)	30(1)
O(6)	-454(1)	3695(1)	5362(1)	36(1)
C(1S)	2008(2)	6980(1)	6189(2)	56(1)
C(2S)	2782(2)	7511(2)	6226(2)	61(1)
O(1S)	2140(1)	6332(1)	5833(1)	51(1)

Table A.9 Bond Lengths [\AA] and Angles [$^\circ$] for 4.12

C(1)-O(1)	1.375(2)
C(1)-C(2)	1.388(2)
C(1)-C(9)	1.398(2)
C(2)-C(3)	1.401(3)
C(2)-H(2)	0.95
C(3)-O(2)	1.374(2)
C(3)-C(4)	1.387(2)
C(4)-C(5)	1.396(2)
C(4)-H(4)	0.95
C(5)-C(9)	1.385(2)
C(5)-C(6)	1.516(2)
C(6)-C(12)	1.559(2)
C(6)-C(7)	1.562(2)
C(6)-H(6)	1
C(7)-C(33)	1.521(2)
C(7)-C(8)	1.561(2)
C(7)-H(7)	1
C(8)-C(9)	1.511(2)
C(8)-C(41)	1.531(2)
C(8)-H(8)	1
C(10)-O(1)	1.428(2)
C(10)-H(10A)	0.98
C(10)-H(10B)	0.98
C(10)-H(10C)	0.98
C(11)-O(2)	1.428(3)
C(11)-H(11A)	0.98
C(11)-H(11B)	0.98
C(11)-H(11C)	0.98
C(12)-C(27)	1.522(2)
C(12)-C(13)	1.527(2)
C(12)-H(12)	1
C(13)-C(14)	1.389(2)
C(13)-C(18)	1.390(2)
C(14)-C(15)	1.392(2)
C(14)-H(14)	0.95
C(15)-C(16)	1.409(2)
C(15)-C(19)	1.543(2)
C(16)-O(3)	1.3807(19)
C(16)-C(17)	1.404(2)
C(17)-C(18)	1.399(2)

C(17)-C(23)	1.545(2)
C(18)-H(18)	0.95
C(19)-C(20)	1.531(2)
C(19)-C(22)	1.541(2)
C(19)-C(21)	1.545(3)
C(20)-H(20A)	0.98
C(20)-H(20B)	0.98
C(20)-H(20C)	0.98
C(21)-H(21A)	0.98
C(21)-H(21B)	0.98
C(21)-H(21C)	0.98
C(22)-H(22A)	0.98
C(22)-H(22B)	0.98
C(22)-H(22C)	0.98
C(23)-C(26)	1.531(2)
C(23)-C(25)	1.538(3)
C(23)-C(24)	1.538(3)
C(24)-H(24A)	0.98
C(24)-H(24B)	0.98
C(24)-H(24C)	0.98
C(25)-H(25A)	0.98
C(25)-H(25B)	0.98
C(25)-H(25C)	0.98
C(26)-H(26A)	0.98
C(26)-H(26B)	0.98
C(26)-H(26C)	0.98
C(27)-C(28)	1.393(2)
C(27)-C(32)	1.394(2)
C(28)-C(29)	1.390(3)
C(28)-H(28)	0.95
C(29)-C(30)	1.375(3)
C(29)-H(29)	0.95
C(30)-C(31)	1.387(3)
C(30)-H(30)	0.95
C(31)-C(32)	1.390(2)
C(31)-H(31)	0.95
C(32)-H(32)	0.95
C(33)-C(34)	1.387(2)
C(33)-C(38)	1.402(2)
C(34)-C(35)	1.398(2)
C(34)-H(34)	0.95

C(35)-O(5)	1.376(2)
C(35)-C(36)	1.380(2)
C(36)-C(37)	1.393(2)
C(36)-H(36)	0.95
C(37)-O(4)	1.367(2)
C(37)-C(38)	1.391(2)
C(38)-H(38)	0.95
C(39)-O(4)	1.419(2)
C(39)-H(39A)	0.98
C(39)-H(39B)	0.98
C(39)-H(39C)	0.98
C(40)-O(5)	1.418(2)
C(40)-H(40A)	0.98
C(40)-H(40B)	0.98
C(40)-H(40C)	0.98
C(41)-C(42)	1.385(2)
C(41)-C(46)	1.387(2)
C(42)-C(43)	1.394(2)
C(42)-H(42)	0.95
C(43)-C(44)	1.405(2)
C(43)-C(47)	1.540(2)
C(44)-O(6)	1.3732(19)
C(44)-C(45)	1.410(2)
C(45)-C(46)	1.398(2)
C(45)-C(51)	1.546(2)
C(46)-H(46)	0.95
C(47)-C(49)	1.533(2)
C(47)-C(50)	1.536(2)
C(47)-C(48)	1.539(2)
C(48)-H(48A)	0.98
C(48)-H(48B)	0.98
C(48)-H(48C)	0.98
C(49)-H(49A)	0.98
C(49)-H(49B)	0.98
C(49)-H(49C)	0.98
C(50)-H(50A)	0.98
C(50)-H(50B)	0.98
C(50)-H(50C)	0.98
C(51)-C(54)	1.525(3)
C(51)-C(52)	1.531(3)
C(51)-C(53)	1.546(3)

C(52)-H(52A)	0.98
C(52)-H(52B)	0.98
C(52)-H(52C)	0.98
C(53)-H(53A)	0.98
C(53)-H(53B)	0.98
C(53)-H(53C)	0.98
C(54)-H(54A)	0.98
C(54)-H(54B)	0.98
C(54)-H(54C)	0.98
O(3)-H(3)	0.8398
O(6)-H(6A)	0.8398
C(1S)-O(1S)	1.427(3)
C(1S)-C(2S)	1.514(3)
C(1S)-H(1SA)	0.99
C(1S)-H(1SB)	0.99
C(2S)-H(2SA)	0.98
C(2S)-H(2SB)	0.98
C(2S)-H(2SC)	0.98
O(1S)-H(1S)	0.8423
O(1)-C(1)-C(2)	124.67(15)
O(1)-C(1)-C(9)	115.50(14)
C(2)-C(1)-C(9)	119.81(15)
C(1)-C(2)-C(3)	119.58(15)
C(1)-C(2)-H(2)	120.2
C(3)-C(2)-H(2)	120.2
O(2)-C(3)-C(4)	123.93(16)
O(2)-C(3)-C(2)	114.54(15)
C(4)-C(3)-C(2)	121.52(15)
C(3)-C(4)-C(5)	117.66(16)
C(3)-C(4)-H(4)	121.2
C(5)-C(4)-H(4)	121.2
C(9)-C(5)-C(4)	121.99(15)
C(9)-C(5)-C(6)	110.37(13)
C(4)-C(5)-C(6)	127.62(15)
C(5)-C(6)-C(12)	110.76(12)
C(5)-C(6)-C(7)	101.92(12)
C(12)-C(6)-C(7)	113.80(12)
C(5)-C(6)-H(6)	110
C(12)-C(6)-H(6)	110
C(7)-C(6)-H(6)	110
C(33)-C(7)-C(8)	113.43(13)

C(33)-C(7)-C(6)	110.12(12)
C(8)-C(7)-C(6)	104.84(12)
C(33)-C(7)-H(7)	109.4
C(8)-C(7)-H(7)	109.4
C(6)-C(7)-H(7)	109.4
C(9)-C(8)-C(41)	113.77(12)
C(9)-C(8)-C(7)	101.21(12)
C(41)-C(8)-C(7)	111.61(12)
C(9)-C(8)-H(8)	110
C(41)-C(8)-H(8)	110
C(7)-C(8)-H(8)	110
C(5)-C(9)-C(1)	119.38(14)
C(5)-C(9)-C(8)	111.81(14)
C(1)-C(9)-C(8)	128.79(15)
O(1)-C(10)-H(10A)	109.5
O(1)-C(10)-H(10B)	109.5
H(10A)-C(10)-H(10B)	109.5
O(1)-C(10)-H(10C)	109.5
H(10A)-C(10)-H(10C)	109.5
H(10B)-C(10)-H(10C)	109.5
O(2)-C(11)-H(11A)	109.5
O(2)-C(11)-H(11B)	109.5
H(11A)-C(11)-H(11B)	109.5
O(2)-C(11)-H(11C)	109.5
H(11A)-C(11)-H(11C)	109.5
H(11B)-C(11)-H(11C)	109.5
C(27)-C(12)-C(13)	111.58(13)
C(27)-C(12)-C(6)	113.54(12)
C(13)-C(12)-C(6)	111.07(12)
C(27)-C(12)-H(12)	106.7
C(13)-C(12)-H(12)	106.7
C(6)-C(12)-H(12)	106.7
C(14)-C(13)-C(18)	117.94(14)
C(14)-C(13)-C(12)	121.30(14)
C(18)-C(13)-C(12)	120.76(14)
C(13)-C(14)-C(15)	122.91(15)
C(13)-C(14)-H(14)	118.5
C(15)-C(14)-H(14)	118.5
C(14)-C(15)-C(16)	116.99(15)
C(14)-C(15)-C(19)	120.57(14)
C(16)-C(15)-C(19)	122.43(14)

O(3)-C(16)-C(17)	116.43(14)
O(3)-C(16)-C(15)	121.14(15)
C(17)-C(16)-C(15)	122.41(14)
C(18)-C(17)-C(16)	117.10(14)
C(18)-C(17)-C(23)	121.38(14)
C(16)-C(17)-C(23)	121.49(14)
C(13)-C(18)-C(17)	122.59(15)
C(13)-C(18)-H(18)	118.7
C(17)-C(18)-H(18)	118.7
C(20)-C(19)-C(22)	106.26(15)
C(20)-C(19)-C(15)	111.47(14)
C(22)-C(19)-C(15)	110.27(14)
C(20)-C(19)-C(21)	106.66(16)
C(22)-C(19)-C(21)	111.34(14)
C(15)-C(19)-C(21)	110.71(14)
C(19)-C(20)-H(20A)	109.5
C(19)-C(20)-H(20B)	109.5
H(20A)-C(20)-H(20B)	109.5
C(19)-C(20)-H(20C)	109.5
H(20A)-C(20)-H(20C)	109.5
H(20B)-C(20)-H(20C)	109.5
C(19)-C(21)-H(21A)	109.5
C(19)-C(21)-H(21B)	109.5
H(21A)-C(21)-H(21B)	109.5
C(19)-C(21)-H(21C)	109.5
H(21A)-C(21)-H(21C)	109.5
H(21B)-C(21)-H(21C)	109.5
C(19)-C(22)-H(22A)	109.5
C(19)-C(22)-H(22B)	109.5
H(22A)-C(22)-H(22B)	109.5
C(19)-C(22)-H(22C)	109.5
H(22A)-C(22)-H(22C)	109.5
H(22B)-C(22)-H(22C)	109.5
C(26)-C(23)-C(25)	106.58(16)
C(26)-C(23)-C(24)	106.95(15)
C(25)-C(23)-C(24)	111.13(15)
C(26)-C(23)-C(17)	111.80(14)
C(25)-C(23)-C(17)	111.09(14)
C(24)-C(23)-C(17)	109.20(14)
C(23)-C(24)-H(24A)	109.5
C(23)-C(24)-H(24B)	109.5

H(24A)-C(24)-H(24B)	109.5
C(23)-C(24)-H(24C)	109.5
H(24A)-C(24)-H(24C)	109.5
H(24B)-C(24)-H(24C)	109.5
C(23)-C(25)-H(25A)	109.5
C(23)-C(25)-H(25B)	109.5
H(25A)-C(25)-H(25B)	109.5
C(23)-C(25)-H(25C)	109.5
H(25A)-C(25)-H(25C)	109.5
H(25B)-C(25)-H(25C)	109.5
C(23)-C(26)-H(26A)	109.5
C(23)-C(26)-H(26B)	109.5
H(26A)-C(26)-H(26B)	109.5
C(23)-C(26)-H(26C)	109.5
H(26A)-C(26)-H(26C)	109.5
H(26B)-C(26)-H(26C)	109.5
C(28)-C(27)-C(32)	117.94(15)
C(28)-C(27)-C(12)	118.86(15)
C(32)-C(27)-C(12)	123.17(14)
C(29)-C(28)-C(27)	120.93(17)
C(29)-C(28)-H(28)	119.5
C(27)-C(28)-H(28)	119.5
C(30)-C(29)-C(28)	120.57(17)
C(30)-C(29)-H(29)	119.7
C(28)-C(29)-H(29)	119.7
C(29)-C(30)-C(31)	119.38(17)
C(29)-C(30)-H(30)	120.3
C(31)-C(30)-H(30)	120.3
C(30)-C(31)-C(32)	120.19(17)
C(30)-C(31)-H(31)	119.9
C(32)-C(31)-H(31)	119.9
C(31)-C(32)-C(27)	120.96(16)
C(31)-C(32)-H(32)	119.5
C(27)-C(32)-H(32)	119.5
C(34)-C(33)-C(38)	119.76(14)
C(34)-C(33)-C(7)	122.55(14)
C(38)-C(33)-C(7)	117.69(14)
C(33)-C(34)-C(35)	119.72(15)
C(33)-C(34)-H(34)	120.1
C(35)-C(34)-H(34)	120.1
O(5)-C(35)-C(36)	123.20(14)

O(5)-C(35)-C(34)	115.71(14)
C(36)-C(35)-C(34)	121.08(15)
C(35)-C(36)-C(37)	118.88(15)
C(35)-C(36)-H(36)	120.6
C(37)-C(36)-H(36)	120.6
O(4)-C(37)-C(38)	124.46(15)
O(4)-C(37)-C(36)	114.49(14)
C(38)-C(37)-C(36)	121.03(15)
C(37)-C(38)-C(33)	119.47(15)
C(37)-C(38)-H(38)	120.3
C(33)-C(38)-H(38)	120.3
O(4)-C(39)-H(39A)	109.5
O(4)-C(39)-H(39B)	109.5
H(39A)-C(39)-H(39B)	109.5
O(4)-C(39)-H(39C)	109.5
H(39A)-C(39)-H(39C)	109.5
H(39B)-C(39)-H(39C)	109.5
O(5)-C(40)-H(40A)	109.5
O(5)-C(40)-H(40B)	109.5
H(40A)-C(40)-H(40B)	109.5
O(5)-C(40)-H(40C)	109.5
H(40A)-C(40)-H(40C)	109.5
H(40B)-C(40)-H(40C)	109.5
C(42)-C(41)-C(46)	118.03(14)
C(42)-C(41)-C(8)	121.67(14)
C(46)-C(41)-C(8)	120.20(14)
C(41)-C(42)-C(43)	122.47(14)
C(41)-C(42)-H(42)	118.8
C(43)-C(42)-H(42)	118.8
C(42)-C(43)-C(44)	117.66(14)
C(42)-C(43)-C(47)	120.28(14)
C(44)-C(43)-C(47)	121.88(14)
O(6)-C(44)-C(43)	115.12(14)
O(6)-C(44)-C(45)	123.14(14)
C(43)-C(44)-C(45)	121.73(14)
C(46)-C(45)-C(44)	117.10(14)
C(46)-C(45)-C(51)	120.95(14)
C(44)-C(45)-C(51)	121.91(14)
C(41)-C(46)-C(45)	122.74(15)
C(41)-C(46)-H(46)	118.6
C(45)-C(46)-H(46)	118.6

C(49)-C(47)-C(50)	106.19(13)
C(49)-C(47)-C(48)	107.75(13)
C(50)-C(47)-C(48)	110.87(13)
C(49)-C(47)-C(43)	111.64(13)
C(50)-C(47)-C(43)	112.04(13)
C(48)-C(47)-C(43)	108.28(13)
C(47)-C(48)-H(48A)	109.5
C(47)-C(48)-H(48B)	109.5
H(48A)-C(48)-H(48B)	109.5
C(47)-C(48)-H(48C)	109.5
H(48A)-C(48)-H(48C)	109.5
H(48B)-C(48)-H(48C)	109.5
C(47)-C(49)-H(49A)	109.5
C(47)-C(49)-H(49B)	109.5
H(49A)-C(49)-H(49B)	109.5
C(47)-C(49)-H(49C)	109.5
H(49A)-C(49)-H(49C)	109.5
H(49B)-C(49)-H(49C)	109.5
C(47)-C(50)-H(50A)	109.5
C(47)-C(50)-H(50B)	109.5
H(50A)-C(50)-H(50B)	109.5
C(47)-C(50)-H(50C)	109.5
H(50A)-C(50)-H(50C)	109.5
H(50B)-C(50)-H(50C)	109.5
C(54)-C(51)-C(52)	109.69(18)
C(54)-C(51)-C(45)	111.54(14)
C(52)-C(51)-C(45)	109.82(14)
C(54)-C(51)-C(53)	104.56(16)
C(52)-C(51)-C(53)	110.29(16)
C(45)-C(51)-C(53)	110.82(15)
C(51)-C(52)-H(52A)	109.5
C(51)-C(52)-H(52B)	109.5
H(52A)-C(52)-H(52B)	109.5
C(51)-C(52)-H(52C)	109.5
H(52A)-C(52)-H(52C)	109.5
H(52B)-C(52)-H(52C)	109.5
C(51)-C(53)-H(53A)	109.5
C(51)-C(53)-H(53B)	109.5
H(53A)-C(53)-H(53B)	109.5
C(51)-C(53)-H(53C)	109.5
H(53A)-C(53)-H(53C)	109.5

H(53B)-C(53)-H(53C)	109.5
C(51)-C(54)-H(54A)	109.5
C(51)-C(54)-H(54B)	109.5
H(54A)-C(54)-H(54B)	109.5
C(51)-C(54)-H(54C)	109.5
H(54A)-C(54)-H(54C)	109.5
H(54B)-C(54)-H(54C)	109.5
C(1)-O(1)-C(10)	117.15(13)
C(3)-O(2)-C(11)	117.07(15)
C(16)-O(3)-H(3)	134.6
C(37)-O(4)-C(39)	117.35(13)
C(35)-O(5)-C(40)	116.59(13)
C(44)-O(6)-H(6A)	131.2
O(1S)-C(1S)-C(2S)	112.60(19)
O(1S)-C(1S)-H(1SA)	109.1
C(2S)-C(1S)-H(1SA)	109.1
O(1S)-C(1S)-H(1SB)	109.1
C(2S)-C(1S)-H(1SB)	109.1
H(1SA)-C(1S)-H(1SB)	107.8
C(1S)-C(2S)-H(2SA)	109.5
C(1S)-C(2S)-H(2SB)	109.5
H(2SA)-C(2S)-H(2SB)	109.5
C(1S)-C(2S)-H(2SC)	109.5
H(2SA)-C(2S)-H(2SC)	109.5
H(2SB)-C(2S)-H(2SC)	109.5
C(1S)-O(1S)-H(1S)	97.9

Table A.10 Torsion Angles [°] for 4.12

O(1)-C(1)-C(2)-C(3)	-177.00(15)
C(9)-C(1)-C(2)-C(3)	1.9(2)
C(1)-C(2)-C(3)-O(2)	179.42(15)
C(1)-C(2)-C(3)-C(4)	0.3(3)
O(2)-C(3)-C(4)-C(5)	179.17(15)
C(2)-C(3)-C(4)-C(5)	-1.8(2)
C(3)-C(4)-C(5)-C(9)	1.2(2)
C(3)-C(4)-C(5)-C(6)	-177.52(15)
C(9)-C(5)-C(6)-C(12)	-103.28(15)
C(4)-C(5)-C(6)-C(12)	75.53(19)
C(9)-C(5)-C(6)-C(7)	18.13(16)
C(4)-C(5)-C(6)-C(7)	-163.06(15)
C(5)-C(6)-C(7)-C(33)	92.78(14)
C(12)-C(6)-C(7)-C(33)	-147.94(13)
C(5)-C(6)-C(7)-C(8)	-29.57(14)
C(12)-C(6)-C(7)-C(8)	89.72(15)
C(33)-C(7)-C(8)-C(9)	-90.26(14)
C(6)-C(7)-C(8)-C(9)	29.91(14)
C(33)-C(7)-C(8)-C(41)	148.38(13)
C(6)-C(7)-C(8)-C(41)	-91.46(14)
C(4)-C(5)-C(9)-C(1)	1.0(2)
C(6)-C(5)-C(9)-C(1)	179.87(13)
C(4)-C(5)-C(9)-C(8)	-177.83(14)
C(6)-C(5)-C(9)-C(8)	1.06(17)
O(1)-C(1)-C(9)-C(5)	176.47(13)
C(2)-C(1)-C(9)-C(5)	-2.5(2)
O(1)-C(1)-C(9)-C(8)	-5.0(2)
C(2)-C(1)-C(9)-C(8)	176.06(15)
C(41)-C(8)-C(9)-C(5)	100.11(15)
C(7)-C(8)-C(9)-C(5)	-19.73(16)
C(41)-C(8)-C(9)-C(1)	-78.55(19)
C(7)-C(8)-C(9)-C(1)	161.61(15)
C(5)-C(6)-C(12)-C(27)	169.17(13)
C(7)-C(6)-C(12)-C(27)	55.05(18)
C(5)-C(6)-C(12)-C(13)	-64.12(17)
C(7)-C(6)-C(12)-C(13)	-178.24(13)
C(27)-C(12)-C(13)-C(14)	67.57(18)
C(6)-C(12)-C(13)-C(14)	-60.21(19)
C(27)-C(12)-C(13)-C(18)	-113.42(16)
C(6)-C(12)-C(13)-C(18)	118.79(15)

C(18)-C(13)-C(14)-C(15)	-0.9(2)
C(12)-C(13)-C(14)-C(15)	178.16(15)
C(13)-C(14)-C(15)-C(16)	-0.4(2)
C(13)-C(14)-C(15)-C(19)	179.76(15)
C(14)-C(15)-C(16)-O(3)	-179.14(15)
C(19)-C(15)-C(16)-O(3)	0.7(2)
C(14)-C(15)-C(16)-C(17)	2.4(2)
C(19)-C(15)-C(16)-C(17)	-177.76(15)
O(3)-C(16)-C(17)-C(18)	178.49(14)
C(15)-C(16)-C(17)-C(18)	-3.0(2)
O(3)-C(16)-C(17)-C(23)	-3.5(2)
C(15)-C(16)-C(17)-C(23)	174.98(15)
C(14)-C(13)-C(18)-C(17)	0.2(2)
C(12)-C(13)-C(18)-C(17)	-178.80(14)
C(16)-C(17)-C(18)-C(13)	1.6(2)
C(23)-C(17)-C(18)-C(13)	-176.36(15)
C(14)-C(15)-C(19)-C(20)	-3.3(2)
C(16)-C(15)-C(19)-C(20)	176.87(16)
C(14)-C(15)-C(19)-C(22)	114.46(17)
C(16)-C(15)-C(19)-C(22)	-65.4(2)
C(14)-C(15)-C(19)-C(21)	-121.88(17)
C(16)-C(15)-C(19)-C(21)	58.3(2)
C(18)-C(17)-C(23)-C(26)	-2.2(2)
C(16)-C(17)-C(23)-C(26)	179.95(16)
C(18)-C(17)-C(23)-C(25)	-121.09(17)
C(16)-C(17)-C(23)-C(25)	61.0(2)
C(18)-C(17)-C(23)-C(24)	115.98(17)
C(16)-C(17)-C(23)-C(24)	-61.9(2)
C(13)-C(12)-C(27)-C(28)	101.00(17)
C(6)-C(12)-C(27)-C(28)	-132.56(15)
C(13)-C(12)-C(27)-C(32)	-77.05(18)
C(6)-C(12)-C(27)-C(32)	49.4(2)
C(32)-C(27)-C(28)-C(29)	1.8(2)
C(12)-C(27)-C(28)-C(29)	-176.37(15)
C(27)-C(28)-C(29)-C(30)	-0.2(3)
C(28)-C(29)-C(30)-C(31)	-1.4(3)
C(29)-C(30)-C(31)-C(32)	1.4(3)
C(30)-C(31)-C(32)-C(27)	0.2(3)
C(28)-C(27)-C(32)-C(31)	-1.8(2)
C(12)-C(27)-C(32)-C(31)	176.29(15)
C(8)-C(7)-C(33)-C(34)	23.1(2)

C(6)-C(7)-C(33)-C(34)	-94.03(17)
C(8)-C(7)-C(33)-C(38)	-156.48(13)
C(6)-C(7)-C(33)-C(38)	86.39(16)
C(38)-C(33)-C(34)-C(35)	2.5(2)
C(7)-C(33)-C(34)-C(35)	-177.09(14)
C(33)-C(34)-C(35)-O(5)	176.78(14)
C(33)-C(34)-C(35)-C(36)	-2.1(2)
O(5)-C(35)-C(36)-C(37)	-178.86(15)
C(34)-C(35)-C(36)-C(37)	-0.1(2)
C(35)-C(36)-C(37)-O(4)	-179.44(15)
C(35)-C(36)-C(37)-C(38)	1.9(3)
O(4)-C(37)-C(38)-C(33)	180.00(15)
C(36)-C(37)-C(38)-C(33)	-1.4(2)
C(34)-C(33)-C(38)-C(37)	-0.8(2)
C(7)-C(33)-C(38)-C(37)	178.84(14)
C(9)-C(8)-C(41)-C(42)	-2.8(2)
C(7)-C(8)-C(41)-C(42)	110.99(16)
C(9)-C(8)-C(41)-C(46)	-179.09(14)
C(7)-C(8)-C(41)-C(46)	-65.32(18)
C(46)-C(41)-C(42)-C(43)	4.4(2)
C(8)-C(41)-C(42)-C(43)	-171.96(14)
C(41)-C(42)-C(43)-C(44)	-1.4(2)
C(41)-C(42)-C(43)-C(47)	173.97(14)
C(42)-C(43)-C(44)-O(6)	175.89(14)
C(47)-C(43)-C(44)-O(6)	0.6(2)
C(42)-C(43)-C(44)-C(45)	-3.4(2)
C(47)-C(43)-C(44)-C(45)	-178.71(15)
O(6)-C(44)-C(45)-C(46)	-174.38(15)
C(43)-C(44)-C(45)-C(46)	4.9(2)
O(6)-C(44)-C(45)-C(51)	3.6(2)
C(43)-C(44)-C(45)-C(51)	-177.14(15)
C(42)-C(41)-C(46)-C(45)	-2.8(2)
C(8)-C(41)-C(46)-C(45)	173.61(14)
C(44)-C(45)-C(46)-C(41)	-1.7(2)
C(51)-C(45)-C(46)-C(41)	-179.68(15)
C(42)-C(43)-C(47)-C(49)	8.6(2)
C(44)-C(43)-C(47)-C(49)	-176.25(15)
C(42)-C(43)-C(47)-C(50)	127.56(16)
C(44)-C(43)-C(47)-C(50)	-57.3(2)
C(42)-C(43)-C(47)-C(48)	-109.86(16)
C(44)-C(43)-C(47)-C(48)	65.30(19)

C(46)-C(45)-C(51)-C(54)	-9.6(2)
C(44)-C(45)-C(51)-C(54)	172.53(17)
C(46)-C(45)-C(51)-C(52)	112.24(19)
C(44)-C(45)-C(51)-C(52)	-65.6(2)
C(46)-C(45)-C(51)-C(53)	-125.65(17)
C(44)-C(45)-C(51)-C(53)	56.5(2)
C(2)-C(1)-O(1)-C(10)	11.1(2)
C(9)-C(1)-O(1)-C(10)	-167.85(13)
C(4)-C(3)-O(2)-C(11)	-0.2(3)
C(2)-C(3)-O(2)-C(11)	-179.28(17)
C(38)-C(37)-O(4)-C(39)	-1.0(2)
C(36)-C(37)-O(4)-C(39)	-179.64(15)
C(36)-C(35)-O(5)-C(40)	17.4(2)
C(34)-C(35)-O(5)-C(40)	-161.44(15)

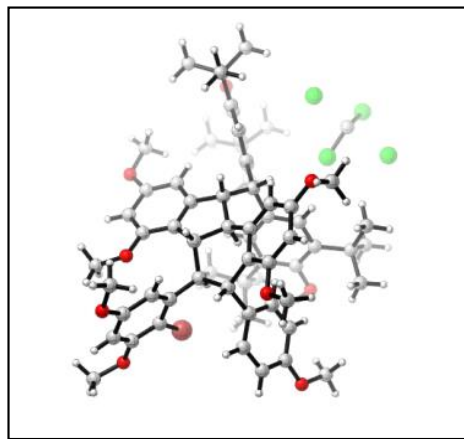
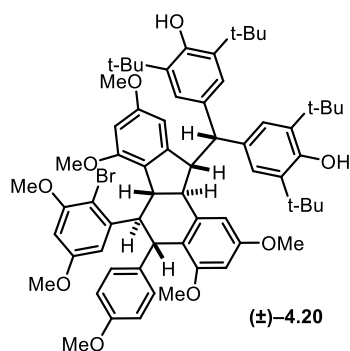


Table A.11 Crystal Data and Structural Refinement for 4.20

Empirical Formula	C ₆₅ H ₇₉ BrCl ₂
Formula Weight	1155.09
Temperature	85(2) K
Wavelength	1.54178 Å
Crystal System	Undefined
Space Group	Undefined
Unit Cell Dimensions	a = 10.0817(3) Å α = 106.414(5)° b = 13.7666(4) Å β = 97.865(8)° c = 23.6123(17) Å γ = 94.332(6)°
Volume	3091.5(3) Å ³
Z	2
Calculated Density	1.241 Mg/m ³
Absorption Coefficient	2.129 mm ⁻¹
F (000)	1220
Crystal Size	0.08 x 0.02 x 0.2 mm
Theta Range for Data Collection	6.74 to 68.21°
Limiting Indices	-12 ≤ h ≤ 12, -16 ≤ k ≤ 16, -28 ≤ l ≤ 28
Reflections Collected	55137
Independent Reflections	10813 [R(int) = 0.1561]
Completeness to Theta	95.6%
Absorption Correction	Semi-empirical from equivalents
Max and Min Transmission	0.9587 to 0.8481
Refinement Method	Full-matrix least-squares on F ²
Data / Restraints / Parameters	10813 / 0 / 391
Goodness-of-Fit on F ²	1.103
Final R Indices [I > 2σ(I)]	R1 = 0.1266, wR2 = 0.3287
R Indices (all data)	R1 = 0.1954, wR2 = 0.3797
Largest Difference Peak and Hole	1.128 and -1.874 (e Å ⁻³)

Table A.12 Atomic coordinates ($\times 10^4$) and equivalent isotropic displacement parameters ($\text{Å}^2 \times 10^3$) for 4.20

U(eq) is defined as one third of the trace of the orthogonalized Uij tensor				
	x	y	z	U(eq)
Br(1)	5790(1)	-1401(1)	7876(1)	64(1)
O(1)	4450(6)	-3308(4)	7931(3)	61(2)
O(2)	486(6)	-2209(5)	8656(3)	75(2)
O(3)	1871(5)	-1374(4)	7144(3)	50(2)
O(4)	1773(5)	-420(4)	5358(3)	51(2)
O(5)	2975(5)	3550(4)	5023(3)	50(2)
O(6)	9820(4)	2348(4)	7882(2)	43(1)
O(7)	3074(5)	5121(4)	9316(3)	47(1)
O(8)	4073(5)	2261(4)	10069(3)	47(1)
O(9)	9843(5)	946(5)	9668(3)	70(2)
C(1)	3817(7)	296(5)	8289(3)	37(2)
C(2)	2886(6)	773(5)	7894(3)	30(1)
C(3)	3635(6)	1848(5)	7979(3)	30(1)
C(4)	3584(6)	2542(5)	8572(3)	30(1)
C(5)	3846(7)	2109(6)	9052(4)	37(2)
C(6)	4212(6)	1039(5)	8957(3)	36(2)
C(7)	3356(7)	-763(6)	8305(4)	45(2)
C(8)	4144(7)	-1584(6)	8133(4)	43(2)
C(9)	3642(8)	-2548(6)	8132(4)	48(2)
C(10)	2442(8)	-2736(7)	8318(4)	55(2)
C(11)	1691(9)	-1944(7)	8490(4)	58(2)
C(12)	2138(8)	-946(6)	8506(4)	48(2)
C(13)	3925(10)	-4322(8)	7869(5)	74(3)
C(14)	-385(11)	-1423(8)	8822(5)	78(3)
C(15)	2657(6)	325(5)	7218(3)	31(1)
C(16)	2161(7)	-671(6)	6858(4)	39(2)
C(17)	1902(7)	-901(6)	6228(4)	40(2)
C(18)	2109(7)	-110(6)	5969(4)	44(2)
C(19)	2581(6)	882(5)	6312(3)	34(2)
C(20)	2853(6)	1083(5)	6938(3)	31(1)
C(21)	1540(10)	-2411(8)	6800(5)	76(3)
C(22)	1831(10)	370(8)	5080(5)	71(3)
C(23)	3224(6)	2120(5)	7399(3)	30(1)
C(24)	4318(6)	2920(5)	7312(3)	32(2)
C(25)	4004(6)	3092(5)	6690(3)	36(2)
C(26)	2806(6)	3472(5)	6532(3)	35(2)
C(27)	2425(6)	3606(5)	5970(3)	36(2)

C(28)	3356(6)	3388(5)	5578(3)	35(2)
C(29)	4575(7)	3008(6)	5715(3)	37(2)
C(30)	4880(7)	2876(6)	6274(4)	40(2)
C(31)	1091(7)	3992(6)	5814(4)	45(2)
C(32)	256(8)	4165(7)	6319(4)	56(2)
C(33)	217(7)	3208(6)	5255(4)	45(2)
C(34)	1354(8)	5018(7)	5674(4)	56(2)
C(35)	5566(7)	2741(6)	5264(4)	42(2)
C(36)	6802(8)	2305(7)	5534(4)	53(2)
C(37)	4947(8)	1916(7)	4676(4)	54(2)
C(38)	6152(8)	3716(6)	5132(4)	50(2)
C(39)	5758(6)	2730(5)	7464(3)	34(2)
C(40)	6679(6)	3496(5)	7850(3)	34(2)
C(41)	8056(6)	3403(5)	7995(3)	31(1)
C(42)	8471(6)	2462(5)	7740(3)	30(1)
C(43)	7579(6)	1639(5)	7338(3)	35(2)
C(44)	6240(6)	1788(5)	7217(3)	32(2)
C(45)	9039(7)	4328(6)	8414(4)	43(2)
C(46)	8308(8)	5258(6)	8655(4)	51(2)
C(47)	10101(8)	4640(6)	8084(4)	48(2)
C(48)	9711(7)	4073(6)	8978(4)	46(2)
C(49)	8065(7)	624(6)	7048(4)	45(2)
C(50)	9134(8)	809(7)	6676(4)	58(2)
C(51)	8714(8)	134(6)	7513(4)	49(2)
C(52)	6921(8)	-136(7)	6636(4)	53(2)
C(53)	3307(7)	3538(6)	8692(4)	38(2)
C(54)	3288(7)	4146(6)	9259(4)	43(2)
C(55)	3528(7)	3727(6)	9746(4)	45(2)
C(56)	3801(7)	2725(6)	9625(4)	41(2)
C(57)	2895(8)	5753(7)	9899(4)	56(2)
C(58)	4028(9)	2817(7)	10679(5)	64(2)
C(59)	5719(7)	1053(6)	9162(4)	40(2)
C(60)	6666(6)	1639(5)	8992(3)	36(2)
C(61)	8031(7)	1623(6)	9149(3)	38(2)
C(62)	8502(8)	1008(6)	9487(4)	50(2)
C(63)	7585(8)	377(7)	9650(4)	57(2)
C(64)	6209(8)	373(7)	9476(4)	51(2)
C(65)	10800(8)	1615(7)	9534(4)	56(2)
C(66)	6680(20)	6243(16)	6914(10)	74(6)
Cl(2)	6949(5)	5159(3)	6939(2)	61(1)
Cl(1)	7560(5)	6786(4)	6436(3)	85(2)

Cl(3)	4937(6)	5894(5)	6364(3)	97(2)
Cl(4)	8544(8)	6847(6)	7520(4)	126(3)

Table A.13 Bond Lengths [Å] and Angles [°] for 4.20

Br(1)-C(8)	1.867(8)
O(1)-C(9)	1.392(10)
O(1)-C(13)	1.414(11)
O(2)-C(11)	1.382(10)
O(2)-C(14)	1.447(12)
O(3)-C(16)	1.365(9)
O(3)-C(21)	1.416(11)
O(4)-C(18)	1.370(10)
O(4)-C(22)	1.421(11)
O(5)-C(28)	1.399(8)
O(5)-H(5A)	0.84
O(6)-C(42)	1.386(7)
O(6)-H(6A)	0.84
O(7)-C(54)	1.347(9)
O(7)-C(57)	1.447(10)
O(8)-C(56)	1.380(9)
O(8)-C(58)	1.437(11)
O(9)-C(62)	1.377(9)
O(9)-C(65)	1.412(10)
C(1)-C(7)	1.508(10)
C(1)-C(2)	1.543(9)
C(1)-C(6)	1.595(11)
C(1)-H(1A)	1
C(2)-C(15)	1.516(10)
C(2)-C(3)	1.557(9)
C(2)-H(2A)	1
C(3)-C(4)	1.465(10)
C(3)-C(23)	1.532(9)
C(3)-H(3A)	1
C(4)-C(53)	1.377(10)
C(4)-C(5)	1.426(9)
C(5)-C(56)	1.389(11)
C(5)-C(6)	1.508(10)
C(6)-C(59)	1.527(9)
C(6)-H(6B)	1

C(7)-C(12)	1.407(11)
C(7)-C(8)	1.428(11)
C(8)-C(9)	1.384(11)
C(9)-C(10)	1.373(12)
C(10)-C(11)	1.374(12)
C(10)-H(10A)	0.95
C(11)-C(12)	1.401(12)
C(12)-H(12A)	0.95
C(13)-H(13A)	0.98
C(13)-H(13B)	0.98
C(13)-H(13C)	0.98
C(14)-H(14A)	0.98
C(14)-H(14B)	0.98
C(14)-H(14C)	0.98
C(15)-C(20)	1.401(9)
C(15)-C(16)	1.405(10)
C(16)-C(17)	1.413(11)
C(17)-C(18)	1.405(11)
C(17)-H(17A)	0.95
C(18)-C(19)	1.385(10)
C(19)-C(20)	1.409(10)
C(19)-H(19A)	0.95
C(20)-C(23)	1.514(10)
C(21)-H(21A)	0.98
C(21)-H(21B)	0.98
C(21)-H(21C)	0.98
C(22)-H(22A)	0.98
C(22)-H(22B)	0.98
C(22)-H(22C)	0.98
C(23)-C(24)	1.574(9)
C(23)-H(23A)	1
C(24)-C(39)	1.508(9)
C(24)-C(25)	1.547(10)
C(24)-H(24A)	1
C(25)-C(26)	1.397(9)
C(25)-C(30)	1.396(11)
C(26)-C(27)	1.396(10)
C(26)-H(26A)	0.95
C(27)-C(28)	1.397(10)
C(27)-C(31)	1.520(10)
C(28)-C(29)	1.404(9)

C(29)-C(30)	1.378(10)
C(29)-C(35)	1.547(11)
C(30)-H(30A)	0.95
C(31)-C(32)	1.528(12)
C(31)-C(33)	1.553(11)
C(31)-C(34)	1.550(11)
C(32)-H(32A)	0.98
C(32)-H(32B)	0.98
C(32)-H(32C)	0.98
C(33)-H(33A)	0.98
C(33)-H(33B)	0.98
C(33)-H(33C)	0.98
C(34)-H(34A)	0.98
C(34)-H(34B)	0.98
C(34)-H(34C)	0.98
C(35)-C(36)	1.560(10)
C(35)-C(37)	1.540(11)
C(35)-C(38)	1.555(11)
C(36)-H(36A)	0.98
C(36)-H(36B)	0.98
C(36)-H(36C)	0.98
C(37)-H(37A)	0.98
C(37)-H(37B)	0.98
C(37)-H(37C)	0.98
C(38)-H(38A)	0.98
C(38)-H(38B)	0.98
C(38)-H(38C)	0.98
C(39)-C(40)	1.371(9)
C(39)-C(44)	1.416(10)
C(40)-C(41)	1.407(9)
C(40)-H(40A)	0.95
C(41)-C(42)	1.388(10)
C(41)-C(45)	1.554(10)
C(42)-C(43)	1.414(9)
C(43)-C(44)	1.384(9)
C(43)-C(49)	1.522(11)
C(44)-H(44A)	0.95
C(45)-C(47)	1.512(11)
C(45)-C(48)	1.553(10)
C(45)-C(46)	1.534(11)
C(46)-H(46A)	0.98

C(46)-H(46B)	0.98
C(46)-H(46C)	0.98
C(47)-H(47A)	0.98
C(47)-H(47B)	0.98
C(47)-H(47C)	0.98
C(48)-H(48A)	0.98
C(48)-H(48B)	0.98
C(48)-H(48C)	0.98
C(49)-C(52)	1.519(10)
C(49)-C(50)	1.531(12)
C(49)-C(51)	1.540(10)
C(50)-H(50A)	0.98
C(50)-H(50B)	0.98
C(50)-H(50C)	0.98
C(51)-H(51A)	0.98
C(51)-H(51B)	0.98
C(51)-H(51C)	0.98
C(52)-H(52A)	0.98
C(52)-H(52B)	0.98
C(52)-H(52C)	0.98
C(53)-C(54)	1.368(11)
C(53)-H(53A)	0.95
C(54)-C(55)	1.425(11)
C(55)-C(56)	1.385(11)
C(55)-H(55A)	0.95
C(57)-H(57A)	0.98
C(57)-H(57B)	0.98
C(57)-H(57C)	0.98
C(58)-H(58A)	0.98
C(58)-H(58B)	0.98
C(58)-H(58C)	0.98
C(59)-C(60)	1.377(10)
C(59)-C(64)	1.426(11)
C(60)-C(61)	1.380(9)
C(60)-H(60A)	0.95
C(61)-C(62)	1.385(10)
C(61)-H(61A)	0.95
C(62)-C(63)	1.388(12)
C(63)-C(64)	1.391(11)
C(63)-H(63A)	0.95
C(64)-H(64A)	0.95

C(65)-H(65A)	0.98
C(65)-H(65B)	0.98
C(65)-H(65C)	0.98
C(66)-Cl(2)	1.55(2)
C(66)-Cl(1)	1.81(2)
C(66)-Cl(3)	1.97(2)
C(66)-Cl(4)	2.15(2)
C(9)-O(1)-C(13)	117.0(7)
C(11)-O(2)-C(14)	117.8(7)
C(16)-O(3)-C(21)	118.5(7)
C(18)-O(4)-C(22)	115.5(7)
C(28)-O(5)-H(5A)	109.5
C(42)-O(6)-H(6A)	109.5
C(54)-O(7)-C(57)	117.9(7)
C(56)-O(8)-C(58)	119.5(7)
C(62)-O(9)-C(65)	117.1(6)
C(7)-C(1)-C(2)	117.7(5)
C(7)-C(1)-C(6)	109.4(6)
C(2)-C(1)-C(6)	111.2(6)
C(7)-C(1)-H(1A)	105.9
C(2)-C(1)-H(1A)	105.9
C(6)-C(1)-H(1A)	105.9
C(15)-C(2)-C(3)	101.6(5)
C(15)-C(2)-C(1)	119.9(6)
C(3)-C(2)-C(1)	104.9(5)
C(15)-C(2)-H(2A)	109.9
C(3)-C(2)-H(2A)	109.9
C(1)-C(2)-H(2A)	109.9
C(4)-C(3)-C(23)	122.8(6)
C(4)-C(3)-C(2)	111.2(6)
C(23)-C(3)-C(2)	107.0(5)
C(4)-C(3)-H(3A)	104.8
C(23)-C(3)-H(3A)	104.8
C(2)-C(3)-H(3A)	104.8
C(53)-C(4)-C(5)	119.5(7)
C(53)-C(4)-C(3)	125.9(6)
C(5)-C(4)-C(3)	114.5(6)
C(56)-C(5)-C(4)	117.4(7)
C(56)-C(5)-C(6)	120.1(7)
C(4)-C(5)-C(6)	122.4(7)
C(59)-C(6)-C(5)	110.8(6)

C(59)-C(6)-C(1)	108.4(6)
C(5)-C(6)-C(1)	115.7(6)
C(59)-C(6)-H(6B)	107.2
C(5)-C(6)-H(6B)	107.2
C(1)-C(6)-H(6B)	107.2
C(12)-C(7)-C(8)	118.9(7)
C(12)-C(7)-C(1)	119.5(7)
C(8)-C(7)-C(1)	121.6(7)
C(9)-C(8)-C(7)	118.9(7)
C(9)-C(8)-Br(1)	119.4(6)
C(7)-C(8)-Br(1)	121.7(6)
C(10)-C(9)-C(8)	122.4(8)
C(10)-C(9)-O(1)	122.8(7)
C(8)-C(9)-O(1)	114.8(7)
C(11)-C(10)-C(9)	118.6(8)
C(11)-C(10)-H(10A)	120.7
C(9)-C(10)-H(10A)	120.7
C(10)-C(11)-O(2)	114.5(8)
C(10)-C(11)-C(12)	122.2(9)
O(2)-C(11)-C(12)	123.2(9)
C(7)-C(12)-C(11)	118.8(8)
C(7)-C(12)-H(12A)	120.6
C(11)-C(12)-H(12A)	120.6
O(1)-C(13)-H(13A)	109.5
O(1)-C(13)-H(13B)	109.5
H(13A)-C(13)-H(13B)	109.5
O(1)-C(13)-H(13C)	109.5
H(13A)-C(13)-H(13C)	109.5
H(13B)-C(13)-H(13C)	109.5
O(2)-C(14)-H(14A)	109.5
O(2)-C(14)-H(14B)	109.5
H(14A)-C(14)-H(14B)	109.5
O(2)-C(14)-H(14C)	109.5
H(14A)-C(14)-H(14C)	109.5
H(14B)-C(14)-H(14C)	109.5
C(20)-C(15)-C(16)	118.3(7)
C(20)-C(15)-C(2)	111.3(6)
C(16)-C(15)-C(2)	130.0(6)
O(3)-C(16)-C(15)	117.0(7)
O(3)-C(16)-C(17)	122.4(7)
C(15)-C(16)-C(17)	120.5(7)

C(16)-C(17)-C(18)	118.9(7)
C(16)-C(17)-H(17A)	120.6
C(18)-C(17)-H(17A)	120.6
C(19)-C(18)-O(4)	124.5(7)
C(19)-C(18)-C(17)	122.1(8)
O(4)-C(18)-C(17)	113.3(7)
C(18)-C(19)-C(20)	117.7(7)
C(18)-C(19)-H(19A)	121.2
C(20)-C(19)-H(19A)	121.2
C(15)-C(20)-C(19)	122.5(6)
C(15)-C(20)-C(23)	110.6(6)
C(19)-C(20)-C(23)	126.6(6)
O(3)-C(21)-H(21A)	109.5
O(3)-C(21)-H(21B)	109.5
H(21A)-C(21)-H(21B)	109.5
O(3)-C(21)-H(21C)	109.5
H(21A)-C(21)-H(21C)	109.5
H(21B)-C(21)-H(21C)	109.5
O(4)-C(22)-H(22A)	109.5
O(4)-C(22)-H(22B)	109.5
H(22A)-C(22)-H(22B)	109.5
O(4)-C(22)-H(22C)	109.5
H(22A)-C(22)-H(22C)	109.5
H(22B)-C(22)-H(22C)	109.5
C(20)-C(23)-C(3)	102.6(5)
C(20)-C(23)-C(24)	120.3(6)
C(3)-C(23)-C(24)	111.5(5)
C(20)-C(23)-H(23A)	107.2
C(3)-C(23)-H(23A)	107.2
C(24)-C(23)-H(23A)	107.2
C(39)-C(24)-C(25)	112.9(6)
C(39)-C(24)-C(23)	114.9(5)
C(25)-C(24)-C(23)	111.8(5)
C(39)-C(24)-H(24A)	105.4
C(25)-C(24)-H(24A)	105.4
C(23)-C(24)-H(24A)	105.4
C(26)-C(25)-C(30)	118.2(7)
C(26)-C(25)-C(24)	119.7(7)
C(30)-C(25)-C(24)	122.1(6)
C(25)-C(26)-C(27)	123.0(7)
C(25)-C(26)-H(26A)	118.5

C(27)-C(26)-H(26A)	118.5
C(28)-C(27)-C(26)	115.8(6)
C(28)-C(27)-C(31)	123.2(7)
C(26)-C(27)-C(31)	121.0(7)
C(27)-C(28)-O(5)	115.1(6)
C(27)-C(28)-C(29)	123.3(7)
O(5)-C(28)-C(29)	121.5(7)
C(30)-C(29)-C(28)	117.9(7)
C(30)-C(29)-C(35)	119.8(6)
C(28)-C(29)-C(35)	122.2(7)
C(29)-C(30)-C(25)	121.6(7)
C(29)-C(30)-H(30A)	119.2
C(25)-C(30)-H(30A)	119.2
C(32)-C(31)-C(27)	112.7(7)
C(32)-C(31)-C(33)	107.1(6)
C(27)-C(31)-C(33)	110.4(7)
C(32)-C(31)-C(34)	107.9(7)
C(27)-C(31)-C(34)	109.8(6)
C(33)-C(31)-C(34)	108.7(6)
C(31)-C(32)-H(32A)	109.5
C(31)-C(32)-H(32B)	109.5
H(32A)-C(32)-H(32B)	109.5
C(31)-C(32)-H(32C)	109.5
H(32A)-C(32)-H(32C)	109.5
H(32B)-C(32)-H(32C)	109.5
C(31)-C(33)-H(33A)	109.5
C(31)-C(33)-H(33B)	109.5
H(33A)-C(33)-H(33B)	109.5
C(31)-C(33)-H(33C)	109.5
H(33A)-C(33)-H(33C)	109.5
H(33B)-C(33)-H(33C)	109.5
C(31)-C(34)-H(34A)	109.5
C(31)-C(34)-H(34B)	109.5
H(34A)-C(34)-H(34B)	109.5
C(31)-C(34)-H(34C)	109.5
H(34A)-C(34)-H(34C)	109.5
H(34B)-C(34)-H(34C)	109.5
C(36)-C(35)-C(29)	110.6(7)
C(36)-C(35)-C(37)	105.5(7)
C(29)-C(35)-C(37)	113.6(6)
C(36)-C(35)-C(38)	105.8(6)

C(29)-C(35)-C(38)	110.6(7)
C(37)-C(35)-C(38)	110.4(7)
C(35)-C(36)-H(36A)	109.5
C(35)-C(36)-H(36B)	109.5
H(36A)-C(36)-H(36B)	109.5
C(35)-C(36)-H(36C)	109.5
H(36A)-C(36)-H(36C)	109.5
H(36B)-C(36)-H(36C)	109.5
C(35)-C(37)-H(37A)	109.5
C(35)-C(37)-H(37B)	109.5
H(37A)-C(37)-H(37B)	109.5
C(35)-C(37)-H(37C)	109.5
H(37A)-C(37)-H(37C)	109.5
H(37B)-C(37)-H(37C)	109.5
C(35)-C(38)-H(38A)	109.5
C(35)-C(38)-H(38B)	109.5
H(38A)-C(38)-H(38B)	109.5
C(35)-C(38)-H(38C)	109.5
H(38A)-C(38)-H(38C)	109.5
H(38B)-C(38)-H(38C)	109.5
C(40)-C(39)-C(44)	116.8(6)
C(40)-C(39)-C(24)	120.0(7)
C(44)-C(39)-C(24)	123.1(6)
C(39)-C(40)-C(41)	123.9(7)
C(39)-C(40)-H(40A)	118
C(41)-C(40)-H(40A)	118
C(40)-C(41)-C(42)	116.8(6)
C(40)-C(41)-C(45)	120.4(6)
C(42)-C(41)-C(45)	122.8(6)
O(6)-C(42)-C(43)	119.8(6)
O(6)-C(42)-C(41)	117.8(6)
C(43)-C(42)-C(41)	122.3(6)
C(44)-C(43)-C(42)	117.6(7)
C(44)-C(43)-C(49)	120.9(6)
C(42)-C(43)-C(49)	121.5(6)
C(43)-C(44)-C(39)	122.5(6)
C(43)-C(44)-H(44A)	118.7
C(39)-C(44)-H(44A)	118.7
C(47)-C(45)-C(48)	110.4(6)
C(47)-C(45)-C(46)	107.8(6)
C(48)-C(45)-C(46)	105.1(7)

C(47)-C(45)-C(41)	110.5(7)
C(48)-C(45)-C(41)	110.7(6)
C(46)-C(45)-C(41)	112.1(6)
C(45)-C(46)-H(46A)	109.5
C(45)-C(46)-H(46B)	109.5
H(46A)-C(46)-H(46B)	109.5
C(45)-C(46)-H(46C)	109.5
H(46A)-C(46)-H(46C)	109.5
H(46B)-C(46)-H(46C)	109.5
C(45)-C(47)-H(47A)	109.5
C(45)-C(47)-H(47B)	109.5
H(47A)-C(47)-H(47B)	109.5
C(45)-C(47)-H(47C)	109.5
H(47A)-C(47)-H(47C)	109.5
H(47B)-C(47)-H(47C)	109.5
C(45)-C(48)-H(48A)	109.5
C(45)-C(48)-H(48B)	109.5
H(48A)-C(48)-H(48B)	109.5
C(45)-C(48)-H(48C)	109.5
H(48A)-C(48)-H(48C)	109.5
H(48B)-C(48)-H(48C)	109.5
C(52)-C(49)-C(43)	111.5(6)
C(52)-C(49)-C(50)	108.3(7)
C(43)-C(49)-C(50)	108.5(7)
C(52)-C(49)-C(51)	108.1(6)
C(43)-C(49)-C(51)	112.4(7)
C(50)-C(49)-C(51)	107.8(6)
C(49)-C(50)-H(50A)	109.5
C(49)-C(50)-H(50B)	109.5
H(50A)-C(50)-H(50B)	109.5
C(49)-C(50)-H(50C)	109.5
H(50A)-C(50)-H(50C)	109.5
H(50B)-C(50)-H(50C)	109.5
C(49)-C(51)-H(51A)	109.5
C(49)-C(51)-H(51B)	109.5
H(51A)-C(51)-H(51B)	109.5
C(49)-C(51)-H(51C)	109.5
H(51A)-C(51)-H(51C)	109.5
H(51B)-C(51)-H(51C)	109.5
C(49)-C(52)-H(52A)	109.5
C(49)-C(52)-H(52B)	109.5

H(52A)-C(52)-H(52B)	109.5
C(49)-C(52)-H(52C)	109.5
H(52A)-C(52)-H(52C)	109.5
H(52B)-C(52)-H(52C)	109.5
C(4)-C(53)-C(54)	122.8(7)
C(4)-C(53)-H(53A)	118.6
C(54)-C(53)-H(53A)	118.6
O(7)-C(54)-C(53)	116.6(7)
O(7)-C(54)-C(55)	124.6(8)
C(53)-C(54)-C(55)	118.8(8)
C(56)-C(55)-C(54)	118.5(8)
C(56)-C(55)-H(55A)	120.7
C(54)-C(55)-H(55A)	120.7
O(8)-C(56)-C(5)	114.5(7)
O(8)-C(56)-C(55)	122.5(8)
C(5)-C(56)-C(55)	123.0(7)
O(7)-C(57)-H(57A)	109.5
O(7)-C(57)-H(57B)	109.5
H(57A)-C(57)-H(57B)	109.5
O(7)-C(57)-H(57C)	109.5
H(57A)-C(57)-H(57C)	109.5
H(57B)-C(57)-H(57C)	109.5
O(8)-C(58)-H(58A)	109.5
O(8)-C(58)-H(58B)	109.5
H(58A)-C(58)-H(58B)	109.5
O(8)-C(58)-H(58C)	109.5
H(58A)-C(58)-H(58C)	109.5
H(58B)-C(58)-H(58C)	109.5
C(60)-C(59)-C(64)	117.0(6)
C(60)-C(59)-C(6)	121.2(6)
C(64)-C(59)-C(6)	121.4(6)
C(59)-C(60)-C(61)	122.0(7)
C(59)-C(60)-H(60A)	119
C(61)-C(60)-H(60A)	119
C(60)-C(61)-C(62)	120.7(7)
C(60)-C(61)-H(61A)	119.6
C(62)-C(61)-H(61A)	119.6
C(63)-C(62)-O(9)	115.7(7)
C(63)-C(62)-C(61)	119.3(7)
O(9)-C(62)-C(61)	124.9(7)
C(62)-C(63)-C(64)	119.8(8)

C(62)-C(63)-H(63A)	120.1
C(64)-C(63)-H(63A)	120.1
C(63)-C(64)-C(59)	121.0(8)
C(63)-C(64)-H(64A)	119.5
C(59)-C(64)-H(64A)	119.5
O(9)-C(65)-H(65A)	109.5
O(9)-C(65)-H(65B)	109.5
H(65A)-C(65)-H(65B)	109.5
O(9)-C(65)-H(65C)	109.5
H(65A)-C(65)-H(65C)	109.5
H(65B)-C(65)-H(65C)	109.5
Cl(2)-C(66)-Cl(1)	117.6(14)
Cl(2)-C(66)-Cl(3)	99.6(11)
Cl(1)-C(66)-Cl(3)	95.1(10)
Cl(2)-C(66)-Cl(4)	88.6(10)
Cl(1)-C(66)-Cl(4)	81.1(8)
Cl(3)-C(66)-Cl(4)	171.8(12)

Table A.14 Torsion Angles [°] for 4.20

C(7)-C(1)-C(2)-C(15)	-67.2(9)
C(6)-C(1)-C(2)-C(15)	165.4(5)
C(7)-C(1)-C(2)-C(3)	179.6(7)
C(6)-C(1)-C(2)-C(3)	52.3(7)
C(15)-C(2)-C(3)-C(4)	161.7(5)
C(1)-C(2)-C(3)-C(4)	-72.7(7)
C(15)-C(2)-C(3)-C(23)	25.2(7)
C(1)-C(2)-C(3)-C(23)	150.8(6)
C(23)-C(3)-C(4)-C(53)	-7.1(10)
C(2)-C(3)-C(4)-C(53)	-135.6(6)
C(23)-C(3)-C(4)-C(5)	172.7(5)
C(2)-C(3)-C(4)-C(5)	44.2(7)
C(53)-C(4)-C(5)-C(56)	0.4(9)
C(3)-C(4)-C(5)-C(56)	-179.5(6)
C(53)-C(4)-C(5)-C(6)	-177.4(6)
C(3)-C(4)-C(5)-C(6)	2.7(9)
C(56)-C(5)-C(6)-C(59)	-73.7(9)
C(4)-C(5)-C(6)-C(59)	104.0(7)
C(56)-C(5)-C(6)-C(1)	162.4(6)
C(4)-C(5)-C(6)-C(1)	-19.8(9)

C(7)-C(1)-C(6)-C(59)	92.3(7)
C(2)-C(1)-C(6)-C(59)	-135.9(6)
C(7)-C(1)-C(6)-C(5)	-142.6(6)
C(2)-C(1)-C(6)-C(5)	-10.9(8)
C(2)-C(1)-C(7)-C(12)	-60.1(10)
C(6)-C(1)-C(7)-C(12)	68.1(8)
C(2)-C(1)-C(7)-C(8)	121.3(8)
C(6)-C(1)-C(7)-C(8)	-110.4(8)
C(12)-C(7)-C(8)-C(9)	4.2(12)
C(1)-C(7)-C(8)-C(9)	-177.2(7)
C(12)-C(7)-C(8)-Br(1)	-178.7(6)
C(1)-C(7)-C(8)-Br(1)	-0.1(11)
C(7)-C(8)-C(9)-C(10)	-3.2(13)
Br(1)-C(8)-C(9)-C(10)	179.7(7)
C(7)-C(8)-C(9)-O(1)	177.1(7)
Br(1)-C(8)-C(9)-O(1)	0.0(10)
C(13)-O(1)-C(9)-C(10)	6.1(12)
C(13)-O(1)-C(9)-C(8)	-174.3(8)
C(8)-C(9)-C(10)-C(11)	2.5(13)
O(1)-C(9)-C(10)-C(11)	-177.9(8)
C(9)-C(10)-C(11)-O(2)	178.6(8)
C(9)-C(10)-C(11)-C(12)	-2.9(14)
C(14)-O(2)-C(11)-C(10)	-177.8(8)
C(14)-O(2)-C(11)-C(12)	3.7(13)
C(8)-C(7)-C(12)-C(11)	-4.6(12)
C(1)-C(7)-C(12)-C(11)	176.8(7)
C(10)-C(11)-C(12)-C(7)	4.0(13)
O(2)-C(11)-C(12)-C(7)	-177.6(8)
C(3)-C(2)-C(15)-C(20)	-15.4(7)
C(1)-C(2)-C(15)-C(20)	-130.3(6)
C(3)-C(2)-C(15)-C(16)	172.1(7)
C(1)-C(2)-C(15)-C(16)	57.2(9)
C(21)-O(3)-C(16)-C(15)	-171.8(7)
C(21)-O(3)-C(16)-C(17)	12.1(11)
C(20)-C(15)-C(16)-O(3)	-174.5(6)
C(2)-C(15)-C(16)-O(3)	-2.5(11)
C(20)-C(15)-C(16)-C(17)	1.7(10)
C(2)-C(15)-C(16)-C(17)	173.7(6)
O(3)-C(16)-C(17)-C(18)	174.0(7)
C(15)-C(16)-C(17)-C(18)	-2.0(11)
C(22)-O(4)-C(18)-C(19)	-4.9(11)

C(22)-O(4)-C(18)-C(17)	173.8(7)
C(16)-C(17)-C(18)-C(19)	1.1(11)
C(16)-C(17)-C(18)-O(4)	-177.5(6)
O(4)-C(18)-C(19)-C(20)	178.5(6)
C(17)-C(18)-C(19)-C(20)	0.0(11)
C(16)-C(15)-C(20)-C(19)	-0.5(10)
C(2)-C(15)-C(20)-C(19)	-174.0(6)
C(16)-C(15)-C(20)-C(23)	173.0(6)
C(2)-C(15)-C(20)-C(23)	-0.4(7)
C(18)-C(19)-C(20)-C(15)	-0.3(10)
C(18)-C(19)-C(20)-C(23)	-172.8(6)
C(15)-C(20)-C(23)-C(3)	16.3(7)
C(19)-C(20)-C(23)-C(3)	-170.4(6)
C(15)-C(20)-C(23)-C(24)	140.8(6)
C(19)-C(20)-C(23)-C(24)	-46.0(9)
C(4)-C(3)-C(23)-C(20)	-155.9(6)
C(2)-C(3)-C(23)-C(20)	-25.6(7)
C(4)-C(3)-C(23)-C(24)	74.0(8)
C(2)-C(3)-C(23)-C(24)	-155.7(6)
C(20)-C(23)-C(24)-C(39)	-78.0(8)
C(3)-C(23)-C(24)-C(39)	42.1(9)
C(20)-C(23)-C(24)-C(25)	52.4(8)
C(3)-C(23)-C(24)-C(25)	172.5(6)
C(39)-C(24)-C(25)-C(26)	-167.6(6)
C(23)-C(24)-C(25)-C(26)	61.1(9)
C(39)-C(24)-C(25)-C(30)	12.7(10)
C(23)-C(24)-C(25)-C(30)	-118.7(7)
C(30)-C(25)-C(26)-C(27)	2.6(10)
C(24)-C(25)-C(26)-C(27)	-177.2(6)
C(25)-C(26)-C(27)-C(28)	-3.4(10)
C(25)-C(26)-C(27)-C(31)	178.1(7)
C(26)-C(27)-C(28)-O(5)	-178.5(6)
C(31)-C(27)-C(28)-O(5)	0.0(10)
C(26)-C(27)-C(28)-C(29)	3.2(11)
C(31)-C(27)-C(28)-C(29)	-178.4(7)
C(27)-C(28)-C(29)-C(30)	-2.2(11)
O(5)-C(28)-C(29)-C(30)	179.6(6)
C(27)-C(28)-C(29)-C(35)	178.0(7)
O(5)-C(28)-C(29)-C(35)	-0.2(11)
C(28)-C(29)-C(30)-C(25)	1.2(11)
C(35)-C(29)-C(30)-C(25)	-179.0(7)

C(26)-C(25)-C(30)-C(29)	-1.4(11)
C(24)-C(25)-C(30)-C(29)	178.3(6)
C(28)-C(27)-C(31)-C(32)	179.7(7)
C(26)-C(27)-C(31)-C(32)	-1.9(10)
C(28)-C(27)-C(31)-C(33)	59.9(9)
C(26)-C(27)-C(31)-C(33)	-121.7(7)
C(28)-C(27)-C(31)-C(34)	-59.9(10)
C(26)-C(27)-C(31)-C(34)	118.4(8)
C(30)-C(29)-C(35)-C(36)	2.0(9)
C(28)-C(29)-C(35)-C(36)	-178.2(7)
C(30)-C(29)-C(35)-C(37)	120.4(8)
C(28)-C(29)-C(35)-C(37)	-59.8(9)
C(30)-C(29)-C(35)-C(38)	-114.9(7)
C(28)-C(29)-C(35)-C(38)	65.0(9)
C(25)-C(24)-C(39)-C(40)	102.2(8)
C(23)-C(24)-C(39)-C(40)	-128.0(7)
C(25)-C(24)-C(39)-C(44)	-76.4(8)
C(23)-C(24)-C(39)-C(44)	53.4(10)
C(44)-C(39)-C(40)-C(41)	1.9(11)
C(24)-C(39)-C(40)-C(41)	-176.8(7)
C(39)-C(40)-C(41)-C(42)	-2.1(11)
C(39)-C(40)-C(41)-C(45)	177.2(7)
C(40)-C(41)-C(42)-O(6)	-179.3(6)
C(45)-C(41)-C(42)-O(6)	1.4(10)
C(40)-C(41)-C(42)-C(43)	2.1(11)
C(45)-C(41)-C(42)-C(43)	-177.2(7)
O(6)-C(42)-C(43)-C(44)	179.4(6)
C(41)-C(42)-C(43)-C(44)	-2.1(11)
O(6)-C(42)-C(43)-C(49)	-0.6(11)
C(41)-C(42)-C(43)-C(49)	177.9(7)
C(42)-C(43)-C(44)-C(39)	1.9(11)
C(49)-C(43)-C(44)-C(39)	-178.1(7)
C(40)-C(39)-C(44)-C(43)	-1.8(11)
C(24)-C(39)-C(44)-C(43)	176.8(7)
C(40)-C(41)-C(45)-C(47)	-117.0(8)
C(42)-C(41)-C(45)-C(47)	62.3(9)
C(40)-C(41)-C(45)-C(48)	120.3(7)
C(42)-C(41)-C(45)-C(48)	-60.4(10)
C(40)-C(41)-C(45)-C(46)	3.3(10)
C(42)-C(41)-C(45)-C(46)	-177.4(7)
C(44)-C(43)-C(49)-C(52)	0.0(11)

C(42)-C(43)-C(49)-C(52)	180.0(7)
C(44)-C(43)-C(49)-C(50)	119.3(7)
C(42)-C(43)-C(49)-C(50)	-60.7(9)
C(44)-C(43)-C(49)-C(51)	-121.6(8)
C(42)-C(43)-C(49)-C(51)	58.4(9)
C(5)-C(4)-C(53)-C(54)	0.8(10)
C(3)-C(4)-C(53)-C(54)	-179.4(6)
C(57)-O(7)-C(54)-C(53)	173.2(6)
C(57)-O(7)-C(54)-C(55)	-8.6(10)
C(4)-C(53)-C(54)-O(7)	176.6(6)
C(4)-C(53)-C(54)-C(55)	-1.7(11)
O(7)-C(54)-C(55)-C(56)	-176.8(6)
C(53)-C(54)-C(55)-C(56)	1.4(10)
C(58)-O(8)-C(56)-C(5)	-178.7(6)
C(58)-O(8)-C(56)-C(55)	2.3(10)
C(4)-C(5)-C(56)-O(8)	-179.6(5)
C(6)-C(5)-C(56)-O(8)	-1.8(9)
C(4)-C(5)-C(56)-C(55)	-0.6(10)
C(6)-C(5)-C(56)-C(55)	177.2(6)
C(54)-C(55)-C(56)-O(8)	178.7(6)
C(54)-C(55)-C(56)-C(5)	-0.2(11)
C(5)-C(6)-C(59)-C(60)	-48.0(10)
C(1)-C(6)-C(59)-C(60)	79.9(9)
C(5)-C(6)-C(59)-C(64)	139.6(8)
C(1)-C(6)-C(59)-C(64)	-92.5(9)
C(64)-C(59)-C(60)-C(61)	-4.0(12)
C(6)-C(59)-C(60)-C(61)	-176.8(7)
C(59)-C(60)-C(61)-C(62)	0.1(13)
C(65)-O(9)-C(62)-C(63)	-176.9(9)
C(65)-O(9)-C(62)-C(61)	4.7(14)
C(60)-C(61)-C(62)-C(63)	2.2(14)
C(60)-C(61)-C(62)-O(9)	-179.5(8)
O(9)-C(62)-C(63)-C(64)	-178.7(8)
C(61)-C(62)-C(63)-C(64)	-0.3(14)
C(62)-C(63)-C(64)-C(59)	-3.8(14)
C(60)-C(59)-C(64)-C(63)	5.9(13)
C(6)-C(59)-C(64)-C(63)	178.6(8)

REFERENCES CITED:

- (1) Global Nutraceuticals Market Players to Find Promising Growth Opportunities in Asia Pacific <http://www.transparencymarketresearch.com/pressrelease/global-nutraceuticals-product-market.htm>.
- (2) Ames, B. N.; Shigenaga, M. K.; Hagen, T. M. Oxidants, Antioxidants, and the Degenerative Diseases of Aging. *Proc. Natl. Acad. Sci.* **1993**, *90* (17), 7915–7922.
- (3) Valko, M.; Leibfritz, D.; Moncol, J.; Cronin, M. T. D.; Mazur, M.; Telser, J. Free Radicals and Antioxidants in Normal Physiological Functions and Human Disease. *Int. J. Biochem. Cell Biol.* **2007**, *39* (1), 44–84.
- (4) Siemann, E. H.; Creasy, L. L. Concentration of the Phytoalexin Resveratrol in Wine. *Am. J. Enol. Vitic.* **1992**, *43* (1), 49–52.
- (5) Renaud, S.; de Lorgeril, M. Wine, Alcohol, Platelets, and the French Paradox for Coronary Heart Disease. *The Lancet* **1992**, *339* (8808), 1523–1526.
- (6) Law, M.; Stampfer, M.; Barker, D. J. P.; Mackenbach, J. P.; Wald, N.; Rimm, E.; Kunst, A. E. Why Heart Disease Mortality Is Low in France: The Time Lag Explanation. *BMJ* **1999**, *318* (7196), 1471–1480.
- (7) Fuchs, F. D.; Chambless, L. E. Is the Cardioprotective Effect of Alcohol Real? *Alcohol* **2007**, *41* (6), 399–402.
- (8) Walton, A. G. Are Red Wine And Chocolate Not So Healthy After All? <http://www.forbes.com/sites/alicegwalton/2014/05/12/new-study-questions-benefit-of-chocolate-and-red-wine-antioxidant/>.
- (9) Vogt, T. Phenylpropanoid Biosynthesis. *Mol. Plant* **2010**, *3* (1), 2–20.
- (10) Schöppner, A.; Kindl, H. Purification and Properties of a Stilbene Synthase from Induced Cell Suspension Cultures of Peanut. *J. Biol. Chem.* **1984**, *259* (11), 6806–6811.
- (11) Vannozzi, A.; Dry, I. B.; Fasoli, M.; Zenoni, S.; Lucchin, M. Genome-Wide Analysis of the Grapevine Stilbene Synthase Multigenic Family: Genomic Organization and Expression Profiles upon Biotic and Abiotic Stresses. *BMC Plant Biol.* **2012**, *12* (1), 130.
- (12) Ingham, J. L. 3,5,4'-Trihydroxystilbene as a Phytoalexin from Groundnuts (*Arachis hypogaea*). *Phytochemistry* **1976**, *15* (11), 1791–1793.
- (13) Flamini, R.; Mattivi, F.; Rosso, M. D.; Arapitsas, P.; Bavaresco, L. Advanced Knowledge of Three Important Classes of Grape Phenolics: Anthocyanins, Stilbenes and Flavonols. *Int. J. Mol. Sci.* **2013**, *14* (10), 19651–19669.
- (14) Regev-Shoshani, G.; Shoseyov, O.; Bilkis, I.; Kerem, Z. Glycosylation of Resveratrol Protects It from Enzymic Oxidation. *Biochem. J.* **2003**, *374* (Pt 1), 157–163.
- (15) Sako, M.; Hosokawa, H.; Ito, T.; Inuma, M. Regioselective Oxidative Coupling of 4-Hydroxystilbenes: Synthesis of Resveratrol and ϵ -Viniferin (E)-Dehydrodimers. *J. Org. Chem.* **2004**, *69* (7), 2598–2600.
- (16) Yang, N.-C.; Lee, C.-H.; Song, T.-Y. Evaluation of Resveratrol Oxidation in Vitro and the Crucial Role of Bicarbonate Ions. *Biosci. Biotechnol. Biochem.* **2010**, *74* (1), 63–68.
- (17) Corduneanu, O.; Janeiro, P.; Brett, A. M. O. On the Electrochemical Oxidation of Resveratrol. *Electroanalysis* **2006**, *18* (8), 757–762.

- (18) Lamb, C.; Dixon, R. A. The Oxidative Burst in Plant Disease Resistance. *Annu. Rev. Plant Physiol. Plant Mol. Biol.* **1997**, *48* (1), 251–275.
- (19) Keylor, M. H.; Matsuura, B. S.; Stephenson, C. R. J. Chemistry and Biology of Resveratrol-Derived Natural Products. *Chem. Rev.* **2015**, *115* (17), 8976–9027.
- (20) Solomon, E. I.; Sundaram, U. M.; Machonkin, T. E. Multicopper Oxidases and Oxygenases. *Chem. Rev.* **1996**, *96* (7), 2563–2606.
- (21) Breuil, A.-C.; Adrian, M.; Pirio, N.; Meunier, P.; Bessis, R.; Jeandet, P. Metabolism of Stilbene Phytoalexins by *Botrytis Cinerea*: 1. Characterization of a Resveratrol Dehydrodimer. *Tetrahedron Lett.* **1998**, *39* (7), 537–540.
- (22) Pezet, R. Purification and Characterization of a 32-kDa Laccase-like Stilbene Oxidase Produced by *Botrytis Cinerea* Pers.:Fr. *FEMS Microbiol. Lett.* **1998**, *167* (2), 203–208.
- (23) Cichewicz, R. H.; Kouzi, S. A.; Hamann, M. T. Dimerization of Resveratrol by the Grapevine Pathogen *Botrytis Cinerea*. *J. Nat. Prod.* **2000**, *63* (1), 29–33.
- (24) Isaac, I. S.; Dawson, J. H. Haem Iron-Containing Peroxidases. *Essays Biochem.* **1999**, *34*, 51–69.
- (25) Langcake, P.; Pryce, R. J. Oxidative Dimerisation of 4-Hydroxystilbenes in Vitro: Production of a Grapevine Phytoalexin Mimic. *J. Chem. Soc. Chem. Commun.* **1977**, No. 7, 208–210.
- (26) Langcake, P.; Pryce, R. J. A New Class of Phytoalexins from Grapevines. *Experientia* **1977**, *33* (2), 151–152.
- (27) Takaya, Y.; Terashima, K.; Ito, J.; He, Y.-H.; Tateoka, M.; Yamaguchi, N.; Niwa, M. Biomimic Transformation of Resveratrol. *Tetrahedron* **2005**, *61* (43), 10285–10290.
- (28) Li, C.; Lu, J.; Xu, X.; Hu, R.; Pan, Y. pH-Switched HRP-Catalyzed Dimerization of Resveratrol: A Selective Biomimetic Synthesis. *Green Chem.* **2012**, *14* (12), 3281–3284.
- (29) Ducrot, P.-H.; Kollmann, A.; Bala, A. E.; Majira, A.; Kerhoas, L.; Delorme, R.; Einhorn, J. Cyphostemmins A-B, Two New Antifungal Oligostilbenes from *Cyphostemma Crotalarioides* (Vitaceae). *Tetrahedron Lett.* **1998**, *39* (52), 9655–9658.
- (30) Adesanya, S. A.; Nia, R.; Martin, M.-T.; Boukamcha, N.; Montagnac, A.; Païs, M. Stilbene Derivatives from *Cissus Quadrangularis*. *J. Nat. Prod.* **1999**, *62* (12), 1694–1695.
- (31) Langcake, P. Disease Resistance of *Vitis* Spp. and the Production of the Stress Metabolites Resveratrol, ϵ -Viniferin, α -Viniferin and Pterostilbene. *Physiol. Plant Pathol.* **1981**, *18* (2), 213–226.
- (32) Lins, A. P.; Ribeiro, M. N. D. S.; Gottlieb, O. R.; Gottlieb, H. E. Gnetins: Resveratrol Oligomers From *Gnetum* Species. *J. Nat. Prod.* **1982**, *45* (6), 754–761.
- (33) Davin, L. B.; Wang, H.-B.; Crowell, A. L.; Bedgar, D. L.; Martin, D. M.; Sarkanen, S.; Lewis, N. G. Stereoselective Bimolecular Phenoxy Radical Coupling by an Auxiliary (Dirigent) Protein Without an Active Center. *Science* **1997**, *275* (5298), 362–367.
- (34) Kim, K.-W.; Smith, C. A.; Daily, M. D.; Cort, J. R.; Davin, L. B.; Lewis, N. G. Trimeric Structure of (+)-Pinoresinol-Forming Dirigent Protein at 1.95 Å Resolution with Three Isolated Active Sites. *J. Biol. Chem.* **2015**, *290* (3), 1308–1318.
- (35) Cichewicz, R. H.; Kouzi, S. A. Resveratrol Oligomers: Structure, Chemistry, and Biological Activity. In *Studies in Natural Products Chemistry*; Atta-ur-Rahman, Ed.; Bioactive Natural Products; Elsevier, 2002; Vol. Volume 26, Part G, pp 507–579.

- (36) Pezet, R.; Gindro, K.; Viret, O.; Spring, J.-L. Glycosylation and Oxidative Dimerization of Resveratrol Are Respectively Associated to Sensitivity and Resistance of Grapevine Cultivars to Downy Mildew. *Physiol. Mol. Plant Pathol.* **2004**, *65* (6), 297–303.
- (37) Pickel, B.; Constantin, M.-A.; Pfannstiel, J.; Conrad, J.; Beifuss, U.; Schaller, A. An Enantiocomplementary Dirigent Protein for the Enantioselective Laccase-Catalyzed Oxidative Coupling of Phenols. *Angew. Chem. Int. Ed.* **2010**, *49* (1), 202–204.
- (38) Suzuki, K.; Shimizu, T.; Kawabata, J.; Mizutani, J. New 3, 5, 4'-Trihydroxystilbene (Resveratrol) Oligomers from *Carex Fedia* Nees Var. *Miyabei* (Franchet) T. Koyama (Cyperaceae). *Agric. Biol. Chem.* **1987**, *51* (4), 1003–1008.
- (39) Jiang, L.; He, S.; Sun, C.; Pan, Y. Selective Singlet Oxygen Quenchers, Oligostilbenes, from *Vitis Wilsonae*: Structural Identification and Biogenetic Relationship. *Phytochemistry* **2012**, *77*, 294–303.
- (40) Sarker, S. D.; Whiting, P.; Dinan, L.; Šik, V.; Rees, H. H. Identification and Ecdysteroid Antagonist Activity of Three Resveratrol Trimers (Suffruticosols A, B and C) from *Paeonia Suffruticosa*. *Tetrahedron* **1999**, *55* (2), 513–524.
- (41) Wang, S.-G.; Ma, D.-Y.; Hu, C.-Q. Two New Oligostilbenes from *Caragana Sinica*. *J. Asian Nat. Prod. Res.* **2004**, *6* (4), 241–248.
- (42) Jang, M.; Cai, L.; Udeani, G. O.; Slowing, K. V.; Thomas, C. F.; Beecher, C. W. W.; Fong, H. H. S.; Farnsworth, N. R.; Kinghorn, A. D.; Mehta, R. G.; Moon, R. C.; Pezzuto, J. M. Cancer Chemopreventive Activity of Resveratrol, a Natural Product Derived from Grapes. *Science* **1997**, *275* (5297), 218–220.
- (43) Bhat, K. P. I.; Pezzuto, J. M. Cancer Chemopreventive Activity of Resveratrol. *Ann. N. Y. Acad. Sci.* **2002**, *957* (1), 210–229.
- (44) Howitz, K. T.; Bitterman, K. J.; Cohen, H. Y.; Lamming, D. W.; Lavu, S.; Wood, J. G.; Zipkin, R. E.; Chung, P.; Kisielewski, A.; Zhang, L.-L.; Scherer, B.; Sinclair, D. A. Small Molecule Activators of Sirtuins Extend *Saccharomyces Cerevisiae* Lifespan. *Nature* **2003**, *425* (6954), 191–196.
- (45) Wood, J. G.; Rogina, B.; Lavu, S.; Howitz, K.; Helfand, S. L.; Tatar, M.; Sinclair, D. Sirtuin Activators Mimic Caloric Restriction and Delay Ageing in Metazoans. *Nature* **2004**, *430* (7000), 686–689.
- (46) Baur, J. A.; Pearson, K. J.; Price, N. L.; Jamieson, H. A.; Lerin, C.; Kalra, A.; Prabhu, V. V.; Allard, J. S.; Lopez-Lluch, G.; Lewis, K.; Pistell, P. J.; Poesala, S.; Becker, K. G.; Boss, O.; Gwinn, D.; Wang, M.; Ramaswamy, S.; Fishbein, K. W.; Spencer, R. G.; Lakatta, E. G.; Le Couteur, D.; Shaw, R. J.; Navas, P.; Puigserver, P.; Ingram, D. K.; de Cabo, R.; Sinclair, D. A. Resveratrol Improves Health and Survival of Mice on a High-Calorie Diet. *Nature* **2006**, *444* (7117), 337–342.
- (47) Sajish, M.; Schimmel, P. A Human tRNA Synthetase Is a Potent PARP1-Activating Effector Target for Resveratrol. *Nature* **2015**, *519* (7543), 370–373.
- (48) He, S.; Yan, X. From Resveratrol to Its Derivatives: New Sources of Natural Antioxidant. *Curr. Med. Chem.* **2013**, *20* (8), 1005–1017.
- (49) Carrizzo, A.; Forte, M.; Damato, A.; Trimarco, V.; Salzano, F.; Bartolo, M.; Maciag, A.; Puca, A. A.; Vecchione, C. Antioxidant Effects of Resveratrol in Cardiovascular, Cerebral and Metabolic Diseases. *Food Chem. Toxicol.* **2013**, *61*, 215–226.
- (50) Aggarwal, B. B.; Bhardwaj, A.; Aggarwal, R. S.; Seeram, N. P.; Shishodia, S.; Takada, Y. Role of Resveratrol in Prevention and Therapy of Cancer: Preclinical and Clinical Studies. *Anticancer Res.* **2004**, *24* (5A), 2783–2840.

- (51) Das, M.; Das, D. K. Resveratrol and Cardiovascular Health. *Phytochem. Cardiovasc. Prot.* **2010**, *31* (6), 503–512.
- (52) Beher, D.; Wu, J.; Cumine, S.; Kim, K. W.; Lu, S.-C.; Atangan, L.; Wang, M. Resveratrol Is Not a Direct Activator of SIRT1 Enzyme Activity. *Chem. Biol. Drug Des.* **2009**, *74* (6), 619–624.
- (53) Pacholec, M.; Bleasdale, J. E.; Chrnyk, B.; Cunningham, D.; Flynn, D.; Garofalo, R. S.; Griffith, D.; Griffor, M.; Loulakis, P.; Pabst, B.; Qiu, X.; Stockman, B.; Thanabal, V.; Varghese, A.; Ward, J.; Withka, J.; Ahn, K. SRT1720, SRT2183, SRT1460, and Resveratrol Are Not Direct Activators of SIRT1. *J. Biol. Chem.* **2010**, *285* (11), 8340–8351.
- (54) Hubbard, B. P.; Gomes, A. P.; Dai, H.; Li, J.; Case, A. W.; Considine, T.; Riera, T. V.; Lee, J. E.; E, S. Y.; Lamming, D. W.; Pentelute, B. L.; Schuman, E. R.; Stevens, L. A.; Ling, A. J. Y.; Armour, S. M.; Michan, S.; Zhao, H.; Jiang, Y.; Sweitzer, S. M.; Blum, C. A.; Disch, J. S.; Ng, P. Y.; Howitz, K. T.; Rolo, A. P.; Hamuro, Y.; Moss, J.; Perni, R. B.; Ellis, J. L.; Vlasuk, G. P.; Sinclair, D. A. Evidence for a Common Mechanism of SIRT1 Regulation by Allosteric Activators. *Science* **2013**, *339* (6124), 1216–1219.
- (55) Mitchell, S. J.; Martin-Montalvo, A.; Mercken, E. M.; Palacios, H. H.; Ward, T. M.; Abulwerdi, G.; Minor, R. K.; Vlasuk, G. P.; Ellis, J. L.; Sinclair, D. A.; Dawson, J.; Allison, D. B.; Zhang, Y.; Becker, K. G.; Bernier, M.; de Cabo, R. The SIRT1 Activator SRT1720 Extends Lifespan and Improves Health of Mice Fed a Standard Diet. *Cell Rep.* **2014**, *6* (5), 836–843.
- (56) Pezzuto, J. M. The Phenomenon of Resveratrol: Redefining the Virtues of Promiscuity. *Ann. N. Y. Acad. Sci.* **2011**, *1215* (1), 123–130.
- (57) Vang, O.; Ahmad, N.; Baile, C. A.; Baur, J. A.; Brown, K.; Csiszar, A.; Das, D. K.; Delmas, D.; Gottfried, C.; Lin, H.-Y.; Ma, Q.-Y.; Mukhopadhyay, P.; Nalini, N.; Pezzuto, J. M.; Richard, T.; Shukla, Y.; Surh, Y.-J.; Szekeres, T.; Szkudelski, T.; Walle, T.; Wu, J. M. What Is New for an Old Molecule? Systematic Review and Recommendations on the Use of Resveratrol. *PLoS ONE* **2011**, *6* (6), e19881.
- (58) Walle, T. Bioavailability of Resveratrol. *Ann. N. Y. Acad. Sci.* **2011**, *1215* (1), 9–15.
- (59) Francioso, A.; Mastromarino, P.; Masci, A.; d'Erme, M.; Mosca, L. Chemistry, Stability and Bioavailability of Resveratrol. *Med. Chem.* **2014**, *10* (3), 237–245.
- (60) Yamada, M.; Hayashi, K.; Ikeda, S.; Tsutsui, K.; Tsutsui, K.; Ito, T.; Inuma, M.; Nozaki, H. Inhibitory Activity of Plant Stilbene Oligomers against DNA Topoisomerase II. *Biol. Pharm. Bull.* **2006**, *29* (7), 1504–1507.
- (61) Lee, S.; Yoon, K. D.; Lee, M.; Cho, Y.; Choi, G.; Jang, H.; Kim, B.; Jung, D.-H.; Oh, J.-G.; Kim, G.-W.; Oh, J.-W.; Jeong, Y.-J.; Kwon, H. J.; Bae, S. K.; Min, D.-H.; Windisch, M. P.; Heo, T.-H.; Lee, C. Identification of a Resveratrol Tetramer as a Potent Inhibitor of Hepatitis C Virus Helicase. *Br. J. Pharmacol.* **2016**, *173* (1), 191–211.
- (62) Vilums, M.; Heuberger, J.; Heitman, L. H.; IJzerman, A. P. Indanes—Properties, Preparation, and Presence in Ligands for G Protein Coupled Receptors. *Med. Res. Rev.* **2015**, *35* (6), 1097–1126.
- (63) Cosenzi, A. Enrasentan, an Antagonist of Endothelin Receptors. *Cardiovasc. Drug Rev.* **2003**, *21* (1), 1–16.
- (64) Liu, J. Y.; Ye, Y. H.; Wang, L.; Shi, D. H.; Tan, R. X. New Resveratrol Oligomers from the Stem Bark of *Hopea Hainanensis*. *Helv. Chim. Acta* **2005**, *88* (11), 2910–2917.

- (65) Johari, A. T. T. Antioxidant, Antimicrobial and Cytotoxic Activities of Resveratrol Oligomers of Shorea Macroptera Dyer. *Aust. J. Basic Appl. Sci.* **2012**, *6* (8), 431–436.
- (66) Patcharamun, W.; Sichaem, J.; Siripong, P.; Khumkratok, S.; Jong-aramruang, J.; Tippyang, S. A New Dimeric Resveratrol from the Roots of Shorea Roxburghii. *Fitoterapia* **2011**, *82* (3), 489–492.
- (67) Ito, T.; Akao, Y.; Yi, H.; Ohguchi, K.; Matsumoto, K.; Tanaka, T.; Iinuma, M.; Nozawa, Y. Antitumor Effect of Resveratrol Oligomers against Human Cancer Cell Lines and the Molecular Mechanism of Apoptosis Induced by Vaticanol C. *Carcinogenesis* **2003**, *24* (9), 1489–1497.
- (68) Colin, D.; Gimazane, A.; Lizard, G.; Izard, J.-C.; Solary, E.; Latruffe, N.; Delmas, D. Effects of Resveratrol Analogs on Cell Cycle Progression, Cell Cycle Associated Proteins and 5-Fluoro-Uracil Sensitivity in Human Derived Colon Cancer Cells. *Int. J. Cancer* **2009**, *124* (12), 2780–2788.
- (69) Ito, T.; Akao, Y.; Tanaka, T.; Iinuma, M.; Nozawa, Y. Vaticanol C, a Novel Resveratrol Tetramer, Inhibits Cell Growth through Induction of Apoptosis in Colon Cancer Cell Lines. *Biol. Pharm. Bull.* **2002**, *25* (1), 147–148.
- (70) Marel, A.-K.; Lizard, G.; Izard, J.-C.; Latruffe, N.; Delmas, D. Inhibitory Effects of Trans-Resveratrol Analogs Molecules on the Proliferation and the Cell Cycle Progression of Human Colon Tumoral Cells. *Mol. Nutr. Food Res.* **2008**, *52* (5), 538–548.
- (71) Chowdhury, S. A.; Kishino, K.; Satoh, R.; Hashimoto, K.; Kikuchi, H.; Nishikawa, H.; Shirataki, Y.; Sakagami, H. Tumor-Specificity and Apoptosis-Inducing Activity of Stilbenes and Flavonoids. *Anticancer Res.* **2005**, *25* (3B), 2055–2063.
- (72) Ito, T.; Tanaka, T.; Nakaya, K.; Iinuma, M.; Takahashi, Y.; Naganawa, H.; Ohyama, M.; Nakanishi, Y.; Bastow, K. F.; Lee, K.-H. A Novel Bridged Stilbenoid Trimer and Four Highly Condensed Stilbenoid Oligomers in Vatica Rassak. *Tetrahedron* **2001**, *57* (34), 7309–7321.
- (73) Seo, E.-K.; Chai, H.; Constant, H. L.; Santisuk, T.; Reutrakul, V.; Beecher, C. W. W.; Farnsworth, N. R.; Cordell, G. A.; Pezzuto, J. M.; Kinghorn, A. D. Resveratrol Tetramers from Vatica Diospyroides. *J. Org. Chem.* **1999**, *64* (19), 6976–6983.
- (74) Ohyama, M.; Tanaka, T.; Ito, T.; Iinuma, M.; Bastow, K. F.; Lee, K.-H. Antitumor Agents 200.1 Cytotoxicity of Naturally Occurring Resveratrol Oligomers and Their Acetate Derivatives. *Bioorg. Med. Chem. Lett.* **1999**, *9* (20), 3057–3060.
- (75) Ito, T.; Tanaka, T.; Nakaya, K.; Iinuma, M.; Takahashi, Y.; Naganawa, H.; Ohyama, M.; Nakanishi, Y.; Bastow, K. F.; Lee, K.-H. A New Resveratrol Octamer, Vateriaphenol A, in Vateria Indica. *Tetrahedron Lett.* **2001**, *42* (34), 5909–5912.
- (76) Qiao, H.; Chen, X.; Xu, L.; Wang, J.; Zhao, G.; Hou, Y.; Ge, H. M.; Tan, R.-X.; Li, E. Antitumor Effects of Naturally Occurring Oligomeric Resveratrol Derivatives. *FASEB J.* **2013**, *27* (11), 4561–4571.
- (77) Choi, C.-W.; Choi, Y.-H.; Cha, M.-R.; Yoo, D.-S.; Kim, Y.-S.; Yon, G.-H.; Choi, S.-U.; Kim, Y.-H.; Ryu, S.-Y. A New Glycoside of Resveratrol Dimer from Stem Bark of Vitis Vinifera. *Bull. Korean Chem. Soc.* **2010**, *31* (11), 3448–3450.
- (78) Wibowo, A.; Ahmat, N.; Hamzah, A. S.; Sufian, A. S.; Ismail, N. H.; Ahmad, R.; Jaafar, F. M.; Takayama, H. Malaysianol A, a New Trimer Resveratrol Oligomer from the Stem Bark of Dryobalanops Aromatica. *Fitoterapia* **2011**, *82* (4), 676–681.
- (79) Sheng, Z. Effects of Miyabenol C on Protein Kinase C in Two Lung Carcinoma Cell Lines. *Shanghai Yike Daxue Xuebao* **1999**, *26* (6), 395.

- (80) Zhi, S.; Guang, X. Growth Inhibitory Effect of Stilbenoids on Lung Cancer Lines. *Shanghai Yike Daxue Xuebao* **1998**, *25*, 327–330.
- (81) González-Sarriás, A.; Gromek, S.; Niesen, D.; Seeram, N. P.; Henry, G. E. Resveratrol Oligomers Isolated from Carex Species Inhibit Growth of Human Colon Tumorigenic Cells Mediated by Cell Cycle Arrest. *J. Agric. Food Chem.* **2011**, *59* (16), 8632–8638.
- (82) Kim, H.-J.; Lee, W.-J.; Park, Y.-H.; Cho, S.-H.; Choi, S.-W. Differential Effects of Resveratrol and Its Oligomers Isolated from Seeds of Paeonia Lactiflora (Peony) on Proliferation of MCF - 7 and ROS 17 / 2.8 Cells. *J. Food Sci. Nutr.* **2003**, *8* (4), 356–364.
- (83) Kim, H.; Chang, E.; Bae, S.; Shim, S.; Park, H.; Rhee, C.; Park, J.; Choi, S. Cytotoxic and Antimutagenic Stilbenes from Seeds of Paeonia Lactiflora. *Arch. Pharm. Res.* **2002**, *25* (3), 293–299.
- (84) Xuan, L.; Shi, J.; Yao, C.; Bai, J.; Qu, F.; Zhang, J.; Hou, Q. Vam3, a Resveratrol Dimer, Inhibits Cigarette Smoke-Induced Cell Apoptosis in Lungs by Improving Mitochondrial Function. *Acta Pharmacol. Sin.* **2014**, *35* (6), 779–791.
- (85) Lim, K. G.; Gray, A. I.; Pyne, S.; Pyne, N. J. Resveratrol Dimers Are Novel Sphingosine Kinase 1 Inhibitors and Affect Sphingosine Kinase 1 Expression and Cancer Cell Growth and Survival. *Br. J. Pharmacol.* **2012**, *166* (5), 1605–1616.
- (86) Li, L.; Henry, G. E.; Seeram, N. P. Identification and Bioactivities of Resveratrol Oligomers and Flavonoids from Carex Folliculata Seeds. *J. Agric. Food Chem.* **2009**, *57* (16), 7282–7287.
- (87) Cheng, Y.-Q.; Jiang, R.; Huang, W.; Wei, W.; Chen, C.-J.; Tan, R.-X.; Ge, H.-M. Hopeachinols E–K, Novel Oligostilbenoids from the Stem Bark of Hopea Chinensis. *RSC Adv.* **2014**, *4* (55), 28901–28907.
- (88) Shibata, M.-A.; Akao, Y.; Shibata, E.; Nozawa, Y.; Ito, T.; Mishima, S.; Morimoto, J.; Otsuki, Y. Vaticanol C, a Novel Resveratrol Tetramer, Reduces Lymph Node and Lung Metastases of Mouse Mammary Carcinoma Carrying p53 Mutation. *Cancer Chemother. Pharmacol.* **2007**, *60* (5), 681–691.
- (89) Colin, D.; Lancon, A.; Delmas, D.; Lizard, G.; Abrossinow, J.; Kahn, E.; Jannin, B.; Latruffe, N. Antiproliferative Activities of Resveratrol and Related Compounds in Human Hepatocyte Derived HepG2 Cells Are Associated with Biochemical Cell Disturbance Revealed by Fluorescence Analyses. *Biochimie* **2008**, *90* (11–12), 1674–1684.
- (90) Muhtadi; Hakim, E. H.; Juliawaty, L. D.; Syah, Y. M.; Achmad, S. A.; Latip, J.; Ghisalberti, E. L. Cytotoxic Resveratrol Oligomers from the Tree Bark of Dipterocarpus Hasseltii. *Fitoterapia* **2006**, *77* (7–8), 550–555.
- (91) Ohguchi, K.; Akao, Y.; Matsumoto, K.; Tanaka, T.; Ito, T.; Inuma, M.; Nozawa, Y. Vaticanol C-Induced Cell Death Is Associated with Inhibition of Pro-Survival Signaling in HL60 Human Leukemia Cell Line. *Biosci. Biotechnol. Biochem.* **2005**, *69* (2), 353–356.
- (92) Quiney, C.; Dauzonne, D.; Kern, C.; Fourneron, J.-D.; Izard, J.-C.; Mohammad, R. M.; Kolb, J.-P.; Billard, C. Flavones and Polyphenols Inhibit the NO Pathway during Apoptosis of Leukemia B-Cells. *Leuk. Res.* **2004**, *28* (8), 851–861.
- (93) Barjot, C.; Tournaire, M.; Castagnino, C.; Vigor, C.; Vercauteren, J.; Rossi, J.-F. Evaluation of Antitumor Effects of Two Vine Stalk Oligomers of Resveratrol on a Panel of Lymphoid and Myeloid Cell Lines: Comparison with Resveratrol. *Life Sci.* **2007**, *81* (23–24), 1565–1574.

- (94) Kang, J. H.; Park, Y. H.; Choi, S. W.; Yang, E. K.; Lee, W. J. Resveratrol Derivatives Potently Induce Apoptosis in Human Promyelocytic Leukemia Cells. *Exp. Mol. Med.* **2003**, *35* (6), 467–474.
- (95) Ito, T.; Tanaka, T.; Ali, Z.; Akao, Y.; Nozawa, Y.; Takahashi, Y.; Sawa, R.; Nakaya, K.; Murata, J.; Darnaedi, D.; Iinuma, M. A New Resveratrol Hexamer from *Upuna Borneensis*. *Heterocycles* **2004**, *63* (1), 129.
- (96) Ito, T.; Iliya, I.; Tanaka, T.; Nakaya, K.; Akao, Y.; Nozawa, Y.; Murata, J.; Darnaedi, D.; Iinuma, M. Stilbenoids from Leaves of *Upuna Borneensis*. *Heterocycles* **2005**, *65* (1), 173–179.
- (97) Iliya, I.; Akao, Y.; Matsumoto, K.; Nakagawa, Y.; Zulfiqar, A.; Ito, T.; Oyama, M.; Murata, H.; Tanaka, T.; Nozawa, Y.; Iinuma, M. Growth Inhibition of Stilbenoids in Welwitschiaceae and Gnetaceae through Induction of Apoptosis in Human Leukemia HL60 Cells. *Biol. Pharm. Bull.* **2006**, *29* (7), 1490–1492.
- (98) Jang, M.; Cho, E. J.; Piao, X.-L. Protective Effects of Resveratrol Oligomers from *Vitis Amurensis* against Sodium Nitroprusside-Induced Neurotoxicity in Human Neuroblastoma SH-SY5Y Cells. *Arch. Pharm. Res.* **2014**, 1–7.
- (99) Mishima, S.; Matsumoto, K.; Futamura, Y.; Araki, Y.; Ito, T.; Tanaka, T.; Iinuma, M.; Nozawa, Y.; Akao, Y. Antitumor Effect of Stilbenoids from *Vateria Indica* against Allografted Sarcoma S-180 in Animal Model. *J. Exp. Ther. Oncol.* **2003**, *3* (5), 283–288.
- (100) Lee, E.-O.; Kwon, B.-M.; Song, G.-Y.; Chae, C.-H.; Kim, H.-M.; Shim, I.-S.; Ahn, K.-S.; Kim, S.-H. Heyneanol A Induces Apoptosis via Cytochrome c Release and Caspase Activation in Human Leukemic U937 Cells. *Life Sci.* **2004**, *74* (18), 2313–2326.
- (101) Sheppard, T. D. Strategies for the Synthesis of 2,3-Dihydrobenzofurans. *J. Chem. Res.* **2011**, *35* (7), 377–385.
- (102) Di Micco, S.; Spatafora, C.; Cardullo, N.; Riccio, R.; Fischer, K.; Pergola, C.; Koeberle, A.; Werz, O.; Chalal, M.; Vervandier-Fasseur, D.; Tringali, C.; Bifulco, G. 2,3-Dihydrobenzofuran Privileged Structures as New Bioinspired Lead Compounds for the Design of mPGES-1 Inhibitors. *Bioorg. Med. Chem.* **2016**, *24* (4), 820–826.
- (103) Illuminati, G.; Mandolini, L. Ring Closure Reactions of Bifunctional Chain Molecules. *Acc. Chem. Res.* **1981**, *14* (4), 95–102.
- (104) Bråkenhielm, E.; Cao, R.; Cao, Y. Suppression of Angiogenesis, Tumor Growth, and Wound Healing by Resveratrol, a Natural Compound in Red Wine and Grapes. *FASEB J.* **2001**, *15* (10), 1798–1800.
- (105) Subbaramaiah, K.; Chung, W. J.; Michaluart, P.; Telang, N.; Tanabe, T.; Inoue, H.; Jang, M.; Pezzuto, J. M.; Dannenberg, A. J. Resveratrol Inhibits Cyclooxygenase-2 Transcription and Activity in Phorbol Ester-Treated Human Mammary Epithelial Cells. *J. Biol. Chem.* **1998**, *273* (34), 21875–21882.
- (106) Billard, C.; Izard, J.-C.; Roman, V.; Kern, C.; Mathiot, C.; Mentz, F.; Kolb, J.-P. Comparative Antiproliferative and Apoptotic Effects of Resveratrol, ϵ -Viniferin and Vine-Shots Derived Polyphenols (Vineatrols) on Chronic B Lymphocytic Leukemia Cells and Normal Human Lymphocytes. *Leuk. Lymphoma* **2002**, *43* (10), 1991–2002.
- (107) Zghonda, N.; Yoshida, S.; Araki, M.; Kusunoki, M.; Mliki, A.; Ghorbel, A.; Miyazaki, H. Greater Effectiveness of ϵ -Viniferin in Red Wine Than Its Monomer Resveratrol for Inhibiting Vascular Smooth Muscle Cell Proliferation and Migration. *Biosci. Biotechnol. Biochem.* **2011**, *75* (7), 1259–1267.

- (108) Paine, A.; Eiz-Vesper, B.; Blasczyk, R.; Immenschuh, S. Signaling to Heme Oxygenase-1 and Its Anti-Inflammatory Therapeutic Potential. *Biochem. Pharmacol.* **2010**, *80* (12), 1895–1903.
- (109) Martin, D.; Rojo, A. I.; Salinas, M.; Diaz, R.; Gallardo, G.; Alam, J.; Galarreta, C. M. R. de; Cuadrado, A. Regulation of Heme Oxygenase-1 Expression through the Phosphatidylinositol 3-Kinase/Akt Pathway and the Nrf2 Transcription Factor in Response to the Antioxidant Phytochemical Carnosol. *J. Biol. Chem.* **2004**, *279* (10), 8919–8929.
- (110) Xu, G.; Zhang, L. P.; Chen, L. F.; Hu, C. Q. Inhibition of protein kinase C by stilbenoids. *Yao Xue Xue Bao* **1994**, *29* (11), 818–822.
- (111) Kulanthaivel, P. Naturally Occurring Protein Kinase C Inhibitors; II. Isolation of Oligomeric Stilbenes from. *Planta Med.* **1995**, *61* (1), 41–44.
- (112) Lee, S.-H.; Shin, N.-H.; Kang, S.-H.; Park, J.; Chung, S.; Min, K.; Kim, Y. α -Viniferin: A Prostaglandin H2 Synthase Inhibitor from Root of *Carex Humilis*. *Planta Med.* **1998**, *64* (3), 204–207.
- (113) Chung, E. Y.; Kim, B. H.; Lee, M. K.; Yun, Y.-P.; Lee, S. H.; Min, K. R.; Kim, Y. Anti-Inflammatory Effect of the Oligomeric Stilbene Alpha-Viniferin and Its Mode of the Action through Inhibition of Cyclooxygenase-2 and Inducible Nitric Oxide Synthase. *Planta Med.* **2003**, *69* (8), 710–714.
- (114) Dilshara, M. G.; Lee, K.-T.; Kim, H. J.; Lee, H.-J.; Choi, Y. H.; Lee, C.-M.; Kim, L. K.; Kim, G.-Y. Anti-Inflammatory Mechanism of α -Viniferin Regulates Lipopolysaccharide-Induced Release of Proinflammatory Mediators in BV2 Microglial Cells. *Cell. Immunol.* **2014**, *290* (1), 21–29.
- (115) Tsukamoto, T.; Nakata, R.; Tamura, E.; Kosuge, Y.; Kariya, A.; Katsukawa, M.; Mishima, S.; Ito, T.; Inuma, M.; Akao, Y.; Nozawa, Y.; Arai, Y.; Namura, S.; Inoue, H. Vatanol C, a Resveratrol Tetramer, Activates PPAR α and PPAR β/δ in Vitro and in Vivo. *Nutr. Metab.* **2010**, *7* (1), 46.
- (116) Ohguchi, K.; Tanaka, T.; Ito, T.; Inuma, M.; Matsumoto, K.; Akao, Y.; Nozawa, Y. Inhibitory Effects of Resveratrol Derivatives from Dipterocarpaceae Plants on Tyrosinase Activity. *Biosci. Biotechnol. Biochem.* **2003**, *67* (7), 1587–1589.
- (117) Sung, S. H.; Kang, S. Y.; Lee, K. Y.; Park, M. J.; Kim, J. H.; Park, J. H.; Kim, Y. C.; Kim, J.; Kim, Y. C. Alpha-Viniferin, a Stilbene Trimer from *Caragana Chamglague*, Inhibits Acetylcholinesterase. *Biol. Pharm. Bull.* **2002**, *25* (1), 125–127.
- (118) Bobrowska-Hägerstrand, M.; Lillås, M.; Mrówczyńska, L.; Wróbel, A.; Shirataki, Y.; Motohashi, N.; Hägerstrand, H. Resveratrol Oligomers Are Potent MRP1 Transport Inhibitors. *Anticancer Res.* **2006**, *26* (3A), 2081–2084.
- (119) Munoz, M.; Henderson, M.; Haber, M.; Norris, M. Role of the MRP1/ABCC1 Multidrug Transporter Protein in Cancer. *IUBMB Life* **2007**, *59* (12), 752–757.
- (120) Chung, E. Y.; Roh, E.; Kwak, J.-A.; Lee, H.-S.; Lee, S. H.; Lee, C.-K.; Han, S.-B.; Kim, Y. Alpha-Viniferin Suppresses the Signal Transducer and Activation of Transcription-1 (STAT-1)–Inducible Inflammatory Genes in Interferon-Gamma-Stimulated Macrophages. *J. Pharmacol. Sci.* **2010**, *112* (4), 405–414.
- (121) Bach, E. A.; Aguet, M.; Schreiber, R. D. THE IFN γ Receptor: A Paradigm for Cytokine Receptor Signaling. *Annu. Rev. Immunol.* **1997**, *15* (1), 563–591.
- (122) Chang, F.; Steelman, L. S.; Lee, J. T.; Shelton, J. G.; Navolanic, P. M.; Blalock, W. L.; Franklin, R. A.; McCubrey, J. A. Signal Transduction Mediated by the

- Ras/Raf/MEK/ERK Pathway from Cytokine Receptors to Transcription Factors: Potential Targeting for Therapeutic Intervention. *Leukemia* **2003**, *17* (7), 1263–1293.
- (123) Courtney, K. D.; Corcoran, R. B.; Engelman, J. A. The PI3K Pathway As Drug Target in Human Cancer. *J. Clin. Oncol.* **2010**, *28* (6), 1075–1083.
- (124) Amorati, R.; Ferroni, F.; Pedulli, G. F.; Valgimigli, L. Modeling the Co-Antioxidant Behavior of Monofunctional Phenols. Applications to Some Relevant Compounds. *J. Org. Chem.* **2003**, *68* (25), 9654–9658.
- (125) Matsuura, B. S.; Keylor, M. H.; Li, B.; Lin, Y.; Allison, S.; Pratt, D. A.; Stephenson, C. R. J. A Scalable Biomimetic Synthesis of Resveratrol Dimers and Systematic Evaluation of Their Antioxidant Activities. *Angew. Chem. Int. Ed.* **2015**, *54* (12), 3754–3757.
- (126) Itoh, K.; Wakabayashi, N.; Katoh, Y.; Ishii, T.; Igarashi, K.; Engel, J. D.; Yamamoto, M. Keap1 Represses Nuclear Activation of Antioxidant Responsive Elements by Nrf2 through Binding to the Amino-Terminal Neh2 Domain. *Genes Dev.* **1999**, *13* (1), 76–86.
- (127) Hong, F.; Sekhar, K. R.; Freeman, M. L.; Liebler, D. C. Specific Patterns of Electrophile Addition Trigger Keap1 Ubiquitination and Nrf2 Activation. *J. Biol. Chem.* **2005**, *280* (36), 31768–31775.
- (128) Suzuki, T.; Motohashi, H.; Yamamoto, M. Toward Clinical Application of the Keap1–Nrf2 Pathway. *Trends Pharmacol. Sci.* **2013**, *34* (6), 340–346.
- (129) Magesh, S.; Chen, Y.; Hu, L. Small Molecule Modulators of Keap1-Nrf2-ARE Pathway as Potential Preventive and Therapeutic Agents. *Med. Res. Rev.* **2012**, *32* (4), 687–726.
- (130) Fourquet, S.; Guerois, R.; Biard, D.; Toledano, M. B. Activation of NRF2 by Nitrosative Agents and H₂O₂ Involves KEAP1 Disulfide Formation. *J. Biol. Chem.* **2010**, *285* (11), 8463–8471.
- (131) Hourihan, J. M.; Kenna, J. G.; Hayes, J. D. The Gasotransmitter Hydrogen Sulfide Induces Nrf2-Target Genes by Inactivating the Keap1 Ubiquitin Ligase Substrate Adaptor Through Formation of a Disulfide Bond Between Cys-226 and Cys-613. *Antioxid. Redox Signal.* **2012**, *19* (5), 465–481.
- (132) Forman, H. J.; Davies, K. J. A.; Ursini, F. How Do Nutritional Antioxidants Really Work: Nucleophilic Tone and Para-Hormesis versus Free Radical Scavenging in Vivo. *Free Radic. Biol. Med.* **2014**, *66*, 24–35.
- (133) Jeffrey, J. L.; Sarpong, R. Concise Synthesis of Pauciflorol F Using a Larock Annulation. *Org. Lett.* **2009**, *11* (23), 5450–5453.
- (134) Nicolaou, K. C.; Wu, T. R.; Kang, Q.; Chen, D. Y.-K. Total Synthesis of Hopeahainol A and Hopeanol. *Angew. Chem. Int. Ed.* **2009**, *48* (19), 3440–3443.
- (135) Nicolaou, K. C.; Kang, Q.; Wu, T. R.; Lim, C. S.; Chen, D. Y.-K. Total Synthesis and Biological Evaluation of the Resveratrol-Derived Polyphenol Natural Products Hopeanol and Hopeahainol A. *J. Am. Chem. Soc.* **2010**, *132* (21), 7540–7548.
- (136) Snyder, S. A.; Zografos, A. L.; Lin, Y. Total Synthesis of Resveratrol-Based Natural Products: A Chemoselective Solution. *Angew. Chem. Int. Ed.* **2007**, *46* (43), 8186–8191.
- (137) Snyder, S. A.; Breazzano, S. P.; Ross, A. G.; Lin, Y.; Zografos, A. L. Total Synthesis of Diverse Carbogenic Complexity within the Resveratrol Class from a Common Building Block. *J. Am. Chem. Soc.* **2009**, *131* (5), 1753–1765.
- (138) Snyder, S. A.; Gollner, A.; Chiriac, M. I. Regioselective Reactions for Programmable Resveratrol Oligomer Synthesis. *Nature* **2011**, *474* (7352), 461–466.

- (139) Snyder, S. A.; Wright, N. E.; Pflueger, J. J.; Breazzano, S. P. Total Syntheses of Heimiol A, Hopeahainol D, and Constrained Analogues. *Angew. Chem. Int. Ed.* **2011**, *50* (37), 8629–8633.
- (140) Snyder, S. A.; Brill, Z. G. Structural Revision and Total Synthesis of Caraphenol B and C. *Org. Lett.* **2011**, *13* (20), 5524–5527.
- (141) Snyder, S. A.; Thomas, S. B.; Mayer, A. C.; Breazzano, S. P. Total Syntheses of Hopeanol and Hopeahainol A Empowered by a Chiral Brønsted Acid Induced Pinacol Rearrangement. *Angew. Chem. Int. Ed.* **2012**, *51* (17), 4080–4084.
- (142) Wright, N. E.; Snyder, S. A. 9-Membered Carbocycle Formation: Development of Distinct Friedel–Crafts Cyclizations and Application to a Scalable Total Synthesis of (±)-Caraphenol A. *Angew. Chem.* **2014**, *126* (13), 3477–3481.
- (143) Jepsen, T. H.; Thomas, S. B.; Lin, Y.; Stathakis, C. I.; de Miguel, I.; Snyder, S. A. Harnessing Quinone Methides: Total Synthesis of (±)-Vaticanol A. *Angew. Chem. Int. Ed.* **2014**, *53* (26), 6747–6751.
- (144) Klotter, F.; Studer, A. Total Synthesis of Resveratrol-Based Natural Products Using a Palladium-Catalyzed Decarboxylative Arylation and an Oxidative Heck Reaction. *Angew. Chem. Int. Ed.* **2014**, *53* (9), 2473–2476.
- (145) Kuttruff, C. A.; Eastgate, M. D.; Baran, P. S. Natural Product Synthesis in the Age of Scalability. *Nat. Prod. Rep.* **2014**, *31* (4), 419–432.
- (146) Robinson, R. LXIII.—A Synthesis of Tropinone. *J. Chem. Soc. Trans.* **1917**, *111* (0), 762–768.
- (147) Newman, D. J.; Cragg, G. M. Natural Products As Sources of New Drugs over the 30 Years from 1981 to 2010. *J. Nat. Prod.* **2012**, *75* (3), 311–335.
- (148) Cragg, G. M.; Grothaus, P. G.; Newman, D. J. New Horizons for Old Drugs and Drug Leads. *J. Nat. Prod.* **2014**, *77* (3), 703–723.
- (149) Nicotra, S.; Cramarossa, M. R.; Mucci, A.; Pagnoni, U. M.; Riva, S.; Forti, L. Biotransformation of Resveratrol: Synthesis of Trans-Dehydrodimers Catalyzed by Laccases from Myceliophthora Thermophyla and from Trametes Pubescens. *Tetrahedron* **2004**, *60* (3), 595–600.
- (150) Ponzoni, C.; Beneventi, E.; Cramarossa, M. R.; Raimondi, S.; Trevisi, G.; Pagnoni, U. M.; Riva, S.; Forti, L. Laccase-Catalyzed Dimerization of Hydroxystilbenes. *Adv. Synth. Catal.* **2007**, *349* (8–9), 1497–1506.
- (151) Wang, M.; Jin, Y.; Ho, C.-T. Evaluation of Resveratrol Derivatives as Potential Antioxidants and Identification of a Reaction Product of Resveratrol and 2,2-Diphenyl-1-Picrylhydrazyl Radical. *J. Agric. Food Chem.* **1999**, *47* (10), 3974–3977.
- (152) Shang, Y.-J.; Qian, Y.-P.; Liu, X.-D.; Dai, F.; Shang, X.-L.; Jia, W.-Q.; Liu, Q.; Fang, J.-G.; Zhou, B. Radical-Scavenging Activity and Mechanism of Resveratrol-Oriented Analogues: Influence of the Solvent, Radical, and Substitution. *J. Org. Chem.* **2009**, *74* (14), 5025–5031.
- (153) Fan, G.-J.; Liu, X.-D.; Qian, Y.-P.; Shang, Y.-J.; Li, X.-Z.; Dai, F.; Fang, J.-G.; Jin, X.-L.; Zhou, B. 4,4'-Dihydroxy-Trans-Stilbene, a Resveratrol Analogue, Exhibited Enhanced Antioxidant Activity and Cytotoxicity. *Bioorg. Med. Chem.* **2009**, *17* (6), 2360–2365.
- (154) Song, T.; Zhou, B.; Peng, G.-W.; Zhang, Q.-B.; Wu, L.-Z.; Liu, Q.; Wang, Y. Aerobic Oxidative Coupling of Resveratrol and Its Analogues by Visible Light Using

- Mesoporous Graphitic Carbon Nitride (Mpg-C₃N₄) as a Bioinspired Catalyst. *Chem. – Eur. J.* **2014**, *20* (3), 678–682.
- (155) Panzella, L.; De Lucia, M.; Amalfitano, C.; Pezzella, A.; Evidente, A.; Napolitano, A.; d’Ischia, M. Acid-Promoted Reaction of the Stilbene Antioxidant Resveratrol with Nitrite Ions: Mild Phenolic Oxidation at the 4’-Hydroxystyryl Sector Triggering Nitration, Dimerization, and Aldehyde-Forming Routes. *J. Org. Chem.* **2006**, *71* (11), 4246–4254.
- (156) Yao, C.-S.; Lin, M.; Wang, Y.-H. Synthesis of the Active Stilbenoids by Photooxidation Reaction of Trans- ϵ -Viniferin. *Chin. J. Chem.* **2004**, *22* (11), 1350–1355.
- (157) Velu, S. S.; Buniyamin, I.; Ching, L. K.; Feroz, F.; Noorbacha, I.; Gee, L. C.; Awang, K.; Wahab, I. A.; Weber, J.-F. F. Regio- and Stereoselective Biomimetic Synthesis of Oligostilbenoid Dimers from Resveratrol Analogues: Influence of the Solvent, Oxidant, and Substitution. *Chem. - Eur. J.* **2008**, *14* (36), 11376–11384.
- (158) Hong, F.-J.; Low, Y.-Y.; Chong, K.-W.; Thomas, N. F.; Kam, T.-S. Biomimetic Oxidative Dimerization of Anodically Generated Stilbene Radical Cations: Effect of Aromatic Substitution on Product Distribution and Reaction Pathways. *J. Org. Chem.* **2014**, *79* (10), 4528–4543.
- (159) Wang, G.-W.; Wang, H.-L.; Capretto, D. A.; Han, Q.; Hu, R.-B.; Yang, S.-D. Tf₂O-Catalyzed Friedel–Crafts Alkylation to Synthesize Dibenzo[a,d]cycloheptene Cores and Application in the Total Synthesis of Diptoindonesin D, Pauciflorial F, and (\pm)-Ampelopsin B. *Tetrahedron* **2012**, *68* (26), 5216–5222.
- (160) Lewis, N.; Morgan, I. A Facile and Mild De-Tert-Butylation Reaction. *Synth. Commun.* **1988**, *18* (15), 1783–1793.
- (161) Saleh, S. A.; Tashtoush, H. I. De-Tert-Butylation of Substituted Arenes. *Tetrahedron* **1998**, *54* (47), 14157–14177.
- (162) Müller, E.; Mayer, R.; Spanagel, H.-D.; Scheffler, K. Über Sauerstoffradikale, XIX. Dehydrierung Hydroxyphenyl-Substituierter Äthylene. *Justus Liebigs Ann. Chem.* **1961**, *645* (1), 53–65.
- (163) Becker, H. D. New Stable Phenoxy Radicals. Oxidation of Hydroxystilbenes. *J. Org. Chem.* **1969**, *34* (5), 1211–1215.
- (164) Sarkanen, K. V.; Wallis, A. F. A. Oxidative Dimerizations of (E)- and (Z)-Isoeugenol (2-Methoxy-4-pro-Penylphenol) and (E)- and (Z)-2,6-Dimethoxy-4-Propenylphenol. *J. Chem. Soc. [Perkin 1]* **1973**, No. 0, 1869–1878.
- (165) Li, W.; Li, H.; Li, Y.; Hou, Z. Total Synthesis of (\pm)-Quadrangularin A. *Angew. Chem. Int. Ed.* **2006**, *45* (45), 7609–7611.
- (166) Li, W.; Li, H.; Luo, Y.; Yang, Y.; Wang, N. Biosynthesis of Resveratrol Dimers by Regioselective Oxidative Coupling Reaction. *Synlett* **2010**, *4*, 1247–1250.
- (167) Yang, Y.; Liu, Q.; Chen, P.; Li, W. FeCl₃·6H₂O Oxidation of Protected Resveratrol for the Synthesis of Tetraarylfuran-Type Oligostilbenes. *Tetrahedron Lett.* **2014**, *55* (32), 4455–4457.
- (168) Ramberg, L.; Bäcklund, B. The Reactions of Some Monohalogen Derivatives of Diethyl Sulfone. *Ark. Kemi Minerat Geol* **1940**, *13A*, 50.
- (169) Meyers, C. Y.; Malte, A. M.; Matthews, W. S. Ionic Reactions of Carbon Tetrachloride. Survey of Reactions with Ketones, Alcohols, and Sulfones. *J. Am. Chem. Soc.* **1969**, *91* (26), 7510–7512.

- (170) Chou, C.-M.; Chatterjee, I.; Studer, A. Stereospecific Palladium-Catalyzed Decarboxylative C(sp³)–C(sp²) Coupling of 2,5-Cyclohexadiene-1-Carboxylic Acid Derivatives with Aryl Iodides. *Angew. Chem. Int. Ed.* **2011**, *50* (37), 8614–8617.
- (171) Zhong, C.; Zhu, J.; Chang, J.; Sun, X. Concise Total Syntheses of (±)isopaucifloral F, (±)quadrangularin A, and (±)pallidol. *Tetrahedron Lett.* **2011**, *52* (22), 2815–2817.
- (172) Prier, C. K.; Rankic, D. A.; MacMillan, D. W. C. Visible Light Photoredox Catalysis with Transition Metal Complexes: Applications in Organic Synthesis. *Chem. Rev.* **2013**, *113* (7), 5322–5363.
- (173) Tucker, J. W.; Stephenson, C. R. J. Shining Light on Photoredox Catalysis: Theory and Synthetic Applications. *J. Org. Chem.* **2012**, *77* (4), 1617–1622.
- (174) Kalyanasundaram, K. Photophysics, Photochemistry and Solar Energy Conversion with tris(bipyridyl)ruthenium(II) and Its Analogues. *Coord. Chem. Rev.* **1982**, *46*, 159–244.
- (175) Juris, A.; Balzani, V.; Barigelletti, F.; Campagna, S.; Belser, P.; von Zelewsky, A. Ru(II) Polypyridine Complexes: Photophysics, Photochemistry, Electrochemistry, and Chemiluminescence. *Coord. Chem. Rev.* **1988**, *84*, 85–277.
- (176) Beatty, J. W.; Stephenson, C. R. J. Amine Functionalization via Oxidative Photoredox Catalysis: Methodology Development and Complex Molecule Synthesis. *Acc. Chem. Res.* **2015**, *48* (5), 1474–1484.
- (177) Lowry, M. S.; Goldsmith, J. I.; Slinker, J. D.; Rohl, R.; Pascal, R. A.; Malliaras, G. G.; Bernhard, S. Single-Layer Electroluminescent Devices and Photoinduced Hydrogen Production from an Ionic Iridium(III) Complex. *Chem. Mater.* **2005**, *17* (23), 5712–5719.
- (178) Nguyen, J. D.; Tucker, J. W.; Konieczynska, M. D.; Stephenson, C. R. J. Intermolecular Atom Transfer Radical Addition to Olefins Mediated by Oxidative Quenching of Photoredox Catalysts. *J. Am. Chem. Soc.* **2011**, *133* (12), 4160–4163.
- (179) Tucker, J. W.; Narayanam, J. M. R.; Shah, P. S.; Stephenson, C. R. J. Oxidative Photoredox Catalysis: Mild and Selective Deprotection of PMB Ethers Mediated by Visible Light. *Chem. Commun.* **2011**, *47* (17), 5040–5042.
- (180) Collin, J.-P.; Dixon, I. M.; Sauvage, J.-P.; Williams, J. A. G.; Barigelletti, F.; Flamigni, L. Synthesis and Photophysical Properties of Iridium(III) Bisterpyridine and Its Homologues: A Family of Complexes with a Long-Lived Excited State. *J. Am. Chem. Soc.* **1999**, *121* (21), 5009–5016.
- (181) Leslie, W.; Batsanov, A. S.; Howard, J. A. K.; Williams, J. A. G. Cross-Couplings in the Elaboration of Luminescent Bis-Terpyridyl Iridium Complexes: The Effect of Extended or Inhibited Conjugation on Emission. *Dalton Trans.* **2004**, No. 4, 623–631.
- (182) Turro, N. J.; Ramamurthy, V.; Sciano, J. C. Modern Molecular Photochemistry of Organic Molecules; University Science Books: Sausalito, Calif, 2010; pp 1001–1042.
- (183) Toteva, M. M.; Richard, J. P. The Generation and Reactions of Quinone Methides. In *Advances in Physical Organic Chemistry*; John P. Richard, Ed.; Academic Press, 2011; Vol. Volume 45, pp 39–91.
- (184) Gordon, H. L.; Freeman, S.; Hudlicky, T. Stability Relationships in Bicyclic Ketones. *Synlett* **2005**, No. 19, 2911–2914.
- (185) Yoshino, H.; Tsuchiya, Y.; Saito, I.; Tsujii, M. Promoting Effect of Pentamethylbenzene on the Deprotection of O-Benzyltyrosine and Epsilon-Benzylloxycarbonyllysine with Trifluoroacetic Acid. *Chem. Pharm. Bull. (Tokyo)* **1987**, *35* (8), 3438–3441.

- (186) Okano, K.; Okuyama, K.; Fukuyama, T.; Tokuyama, H. Mild Debenzylation of Aryl Benzyl Ether with BCl_3 in the Presence of Pentamethylbenzene as a Non-Lewis-Basic Cation Scavenger. *Synlett* **2008**, No. 13, 1977–1980.
- (187) Porter, N. A. Mechanisms for the Autoxidation of Polyunsaturated Lipids. *Acc. Chem. Res.* **1986**, *19* (9), 262–268.
- (188) Pratt, D. A.; Tallman, K. A.; Porter, N. A. Free Radical Oxidation of Polyunsaturated Lipids: New Mechanistic Insights and the Development of Peroxyl Radical Clocks. *Acc. Chem. Res.* **2011**, *44* (6), 458–467.
- (189) Yin, H.; Xu, L.; Porter, N. A. Free Radical Lipid Peroxidation: Mechanisms and Analysis. *Chem. Rev.* **2011**, *111* (10), 5944–5972.
- (190) Halliwell, B.; Gutteridge, J. *Free Radicals in Biology and Medicine*, Fourth Edition.; Oxford University Press, 2007.
- (191) Burton, G. W.; Ingold, K. U. Vitamin E: Application of the Principles of Physical Organic Chemistry to the Exploration of Its Structure and Function. *Acc. Chem. Res.* **1986**, *19* (7), 194–201.
- (192) Ingold, K. U.; Pratt, D. A. Advances in Radical-Trapping Antioxidant Chemistry in the 21st Century: A Kinetics and Mechanisms Perspective. *Chem. Rev.* **2014**, *114* (18), 9022–9046.
- (193) Li, B.; Pratt, D. A. Methods for Determining the Efficacy of Radical-Trapping Antioxidants. *Free Radic. Biol. Med.* **2015**, *82*, 187–202.
- (194) R, A.; Luca Valgimigli. Advantages and Limitations of Common Testing Methods for Antioxidants. *Free Radic. Res.* **2015**, *49*, 633–649.
- (195) Foti, M. C. Use and Abuse of the DPPH• Radical. *J. Agric. Food Chem.* **2015**, *63* (40), 8765–8776.
- (196) Roschek, B.; Tallman, K. A.; Rector, C. L.; Gillmore, J. G.; Pratt, D. A.; Punta, C.; Porter, N. A. Peroxyl Radical Clocks. *J. Org. Chem.* **2006**, *71* (9), 3527–3532.
- (197) Hanthorn, J. J.; Pratt, D. A. Peroxyesters As Precursors to Peroxyl Radical Clocks. *J. Org. Chem.* **2012**, *77* (1), 276–284.
- (198) Haidasz, E. A.; Van Kessel, A. T. M.; Pratt, D. A. A Continuous Visible Light Spectrophotometric Approach To Accurately Determine the Reactivity of Radical-Trapping Antioxidants. *J. Org. Chem.* **2016**, *81* (3), 737–744.
- (199) Tallman, K. A.; Pratt, D. A.; Porter, N. A. Kinetic Products of Linoleate Peroxidation: Rapid β -Fragmentation of Nonconjugated Peroxyls. *J. Am. Chem. Soc.* **2001**, *123* (47), 11827–11828.
- (200) Tallman, K. A.; Roschek, B.; Porter, N. A. Factors Influencing the Autoxidation of Fatty Acids: Effect of Olefin Geometry of the Nonconjugated Diene. *J. Am. Chem. Soc.* **2004**, *126* (30), 9240–9247.
- (201) Krumova, K.; Friedland, S.; Cosa, G. How Lipid Unsaturation, Peroxyl Radical Partitioning, and Chromanol Lipophilic Tail Affect the Antioxidant Activity of α -Tocopherol: Direct Visualization via High-Throughput Fluorescence Studies Conducted with Fluorogenic α -Tocopherol Analogues. *J. Am. Chem. Soc.* **2012**, *134* (24), 10102–10113.
- (202) Barclay, L. R. C. 1992 Syntex Award Lecture Model Biomembranes: Quantitative Studies of Peroxidation, Antioxidant Action, Partitioning, and Oxidative Stress. *Can. J. Chem.* **1993**, *71* (1), 1–16.

- (203) Niki, E.; Noguchi, N. Dynamics of Antioxidant Action of Vitamin E. *Acc. Chem. Res.* **2004**, *37* (1), 45–51.
- (204) Jeandet, P.; Hébrard, C.; Deville, M.-A.; Cordelier, S.; Dorey, S.; Aziz, A.; Crouzet, J. Deciphering the Role of Phytoalexins in Plant-Microorganism Interactions and Human Health. *Molecules* **2014**, *19* (11), 18033–18056.
- (205) Harborne, J. B. The Role of Phytoalexins in Natural Plant Resistance. In *Natural Resistance of Plants to Pests*; ACS Symposium Series; American Chemical Society, 1986; Vol. 296, pp 22–35.
- (206) Snyder, S. A.; ElSohly, A. M.; Kontes, F. Synthetic Approaches to Oligomeric Natural Products. *Nat. Prod. Rep.* **2011**, *28* (5), 897–924.
- (207) Jansen, D. J.; Shenvi, R. A. Synthesis of Medicinally Relevant Terpenes: Reducing the Cost and Time of Drug Discovery. *Future Med. Chem.* **2014**, *6* (10), 1127–1148.
- (208) Niwa, M.; He, Y.-H.; Takaya, Y.; Terashima, K. Determination of Absolute Structure of (+)-Davidiol A. *Heterocycles* **2006**, *68* (1), 93.
- (209) Wilkens, A.; Paulsen, J.; Wray, V.; Winterhalter, P. Structures of Two Novel Trimeric Stilbenes Obtained by Horseradish Peroxidase Catalyzed Biotransformation of Trans-Resveratrol and (–)- ϵ -Viniferin. *J. Agric. Food Chem.* **2010**, *58* (11), 6754–6761.
- (210) Takaya, Y.; Yan, K.-X.; Terashima, K.; He, Y.-H.; Niwa, M. Biogenetic Reactions on Stilbenetetramers from Vitaceae Plants. *Tetrahedron* **2002**, *58* (45), 9265–9271.
- (211) Johnson, A. W.; LaCount, R. B. The Chemistry of Ylids. VI. Dimethylsulfonium Fluorenylide—A Synthesis of Epoxides I. *J. Am. Chem. Soc.* **1961**, *83* (2), 417–423.
- (212) Corey, E. J.; Chaykovsky, M. Dimethylsulfonium Methylide ((CH₃)₂SOCH₂) and Dimethylsulfonium Methylide ((CH₃)₂SCH₂). Formation and Application to Organic Synthesis. *J. Am. Chem. Soc.* **1965**, *87* (6), 1353–1364.
- (213) Meinwald, J.; Labana, S. S.; Chadha, M. S. Peracid Reactions. III. The Oxidation of Bicyclo [2.2.1]heptadiene. *J. Am. Chem. Soc.* **1963**, *85* (5), 582–585.
- (214) Poss, C. S.; Schreiber, S. L. Two-Directional Chain Synthesis and Terminus Differentiation. *Acc. Chem. Res.* **1994**, *27* (1), 9–17.
- (215) Magnuson, S. R. Two-Directional Synthesis and Its Use in Natural Product Synthesis. *Tetrahedron* **1995**, *51* (8), 2167–2213.
- (216) Staunton, J.; Weissman, K. J. Polyketide Biosynthesis: A Millennium Review. *Nat. Prod. Rep.* **2001**, *18* (4), 380–416.
- (217) Turro, N. J.; Lei, X.; Jockusch, S.; Li, W.; Liu, Z.; Abrams, L.; Ottaviani, M. F. EPR Investigation of Persistent Radicals Produced from the Photolysis of Dibenzyl Ketones Adsorbed on ZSM-5 Zeolites. *J. Org. Chem.* **2002**, *67* (8), 2606–2618.
- (218) Griller, D.; Ingold, K. U. Persistent Carbon-Centered Radicals. *Acc. Chem. Res.* **1976**, *9* (1), 13–19.
- (219) Gomberg, M. Triphenylmethyl, Ein Fall von Dreiwerthigem Kohlenstoff. *Berichte Dtsch. Chem. Ges.* **1900**, *33* (3), 3150–3163.
- (220) Gomberg, M. An Instance of Trivalent Carbon: Triphenylmethyl. *J. Am. Chem. Soc.* **1900**, *22* (11), 757–771.
- (221) McBride, J. M. The Hexaphenylethane Riddle. *Tetrahedron* **1974**, *30* (14), 2009–2022.
- (222) Ito, J.; Takaya, Y.; Oshima, Y.; Niwa, M. New Oligostilbenes Having a Benzofuran from *Vitis Vinifera* “Kyohou.” *Tetrahedron* **1999**, *55* (9), 2529–2544.

- (223) Kim, I.; Choi, J. A Versatile Approach to Oligostilbenoid Natural Products – Synthesis of Permethylated Analogues of Viniferifuran, Malibatol A, and Shoreaphenol. *Org. Biomol. Chem.* **2009**, *7* (13), 2788–2795.
- (224) Lindgren, A. E. G.; Öberg, C. T.; Hillgren, J. M.; Elofsson, M. Total Synthesis of the Resveratrol Oligomers (±)-Ampelopsin B and (±)- ϵ -Viniferin. *Eur. J. Org. Chem.* **2016**, *2016* (3), 426–429.
- (225) Liégault, B.; Lapointe, D.; Caron, L.; Vlassova, A.; Fagnou, K. Establishment of Broadly Applicable Reaction Conditions for the Palladium-Catalyzed Direct Arylation of Heteroatom-Containing Aromatic Compounds. *J. Org. Chem.* **2009**, *74* (5), 1826–1834.
- (226) Kim, K.; Kim, I. Total Synthesis of Diptoindonesin G via a Highly Efficient Domino Cyclodehydration/Intramolecular Friedel–Crafts Acylation/Regioselective Demethylation Sequence. *Org. Lett.* **2010**, *12* (22), 5314–5317.
- (227) Wohl, A. Bromierung Ungesättigter Verbindungen Mit N-Brom-Acetamid, Ein Beitrag Zur Lehre Vom Verlauf Chemischer Vorgänge. *Berichte Dtsch. Chem. Ges. B Ser.* **1919**, *52* (1), 51–63.
- (228) Ziegler, K.; Schenck, G.; Krockow, E. W.; Siebert, A.; Wenz, A.; Weber, H. Die Synthese Des Cantharidins. *Justus Liebigs Ann. Chem.* **1942**, *551* (1), 1–79.
- (229) Michaelis, A.; Kaehne, R. Ueber Das Verhalten Der Jodalkyle Gegen Die Sogen. Phosphorigsäureester Oder O-Phosphine. *Berichte Dtsch. Chem. Ges.* **1898**, *31* (1), 1048–1055.
- (230) Ishihara, K.; Kubota, M.; Kurihara, H.; Yamamoto, H. Scandium Trifluoromethanesulfonate as an Extremely Active Acylation Catalyst. *J. Am. Chem. Soc.* **1995**, *117* (15), 4413–4414.
- (231) Klebe, J. F.; Finkbeiner, H.; White, D. M. Silylations with Bis(trimethylsilyl)acetamide, a Highly Reactive Silyl Donor. *J. Am. Chem. Soc.* **1966**, *88* (14), 3390–3395.
- (232) Gibian, M. J.; Corley, R. C. Organic Radical-Radical Reactions. Disproportionation vs. Combination. *Chem. Rev.* **1973**, *73* (5), 441–464.
- (233) Soldi, C.; Lamb, K. N.; Squitieri, R. A.; González-López, M.; Di Maso, M. J.; Shaw, J. T. Enantioselective Intramolecular C–H Insertion Reactions of Donor–Donor Metal Carbenoids. *J. Am. Chem. Soc.* **2014**, *136* (43), 15142–15145.
- (234) Davies, H. M. L.; Grazini, M. V. A.; Aouad, E. Asymmetric Intramolecular C–H Insertions of Aryldiazoacetates. *Org. Lett.* **2001**, *3* (10), 1475–1477.
- (235) Saito, H.; Oishi, H.; Kitagaki, S.; Nakamura, S.; Anada, M.; Hashimoto, S. Enantio- and Diastereoselective Synthesis of Cis-2-Aryl-3-Methoxycarbonyl-2,3-Dihydrobenzofurans via the Rh(II)-Catalyzed C–H Insertion Process. *Org. Lett.* **2002**, *4* (22), 3887–3890.
- (236) Natori, Y.; Tsutsui, H.; Sato, N.; Nakamura, S.; Nambu, H.; Shiro, M.; Hashimoto, S. Asymmetric Synthesis of Neolignans (–)-Epi-Conocarpan and (+)-Conocarpan via Rh(II)-Catalyzed C–H Insertion Process and Revision of the Absolute Configuration of (–)-Epi-Conocarpan. *J. Org. Chem.* **2009**, *74* (11), 4418–4421.
- (237) Kurosawa, W.; Kan, T.; Fukuyama, T. Stereocontrolled Total Synthesis of (–)-Ephedradine A (Orantine). *J. Am. Chem. Soc.* **2003**, *125* (27), 8112–8113.
- (238) O'Malley, S. J.; Tan, K. L.; Watzke, A.; Bergman, R. G.; Ellman, J. A. Total Synthesis of (+)-Lithospermic Acid by Asymmetric Intramolecular Alkylation via Catalytic C–H Bond Activation. *J. Am. Chem. Soc.* **2005**, *127* (39), 13496–13497.
- (239) Koizumi, Y.; Kobayashi, H.; Wakimoto, T.; Furuta, T.; Fukuyama, T.; Kan, T. Total Synthesis of (–)-Serotobenine. *J. Am. Chem. Soc.* **2008**, *130* (50), 16854–16855.

- (240) Wakimoto, T.; Miyata, K.; Ohuchi, H.; Asakawa, T.; Nukaya, H.; Suwa, Y.; Kan, T. Enantioselective Total Synthesis of Aiperidine. *Org. Lett.* **2011**, *13* (10), 2789–2791.
- (241) Reddy, R. P.; Lee, G. H.; Davies, H. M. L. Dirhodium Tetracarboxylate Derived from Adamantylglycine as a Chiral Catalyst for Carbenoid Reactions. *Org. Lett.* **2006**, *8* (16), 3437–3440.
- (242) Kurosawa, W.; Kan, T.; Fukuyama, T. An Efficient Synthesis of Optically Active *Trans*-2-Aryl-2,3-Dihydrobenzofuran-3-carboxylic Acid Esters via C-H Insertion Reaction. *Synlett* **2003**, No. 7, 1028–1030.
- (243) Gore, P. H. The Friedel-Crafts Acylation Reaction and Its Application to Polycyclic Aromatic Hydrocarbons. *Chem. Rev.* **1955**, *55* (2), 229–281.
- (244) Newman, M. S.; Muth, C. W. The Behavior of 3-Methylphthalic Anhydride in Friedel—Crafts and Grignard Condensations. III. *J. Am. Chem. Soc.* **1950**, *72* (11), 5191–5193.
- (245) Mamone, P.; Danoun, G.; Gooßen, L. J. Rhodium-Catalyzed Ortho Acylation of Aromatic Carboxylic Acids. *Angew. Chem. Int. Ed.* **2013**, *52* (26), 6704–6708.
- (246) Little, A.; Porco, J. A. Total Syntheses of Graphisin A and Sydowinin B. *Org. Lett.* **2012**, *14* (11), 2862–2865.
- (247) O’Keefe, B. M.; Simmons, N.; Martin, S. F. Facile Access to Sterically Hindered Aryl Ketones via Carbonylative Cross-Coupling: Application to the Total Synthesis of Luteolin. *Tetrahedron* **2011**, *67* (24), 4344–4351.
- (248) Alder, K.; Rickert, H. F. Zur Kenntnis Der Dien-Synthese. I. Über Eine Methode Der Direkten Unterscheidung Cyclischer Penta- Und Hexa-Diene. *Justus Liebigs Ann. Chem.* **1936**, *524* (1), 180–189.
- (249) Danishefsky, S.; Singh, R. K.; Gammill, R. B. Diels-Alder Reactions of 1,1-Dimethoxy-3-Trimethylsilyloxy-1,3-Butadiene. *J. Org. Chem.* **1978**, *43* (2), 379–380.
- (250) Yang, Z.-Q.; Danishefsky, S. J. A Concise Route to Benzofused Macrolactones via Ynolides: Cyclopropanadicol. *J. Am. Chem. Soc.* **2003**, *125* (32), 9602–9603.
- (251) Dai, M.; Sarlah, D.; Yu, M.; Danishefsky, S. J.; Jones, G. O.; Houk, K. N. Highly Selective Diels-Alder Reactions of Directly Connected Enyne Dienophiles. *J. Am. Chem. Soc.* **2006**, *129* (3), 645–657.
- (252) Yoshino, T.; Ng, F.; Danishefsky, S. J. A Total Synthesis of Xestodecalactone A and Proof of Its Absolute Stereochemistry: Interesting Observations on Dienophilic Control with 1,3-Disubstituted Nonequivalent Allenes. *J. Am. Chem. Soc.* **2006**, *128* (43), 14185–14191.
- (253) Pünner, F.; Schieven, J.; Hilt, G. Synthesis of Fluorenone and Anthraquinone Derivatives from Aryl- and Aroyl-Substituted Propiolates. *Org. Lett.* **2013**, *15* (18), 4888–4891.
- (254) Bürgi, H. B.; Dunitz, J. D.; Lehn, J. M.; Wipff, G. Stereochemistry of Reaction Paths at Carbonyl Centres. *Tetrahedron* **1974**, *30* (12), 1563–1572.
- (255) Lin, Y. Studies towards Selective Synthesis of Resveratrol-Based Oligomeric Natural Products, Columbia University, 2012.
- (256) Tebbe, F. N.; Parshall, G. W.; Reddy, G. S. Olefin Homologation with Titanium Methylene Compounds. *J. Am. Chem. Soc.* **1978**, *100* (11), 3611–3613.
- (257) Nicolaou, K. C.; Koide, K.; Bunnage, M. E. Total Synthesis of Balanol and Designed Analogues. *Chem. – Eur. J.* **1995**, *1* (7), 454–466.
- (258) Bordwell, F. G. Equilibrium Acidities in Dimethyl Sulfoxide Solution. *Acc. Chem. Res.* **1988**, *21* (12), 456–463.

- (259) Zhang, X. M.; Bordwell, F. G. Equilibrium Acidities and Homolytic Bond Dissociation Energies of the Acidic Carbon-Hydrogen Bonds in P-Substituted Triphenylphosphonium Cations. *J. Am. Chem. Soc.* **1994**, *116* (3), 968–972.
- (260) Luo, H.-F.; Zhang, L.-P.; Hu, C.-Q. Five Novel Oligostilbenes from the Roots of *Caragana Sinica*. *Tetrahedron* **2001**, *57* (23), 4849–4854.
- (261) Ito, T.; Abe, N.; Oyama, M.; Inuma, M. Oligostilbenoids from Dipterocarpaceae Plants: A New Resveratrol Tetramer from *Vateria Indica* and the Revised Structure of Isohopeaphenol. *Helv. Chim. Acta* **2008**, *91* (10), 1989–1998.
- (262) Sotheeswaran, S.; Champika Diyasena, M. N.; Leslie Gunatilaka, A. A.; Bokel, M.; Kraus, W. Further Evidence for the Structure of Vaticaffinol and a Revision of Its Stereochemistry. *Phytochemistry* **1987**, *26* (5), 1505–1507.
- (263) Yamada, M.; Hayashi, K.; Hayashi, H.; Ikeda, S.; Hoshino, T.; Tsutsui, K.; Tsutsui, K.; Inuma, M.; Nozaki, H. Stilbenoids of *Kobresia Nepalensis* (Cyperaceae) Exhibiting DNA Topoisomerase II Inhibition. *Phytochemistry* **2006**, *67* (3), 307–313.
- (264) Kaburagi, Y.; Kishi, Y. Operationally Simple and Efficient Workup Procedure for TBAF-Mediated Desilylation: Application to Halichondrin Synthesis. *Org. Lett.* **2007**, *9* (4), 723–726.
- (265) Ohyama, M.; Tanaka, T.; Inuma, M.; Burandt, C. L. Phenolic Compounds Isolated from the Roots of *Sophora Stenophylla*. *Chem. Pharm. Bull. (Tokyo)* **1998**, *46* (4), 663–668.
- (266) Abe, N.; Ito, T.; Ohguchi, K.; Nasu, M.; Masuda, Y.; Oyama, M.; Nozawa, Y.; Ito, M.; Inuma, M. Resveratrol Oligomers from *Vatica Albiramis*. *J. Nat. Prod.* **2010**, *73* (9), 1499–1506.
- (267) Vincenti, M. P.; Brinckerhoff, C. E. Signal Transduction and Cell-Type Specific Regulation of Matrix Metalloproteinase Gene Expression: Can MMPs Be Good for You? *J. Cell. Physiol.* **2007**, *213* (2), 355–364.
- (268) Hande, K. R. Etoposide: Four Decades of Development of a Topoisomerase II Inhibitor. *Eur. J. Cancer* **1998**, *34* (10), 1514–1521.
- (269) Organization, W. H.; others. WHO Model List of Essential Medicines: 17th List, March 2011. **2011**.
- (270) Hu, J.; Lin, T.; Xu, J.; Ding, R.; Wang, G.; Shen, R.; Zhang, Y.; Chen, H. Polyphenols Isolated from Leaves of *Vitis Thunbergii* Var. *Taiwaniana* Regulate APP Related Pathway. *Bioorg. Med. Chem. Lett.* **2016**, *26* (2), 505–511.
- (271) Niwa, M.; Ito, J.; Oshima, Y. A New Hydroxystilbene Tetramer Named Isohopeaphenol from *Vitis Vinifera* “Kyohou.” *Heterocycles* **1997**, *45* (9), 1809.
- (272) Coggon, P.; King, T. J.; Wallwork, S. C. The Structure of Hopeaphenol. *Chem. Commun. Lond.* **1966**, No. 13, 439–440.
- (273) Coggon, P.; McPhail, A. T.; Wallwork, S. C. Structure of Hopeaphenol: X-Ray Analysis of the Benzene Solvate of Dibromodeca-O-Methylhopeaphenol. *J. Chem. Soc. B Phys. Org.* **1970**, No. 0, 884–897.
- (274) Kawabata, J.; Fukushi, E.; Hara, M.; Mizutani, J. Detection of Connectivity between Equivalent Carbons in a C₂ Molecule Using Isotopomeric Asymmetry: Identification of Hopeaphenol in *Carex Pumila*. *Magn. Reson. Chem.* **1992**, *30* (1), 6–10.
- (275) Su, P.-S.; Doerksen, R. J.; Chen, S.-H.; Sung, W.-C.; Juan, C.-C.; Rawendra, R. D. S.; Chen, C.-R.; Li, J.-W.; Aisha; Huang, T.-C.; Liao, M.-H.; Chang, C.-I.; Hsu, J.-L. Screening and Profiling Stilbene-Type Natural Products with Angiotensin-Converting

- Enzyme Inhibitory Activity from *Ampelopsis Brevipedunculata* Var. *Hancei* (Planch.) Rehder. *J. Pharm. Biomed. Anal.* **2015**, *108*, 70–77.
- (276) Zetterström, C. E.; Hasselgren, J.; Salin, O.; Davis, R. A.; Quinn, R. J.; Sundin, C.; Elofsson, M. The Resveratrol Tetramer (-)-Hopeaphenol Inhibits Type III Secretion in the Gram-Negative Pathogens *Yersinia Pseudotuberculosis* and *Pseudomonas Aeruginosa*. *PLoS ONE* **2013**, *8* (12), e81969.
- (277) Davis, R. A.; Beattie, K. D.; Xu, M.; Yang, X.; Yin, S.; Holla, H.; Healy, P. C.; Sykes, M.; Shelper, T.; Avery, V. M.; Elofsson, M.; Sundin, C.; Quinn, R. J. Solving the Supply of Resveratrol Tetramers from Papua New Guinean Rainforest Anisoptera Species That Inhibit Bacterial Type III Secretion Systems. *J. Nat. Prod.* **2014**, *77* (12), 2633–2640.
- (278) Empl, M. T.; Macke, S.; Winterhalter, P.; Puff, C.; Lapp, S.; Stoica, G.; Baumgärtner, W.; Steinberg, P. The Growth of the Canine Glioblastoma Cell Line D-GBM and the Canine Histiocytic Sarcoma Cell Line DH82 Is Inhibited by the Resveratrol Oligomers Hopeaphenol and r2-Viniferin. *Vet. Comp. Oncol.* **2014**, *12* (2), 149–159.
- (279) Wang, S.; Ma, D.; Hu, C. Three New Compounds from the Aerial Parts of *Caragana Sinica*. *Helv. Chim. Acta* **2005**, *88* (8), 2315–2321.
- (280) Oshima, Y.; Ueno, Y.; Hisamichi, K.; Takeshita, M. Ampelopsins F and G, Novel Bridged Plant Oligostilbenes from *Ampelopsis Brevipedunculata* Var. *Hancei* Roots (Vitaceae). *Tetrahedron* **1993**, *49* (26), 5801–5804.
- (281) Tanaka, T.; Ito, T.; Nakaya, K.; Inuma, M.; Riswan, S. Oligostilbenoids in Stem Bark of *Vatica Rassak*. *Phytochemistry* **2000**, *54* (1), 63–69.
- (282) Vanderwal, C. D.; Jacobsen, E. N. Enantioselective Formal Hydration of α,β -Unsaturated Imides by Al-Catalyzed Conjugate Addition of Oxime Nucleophiles. *J. Am. Chem. Soc.* **2004**, *126* (45), 14724–14725.
- (283) Edwards, H. J.; Hargrave, J. D.; Penrose, S. D.; Frost, C. G. Synthetic Applications of Rhodium Catalysed Conjugate Addition. *Chem. Soc. Rev.* **2010**, *39* (6), 2093.
- (284) Vuagnoux-d'Augustin, M.; Alexakis, A. Copper-Catalyzed Asymmetric Conjugate Addition of Trialkylaluminium Reagents to Trisubstituted Enones: Construction of Chiral Quaternary Centers. *Chem. - Eur. J.* **2007**, *13* (34), 9647–9662.
- (285) Gilman, H.; Jones, R. G.; Woods, L. A. The Preparation of Methylcopper and Some Observations on the Decomposition of Organocopper Compounds. *J. Org. Chem.* **1952**, *17* (12), 1630–1634.
- (286) Krasovskiy, A.; Knochel, P. A LiCl-Mediated Br/Mg Exchange Reaction for the Preparation of Functionalized Aryl- and Heteroarylmagnesium Compounds from Organic Bromides. *Angew. Chem. Int. Ed.* **2004**, *43* (25), 3333–3336.
- (287) Yamamoto, Y.; Tanaka, M.; Ibuka, T.; Chounan, Y. Higher Order Zinc Cuprate Reagents. Very High 1,3-Chirality Transfer Reaction of Gamma-(Mesyloxy)-Alpha,beta-Unsaturated Carbonyl Derivatives. *J. Org. Chem.* **1992**, *57* (3), 1024–1026.
- (288) Fukuhara, K.; Urabe, H. Iron-Catalyzed 1,6-Addition of Aryl Grignard Reagents to 2,4-Dienoates and -Dienamides. *Tetrahedron Lett.* **2005**, *46* (4), 603–606.
- (289) Luche, J.-L.; Petrier, C.; Lansard, J. P.; Greene, A. E. Ultrasound in Organic Synthesis. 4. A Simplified Preparation of Diarylzinc Reagents and Their Conjugate Addition to Alpha-Enones. *J. Org. Chem.* **1983**, *48* (21), 3837–3839.
- (290) Corey, E. J.; Boaz, N. W. Evidence for a Reversible D, π -Complexation, β -Cupration Sequence in the Conjugate Addition Reaction of Gilman Reagents with α,β -Enones. *Tetrahedron Lett.* **1985**, *26* (49), 6015–6018.

- (291) Corey, E. J.; Boaz, N. W. The Reactions of Combined Organocuprate-Chlorotrimethylsilane Reagents with Conjugated Carbonyl Compounds. *Tetrahedron Lett.* **1985**, 26 (49), 6019–6022.
- (292) Yamamoto, Y.; Maruyama, K. RCu.BF₃. 3. Conjugate Addition to Previously Unreactive Substituted Enoate Esters and Enoic Acids. *J. Am. Chem. Soc.* **1978**, 100 (10), 3240–3241.
- (293) Shizuri, Y.; Nakamura, K.; Yamamura, S. Reactions of Alkenes with Unstable Cations Electrogenerated from Phenols. *J. Chem. Soc. Chem. Commun.* **1985**, No. 9, 530–531.
- (294) Gates, B. D.; Dalidowicz, P.; Tebben, A.; Wang, S.; Swenton, J. S. Mechanistic Aspects and Synthetic Applications of the Electrochemical and Iodobenzene Bistrifluoroacetate Oxidative 1,3-Cycloadditions of Phenols and Electron-Rich Styrene Derivatives. *J. Org. Chem.* **1992**, 57 (7), 2135–2143.
- (295) Huang, Z.; Jin, L.; Feng, Y.; Peng, P.; Yi, H.; Lei, A. Iron-Catalyzed Oxidative Radical Cross-Coupling/Cyclization between Phenols and Olefins. *Angew. Chem. Int. Ed.* **2013**, 52 (28), 7151–7155.
- (296) Blum, T. R.; Zhu, Y.; Nordeen, S. A.; Yoon, T. P. Photocatalytic Synthesis of Dihydrobenzofurans by Oxidative [3+2] Cycloaddition of Phenols. *Angew. Chem. Int. Ed.* **2014**, 53 (41), 11056–11059.
- (297) Bérard, D.; Giroux, M.-A.; Racicot, L.; Sabot, C.; Canesi, S. Intriguing Formal [2+3] Cycloaddition Promoted by a Hypervalent Iodine Reagent. *Tetrahedron* **2008**, 64 (32), 7537–7544.
- (298) Kawabata, J.; Mishima, M.; Kurihara, H.; Mizutani, J. Stereochemistry of Two Tetrastilbenes from Carex Species. *Phytochemistry* **1995**, 40 (5), 1507–1510.